Thermal conductivity tensor from lattice excitations : theory of inelastic scattering of phonons in quantum materials

Léo Mangeolle

Numéro National de Thèse : 2022ENSL0011

THESE
en vue de l'obtention du grade de Docteur, délivré par
l'ECOLE NORMALE SUPERIEURE DE LYON

École Doctorale N° 52
Physique et Astrophysique de Lyon (PHAST)

Discipline : Physique

Soutenue publiquement le 19/09/2022, par :
Léo MANGEOLLE

Thermal conductivity tensor from lattice excitations: theory of inelastic scattering of phonons in quantum materials

Tenseur de conductivité thermique par les excitations du réseau : théorie de la diffusion inélastique des phonons dans les matériaux quantiques

---

Après l'avis de :

BRENIG, Wolfram	Professeur	Technische Universität Braunschweig
PERKINS, Natalia	Professeure	University of Minnesota

Devant le jury composé de :

PERKINS, Natalia	Professeure	University of Minnesota	Rapporteure
BALENTS, Leon	Professeur	University of California Santa Barbara	Examinateur
BEHNIA, Kamran	DR CNRS	LPEM ESPCI	Examinateur
HOLDSWORTH, Peter	PR	ENS de Lyon	Examinateur
SACHDEV, Subir	Professeur	Harvard University	Examinateur
VALENTÍ, Roser	Professeure	Goethe-Universität Frankfurt am Main	Examinatrice
SAVARY, Lucile	CR CNRS	LP ENS de Lyon	Directrice de thèse

Acknowledgements

My first thanks go to my PhD advisor, Lucile Savary.

First, of course, for undertaking and supervising the project which now constitutes the bulk of this thesis. This challenging thesis subject made me discover and learn many different aspects of condensed matter physics, and I am very grateful for this.

Also, for suggesting many great ideas to follow, especially when I was having trouble with a calculation or did not quite know "what to do next". And most of all, for her patience answering my numerous questions on various subjects.

Last but not least, for the extraordinary opportunities she offered me to participate to schools and conferences, and thus to learn many things and to present my work. I am especially grateful for this too.

It is my pleasure to thank Leon Balents, who was much involved at many stages of this work, and who provided many great ideas and suggestions about all aspects of the project.

Thanks not only for helping me understand the big picture of it, but also for delving into the technicalities of the physics, and even helping me with subtle details of integral analysis.

Thanks also for kindly answering numerous naïve questions from me, and for being a member of my defense committee.

I am very grateful to Wolfram Brenig, for agreeing to review my dissertation, and for the interest he showed in the work presented in this thesis, at the occasion of the HFM2022 conference in Paris.

I am equally grateful to Natalia Perkins, for agreeing to review my dissertation, for very stimulating discussion we had and suggestions she made during HFM2022, and for being a member of my defense committee.

I want to thank Kamran Behnia for agreeing to be a member of my defense committee. I also acknowledge the interest he showed, and the many insightful questions he asked, at my *comité de suivi de thèse*.

Many thanks to Roser Valentí, for agreeing to be a member of my defense committee, for the enthusiasm she showed about the work presented here, and for her encouragements to pursue this research.

I want to thank Subir Sachdev for agreeing to be a member of my defense committee. I also acknowledge a stimulating discussion at Collège de France.

I thank Peter Holdsworth for being a member of my defense committee. I also thank him for being my official *directeur de thèse* for a while. Last but not least, I thank him heartily for suggesting that I should do my PhD under Lucile's supervision.

I acknowledge financial support:

- from the ENS de Lyon through a CDSN scholarship;
- from the ED PhAst through an *ad hoc* contribution;
- from the ANR through the grant ANR-18-ERC2-0003-01 (QUANTEM);
- from the ERC through the grant ERC-starting-853116 (TRANSPORT).

Converting these fundings into extraordinary working conditions was made possible by the lab's administration staff, especially Nadine Clervaux and Laurence Mauduit, whom I wish to thank heartily. I should also apologize for contributing to transform L. M.'s office into a travel agency.

To continue on working conditions, a key participant in the lab's social life in the past three years was SARS-CoV-2, whom I do not particularly wish to thank.

On a brighter note, I would like to thank Aubin Archambault *et ses équipes*, especially Thomas Boquet, for voluntarily taking charge of the coffee supply of the laboratory.

Thanks also to the former and current directors of the theoretical physics team, Jean-Michel Maillet and David Carpentier, and to the director of the physics laboratory, Jean-Christophe Géminard.

Thanks finally to my *référente de thèse* Cendrine Moskalenko.

During my PhD, I have had the privilege to count among my close colleagues Baptiste Bermond, Seydou Diop and Urban Seifert. I have learned and benefited very much from the numerous (yet perhaps too few) discussions that we have had on various subjects, including (but not restricted to) thermal transport, magnetism, geometric phases, emergent gauge theories in spin systems, condensed matter theory, physics in general, and a fair number of other topics, many of which are neither closely nor vaguely related to this thesis.

I also want to thank the regular attendees, speakers and co-organisers of the Condensed Matter Students Weekly Meeting for their enthusiasm, motivation, involvement, and for sharing so many interesting bits of physics with everyone. Thanks to B. B., Eric Brillaux, Victor Dansage, S. D., Geoffroy Haeseler, Lucien Jezequel, Jacquelin Luneau, Nicolas Perez, U. S., Hubert Souquet-Basiège, Youssef Trifa and Harriet Walsh.

I should probably thank my neighbours of the M7.112.5 office for tolerating me. Thanks to Charles-Gérard Lucas, J. L., Thomas Basset, G. H., Alexis Poncet, S. D., Marcelo Guzmán, and to B. B. as a *de facto* part-time occupant.

Finally, it is *de rigueur*, and my pleasure, to thank all my collegues in the physics laboratory, whose names the margin is unfortunately too narrow to contain.

I dedicate this thesis to my family and friends.

Abstract

Probing quantum materials is important. Only thanks to a detailed understanding of materials and phenomena can one hope to manipulate them. In fact, understanding the organization of atoms and the "hidden" electronic structures in crystals has been one of the main endeavors of solid state physics since its very beginnings. Crystalline orders (e.g. via X-ray scattering) and magnetic orders (e.g. via neutron scattering) of materials have been investigated for decades. More recently, other types of orders falling out of the Landau paradigm of symmetry breaking (e.g. topological orders and fractional excitations) have been discovered. These rely deeply on the quantum nature of the underlying degrees of freedom (namely, electrons), and will be of prominent importance in the development of new technologies. Such behaviors are often looked for in novel synthetic materials, grown in the laboratory. The main issue then becomes to probe and characterize these new quantum materials, in search of interesting properties.

However, probing quantum materials is hard. The large diversity of behaviors that electrons can collectively adopt in solids can only be probed via a handful of experimental methods, each with its own (sometimes narrow) range of applicability. Thermal transport is a universal probe, in that any particle, more generally any mobile excitation of the hamiltonian, contributes to it to some extent. A challenge, both theoretical and experimental, then consists of separating the different contributions to thermal conductivity, so as to identify which kind of excitations account for (part of) the energy transport in a given material.

What is sometimes perceived as a thorn in the side of any attempt at interpreting a thermal transport measurement is the inevitable presence of phonons. Indeed, in any crystal, phonons propagate and carry energy, and acoustic (i.e. linearly dispersing) phonons survive down to zero temperature. Therefore it is crucial to understand in detail thermal conductivity due to phonons.

One of the purposes of this thesis is to show that, in fact, the thermal conductivity of phonons itself contains valuable information about all the other excitations of the material. Indeed, all the degrees of freedom in a solid are to some extent coupled to the lattice, i.e. to the phonons. In this work, I show how the latter, whose thermal conductivity is usually dominant in electrical insulators, can consequently be used as a probe of all the *other* degrees of freedom. More precisely, I show that the phonon thermal conductivity contains information about dynamical correlation functions of all other excitations. Because thermodynamics imposes certain reciprocity and detailed balance relations, the form of

these correlation functions is highly constrained. In particular, I show that the thermal *Hall* conductivity of phonons is related entirely to non-gaussian correlation functions. It thereby provides direct information about structures richer than gaussian correlations, which almost systematically dominate the signal in other types of measurements.

It is well known that Hall conductivity coefficients vanish in the presence of given symmetries, such as some mirror symmetries and, crucially, time reversal. Therefore in insulators, where most of the excitations are electrically neutral, the existence of a thermal Hall effect is far from obvious. Even less obvious is the existence of a *phonon* Hall effect, since phonons carry neither charge nor spin through which they could "feel" magnetic fields. In this work, I elucidate mechanisms whereby a phonon Hall effect is generated in insulators. In particular, I consider a two-dimensional Néel antiferromagnet on the square lattice, and a disordered magnetic phase (a spin liquid) with fermionic excitations.

Contents

Chapter 1

Introduction

1.1 Motivation for the study of thermal transport by phonons

1.1.1 Transport properties in condensed matter

Arguably one of the experimental challenges of solid state physics consists in measuring the microscopic properties of crystalline materials. Experimental probes can be roughly divided in three kinds: spectroscopic, where one studies the absorptivity, emissivity and scattering properties of a material for a certain kind of excitation (light, neutrons); thermodynamic measurements, such as specific heat or magnetic susceptibility; and transport experiments. Here we focus on the latter.

1.1.1.1 An example: the early theory of electronic conduction

The study of transport properties of materials has been instrumental in elaborating the theories which are now the fundamentals of solid state physics. A major historical example is charge transport. In that case, the phenomenological formula relating the charge current J^μ to the applied electric field E^ν, $J^\mu = \sigma^{\mu\nu} E^\nu$, which is Kirchhoff's microscopic formulation of Ohm's law, was established before the underlying mechanisms accounting for the electric conductivity tensor $\boldsymbol{\sigma}$ were known. Experimental data on electric conductivity in a variety of materials could thus be used as a basis for theoretical models thereof.

An instance of this is the theory of electronic transport in metals, initially proposed by Drude [Drude, 1900] soon after the discovery of the electron. Experiments on conductivity in narrow wires then led to a correction of the electrons' mean free path by two orders of magnitude from that predicted by Drune, and to the theory of Sommerfeld [Sommerfeld, 1928], who correctly evaluated the Fermi velocity for a sea of free fermions – two orders of magnitude larger than the velocity predicted by the Maxwell-Boltzmann kinetic theory of gases. Subsequent developments were made by Bloch [Bloch, 1929], who introduced the notion of electron bands (labeled by s) and thus the electron group velocity $v^\mu_{s\mathbf{k}} = \partial\epsilon_{s\mathbf{k}}/\partial k_\mu$ and the effective mass $m^*_s = \left|\partial^2\epsilon_{s\mathbf{k}}/\partial k_\mu \partial k_\nu\right|^{-1}$.

1.1.1.2 A few more modern examples

More exotic phenomena in solid state physics were also discovered thanks to conductivity measurements. In particular, the temperature dependence of the resistivity $\rho(T)$ played a key role in these breakthroughs.

Perhaps one of the most famous examples is the experimental discovery that in conventional metals, especially Hg, the resistivity drops to zero below a given critical temperature T_c. [Onnes, 1911] This property could later be interpreted as the hallmark of a new phase of matter [London, 1937], and the power-law behavior $\rho(T) \propto \sqrt{T - T_c}$ in terms of critical exponents following Laudau's theory of phase transitions. A satisfactory microscopic mechanism was found much later [Bardeen et al., 1957], which shed new light onto the physics of electron-phonon interactions. [Fröhlich, 1952]

Another example is the experimental discovery of a resistivity minimum at low temperatures in certain alloys in the presence of magnetic impurities [De Haas et al., 1934]. Much later, an explanation was proposed, which involved a new microscopic mechanism of interaction between conduction electrons and localized magnetic moments [Kondo, 1964]. This, in turn, led to a deeper understanding of the formation of a local Fermi liquid near a magnetic impurity (a "Kondo singlet") [Nozières, 1974].

More recently, a linear $\rho(T)$ behavior was found in some compounds, in particular the "strange metal" phase of the cuprates. Such a behavior, in the very large temperature limit of metals – the "bad metal" limit, beyond the Mott-Ioffe-Regel bound [Mott, 1960, Ioffe and Regel, 1960] –, is known to correspond to the breakdown of the Fermi liquid theory and of the quasiparticle construction, which generally predicts $\rho(T) \sim T^2$. This linear behavior was also measured at quite low temperature in doped perovskites [Lin et al., 2017]. More generally, understanding the relation between a linear resistivity at much lower temperatures, like in the cuprates, and non-Fermi-liquid behavior is an active subject of theoretical research. [Chowdhury et al., 2021]

1.1.1.3 Insights from $\rho(T)$ in metals

Even in conventional metals, the form of the electrical resistivity as a function of temperature can be far from simple, with different contributions resulting from different physical processes. Various contributions to $\rho(T)$ are summarized in the Bloch-Grüneisen formula [Bloch, 1930, Grüneisen, 1933]:

$$\rho(T) = \rho(0) + A_n \left(\frac{T}{\Theta_R}\right)^n \int_0^{\Theta_R/T} \mathrm{d}u \frac{u^n}{(e^u - 1)(1 - e^{-u})}. \tag{1.1}$$

In this formula, $\rho(0)$ is the residual zero-temperature resistivity due to boundary scattering and static defects, and $\Theta_R = 2\hbar v_{\mathrm{ph}} v_F / k_B$ is the Bloch temperature, with v_{ph} the sound velocity and v_F the Fermi velocity. The index n corresponds to the dominant electron-phonon scattering process: $n = 5$ for the usual scattering of conduction electrons by phonons, $n = 3$ for $s - d$ electron scattering, and $n = 2$ for electron-electron interactions – or more generally quasiparticle interactions in Landau's Fermi liquid theory. When several physical pro-

cesses contribute to the electrical resistivity, their scattering rates, and therefore their electrical resistivities, add up; this is the content of Matthiessen's rule. [Matthiessen and Vogt, 1864]. Then, two limits can be considered in Eq. (1.1): when $T \ll \Theta_R$, the integral depends little on T so that $\rho(T) \propto T^n$; meanwhile when $T \gg \Theta_R$, the denominator in the integrand can be expanded at small u, yielding $\rho(T) \propto T^1$. Such arguments, often used in experiment to determine the temperature scaling of the conductivity depending on the dominant scattering process and ratios between quantities such as T/Θ_R, will be pervasive in the following.

Conversely, knowledge about the temperature dependence of the conductivity in a given material, and especially about the crossovers between two different behaviors, provides important insight about the scattering processes at work, and the value of material-dependent physical parameters such as Θ_R.

1.1.2 Thermal transport and the lattice contribution

1.1.2.1 Definition of the thermal conductivity

In this thesis, I focus on thermal transport, i.e. the transport of energy, which is always a conserved quantity in time-translational invariant physical theories. Its linear response coefficient is the thermal conductivity tensor, $\kappa^{\mu\nu}$, which relates the energy current j^μ to the gradient of temperature $\partial_\nu T$ through Fourier's law [Fourier et al., 1822]:

$$j^\mu = -\kappa^{\mu\nu}\partial_\nu T, \tag{1.2}$$

which is the analogous to Ohm's law in the case of energy conduction. Equivalently, one defines the thermal resistivity tensor $\boldsymbol{\varrho} = \boldsymbol{\kappa}^{-1}$ as the inverse of the thermal conductivity tensor.

1.1.2.2 Phenomenology in metals and insulators

A rough estimate of the longitudinal thermal conductivity in a solid can be obtained for well-defined energy-carrying particles with population density n and elementary specific heat c_v. Indeed their total increase of internal energy U through displacement in a temperature gradient is $\partial_t U = nc_v v^\mu \partial_\mu T$, and the corresponding average energy current density is $J_\mu = -nc_v\tau\frac{v^2}{3}\partial_\mu T$, where τ is the typical scattering time of a particle. This yields the longitudinal thermal conductivity

$$\kappa_L \approx \frac{1}{3}\sum_j c_{v,j} v_j l_j, \tag{1.3}$$

where j indexes the different particle flavors involved in energy transport. Here $l_j = v_j\tau_j$ is the mean free path with τ_j the average scattering time of the j particles. [Peierls, 1955, Kittel, 1953]

In conventional metals, thermal conductivity is usually dominated by the electronic contributions, because of the large Fermi velocity. Since then both energy and charge are carried by the same quasiparticles, this results in the

Wiedemann-Franz law [Franz and Wiedemann, 1853]: $\boldsymbol{\kappa} = \frac{\pi^2}{3}(\frac{k_B}{e})^2 T\boldsymbol{\sigma}$; the latter states that the thermal and electrical conductivity tensors are proportional to each other. In particular, the Bloch-Grüneisen formula Eq. (1.1) can be straightforwardly translated to give the temperature dependence of the *thermal* resistivity, in any material where the Wiedemann-Franz law applies.

In insulators, mobile electrons can no longer be the main energy carriers. Thermal conductivity in insulators results from energy transport by various *neutral* excitations, which therefore do not enforce the Wiedemann-Franz law. [Ziman, 1960] In particular, at low temperatures, only those excitations which have a vanishingly small energy at long wavelengths can significantly contribute to the thermal conductivity. This includes the slow modes associated with broken continuous symmetries – in particular, acoustic phonons are usually among the main energy carriers in any insulator. Other low-energy excitations include spin waves in ordered magnetic materials, or emergent gapless neutral fermions in some disordered antiferromagnets. Further contributions can come from gapped particles such as optical phonons, gapped spin excitations, etc. In this work, I focus on the role of phonons in energy transport.

1.1.2.3 Phonons and their role in thermal conduction

Phonons are defined by the canonical quantization of the lattice displacement field [Ashcroft and Mermin, 1976]:

$$a_{n\mathbf{k}} = \frac{1}{\sqrt{N_{\text{uc}}}} \sum_{\mathbf{r}} e^{-i\mathbf{k}\cdot\mathbf{r}} \boldsymbol{\varepsilon}_n^c(\mathbf{k}) \cdot \left[\sqrt{\frac{M^c \omega_n(\mathbf{k})}{2\hbar}} \boldsymbol{u}^c(\mathbf{r}) + i \sqrt{\frac{(M^c \omega_n(\mathbf{k}))^{-1}}{2\hbar}} \boldsymbol{p}^c(\mathbf{r}) \right]. \tag{1.4}$$

In Eq. (1.4), n is the phonon band index, $\mathbf{k}$ the phonon momentum, N_{uc} is the number of unit cells, c indexes the different atoms in the unit cell with mass M^c, $u^c(\mathbf{r})$ is the displacement of atom c in the unit cell with average location $\mathbf{r}$, and $p^c(\mathbf{r})$ is the momentum of the said atom – which is canonically conjugate to $u^c(\mathbf{r})$, namely $[\hat{u}^a_\mu(\mathbf{r}), \hat{p}^b_\nu(\mathbf{r'})] = i\hbar\delta_{ab}\delta_{\mu\nu}\delta_{\mathbf{r},\mathbf{r}'}$. Finally, $\boldsymbol{\varepsilon}_n^c(\mathbf{k})$ is the polarization vector of atom c in phonon band n, which satisfies $\sum_n [\boldsymbol{\varepsilon}^a_n(\mathbf{k})^*]_\mu [\boldsymbol{\varepsilon}^b_n(\mathbf{k})]_\nu = \delta_{ab}\delta_{\mu\nu}$. From this definition, it follows that $[a_{n\mathbf{k}}, a^\dagger_{n'\mathbf{k}'}] = \delta_{nn'}\delta_{\mathbf{k},\mathbf{k}'}$, i.e. the phonons are well-defined canonical bosons.

In contrast to other quasiparticles which can emerge e.g. in magnetic phases, phonons (as the vibration modes of the lattice) are always present in a crystal. Moreover, the polarization index ranges in $n = 1, .., 3p$ where p is the number of atoms in the unit cell, so that there are typically many excited phonon modes as compared to other excitations. In particular, the three acoustic phonons, which are the Goldstone modes [Goldstone et al., 1962] associated with the translational symmetries broken by crystalline order, remain present down to zero energy (i.e. zero temperature), and therefore contribute to the thermal conductivity down to the lowest temperatures.

The thermal conductivity of phonons depends on the interactions of phonons with all other degrees of freedom present in the material, as well as with the sample boundaries, etc. Analogously to Matthiessen's rule, the phonons' scattering

rate τ^{-1} is the sum of all the partial scattering rates resulting from different scattering processes. [Tritt, 2004] This can be written in compact form as a formula similar to the Bloch-Grüneisen one for the lattice thermal conductivity $\kappa(T)$, see for instance [Klemens, 1951].

1.1.2.4 Usually dominant contributions to the phonon resistivity: purely from the lattice

Early in the theory of lattice thermal conductivity, it was realized by Peierls [Peierls, 1929] that a pure theory of harmonic phonons yields an infinite thermal conductivity (i.e. zero resistivity). This can be understood, for instance, from Eq. (1.3) with a vanishing phonon scattering rate, $\tau^{-1} \to 0$. However, the argument is in fact more general, and holds even in the presence of inter-phonon interactions (related to phonon anharmonicity [Ashcroft and Mermin, 1976]), as long as only "normal" (N) processes, i.e. processes which conserve the total phonon momentum, are involved. [Ziman, 1960, Krumhansl, 1965] At large temperatures, Peierls understood the prominent role of the (U) "umklapp-prozesse", which are interactions between (at least) three phonons where the total momentum is only conserved up to a reciprocal lattice vector $\mathbf{K}$, i.e. $\mathbf{p}_1 = \mathbf{p}_2 + \mathbf{p}_3 + \mathbf{K}$. More details concerning U-processes and phonon anharmonicity, as well as many references, are provided in [Han and Klemens, 1993]. The contribution of U-processes to the thermal resistivity is exponential, $\rho_{\mathrm{U}}(T) \sim e^{-\theta_{\mathrm{D}}/T}$ with θ_{D} the Debye temperature; this accounts for the decay of thermal conductivity at temperatures larger than θ_{D}, but does not explain why thermal conductivity vanishes at $T \to 0$.

A power-law behavior $\kappa_L(T) \sim T^3$ at low temperatures can be obtained from Eq. (1.3) assuming a constant scattering rate τ. This can follow, notably, from phonon scattering on the boundaries of the sample. An elegant derivation of the corresponding τ was proposed by Casimir [Casimir, 1938], using the direct analogy between a phonon gas and a photon gas, whose energy transport (i.e. radiation) properties are well known and given by the Stefan-Boltzmann law. Since naturally $\lim_{L\to\infty} \tau_{\mathrm{boundary}} = \infty$, where L is the smallest dimension of the sample, this term can only play a role in samples with at least one small dimension.

1.1.2.5 Many more contributions purely from the lattice

Beside these two contributions, many other scattering processes can contribute to the phonon thermal conductivity, some of which are summarized in [Tritt, 2004]; see also the review paper by [Carruthers, 1961].

Three-phonon N-processes were considered by Callaway [Callaway, 1959]; although these alone cannot yield a finite thermal resistivity (because of the Peierls argument described above), they still play a role through a phonon relaxation rate $\tau^{-1} \propto \omega^2 T^3$, which puts a bound on the validity of Matthiessen's rule [Krumhansl, 1965, Tritt, 2004]. Finally, it should be mentioned that phonon scattering by a quadratic band of conduction electrons was considered in [Ziman, 1956].

The phonon scattering rate due to point-like defects in the lattice, be it a local substitution by an atom of different mass or a local change of the elastic constant, was calculated by Klemens [Klemens, 1955]; in both cases, $\tau^{-1} \propto \omega^4$, where ω is the phonon frequency. The same author also calculated the scattering rate due to screw and edge dislocations, which behaves like $\tau^{-1} \propto \omega^1$ – this recovers Nabarro's result [Nabarro, 1951]. He also considered phonon scattering by grain boundaries, which yields (like in [Casimir, 1938]) a constant scattering rate $\tau^{-1} \sim v_{\mathrm{ph}}/L$, where now the typical distance L depends on many features of the grain boundaries and is not related to the size of the sample.

1.1.3 Thermal Hall conductivity and the role of symmetries

In this work, I am particularly interested in the thermal Hall conductivity tensor, $\boldsymbol{\kappa}_{\mathrm{H}} = \frac{1}{2}\left(\boldsymbol{\kappa} - \boldsymbol{\kappa}^{\mathrm{T}}\right)$, and the thermal Hall resistivity tensor, $\boldsymbol{\varrho}_{\mathrm{H}} = \frac{1}{2}\left(\boldsymbol{\varrho} - \boldsymbol{\varrho}^{\mathrm{T}}\right)$. The thermal Hall conductivity tensor has several unusual properties. For instance, by definition, it does not contribute to the entropy production, since the latter is proportional to $-\mathbf{j} \cdot \boldsymbol{\nabla} T$, with $\mathbf{j}$ the energy current. I will also show in the following that it is primarily related to non-time-ordered four-point correlators, instead of two-point correlations as is customary in linear response theory (see 1.2.3 below). I will also consider in detail its symmetry properties, in particular its behavior under the time reversal operation.

1.1.3.1 Time reversal symmetry

The time reversal operator, $\hat{\Theta}$, is an anti-unitary operator which can be decomposed as $\hat{\Theta} = \hat{\mathcal{U}}\hat{K}$, where $\hat{K}$ stands for complex conjugation (i.e. $\hat{K}\Psi\hat{K}^{-1} = \Psi^*$ for a complex function Ψ) and $\hat{\mathcal{U}}$ is a unitary operator. [Sakurai, 1994] In the case of a spin $\frac{1}{2}$ system, time reversal acts as $\hat{\Theta}\boldsymbol{\sigma}\hat{\Theta}^{-1} = -\boldsymbol{\sigma}$. Thus the operator $\mathcal{U}$ must anticommute with both σ^x and σ^z, and commute with σ^y; therefore a possible choice is $\mathcal{U} = \sigma^y$.[Wigner, 1959]

Time reversal plays an important role in thermal transport. Indeed, a quasiparticle energy $\omega_{n\mathbf{k}}$ is even under $\hat{\Theta}$ while its velocity $v_{n\mathbf{k}}$ is odd, so $\hat{\Theta}\mathbf{j}_{n\mathbf{k}}\hat{\Theta}^{-1} := \hat{\Theta} v_{n\mathbf{k}}\omega_{n\mathbf{k}}\hat{\Theta}^{-1} = -\mathbf{j}_{n\mathbf{k}}$: a quasiparticle energy current is odd under time reversal. Note that applying time reversal naïvely to both sides of Fourier's law, Eq.(1.2), would lead one to conclude that the whole thermal conductivity tensor $\boldsymbol{\kappa}$ is odd under time reversal. This is because *dissipative* quantities are not straightforwardly described in the framework of unitary time evolution where $\hat{\Theta}$ is well defined. By contrast, this naïve approach yields the correct result in the case of the thermal *Hall* conductivity tensor, which is non-dissipative and indeed vanishes in the presence of time reversal as a symmetry of the system – these properties can be derived rigorously using Kubo's formula and the Lehmann representation. Consequently, time reversal symmetry (TRS) is an obstruction to the existence of a thermal Hall effect. In this work, I also consider time reversal as an *effective* symmetry of the system of energy-carrying quasiparticles. In other words, "does the energy carrying (phonon) system know about the lack of time reversal symmetry in the *entire* system?", or more precisely "does the *effective* theory describing the phonon system (with the Q fields "integrated out") lack

TRS?". This will prove crucial in the case of phonons which, being electrically neutral, do not couple directly to the magnetic field.

1.1.3.2 Onsager-Casimir relations

Linear response coefficients are also strongly constrained by close-to-equilibrium thermodynamic identities. In time-reversal-invariant systems, these are the Onsager relations. [Onsager, 1931] The latter are statements about sets of conserved extensive quantities E_i, labeled by i, with conserved current $\vec{J_i}$, each of which is the thermodynamic conjugate of an intensive quantity ϕ_i (so that $\mathrm{d}S = \sum_i \phi_i \mathrm{d}E_i$). Then one can show that the linear response coefficients L_{ij} appearing in the linear response equation $J_i^\mu = L_{ij}\partial^\mu \phi_j$ satisfy the reciprocity relations $L_{ij} = L_{ji}$. [Callen, 1985, Pottier, 2009]

As was emphasized by Casimir [Casimir, 1945], strictly speaking the Onsager relations directly apply to conductivity tensors only in one-dimensional systems. Indeed, in the continuity equation $\partial_t E_i + \partial_\mu J_i^\mu = 0$ (with implicit summation over $\mu = x, y, z$ the spatial coordinate index) the i index is not a spatial orientation x, y, z of a conductivity tensor, as would be necessary for L_{ij} to be one. In 1D this not an issue, since then one of the linear response equations reads $J_i^x = L_{ii}\partial^x \phi_i$ (and the conductivity coefficient L_{ii} is a "scalar" with respect to x). Onsager's argument was nevertheless adapted in [De Groot and Mazur, 1984] (and proven more rigorously in [Garrod and Hurley, 1983]). The authors established the following result (still named after Onsager in the literature): in a time-reversal-invariant system, a conductivity tensor must be symmetric, namely $\sigma^{\mu\nu} = \sigma^{\nu\mu}$.

A further generalization to systems without time-reversal symmetry was given by Casimir [Casimir, 1945]; if ϵ_i, ϵ_j denote the signature of E_i, ϕ_j under time reversal, the linear response coefficients satisfy the Onsager-Casimir relation, $L_{ij}(\mathbf{B}) = \epsilon_i \epsilon_j L_{ji}(-\mathbf{B})$. Here $\mathbf{B}$ stands for all TR-odd parameters such as the magnetic field, magnetization, angular velocity of the sample, etc. An extension of this relation to the thermal conductivity tensor establishes that

$$\kappa^{\mu\nu}(\mathbf{B}) = \kappa^{\nu\mu}(-\mathbf{B}). \tag{1.5}$$

In particular, a thermal Hall conductivity can only exist if time reversal is broken. A brief review of Onsager-Casimir arguments applied to transport properties, and an extension thereof to boundary transport (with the same conclusions), is due to Büttiker. [Buttiker, 1988]

1.1.3.3 Other symmetries from the Curie principle

In addition to the Onsager relations, some symmetry properties of the conductivity tensor come simply from a direct application of the Curie principle of symmetry. In particular, if the system possesses a mirror symmetry with respect to the (x, z) plane, or the (y, z) plane, or the $(\frac{x+y}{\sqrt{2}}, z)$ plane, then it is easy to see from Fourier's law (i.e. the very definition of the conductivity tensor) that $\kappa_{\mathrm{H}}^{xy} = 0$. A more general analysis, based on the representation theory of the D_{4h} group, is provided in Sec.3.

In the case where energy is solely carried by the phonons, a very important (although simple and intuitive) result, which I want to emphasize, is that the above argument still holds true provided that the said transformations are symmetries of the *phonon system*, even if they are not symmetries of the entire system. Here "the phonon system" means the theory of the phonons and of all the degrees of freedom which they couple to. In other words, a phonon Hall effect can only exist if the symmetries mentioned above are broken either by the phonons themselves, or by at least one degree of freedom coupled to the lattice – note that this is a necessary condition but not a sufficient one.

Finally, note that the pure phonon theory – i.e. the dynamical theory of the lattice alone – inherits all the symmetry properties of the lattice. This includes mirror symmetries if the lattice has them, and most importantly, time reversal symmetry in any lattice. [Maradudin and Vosko, 1968] Therefore, the pure phonon system can never exhibit a thermal Hall effect.

This makes the possibility of phonon thermal Hall conductivity an interesting theoretical question, which is a central focus of this thesis. For a phonon Hall effect to exist, time reversal – along with symmetries such as mirror, if they are present in the pure lattice theory – must be broken indirectly, through coupling the lattice to other degrees of freedom. In the following, I derive expressions for the phonon thermal Hall conductivity in terms of these other degrees of freedom, both as fully general formulae and explicitly in particular cases of special relevance.

1.1.4 Experimental aspects

1.1.4.1 Schematic experimental setup and method

Thermal conductivity coefficient measurements are usually performed using experimental setups similar to that represented pictorially in Fig.1.1.

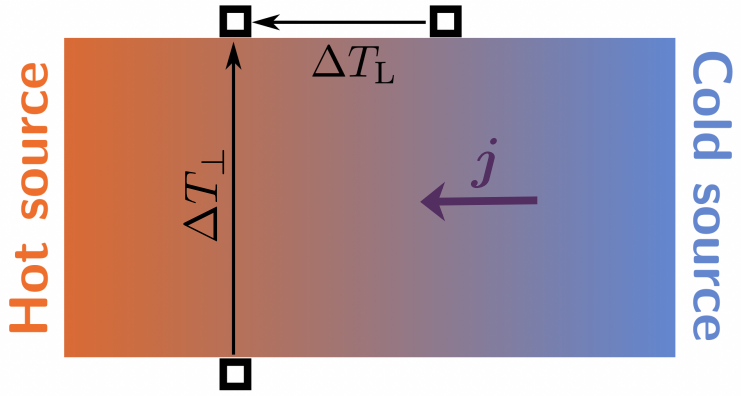

Figure 1.1: Schematic experimental setup for thermal conductivity measurement. The three black empty squares represent contact points where the temperature T is measured, and $\boldsymbol{j}$ is the energy current.

The experimentally tunable parameter is the total energy flux sent through

the sample – from which the local energy current $\boldsymbol{j}$ can be deduced in the permanent regime since it is divergenceless. Another tunable parameter is the applied magnetic field $\mathbf{H}$, which is important for instance in thermal Hall conductivity measurements.

Temperature is the parameter which is measured; it is probed simultaneously – note that this is not a strong requirement since usually experiments are carried out in the permanent regime – at (at least) three different contact points, as represented in the figure. To extract the thermal conductivity tensor, temperature differences in the directions parallel to the current (ΔT_L) and perpendicular to it ($\Delta T_\perp$) are needed, which are accessible directly by a voltage measurement in a thermocouple. This is based on the Seebeck effect, which provides a proportionality relation between the measured voltage and ΔT. The proportionality coefficient is a property of the metals in the contacts, tabulated with very good accuracy.

From ΔT_L, the longitudinal conductivity coefficient κ^{xx} is easily determined (here x is the longitudinal direction, i.e. the horizontal direction in Fig.1.1). Meanwhile, $\Delta T_\perp$ only gives access to the transverse thermal conductivity coefficient κ^{yx}, and not directly to the thermal *Hall* coefficient $\kappa_{\mathrm{H}}^{xy} = \frac{1}{2}(\kappa^{xy} - \kappa^{yx})$. Experimentally it is not feasible to simply rotate the sample by 90 degrees with respect to the energy current, so that κ^{yx} cannot be measured directly. Fortunately, the aforementioned Onsager-Casimir relation implies that $\kappa^{xy}(-\mathbf{H}) = \kappa^{yx}(\mathbf{H})$, so that by experimentally reversing the magnetic field it is possible to subtract the symmetric component of the conductivity tensor, and thus obtain the proper *Hall* conductivity.

It is worth mentioning that the contacts are contacts with the *lattice*. Therefore, any measurement, notably a temperature measurement, ought to involve phonons, even though energy is partly or even mostly carried by "electronic" (in a broad sense) degrees of freedom. Therefore, the question of thermal equilibration between the "electronic" system and the lattice is an important question with direct experimental implications. [Ye et al., 2018]

1.1.4.2 Recent experimental results

Thermal conductivity in insulators has become recently of great experimental interest, in the wake of several important experiments looking to probe neutral excitations in quantum materials. The current lack of precise theoretical understanding of any of these experiments also motivates this thesis. In Tables 1.1,1.2 I review the known experimental values in many insulating compounds, grouped in (quite arbitrary, but hopefully relevant) families. The value of H is taken as large as possible, provided that the values of both κ_H and κ_L are known for this magnetic field. The value of T is taken close to the Hall conductivity peak, which means a maximum of κ_H or κ_H/T depending on the cited papers. In the latter case (κ_H/T), the temperature in the table is indicated with a star – see for instance $Tb_2Ti_2O_7$. When κ_H is zero, the value of T is taken equal to that of a similar material with finite κ_H, as a means of comparison – see for instance $Y_2Ti_2O_7$. In the case of a single temperature measurement (e.g. for the

	Material	$\kappa_L(H,T)$ (W/K/m)	$\kappa_H(H,T)$ (mW/K/m)	H (T)	T (K)	Reference(s)
Pyrochlore materials	$Tb_2Ti_2O_7$	0.27	1.2	12	$15^\star$	[Hirschberger et al., 2015b]
	$(Tb_{.3}Y_{.7})_2Ti_2O_7$	≈ 0.5	3.0	12	$11^\star$	[Hirokane et al., 2019]
	$Y_2Ti_2O_7$	18	0	8.0	$15^\star$	[Hirschberger et al., 2015b, Li et al., 2013]
	$Lu_2V_2O_7$	0.7	≈ 1	0.1	50	[Onose et al., 2010, Ideue et al., 2012]
	$Ho_2V_2O_7$	1.0	≈ 0.5	0.1	50	[Ideue et al., 2012]
	$In_2Mn_2O_7$	3.1	≈ -2	0.1	102	[Ideue et al., 2012]
	See also [Kolland et al., 2012, Toews et al., 2013] for studies of κ_L in several other compounds.					
Perovskites	$Fe_2Mo_3O_8$	5.0	27	10	45	[Ideue et al., 2017]
	$(Zn_{1/8}Fe_{7/8})_2Mo_3O_8$	9.0	30	0.1	30	[Ideue et al., 2017]
	$SrTiO_3$	36	80	12	20	[Martelli et al., 2018, Li et al., 2020a]
	$KTaO_3$	32	2	12	30	[Martelli et al., 2018, Li et al., 2020a]
	$BiMnO_3$	≈ 2.7	≈ -0.7	0.1	48	[Ideue et al., 2012]
	$YTiO_3$	≈ 2.7	0	0.1	48	[Ideue et al., 2012]
	La_2TiMnO_6	≈ 0.4	0	0.1	48	[Ideue et al., 2012]
	$Ba_3CuSb_2O_9$	0.8	-0.08	15	50	[Sugii et al., 2017]
Others	VI_3	4.0	≈ 10	>0.1	20	[Zhang et al., 2021a]
	Cu_3TeO_6	$3.3 \cdot 10^2$	$-1.1 \cdot 10^3$	15	20	[Chen et al., 2021]

Table 1.1: Experimental results for the longitudinal and Hall thermal conductivity of several insulators, at fixed temperature T – corresponding approximately to the peak in κ_H, see text – and fixed magnetic field H. At T, the $\star$ symbol indicates a peak of κ_H/T while the absence thereof indicates a peak of κ_H.

	Material	$\kappa_{\mathrm{L}}(H,T)$ (W/K/m)	$\kappa_{\mathrm{H}}(H,T)$ (mW/K/m)	H (T)	T (K)	Reference(s)
Rare-earth garnets	$Tb_3Ga_5O_{12}$	0.19	$2.0 \cdot 10^{-2}$	3	$5.1^{\diamond}$	[Strohm et al., 2005] [Inyushkin and Taldenkov, 2007]
	$(Tb_{.3}Y_{.7})_3Ga_5O_{12}$	0.1	$9.5 \cdot 10^{-2}$	10	$8.0^{\star}$	[Hirokane et al., 2019]
Spin liquid candidates	dmit-131	0.05	?	0–10	$2^{\star}$	[Bourgeois-Hope et al., 2019] [Ni et al., 2019]
		See also [Yamashita et al., 2010] where quantitatively different values are obtained.				
	α-$RuCl_3$	15	8	12	$20^{\star}$	[Kasahara et al., 2018b]
		8	3.5	16	35	[Hentrich et al., 2019]
		See also [Czajka et al., 2022, Bruin et al., 2022a] for consistent results at lower T.				
Cuprates	La_2CuO_4	12	-38	15	$20^{\star}$	[Grissonnanche et al., 2019]
	$Sr_2CuO_2Cl_2$	7	-21	15	$20^{\star}$	[Boulanger et al., 2020]
	Nd_2CuO_4	56	-200	15	$20^{\star}$	[Boulanger et al., 2020]
	Note that doped cuprates are explored in [Grissonnanche et al., 2020, Boulanger et al., 2022].					
Kagome materials	Cu(1,3-bdc)	≈ 0.07	≈ 0.2	0.1	$0.82^{\star}$	[Hirschberger et al., 2015a]
	Volborthite	1.9	-0.66	15	$22^{\star}$	[Watanabe et al., 2016]
	Ca-Kapellasite	≈ 0.2	≈ 1	15	$20^{\star}$	[Doki et al., 2018]
	Cd-Kapellasite	1.7	11	15	$10^{\star}$	[Akazawa et al., 2020]

Table 1.2: Experimental results for the longitudinal and Hall thermal conductivity of several insulators, at fixed temperature T – corresponding approximately to the peak in κ_H, see text – and fixed magnetic field H. At T, the $\star$ symbol indicates a peak of κ_H/T while the absence thereof indicates a peak of κ_H. The $\diamond$ symbol indicates a single temperature measurement.

early experiments on $Tb_3Ga_5O_{12}$) I used the symbol $T^\diamond$. References where only κ_L is presented, or where only a range of temperatures below the κ_H peak is explored, are mentioned as comments but their results are not displayed in the table. A notable exception to the above is the case of the spin liquid candidate dmit-131, where κ_H is not known as far as I can tell; the displayed temperature is then defined with respect to the peak of κ_L (here, in fact, κ_L/T). When experimental results present a discrepancy between different papers (as is the case for dmit-131), I displayed the most recent results.

Note that Tables 1.1,1.2 are inspired, and parts of them are adapted, from a few summaries which already exist in the literature: [Chen et al., 2021, Ideue et al., 2017]. In the following I provide some more detail about the data displayed in the tables, and their possible interpretations as given in the referenced experimental papers – and the theory literature when it exists.

In the following I use the word "large" (as a qualifier for κ_H) as it is used in the experimental literature. This means sometimes that κ_H is large on an absolute scale (i.e. typically $|\kappa_H| \gtrsim 10$ mW/K/m), sometimes that κ_H is large *relatively* to κ_L (i.e. typically $|\kappa_H|/\kappa_L \gtrsim 10^{-3}$), sometimes both.

(i) Rare-earth garnets These are the first insulators where a "large" thermal Hall signal was measured, in the pioneering experiments of [Strohm et al., 2005, Inyushkin and Taldenkov, 2007] with $Tb_3Ga_5O_{12}$ (and a variant thereof), in which magnetism is carried by the localized spins of Tb^{3+} ions – plus those of superstoechiometric Tb^{3+} impurities. The temperatures where these experiments were conducted are much above the Néel temperature. Since in the paramagnetic phase the low-energy modes which can efficiently carry energy do not include spin waves, this thermal Hall effect was soon identified as a phonon contribution. The mechanism whereby phonons, by interacting with magnetic impurities, can acquire chirality and contribute a finite Hall conductivity, was investigated theoretically in [Mori et al., 2014].

(ii) Pyrochlores A thermal Hall effect was found in several pyrochlore materials displaying various magnetic behaviors. A finite thermal Hall effect was for instance measured in $Lu_2V_2O_7, Ho_2V_2O_7$ and $In_2Mn_2O_7$, which at the considered temperatures are ferromagnetic [Ideue et al., 2012]. It is interesting to note that $\kappa_{\rm H}$ can be positive or negative, depending on the material. A quite large thermal Hall conductivity was also measured in the "quantum spin ice" material $Tb_2Ti_2O_7$, while the signal seems to vanish in $Y_2Ti_2O_7$ which is non-magnetic [Hirschberger et al., 2015b] – this is in accordance with the necessity to break time-reversal symmetry to obtain a nonzero Hall effect. It is also interesting that the "intermediate" compound $(Tb_{.3}Y_{.7})_2Ti_2O_7$ has a larger peak thermal Hall conductivity (at about the same temperature) than the "pure" magnetic compound $Tb_2Ti_2O_7$. [Hirokane et al., 2019]

(iii) Kagome materials Thermal Hall conductivity signals – again of both signs – have been measured in kagome materials, such as the layered ferromagnet Cu(1,3-bdc) [Hirschberger et al., 2015a], both above and below its Curie

temperature. More exotic magnetic phases in kagome frustrated antiferromagnets were also explored: in volborthite, suspected of hosting a gapless spin liquid [Watanabe et al., 2016]; in Ca-Kapellasite [Doki et al., 2018] and Cd-Kapellasite [Akazawa et al., 2020], which seem to be well approximated by the kagome Heisenberg antiferromagnet model. A derivation of the *magnon* thermal Hall effect in the latter material is proposed in [Mook et al., 2019]. As for *phonons*, it is worth mentioning that the lattice dynamics in herbertsmithite was recently investigated, both experimentally and by *ab initio* DFT calculations, in [Li et al., 2020b].

(iv) Spin liquid candidates In the layered triangular organic dmit-131, the linear (or affine) behavior of $\kappa_L(T)$ was suggested to bear the hallmark of exotic phenomena [Yamashita et al., 2010], and was further investigated recently [Ni et al., 2019, Bourgeois-Hope et al., 2019]. Meanwhile, the nature of the energy carriers responsible for this signal remains so far unclear, and the role played by phonons has not yet been identified – note that in Chapter 4, a series of arguments are presented, which might shed light on this particular aspect.

The thermal Hall conductivity of the famous Kitaev compound α-$RuCl_3$ has been the focus of intense experimental activity over a large range of temperatures [Kasahara et al., 2018b, Hentrich et al., 2019]. The longitudinal thermal conductivity too was reported to be unusual [Hentrich et al., 2018]. Temperatures below the peak of κ_{H} were explored more specifically in [Czajka et al., 2022, Bruin et al., 2022a], partly motivated by the reported measurement of a Hall conductivity plateau at half-quantization [Kasahara et al., 2018a]. Magnetoelastic coupling in α-$RuCl_3$ was investigated in [Kaib et al., 2021] using first-principles methods. The particular role played by phonons in Kitaev materials was studied in a series of theoretical papers [Metavitsiadis and Brenig, 2020, Ye et al., 2020, Feng et al., 2021, Feng et al., 2022]. One of these partly addresses the phonon thermal Hall conductivity via the phonon Hall viscosity, while [Ye et al., 2021] emphasizes the role that phonons play in the *majorana* Hall conductivity.

Besides, [Koyama and Nasu, 2021] addresses the question of magnon Hall conductivity in related (Heisenberg-Kitaev) compounds where magnetic ordering has developed.

(v) Perovskites Measurements on the thermal Hall conductivity of the perovskite $Ba_3CuSb_2O_9$ are reported in [Sugii et al., 2017]. Because spin excitations are gapped in this material, thermal Hall transport was argued to be due to the phonons. This is also supported by the spin-lattice coupling being particularly strong in this compound. In fact, since this is known to be the case in several perovskites, most of the thermal conductivity features in these compounds have been attributed to the phonons.

In particular, an unusual behavior of the longitudinal thermal conductivity was found in the $SrTiO_3$ compound, which is insulating, nonmagnetic and nearly ferroelectric (a "quantum paraelectric") [Martelli et al., 2018]. This ma-

terial also appears to exhibit an unusually large thermal Hall conductivity, as shown in [Li et al., 2020a]; this paper identifies quite conclusively this signal as a phonon Hall effect. A much smaller (although, arguably still quite large) κ_{H} signal was also measured in the structurally very similar material $KTaO_3$. The phenomenology of phonon thermal Hall transport near the ferroelectric transition in the presence of large quantum fluctuations was subsequently discussed theoretically in [Chen et al., 2020].

Other experimental studies include the multiferroic $Fe_2Mo_3O_8$, which exhibits spontaneous electric polarization and ferrimagnetic ordering, and strong magnetoelectric coupling; a very large Hall conductivity was found in this compound and another parent multiferroic. [Ideue et al., 2017]

Thermal Hall conductivity measurements have also been conducted on several perovskite ferromagnets, namely $YTiO_3$, La_2TiMnO_6 and $BiMnO_3$. While a finite signal was indeed measured in the latter, the two others do not exhibit a measurable thermal Hall effect; this was interpreted as a magnon Hall effect (or the absence thereof) [Ideue et al., 2012], which arguably has little to do with the phenomenology of the other perovskite materials cited so far.

(vi) Cuprates Even in conventional magnets, such as the undoped La_2CuO_4 cuprate, a surprisingly large thermal Hall conductivity was found [Grissonnanche et al., 2019]. A striking feature of this signal is that it remains large in a vast region of the phase diagram, being of the same order of magnitude in the Mott insulator phase, the pseudogap regime and deep in the metallic phase. The thermal Hall conductivity was also shown to be little sensitive to the choice of the Hall plane, i.e. $\kappa^{xy} \approx \kappa^{xz}$ [Grissonnanche et al., 2020]. Because of the layered structure of magnetic ordering in these materials, this conclusively shows that magnons (or any other spin/electronic excitations) cannot account for this signal, which thus corresponds to a large *phonon* thermal Hall effect. A large κ_{H}^{xy} was also measured in the undoped cuprate $Sr_2CuO_2Cl_2$, and an exceptionally large one in Nd_2CuO_4 [Boulanger et al., 2020]. Interestingly, κ_{H}^{xy} has the same negative sign in these three materials, which is opposite to what would be expected from the Wiedemann-Franz law at finite doping, if the thermal Hall effect were of electronic origin – this was investigated further in [Boulanger et al., 2022]. This may indicate that a similar mechanism is responsible for the (phonon) thermal Hall effect in all three cuprates, and that it survives beyond the Mott insulating phase, as a negative signal is also found in the pseudogap phase [Grissonnanche et al., 2019].

(vii) Others Recently, an exceptionally large κ_{H}, presumably of phononic origin, was found in the 3D collinear antiferromagnet Cu_3TeO_6 with cubic symmetry, and reported in [Chen et al., 2021]. The authors argue that this result is striking, because it shows that no special properties such as ferroelectricity, strong correlations, or the presence of magnetic impurities are required to generate a very large thermal Hall conductivity. Indeed, the authors argue that Cu_3TeO_6 (and their samples in particular) lack all of these. Moreover, the effect survives above the Néel temperature. Some insight on these results can proba-

bly be gained from Chapter 3. There, we compute κ_H from phonon scattering in a 2D Néel collinear antiferromagnet with tetragonal symmetry; the coupling mechanism which we identify, whereby chirality is transferred to the phonons, depends strongly on anisotropies of the spin model (whose symmetries would also apply to the cubic case) but not much on the dimensionality of the spin waves (Cu_3TeO_6 is a 3D magnet). Moreover, as we emphasize in Chapter 2, the phonon Hall conductivity calculated in our approach depends on *dynamical* four-point correlation functions of the spin degrees of freedom. These may indeed survive above the Néel temperature, even though the *static* correlations do not: the general framework which we develop in Chapter 2 might be a good starting point to explain the large thermal Hall conductivity of Cu_3TeO_6.

For the sake of completeness, I note here that a finite κ_{H} was found in the 2D van der Waals ferromagnet VI_3. The authors argue that it might be of similar origin as in kagome magnets, namely that this anomalous thermal Hall effect is driven by the magnon band topology.[Zhang et al., 2021a] They also claim that phonons should play a role at lower temperatures.

1.1.4.3 Motivation

The present work is motivated by the fact that phonons should always be considered good candidates to account for a thermal conductivity signal, and the latter begs for a thorough theoretical understanding. It is therefore important to understand precisely the role played by phonons in thermal conduction, especially as far as subtle effects such as thermal Hall conductivity are concerned, for two essential reasons: (1) they might indeed be responsible for the signal, perhaps via a subtle interaction with other excitations, which can thus be probed through the phonon thermal transport; or (2) they might not be the only energy carriers, in which case being able to subtract their contribution from the experimental signal could prove very helpful. In this work, I focus on the role of phonons in thermal transport, and show that the phonon thermal conductivity tensor (in particular its Hall component) contains valuable information about interactions and correlations in the material.

1.2 Theoretical approaches to thermal conductivity

1.2.1 Hydrodynamical approach to transport theory

Several theoretical frameworks have been developed to study transport properties of quantum systems; I review some of their properties and differences in Sec. 1.2.3. In the present work, we use the hydrodynamical approach. The latter relies strongly on the concept of a quasiparticle [Landau, 1957]. The transported quantity (charge, energy, etc) is assumed to be carried by well-defined excitations called quasiparticles, whose energy is a narrowly peaked function of momentum and whose self-energy has a very small imaginary part. In other words, the quasiparticle's velocity divided by the width of the spectral function peak (which gives an estimate of the mean free path) is very large compared to

the quasiparticle's wavelength. [Coleman, 2015] This is true for phonons[1].

1.2.1.1 Hydrodynamic equations from quantum field theory

Hydrodynamic equations can be derived as an approximation from exact quantum field-theoretical formulas, notably in the Schwinger-Baym-Kadanoff formalism [Kadanoff and Baym, 1962, Prange and Kadanoff, 1964], or the closely related Keldysh formulation [Keldysh et al., 1965]. For a parallel derivation of some of our results from the Keldysh formalism, see App. 5.1. More recent discussions of this formalism, and of the derivation of "quantum Boltzmann equations" therefrom, are in [Mahan, 1987, Kamenev, 2011].

I want to emphasize an important step in the derivation. Green's functions and self-energies are a priori functions of four variables $(\mathbf{r}, t, \mathbf{p}, \omega)$: they are obtained by a Wigner transform of the two-point correlation functions, where $\mathbf{r}, t$ account for the slow variations of statistical properties while $\mathbf{p}, \omega$ contain information about fast variations of the quantum fields. The hydrodynamic approximation consists in removing the ω dependence from G, Σ, etc. This corresponds to assuming that the spectral function of the excitations is a pure Dirac delta distribution located at $\omega(\mathbf{p})$, so that $\mathbf{p}$ and the dispersion relation contain all the information about the quasiparticles. [Hänsch and Mahan, 1983] This assumption leads to considerable simplifications of the problem, while maintaining a very accurate description of the transport properties, as these are usually mainly governed by slowly-varying, classical statistical quantities [Chaikin et al., 1995] (with the notable exception of coherent effects in mesoscopic physics, as I mention later).

Therefore the hydrodynamic approach is often referred to as "semiclassical". This is also because the hydrodynamical equation is ultimately an equation of motion for the particle population density, which is essentially a classical function, as it appears on the diagonal of the density matrix. Note, nonetheless, that semiclassical kinetic equations for the full density matrix can also be derived. [Sekine and Nagaosa, 2020]. For completeness, I should mention that it is also possible, starting from Kubo formulae (or related formulations), to derive Boltzmann (or related) hydrodynamic equations. This was shown, notably, by Eliashberg [Eliashberg, 1962]. The two approaches have been shown to yield identical results in some cases [Gangadharaiah et al., 2010, Chen and Su, 1989].

1.2.1.2 Boltzmann's equation

From the above, it follows that the out-of-equilibrium dynamics of a system of well-defined quasiparticles indexed by momentum $\mathbf{k}$ and an extra index n can be described using Boltzmann's equation. The latter is valid provided that quasiparticles are well defined, so that their one-particle distribution function $N_{n\mathbf{k}}(\mathbf{r}, t)$ yields an accurate description of their statistical properties. Then, the equation of evolution for $N_{n\mathbf{k}}(\mathbf{r}, t)$ is Boltzmann's equation:

$$\left[\partial_t + \boldsymbol{v}_{n\mathbf{k}} \cdot \boldsymbol{\nabla}_{\mathbf{r}} + \boldsymbol{f}_{n\mathbf{k}} \cdot \boldsymbol{\nabla}_{\mathbf{k}}\right] N_{n\mathbf{k}}(\mathbf{r}, t) = \mathcal{C}_{n\mathbf{k}}\left[\{N_{n'\mathbf{k}'}\}\right]. \tag{1.6}$$

[1] (except in a few cases like the polaron limit, which I mention later)

On the left-hand-side, $\boldsymbol{v}_{n\mathbf{k}}$ is the group velocity of the $(n, \mathbf{k})$ quasiparticle, defined by $v^{\mu}_{n\mathbf{k}} = \partial_{k^\mu} \epsilon_{n\mathbf{k}}$ where $\epsilon_{n\mathbf{k}}$ is the quasiparticle's energy; and $\boldsymbol{f}_{n\mathbf{k}}$ is a generalized force felt by the $(n, \mathbf{k})$ quasiparticle. It can be a genuine force (for instance $\boldsymbol{f}_{n\mathbf{k}} = -e(\mathbf{E} + \boldsymbol{v}_{n\mathbf{k}} \times \mathbf{B})$ if the quasiparticles are electrons) or an emergent force proportional to the Berry curvature of the quasiparticle band – see pioneering works by Wannier, Kohn and Luttinger [Luttinger, 1951, Luttinger and Kohn, 1955, Kohn, 1959, Wannier, 1962] and a more recent review reinterpreting these results in modern terms [Xiao et al., 2010].

In the right-hand-side, $\mathcal{C}_{n\mathbf{k}}[\{N_{n'\mathbf{k}'}\}]$ is the *collision integral*, accounting for collisions (i.e. interactions) between quasiparticles and other degrees of freedom, or between quasiparticles. Crucially, the collision integral depends on all the out-of-equilibrium quasiparticle populations $N_{n'\mathbf{k}'}(\mathbf{r}, t)$, so that Eq.(1.6) (for all $n, \mathbf{k}$) is a system of (a priori nonlinear) equations with unknowns $N_{n'\mathbf{k}'}(\mathbf{r}, t)$.

In the present work, we use Boltzmann's equation to describe the out-of-equilibrium dynamics of phonons. In our case $\mathbf{k}$ is the phonon momentum, n is a band index, and we neglect the $\boldsymbol{f}_{n\mathbf{k}} \cdot \boldsymbol{\nabla}_{\mathbf{k}}$ term since we focus on the role of scattering, i.e. the $\mathcal{C}_{n\mathbf{k}}$ side of the equation.

1.2.1.3 Thermal conductivity from Boltzmann's equation

Energy transport by phonons, in particular, can be studied through Boltzmann's equation – which in this context is sometimes called the Boltzmann-Peierls equation. [Peierls, 1955, Krumhansl, 1965] The gradient of temperature typically appears in the lhs by rewriting $\boldsymbol{\nabla}_{\mathbf{r}} = \boldsymbol{\nabla}_{\mathbf{r}} T \cdot \frac{\partial}{\partial T}$, but some authors prefer using Luttinger's trick [Luttinger, 1964] (analogous to the usual minimal coupling for charged particles – see Sec. 1.2.3 for a discussion) to make it appear in the $\boldsymbol{\nabla}_{\mathbf{k}}$ term.

Meanwhile, expanding the out-of-equilibrium quasiparticle populations around the equilibrium solution, $N_{n\mathbf{k}} = N^{\mathrm{eq}}_{n\mathbf{k}} + \delta N_{n\mathbf{k}}$ and keeping only the linear order in the expansion of the collision integral, Eq.(1.6) (for all $n, \mathbf{k}$) becomes a system of *linear* equations with unknowns $\delta N_{n\mathbf{k}}(\mathbf{r}, t)$. This is sometimes referred to as Callaway's procedure [Callaway, 1959], and this is what we follow in the present work.

Solving the aforementioned system of equations, which schematically is of the form $\mathsf{X}_i = \mathsf{M}_{ij} \delta N_j$ for some quantities $\mathsf{X}_i, \mathsf{M}_{ij}$, provides the out-of-equilibrium populations $\delta N_{n\mathbf{k}}$ – here the index i, j stands for $(n, \mathbf{k})$ the phonon band and momentum. This is a trivial step when only the lowest-order contributions to κ_L are considered, because in that case the problem's matrix M is diagonal with coefficients $\mathsf{M}_{ii} = \mathsf{M}_{n\mathbf{k},n\mathbf{k}} = -\tau^{-1}_{n\mathbf{k}}$, the phonon "Drude-like" scattering rates. More generally, in the following we use the fact that for a matrix M with dominant diagonal (i.e. $|\mathsf{M}_{ii}| \gg |\mathsf{M}_{j\neq k}|$), to linear order in the off-diagonal coefficients $[\mathsf{M}^{-1}]_{ij} \approx -(-1)^{\delta_{ij}} \mathsf{M}^{-1}_{ii} \mathsf{M}_{ij} \mathsf{M}^{-1}_{jj}$. This solves the problem to linear order in the perturbed populations, i.e. to the order of linear response. From the out-of-equilibrium phonon populations $\delta N_{n\mathbf{k}}$, the phonon energy currents $j^{\mu} = \sum_{n\mathbf{k}} v^{\mu}_{n\mathbf{k}} \epsilon_{n\mathbf{k}} \delta N_{n\mathbf{k}}$ are deduced as a function of $\partial_\nu T$; this gives access to the linear response coefficients $\boldsymbol{\kappa}$ and $\boldsymbol{\varrho}$, as is shown in Chapters 2 and 3. In fact this

procedure is general and could apply to other bosons as well; however, I have argued in Sec.1.1.4 that phonons as energy carriers are of particular relevance.

1.2.2 Scattering theory and correlation functions

1.2.2.1 Master equation

The collision integral can be obtained, under certain approximations which are discussed with great detail in [Pottier, 2009] in the context of Markov chains, from the "master equations" for the population density. Quite generally, given a population or probability density ρ_r, its collision integral is given by the master equation:

$$\mathrm{D}_t \rho_r = \sum_{r'} \left\{ \Gamma_{r \leftarrow r'} \rho_{r'} - \Gamma_{r \to r'} \rho_r \right\}. \tag{1.7}$$

In the above, D_t is the particle derivative appearing in the lhs of Boltzmann's equation, r is a generic index for quantum states, and $\Gamma_{r \leftarrow r'} = \Gamma_{r' \to r}$ are transition rates between the states indexed by r and r'. We apply this master equation to express the collision integral of phonons. In this case, the quantum states $|r\rangle$ are the full many-body states of the entire system of phonons and all other degrees of freedom. The density ρ must then be understood as labeled by an extra phonon index, $n\mathbf{k}$, so that $\rho_r \equiv N_{n\mathbf{k}}(|r\rangle)$ is the population of $(n, \mathbf{k})$ phonons in the $|r\rangle$ many-body quantum state. Here we make the assumption that the phonons are good particles, defined independently from any other degree of freedom, so that it is possible to express the state of the full system in a basis where the number of phonons is always a well defined quantity. This also makes it possible to consider $\overline{N}_{n\mathbf{k}}$, the population of $(n, \mathbf{k})$ phonons averaged over all the many-body quantum states, and to deduce its collision integral $\mathcal{C}_{n\mathbf{k}}$ from the master equation Eq. (1.7). In fact, $N_{n\mathbf{k}}$ in Boltzmann's equation Eq.(1.6) should be understood as $\overline{N}_{n\mathbf{k}}$. More details are given in Chap.2.

1.2.2.2 Fermi's golden rule

The transition rates Γ appearing in the collision integral (cf Eq. 1.7) can be evaluated using scattering theory [Lifschitz and Pitajewski, 1983, Baym, 1969]. The latter is a particular instance of time-dependent perturbation theory, i.e. the problem of solving $H = H_0 + V$ where H_0 is soluble and V is an (arguably small) interaction term, where the interaction is a collision. This last statement means that the system is assumed to be non-interacting at $t \to \pm\infty$, and only at intermediate times (i.e. when the "collision" happens) does the interaction manifest itself. This assumption achieves considerable simplification of the perturbation problem. The scattering rate $\Gamma_{\mathtt{i} \to \mathtt{f}}$ between the initial $|\mathtt{i}\rangle$ and final $|\mathtt{f}\rangle$ states (defined in the unperturbed theory) is expressed using Fermi's golden rule,

$$\Gamma_{\mathtt{i} \to \mathtt{f}} = \frac{2\pi}{\hbar} |T_{\mathtt{fi}}|^2 \delta(E_{\mathtt{f}} - E_{\mathtt{i}}). \tag{1.8}$$

In this formula, $E_{\mathtt{f}}$ and $E_{\mathtt{i}}$ are the unperturbed energies of the $\mathtt{i}, \mathtt{f}$ states, and $T_{\mathtt{fi}}$ are matrix elements of the T-matrix. The latter is defined from the S-matrix

via the formula $S_{\mathtt{fi}} = \delta_{\mathtt{f,i}} - 2\pi i\delta(E_{\mathtt{f}} - E_{\mathtt{i}})T_{\mathtt{fi}}$. The S-matrix, in the interaction picture, reads $S_{\mathtt{fi}} = \langle \mathtt{f}|U(+\infty, -\infty)|\mathtt{i}\rangle$, with $U(t, t')$ the quantum evolution operator in the interaction picture.

1.2.2.3 Scattering theory

The central result of scattering theory is the Lippman-Schwinger equation, which formulated in terms of the T-matrix reads [Merzbacher, 1961]:

$$T_{\mathtt{fi}} = \langle \mathtt{f}|V|\mathtt{i}\rangle + \frac{1}{\hbar}\sum_{\mathtt{n}} \frac{\langle \mathtt{f}|V|\mathtt{n}\rangle T_{\mathtt{fi}}}{E_{\mathtt{i}} - E_{\mathtt{n}} + i\eta}, \tag{1.9}$$

where $\eta \to 0^+$ is a regularization keeping track of the time-ordering of the evolution operator U. By iterating the formula, one obtains the Born's expansion [Cohen-Tannoudji et al., 1997] of the T-matrix:

$$T_{\mathtt{fi}} = \langle \mathtt{f}|V|\mathtt{i}\rangle + \frac{\langle \mathtt{f}|V|\mathtt{n}\rangle\langle \mathtt{n}|V|\mathtt{i}\rangle}{E_{\mathtt{i}} - E_{\mathtt{n}} + i\eta} + \sum_{k=2}^{\infty} \langle \mathtt{f}|V\left(\frac{1}{E_{\mathtt{i}} - H_0 + i\eta}V\right)^k|\mathtt{i}\rangle. \tag{1.10}$$

The initial assumptions of scattering theory thus appear to considerably simplify the perturbation expansion. Indeed, the form Eq.(1.10) is both much simpler than the usual Rayleigh-Schrödinger expansion, and much more tractable than the seemingly simple Brillouin-Wigner expansion, since here all the energies appearing in the denominators are *unperturbed* energies. In our treatment of energy transport by phonons, we will keep only the first two terms of the expansion, thus making the second-order Born's approximation (although for completeness we also use the third-order contribution in an appendix), in Chapter 3.

1.2.2.4 Scattering rates as correlation functions

In this thesis, I use scattering theory to express the phonon collision integral in terms of scattering rates, resulting from the phonon interactions with generic fields Q; the interaction hamiltonian is

$$V = \sum_{n\mathbf{k}} a^\dagger_{n\mathbf{k}} Q^\dagger_{n\mathbf{k}} + \text{h.c.} \quad + \ldots, \tag{1.11}$$

where n is a phonon band index, $\mathbf{k}$ momentum, and "+..." includes terms with a larger number of phonon operators. Here I want to emphasize that Q can be *any* operator, which in practice can contain any number of particle creation-annihilation operators. Please note that $Q_{n\mathbf{k}}$ in Eq.(1.11) also includes the coupling strength. In fact, Q may even involve phonons, so long as they belong to bands which are not spanned by the n index – see below for a comment on this.

An important result, which I then use extensively in the applications, is that the phonon scattering rates can be expressed in terms of correlation functions of the Q operators. This can be derived in the basis $\{|n\rangle\}$ of eigenstates of the Hamiltonian of the Q system, sometimes called the Lehmann representation. [Bruus and Flensberg, 2004]

Let us consider $\Gamma_{n\to m}(\omega) = 2\pi \left|\langle n|Q|m\rangle\right|^2 \delta(E_n - E_m + \omega)$. This is the scattering rate of the process whereby the Q system transitions from state n to state m while a phonon of energy $\hbar\omega$ is absorbed. It was obtained from Fermi's golden rule and the first Born approximation.

Let us now consider the quantity $\frac{1}{Z}\sum_{n,m} e^{-\beta E_n}\Gamma_{n\to m}(\omega)$, where $Z = \sum_n e^{-\beta E_n}$ is the partition function of the Q system. Using the Heisenberg picture for time-evolved operators, $Q(t) = e^{iHt}Qe^{-iHt}$, along with the integral representation of the Dirac delta distribution, $\delta(\Omega) = \frac{1}{2\pi}\int \mathrm{d}t e^{i\Omega t}$, it follows that

$$\frac{2\pi}{Z}\sum_{n,m} e^{-\beta E_n}\left|\langle n|Q|m\rangle\right|^2 \delta(E_n - E_m + \omega) = \int \mathrm{d}t e^{i\omega t}\left\langle Q(t)Q(0)\right\rangle_\beta , \qquad (1.12)$$

where $\langle\cdot\rangle_\beta$ denotes the thermal average at inverse temperature β.

In the present work, we find that the phonon diagonal scattering rate – which can be identified with the Drude inverse scattering time $\tau^{-1}_{n\mathbf{k}}$, see Sec.1.2.1.3 – is expressed in terms of two-point equilibrium correlation functions of the $Q_{n\mathbf{k}}$ degrees of freedom, with the specific form

$$D^{(1)}_{n\mathbf{k}} = -\frac{1}{\hbar^2}\int dt\, e^{-i\omega_{n\mathbf{k}}t}\left\langle [Q_{n\mathbf{k}}(t), Q^\dagger_{n\mathbf{k}}(0)]\right\rangle_\beta . \qquad (1.13)$$

This identifies (up to a factor of π) as the spectral function of the $Q_{n\mathbf{k}}$ excitations, evaluated at $\omega_{n\mathbf{k}}$ frequency of the $(n,\mathbf{k})$ phonon. Here the $\langle\cdot\rangle_\beta$ average is the expectation value, at finite temperature, computed with the *free* action of the $Q_{n\mathbf{k}}$ excitations, decoupled from the phonons.

Similar formulae have been derived in neutron scattering theory. [Squires, 2012] In this context, the neutron cross-section is related to two-point correlations of the magnetic texture, and the relation is very similar to Eq.(1.13).

In this thesis, I go beyond the first Born approximation, and show how phonon scattering rates obtained from the second Born approximation can be expressed as correlation functions as well. This makes use of the formula $\frac{1}{\Omega+i0^+} = \mathrm{PP}\frac{1}{\Omega} - i\pi\delta(\Omega)$ among other identities, where PP is Cauchy's principal part. The result is that, at second Born's order, four-point correlation functions of the Q operators are involved, which are not time-ordered. This is one of the main results presented in Chap.2; I formulate it more explicitly below, after a few preliminary comments.

1.2.2.5 Detailed balance relations

Certain relations on the scattering rates are directly required by the assumption which we make, that all degrees of freedom Q are at thermal equilibrium, while only phonons are out of equilibrium. [2] Their correlation functions are

[2] This would be an important caveat, should $Q_{n\mathbf{k}}$ involve phonons (from bands which, as we have already emphasized, cannot be spanned by the index n). Then, our approach requires that the phonons involved in Q relax much faster to equilibrium than the ones spanned by n; in some cases this might apply to acoustic vs optical phonons. In other cases, other methods should be used – see e.g. Sec.1.2.3.6.

therefore related by the Kubo-Martin-Schwinger relations: their structure factor $S(\omega) := \int_{-\infty}^{+\infty} \mathrm{d}t\, e^{i\omega t}\langle Q(t)Q(0)\rangle$ can be easily shown to satisfy the relation $S(\omega) = S(-\omega)e^{\beta\hbar\omega}$. [Pottier, 2009] The latter can also be understood as a consequence of the quantum fluctuation-dissipation theorem. It is a well-known fact – for instance in the theory of thermal neutron scattering [Squires, 2012] – that these identities between *two-point equilibrium correlators*, once plugged into Fermi's golden rule at first Born's order as outlined above, become relations about *transition rates*. In this guise, they are known as detailed-balance relations, and take the following form:

$$e^{-\beta\hbar E_{\mathtt{i}}}\Gamma_{\mathtt{i}\to\mathtt{f}} = e^{-\beta\hbar E_{\mathtt{f}}}\Gamma_{\mathtt{f}\to\mathtt{i}}. \tag{1.14}$$

Here the states $|\mathtt{i}\rangle, |\mathtt{f}\rangle$ are eigenstates of the hamiltonian with energies $E_{\mathtt{i}}, E_{\mathtt{f}}$. Clearly, the detailed-balance relations express the fact that at equilibrium, the probabilities to transition from $|\mathtt{i}\rangle$ to $|\mathtt{f}\rangle$ and from $|\mathtt{f}\rangle$ to $|\mathtt{i}\rangle$ exactly compensate each other, so that the system is indeed at equilibrium.

In the following, I will show that similar relations can be derived for certain kinds of *four*-point correlation functions (and their associated two-particle transition rates), as generated by the second Born's approximation and Fermi's golden rule.

1.2.2.6 The particular case of thermal Hall conductivity

A central result of our work is that, in the phonon thermal *Hall* conductivity, the contribution of two-point correlations like Eq.(1.13) adds up to zero. Only four-point correlations with a very specific structure ultimately contribute to $\boldsymbol{\kappa}_H$ – along with yet higher-order correlations. The corresponding scattering rates read

$$\begin{aligned}\mathfrak{W}^{\ominus,qq'}_{n\mathbf{k}n'\mathbf{k}'} = \frac{2N_{\mathrm{uc}}}{\hbar^4}\mathfrak{Re}\int \mathrm{d}t_1\mathrm{d}t_2\mathrm{d}t\ \mathrm{sign}(t_2)\ e^{i\left[\Sigma^{q,q'}_{n\mathbf{k}n'\mathbf{k}'}t+\Delta^{q,q'}_{n\mathbf{k}n'\mathbf{k}'}(t_1+t_2)\right]} \\ \left\langle\left[Q^{-q}_{n\mathbf{k}}(-t-t_2), Q^{-q'}_{n'\mathbf{k}'}(-t+t_2)\right]\left\{Q^{q'}_{n'\mathbf{k}'}(-t_1), Q^{q}_{n\mathbf{k}}(t_1)\right\}\right\rangle,\end{aligned} \tag{1.15}$$

where $q, q' = \pm$, we use the convention $Q^+ = Q^\dagger, Q^- = Q$, N_{uc} is the total number of unit cells, $\Sigma^{q,q'}_{n\mathbf{k}n'\mathbf{k}'} = q\omega_{n\mathbf{k}} + q'\omega_{n'\mathbf{k}'}$ and $\Delta^{q,q'}_{n\mathbf{k}n'\mathbf{k}'} = q\omega_{n\mathbf{k}} - q'\omega_{n'\mathbf{k}'}$.

This nontrivial result entails that the phonon Hall conductivity is a probe of rich structures of the material, which appear in $\boldsymbol{\kappa}_H$ unobscured by e.g. two-point correlations.

Here a few comments are in order. The time points at which operators are evolved, and the phonon energies in the exponentials, are imposed by the perturbation theory at second Born's order, and our assumption that the phonons can be "factorised", being well defined independently from the Q system – this is shown more clearly in the appendices of Chap. 3. The presence of x commutators, $2-x$ anticommutators, and x sign functions, for x between 0 and 2, is due to certain symmetries of scattering theory (typically, $|\langle n|Q|m\rangle|^2 = |\langle m|Q^\dagger|n\rangle|^2$) and our representation of delta functions and energy denominators as time integrals. The particular structure with one commutator, one anticommutator, and

one sign function, is imposed by the generalized detailed-balance identity

$$\mathfrak{W}^{\ominus,q,q'}_{n\mathbf{k}n'\mathbf{k}'} = -e^{-\beta(q\omega_{n\mathbf{k}}+q'\omega_{n'\mathbf{k}'})}\mathfrak{W}^{\ominus,-q,-q'}_{n\mathbf{k}n'\mathbf{k}'} \tag{1.16}$$

and related formulae. Their derivation is exposed with greater detail in Chap.2.

1.2.2.7 Wick's theorem

To summarize, we have shown show that the thermal conductivity of phonons can be expressed in terms of two-point and four-point finite-temperature correlation functions of certain composite operators Q. We then consider Q to be a product of two (bosonic or fermionic) operators; thus, correlations with four to eight fields must be computed. Computing correlation functions of any (even) number of fields larger than two is a priori a difficult task. A dramatic simplification occurs when the fields have a quadratic hamiltonian: in that case, Wick's theorem [Wick, 1950] can be used. This theorem has several formulations. [Evans and Steer, 1996] One of these expresses the finite-temperature correlation of $2n$ fields $\varphi_k, \varphi^\dagger_{k'}$, $k = 1,..,n$, $k' = 1,..,n$, as the (signed in the fermionic case) sum of all products of n two-field correlations:

$$\begin{aligned}&\left\langle \varphi_1(\tau_1)\dots\varphi_n(\tau_n)\varphi^\dagger_{n'}(\tau_{n'})\dots\varphi^\dagger_{1'}(\tau_{1'})\right\rangle \\ &= \sum_{P\in\mathfrak{S}_n} \epsilon_\pm(P)\langle\varphi_1(\tau_1)\varphi^\dagger_{P(1)'}(\tau_{P(1)'})\rangle\dots\langle\varphi_n(\tau_n)\varphi^\dagger_{P(n)'}(\tau_{P(n)'})\rangle.\end{aligned} \tag{1.17}$$

Here $P \in \mathfrak{S}_n$ is a permutation of n elements, $\epsilon_\pm(P)$ is either $+1$ if the φ fields are bosonic, or the signature of the permutation P if the φ fields are fermionic. In this version of the theorem, the correlation functions need not be time-ordered. The $\varphi, \varphi^\dagger$ fields are free but need not diagonalize the (quadratic) hamiltonian, and only $\langle\varphi_i\varphi_j\rangle = 0 = \langle\varphi^\dagger_i\varphi^\dagger_j\rangle$ is assumed. Provided that Q is expressed as a product of any number of free fields (in our case, two), it is thus possible to compute explicitly correlations like in Eq. (1.15).

1.2.2.8 Consequences of symmetries of the *scattering rates*

In the present work, we thus obtain detailed and explicit expressions for the skew-scattering rate $\mathfrak{W}^{\ominus,qq'}_{n\mathbf{k}n'\mathbf{k}'}$, as it appears in the collision integral. From this, we deduce an explicit formula for the thermal Hall conductivity tensor, namely

$$\kappa^{\mu\nu}_{\mathrm{H}} = \frac{\hbar^2}{k_B T^2}\frac{1}{V}\sum_{n\mathbf{k}n'\mathbf{k}'} J^\mu_{n\mathbf{k}} K^{\mathrm{H}}_{n\mathbf{k},n'\mathbf{k}'} J^\nu_{n'\mathbf{k}'}, \tag{1.18}$$

where $J^\mu_{n\mathbf{k}} = N^{\mathrm{eq}}_{n\mathbf{k}}\omega_{n\mathbf{k}}v^\mu_{n\mathbf{k}}$ is the equilibrium phonon current, and $N^{\mathrm{eq}}_{n\mathbf{k}}$ is the equilibrium bosonic distribution. To keep the discussion simple, I do not provide the expression of $K^{\mathrm{H}}_{n\mathbf{k},n'\mathbf{k}'}$ in this introduction, and simply mention that it is proportional to $\mathfrak{W}^{\ominus,qq'}_{n\mathbf{k}n'\mathbf{k}'}$. The nonvanishing of the Hall conductivity depends crucially on the symmetry properties of the kernel $K^{\mathrm{H}}_{n\mathbf{k},n'\mathbf{k}'}$. For instance, if the relation $K^{\mathrm{H}}_{n\mathbf{k},n'\mathbf{k}'} = K^{\mathrm{H}}_{n-\mathbf{k},n'-\mathbf{k}'}$ is verified, then it is easy to see that $\kappa_{\mathrm{H}} = 0$.

In Sec. 3, we show that this is a manifestation of time reversal symmetry being *effectively* preserved in the phonon scattering rates (even though it might be broken in the full system). One can proceed similarly with mirror symmetries; a discussion including general group-theoretical statements and some nontrivial examples is presented in Sec. 3.

1.2.3 Other approaches to transport theory

I will now review some other methods which are commonly used to solve transport problems, which we do not use in the present work.

1.2.3.1 The Kubo formulae

Another traditional approach to the theory of transport (and more generally linear response) coefficients is via Kubo's formulae, derived in several different contexts in [Kubo, 1957, Kubo et al., 1957, Mori, 1958]. These are valid in full generality in the theory of linear response; namely, for a perturbed hamiltonian $\hat{H}(t) = \hat{H}_0 - F(t)\hat{A}$ where $F(t)$ is a function of time and $\hat{A}$ a hermitian operator, the response of some other hermitian observable $\hat{B}$ is given by $\langle \hat{B}(t) \rangle = \int \mathrm{d}t' \chi_{BA}(t-t')F(t')$. Here χ_{BA} is the generalized susceptibility, and the expectation $\langle \cdot \rangle$ is relative to the perturbed density matrix. Kubo's formulae express the linear response coefficient (i.e. the susceptibility) in terms of a two-point correlation:

$$\chi_{BA}(t) = \Theta(t) \int_0^\beta \mathrm{d}\lambda \langle \dot{A}(-i\hbar\lambda)\hat{B}(t) \rangle_0, \tag{1.19}$$

where $\Theta(t)$ is the Heaviside function ensuring the response's causality, $\dot{A}$ is the time derivative of $\hat{A}$, operators are time-evolved in the Heisenberg picture, and the expectation $\langle \cdot \rangle_0$ is relative to the unperturbed density matrix. [Pottier, 2009]

The particular case of transport coefficients can be obtained as follows: $F(t)$ is an external classical field, $\hat{A}$ is the position operator weighted by the local charge (so that $\dot{A}$ is a current operator), and $\hat{B}$ is a current operator. Consequently χ_{BA} is a conductivity coefficient. Kubo's formula Eq. (1.19) thus expresses conductivity coefficients in terms of equilibrium two-point current-current correlations, as is well known in special cases such as the electric conductivity $\sigma_{\mu\nu}$ or thermal conductivity $\kappa_{\mu\nu}$.

1.2.3.2 Remark about thermal transport

It is worth noting that, although Kubo's formula in its final form does not make explicit reference to the perturbation term $-F(t)\hat{A}$ in the Hamiltonian, an implicit assumption is that there exists a classical external field $F(t)$ under which particles are charged. For instance, in the case of electric conductivity (the Kubo-Nakabo formula), $F(t) := E_\nu(t)$ is the electric field and $\hat{A} := \sum_i q_i \hat{r}_i^\nu$, where i indexes small volume elements, ν a spatial direction, and q_i is the charge of the elementary volume.

The case of thermal transport is more subtle. Indeed, while one can define $\hat{A} := \sum_i h_i \hat{r}_i^\nu$ (with h_i the elementary volume's energy, playing the same role as the local charge), it is unclear what the classical field $F(t)$ should be. Therefore the validity of Kubo's formula for thermal transport is a priori questionable. However, an argument known as "Luttinger's trick" [Luttinger, 1964], based on the fact that such an $F(t)$ exists in general relativity, proves that one can safely apply Kubo's formula to thermal transport as well. Then, the thermal conductivity tensor is expressed in terms of a (thermal current - thermal current) two-point correlation function at equilibrium.

The expression of linear response coefficients provided by Kubo's formula is *exact*. However, the current-current correlation which it involves contains, in principle, all the diagrams generated by the energy-carrying-quasiparticle interactions with all the other degrees of freedom in the theory. Starting from Kubo's formula, is therefore often necessary to make subsequent approximations.

1.2.3.3 Approximation schemes from Kubo's formulae: memory matrix formalism

One instance of such approximation schemes is the "memory matrix formalism", first introduced in [Mori, 1965] and applied successfully to several transport problems, especially in one dimension [Shimshoni et al., 2003, Giamarchi, 1991]. This method is a particular choice of self-consistent perturbative expansion derived from Kubo's formula [Götze and Wölfle, 1972]; it consists in rewriting Kubo's formula while implementing an effective separation between faster modes and slower modes. The latter are the ones which efficiently carry conserved quantities such as charge and energy. [Forster, 1975, Chaikin et al., 1995] Therefore, the memory matrix formalism can be understood as a generalization of a hydrodynamic approach, applicable in cases where quasiparticles are not well-defined, such as strange metals [Lucas and Sachdev, 2015], other non-Fermi liquids and other models where the Wiedemann-Franz law breaks down [Mahajan et al., 2013].

In the present work, we do not resort to this formalism, which usually requires to carry out uncontrolled approximations, and is unnecessary in our case. Phonons in our derivation are treated as well-defined quasiparticles, so that their out-of-equilibrium dynamics is well described by the familiar (and slightly simpler) framework of Boltzmann's equation. In particular, the phonons' collision integral can be computed directly from scattering theory, and has a direct physical interpretation.

1.2.3.4 Approximation schemes from Kubo's formulae: Kubo-Streda formula and diagrammatics

Another set of approximation schemes used to compute the Kubo formula consist of resumming only certain subsets of diagrams in the perturbative expansion of the correlator. This is used, in particular, in mesoscopic physics, where diagrams with high-order vertex corrections can become relevant in some cases such as localization effects. [Rammer and Smith, 1986, Coleman, 2015] This is usually

made easier by using certain rewritings of the Kubo formula – e.g. "Kubo-Streda formulae" – in terms of retarded and advanced Green's functions [Akkermans and Montambaux, 2007]; then, statistical properties of the disorder can help in identifying the most relevant diagrams.

We do not resort to this method in the present work for three reasons. First, as mentioned just before, it is mostly relevant in situations with disorder where high-order vertex corrections are important, which is sometimes the case with electrons but less often with phonons as far as I am aware. Second, like the memory matrix formalism, it lacks the simplicity of the Boltzmann equation formalism. Third, this method was engineered to deal with problems where interaction vertices have at least three legs. Because we leave Q unspecified, the number of legs is also arbitrary, and the method unpractical.

1.2.3.5 Single-particle descriptions

In contrast to the above approaches, where vertex corrections often play an important role, some successful approaches to quantum transport – especially electronic transport – use a single-particle viewpoint, where the response function is computed at the one-loop order using approaches like the random phase approximation. [Bruus and Flensberg, 2004] These calculations are thus sometimes called "semiclassical", because they consider well-defined quasiparticles in an equilibrium field-theoretical framework, while replacing the bare propagator of the initial quasiparticle by a dressed propagator with a finite self-energy. [Rammer and Smith, 1986, Rammer, 1991] The latter has a real part, accounting for an energy shift as well as non-dissipative effects such as the single-particle Berry curvature, and an imaginary part, governing the quasiparticle lifetime and accounting for dissipative effects.

Such single-particle approaches are particularly well defined when the said quasiparticles are electrons in a metal, because their very small mass (or correspondingly the inverse of their very large Fermi velocity) is a suitable small parameter guaranteeing that loop corrections to the propagator can be neglected; this is the essence of Migdal's theorem [Migdal, 1958]. By contrast, no such controlled approximation exists for phonons. Moreover, and most importantly, these are bosons instead of fermions, and their particle number is not conserved, so that many-particle approaches are more likely to yield accurate results in their case. This is why, in the present work, we prefer to study the out-of-equilibrium dynamics in a framework where the particle number is treated explicitly as the unknown of the problem, which is the essence of Boltzmann's equation.

1.2.3.6 Coupled systems of quasiparticles out of equilibrium

Our hydrodynamical derivation of thermal transport by phonons relies on the assumption that phonons are long-lived modes which alone carry the out-of-equilibrium current. Other degrees of freedom coupled to them are treated as short-lived modes, which relax much more rapidly to equilibrium. Thus the phonon populations $\delta N_{n\mathbf{k}}$ are out of equilibrium, whereas the $Q_{n\mathbf{k}}$ degrees of

freedom have *equilibrium* correlations and dynamics – which are directly involved in the phonon scattering rates.

Other approaches, such as "thermal drag" considerations [Bartsch and Brenig, 2013], treat both the energy carriers (say, the phonons) and the other degrees of freedom (say, magnons) in a combined out-of-equilibrium framework. The thermal transport in the system is then obtained by solving a system of two (or more) coupled Boltzmann equations, one for each nonequilibrium population of particles. See for instance [Gangadharaiah et al., 2010], where this approach was used to reconcile the general Kubo formula for the *full* thermal current of both phonon and magnon quasiparticles with the formalism of Boltzmann's equation – both approaches yielding the very same result for the longitudinal thermal conductivity, at the perturbative order considered.

This approach would be well-suited to study the out-of-equilibrium dynamics of phonons coupled to *known* quasiparticles. [3] Here, we are interested in a case where the other degree of freedom, Q, is not specified – and might well have no quasiparticles at all. This is why we do not resort to this formalism in the present work.

1.2.4 Other mechanisms for (phonon) thermal Hall conductivity

Here, for completeness, I briefly review some approaches to thermal Hall conductivity (some of which involve phonons, in various ways) which we do not follow in the present work.

1.2.4.1 Thermal Hall current of spin excitations

Thermal Hall effect in quantum magnets has been considered by several authors, in the case where the transverse energy current is not carried by phonons but by magnetic excitations. In this context, it is usually called anomalous thermal Hall effect. [Katsura et al., 2010] It was shown by several authors [Samajdar et al., 2019, Han et al., 2019, Han and Lee, 2017] that thermal Hall conductivity by magnetic excitations in magnets is made possible by the presence of a spin chirality in the magnetic texture. These results could be interpreted as the manifestation of the magnon Berry curvature. [Matsumoto and Murakami, 2011, Murakami and Okamoto, 2017] In fact, although spin chirality was shown to enhance the magnon thermal Hall effect in some models [Koyama and Nasu, 2021], it does not seem to be a necessary ingredient: see [Mook et al., 2019] for some arguments based on symmetry, and [Teng et al., 2020] for a study in a magnetically disordered phase.

From the existence of a thermal Hall conductivity for magnetic excitations, in particular magnons, it becomes a priori possible for the phonons to exhibit a thermal Hall conductivity as well. Indeed, since the seminal work of Holstein [Holstein, 1959a, Holstein, 1959b], it has been known that strongly interacting

[3] In particular, this would be an appropriate framework to study the interaction between several phonon branches, in cases where the separation outlined in the footnote of Sec. 1.2.2.5 cannot apply.

phonons and magnons can merge into emergent quasiparticles known as polarons [Mahan, 1981]. This results from the fact that a quadratic hamiltonian of magnon and phonon operators can be readily diagonalized by means of a Bogoliubov transformation, whose eigenstates are a new type of bosons interpolating between the initial two families of bosons. This effect, however, cannot yield a large contribution to thermal transport at low temperatures. Indeed, the phase space of such phonon-magnon interactions is typically very small: the constraint of both energy and momentum conservation by the interaction requires a crossing between the bare phonon and magnon bands. [White et al., 1965] This, for acoustic phonons and (almost) gapless magnons, can only occur close to zero energy and momentum – where no current is carried –, except if magnons and phonons have similar velocities, as was studied in $FeCl_2$ [Laurence and Petitgrand, 1973] and FeF_2 [Lovesey, 1972].

These approaches are of course completely distinct from our problem, since phonons are not the energy carriers there. Now I will consider more specifically approaches to the *phonon* thermal Hall conductivity, which have been proposed in the literature. In the following cases, phonons remain well-defined quasiparticles (as opposed to the polaron case, notably) and are alone responsible for the transport of energy through the sample. Other excitations or quasiparticles may still interact with the phonons (and e.g. scatter them), but their role as energy carriers is not considered.

1.2.4.2 Phonon Berry curvature from Raman-type interactions

A model for thermal Hall conductivity has been proposed in paramagnetic dielectrics, based on a Raman-type coupling between the unit cell orbital momentum and the local magnetization in the presence of a magnetic field. [Sheng et al., 2006, Kagan and Maksimov, 2008] I briefly explain the physical origin of this mechanism in Sec. 1.3.3. This interaction appears as a two-phonon term in the energy current, and directly enters the thermal conductivity via Kubo's formula. This mechanism involves explicitly the local magnetization $\boldsymbol{m}$ and the unit cell angular momentum $\boldsymbol{p}$, namely $H' = \boldsymbol{m} \cdot (\boldsymbol{u} \times \boldsymbol{p})$ with $\boldsymbol{u}$ the displacement field. In a single-particle picture, this H' can also be interpreted as a redefinition of the phonon energies, including a time-reversal-breaking term responsible for a thermal Hall conductivity.

This single-particle contribution was subsequently interpreted in terms of the Berry curvature of the phonon bands. [Qin et al., 2012, Zhang et al., 2010] This is why it is often referred to as an *intrinsic* phonon thermal Hall conductivity, although the breaking of time reversal is provided by the local magnetization appearing in the Raman coupling. Note, however, that this mechanism is also possible in *nonmagnetic* materials, if one considers deviations from the Born-Oppenheimer approximation for the charged nuclei of the lattice, subject to a Lorentz force in an external magnetic field. [Saito et al., 2019]

This approach is very similar to the next one. I comment on their common interpretation in the next subsection.

1.2.4.3 Phonon Hall viscosity

A related approach to the phonon thermal Hall effect uses the concept of phonon Hall viscosity (PHV) [Barkeshli et al., 2012]. This is the coefficient $\eta^H_{\alpha\beta\gamma\delta}$ appearing in the antisymmetric, time-reversal-odd term $\mathcal{L}_{\text{phv}} = \eta^H_{\alpha\beta\gamma\delta}\left(\mathcal{E}^{\alpha\beta}\dot{\mathcal{E}}^{\gamma\delta} - \dot{\mathcal{E}}^{\alpha\beta}\mathcal{E}^{\gamma\delta}\right)$ in the strain field's lagrangean, where $\mathcal{E}$ is the strain field and $\dot{\mathcal{E}}$ its time derivative. [Ye et al., 2021] Such a term in the phonon's action is usually obtained by integrating out other degrees of freedom coupled to the phonons and sensitive to the breaking of time reversal. For instance, in [Zhang et al., 2021b], these other degrees of freedom are spinons in a chiral spin liquid – with a Zeeman coupling of the spins to an external magnetic field and a spin chirality term $\mathbf{S}_i \cdot (\mathbf{S}_j \times \mathbf{S}_k)$ around triangular plaquettes –, and the resulting phonon Hall viscosity is explicitly calculated. In [Feng et al., 2021], these other degree of freedom are the emergent Majorana fermions in the Kitaev spin liquid; in the presence of a magnetic field these exhibit a chirality, which is transferred to the phonons as a PHV coefficient. Finally, in [Zhang et al., 2019], these other degrees of freedom are magnons, made chiral by a staggered Dzyaloshinskii-Moriya interaction in the presence of a magnetic field (however the PHV is not explicitly calculated, and only the thermal current is "renormalized" accordingly). The phonon Hall viscosity term is a non-dissipative contribution to the phonon's action; it thus provides an intrinsic, single-particle contribution to the phonon Hall conductivity.

This approach and the previous one both account for an intrinsic contribution to the conductivity. In Boltzmann's equation their effect would appear as a force term $\boldsymbol{f}_{n\mathbf{k}} \cdot \boldsymbol{\nabla}_{\mathbf{k}}$, since a Berry curvature has the interpretation of a force of geometric origin. While such approaches have led to interesting findings in the theory of phonon Hall conductivity, they are known [Ye et al., 2021] to yield a very small phonon Hall effect if not enhanced by an extrinsic mechanism [Guo and Sachdev, 2021]. In this work, on the contrary, we focus on that other side of Boltzmann's equation that can generate a phonon Hall effect, namely the collision integral $\mathcal{C}_{n\mathbf{k}}$, which is a different problem.

1.2.4.4 Extrinsic phonon Hall effect from scattering by impurities

Finally, many works focus on phonon scattering by defects. This was studied in the case of magnetic impurities, where the breaking of time reversal by the external magnetic field is directly mediated by the impurities' inner structure. Energy transport was studied both via Boltzmann's equation [Mori et al., 2014, Sun et al., 2021] and via Kubo's formula [Guo et al., 2022]. Phonon scattering by defects was also studied in the case of "simple" ionic crystals in [Flebus and MacDonald, 2021], where the breaking of time reversal comes from the Lorentz force felt by moving charged defects. Finally, phonon scattering by defects was studied in a recent work [Guo and Sachdev, 2021], as a means to enhance an already existing phonon Hall effect (generated by an ansatz phonon Hall viscosity term) through resonant skew-scattering.

These works provide mechanisms which can explain phonon thermal Hall conductivity in materials with a specific model for defects. These defects are,

almost by definition, independent objects, and translational invariance is thus explicitly broken in the derivation. In the following, on the contrary, we show how the thermal conductivity of phonons coupled to degrees of freedom $Q_{n\mathbf{k}}$ provides information about the *correlations* between the Q objects, which may as well be (periodic) defects or continuous fields in the description which we use. In particular, we apply our formalism to continuous fields (both bosonic and fermionic). Thus we are focusing on the clean limit, which is a different problem to that studied in the works cited above.

1.2.4.5 Remark about a pioneering work on phonon Hall effect

Here, a remark about the work of [Mori et al., 2014] is in order. Indeed, in this paper, the phonon Hall conductivity in rare-earth garnets is computed using the Boltzmann's equation formalism and scattering theory. Application of the formalism introduced in this thesis to defects in rare-earth garnets would provide a generalization of the results of the cited paper in at least two respects.

First, the model of spin-strain interaction which the authors of [Mori et al., 2014] consider is a particular case of our Eq.(1.11), where the field $Q_{n\mathbf{k}}$ is a composite of spin operators localized at the impurity, and thus does not depend on $\mathbf{k}$. Nevertheless, correlations of the impurities' positions are introduced, in an *ad hoc* manner, at the end of their derivation, and appear to be necessary for a net phonon Hall conductivity to appear. Our formalism, where $Q_{n\mathbf{k}}$ is a priori momentum-dependent, provides a natural framework where such effects of impurity positional correlations can be incorporated.

Second, the scattering rates considered in [Mori et al., 2014] are those of a particular type of scattering events, where one phonon is absorbed and one phonon is emitted. Although these appear to be sufficient to capture a phonon Hall effect, they arise at the same perturbative order as processes where two phonons are emitted or two phonons are absorbed. In our derivation, all such processes are considered, so that we provide the complete expression of scattering rates at second order in perturbation theory. We also consider carefully the detailed balance relations between these scattering rates, which provides an interpertation, in terms of general properties of linear response, of the cancellation of $W_{\mathbf{k}\to\mathbf{k}'}f_{\mathbf{k}} - W_{\mathbf{k}'\to\mathbf{k}}f_{\mathbf{k}'}$ (in the notations of [Mori et al., 2014]).

1.3 Dynamics, correlations and phonons in Néel antiferromagnets

In this section, I briefly introduce some concepts which we use in the bulk of this thesis, when studying the dynamics and correlations in antiferromagnets in general, and 2D tetragonal collinear Néel antiferromagnets in particular.

1.3.1 Introduction to antiferromagnetism

1.3.1.1 A rough definition

Antiferromagnetism is a form of magnetic ordering, i.e. a magnetic phase characterized by long-range spin-spin correlations, which does not exhibit any net spontaneous magnetization: $\langle \boldsymbol{S}_{\text{tot}} \rangle = \mathbf{0}$. The order parameter is not the local net magnetization vector $\langle \boldsymbol{S}(\mathbf{r}) \rangle$, and its orientation is site-dependent. For instance, the Néel order on a bipartite lattice is characterized by a finite staggered magnetization $\sum_{\mathbf{r}} \langle (-1)^{\mathbf{r}} \boldsymbol{S}(\mathbf{r}) \rangle$, where $(-1)^{\mathbf{r}}$ alternates between neighboring sites.

Antiferromagnetic ordering typically arises as the classical ground state of magnetic models like

$$H_{\text{mag}} = \sum_{\mathbf{r},\mathbf{r}'} \sum_{a,b} J^{ab}_{\mathbf{r},\mathbf{r}'} S^a_{\mathbf{r}} S^b_{\mathbf{r}'}, \tag{1.20}$$

where $a, b = x, y, z$ is the spin orientation index and $J^{ab}_{\mathbf{r},\mathbf{r}'}$ the magnetic exchange constant between spins at sites $\mathbf{r}$ and $\mathbf{r}'$, for large *positive* isotropic exchange J_{iso} between nearest neighbors.

1.3.1.2 Where to find it

Antiferromagnetism is most common in insulators.

A first way to see this is as follows. Starting from the Hubbard model,

$$H_{tU} = -t \sum_{\langle \mathbf{r},\mathbf{r}' \rangle, \sigma} c^\dagger_{\mathbf{r},\sigma} c_{\mathbf{r}',\sigma} + U \sum_{\mathbf{r}} n_{\mathbf{r},\uparrow} n_{\mathbf{r},\downarrow}, \tag{1.21}$$

due to the strong electron-electron repulsion the system undergoes a Mott metal-insulator transition as U/t increases [Mott, 1960, Marino, 2017]. The electrons are then localized on atomic orbitals, and can only hop between sites via virtual processes. Second order perturbation theory in large U/t, around the ground state in which each orbital is half-filled, leads to an antiferromagnetic interaction (i.e. a positive $J^{\text{iso}} \sim t^2/U$ exchange) between neighboring spins. This is the Anderson superexchange mechanism. [Anderson, 1959]

A second way to see this is to start from the Fermi surface description of conduction electrons. At specific fillings (notably, half-filling), the existence of nesting wavevectors between opposite sides of the Fermi surface is responsible for an antiferromagnetic instability of the Fermi surface, and a (typically, twofold) enlargement of the unit cell. [Fradkin, 2013, Mahan, 1981]. This changes the filling by a multiplicative factor (typically, 2), and leads to an ("Slater", band) insulating state.

In both cases the insulating state is associated with some form of antiferromagnetism. By contrast, the Stoner mechanism [Stoner, 1938], whereby a Fermi sea of itinerant electrons spontaneously spin-polarizes due to Pauli exclusion, leads to ferromagnetic exchange ($J^{\text{iso}} < 0$).

Antiferromagnetism can also be induced in the presence of itinerant electrons by RKKY interactions [Yosida, 1957, Coleman, 2015]. Conversely, ferromagnetism can of course also be induced in insulators, for instance by dipolar interactions between two orthogonal orbitals, or by superexchange between one

half-filled and one filled or empty orbitals, following the Goodenough-Kanamori rules [Goodenough, 1955, Kanamori, 1959]. Notably, this is the case in perovskite materials.

1.3.1.3 What to expect from an antiferromagnetic ansatz

It should be noted that antiferromagnetism is not a priori a good description of the quantum ground state. For instance, the Néel state on a bipartite lattice

$$|N\rangle = \left(\bigotimes_{\mathbf{r}\ \text{even}} |\uparrow^z\rangle \right) \otimes \left(\bigotimes_{\mathbf{r}\ \text{odd}} |\downarrow^z\rangle \right) \tag{1.22}$$

is not an eigenstate of the hamiltonian Eq.(1.20) – even with only isotropic exchange. [Anderson, 1952] Exact solutions (especially in 1D systems) for some antiferromagnetic models exist, such as the Bethe and Lieb-Schultz-Mattis solutions for spin chains [Bethe, 1931, Lieb et al., 1961], which show that the true quantum ground state is not well described by the Néel ansatz.

However, while the antiferromagnetic classical ground state is not exact, it may still lie in the same phase as the true ground state. Moreover, the *excitations* above the ground states are well captured by spin wave theory above the Néel classical order [Kubo, 1952]. It is therefore possible to understand with good accuracy the quantum dynamics and correlations of the spins above the ground state, starting from a rough approximation thereof by a classical antiferromagnetic ansatz. [Anderson, 1952] This is even true in some two-dimensional antiferromagnets, which are very common and particularly well described by classical spin wave theory [Auerbach, 1994], e.g. layered materials such as cuprates below their Néel temperature [Stein et al., 1996], even though such a phase is in principle forbidden by the Berezinskii-Hohenberg-Mermin-Wagner theorem [Berezinskii, 1971, Berezinskii, 1972].

In the remainder of this section, we therefore describe the spin dynamics of a 2D magnet on the square lattice using a low-energy theory for spin waves above a classical Néel order.

1.3.2 Spin waves from a nonlinear sigma-model

1.3.2.1 Low-energy approximation of the local spins

To derive the low-energy theory of a collinear $S = 1/2$ antiferromagnet, it is useful to rewrite the local spin operators in terms of two fields, the staggered magnetization $\mathbf{n}(\mathbf{r})$ and the net magnetization $\mathbf{m}(\mathbf{r})$:

$$\mathbf{S}(\mathbf{r}) = (-1)^{\mathbf{r}} S\mathbf{n}(\mathbf{r}) + \mathbf{m}(\mathbf{r}), \tag{1.23}$$

where $(-1)^{\mathbf{r}}$ changes signs between neighboring sites (here I assume a bipartite lattice). This is referred to as Haldane's mapping in the literature. [Haldane, 1983b, Haldane, 1983a] The classical spin vector $\mathbf{S}(\mathbf{r})$ is assumed to be of fixed length $S = 1/2$, which is enforced by assuming the local constraints $\mathbf{n} \cdot \mathbf{m} = 0$ as well as $\mathbf{n}^2 + \mathbf{m}^2/S^2 = 1$. In terms of the spin operator, one should notice that

the quantum rotor algebra [Sachdev, 2011] for the $\mathbf{n}, \mathbf{m}$ fields, $[\mathrm{m}^\mu(\mathbf{r}), \mathrm{n}^\nu(\mathbf{r}')] = i\epsilon^{\mu\nu\lambda}\delta_{\mathbf{r},\mathbf{r}'}\mathrm{n}^\lambda(\mathbf{r})$, $[\mathrm{m}^\mu(\mathbf{r}), \mathrm{m}^\nu(\mathbf{r}')] = i\epsilon^{\mu\nu\lambda}\delta_{\mathbf{r},\mathbf{r}'}\mathrm{m}^\lambda(\mathbf{r})$, $[\mathrm{n}^\mu(\mathbf{r}), \mathrm{n}^\nu(\mathbf{r}')] = 0$, reproduces the spin algebra $[S^\mu(\mathbf{r}), S^\nu(\mathbf{r}')] = i\epsilon^{\mu\nu\lambda}\delta_{\mathbf{r},\mathbf{r}'}S^\lambda(\mathbf{r})$.

1.3.2.2 Expansion around the classical order

For concreteness, let us now assume Néel ordering along the $\hat{\mathbf{x}}$ axis, such that the classical ground state is $\mathbf{n}_0 = \hat{\mathbf{x}}, \mathbf{m}_0 = \mathbf{0}$. The low-energy theory is obtained by expanding the spin field at linear order around this classical state, namely $\mathbf{n} = \mathbf{n}_0 + \boldsymbol{n}$ and $\mathbf{m} = \boldsymbol{m}$, where now $\boldsymbol{m}, \boldsymbol{n}$ are small perturbations. Plugging this into constraint equations on $\mathbf{m}, \mathbf{n}$, the components m_x and n_x become functions of (m_y, m_z, n_y, n_z). Moreover, it is clear that at linear order in the perturbation, $m_x \approx 0 \approx n_x$. The commutation relations for the four remaining fields are $[m_y(\mathbf{r}), n_z(\mathbf{r}')] = i\delta_{\mathbf{r},\mathbf{r}'} = -[m_z(\mathbf{r}), n_y(\mathbf{r}')]$ and $[m_y(\mathbf{r}), m_z(\mathbf{r}')] = 0 = [n_y(\mathbf{r}), n_z(\mathbf{r}')]$. The two Goldstone modes associated with the spontaneous breaking of $O(3)$ rotational symmetry by the Néel order, n_y and n_z, are thus (in this linear approximation) independent, and their canonical momenta are $-m_z$ and m_y, respectively. It is thus possible to perform a canonical quantization of these fields in terms of bosonic operators, $b_{\ell\mathbf{k}}$ and $b^\dagger_{\ell\mathbf{k}}$, which are identified as magnon creation-annihilation operators, where $\ell = 0, 1$ is a magnon flavor index. Then, all the magnon correlations can be computed – these are free bosons, once their hamiltonian is specified.

Here, for simplicity I assumed that the classical configuration is a Néel order along the $\hat{\mathbf{x}}$ axis. This is not enough to warrant a nonzero phononic thermal Hall effect: one can understand this from the fact that time reversal followed by a translation by half a magnetic unit cell is a symmetry of the system, which forbids any Hall conductivity. Therefore, in the next chapters, we will include an external magnetic field $\boldsymbol{h}$. In response, the spins are slightly tilted off the Néel axis toward the direction of $\boldsymbol{h}$; this is captured by a nonzero $\mathbf{m}_0$ value. The spin wave expansion which I described above can still be performed around this new classical order, without any further conceptual difficulty. Details are provided in Chapter 3.

1.3.2.3 Phenomenological model from symmetries

The semiclassical action for a Heisenberg magnet can also be derived from the path integral, and is known to be the nonlinear sigma-model [Fradkin, 2013, Marino, 2017]. The representation of spins using coherent states produces a topological (Wess-Zumino) term in the action, which in the antiferromagnetic case takes the simple form $\mathbf{m} \times \partial_t \mathbf{n}$, where the $\mathbf{m}$ and $\mathbf{n}$ fields identify as those of Sec.1.3.2.1. This has the familiar form $\boldsymbol{x} \cdot \dot{\boldsymbol{p}}$ of the kinetic term of canonical position and momentum variables, which confirms the identification of "position" and "momentum" variables made in Sec.1.3.2.2 above. [Auerbach, 1994] Thus, in the antiferromagnetic case it is sufficient to know the nonlinear sigma

hamiltonian, which can be written on symmetry grounds:

$$\mathcal{H}_{\mathrm{nl}\sigma} = \frac{\rho}{2}\left(|\underline{\boldsymbol{\nabla}} n_y|^2 + |\underline{\boldsymbol{\nabla}} n_z|^2\right) + \frac{1}{2\chi}(m_y^2 + m_z^2) + \sum_{a,b=y,z}\left(\frac{\Gamma_{ab}}{2} + \frac{\chi}{2}h_a h_b\right) n_a n_b. \tag{1.24}$$

If $\boldsymbol{\Gamma} = \mathbf{0} = \boldsymbol{h}$, the slow field $\boldsymbol{n}$ is indeed a gapless mode, while the fast field $\boldsymbol{m}$ remains gapped, as is the case for half-integer Heisenberg antiferromagnets. Here I used the words "slow" and "fast" in the traditional sense of [Chaikin et al., 1995]: a "slow" variable appears in the hamiltonian predominantly through its spatial derivatives, while a "fast" variable appears predominantly within a mass term.

The first two terms of the hamiltonian Eq. (1.24) form the simplest quadratic hamiltonian with linear soft modes n_y, n_z and fast modes m_y, m_z, with the same symmetries as the magnetically ordered phase (recall we choose it to be antiferromagnetic on the square lattice, with a Néel axis along the $\hat{\mathbf{x}}$ direction). Note that in Eq. (1.24) the $-\boldsymbol{m}\cdot\boldsymbol{h}$ coupling is effectively taken into account in the possibly nonzero expectation value $\langle\boldsymbol{m}\rangle$ (and we disregard the modification of the value of the gap of the fast mode $\boldsymbol{m}$ due to $\boldsymbol{h}$).

The third and fourth terms give a (small) mass to the Goldstone modes, and are a priori not diagonal in the (n_y, n_z) basis. In particular, the fourth term captures the coupling between an external applied field $\boldsymbol{h}$ and the slow mode $\boldsymbol{n}$, so that there exists an explicit dependence of the magnon gap on the magnetic field.

When the external magnetic field is oriented purely along the $\hat{\mathbf{y}}$ axis or purely along the $\hat{\mathbf{z}}$ axis, then the combination of a C_2 rotation around the field's axis and a translation by half a magnetic unit cell is a symmetry of the system, under which the last two terms of Eq. (1.24) for $a \neq b$ are not invariant. Therefore, this symmetry restores the independence of the n_y, n_z fields, which are then indeed the eigenmodes of the low-energy hamiltonian Eq. (1.24).

We use this method in the next two chapters to write down the effective dynamics for the spin variables interacting with the phonons.

1.3.2.4 Derivation from the microscopic theory

This low-energy theory can also be derived directly from a microscopic model, such as a spin hamiltonian of the form Eq. (1.20). For instance, ρ and χ can be derived from the magnetic exchange constant in the Heisenberg spin model, namely $\rho = 2JS^2$ and $\chi^{-1} = 4J\mathfrak{a}^2$ with $\mathfrak{a}$ the lattice spacing.

Similarly, the third term in our continuous hamiltonian Eq. (1.24) originates from anisotropies in the spin model. These anisotropies are due to spin-orbit coupling, which breaks the $O(3)$ spin rotational invariance while preserving the crystalline symmetries. The Γ_{ab} parameters can be derived, for instance, from an XXZ interaction between neighboring spins, as I show in Chap.3.

Finally, the last term is written on symmetry grounds (as the lowest-order term preserving the C_2 symmetry mentioned above), but the value of the $\chi/2$ constant can be derived from the continuous description above (see Chap.3, appendices), or it can be identified from microscopics [Benfatto and Silva Neto, 2006].

1.3.3 Magnetoelastic coupling

Here I review a few theoretical descriptions of magnetoelastic (i.e. spin-lattice) coupling in ordered magnets. In particular, I briefly present the method used in the next two chapters.

1.3.3.1 Generic coupling to boson bilinears

In Chapters 2 and 3, we consider the case where the $Q_{n\mathbf{k}}$ operators are bilinears of bosonic creation-annihilation operators, so that the interaction hamiltonian takes schematically the form $H_{\text{int}} = (a^\dagger + a)(b^\dagger b^\dagger + bb + b^\dagger b)$, where $a^\dagger$ is the phonon creation operator and $b^\dagger$ that of the other bosons. A term of the form $(a^\dagger + a)(b^\dagger + b)$ could in principle be included, but it can be readily removed from the interaction through a redefinition of the a and b operators. Indeed, as mentioned in Sec.1.2.4.1, the phonon-boson hamiltonian restricted to its quadratic order H_0 is always diagonalizable by means of a Bogoliubov transformation, so that a and b are its eigenbosons: H_0 contains $a^\dagger a$ and $b^\dagger b$ terms, but no mixed $(a^\dagger b, \dots)$ terms. Therefore H_{int} as written above is the lowest-order nontrivial interaction term that can be written between one phonon a and bosons b.

This was also the starting point in [Chernyshev and Brenig, 2015, Gangadharaiah et al., 2010], which considered the longitudinal conductivity of coupled phonon-magnon systems. Here we do not yet specify the nature of the b bosons, and compute the Hall conductivity as well. Importantly, all the information about the original quasiparticles and their dynamics is contained within the coupling constants. In Chap.3 these are denoted $\mathcal{B}$, so that

$$Q^q_{n\mathbf{k}} = \frac{1}{\sqrt{N_{\text{uc}}}} \sum_{\substack{\mathbf{p},\ell_1,\ell_2 \\ q_1,q_2=\pm}} \mathcal{B}^{n,\ell_1,\ell_2|q_1q_2q}_{\mathbf{k};\mathbf{p}} \; b^{q_1}_{\ell_1,\mathbf{p}+\frac{q}{2}\mathbf{k}} b^{q_2}_{\ell_2,-\mathbf{p}+\frac{q}{2}\mathbf{k}}. \tag{1.25}$$

Here $q, q_{1,2} = \pm$, $\ell_{1,2}$ is a boson valley index, and the b bosons are eigenbosons of the free hamiltonian H_0. Note that the breaking of time reversal and other symmetries which are obstacles to a phonon Hall effect is solely contained within the $\mathcal{B}$ coupling coefficients. A realistic theory of phonon thermal Hall conductivity thus requires a detailed understanding of these phonon-boson coupling constants and their symmetries; we undertake this task in the present work, both in general terms and more specifically in the case of phonon-magnon interactions.

1.3.3.2 Phonon-magnon coupling from the microscopic model

The existence of a coupling between phonons and magnons – or, in fact, between the displacement field $\boldsymbol{u}$ and spins – can be understood intuitively from simple considerations. The magnetic exchange constants $J^{ab}_{\mathbf{r},\mathbf{r}'}$ appearing in the spin hamiltonian Eq.(1.20) depend strongly on the distance between the sites $\mathbf{r}, \mathbf{r}'$ – in fact exponentially so, as they are typically proportional to an overlap of atomic orbitals[4]. Therefore, the displacement field $\boldsymbol{u}$ is coupled to the spins

[4] except, notably, dipolar interactions between spins; these are only polynomial wrt the distance.

already at first order in the Taylor expansion of H_{mag}, through an interaction term of the form $H' = \boldsymbol{u} \cdot \boldsymbol{\nabla} J^{ab} S^a S^b$. This intuitive approach was followed in [Cottam, 1974] to study the longitudinal phonon thermal conductivity in a Heisenberg magnet. More recently it was used in [Ye et al., 2020] to study the dynamics of phonons in the Kitaev spin liquid. The same authors and coworkers explored the consequences of spin-phonon coupling in this phase in terms of specific heat, sound attenuation and phonon Hall viscosity in [Feng et al., 2021], and of Raman spectroscopy in [Feng et al., 2022].

The same form of coupling was also used in [Zhang et al., 2019] to study the phonon thermal Hall conductivity in a collinear ferromagnet. In the latter, it is worth noting that an external magnetic field as well as a strongly anisotropic magnetic exchange (namely, a staggered Dzyaloshinskii-Moriya interaction) are involved in κ_{H}.

Finally, we note that the same form of coupling was used in [Ferrari et al., 2021] to study the role of phonons in the dynamics of frustrated magnetic models.

This intuitive derivation from the spin hamiltonian assumes implicitly a Born-Oppenheimer approximation, because in principle the local spins $\boldsymbol{S}_{\mathbf{r}}$ become ill-defined quantities if the dynamics of $\boldsymbol{u}$ happens on the same timescales as the dynamics of electronic orbitals. Because of the very small ratio m/M, with m the electron's mass and M the typical mass of the lattice ions, the lattice motion can always be treated as very slow and this intuitive approach is well-founded. This assumption is also made in [Lovesey, 1972], which uses a similar derivation as above, but at the more fundamental level of Coulomb interactions between electronic orbitals, to account for the longitudinal conductivity of phonons in antiferromagnets.

1.3.3.3 Phenomenological expansion in terms of $\boldsymbol{u}$ and $\boldsymbol{p}$

A more phenomenological approach consists in writing all possible coupling terms allowed by symmetry, up to a given order in powers of the displacement field $\boldsymbol{u}$ or of $\boldsymbol{p}$ its conjugate momentum, $[\boldsymbol{u}, \boldsymbol{p}] = i$ (i.e. in the number of phonons involved, see Eq. (1.4)). A list of the lowest-order terms allowed by time reversal symmetry is provided in [Ioselevich and Capellmann, 1995]:

$$H_{\text{int}} = \sum_{\mathbf{r},\mathbf{r}'} S^a_{\mathbf{r}} \left[B^{1|ab}_{\mathbf{r},\mathbf{r}'} \; p^b_{\mathbf{r}'} + u^b_{\mathbf{r}'} \sum_{\mathbf{r}''} \left(B^{2|abc}_{\mathbf{r},\mathbf{r}',\mathbf{r}''} \; S^c_{\mathbf{r}''} + B^{3|abc}_{\mathbf{r},\mathbf{r}',\mathbf{r}''} \; p^c_{\mathbf{r}''} \right) \right] \tag{1.26}$$

where the Bs are phenomenological coupling parameters. Note that the dependence on a, b, c spatial indices is constrained by spatial symmetries of the crystal. This is because the larger symmetry group of the "initial" spin operators, corresponding to the symmetries of the non-interacting magnetic ions, is broken by crystal fields and spin-orbit coupling down to the spatial symmetry group of the crystal. [Laurence and Petitgrand, 1973]

The first term in Eq.(1.26) can be derived as a coupling between the local spin and the magnetic field generated by the oscillatory motion of the ions; the coupling parametr $B^{1|ab}_{\mathbf{r},\mathbf{r}'}$ is thus typically proportional to v_{ion}/c (with c the speed of light), and as such is utterly negligible.

The third term in Eq.(1.26) corresponds to the Raman coupling which I mentioned in Sec.1.2.4; its derivation as a coupling between the local spin $\boldsymbol{S}_{\mathbf{r}}$ and time-dependent crystal fields – or equivalently between $\boldsymbol{S}_{\mathbf{r}}$ and $\boldsymbol{L}_{\mathbf{r}'} := \boldsymbol{u}_{\mathbf{r}'} \times \boldsymbol{p}_{\mathbf{r}'}$ the unit cell angular momentum – is discussed in [Manenkov and Orbach, 1966, Abragam and Bleaney, 1970]. This is a two-phonon term which has been shown to generate a finite, but small, phonon Hall viscosity.

Finally, the second term in Eq.(1.26) is a one-phonon term which corresponds to the intuitive picture given above in terms of spatial derivative of magnetic exchange. Since it has the smallest number of phonon operators, and is thus the most likely to contribute to the phonon skew-scattering rate at low temperatures, this is the term which we consider in more detail in the following.

1.3.3.4 Phenomenological expansion with tetragonal symmetry

In this case, we do not consider directly the local spins $\boldsymbol{S}_{\mathbf{r}}$ but rather the slowly varying fields $\mathbf{m}, \mathbf{n}$ of the nonlinear sigma-model. To derive the coupling between one phonon operator and two such fields, we follow the method outlined above: we write down all interaction terms between the strain tensor and bilinears of the $\mathbf{m}, \mathbf{n}$ fields which are allowed by symmetries.[5]

This method requires to select a crystal symmetry group; we choose the largest tetragonal symmetry group, D_{4h}, which is for instance that of the low-temperature crystalline phase of La_2CuO_4. Because the form of the coupling shoud not depend a priori on the magnetic phase, the symmetry group of the spin variables – which is also that of the crystal itself, because of the aforementioned spin-orbit and crystal-field effects – is the largest possible one, i.e. that of the paramagnetic phase. The interaction hamiltonian then takes the following form:

$$H'_{\text{tetra}} = \sum_{\mathbf{r}} \sum_{\alpha,\beta=x,y,z} \sum_{a,b=x,y,z} \mathcal{E}^{\alpha\beta}_{\mathbf{r}} \left(\Lambda^{(\mathrm{n}),\alpha\beta}_{ab} \mathrm{n}_a \mathrm{n}_b + \Lambda^{(\mathrm{m}),\alpha\beta}_{ab} \frac{\mathrm{m}_a \mathrm{m}_b}{n_0^2} \right) \Big|_{\mathbf{r}}, \qquad (1.27)$$

where n_0 is the ordered antiferromagnetic moment density. Here each $\Lambda^{(\xi)}$ tensor, which we define to be symmetric in both ab (direction in spin space) and $\alpha\beta$ (direction in real space) variables, has seven independent coefficients, which are related by symmetries. All technical details are provided in the appendices of Chapter 3. Note also that $\mathrm{m}^a\mathrm{n}^b$ couplings are forbidden by the combination of time reversal and translation by one (lattice) unit cell.

The last step in our derivation of the phonon-magnon interaction consists in expanding the $\mathbf{m}, \mathbf{n}$ fields around the classically ordered configuration $\mathbf{m}_0, \mathbf{n}_0$, which comprises the Néel antiferromagnetic spontaneous ordering and the paramagnetic response to an applied external magnetic field. I outlined this procedure in Sec.1.3.2.2. The choice of the Néel vector along the crystal's $\hat{\mathbf{x}}$ axis, and

[5] In principle, one could also consider coupling of the magnetic fluctuations to the "small rotation tensor", which is the antisymmetric cousin of the strain tensor: $\Omega_{\mu\nu} := \frac{1}{2}(\partial_\mu u_\nu - \partial_\nu u_\mu)$. Because of global rotational invariance, the latter does not appear in the hamiltonian of linear elasticity, and only manifests itself at higher orders in the theory of elasticity. Thus we expect it to yield much smaller contributions than the strain tensor to the magnetoelastic coupling, as it already yields much smaller contributions to pure elasticity itself. Therefore, we consider only the symmetric strain tensor in the magnetoelastic hamiltonian density.

of the applied magnetic field along either of the $(\hat{\mathbf{y}}, \hat{\mathbf{z}})$ axes, makes more explicit the role of anisotropic couplings – such as XXZ exchange – and spin-orbit coupling in the phonon Hall effect. In Chapter 3, we show precisely which of the $\Lambda^{(\xi)}$ coupling constants are involved in κ_{H}, and what this implies, notably, in terms of the temperature and field dependences of the conductivity. In particular, the sign of κ_{H} is determined by a nontrivial combination of these parameters.

1.3.3.5 Remark about a pioneering work on spin-phonon coupling

Here, a remark about the work of [Cottam, 1974] is in order. There, the author uses the method outlined in Sec. 1.3.3.2 to study the interactions between phonons and magnons in a Heisenberg antiferromagnet. The interaction kernel has one phonon line and two (each incoming or outgoing) magnon lines, and is therefore a particular case of our interaction Eq.(1.25) where the coupling is isotropic in spin space.

The author computes, among other quantities, the phonon self-energy arising from this phonon-magnon interaction, and in particular the phonon damping rate τ^{-1}. We also compute this quantity, which we denote $D_{n\mathbf{k}}$, except that our result corresponds to the one-loop diagram in the expansion. Therefore our result coincides with that of [Cottam, 1974] only at leading order in the perturbation expansion.

On the other hand, our result for the phonon longitudinal thermal conductivity is more general than that of [Cottam, 1974], where only a Heisenberg exchange is considered. This corresponds, in our Eq.(1.27), to considering $\Lambda_{ab}^{(\xi),\alpha\beta} \propto \delta_{ab}$. By contrast, we consider the most general exchange allowed by symmetry. This enables us to derive the scaling behavior $\kappa_{\mathrm{L}}(T)$ for the full temperature scale, while Cottam's result captures only the high-temperature limit. Moreover, as mentioned in the previous subsubsection, we show that the phonon *Hall* conductivity arises from coupling constants which are anisotropic in spin space, so that the model considered in [Cottam, 1974] leads to a vanishing phonon Hall effect.

1.4 Dynamics, correlations and phonons in insulators with emergent fermions

In this section, I briefly introduce some concepts which are used in the fourth chapter of this thesis, when studying the dynamics and correlations in disordered antiferromagnets with neutral fermionic excitations.

1.4.1 Fermionic phases in insulators

1.4.1.1 Disordered magnetic phases and fractional excitations

The previous section dealt with models where antiferromagnetic exchange between neighboring spins on the square lattice induced the formation of a Néel-ordered phase. However, antiferromagnetic exchange sometimes favors *disor-*

dered phases at low temperatures. This occurs especially on frustrated lattices [Balents, 2010], such as the two-dimensional triangular and kagome lattices or the three-dimensional pyrochlore lattice. This property has been kown for a very long time, even at the classical level with purely Ising spins: see for instance the extensive entropy in the ground state of water ice [Pauling, 1935] – this is in the pyrochlore lattice – or the disordered phase down to zero temperature of the triangular lattice Ising model [Wannier, 1950].

An extension of this concept to quantum magnetic phases was proposed by Anderson, in the particular case of the resonating valence bond state [Anderson, 1973]. This led to the more general concept of quantum spin liquids, which have attracted much interest in the last few decades; two recent reviews are [Savary and Balents, 2016, Zhou et al., 2017]. One pervasive feature of spin liquids is the existence of fractional excitations, i.e. emergent degrees of freedom whose charge, spin, central charge, or statistics are a fraction of that of the initial degrees of freedom of the model. [Wen, 2004] In the following, I will be particularly interested in emergent fermionic phases of quantum magnets. The physics of such systems is well described in terms of emergent neutral fermions, even though (1) the initial model was written purely in terms of local spins – which have bosonic statistics – and (2) the elementary constituents of any such degrees of freedom are always electrons, and it is far from obvious how neutral fermions could be built out of electrons while not contradicting the spin-statistics theorem.

1.4.1.2 Parton representation of spin models

To theoretically describe spin liquids, and more generally phases of matter hosting emergent fractional excitations, it is often useful to resort to parton constructions. In Sec. 4 of this thesis, we resort to the Abrikosov fermion representation of spin operators, which are the fermionic counterpart of Schwinger bosons [Auerbach, 1994], and were first introduced in the context of Kondo problems [Abrikosov, 1965]. Introducing fermion operators $\psi_{\mathbf{r}\alpha}, \psi^\dagger_{\mathbf{r}\alpha}$, where $\alpha = \uparrow, \downarrow$ is a spin-$\frac{1}{2}$ index (although this construction can be generalized to higher spin [Coleman, 2015]), it is possible to construct spin operators from these "partons":

$$\boldsymbol{S}_{\mathbf{r}} = \frac{1}{2} \sum_{\alpha\beta} \psi^\dagger_{\mathbf{r}\alpha} \boldsymbol{\sigma}_{\alpha\beta} \psi_{\mathbf{r}\beta}. \tag{1.28}$$

This construction faithfully reproduces the spin *operators*: provided that the fermionic algebra $\left\{\psi_{\alpha\mathbf{r}}, \psi^\dagger_{\beta\mathbf{r}'}\right\} = \delta_{\alpha\alpha'}\delta_{\mathbf{r},\mathbf{r}'}$ is satisfied, the spin algebra $[S^\mu, S^\nu] = i\epsilon^{\mu\nu\lambda}S^\lambda$ holds.

This construction also faithfully reproduces the *states* of a spin-$\frac{1}{2}$ system, provided that the local constraint $\psi^\dagger_{\mathbf{r}\alpha}\psi_{\mathbf{r}\alpha} = 1 \quad \forall \mathbf{r}$ is enforced exactly at each site (this ensures that the Hilbert space has two dimensions instead of four, as would be the case without the constraint). [Baskaran and Anderson, 1988, Marston and Affleck, 1989]. This local constraint can be implemented by means of a Gutzwiller projection (i.e. a projection onto the space of "physical" states where the constraint is satisfied), or via a Lagrange multiplier term, $-A^0_{\mathbf{r}}(f^\dagger_{\alpha\mathbf{r}} f_{\alpha\mathbf{r}} -$

1), where functional integration over the time fluctuations of $A^0_{\mathbf{r}}$ enforces the constraint.

1.4.1.3 Redundancy and constraint as gauge theories

Besides, two sets of $SU(2)$ operations can act on this fermionic representation. First, the rotations of the physical spin, which transform $S^\mu_{\mathbf{r}} \to R^{\mu\nu} S^\nu_{\mathbf{r}}$; these are physical symmetry operations, which can be broken by the initial spin model in the presence of spin-orbit coupling, or spontaneously in some magnetic phases. Second, there is an $SU(2)$ redundancy in the above description of spins in terms of Abrikosov fermions, i.e. a set of $SU(2)$ gauge transformations which modify the fermion operators ($f^\dagger_\uparrow \to \alpha f^\dagger_\uparrow + \beta f_\downarrow$, etc) but not the physical spin $\boldsymbol{S}_{\mathbf{r}} \to \mathbf{S}_{\mathbf{r}}$. In some phases this $SU(2)$ gauge symmetry is broken down to $U(1)$, e.g. by a Higgs mechanism whereby some components of the gauge field are gapped out.[Wen, 2004] In such phases, the low-energy theory retains a $U(1)$ gauge invariance $\psi_{\alpha\mathbf{r}} \to e^{i\theta(\mathbf{r})}\psi_{\alpha\mathbf{r}}$, and the fermions are coupled to a lattice gauge vector potential $A_{\mathbf{r},\mathbf{r}'}$. The latter contains the space components of the full $D = d + 1$ emergent gauge field, while $A^0_{\mathbf{r}}$ is the time component.

The existence of phases of spin models well described by a $U(1)$ gauge theory can be questioned. Indeed, in $D = 2 + 1$ the existence of deconfined $U(1)$ *pure* gauge theories is forbidden because of the strong fluctuations of the gauge field, in particular by the proliferation of instantons [Polyakov, 1977]. However, in the presence of matter fields, $D = 2 + 1$ abelian gauge theories have been shown to be stable in several cases [Hermele et al., 2004]. This, as shown already by Ioffe and Larkin [Ioffe and Larkin, 1989], is due to the fact that the presence of charges modifies the action of the gauge field, in particular in the form of Landau damping – see Sec. 1.4.2 for further details, so that the instantons' action becomes infinite, and the deconfined emergent electromagnetism is stable.

1.4.1.4 Free fermion theory from a mean-field ansatz

The above procedure (plugging Eq. (1.28) into Eq. (1.20)) replaces the spin hamiltonian by a four-fermion interaction. It is then possible to decouple this interaction in various mean-field channels, for instance by means of a Hubbard-Stratonovich transformation [Hubbard, 1959, Stratonovich, 1957]. Different theories obtained from different mean-field decoupling channels can subsequently be interpreted as describing different emergent fermionic phases [Nagaosa and Lee, 1990, Lee and Nagaosa, 1992, Lee et al., 2006]. Note that although the hamiltonian is now quadratic in the fermions, they are not really free fermions since they are still coupled to the fluctuating gauge field.

A next approximation step often consists in neglecting the time fluctuations of the $A^0_{\mathbf{r}}(\tau)$ gauge field. Then, the local constraint of single occupancy is only enforced *on average, in the ground state*, and the consequence is that $A^0_{\mathbf{r}}$ acts only as a local chemical potential for the fermions [Nagaosa, 1999]. Whether this approximation is also true (for a given gauge choice) for the spatial components $A_{\mathbf{r},\mathbf{r}'}$ of the gauge field, and which ansatz is taken for the corresponding expectation values, leads to a panoply of different quantum phases. [Wen, 2004]

One particular instance of such an emergent fermionic phase is a spinon Fermi surface spin liquid, in which the essentially free spinons exhibit a Fermi surface and are charged under an emergent $U(1)$ gauge field. This phase has been argued to occur in two-dimensional models of strongly correlated electrons [Marston and Affleck, 1989], and to be stable against gauge field fluctuations [Lee, 2008].

In Chapter 4, we also consider the case of Dirac fermions in two dimensions. These are of course well known in the context of graphene, and they also theoretically emerge in (insulating) magnetic phases, for instance in the π-flux phase of the model described above[Fradkin, 2013, Wen, 2004, Misguich, 2011]. In the latter case, the mean-field ansatz for the emergent gauge field displays a uniform magnetic flux per plaquette. Such a phase has also been argued to be stable if the matter fields satisfy some conditions [Hermele et al., 2004].

1.4.2 Dynamics of the emergent gauge field

I now consider more specifically the case of a $U(1)$ spinon Fermi surface [Ioffe and Larkin, 1989, Kim et al., 1994]. The physics is that of a Fermi sea of fermions charged under a $U(1)$ gauge field, and is therefore very similar to electrodynamics in metals [Abrikosov et al., 1976, Lifshitz and Pitaevskii, 1980] – except that the values of the fundamental constants are very different.

The fermions are coupled to the gauge field via the minimal coupling term, $\mathcal{L}_{\text{mc}} = -\boldsymbol{j} \cdot \boldsymbol{A}$, where $\boldsymbol{j} \sim f^\dagger \boldsymbol{\nabla} f$ is the fermion current and $\boldsymbol{A}$ the vector potential. Diagrammatically, the minimal coupling can therefore be represented as a vertex with one gauge boson line and one incoming, one outgoing fermion lines. This, as is well known from the quantum theory of the electron gas, leads to a renormalization of the gauge field's propagator. The latter is traditionally treated in the random phase approximation, and the renormalized dielectric constant is expressed in terms of the fermion "polarization bubbles". [Bruus and Flensberg, 2004]

Thus the emergent electromagnetic field, because of its interaction with the spinon Fermi surface, has the same propagator as an electromagnetic wave in a metal, at low momentum and frequency. Namely, its scalar (time) component acquires a mass because of Debye screening, while the vector field's action contains a Landau damping term, which accounts for the wave's dissipation by fermion-hole pair fluctuations. [Giuliani and Vignale, 2005]

At the end of Chapter 4, we consider the coupling of phonons directly to the emergent electromagnetic field. The latter has a quadratic action – once the fermions have been integrated out, yielding the aforementioned mass and damping terms. Therefore the two-point correlator involved in the phonon's longitudinal thermal conductivity, Eq.(1.13), can be directly evaluated from the action, either by analytic continuation [Coleman, 2015] or by performing a Matsubara summation [Matsubara, 1955] and a Fourier transform.

1.4.3 Magnetoelastic couplings

1.4.3.1 Generic coupling to fermion bilinears

Like in the previous section, where the coupling of a phonon operator to boson bilinears contributed to the phonons' collision integral, in Chapter 4 we consider the coupling of a phonon operator to fermion bilinears. We write an interaction hamiltonian of the form $H_{\text{int}} \sim \mathcal{B}(a^\dagger + a) f^\dagger f$, with f the fermion destruction operator and $\mathcal{B}$ a generic coupling constant:

$$Q_{n\mathbf{k}} = \sum_{\mathbf{p},\ell,\ell'} \mathcal{B}^{n,\ell,\ell'}_{\mathbf{k};\mathbf{p}} \; f^\dagger_{\ell,\mathbf{p}} f_{\ell',\mathbf{p}+\mathbf{k}}. \tag{1.29}$$

$H_{\text{int}} = a^\dagger Q^\dagger + \text{h.c.}$ is the most general hamiltonian with one phonon operator and two fermion operators which conserves the total fermion number – i.e. the system's total charge with respect to the $U(1)$ gauge theory. Like in the bosonic case, ℓ, ℓ' is a fermion flavor index and the free fermion hamiltonian is diagonal in the f basis. Note that our calculations are valid regardless of the nature of the fermions, which may just as well be spinons coupled to an emergent electromagnetism, or mobile electrons coupled to "true" electromagnetism.

Our calculation of the phonon's longitudinal conductivity involves two-point correlations of the form Eq.(1.13), which more precisely can be identified to the $Q_{n\mathbf{k}}$ field's spectral function. Since here we have $Q \sim f^\dagger f$ (so that $Q_{n\mathbf{k}}$ can be schematically interpreted as a fermion current or density), this calculation involves the same "bubble" diagram as mentioned in the previous subsection, with a phonon line instead of a photon line. In both cases, this amounts to computing a quantity very similar to the Lindhard function [Coleman, 2015] of a sea of non-interacting fermions.

1.4.3.2 Phonon-spinon coupling from the microscopic model

Now again, I consider more specifically the case of a spinon Fermi surface $U(1)$ spin liquid. Then, the above fermions are spinons, defined from underlying spins via the parton construction Eq.(1.28). The coupling constant $\mathcal{B}$, similarly to the magnons' case, can be obtained from spatial derivatives of the magnetic exchange constants of the initial spin model Eq.(1.20). The phonon-spin coupling thus obtained, $H' \sim (a + a^\dagger) SS$, can then be expanded in terms of Abrikosov fermions, yielding an interaction of the form $H' \sim f^\dagger f (a + a^\dagger) f^\dagger f$. The mean-field treatment outlined in Sec.1.4.1 completes the derivation. A very similar derivation was proposed in [Zhang et al., 2021b], where the phonon-spinon coupling constant is derived directly from spatial derivatives of the spinon hopping amplitudes $t_{\mathbf{r},\mathbf{r}'}$.

1.4.3.3 Specific terms: Dzyaloshinskii-Moriya and Rashba couplings

In addition to the Heisenberg exchange between spins, we also introduced a Dzyaloshinskii-Moriya interaction – namely, a contribution of the form $H_{\text{DM}} = \sum_{\mathbf{r},\mathbf{r}' \text{ n.n.}} J_D (\boldsymbol{S}_\mathbf{r} \times \boldsymbol{S}_{\mathbf{r}'}) \cdot \hat{\mathbf{D}}(\mathbf{r} - \mathbf{r}')$ to the initial spin hamiltonian Eq.(1.20). Here

J_D is the strength of the Dzyaloshinskii-Moriya interaction, and we choose a particular bond-dependent $\hat{\mathbf{D}}(\mathbf{r}-\mathbf{r}') = (\hat{\boldsymbol{z}} \times [\mathbf{r}-\mathbf{r}'])$ always orthogonal to the bond. For such an interaction to exist, inversion symmetry must be broken; depending on the lattice, this is also the case for other discrete (for instance, mirror) symmetries.

Once treated following the procedure described in Sec.1.4.1.4, the Dzyaloshinskii-Moriya interaction between *spins* becomes an interaction between *spinons* which takes the form of a Rashba term, i.e. $H_{\mathrm{DM}} \longrightarrow H_{\mathrm{R}} = \alpha_{\mathrm{R}}\, f^{\dagger}_{\mathbf{p}}\, \hat{\boldsymbol{z}} \cdot (\mathbf{p} \times \boldsymbol{\sigma})\, f_{\mathbf{p}}$ in the free spinons' hamiltonian. The Rashba term is a typical spin-orbit effect in electronic conductors, which can be derived by a simple argument in the case of electrons; here is an outline of this argument. [Petersen and Hedegård, 2000] The starting point is an electron orbiting in the xy plane and placed in an electric field $\mathbf{E} = E_0 \hat{\boldsymbol{z}}$. While inversion symmetry in the xy plane seems to be preserved, it is actually broken in the electron's rest frame because of special relativity – here it is worth recalling that spin-orbit couplings are essentially relativistic effects [Atkins and de Paula, 2014]. The electron interacts with an effective magnetic field $\mathbf{B}_{\mathrm{eff}} = \gamma \boldsymbol{v} \times \mathbf{E}$, and the corresponding Zeeman interaction takes the form of a Rashba term, $H_{\mathrm{soc}} = \alpha_{\mathrm{R}} (\mathbf{p} \times \boldsymbol{\sigma}) \cdot \hat{\boldsymbol{z}}$ with a coupling constant $\alpha_{\mathrm{R}} \propto E_0 \mu_{\mathrm{B}}/m$.

1.4.3.4 Phenomenological phonon-photon coupling

Finally, as already mentioned, for completeness we also consider the coupling between phonons and the emergent electromagnetic field – that is to say, the electric or the magnetic field, since phonons can only couple to gauge-invariant quantities. We consider a general, phenomenological interaction between the phonons and the electric field only. This coupling requires a lack of inversion symmetry (either inherited from the lattice structure itself, or occurs spontaneously in the spin liquid's mean-field ansatz) but not of time reversal. In turn, this coupling does not contribute to the phonon Hall conductivity. Nonetheless it produces a contribution to the longitudinal thermal conductivity, which we compute in Sec.4.H.

1.5 Summary of the following chapters

In this thesis, I study the thermal transport induced by the intrinsic scattering of phonons by a generic quantum degree of freedom. This means a field Q, whose correlations are a priori completely general, and whose coupling to the phonons is constrained only by unitarity and translational invariance. The scattering rates resulting from this interaction have direct consequences on the phonon thermal conductivity tensor. We compute them in the framework of quantum scattering theory. Then, we study the phonon out-of-equilibrium dynamics via kinetic theory, in particular Boltzmann's equation.

At lowest order, the diagonal scattering rate, which determines the longitudinal conductivity, is controlled by two-point correlation functions of the Q field. A central result of our work is that off-diagonal scattering rates which are

involved in the thermal Hall conductivity do involve at least three-point correlation functions (and at least four-point correlators in the case of one-phonon interactions). We obtain general and explicit expressions for these correlations, carefully isolating those contributions that are specific to the Hall conductivity. From these, we provide a general discussion of how symmetries of the system on the one hand, and local thermal equilibrium on the other hand, imply important constraints on the thermal conductivity tensor and in particular its Hall component.

We then compute explicitly these two-point and four-point correlation functions, and the thermal transport coefficients which follow from them, in the case of a completely generic interaction between one phonon and two bosonic creation-annihilation operators. The coupling strength is only constrained by hermiticity and translational invariance. To illustrate this formalism with a concrete example, we then consider the specific case of a two-dimensional antiferromagnet with tetragonal symmetry. In this case, the Q field is a composite of two magnon creation-annihilation operators, which arises from spin-lattice coupling. We assume that the low-energy dynamics of spins, from which we compute the aforementioned correlation functions, is given by a nonlinear sigma-model. We consider the most general coupling between the low-energy magnetization fields and the strain tensor allowed by symmetry. This model allows for an analytical calculation of the scattering rates, which we perform. We then analyze the integrals involved in the theoretical expression of thermal conductivity (both longitudinal and Hall) in terms of these scattering rates; from this we can extract the temperature dependence of thermal conductivity, which depends on various parameters of the model. We then evaluate these same integrals numerically. Thereby we show explicitly that our results account for a nonzero thermal Hall conductivity due to inelastic phonon-magnon scattering. Chapter 2 provides a compact and streamlined presentation of our main results, while Chapter 3 contains detailed discussions, derivations and generalizations of various aspects.

In Chapter 4, we apply our general results to fermions. To do so, we then compute the very same two-point and four-point correlation functions, and the resulting thermal transport coefficients, in the case of an interaction between phonons and fermions. The interaction vertex involves one phonon operator and a number-preserving fermion bilinear; the coupling is again completely generic and only constrained by hermiticity and translational invariance. We compute explicitly the diagonal and off-diagonal scattering rates generated by this interaction. This is performed analytically in two tractable cases: fermions with a linear dispersion (and at any filling), and a Fermi surface of fermions with a quadratic dispersion. As a concrete example, and in order to elucidate the role of correlations in a magnetically disordered phase, we then consider the particular case of a $U(1)$ spinon Fermi surface spin liquid. We propose a model of spin-lattice interaction which, in the emergent fermionic phase, accounts for a phonon Hall effect induced by scattering with fermion bilinears. We show explicitly that this model meets all the symmetry requirements for a phonon Hall effect to exist. Finally, the emergent electromagnetic field associated with the spinons can fluctuate and interact with the lattice as well. For completeness, we thus

propose a phenomenological phonon-photon coupling, and explicitly compute its contribution to the lattice thermal conductivity.

A final appendix, Sec. 5.1, describes an alternative derivation of some of our general results using the Keldysh formalism. There, we discuss in particular the set of physical assumptions leading from the exact equations of quantum dynamics to hydrodynamics and Boltzmann's equation.

1.6 Outlook

1.6.1 Summary

In this work, we focused on the thermal transport by phonons governed by their collisions with other degrees of freedom. Our derivations were entirely analytical, based on the assumptions of hydrodynamics, perturbation theory in the second Born approximation, and within linear response. Analytical calculation of the eight-boson and eight-fermion correlation functions were tractable using Wick's theorem because we considered quadratic hamiltonians. The bosonic and fermionic dispersion relations which we considered also allowed for analytical solutions of the energy conservation constraints. Except for these few assumptions, our derivations are general and apply to a wide range of models. In the bosonic case, we considered the particular case of a 2D Néel antiferromagnet with tetragonal symmetry, but our calculations could be easily adapted to many other models of ordered magnets with spin waves as low-energy excitations. In the fermionic case, we kept the discussion as general as possible, so that it applies to any free fermions with either linear or quadratic dispersion. We presented a microscopic derivation in the case of a 2D spinon Fermi surface $U(1)$ spin liquid, which could be adapted to other cases as well.

1.6.2 Possible applications

It would be interesting to apply the formalism introduced here to other problems.

For instance, we derive general formulae for phonon transport due to phonon-fermions scattering, which we then apply to a specific case of *neutral* fermions. A possible extension of our work would be to consider *charged* fermions[6], which in particular might shed light onto the phenomenon of quantum oscillations of the thermal conductivity. This is a problem of current interest, partly because such oscillations were reported recently in α-$RuCl_3$ [Czajka et al., 2021, Bruin et al., 2022b].

It would also be interesting to consider models with different kinds of orders or excitations which are not covered in this thesis. In quantum magnets, for

[6] In the sense that the Aharonov-Bohm phase accumulated by fermions as they move around is not negligible (e.g. it cannot be gauged out). Equivalently, it means that the lack of translational symmetry due to the space-dependent gauge field impacts the fermion dynamics and (technically) their quantization. This may refer to "true" electromagnetism, or another gauge theory. For instance, spinons are neutral for standard electromagnetism but *a priori* charged under an emergent $U(1)$ gauge theory. However, in the zero-flux phase they feel no Aharonov-Bohm phase, and are also "neutral" in that sense.

instance, phonon thermal transport and in particular the phonon Hall effect in skyrmion phases [Mühlbauer et al., 2009], or the influence of vortex dynamics [Seifert et al., 2022] in 2D magnets on thermal transport, could be investigated.

Our formalism could also be applied to instances of $Q_{n\mathbf{k}}$ which involve other degrees of freedom than spin. For instance, the local electrical polarization was shown to play a role in the phonon Hall conductivity in a theoretical model [Chen et al., 2020]. There, its role on the phonon band geometry (in particular, the phonon Hall viscosity) was studied, but the resulting *collisional* thermal transport remains thus far an open question.

1.6.3 Possible extensions

Our formal results could also be extended in several ways.

Notably, I have already mentioned that phonon-phonon interactions can be considered within our formalism, under certain conditions. When these conditions are not fulfilled, "thermal drag" [Bartsch and Brenig, 2013] methods may be used, where a *system* of Boltzmann's equations is considered – one for each flavor of energy carriers. Therefore it would be interesting to extend our results to the problem of several systems of energy carriers, interacting with each other and with other fields Q relaxing rapidly to equilibrium.

Also, in the present work, disorder is introduced in the form of a diagonal scattering rate $\breve{D}_{n\mathbf{k}}$, which adds up to the calculated $D^{(1)}_{n\mathbf{k}}$ following Matthiessen's rule, and which we take to be a constant in our numerical evaluations. Our results could be extended by including disorder in a more systematic way, e.g. by introducing the scattering of phonons with impurities as an extra term in the perturbation hamiltonian H'.

1.6.4 Numerics

As already mentioned, the calculations presented in this thesis are analytical. This includes the sections where we apply our general formulae to given specific problems, which were analytically tractable. However, numerics could be introduced at several stages in applications of our general results to other (or the same) problems, and prove very helpful.

First, numerics are needed to evaluate momentum integrals. Indeed, the general expressions we derived for the thermal conductivities $\kappa_{\mathrm{L}}, \kappa_{\mathrm{H}}$ involve 3- and 6-dimensional integration over phonon momenta, respectively. In addition, the phonon scattering rates also involve integration over "internal momenta" of the bosons/fermions that interact with phonons. In the particular case of 2D magnons in a Néel antiferromagnet, we evaluated these multidimensional integrals numerically by a C code using the Cuba and Cubature libraries [Hahn, 2005], but a more general numerical implementation adaptable to other cases is missing. Moreover, the aforementioned integral over "internal momenta" is partly collapsed, due to the energy conservation constraints. In our applications to gapped magnons, Dirac fermions and quadratic fermions, we were able to perform this analytically, thanks to the specific shape of the dispersion rela-

tions. It would be desirable (and in some sense "straightforward") to turn our codes into a more general toolbox for other magnets.

Second, because our general formalism applies to *any* operator $Q_{n\mathbf{k}}$, a wider set of applications will become accessible through the calculation of interacting correlation functions from numerical simulations. Indeed, here, we considered particular instances of Q fields coupled to the phonons where $Q_{n\mathbf{k}}$ is expressed as a bilinear of free particles (bosons and fermions). Consequently, their two- and four-point correlation functions could be computed analytically using Wick's theorem.[7] However, this is not possible for general degrees of freedom $Q_{n\mathbf{k}}$ which do not have a quadratic hamiltonian. To compute the Q correlation functions involved in the scattering rates, and in particular the specific correlation functions with structure $\langle[Q(t), Q(0)]\rangle$ and $\langle[Q(-t-t_1), Q(-t+t_1)]\{Q(-t_2), Q(+t_2)\}\rangle$ that we have identified, it will be crucial to access the latter from numerical simulations such as DMRG, QMC, ED, DMFT...

Third, numerics could be instrumental in estimating microscopic parameters. Here, in our numerical evaluation of the integrals, the values which we assigned to the spin-lattice coupling constants were only rough estimates of the values they might have in a given material. From our work, it appears that spin-lattice coupling constants typically appear in the thermal conductivity tensor as intricate combinations, so that even the *sign* of the thermal Hall conductivity depends nontrivially on these parameters. This, in turn, implies that extracting the value of each spin-lattice coupling constant independently, e.g. from experimental data, should be hard. Indeed, spin-lattice coupling constants are typically not tabulated quantities. To obtain correct estimates of the values of these constants (as well as other microscopic parameters) in a given material, a promising way would be to resort to numerics. In particular, *ab initio* calculations based e.g. on DFT have been successfully applied to such problems [Riedl et al., 2019], and could become an important tool in the theory of phonon thermal conductivity in quantum materials (be they magnetic or not).

1.6.5 Experiments

Where to look for a "large" phonon Hall conductivity (in the sense of large κ_H/κ_L) in insulators? Although a complete answer to this question is not known, I have emphasized in this thesis that any mechanism whereby the phonons can "feel" the lack of time reversal and mirror symmetries is certainly a good starting point. In our application to a Néel antiferromagnet, spin-orbit coupling was a key ingredient in that regard, and we showed that κ_{H} in that case is proportional to a combination of anisotropic magnetic exchange constants.

Phonon thermal Hall effects are often considered a measure of the chirality of phonons. In fact, we have emphasized that ϱ_{H} is a more proper measure thereof than κ_{H}, since it does not depend on diagonal scattering rates $D_{n\mathbf{k}}$, at least in the dirty limit where these are well approximated by an isotropic Drude rate

[7] In fact, in the bosonic case where we considered all possible boson bilinears $(b^\dagger b^\dagger, b^\dagger b, bb)$ in Q, even the Wick's theorem expansion of the eight-boson correlator was performed with the help of mathematica, because of the large number of terms in the expansion.

τ^{-1}. More generally, the information carried by ϱ_{H} or κ_{H} may only be correctly interpreted if the *diagonal* scattering rates (involved, notably, in κ_L) are well characterized. This may involve other types of measurements, such as that of specific heat. [Martelli et al., 2018]

Finally, where could one *want to* measure thermal Hall conductivity? As discussed at length in this thesis, the scattering-induced phonon thermal Hall effect probes a specific kind of four-point correlation functions which are entirely non-gaussian. Therefore, it might be an interesting tool to characterize materials exhibiting weak signatures for other experimental methods, where mainly two-point correlations are probed, and whose signal is typically dominated by gaussian fluctuations. In particular, thermal Hall conductivity might be usefully measured in materials that exhibit disordered magnetic phases, quantum phases without quasiparticles, etc.

Chapter 2

Phonon thermal Hall conductivity from scattering with collective fluctuations

Because electrons and ions form a coupled system, it is a priori clear that the dynamics of the lattice should reflect symmetry breaking within the electronic degrees of freedom. This has been recently clearly evidenced for the case of time-reversal and mirror symmetry breakings by observations of a large phononic thermal Hall effect in many strongly correlated electronic materials. The mechanism by which time-reversal breaking and chirality is communicated to the lattice is, however, far from evident. In this paper we discuss how this occurs via many-body scattering of phonons by collective modes: a consequence of non-Gaussian correlations of the latter modes. We derive fundamental new results for such skew (i.e. chiral) scattering and the consequent thermal Hall conductivity. We emphasize that these results apply to any collective variables in any phase of matter, electronic, magnetic or neither, highly fluctuating and correlated, or not. As a proof of principle, we compute general formulae for the above quantities for ordered antiferromagnets. From the latter we obtain the scaling behavior of the phonon thermal Hall effect in clean antiferromagnets. The calculations show several different regimes and give quantitative estimates of similar order to that seen in recent experiments.

2.1 Introduction

Thermal conductivity is the most ubiquitous transport coefficient, being well-defined in any system with sufficiently local interactions, irrespective of the nature of the specific low energy degrees of freedom. It is particularly im-

portant therefore in systems for which charge transport is either strongly suppressed (i.e. insulators) or singular (i.e. superconductors). Moreover, the thermal *Hall* conductivity plays a particularly special role in the theory of exotic topological phases, as it can be related to the chiral central charge, to the presence of edge modes, etc. For all of the above reasons, experiments on thermal conductivity have played a pre-eminent role in establishing the nature of the most interesting strongly correlated states of matter. A few notable examples are the observation of metallic-like transport in an organic spin liquid [Yamashita et al., 2010], a quantized thermal Hall effect in the Kitaev material α-$RuCl_3$ [Kasahara et al., 2018a], taken as evidence for Majorana fermion edge states, and an exceptionally large and yet unexplained thermal Hall effect in under-doped cuprate high-temperature superconducting materials [Grissonnanche et al., 2019, Boulanger et al., 2020].

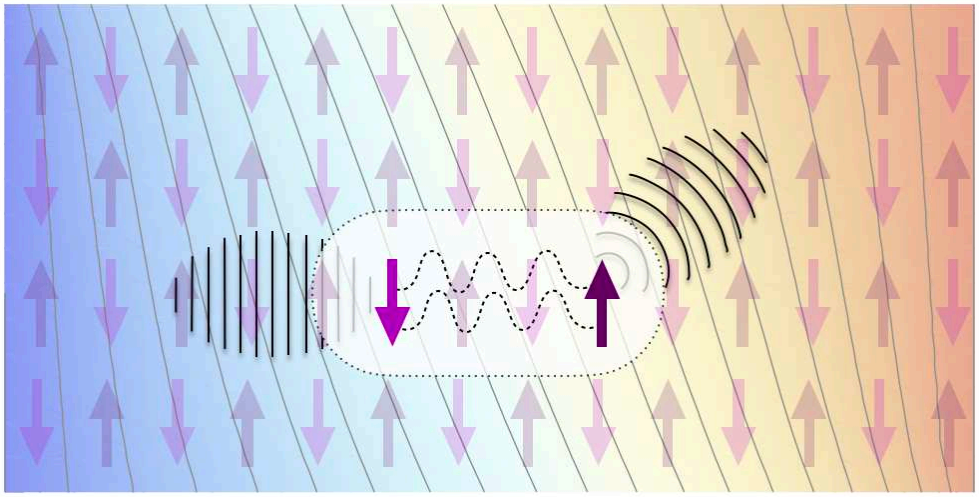

Figure 2.1: Illustration of a scattering mechanism responsible for a Hall effect. Only scattering processes which involve at least two (virtual) collisions with collective fluctuations can contribute to a Hall effect.

Arguably the Achilles heel of thermal conductivity measurements is the contribution of lattice vibrations/phonons to heat transport. Phonons are present in any solid, and indeed, except at very low temperature, usually dominate the thermal properties of materials. A common approach to this fact is to attempt to separate electronic and lattice contributions by some subtraction scheme, for example based on measuring two electronically different but vibrationally similar analog materials, or on dependences on temperature, field, etc., which might be attributed uniquely to only one of the lattice or electronic degrees of freedom. Of particular significance in this regard is the thermal Hall effect, which by Onsager relations can only exist when time-reversal symmetry is broken [Casimir, 1945]. The Hall conductivity is captured by the antisymmetric components of the thermal conductivity tensor $\boldsymbol{\kappa}$, namely

$$\kappa_H^{\mu\nu}(T, \boldsymbol{H}, \cdots) = (\kappa^{\mu\nu} - \kappa^{\nu\mu})/2. \tag{2.1}$$

It has been often assumed that the charge neutrality of phonons and the large ionic mass are sufficient to prevent them from coupling effectively to internal or external magnetic fields, and therefore that large thermal Hall signals must arise uniquely from the electrons in a material. Many recent theoretical works have thus focused on the thermal Hall conductivity of spin excitations [Katsura et al., 2010, Han and Lee, 2017, Han et al., 2019, Samajdar et al., 2019, Teng et al., 2020], in particular spin waves [Matsumoto and Murakami, 2011, Murakami and Okamoto, 2017, Mook et al., 2019, Koyama and Nasu, 2021].

Recent experiments, however, have conclusively shown that this assumption is incorrect, via the simplest and most persuasive of arguments [Hirokane et al., 2019, Li et al., 2020a, Chen et al., 2021]. In particular, studies of materials which are electronically (or magnetically) two-dimensional have observed that the thermal Hall conductivity is three-dimensional, and remains large when the thermal current within the sample is normal to the two-dimensional planes [Grissonnanche et al., 2020]. One has no choice but to conclude that the transported heat is carried by phonons.

The problem posed by these observations is then to understand how lattice vibrations "sense" time reversal symmetry breaking. This must indeed be by an indirect process, as ultimately it is the electrons which interact directly and significantly with magnetic fields. In principle there are two broad ways in which the transfer of information, i.e. the breaking of time-reversal symmetry, can occur from electrons to the lattice. First, it can occur via the quasi-adiabatic adaptation of electronic states to slow phonon motions, which may modify the phonon dispersion relations and generate dynamical Berry phases [Sheng et al., 2006, Kagan and Maksimov, 2008, Zhang et al., 2019, Chen et al., 2020]. While this is certainly possible in principle, numerous estimates indicate that this mechanism is unlikely to explain the large magnitude of thermal Hall signals seen in experiments. The second type of information transfer, depicted in Fig. 2.1, is through scattering of phonons from the electronic modes, which can be "chiral" when the latter break time-reversal and reflection symmetries. In the electrical anomalous Hall effect, such "skew scattering" is known to dominate in the most highly conducting samples [Saito et al., 2019], and for similar reasons, we expect it to do so for heat transport when thermal conductivity is large.

With this in mind, it is critical to ask how time-reversal symmetry breaking of electronic degrees of freedom is communicated *via scattering* to phonons in clean systems. We assume perturbative coupling of some set of collective fields Q to the lattice, which is generally valid away from the limit of polaron formation [Holstein, 1959a, Holstein, 1959b]. To account for the diversity of different electronic and magnetic phases being studied, we allow the fields Q to be *general*, restricted only by the requirements of unitarity of quantum mechanics and equilibrium. We show that the full scattering data needed to understand the thermal conductivity (both longitudinal and Hall components) can be obtained from the time and space-dependent correlation functions of the Q fields. Crucially, we show that *the standard two-point correlation functions of Q give vanishing contributions to skew scattering and the Hall effect.* Consequently the skew scattering can be attributed entirely to *non-Gaussian* fluctuations of

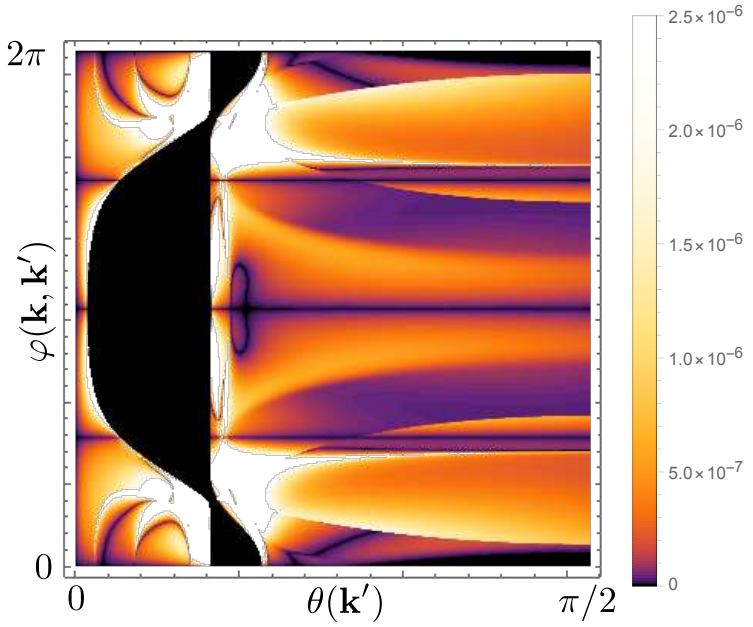

Figure 2.2: Calculated skew-scattering rate $\mathfrak{W}^{\ominus,-+}_{n\mathbf{k}n'\mathbf{k}'}/\gamma_0$ (see Eqs. (2.10, 2.19)) to transfer a phonon in mode $n'\mathbf{k}'$ into mode $n\mathbf{k}$ induced by coupling the lattice to a two dimensional antiferromagnet. The density plot shows the angular dependence as a function of $\theta(\mathbf{k}') \in [0, \pi/2]$ (horizontal axis) and $\varphi(\mathbf{k}, \mathbf{k}') = \phi(\mathbf{k}') - \phi(\mathbf{k})$ (vertical axis) for fixed $|\mathbf{k}'| = 0.8/\mathfrak{a}$, $k_x = 0.2/\mathfrak{a}$, $k_y = 0$, $k_z = 0.1/\mathfrak{a}$, $\boldsymbol{m}_0 = 0.05\hat{\mathbf{z}}$ and temperature $T = 0.5T_0$. Here $\mathfrak{a}$ is the in-layer lattice spacing, $\phi(\mathbf{k}^{(\prime)})$ and $\theta(\mathbf{k}^{(\prime)})$ are the azimuthal and polar angles of $\mathbf{k}^{(\prime)}$, defined in the usual way. Note that the colorbar is not scaled linearly.

the collective modes. This is a challenge theoretically (because as we discuss below, beyond-Gaussian fluctuations are significantly more complex than Gaussian ones) but also an opportunity. The absence of lower-order contributions to skew scattering means that the latter provides a direct probe of non-Gaussianity, which does not require any subtraction! This suggests the prospect of using measures of skew scattering of phonons, such as the thermal Hall effect, as a means to interrogate the rich higher order correlations of electronic modes.

In this paper, we identify the corresponding higher order correlation functions which relate the multi-phonon scattering rates to the fluctuations of the collective modes. These are complicated objects which depend upon several time and space coordinates, or equivalently multiple frequencies and wavevectors. We show how to extract the essentially antisymmetric part of these correlations which uniquely contribute to the Hall effect, using symmetry and detailed balance relations, which generalize well-known and ubiquitously important laws that are used to analyze two-point correlations throughout physics [Onsager, 1931, Squires, 2012, Buttiker, 1988]. This provides a recipe which can be applied in diverse systems, telling what must be known about the electronic modes coupled to the lattice and how to use that data to obtain an understanding of the thermal Hall effect of phonons. Notably, the results are valid irrespective of the nature of the phase of matter hosting the collective fields: it may be strongly fluctuating, highly correlated, or even have no quasiparticles at all. This contrasts greatly with prior theories of phonon skew scattering which are based on very specific models of electronic modes [Lovesey, 1972, Laurence and Petitgrand, 1973].

To demonstrate the methodology and as a proof of principle, we also apply the general results to the case of an ordered antiferromagnet, in which case the Q fields correspond to magnetic fluctuations which can be decomposed into composites of magnons. The result is a richly structured skew scattering rate, visualized in Fig. 3.5.6. Validating the general formulation, we obtain a non-vanishing thermal Hall effect when all the symmetry criteria (which we establish) are satisfied, and we explicitly show that within a minimal model of an antiferromagnet with strictly two-dimensional magnetic correlations, the thermal Hall effect is three-dimensional and its magnitude is roughly independent of whether the thermal currents are within or normal to the magnetic planes.

2.2 Scattering and correlation functions

In this section, we present the main results for the scattering rates of phonons due to collective modes. We limit the discussion here to the simplest case in which the coupling is linear in phonon creation/annihilation operators $a^\dagger_{n\mathbf{k}}, a_{n\mathbf{k}}$. Then, the coupling Hamiltonian is

$$H' = \sum_{n\mathbf{k}} \left(a^\dagger_{n\mathbf{k}} Q^\dagger_{n\mathbf{k}} + a_{n\mathbf{k}} Q_{n\mathbf{k}} \right), \tag{2.2}$$

where $Q_{n\mathbf{k}}$ describes the collective mode arising from electronic degrees of freedom, coupled to the n^{th} phonon polarization. For brevity, we subsume any

electron-phonon coupling constant into $Q_{n\mathbf{k}}$. We carry out a perturbative analysis of H', so $Q_{n\mathbf{k}}$ may be regarded as "small".

2.2.1 Formulation

Our aim is to calculate the necessary terms in the collision integral $\mathcal{C}_{n\mathbf{k}}$ of the phonon Boltzmann equation,

$$\partial_t \overline{N}_{n\mathbf{k}} + \boldsymbol{v}_{n\mathbf{k}} \cdot \boldsymbol{\nabla}_{\mathbf{r}} \overline{N}_{n\mathbf{k}} = \mathcal{C}_{n\mathbf{k}}[\{\overline{N}_{n'\mathbf{k}'}\}] \tag{2.3}$$

where $\overline{N}_{n\mathbf{k}}$ is the non-equilbrium average occupation number of phonons in polarization mode n and quasi-momentum $\mathbf{k}$ with velocity $\boldsymbol{v}_{n\mathbf{k}} = \boldsymbol{\nabla}_{\mathbf{k}}\omega_{n\mathbf{k}}$, where $\omega_{n\mathbf{k}}$ is the $(n, \mathbf{k})$ phonon dispersion relation. Once the collision integral is known, the Boltzmann equation can be solved in a standard manner by linearizing around the equilibrium distribution, to obtain the non-equilibrium change and thereby the transport current to linear order in the temperature gradient.

We now summarize the method used to obtain the collision integral from the microscopic quantum dynamics and Eq. (2.2). The basic procedure is to determine the *many body* transition rate between microstates in the combined phonon-electron system using the scattering matrix (T) expansion, and from there, use the equilibrium distribution for the electronic subsystem to evaluate the rate of change of the mean occupation probabilities of phonon states that enter the Boltzmann equation.

We begin with the Born expansion [Landau and Lifshitz, 1958]:

$$T_{\mathtt{i}\to\mathtt{f}} = T_{\mathtt{fi}} = \langle \mathtt{f}|H'|\mathtt{i}\rangle + \sum_{\mathtt{n}} \frac{\langle \mathtt{f}|H'|\mathtt{n}\rangle\langle \mathtt{n}|H'|\mathtt{i}\rangle}{E_{\mathtt{i}} - E_{\mathtt{n}} + i\eta} + \cdots, \tag{2.4}$$

where the $|\mathtt{i}\rangle, |\mathtt{f}\rangle, |\mathtt{n}\rangle$ states are product states in the Q (index s) and phonon (index p) Hilbert space, $|\mathtt{g}\rangle = |g_s\rangle|g_p\rangle$ for $g = i, f, n$, and $E_{\mathtt{g}}$ is the energy of the unperturbed Hamiltonians of the Q and phonons in state $\mathtt{g}$. $\eta \to 0^+$ is a small regularization parameter.

The rate of transitions from state $\mathtt{i}$ to state $\mathtt{f}$ is obtained using Fermi's golden rule,

$$\Gamma_{\mathtt{i}\to\mathtt{f}} = \frac{2\pi}{\hbar} |T_{\mathtt{i}\to\mathtt{f}}|^2 \delta(E_{\mathtt{i}} - E_{\mathtt{f}}). \tag{2.5}$$

Note that $\Gamma_{\mathtt{i}\to\mathtt{f}}$ is a transition rate in the full combined phonon-Q system. By assuming equilibrium for the electronic modes, we obtain the transition rates within the phonon subsystem,

$$\tilde{\Gamma}_{i_p\to f_p} = \sum_{i_s f_s} \Gamma_{\mathtt{i}\to\mathtt{f}}\, p_{i_s}, \tag{2.6}$$

with $p_{i_s} = \frac{1}{Z_s} e^{-\beta E_{i_s}}$. This in turn determines the collision integral through the master equation

$$\mathcal{C}_{n\mathbf{k}} = \sum_{i_p, f_p} \tilde{\Gamma}_{i_p\to f_p} \left(N_{n\mathbf{k}}(f_p) - N_{n\mathbf{k}}(i_p)\right) p_{i_p}, \tag{2.7}$$

where $p_{i_p} = \sum_{i_s} p_{\mathtt{i}}$, where $p_{\mathtt{i}}$ is the probability to find the system in state $\mathtt{i}$.

2.2.2 Result

To carry out the above procedure, we first express the microscopic processes generated in the Born expansion, Eq. (2.4), and insert them into the square in Eq. (2.5). Then the sums over electronic states i_s, f_s in Eq. (2.6) can be converted into dynamical multi-time correlation functions of the Q operators. The corresponding technical manipulations are described in Appendix 2.A. The leading result for the longitudinal conductivity (symmetric part of the tensor) is dominated by diagonal scattering (absorption or emission of a single phonon), and is given by

$$\kappa_L^{\mu\nu} = \frac{\hbar^2}{k_B T^2} \frac{1}{V} \sum_{n\mathbf{k}} \frac{\omega_{n\mathbf{k}}^2 v_{n\mathbf{k}}^\mu v_{n\mathbf{k}}^\nu}{4 D_{n\mathbf{k}} \sinh^2(\beta\hbar\omega_{n\mathbf{k}}/2)}. \tag{2.8}$$

For the Hall effect, the important contributions are those from the second order terms in the Born expansion, which generate processes in which a phonon is scattered from one state to another, or in which pairs of phonons are created or annihilated. Using Eq. (2.7) then leads to off-diagonal terms in the collision integral, i.e. contributions to $\mathcal{C}_{n\mathbf{k}}$ proportional to $N_{n'\mathbf{k}'}$ with $n'\mathbf{k}' \neq n\mathbf{k}$. The desired "skew" scattering contributions, roughly speaking, correspond to processes in which $\mathbf{k}$ is preferentially deflected "to the right" of $\mathbf{k}'$, for example.

More precisely, we define an anti-symmetric scattering rate $\mathfrak{W}^{\ominus,+,q}_{n\mathbf{k},n'\mathbf{k}'}$ in such a way that it controls the anti-symmetric (Hall) part of the thermal conductivity tensor, $\kappa_H^{\mu\nu} = -\kappa_H^{\nu\mu}$:

$$\begin{aligned} \kappa_H^{\mu\nu} = {} & \frac{\hbar^2}{k_B T^2} \frac{1}{V} \sum_{n\mathbf{k}n'\mathbf{k}'} \\ & \times J^\mu_{n\mathbf{k}} \frac{e^{\beta\hbar\omega_{n\mathbf{k}}/2}}{2D_{n\mathbf{k}}} \left(\frac{1}{N_{\mathrm{uc}}} \sum_{q=\pm} \frac{\left(e^{\beta\hbar\omega_{n\mathbf{k}}} - e^{q\beta\hbar\omega_{n'\mathbf{k}'}}\right) \mathfrak{W}^{\ominus,+,q}_{n\mathbf{k},n'\mathbf{k}'}}{\sinh(\beta\hbar\omega_{n\mathbf{k}}/2)\sinh(\beta\hbar\omega_{n'\mathbf{k}'}/2)} \right) \frac{e^{\beta\hbar\omega_{n'\mathbf{k}'}/2}}{2D_{n'\mathbf{k}'}} J^\nu_{n'\mathbf{k}'}, \end{aligned} \tag{2.9}$$

where

$$\begin{aligned} \mathfrak{W}^{\ominus,qq'}_{n\mathbf{k}n'\mathbf{k}'} = {} & \frac{2N_{\mathrm{uc}}}{\hbar^4} \mathfrak{Re} \int_{t,t_1,t_2} e^{i[\Sigma^{q,q'}_{n\mathbf{k}n'\mathbf{k}'} t + \Delta^{q,q'}_{n\mathbf{k}n'\mathbf{k}'}(t_1+t_2)]} \mathrm{sign}(t_2) \\ & \left\langle \left[Q^{-q}_{n\mathbf{k}}(-t-t_2), Q^{-q'}_{n'\mathbf{k}'}(-t+t_2) \right] \left\{ Q^{q'}_{n'\mathbf{k}'}(-t_1), Q^{q}_{n\mathbf{k}}(t_1) \right\} \right\rangle, \end{aligned} \tag{2.10}$$

and

$$D_{n\mathbf{k}} = -\frac{1}{\hbar^2} \int dt\, e^{-i\omega_{n\mathbf{k}}t} \left\langle [Q_{n\mathbf{k}}(t), Q^\dagger_{n\mathbf{k}}(0)] \right\rangle_\beta + \breve{D}_{n\mathbf{k}}. \tag{2.11}$$

Here $\mu, \nu = x, y, z$ and we defined the phonon current $J^\mu_{n\mathbf{k}} = N^{\mathrm{eq}}_{n\mathbf{k}}\, \omega_{n\mathbf{k}} v^\mu_{n\mathbf{k}}$, and $N^{\mathrm{eq}}_{n\mathbf{k}}$ is the number of phonons in mode $n\mathbf{k}$ in thermal equilibrium. Eq. (2.11) gives the leading order result for the diagonal scattering rate $D_{n\mathbf{k}}$, which enters Eq. (2.9). In general it includes contributions $\breve{D}_{n\mathbf{k}}$ from other scattering channels (e.g. impurities) and higher-order contributions. In Eq. (2.10) we introduced the notation $Q^+_{n\mathbf{k}} = Q^\dagger_{n\mathbf{k}}$ and $Q^-_{n\mathbf{k}} = Q_{n\mathbf{k}}$, as well as $\Sigma^{q,q'}_{n\mathbf{k}n'\mathbf{k}'} = q\omega_{n\mathbf{k}} + q'\omega_{n'\mathbf{k}'}$ and $\Delta^{q,q'}_{n\mathbf{k}n'\mathbf{k}'} = q\omega_{n\mathbf{k}} - q'\omega_{n'\mathbf{k}'}$.

Eqs. (2.9,2.10) constitute the central result of this paper. They give a general formula for the skew scattering rate and the thermal Hall conductivity, given Eq. (2.2), assuming small Hall angle (a condition which is nearly always true), valid in any dimension. Even more general formulae valid when electronic modes are coupled to both linear and quadratic functions of the phonons will be given in a separate publication. These results can be applied to any material provided the non-Gaussian correlations of the collective degrees of freedom corresponding to $Q_{n\mathbf{k}}$ are known.

Considerable structure is encoded in Eq. (2.10). It is straightforward to show that the skew scattering vanishes if $Q_{n\mathbf{k}}$ is taken to be Gaussian: in this case, Wick's theorem is obeyed, and its application to Eq. (2.10) implies that $\mathfrak{W}^{\ominus}_{n\mathbf{k}n'\mathbf{k}'}$ is zero if $(n,\mathbf{k}) \neq (n',\mathbf{k}')$. Hence, non-trivial contributions to the skew scattering arise entirely from non-Gaussian correlations. Physically, $\mathfrak{W}^{\ominus,++}$ (resp. $\mathfrak{W}^{\ominus,--}$) corresponds to scattering processes where two phonons are emitted (resp. absorbed), and $\mathfrak{W}^{\ominus,+-}, \mathfrak{W}^{\ominus,-+}$ to processes where one phonon is emitted and one is absorbed. The contribution to the Hall conductivity has been carefully isolated so that the rate obeys the "anti-detailed balance" relation:

$$\mathfrak{W}^{\ominus,qq'}_{n\mathbf{k}n'\mathbf{k}'} = -\, e^{-\beta(q\omega_{n\mathbf{k}}+q'\omega_{n'\mathbf{k}'})}\; \mathfrak{W}^{\ominus,-q-q'}_{n\mathbf{k}n'\mathbf{k}'}, \tag{2.12}$$

as well as

$$\mathfrak{W}^{\ominus,qq'}_{n\mathbf{k}n'\mathbf{k}'} = \mathfrak{W}^{\ominus,q'q}_{n'\mathbf{k}'n\mathbf{k}}. \tag{2.13}$$

The combination of the commutator and anti-commutator in Eq. (2.10) ensures the validity of these relations.

2.3 Application to an ordered antiferromagnet

We now provide an application of the above results to the specific case of an insulating antiferromagnet. This is important as a proof of principle to confirm that the general formula in Eq. (2.10) indeed results in a non-vanishing Hall effect of phonons from skew scattering. It is also a relevant test case as it corresponds to the situation in many recent experiments, and is perhaps the simplest situation in which time-reversal symmetry breaking of spins is communicated to phonons in an insulator.

To model the antiferromagnet, we employ a spin wave description, and for concreteness assume the spin correlations are purely two-dimensional: each layer of spins is presumed completely independent. The latter assumption is not essential but it is illustrative: using it we demonstrate that even when spin correlations are confined to two dimensions, their influence can lead to thermal Hall conductivity with heat current oriented perpendicular to those layers. In any case, the general formulae in the first subsection below can be easily modified for the case of three-dimensional spin waves.

2.3.1 Formulation and general results within linear spin wave theory

The spin waves are described by magnon operators $b^\dagger_{\ell\mathbf{k},z}$ ($b_{\ell\mathbf{k},z}$), which create (annihilate) a magnon in branch ℓ with momentum $\mathbf{k}$ in layer z, whose Hamiltonian is

$$H_m = \sum_{\ell,\mathbf{k},z} \Omega_{\mathbf{k},\ell} b^\dagger_{\ell\mathbf{k},z} b_{\ell\mathbf{k},z}. \tag{2.14}$$

Note that the effect of a magnetic field is already included in H_m, i.e. here the spin wave modes are based on an expansion around the spin order *including* the effect of the field. The collective modes $Q^q_{n\mathbf{k}}$ can be expanded in a series in the spin wave operators, and the dominant contribution to scattering comes from second order [1]:

$$Q^q_{n\mathbf{k}} = \frac{1}{\sqrt{N_{\rm uc}}} \sum_{\substack{\mathbf{p},\ell_1,\ell_2\\ q_1,q_2,z}} \mathcal{B}^{n,\ell_1,\ell_2|q_1q_2q}_{\mathbf{k};\mathbf{p}}\ e^{ik_z z} b^{q_1}_{\ell_1,\mathbf{p}+\frac{q}{2}\mathbf{k},z} b^{q_2}_{\ell_2,-\mathbf{p}+\frac{q}{2}\mathbf{k},z}. \tag{2.15}$$

Here we defined the notations

$$b^+_{\ell,\mathbf{p},z} = b^\dagger_{\ell,\mathbf{p},z}, \qquad\qquad b^-_{\ell,\mathbf{p},z} = b_{\ell,-\mathbf{p},z}. \tag{2.16}$$

Note the minus sign in the momentum in the second relation. This means generally that $\left(b^q_{\ell,\mathbf{p},z}\right)^\dagger = b^{-q}_{\ell,-\mathbf{p},z}$. To make the coefficients unambiguous, we choose the symmetrized form $\mathcal{B}^{n,\ell_1,\ell_2|q_1q_2q}_{\mathbf{k};\mathbf{p}} = \mathcal{B}^{n,\ell_2,\ell_1|q_2q_1q}_{\mathbf{k};-\mathbf{p}}$. Demanding that $Q^+_{n\mathbf{k}} = (Q^-_{n\mathbf{k}})^\dagger$ implies that $\mathcal{B}^{n,\ell_1,\ell_2|q_1q_2+}_{\mathbf{k};\mathbf{p}} = \left(\mathcal{B}^{n,\ell_2,\ell_1|-q_2-q_1-}_{\mathbf{k};\mathbf{p}}\right)^*$.

Eq. (2.14) contains the energy dispersion $\Omega_{\mathbf{k},\ell}$ of the spin waves but their wavefunctions are implicit. That information is encoded in the $\mathcal{B}$ coefficients. To obtain them, one should start with a microscopic spin-lattice coupling, expand it via Holstein-Primakoff bosons, and then use the canonical Bogoliubov transformation which achieves the diagonal form of Eq. (2.14) to express the coupling as in Eq. (2.15). We apply this procedure to a particular case in Sec. 2.3.2. The following general results hold beyond this specific case, and only assume Eqs. (2.14, 2.15) as a starting point.

To proceed to evaluate Eqs. (2.9-2.11), we use Wick's theorem (valid for the free boson Hamiltonian in Eq. (2.14)) to compute the necessary correlation functions, which decomposes them into products of the free-particle two-point function,

$$\begin{aligned}\left\langle b^{q_1}_{\ell_1,\mathbf{p}_1,z_1}(t_1) b^{q_2}_{\ell_2,\mathbf{p}_2,z_2}(t_2)\right\rangle = &\quad \delta_{\ell_1,\ell_2}\delta_{z_1,z_2}\delta_{q_1,-q_2}\delta_{\mathbf{p}_1+\mathbf{p}_2,\mathbf{0}}\\ &\times\ f_{q_2}(\Omega_{\ell_1,q_1\mathbf{p}_1}) e^{-iq_2\Omega_{\ell_2,q_2\mathbf{p}_2}(t_1-t_2)}.\end{aligned} \tag{2.17}$$

Here $f_q(\Omega) = (1+q)/2 + n_{\rm B}(\Omega)$, where $n_{\rm B}(\Omega)$ is the Bose distribution.

[1] A linear term in magnon operators is generically present but does not contribute significantly to scattering due to phase space constraints.

This results in the following expressions for the diagonal and off-diagonal scattering rates:

$$D^{(s)}_{n\mathbf{k}} = \frac{(3-s)\pi}{\hbar^2 N^{\rm 2d}_{\rm uc}} \sum_{\mathbf{p}} \sum_{\ell,\ell'} \frac{\sinh(\frac{\beta}{2}\hbar\omega_{n\mathbf{k}})}{\sinh(\frac{\beta}{2}\hbar\Omega^{\ell,+}_{\mathbf{p}})\sinh(\frac{\beta}{2}\hbar\Omega^{\ell',-s}_{\mathbf{p}+\mathbf{k}})} \times \delta(\omega_{n\mathbf{k}} - \Omega^{\ell,+}_{\mathbf{p}} - s\Omega^{\ell',-s}_{\mathbf{p}+\mathbf{k}}) \left| \mathcal{B}^{n,\ell,\ell'|+s-}_{\mathbf{k};\mathbf{p}+\frac{\mathbf{k}}{2}} \right|^2 , \tag{2.18}$$

where $s = \pm$ and $D_{n\mathbf{k}} = \sum_s D^{(s)}_{n\mathbf{k}} + \breve{D}_{n\mathbf{k}}$, we defined $\Omega^{\ell,q}_{\mathbf{p}} = \Omega_{\ell,q\mathbf{p}}$, and

$$\begin{aligned} \mathfrak{W}^{\ominus,qq'}_{n\mathbf{k},n'\mathbf{k}'} = \frac{64\pi^2}{\hbar^4} \frac{1}{N^{2d}_{\rm uc}} \sum_{\mathbf{p}} \sum_{\{\ell_i,q_i\}} \mathfrak{D}^{nn'|q_1q_2q_3,\ell_1\ell_2\ell_3}_{q\mathbf{k}q'\mathbf{k}',\mathbf{p}} \, \mathfrak{F}^{q_1q_2q_4,\ell_1\ell_2\ell_3}_{q\mathbf{k}q'\mathbf{k}',\mathbf{p}} \\ \times \mathfrak{Im}\Big\{ \mathcal{B}^{n\ell_2\ell_3|q_2q_3q}_{\mathbf{k},\mathbf{p}+\frac{1}{2}q\mathbf{k}+q'\mathbf{k}'} \mathcal{B}^{n'\ell_3\ell_1|-q_3q_1q'}_{\mathbf{k}',\mathbf{p}+\frac{1}{2}q'\mathbf{k}'} \\ \times \mathrm{PP}\Big[\frac{\mathcal{B}^{n\ell_1\ell_4|-q_1q_4-q}_{\mathbf{k},\mathbf{p}+\frac{1}{2}q\mathbf{k}} \mathcal{B}^{n'\ell_4\ell_2|-q_4-q_2-q'}_{\mathbf{k}',\mathbf{p}+q\mathbf{k}+\frac{1}{2}q'\mathbf{k}'}}{\Delta^{qq'}_{n\mathbf{k}n'\mathbf{k}'} + q_1\Omega^{\ell_1,-q_1}_{\mathbf{p}} - q_2\Omega^{\ell_2,q_2}_{\mathbf{p}+q\mathbf{k}+q'\mathbf{k}'} - 2q_4\Omega^{\ell_4,-q_4}_{\mathbf{p}+q\mathbf{k}}} \\ + \frac{\mathcal{B}^{n'\ell_1\ell_4|-q_1-q_4-q'}_{\mathbf{k}',\mathbf{p}+\frac{1}{2}q'\mathbf{k}'} \mathcal{B}^{n\ell_4\ell_2|q_4-q_2-q}_{\mathbf{k},\mathbf{p}+\frac{1}{2}q\mathbf{k}+q'\mathbf{k}'}}{\Delta^{qq'}_{n\mathbf{k}n'\mathbf{k}'} - q_1\Omega^{\ell_1,-q_1}_{\mathbf{p}} + q_2\Omega^{\ell_2,q_2}_{\mathbf{p}+q\mathbf{k}+q'\mathbf{k}'} - 2q_4\Omega^{\ell_4,q_4}_{\mathbf{p}+q'\mathbf{k}'}} \Big] \Big\}, \end{aligned} \tag{2.19}$$

where we used as before $\Sigma^{q,q'}_{n\mathbf{k}n'\mathbf{k}'} = q\omega_{n\mathbf{k}} + q'\omega_{n'\mathbf{k}'}$, $\Delta^{q,q'}_{n\mathbf{k}n'\mathbf{k}'} = q\omega_{n\mathbf{k}} - q'\omega_{n'\mathbf{k}'}$, and we defined the product of delta functions $\mathfrak{D}$ and 'thermal factor' $\mathfrak{F}$:

$$\begin{aligned} \mathfrak{D}^{nn'|q_1q_2q_3,\ell_1\ell_2\ell_3}_{q\mathbf{k}q'\mathbf{k}',\mathbf{p}} &= \delta\left(\Sigma^{qq'}_{n\mathbf{k}n'\mathbf{k}'} + q_1\Omega^{\ell_1,-q_1}_{\mathbf{p}} + q_2\Omega^{\ell_2,q_2}_{\mathbf{p}+q\mathbf{k}+q'\mathbf{k}'}\right) \\ &\quad \delta\left(\Delta^{qq'}_{n\mathbf{k}n'\mathbf{k}'} + 2q_3\Omega^{\ell_3,-q_3}_{\mathbf{p}+q'\mathbf{k}'} - q_1\Omega^{\ell_1,-q_1}_{\mathbf{p}} + q_2\Omega^{\ell_2,q_2}_{\mathbf{p}+q\mathbf{k}+q'\mathbf{k}'}\right), \end{aligned} \tag{2.20}$$

$$\begin{aligned} \mathfrak{F}^{q_1q_2q_4,\ell_1\ell_2\ell_3}_{q\mathbf{k}q'\mathbf{k}',\mathbf{p}} &= q_4\left(2n_{\rm B}(\Omega^{\ell_3,-q_3}_{\mathbf{p}+q'\mathbf{k}'}) + 1\right)\left(2n_{\rm B}(\Omega^{\ell_1,-q_1}_{\mathbf{p}}) + q_1 + 1\right) \\ &\quad \left(2n_{\rm B}(\Omega^{\ell_2,q_2}_{\mathbf{p}+q\mathbf{k}+q'\mathbf{k}'}) + q_2 + 1\right). \end{aligned} \tag{2.21}$$

These formulae make no further assumptions on the nature of the spin wave modes or spin-lattice couplings, and so could be applied to general problems involving spin-lattice coupling using a spin wave approach. Note that although we take the spin wave operators to be free bosons, with Gaussian correlations, the $Q^q_{n\mathbf{k}}$ operator defined through Eq. (2.15) is generally non-Gaussian, as it is bilinear in the b fields.

2.3.2 Square lattice two-sublattice antiferromagnets

Now we evaluate the diagonal and Hall scattering rates specifically for spin waves on the square lattice in low magnetic fields. We assume the magnon dispersions $\Omega_{\ell,\mathbf{k}} = \sqrt{v^2_{\rm m}\underline{k}^2 + \Delta^2_\ell}$ with magnon velocity $v_{\rm m}$ and magnon gaps Δ_ℓ, and take isotropic acoustic phonons with $\omega_{n\mathbf{k}} = v_{\rm ph}\sqrt{\underline{k}^2 + k_z^2}$ (we define $\underline{k} = \sqrt{k_x^2 + k_y^2}$). We obtain the coefficients $\mathcal{B}^{n\ell_1\ell_2|q_1q_2q}_{\mathbf{k};\mathbf{p}}$ from the continuum description of the spin

waves in terms of local fluctuating uniform and staggered magnetization fields, and the symmetry-allowed couplings of these fields to the strain. The expressions for these coefficients are algebraically complicated and some further details are given in Appendix 2.B, with a full exposition of the calculations to be presented in the next chapter. Here instead we sketch the important properties of the coefficients and their origins.

2.3.2.1 Scaling

First, when the temperature is smaller than the magnon gaps, $k_B T \lesssim \Delta_\ell$, all contributions to scattering become exponentially suppressed by thermal factors and the scaling is unimportant. For larger temperatures, the gaps are negligible, and the momentum sum(s) in Eqs. (2.18,2.19) are dominated by momenta of order $k, p \sim k_B T / v_{\mathrm{m}}$. Then the $\mathcal{B}$ coefficients, evaluated for momenta of this order, are sums of three types of contributions:

$$\mathcal{B} \sim \left(\frac{k_B T}{M v_{\mathrm{ph}}^2} \right)^{\frac{1}{2}} n_0^{-1} \left(\lambda_{mm} \frac{\chi k_B T}{n_0} + \lambda_{mn} + \lambda_{nn} \frac{n_0}{\chi k_B T} \right). \tag{2.22}$$

Here M is the mass per unit cell of the solid, n_0 is the ordered (staggered) moment density, χ is the uniform susceptibility, and $\lambda_{mm}, \lambda_{mn}$ and λ_{nn} represent couplings of the strain to exchange terms quadratic in local magnetization fluctuations δm, local staggered magnetization fluctuations δn, and the product of the two, respectively. Microscopically this arises from effects like magnetostriction, the modification of orbital overlaps due to strain-induced bond length and angle changes, etc. The different powers of temperature multiplying the different λ couplings arise from the fact that the order parameter of the antiferromagnet is the staggered magnetization, and therefore its fluctuations are more singular than those of the uniform magnetization, which is, however, still a low energy mode in an antiferromagnet.

Depending upon the relative magnitudes of these different couplings, distinct scalings are observed for the diagonal and off-diagonal scattering rates, and hence for thermal conductivity components. To perform a full evaluation, we use parameters (given explicitly in Appendix 2.B) which describe a typical situation corresponding to weak spin-orbit coupling and correspondingly weak anisotropy of magnetic exchange. In this case, there is a hierarchy that $\lambda_{mm} \gg \lambda_{nn}, \lambda_{mn}$ (which is ultimately a consequence of Goldstone's theorem). Furthermore, in the low field regime, i.e. when the field-induced magnetization m_0 of the antiferromagnet is much smaller than m_s the saturation value, $m_0 \ll m_s$, the mixed coupling λ_{mn} is proportional to m_0 and $\lambda_{mn} \ll \lambda_{nn}$ as well.

These facts allow one to estimate the scalings of the important physical quantities. The longitudinal scattering rate (Eq. (2.18)) scales as

$$D_{n\mathbf{k}} \sim \frac{1}{\tau} \sim T^{d-1} |\mathcal{B}|^2 \sim T^{d+2x}. \tag{2.23}$$

Here d is the dimensionality of the spin system (which we take later equal to $d = 2$ for numerical calculations) while phonons are always three dimensional.

The crucial exponent $x = 1$ occurs in the "high" temperature regime dominated by λ_{mm}, while a crossover to behavior controlled by λ_{nn} with $x = -1$ can occur at lower temperature if the minimum magnon gap is sufficiently small. This behavior corresponds to the longitudinal thermal conductivity (Eq. (2.8)) behaving as

$$\kappa_L \sim T^{3-d-2x}, \tag{2.24}$$

when magnon-phonon scattering dominates the phonon mean free path. Again the power laws apply in certain distinct regimes, and should be pieced together, along with the influence of non-zero gaps and other scattering mechanisms of phonons, to form a complete picture of the thermal conductivity. This is captured in the numerical calculations.

Next, we turn to the thermal Hall effect. It is crucial to keep in mind the *effective* time-reversal symmetry of an antiferromagnet under the combined action of time-reversal and a translation which exchanges the two sublattices. The uniform magnetization is invariant under this symmetry but the staggered magnetization is odd. Consequently, the couplings λ_{mm} and λ_{nn} are even under effective time-reversal, while only λ_{mn} is odd. This implies that the Hall conductivity and Hall scattering rate $\mathfrak{W}^{\ominus,\text{eff}}$, with $\mathfrak{W}^{\ominus,\text{eff},qq'}_{n\mathbf{k},n'\mathbf{k}'} := \mathfrak{W}^{\ominus,qq'}_{n\mathbf{k},n'\mathbf{k}'} + \mathfrak{W}^{\ominus,qq'}_{n-\mathbf{k},n'-\mathbf{k}'}$, which are odd under effective time-reversal, must be proportional to an odd power of λ_{mn}, and to linear order in the magnetic field/average magnetization, these quantities are simply linear in λ_{mn}. From Eq. (2.19) and Eq. (2.22), we therefore obtain

$$\mathfrak{W}^{\ominus,\text{eff}} \sim T^{d-1}\lambda_{mn}\left(\lambda_{mm}T + \lambda_{nn}T^{-1}\right)^3 \sim T^{d-1+3x}. \tag{2.25}$$

The natural definition of a skew scattering rate multiplies the above by a phase-space factor to account for the sum over different final states of the scattering, which gives $1/\tau_{\text{skew}} \sim T^3\mathfrak{W}^{\ominus,\text{eff}} \sim T^{d+2+3x}$.

We would like to emphasize that within any scattering mechanism of phonon thermal Hall effect, the skew scattering rate is a more fundamental measure of the chirality of the phonons than the thermal Hall *conductivity*. This is because the Hall conductivity inevitably involves the combination of the skew and longitudinal scattering rates (in the form $\tau^2/\tau_{\text{skew}}$), and the longitudinal scattering rate of phonons has many other contributions that do not probe chirality, and may have complex dependence on temperature and other parameters that obscure the skew scattering.

Consequently, instead of the thermal Hall conductivity we will discuss the thermal Hall resistivity, ϱ_H, which is simply proportional to $1/\tau_{\text{skew}}$, at least in the simplest view where the angle-dependence of the longitudinal scattering does not spoil its cancellation.

We define the thermal Hall resistivity tensor as usual by the matrix inverse, $\boldsymbol{\varrho} = \boldsymbol{\kappa}^{-1}$. In particular, considering the simplest case of isotropic $\kappa^{\mu\mu} \to \kappa_L$ and $\kappa_L \gg \kappa^{\mu\neq\nu}$, one thus has

$$\varrho_H^{\mu\nu} = \frac{\varrho_{\mu\nu} - \varrho_{\nu\mu}}{2} \approx \frac{-\kappa_{\mu\nu} + \kappa_{\nu\mu}}{2\kappa_L^2} = -\frac{\kappa_H^{\mu\nu}}{\kappa_L^2}. \tag{2.26}$$

The quantity $\varrho_H^{\mu\nu}$ is independent of the scale of the longitudinal scattering, in the sense that under a rescaling $D_{n\mathbf{k}} \to \zeta D_{n\mathbf{k}}$, then $\varrho_H^{\mu\nu}$ is unchanged. If we

assume that $D_{n\mathbf{k}} = 1/\tau$ is $(n, \mathbf{k})$-independent, e.g. as is the case if dominated by some extrinsic effects, then we can readily extract the scaling of the thermal Hall resistivity. One finds

$$\varrho_H \sim \mathfrak{W}^{\ominus,\text{eff}} \sim T^{d-1+3x}, \tag{2.27}$$

which is verified numerically. This scaling behavior should also be roughly true in the presence of more angle-dependent scattering, given the aforementioned independence on the scale of scattering.

Finally, we comment on the role of spin-orbit coupling in the present model. The coefficient λ_{mn} communicates the lack of effective time-reversal and mirror symmetry breaking to the scattering rate $\mathfrak{W}^{\ominus}$, and thereby the Hall resistivity begins at linear order in this coefficient. In the present model, λ_{mn} is also proportional to (symmetric) spin-orbit coupling terms (microscopically, derivatives of such terms with respect to ionic displacement)—see Appendix 2.B. In general, however, for more complex magnetic ordering patterns, a nonzero Hall effect may be obtained from our formulation even in the absence of spin-orbit coupling.

2.3.2.2 Numerical evaluation

It is important to verify that the formulae in Eqs. (2.18,2.19) are sufficient to generate all the expected symmetry-allowed scattering processes and thereby contributions to the thermal Hall conductivity. To do so, we evaluated these formulae numerically, which also allows a test of the scaling predictions above. In the numerical calculations, we took specific values for the microscopic parameters which define the dispersions of the magnons and phonons, as well as those which underlie the $\mathcal{B}$ coefficients, comprising spin-lattice couplings and the mass per unit cell. Eqs. (2.18,2.19,2.8,2.9) were evaluated by a C code using the Cuba and Cubature libraries for numerical integration [Hahn, 2005].

It is convenient to measure energies in units of the phononic energy scale $\epsilon_0 = k_B T_0 = \hbar v_{\text{ph}}/\mathfrak{a}$, which is equal to the Debye temperature up to a factor, and we report thermal conductivities in units of $\kappa_0 = k_B v_{\text{ph}}/\mathfrak{a}^2$, which gives a natural scale for phononic heat transport.

To make our numerical calculations more directly relevant, we loosely chose key dimensionless parameters to loosely match those of Copper Deuteroformate Tetradeuterate (CFTD), a square lattice S=1/2 antiferromagnet which has been intensively studied via neutron scattering [Christensen et al., 2007, Dalla Piazza et al., 2015, Rønnow et al., 2001] due to its convenient scale of exchange which suits such measurements. For our purposes, CFTD has the desirable attribute that the magnon and phonon velocities are comparable (based on an estimate of the sound velocity from the corresponding hydrate [Kameyama et al., 1973]), which creates a significant phase space for magnon-phonon scattering. In particular, we take $v_{\text{m}}/v_{\text{ph}} = 2.5$, while the corresponding ratio in La_2CuO_4, $v_{\text{m}}/v_{\text{ph}}$ is approximately 30. We also use the mass per unit cell M_{uc} appropriate to CFTD. The parameters $n_0 = 1/2$ and $\chi = 1/(4J\mathfrak{a}^2)$ are chosen to be consistent with spin wave theory. We included small magnon gaps, $\Delta_0 = 0.2\epsilon_0$ and $\Delta_1 = 0.04\epsilon_0$. The microscopic spin-lattice couplings were taken consistent with the expectations for

weak spin-orbit coupling, and are given in Appendix 2.B. Finally, we included in the calculations a small constant contribution $\breve{D}_{n\mathbf{k}} \to \gamma_{\text{ext}}$, independent of $(n, \mathbf{k})$, to model additional scattering channels. In very clean monocrystals and in the absence of any other phonon scattering events, $\gamma_{\text{ext}} \sim v_{\text{ph}}/L$ reduces to the rate at which phonons bounce off the boundaries of the sample (of size L). We vary γ_{ext} to show the dependence on these extrinsic effects. For the calculations of the Hall effect we include a small non-zero magnetization in the direction of the applied field, of 1/20th of the saturation magnetization.

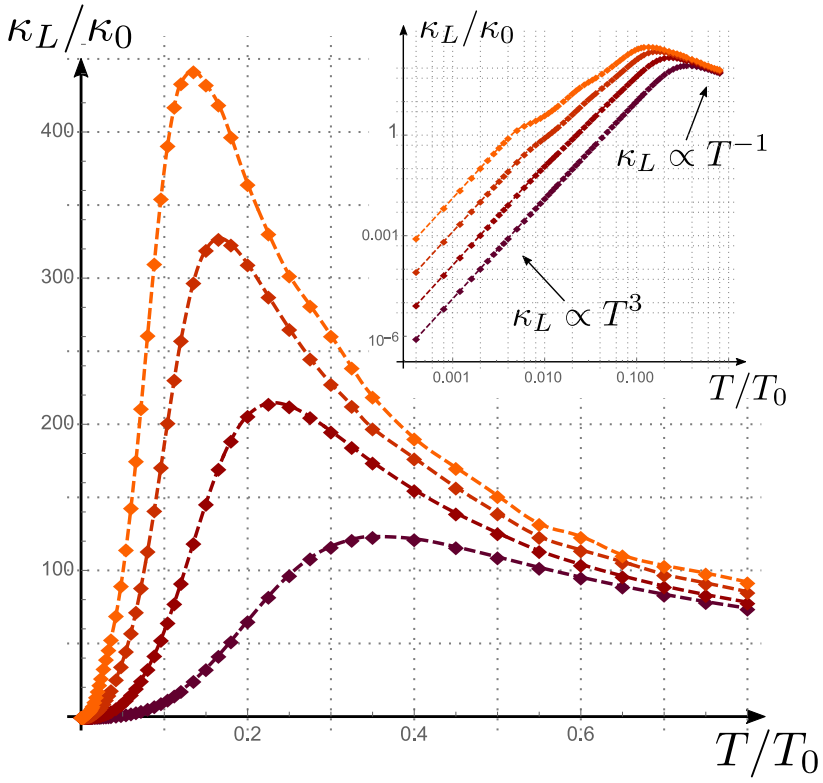

Figure 2.3: Longitudinal thermal conductivity κ_L with respect to temperature T, for four different values of γ_{ext}. (a) Results on an order one temperature scale, with $\gamma_{\text{ext}} = 1 \cdot 10^{-z}(v_{\text{ph}}/\mathfrak{a}), z \in [\![4, 7]\!]$, from darker ($z = 4$) to lighter ($z = 7$) shade. A crossover occurs between two scaling regimes with $x = 1$ and $x = -1$ (see Eq. (2.24)). Inset: log-log plot; the scaling behaviors are consistent with the analysis presented in the text.

Figs. 2.3,2.4 show the results for the longitudinal thermal conductivity versus temperature in zero or low applied magnetic field (the results are insensitive to small magnetizations), for different choices of γ_{ext}. In the first figure, a broad temperature range is shown, which exposes the evolution from an extrinsic scattering regime $\kappa_L \propto T^3$ at low temperature to an intrinsic one $\kappa_L \propto 1/T$ at high temperature. In the second figure, further features emerge related to the scales of the magnon gaps.

Next we turn to the calculations of chiral scattering and the thermal Hall

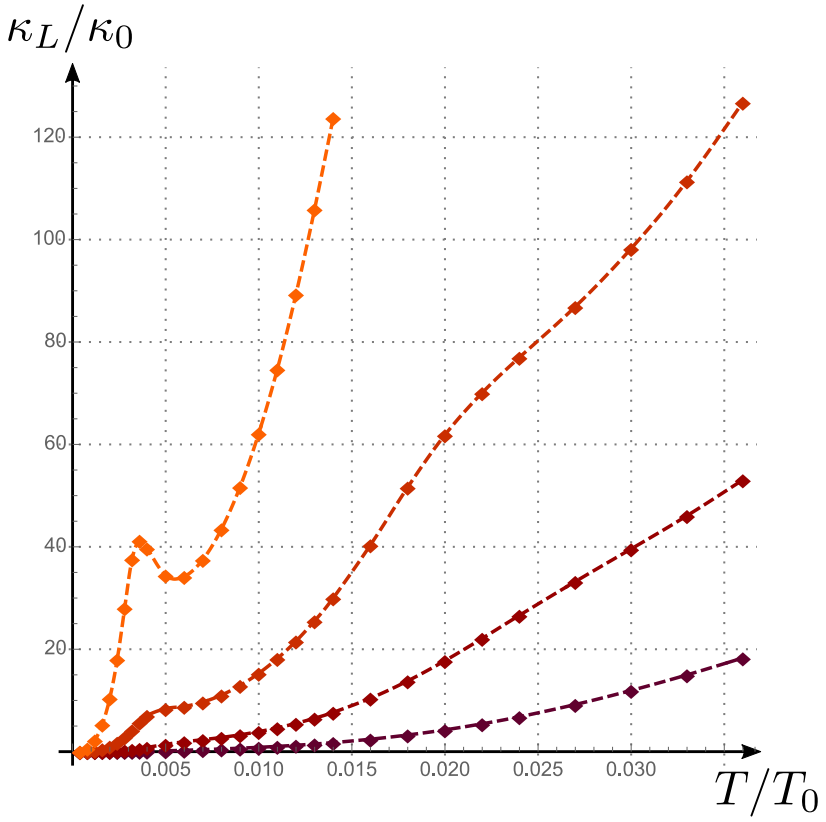

Figure 2.4: Longitudinal thermal conductivity κ_L with respect to temperature T, for four different values of γ_{ext}. Results on a smaller temperature scale, with $\gamma_{\text{ext}} = 1 \cdot 10^{-z}(v_{\text{ph}}/\mathfrak{a}), z \in [\![6, 9]\!]$, from darker ($z = 6$) to lighter ($z = 9$) shade. The peaks are features related to the magnon gaps.

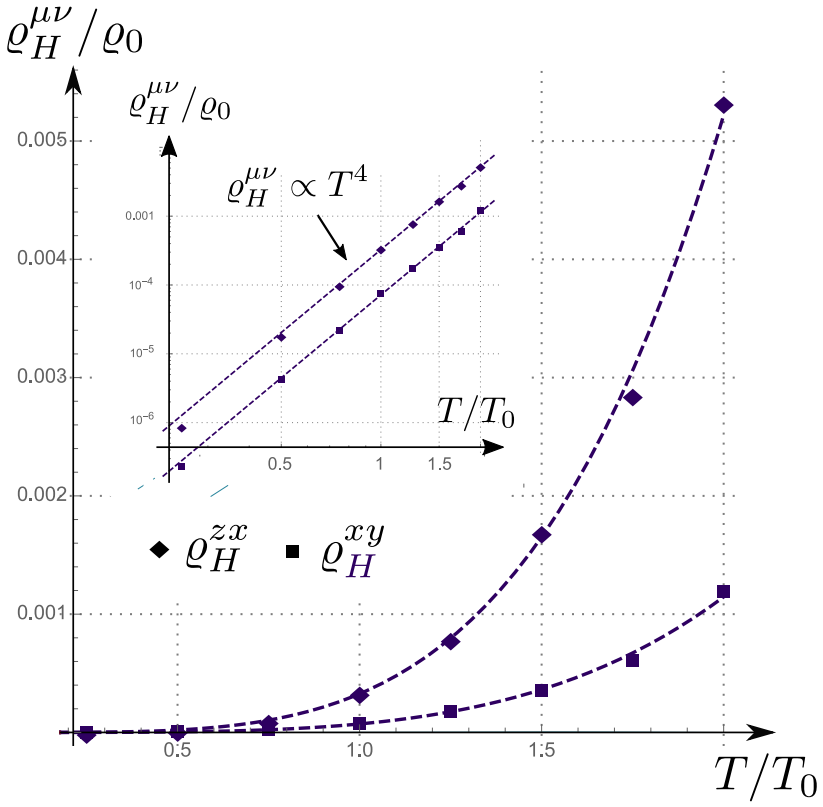

Figure 2.5: Thermal Hall resistivity ϱ_H^{xy} and ϱ_H^{zx} (in units of $\varrho_0 = \kappa_0^{-1}$ with respect to temperature T. The transverse magnetization values (m_0^y, m_0^z) used for computing ϱ_H^{xy} and ϱ_H^{xz} were $(0.0, 0.05)$ and $(0.05, 0.0)$, respectively. Inset: log-log plot; the scaling behavior is consistent with the analysis presented in the text.

effect. Figure 3.5.6 shows a density plot of the Hall scattering rate $\mathfrak{W}^{\ominus,-+}$ as a function of the polar angle of $\mathbf{k}'$, $\theta(\mathbf{k}')$, and of the difference in azimuthal angles of $\mathbf{k}'$ and $\mathbf{k}$, $\varphi(\mathbf{k},\mathbf{k}') = \phi(\mathbf{k}') - \phi(\mathbf{k})$. We see that it has an intricate structure reflecting kinematics and energetics. The thermal Hall resistivity in the constant longitudinal scattering approximation ($D_{n\mathbf{k}} = 1/\tau$ independent of $n, \mathbf{k}$) is plotted in Fig. 2.5 for two different field orientations: for a field along the z axis, normal to the planes, we plot ϱ_H^{xy}, and for a field along the y axis, within the planes, we plot ϱ_H^{zx}. Both curves perfectly fit the T^4 scaling expected theoretically from Eq. (2.27) (using $d = 2, x = 1$) with weak spin-orbit coupling. Notably the magnitudes of the thermal Hall resistivity for the two orientations are comparable, and it is actually *larger* for an *in-plane* field than for an out-of-plane one!

2.4 Conclusion

In this paper, we presented a theory for the skew scattering of phonons coupled to a quantum collective field, which gives rise to a phonon thermal Hall effect. A general formula, given in Eqs. (2.9,2.10), allows the latter to be calculated for *arbitrary* correlations of the collective variable. We then explicitly calculated these correlations for the case in which the collective field is bilinear in canonical bosons, e.g. spin wave operators. A formula with no further assumptions is given in Eq. (2.19). Applying this to the regime of long-wavelength magnons in a square lattice antiferromagnet, we obtained a non-zero thermal Hall effect and its scaling with temperature in various regimes.

While we are not aware of any general results on the intrinsic phonon Hall conductivity due to scattering, there are a number of complementary theoretical papers as well as some prior work which overlap a small part of our results. The specific problem of phonons scattering from magnons was studied long ago to the leading second order in the coupling by Cottam [Cottam, 1974]. That work, which assumed the isotropic SU(2) invariant limit, agrees with our calculations when these assumptions are imposed. The complementary mechanism of intrinsic phonon Hall effect due to phonon Berry curvature was studied by many authors [Qin et al., 2012, Saito et al., 2019, Zhang et al., 2010, Zhang et al., 2021b], including how the phonon Berry curvature is induced by spin-lattice coupling in Ref. [Ye et al., 2021]. The majority of recent theoretical work has concentrated on *extrinsic* effects due to scattering of phonons by defects [Sun et al., 2021, Guo and Sachdev, 2021, Guo et al., 2022, Flebus and MacDonald, 2021]. The pioneering paper of Mori *et al.* [Mori et al., 2014] in particular recognized the importance of higher order contributions to scattering for the Hall effect, and is in some ways a predecessor to our work.

Do the present results explain experiments on the cuprates? We have not attempted a quantitative comparison, for several reasons. This would require some detailed knowledge of spin-lattice couplings. It also is numerically difficult because in the cuprates there is a very large ratio of magnon to phonon velocities (of order 30), which renders the scattering phase space narrow and the integration challenging. Nevertheless, it is interesting to ask about the order of

magnitude of the response. For this comparison, we follow the logic outlined in Sec. 2.3.2.1 in which we argued that the thermal Hall resistivity is a better quantity for which to compare theory and experiment. We obtain the thermal resistivity from the experimental data in Ref. [Grissonnanche et al., 2020] on the undoped material La_2CuO_4: at about 20 K, the longitudinal conductivity $\kappa_{xx} \approx 10$ W/(K m) (from their extended data Figure 2), and the thermal Hall conductivity $\kappa_{xy} \approx 40$ mW/(K m). Using Eq. (2.26) and the the value $\varrho_0^{\rm LCO} \approx 2.6$ K m/W, we then obtain $(\varrho_H/\varrho_0)^{\rm LCO} \approx 1.5 \times 10^{-4}$. This is at least comparable to values in Figure 2.5.

Regardless of whether the intrinsic picture is correct for the cuprates (we think it most proming for systems like CFTD for which there is a good phase space match of phonons and magnons), we believe that a scattering mechanism *of some kind* is very likely at work. Therefore, we would encourage analysis of future experimental data in terms of ϱ_H rather than κ_H.

In a companion paper (next chapter), we will expound on the results of the present paper and give several extensions covering even more general types of coupling of phonons to collective degrees of freedom. There also remain many other related problems that would be interesting to explore, for example the influence of electronic disequilibrium upon the phonons, and vice versa, and the interplay of scattering, presumed here to be dominant, and phononic Berry phases. We hope that the present study provides a theoretical framework to begin to approach these and other intriguing questions.

Appendix

2.A From interaction terms to the collision integral

2.A.1 First Born order

First, we consider only the first term of Born's expansion. The transition rate associated with H' at this order are simply the matrix elements:

$$T^{[1]}_{\mathtt{i}\to\mathtt{f}} = \sum_{n\mathbf{k}q} \sqrt{N^i_{\mathbf{k},n} + \tfrac{q+1}{2}}\ \langle f_s|Q^q_{n\mathbf{k}}|i_s\rangle\ \mathbb{I}(i_p \xrightarrow{q\cdot n\mathbf{k}} f_p), \tag{2.28}$$

where $\mathbb{I}(i_p \xrightarrow{q\cdot n\mathbf{k}} f_p)$ means that the only difference between $|i_p\rangle$ and $|f_p\rangle$ is that there is $q = \pm 1$ more phonon of species $(n, \mathbf{k})$ in the final state.

We then compute the squared matrix element. We have

$$\begin{aligned}\left|T^{[1]}_{\mathtt{i}\to\mathtt{f}}\right|^2 &= \sum_{n\mathbf{k}q} \left(N^i_{\mathbf{k},n} + \tfrac{q+1}{2}\right)\ \mathbb{I}(i_p \xrightarrow{q\cdot n\mathbf{k}} f_p) \\ &\times\ \langle i_s|Q^{-q}_{n\mathbf{k}}|f_s\rangle\langle f_s|Q^q_{n\mathbf{k}}|i_s\rangle.\end{aligned} \tag{2.29}$$

We then enforce the energy conservation $\delta(E_{\mathtt{f}} - E_{\mathtt{i}}) = \delta(q\omega_{n\mathbf{k}} + E_{f_s} - E_{i_s})$ by writing the latter as a time integral, i.e. $\int_{-\infty}^{+\infty} \mathrm{d}t e^{i\omega t} = 2\pi\delta(\omega)$, identify $A(t) = e^{+iHt}Ae^{-iHt}$, use the identity $1 = \sum_{f_s} |f_s\rangle\langle f_s|$, and take the Q field in the initial state to be in thermal equilibrium $p_{i_s} = Z_s^{-1}e^{-\beta E_{i_s}}$. Finally summing over $|i_s\rangle$ and identifying $\langle A\rangle_\beta = Z_s^{-1}\mathrm{Tr}(e^{-\beta H}A)$, we find that the scattering rate between phonon states at first Born's order reads

$$\begin{aligned}\Gamma^{[1];[1]}_{i_p\to f_p} &= \sum_{n\mathbf{k}q} \left(N^i_{n\mathbf{k}} + \tfrac{q+1}{2}\right)\ \mathbb{I}(i_p \xrightarrow{q\cdot n\mathbf{k}} f_p) \\ &\times \int_{-\infty}^{\infty} \mathrm{d}t\, e^{-iq\omega_{n\mathbf{k}}t} \left\langle Q^{-q}_{n\mathbf{k}}(t)\ Q^q_{n\mathbf{k}}(0)\right\rangle_\beta .\end{aligned} \tag{2.30}$$

To arrive at the collision integral, the final step involves summing over final phononic states f_p and taking the average over initial phononic states i_p. First, we notice that a change of variables in $\left\langle Q^{-q}_{n\mathbf{k}}(t)\ Q^q_{n\mathbf{k}}(0)\right\rangle_\beta$ leads to the detailed-balance relation

$$\left\langle Q^{-q}_{n\mathbf{k}}(t)\ Q^q_{n\mathbf{k}}(0)\right\rangle_\beta = \left\langle Q^q_{n\mathbf{k}}(t)\ Q^{-q}_{n\mathbf{k}}(0)\right\rangle_\beta e^{-q\beta\omega_{n\mathbf{k}}}. \tag{2.31}$$

It is then straightforward to show that only the commutator term on the right-hand-side of Eq. (2.30) satisfies this relation. In turn, the final expression for the diagonal of the collision matrix takes the form of the spectral function:

$$D^{[1];[1]}_{n\mathbf{k}} = -\int_{-\infty}^{+\infty} \mathrm{d}t e^{-i\omega_{n\mathbf{k}}t} \left\langle [Q^{-}_{n\mathbf{k}}(t), Q^{+}_{n\mathbf{k}}(0)] \right\rangle_{\beta}, \tag{2.32}$$

as quoted in the main text.

2.A.2 Second Born order

As discussed, the first Born approximation alone does not lead to a nonzero thermal Hall effect. Here we compute that which appears when the Born expansion is taken up to the second Born order. We have

$$\begin{aligned} T^{[1,1]}_{\mathtt{i}\to\mathtt{f}} &= \sum_{n\mathbf{k},n'\mathbf{k}'} \sum_{q,q'=\pm} \sqrt{N^{i}_{n\mathbf{k}} + \tfrac{1+q}{2}} \sqrt{N^{f}_{n'\mathbf{k}'} + \tfrac{1-q'}{2}} \\ &\quad \cdot \sum_{m_s} \frac{\langle f_s | Q^{q'}_{n'\mathbf{k}'} | m_s \rangle \langle m_s | Q^{q}_{n\mathbf{k}} | i_s \rangle}{E_{i_s} - E_{m_s} - q\omega_{\mathbf{k},n} + i\eta} \; \mathbb{I}(i_p \xrightarrow[q'\cdot n'\mathbf{k}']{q\cdot n\mathbf{k}} f_p), \end{aligned} \tag{2.33}$$

The squared T-matrix elements now include cross-terms between the first and second orders of Born's expansion. Here we give details of the calculation of one term, the square of Eq. (2.33), $\left|T^{[1,1]}_{\mathtt{i}\to\mathtt{f}}\right|^2$. In the numerator, the matrix elements of the Q operators can combine themselves in two different ways, which we denote in the following as (a): $\langle i_s|Q^{q}_{n\mathbf{k}}|m_s\rangle\langle m_s|Q^{q'}_{n'\mathbf{k}'}|f_s\rangle\langle f_s|Q^{-q'}_{n'\mathbf{k}'}|m'_s\rangle\langle m'_s|Q^{-q}_{n\mathbf{k}}|i_s\rangle$, and (b): $\langle i_s|Q^{q}_{n\mathbf{k}}|m_s\rangle\langle m_s|Q^{q'}_{n'\mathbf{k}'}|f_s\rangle\langle f_s|Q^{-q}_{n\mathbf{k}}|m'_s\rangle\langle m'_s|Q^{-q'}_{n'\mathbf{k}'}|i_s\rangle$.

We use the following time integral representation of each of the denominators (using a regularized definition of the sign function),

$$\begin{aligned} \frac{1}{x \pm i\eta} &= \mathrm{PP}\frac{1}{x} \mp i\pi\delta(x) \\ &= \frac{1}{2i}\int_{-\infty}^{+\infty} \mathrm{d}t_1 e^{it_1 x}\mathrm{sign}(t_1) \pm \frac{1}{2i}\int_{-\infty}^{+\infty} \mathrm{d}t_1 e^{it_1 x}. \end{aligned} \tag{2.34}$$

and a introduce a third time integral to enforce the energy conservation $E_{\mathtt{f}} - E_{\mathtt{i}} = q'\omega_{n'\mathbf{k}'} + q\omega_{n\mathbf{k}} + E_{f_s} - E_{i_s}$. The product of the denominators (cf. Eq. (2.34)) leads to four terms, which can be labeled by two signs $s, s' = \pm$, and we define, for convenience,

$$\Theta_{ss'}(t_1, t_2) := [-\mathrm{sign}(t_1)]^{\frac{1-s}{2}} \, [\mathrm{sign}(t_2)]^{\frac{1-s'}{2}}. \tag{2.35}$$

Then, the transition rate coming from this part of the total squared matrix element can be written as a sum of eight terms:

$$\Gamma^{[1,1];[1,1]}_{i_p\to f_p} = \sum_{n\mathbf{k},n'\mathbf{k}'} \sum_{q,q'} \left(N^{i}_{n\mathbf{k}} + \tfrac{q+1}{2}\right)\left(N^{i}_{n'\mathbf{k}'} + \tfrac{q'+1}{2}\right) \tag{2.36}$$

$$\times \sum_{s,s'=\pm} \sum_{i=a,b} W^{[1,1];[1,1],(i),ss'}_{n\mathbf{k}q,n'\mathbf{k}'q'} \; \mathbb{I}(i_p \xrightarrow[q'\cdot n'\mathbf{k}']{q\cdot n\mathbf{k}} f_p), \tag{2.37}$$

where we defined (notice the order of the first two operators in the correlator and the sign $t_1 \pm t_2$ in the exponential):

$$W^{[1,1];[1,1],(a),ss'}_{n\mathbf{k}q,n'\mathbf{k}'q'} = \int \mathrm{d}t\mathrm{d}t_1\mathrm{d}t_2\Theta_{ss'}(t_1,t_2)e^{i(q\omega_{n\mathbf{k}}+q'\omega_{n'\mathbf{k}'})t}e^{i(t_1+t_2)(q\omega_{n\mathbf{k}}-q'\omega_{n'\mathbf{k}'})} \cdot \left\langle Q^{-q}_{n\mathbf{k}}(-t-t_2)Q^{-q'}_{n'\mathbf{k}'}(-t+t_2)Q^{q'}_{n'\mathbf{k}'}(-t_1)Q^{q}_{n\mathbf{k}}(+t_1)\right\rangle_\beta \quad (2.38)$$

$$W^{[1,1];[1,1],(b),ss'}_{n\mathbf{k}q,n'\mathbf{k}'q'} = \int \mathrm{d}t\mathrm{d}t_1\mathrm{d}t_2\Theta_{ss'}(t_1,t_2)e^{i(q\omega_{n\mathbf{k}}+q'\omega_{n'\mathbf{k}'})t}e^{i(t_1-t_2)(q\omega_{n\mathbf{k}}-q'\omega_{n'\mathbf{k}'})} \cdot \left\langle Q^{-q'}_{n'\mathbf{k}'}(-t-t_2)Q^{-q}_{n\mathbf{k}}(-t+t_2)Q^{q'}_{n'\mathbf{k}'}(-t_1)Q^{q}_{n\mathbf{k}}(+t_1)\right\rangle_\beta \quad (2.39)$$

One can show the following ("anti-")detailed-balance relations

$$W^{[1,1];[1,1],(a),ss'}_{n\mathbf{k}q,n'\mathbf{k}'q'} = ss'\ W^{[1,1];[1,1],(a),s's}_{n'\mathbf{k}'-q',n\mathbf{k}-q}e^{-\beta(q\omega_{n\mathbf{k}}+q'\omega_{n\mathbf{k}'})}, \quad (2.40)$$

$$W^{[1,1];[1,1],(b),ss'}_{n\mathbf{k}q,n'\mathbf{k}'q'} = ss'\ W^{[1,1];[1,1],(b),s's}_{n\mathbf{k}-q,n'\mathbf{k}'-q'}e^{-\beta(q\omega_{n\mathbf{k}}+q'\omega_{n'\mathbf{k}'})}. \quad (2.41)$$

From this, the same holds for the symmetrized in $n\mathbf{k}q \leftrightarrow n'\mathbf{k}'q'$ scattering rate $\mathcal{W}^{[1,1];[1,1],ss'}_{n\mathbf{k}q,n'\mathbf{k}'q'} = \sum_{i=a,b} W^{[1,1];[1,1],(i),ss'}_{n\mathbf{k}q,n'\mathbf{k}'q'} + (n\mathbf{k}q \leftrightarrow n'\mathbf{k}'q')$, i.e.

$$\mathcal{W}^{[1,1];[1,1],ss'}_{n\mathbf{k}q,n'\mathbf{k}'q'} = ss'\ e^{-\beta(q\omega_{n\mathbf{k}}+q'\omega_{n'\mathbf{k}'})}\mathcal{W}^{[1,1];[1,1],ss'}_{n\mathbf{k}-q,n'\mathbf{k}'-q'}. \quad (2.42)$$

We can then identify

$$\mathfrak{W}^{\ominus,[1,1];[1,1],qq'}_{n\mathbf{k},n'\mathbf{k}'} = N_{\mathrm{uc}}\sum_{s=\pm}\mathcal{W}^{[1,1];[1,1],s,-s}_{n\mathbf{k}q,n'\mathbf{k}'q'}, \quad (2.43)$$

$$\mathfrak{W}^{\oplus,[1,1];[1,1],qq'}_{n\mathbf{k},n'\mathbf{k}'} = N_{\mathrm{uc}}\sum_{s=\pm}\mathcal{W}^{[1,1];[1,1],ss}_{n\mathbf{k}q,n'\mathbf{k}'q'}, \quad (2.44)$$

which, by construction, satisfy

$$\mathfrak{W}^{\sigma,[1,1];[1,1],qq'}_{n\mathbf{k},n'\mathbf{k}'} = \sigma\ e^{-\beta(q\omega_{n\mathbf{k}}+q'\omega_{n'\mathbf{k}'})}\mathfrak{W}^{\sigma,[1,1];[1,1],-q-q'}_{n\mathbf{k},n'\mathbf{k}'}, \quad (2.45)$$

where $\sigma = \oplus$ (resp. $\sigma = \ominus$) indicates that $\mathfrak{W}$ satisfies detailed balance (resp. "anti-detailed balance"). Only $\mathfrak{W}^{\ominus,[1,1];[1,1],qq'}_{n\mathbf{k},n'\mathbf{k}'}$ contributes to the thermal Hall conductivity.

2.B Details of the magnetic model

2.B.1 General symmetry-allowed model

We begin with a semi-microscopic coupling of the local strain tensor $\boldsymbol{\mathcal{E}}_{\mathbf{r}}$ to continuum non-linear sigma model fields: the density m_a of uniform magnetization and n_a of staggered magnetization ($a = x, y, z$). This is

$$\mathcal{H}'_{\mathrm{tetra}}(\mathbf{r}) = \sum_{\substack{\alpha,\beta=x,y,z\\ a,b=x,y,z}}\mathcal{E}^{\alpha\beta}_{\mathbf{r}}\left(\Lambda^{(\mathrm{n}),\alpha\beta}_{ab}\mathrm{n}_a\mathrm{n}_b + \frac{\Lambda^{(\mathrm{m}),\alpha\beta}_{ab}}{n_0^2}\mathrm{m}_a\mathrm{m}_b\right)\Bigg|_{\mathbf{x},z}, \quad (2.46)$$

where n_0 is the ordered moment density. The $\Lambda_{ab}^{(\xi),\alpha\beta}$ coefficients are constrained by the tetragonal symmetry of the crystal. The non-linear sigma model is defined by the constraints $\mathbf{n}\cdot\mathbf{m}=0$ and $\mathbf{n}^2+\mathbf{m}^2/n_0^2=1$.

We expand the above to second order in the *fluctuations* $(\delta m,\delta n)$ around the average values due to both spontaneous ordering and the applied field. We take the Néel vector along $\hat{\boldsymbol{x}}$. Then $\mathrm{n}_x = 1-\frac{1}{2}\sum_{b=y,z}[\delta n_b^2+\frac{1}{n_0^2}(m_0^b+\delta m_b)^2]$, and $\mathrm{m}_x=-\sum_{b=y,z}(m_0^b+\delta m_b)\delta n_b$. Here $\boldsymbol{m}_0$ is the average uniform magnetization, which lies in the $y-z$ plane. We assume $m_0\ll n_0$, so quantities are expressed to linear order in m_0 whenever possible. This gives

$$\mathcal{H}'_{\rm tetra}(\mathbf{r}) \approx \sum_{\alpha\beta}\mathcal{E}_{\mathbf{r}}^{\alpha\beta}\sum_{a,b=y,z}\sum_{\xi,\xi'=0,1}\lambda_{ab;\xi\xi'}^{\alpha\beta}n_0^{-\xi-\xi'}\eta_{a\xi\mathbf{r}}\eta_{b\xi'\mathbf{r}}, \tag{2.47}$$

where $\eta_{a0}=\delta n_a$ and $\eta_{a1}=\delta m_a$, and

$$\begin{aligned}\lambda_{ab;\xi\xi}^{\alpha\beta} &= \Lambda_{ab}^{(\xi),\alpha\beta}-\delta_{ab}\Lambda_{xx}^{(0),\alpha\beta},\\ \lambda_{ab;01}^{\alpha\beta} &= \lambda_{ba;10}^{\alpha\beta}=\frac{-1}{n_0}\left[m_0^a\Lambda_{bx}^{(1),\alpha\beta}+\delta_{ab}m_0^{\overline{a}}\Lambda_{\overline{a}x}^{(1),\alpha\beta}+m_0^b\Lambda_{ax}^{(0),\alpha\beta}\right],\end{aligned} \tag{2.48}$$

where $\overline{y}=z$, $\overline{z}=y$ and we have associated $\xi=\mathrm{n}\Leftrightarrow\xi=0$ and $\xi=\mathrm{m}\Leftrightarrow\xi=1$ in $\Lambda^{(\xi)}$.

Here each $\Lambda^{(\xi)}$ tensor, which we define to be symmetric in both ab and $\alpha\beta$ variables, has seven independent coefficients, which we call $\Lambda_1^{(\xi)}=\Lambda_{xx}^{(\xi),xx}=\Lambda_{yy}^{(\xi),yy}$, $\Lambda_2^{(\xi)}=\Lambda_{yy}^{(\xi),xx}=\Lambda_{xx}^{(\xi),yy}$, $\Lambda_3^{(\xi)}=\Lambda_{zz}^{(\xi),xx}=\Lambda_{zz}^{(\xi),yy}$, $\Lambda_4^{(\xi)}=\Lambda_{xx}^{(\xi),zz}=\Lambda_{yy}^{(\xi),zz}$, $\Lambda_5^{(\xi)}=\Lambda_{zz}^{(\xi),zz}$, $\Lambda_6^{(\xi)}=\Lambda_{xy}^{(\xi),xy}=\Lambda_{xy}^{(\xi),yx}=\Lambda_{yx}^{(\xi),yx}=\Lambda_{yx}^{(\xi),xy}$, $\Lambda_7^{(\xi)}=\Lambda_{xz}^{(\xi),xz}=\Lambda_{xz}^{(\xi),zx}=\Lambda_{zx}^{(\xi),zx}=\Lambda_{zx}^{(\xi),xz}=\Lambda_{yz}^{(\xi),yz}=\Lambda_{yz}^{(\xi),zy}=\Lambda_{zy}^{(\xi),zy}=\Lambda_{zy}^{(\xi),yz}$. All other $\Lambda_{ab}^{(\xi),\alpha\beta}$ are zero. This is the most general coupling allowed by the symmetries of the lattice and of the magnetic order.

To cast this in the form of Eq. (2.2) and Eq. (2.15), we insert the (very standard) free field expressions for the strain and magnetization fluctuations in terms of phonon and magnon creation/annihilation operators, respectively, into Eq. (2.47). For the strain,

$$\mathcal{E}^{\mu\nu}(\mathbf{x})=\frac{1}{\sqrt{V}}\sum_{n\mathbf{k}}\frac{i/2}{\sqrt{2\rho_M\omega_{n\mathbf{k}}}}\left(a_{n\mathbf{k}}+a_{n,-\mathbf{k}}^\dagger\right)\left(k^\mu\varepsilon_{n\mathbf{k}}^\nu+k^\nu\varepsilon_{n\mathbf{k}}^\mu\right)e^{i\mathbf{k}\cdot\mathbf{x}},$$

where ρ_M is the mass density. For the magnetization densities, diagonalization of the nonlinear sigma-model hamiltonian density

$$\begin{aligned}\mathcal{H}_m &= \frac{\rho}{2}\left(|\underline{\boldsymbol{\nabla}}\delta n_y|^2+|\underline{\boldsymbol{\nabla}}\delta n_z|^2\right)\\ &+ \frac{1}{2\chi}(\delta m_y^2+\delta m_z^2)+\sum_{a=y,z}\frac{\chi\Delta_{a-1}^2}{2}\delta n_a^2\end{aligned} \tag{2.49}$$

yields

$$\eta_{a\xi\mathbf{r}}=\sum_{\mathbf{p}}\sum_{\ell=0,1}\sum_{q=\pm}U_{a\xi\ell q}(\mathbf{p})b_{\ell\mathbf{p}}^q e^{i\mathbf{p}\cdot\mathbf{r}}, \tag{2.50}$$

with

$$U_{a\xi\ell q}(\mathbf{p}) = -\delta_{a-1,\ell-\bar{\xi} \bmod 2} F_{\xi q\ell}(\mathbf{p}), \tag{2.51}$$

$$F_{\xi q\ell}(\mathbf{p}) = (iq)^{\bar{\xi}} (-1)^{\bar{\xi}\ell} (\chi \Omega_{\ell \mathbf{p}})^{\xi - \frac{1}{2}}. \tag{2.52}$$

We defined $\bar{\xi} = 1 - \xi$, i.e. $\bar{0} = 1, \bar{1} = 0$, as well as $a = y \Leftrightarrow a - 1 = 0$ and $a = z \Leftrightarrow a - 1 = 1$. In addition, in Eq. (2.49), ρ is the antiferromagnetic spin stiffness, and χ is the magnetic susceptibility. Inserting these definitions into Eq. (2.47), some algebra leads to the form of the text, with the coupling coefficients

$$\mathcal{B}^{n,\ell_1\ell_2|q_1q_2q}_{\mathbf{k};\mathbf{p}} = \frac{iq}{2\sqrt{2M_{\rm uc}}} \sum_{\xi\xi'} n_0^{-\xi-\xi'} \mathcal{L}^{q,\ell_1,\ell_2}_{n\mathbf{k};\xi,\xi'} \, F_{\xi q_1 \ell_1}\left(\mathbf{p} + \frac{q}{2}\mathbf{k}\right) F_{\xi' q_2 \ell_2}\left(-\mathbf{p} + \frac{q}{2}\mathbf{k}\right), \tag{2.53}$$

where

$$\mathcal{L}^{q,\ell_1,\ell_2}_{n\mathbf{k};\xi,\xi'} = \sum_{\alpha,\beta=x,y,z} \hat{\lambda}^{\ell_1\ell_2;\alpha\beta}_{\xi\xi'} \, \frac{k^\alpha (\varepsilon^\beta_{n\mathbf{k}})^q + k^\beta (\varepsilon^\alpha_{n\mathbf{k}})^q}{\sqrt{\omega_{n\mathbf{k}}}}, \tag{2.54}$$

and $\hat{\lambda}^{\ell\ell';\alpha\beta}_{\xi\xi'} = \lambda^{\alpha\beta}_{\ell-\bar{\xi} \bmod 2, \ell'-\bar{\xi}' \bmod 2; \xi\xi'}$.

Note that the λ_{mn} coefficients involved in the Hall conductivity, namely the $\boldsymbol{\lambda}_{ab;01}$ rank-2 tensors, are written explicitly in Eq. (2.48). They are proportional to the net magnetization $\boldsymbol{m}_0$, as is consistent with the fact that they are associated with a time-reversal breaking quantity. One can also observe that they involve only the *anisotropic* coefficients $\Lambda^{(\xi)}_{6,7}$, which in a microscopic derivation arise from spin-orbit coupling, see next chapter.

2.B.2 Numerical implementation

In the numerical implementation, we use values of the parameters roughly appropriate for CFTD, which we provide in Table 3.5.4. The phonon polarization vectors $\boldsymbol{\varepsilon}_{n,\mathbf{k}}$ are chosen to form an orthonormal basis in which $\mathbf{k}$ points along the $[1,1,1]$ axis, so that $\mathbf{k} \cdot \boldsymbol{\varepsilon}_{n,\mathbf{k}} = \frac{|\mathbf{k}|}{\sqrt{3}} \; \forall n$.

$\frac{v_\mathrm{m}}{v_\mathrm{ph}}$	$\chi\epsilon_0\mathfrak{a}^2$	n_0	$\frac{M_\mathrm{uc}v_\mathrm{ph}\mathfrak{a}}{\hbar}$	m_0^x	m_0^y	m_0^z	$\frac{\Delta_0}{\epsilon_0}$	$\frac{\Delta_1}{\epsilon_0}$
2.5	0.19	1/2	$8 \cdot 10^3$	0	0.0 0.05	0.05 0.0	0.2	0.04

ξ	$\Lambda_1^{(\xi)}$	$\Lambda_2^{(\xi)}$	$\Lambda_3^{(\xi)}$	$\Lambda_4^{(\xi)}$	$\Lambda_5^{(\xi)}$	$\Lambda_6^{(\xi)}$	$\Lambda_7^{(\xi)}$
n = 0	12.0	10.0	14.0	10.0	12.0	0.6	0.8
m = 1	−10.0	−12.0	−14.0	−12.0	−10.0	−0.8	−0.6

Table 2.B.1: Numerical values of the fixed dimensionless parameters used in all numerical evaluations. The upper and lower entries for m_0^y and m_0^z correspond to the two cases for calculating ϱ_H^{xy} and ϱ_H^{xz}, respectively. The couplings $\Lambda_i^{(\xi)}$ are given in units of $\epsilon_0/\mathfrak{a}$.

Chapter 3

Thermal conductivity and theory of inelastic scattering of phonons by collective fluctuations

We study the *intrinsic* scattering of phonons by a general quantum degree of freedom, i.e. a fluctuating "field" Q, which may have completely general correlations, restricted only by unitarity and translational invariance. From the induced scattering rates, we obtain the consequences on the thermal conductivity tensor of the phonons. We find that the lowest-order diagonal scattering rate, which determines the longitudinal conductivity, is controlled by two-point correlation functions of the Q field, while the off-diagonal scattering rates involve a minimum of three to four point correlation functions. We obtain general and explicit forms for these correlations which isolate the contributions to the Hall conductivity, and provide a general discussion of the implications of symmetry and equilibrium. We evaluate these two- and four-point correlation functions and hence the thermal transport for the illustrative example of an ordered two dimensional antiferromagnet. In this case the Q field is a composite of magnon operators arising from spin-lattice coupling. A numerical evaluation of the required integrals demonstrates that the results satisfy all the necessary symmetry restrictions but otherwise lead to non-vanishing scattering and Hall effects, and in particular that this mechanism leads to comparable thermal Hall conductivity for thermal currents within and normal to the plane of the antiferromagnetism.

3.1 Introduction

Two-point correlation functions are ubiquitous in the study of condensed matter systems. They are often the building blocks of response functions in scattering and other experiments and appear in Feynman diagrams, as well as Monte Carlo simulations. They are the central elements of linear response theory, as is evident from Kubo's formula [Luttinger, 1964, Chen et al.,]. They are often independent of the arbitrary phase choice of the wave function.

Higher order correlation functions have witnessed renewed interest recently. They arise theoretically in the measurement of chaos. A particular type of four-point correlation function, the "out-of-time-ordered" correlator, has been shown to be related to the Lyapunov exponent, which measures the rate at which the result of a measurement diverges after a weak initial perturbation [Swingle, 2018]. Multi-point correlations also naturally describe non-linear response, e.g. in non-linear optics such as second harmonic generation, and in "multi-dimensional spectroscopy" [Wan and Armitage, 2019]. They may also arise in scattering measurements at resonance, such as RIXS [Ament et al., 2011, Savary and Senthil, 2015]. From a statistical point of view, higher order correlation functions measure the non-Gaussianity of the distribution of an observable. The more strongly correlated a state is, i.e. the more it deviates from a free-particle description, the more significant the non-Gaussianity. Hence multi-point functions are essential harbingers of strong correlations.

In a companion paper, we studied the thermal conductivity due to phonons coupled to another degree of freedom, for example an electronic or a magnetic one, and expressed our results in terms of the correlations of the local observable – e.g. an order parameter – Q coupled to the phonons, e.g. with an interaction hamiltonian density

$$H' = \sum_{n\mathbf{k}} \left(a^\dagger_{n\mathbf{k}} Q^\dagger_{n\mathbf{k}} + a_{n\mathbf{k}} Q_{n\mathbf{k}} \right), \tag{3.1}$$

for the simplest case of linear coupling to the strain tensor. The latter is expressed in terms of phonons, whose creation and annihilation operators in mode $n\mathbf{k}$, i.e. at momentum $\mathbf{k}$ in polarization n are $a^\dagger_{n\mathbf{k}}, a_{n\mathbf{k}}$. Here we consider also quadratic coupling, c.f. Eq. (3.16) (as well as even more general forms in the Appendices), and discuss in considerably more detail the physics and consequences of our results, as well as those of the application to an ordered antiferromagnet we provide. The latter include in particular that the leading diagonal scattering rate is

$$D_{n\mathbf{k}} = -\frac{1}{\hbar^2} \int dt\, e^{-i\omega_{n\mathbf{k}} t} \left\langle [Q_{n\mathbf{k}}(t), Q^\dagger_{n\mathbf{k}}(0)] \right\rangle_\beta + \breve{D}_{n\mathbf{k}}, \tag{3.2}$$

where $\breve{D}_{n\mathbf{k}}$ includes both higher order terms and contributions from other mechanisms such as scattering from impurities, $\langle\cdot\rangle_\beta$ denotes thermal averaging, and $\hbar$ is Planck's constant divided by 2π. This controls the longitudinal (dissipative) part of the thermal conductivity, $\kappa^{\mu\nu}_L = (\kappa^{\mu\nu} + \kappa^{\nu\mu})/2$, which, to the same leading order, is

$$\kappa^{\mu\nu}_L = \frac{\hbar^2}{k_B T^2} \frac{1}{V} \sum_{n\mathbf{k}} \frac{v^\mu_{n\mathbf{k}} \omega^2_{n\mathbf{k}} v^\nu_{n\mathbf{k}}}{4 D_{n\mathbf{k}} \sinh^2(\beta\hbar\omega_{n\mathbf{k}}/2)}, \tag{3.3}$$

for $\mu, \nu = x, y, z$, where V is the volume of the system, T the temperature, $k_{\rm B}$ Boltzmann's constant, $\beta = 1/(k_{\rm B}T)$, and $\omega_{n\mathbf{k}}$ and $\boldsymbol{v}_{n\mathbf{k}} = \boldsymbol{\nabla}_{\mathbf{k}}\omega_{n\mathbf{k}}$ are respectively the phonon frequency and velocity in mode $n\mathbf{k}$. Note that $\kappa_L^{\mu\nu}$ is symmetric in $\mu \leftrightarrow \nu$. We also discuss in great detail, and with numerous symmetry analyses that, by contrast, the thermal Hall conductivity is antisymmetric, and hence completely controlled by off-diagonal scattering, and of fourth order. As explained in Sec. 3.2.2, the fourth order nature of the Hall effect is guaranteed because second order contributions to scattering are equivalent to the first Born approximation, which obeys detailed balance and effectively preserves time-reversal symmetry (see also Ref. [Mori et al., 2014]). Through detailed calculations, we find that the thermal Hall conductivity is controlled by two fourth order correlation functions, schematically

$$\begin{aligned} \mathfrak{W}^{\ominus,++}_{n\mathbf{k}n'\mathbf{k}'} &\sim \left\langle [Q_{n\mathbf{k}}, Q_{n'\mathbf{k}'}]\{Q^\dagger_{n'\mathbf{k}'}, Q^\dagger_{n\mathbf{k}}\}\right\rangle , \\ \mathfrak{W}^{\ominus,+-}_{n\mathbf{k}n'\mathbf{k}'} &\sim \left\langle [Q_{n\mathbf{k}}, Q^\dagger_{n'\mathbf{k}'}]\{Q_{n'\mathbf{k}'}, Q^\dagger_{n\mathbf{k}}\}\right\rangle , \end{aligned} \tag{3.4}$$

reflecting particle-particle and particle-hole type processes. Eq. (3.4) is symbolic, and precise formulae with full details of the time/frequency dependence and Fourier transform conventions are given in Eqs. (3.35,3.34,3.36). Note however the combination of commutator $[\,,]$ and anti-commutator $\{\,,\}$, which imposes the subtle structure that extracts the part of the four-point correlations responsible for a Hall effect. We obtain this structure by isolating the "skew scattering" terms in the phonon Boltzmann equation, which are those which are appropriately antisymmetric in $n\mathbf{k} \leftrightarrow n'\mathbf{k}'$, violate detailed balance, and thereby contribute to a Hall effect.

Then the thermal Hall (antisymmetric) conductivity, $\kappa_H^{\mu\nu} = (\kappa^{\mu\nu} - \kappa^{\nu\mu})/2$, at leading order is expressed as

$$\kappa_H^{\mu\nu} = \frac{\hbar^2}{k_B T^2}\frac{1}{V}\sum_{n\mathbf{k}n'\mathbf{k}'} J^\mu_{n\mathbf{k}} \frac{e^{\beta\hbar\omega_{n\mathbf{k}}/2}}{2D_{n\mathbf{k}}} \left(\frac{1}{N_{\rm uc}} \sum_{q=\pm} \frac{\left(e^{\beta\hbar\omega_{n\mathbf{k}}} - e^{q\beta\hbar\omega_{n'\mathbf{k}'}}\right) \mathfrak{W}^{\ominus,+,q}_{n\mathbf{k},n'\mathbf{k}'}}{\sinh(\beta\hbar\omega_{n\mathbf{k}}/2)\sinh(\beta\hbar\omega_{n'\mathbf{k}'}/2)} \right) \frac{e^{\beta\hbar\omega_{n'\mathbf{k}'}/2}}{2D_{n'\mathbf{k}'}} J^\nu_{n'\mathbf{k}'}, \tag{3.5}$$

where $\mu, \nu = x, y, z$ and we defined the phonon current $J^\mu_{n\mathbf{k}} = N^{\rm eq}_{n\mathbf{k}}\,\omega_{n\mathbf{k}} v^\mu_{n\mathbf{k}}$, and $N^{\rm eq}_{n\mathbf{k}}$ is the number of phonons in mode $n\mathbf{k}$ in thermal equilibrium.

Eqs. (3.2-3.5) summarize the key general results of this chapter and of the next chapter, to leading order for the simplest case of linear coupling of an order parameter to phonons. More general formulae including both linear and quadratic coupling are given in Section 3.3.4. These equations may be applied to obtain the phonon thermal conductivity for *any* system provided the correlations of the quantities Q coupling to phonons are known.

The results in this paper are derived using the Boltzmann equation [Ziman, 1960], applying Fermi's golden rule and the first and second Born approximations to the transition probabilities between initial and final states of the joint observable-and-phonon system. These resulting collision terms can be expressed through multi-point correlation functions of the observable. By solving the Boltzmann equation, and computing the resulting phonon thermal currents, we obtain the results quoted above and their generalizations.

In light of several experimental and theoretical studies [Kasahara et al., 2018a, Ye et al., 2018, Grissonnanche et al., 2019, Grissonnanche et al., 2020] which highlight the major role of phonons in the thermal transport in magnetic systems, we demonstrate our formalism on a model for an ordered two-dimensional antiferromagnet, inspired by experiments on the cuprates [Chernyshev and Brenig, 2015]. In this case the Q fields constitute bilinears of magnon operators. In a separate publication, we will present a second application to a spinon Fermi surface quantum spin liquid [Savary and Balents, 2016] and other fermionic systems, including electronic ones.

3.2 Setup

3.2.1 Derivation

The quasiparticle nature of phonons justifies treating their dynamics within the Boltzmann equation,

$$\partial_t \overline{N}_{n\mathbf{k}} + \boldsymbol{v}_{n\mathbf{k}} \cdot \boldsymbol{\nabla}_{\mathbf{r}} \overline{N}_{n\mathbf{k}} = \mathcal{C}_{n\mathbf{k}}[\{\overline{N}_{n'\mathbf{k}'}\}], \tag{3.6}$$

where $N_{n\mathbf{k}}(i_p) = \langle i_p | a^\dagger_{n\mathbf{k}} a_{n\mathbf{k}} | i_p \rangle$ is the number of $(n, \mathbf{k})$ phonons ($\mathbf{k}$ is the phonon momentum and n an extra phonon label, containing the band index and polarization) in the $|i_p\rangle$ state, $\overline{N}_{n\mathbf{k}} = \sum_{i_p} N_{n\mathbf{k}}(i_p) p_{i_p}$ is the average population, and $\boldsymbol{v}_{n\mathbf{k}} = \boldsymbol{\nabla}_{\mathbf{k}} \omega_{n\mathbf{k}}$, with $\omega_{n\mathbf{k}}$ the dispersion of phonons, is the group velocity of phonons. $\mathcal{C}$ is the "collision integral," which captures in particular the scattering of phonons with other degrees of freedom (Q fields whose coupling to the phonons is given by H' in Eq. (3.1) or more generally by Eq. (3.16)). In turn, using Born's approximation, we have the following perturbative expansion of the scattering matrix:

$$T_{\mathtt{i}\to\mathtt{f}} = T_{\mathtt{f}\mathtt{i}} = \langle \mathtt{f} | H' | \mathtt{i} \rangle + \sum_{\mathtt{n}} \frac{\langle \mathtt{f} | H' | \mathtt{n} \rangle \langle \mathtt{n} | H' | \mathtt{i} \rangle}{E_{\mathtt{i}} - E_{\mathtt{n}} + i\eta} + \cdots, \tag{3.7}$$

where the $|\mathtt{i}, \mathtt{f}, \mathtt{n}\rangle$ states are product states in the Q (index s) and phonon (index p) Hilbert space, $|\mathtt{g}\rangle = |g_s\rangle |g_p\rangle$ for $g = i, f, n$, and $E_{\mathtt{g}}$ is the energy of the unperturbed Hamiltonians of the Q and phonons in state $\mathtt{g}$. $\eta \to 0^+$ is a small regularization parameter. The expression Eq. (3.7) can be derived from time-dependent perturbation (scattering) theory, in which η captures causality and the regularizability of $1/(E_{\mathtt{i}} - E_{\mathtt{n}})$ in the case of a continuous energy spectrum, appropriate for scattering (unbounded) states which we are interested in [Landau and Lifshitz, 1958].

The rate of transitions from state $\mathtt{i}$ to state $\mathtt{f}$ is obtained using Fermi's golden rule,

$$\Gamma_{\mathtt{i}\to\mathtt{f}} = \frac{2\pi}{\hbar} |T_{\mathtt{i}\to\mathtt{f}}|^2 \delta(E_{\mathtt{i}} - E_{\mathtt{f}}). \tag{3.8}$$

Note that $\Gamma_{\mathtt{i}\to\mathtt{f}}$ is a transition rate in the full combined phonon-Q system. This in turn determines the collision integral through the master equation

$$\mathcal{C}_{n\mathbf{k}} = \sum_{i_p, f_p} \tilde{\Gamma}_{i_p \to f_p} \left(N_{n\mathbf{k}}(f_p) - N_{n\mathbf{k}}(i_p) \right) p_{i_p}, \tag{3.9}$$

where $p_{i_p} = \sum_{i_s} p_{\mathtt{i}}$, where $p_{\mathtt{i}} = \frac{1}{Z} e^{-\beta E_{\mathtt{i}}}$ is the probability to find the system in state $\mathtt{i}$, and Z is the partition function of the two subsystems. Here

$$\tilde{\Gamma}_{i_p \to f_p} = \sum_{i_s f_s} \Gamma_{\mathtt{i} \to \mathtt{f}} \, p_{i_s} \tag{3.10}$$

is the transition rate between just phonon states, with $p_{i_s} = \frac{1}{Z_s} e^{-\beta E_{i_s}}$.

3.2.2 Discussion

The above approach is "semiclassical" in two respects. First, it ultimately treats phonons as quasiparticles within a Boltzmann equation. This is justified whenever the scattering rate is small compared to the energy of the particles. Second, we use the Fermi's golden rule relation, Eq. (3.8), to determine the scattering rates. This approximation leads to slight differences from an exact calculation of the quantum rates, but preserves all symmetries and physical processes, and we expect it to capture all the key features of a fully quantum approach. We proceed with the T-matrix approach here which has the advantage of (relative) physical transparency, as every effect can be directly identified with a scattering process.

One can understand the need for effects beyond the first Born approximation entirely through the symmetries of the T-matrix. Specifically, since the time reversal (TR) operator is anti-unitary, and requires complex conjugation, one can see from Eq. (3.7) that under time reversal, TR : $T \mapsto T^\dagger$ ($\eta \to -\eta$ under complex conjugation). Since TR invariance is sufficient to enforce a vanishing Hall effect, the hermiticity of T is enough to guarantee a vanishing Hall effect. From Eq. (3.7), T is indeed always hermitian within the first Born approximation, because H' itself must be hermitian.

Finally, we note that we are focusing on collisional effects, i.e. on *real* transitions induced by interactions, rather than Berry phase contributions, which arise from entirely virtual transitions and manifest as modifications to the semiclassical equations of motion for phonons, e.g. an anomalous velocity. Formally, real transitions are captured within the collision integral on the right hand side of the Boltzmann equation [Mori et al., 2014], while Berry phase contributions enter the left hand side and in the definition of the currents. For phonons, our focus on collisions is justified by strong phase space constraints on the Berry curvature effects which are typical to acoustic bosonic modes. Specifically, as shown in Ref. [Qin et al., 2012], the Berry phase contributions are described by an emergent vector potential which at small momenta must by symmetry be at least second order in gradients, making it a formally "irrelevant" perturbation to the phonon Lagrangian, and strongly suppressing its effects at low temperature [Ye et al., 2021].

3.3 Formal expressions for the thermal conductivity

3.3.1 Formal expressions

To solve Eq. (3.6), we expand $\overline{N}_{n\mathbf{k}} = N^{\rm eq}_{n\mathbf{k}} + \delta\overline{N}_{n\mathbf{k}}$ around the equilibrium distribution $N^{\rm eq}_{n\mathbf{k}}$, which solves Boltzmann's equation at $\boldsymbol{\nabla} T = \mathbf{0}$, keep terms up to linear order in $\delta\overline{N}_{n\mathbf{k}}$ in the collision integral and for convenience separate the diagonal $D_{n\mathbf{k}}$ and off-diagonal $M_{n\mathbf{k},n'\mathbf{k}'}$ parts, i.e. we write the collision integral

$$\mathcal{C}_{n\mathbf{k}} = \sum_{n'\mathbf{k}'} \big(-\delta_{nn'}\delta_{\mathbf{k}\mathbf{k}'} D_{n\mathbf{k}} + M_{n\mathbf{k},n'\mathbf{k}'} \big) \delta\overline{N}_{n'\mathbf{k}'} + O(\delta\overline{N}^2), \tag{3.11}$$

where by definition $M_{n\mathbf{k},n\mathbf{k}} = 0$. The equation $\mathcal{C}_{n\mathbf{k}}[\{N^{\rm eq}_{n'\mathbf{k}'}\}] = 0$ —i.e. the collision integral is zero in equilibrium— should be considered the *definition* of the equilibrium densities $\{N^{\rm eq}_{n'\mathbf{k}'}\}$ of the interacting phonons (see Appendix 3.C.3).

Using Fourier's law,

$$\mathbf{j} = -\boldsymbol{\kappa} \cdot \boldsymbol{\nabla} T = V^{-1} \sum_{n\mathbf{k}} \overline{N}_{n\mathbf{k}} \boldsymbol{v}_{n\mathbf{k}} \omega_{n\mathbf{k}}, \tag{3.12}$$

and formally inverting the collision integral leads to the following expressions for the longitudinal $\kappa^{\mu\mu}_L$, and Hall $\kappa^{\mu\nu}_H$ conductivities (along the μ direction and in the $\mu\nu$ plane, respectively):

$$\kappa^{\mu\nu}_{L/H} = \frac{\hbar^2}{k_B T^2} \frac{1}{V} \sum_{n\mathbf{k}n'\mathbf{k}'} J^{\mu}_{n\mathbf{k}} K^{L/H}_{n\mathbf{k}n'\mathbf{k}'} J^{\nu}_{n'\mathbf{k}'}, \tag{3.13}$$

where $\nu = \mu$ for κ_L. Assuming $\sum_{n'\mathbf{k}'} M_{n\mathbf{k}n'\mathbf{k}'} \ll D_{n\mathbf{k}}$, one can effectively invert the collision integral to obtain the kernels

$$\begin{aligned} K^{L}_{n\mathbf{k}n'\mathbf{k}'} &= \frac{e^{\beta\hbar\omega_{n\mathbf{k}}}}{D_{n\mathbf{k}}} \delta_{nn'}\delta_{\mathbf{k},\mathbf{k}'} \qquad (3.14) \\ &\quad + \frac{e^{\beta\hbar(\omega_{n\mathbf{k}}+\omega_{n'\mathbf{k}'})/2}}{2D_{n\mathbf{k}}D_{n'\mathbf{k}'}} \left(\frac{\sinh(\beta\hbar\omega_{n\mathbf{k}}/2)}{\sinh(\beta\hbar\omega_{n'\mathbf{k}'}/2)} M_{n\mathbf{k},n'\mathbf{k}'} + (n\mathbf{k} \leftrightarrow n'\mathbf{k}') \right), \\ K^{H}_{n\mathbf{k}n'\mathbf{k}'} &= \frac{e^{\beta\hbar(\omega_{n\mathbf{k}}+\omega_{n'\mathbf{k}'})/2}}{2D_{n\mathbf{k}}D_{n'\mathbf{k}'}} \left(\frac{\sinh(\beta\hbar\omega_{n\mathbf{k}}/2)}{\sinh(\beta\hbar\omega_{n'\mathbf{k}'}/2)} M_{n\mathbf{k},n'\mathbf{k}'} - (n\mathbf{k} \leftrightarrow n'\mathbf{k}') \right) \qquad (3.15) \end{aligned}$$

Here we identified the equilibrium phonon current $J^{\mu}_{n\mathbf{k}} = N^{\rm eq}_{n\mathbf{k}} \omega_{n\mathbf{k}} v^{\mu}_{n\mathbf{k}}$, and made the "standard" approximation $\boldsymbol{\nabla}_{\mathbf{r}} \overline{N}_{n\mathbf{k}} \approx \boldsymbol{\nabla}_{\mathbf{r}} N^{\rm eq}_{n\mathbf{k}}$, and looked for a stationary solution ($\partial_t \overline{N} = 0$) to Boltzmann's equation. While the sign of κ_H depends on the details of the system (see later), the second law of thermodynamics imposes $\kappa_L > 0$. Considering Eq. (3.14), we therefore expect $D_{n\mathbf{k}} > 0$.

Clearly, only contributions to $K^{L/H}_{n\mathbf{k},n'\mathbf{k}'}$ which are symmetric (resp. antisymmetric) in exchanging $(n\mathbf{k} \leftrightarrow n'\mathbf{k}')$ contribute to κ_L (resp. κ_H). As a special case, the term diagonal in $n\mathbf{k}, n'\mathbf{k}'$, being symmetric, does not contribute to the Hall conductivity. Below we will isolate the correlation functions of the Q operators which give anti-symmetric (in $n\mathbf{k} \leftrightarrow n'\mathbf{k}'$) contributions to $\frac{\sinh(\beta\hbar\omega_{n\mathbf{k}}/2)}{\sinh(\beta\hbar\omega_{n'\mathbf{k}'}/2)} M_{n\mathbf{k},n'\mathbf{k}'}$, and hence contribute to κ_H. These correspond to scattering processes which violate detailed balance.

3.3.2 Model

To describe the interaction between the phonons and another degree of freedom, we introduce general coupling terms between phonon annihilation (creation) operators $a^{(\dagger)}_{n\mathbf{k}}$ and general, for now unspecified, fields $Q^{\{q_j\}}_{\{n_j,\mathbf{k}_j\}}$ which are operators acting in their own Hilbert space. In what follows we only consider the first two terms of the expansion with respect to phonon operators, i.e. we write the interaction hamiltonian as $H' = H'_{[1]} + H'_{[2]}$, where

$$\begin{aligned} H'_{[1]} &= \sum_{n\mathbf{k}} \sum_{q=\pm} a^q_{n\mathbf{k}} Q^q_{n\mathbf{k}}, \\ H'_{[2]} &= \frac{1}{\sqrt{N_{\mathrm{uc}}}} \sum_{n\mathbf{k}\neq n'\mathbf{k}'} \sum_{q,q'=\pm} a^q_{n\mathbf{k}} a^{q'}_{n'\mathbf{k}'} Q^{qq'}_{n\mathbf{k}n'\mathbf{k}'}, \end{aligned} \tag{3.16}$$

and in the following, we consider Eq. (3.16) as a perturbative expansion with respect to a small parameter λ, such that formally $Q_{n\mathbf{k}} \sim \lambda, Q^{qq'}_{n\mathbf{k}n'\mathbf{k}'} \sim \lambda^2$, etc. Note we consider generalizations of this model in Appendix 3.D.

In the above expression we used $a^+_{n\mathbf{k}} \equiv a^\dagger_{n\mathbf{k}}$ and $a^-_{n\mathbf{k}} \equiv a_{n\mathbf{k}}$. The hermiticity of H' imposes $Q^+_{\{n_i\mathbf{k}_i\}} \equiv Q^\dagger_{\{n_i\mathbf{k}_i\}}$ and $Q^-_{\{n_i\mathbf{k}_i\}} \equiv Q_{\{n_i\mathbf{k}_i\}}$, and for many-phonon terms, we have $Q^{-q_1,\ldots,-q_M}_{\{n_j\mathbf{k}_j\}} = (Q^{q_1\ldots q_M}_{\{n_j\mathbf{k}_j\}})^\dagger$. The single-phonon interaction terms, which may physically be seen as single-phonon scattering off the Q degrees of freedom, corresponds in particular to a coupling of the Q operators to the strain tensor $\mathcal{E}^{\alpha\beta}(\mathbf{r})$,

$$\mathcal{E}^{\alpha\beta}(\mathbf{r}) = \frac{i\hbar^{1/2}}{\sqrt{N_{\mathrm{uc}}}} \sum_{\mathbf{k}n} e^{i\mathbf{k}\cdot\mathbf{r}} \frac{\left(k^\alpha \varepsilon^\beta_{\mathbf{k}n} + k^\beta \varepsilon^\alpha_{\mathbf{k}n}\right)}{\sqrt{2M_{\mathrm{uc}}\omega_{\mathbf{k}n}}} \left(a_{\mathbf{k}n} + a^\dagger_{-\mathbf{k}n}\right), \tag{3.17}$$

where M_{uc} is the unit cell mass and $\boldsymbol{\varepsilon}_{n\mathbf{k}}$ is the polarization vector of the $|n\mathbf{k}\rangle$ phonon. The two-phonon terms capture quadratic coupling of the lattice displacements to the electrons/spins, as is often considered for example in treatments of Raman scattering [Sheng et al., 2006, Kagan and Maksimov, 2008]. A priori, the quadratic terms are much smaller than the linear ones, but the former may be important if they give rise to distinct effects or contribute at a lower order in perturbation theory than the linear ones.

3.3.3 Scattering rates

3.3.3.1 T-matrix elements

The transition matrix elements are $T_{\mathtt{fi}} = \sum_l T^{[l_1,\ldots]}_{\mathtt{fi}}$ (the l_i represent which $H_{[l_i]}$ appear successively in T, so that the number of l_i appearing in $T^{[l_1,\ldots]}_{\mathtt{fi}}$ is the order of the Born approximation used for that term), where

$$T^{[1]}_{\mathtt{i}\to\mathtt{f}} = \sum_{n\mathbf{k}q} \sqrt{N^i_{n\mathbf{k}} + \tfrac{1+q}{2}}\ \langle f_s|Q^q_{n\mathbf{k}}|i_s\rangle\ \mathbb{I}(i_p \xrightarrow{q\cdot n\mathbf{k}} f_p), \tag{3.18}$$

$$T^{[2]}_{\mathtt{i}\to\mathtt{f}} = \frac{1}{\sqrt{N_{\rm uc}}} \sum_{n\mathbf{k}q,n'\mathbf{k}'q'} \sqrt{N^i_{n\mathbf{k}} + \tfrac{1+q}{2}}\sqrt{N^i_{n'\mathbf{k}'} + \tfrac{1+q'}{2}} \tag{3.19}$$

$$\times\langle f_s|Q^{qq'}_{n\mathbf{k}n'\mathbf{k}'}|i_s\rangle\ \mathbb{I}(i_p \xrightarrow[q'\cdot n'\mathbf{k}']{q\cdot n\mathbf{k}} f_p), \tag{3.20}$$

$$T^{[1,1]}_{\mathtt{i}\to\mathtt{f}} = \sum_{n\mathbf{k}q,n'\mathbf{k}'q'} \sqrt{N^i_{n\mathbf{k}} + \tfrac{1+q}{2}}\sqrt{N^f_{n'\mathbf{k}'} + \tfrac{1-q'}{2}} \tag{3.21}$$

$$\times \sum_{m_s} \frac{\langle f_s|Q^{q'}_{n'\mathbf{k}'}|m_s\rangle\langle m_s|Q^q_{n\mathbf{k}}|i_s\rangle}{E_{i_s} - E_{m_s} - q\omega_{n\mathbf{k}} + i\eta}\ \mathbb{I}(i_p \xrightarrow[q'\cdot n'\mathbf{k}']{q\cdot n\mathbf{k}} f_p),$$

and $T^{[1,2]}_{\mathtt{i}\to\mathtt{f}}$ and $T^{[1,1,1]}_{\mathtt{i}\to\mathtt{f}}$ are given in Appendices 3.C.4 and 3.C.5, respectively. Here, $\mathbb{I}(i_p \xrightarrow{q\cdot n\mathbf{k}} f_p)$ (resp. $\mathbb{I}(i_p \xrightarrow[q'\cdot n'\mathbf{k}']{q\cdot n\mathbf{k}} f_p)$) is a large product of delta functions which enforce $N^f_{n''\mathbf{k}''} = N^i_{n''\mathbf{k}''}\ \forall n''\mathbf{k}'' \neq n\mathbf{k}$ (resp. $\forall n''\mathbf{k}'' \neq (n\mathbf{k}, n'\mathbf{k}')$), and $N^f_{n\mathbf{k}} = N^i_{n\mathbf{k}} + q$ (resp. $N^f_{n\mathbf{k}} = N^i_{n\mathbf{k}} + q, N^f_{n'\mathbf{k}'} = N^i_{n'\mathbf{k}'} + q'$). Note that the cases where $n\mathbf{k} = n'\mathbf{k}'$ require a formal correction. However, at any given order in the λ expansion, such terms are smaller than all others by a factor $1/N_{\rm uc}$, where $N_{\rm uc}$ is the number of unit cells, and therefore vanish in the thermodynamic limit. In what follows we thus use $\sum_{n\mathbf{k},n'\mathbf{k}'}$ and $\sum_{n\mathbf{k}\neq n'\mathbf{k}'}$ exchangeably, unless we specify otherwise.

The scattering rate as given by Eq. (3.8), involves the squares of the elements of the total transition matrix (see Appendices 3.C.4, 3.C.5 for computational details). Its full expression to perturbative order λ^4 is

$$\Gamma_{\mathtt{i}\to\mathtt{f}} = \Gamma^{\mathtt{SC}}_{\mathtt{i}\to\mathtt{f}} + \Gamma^{\mathtt{Q1}}_{\mathtt{i}\to\mathtt{f}} + \Gamma^{\mathtt{Q2}}_{\mathtt{i}\to\mathtt{f}}, \tag{3.22}$$

where

$$\begin{aligned}\left[\Gamma^{\mathtt{SC}}_{\mathtt{i}\to\mathtt{f}}\ ;\ \Gamma^{\mathtt{Q2}}_{\mathtt{i}\to\mathtt{f}}\ ;\ \Gamma^{\mathtt{Q1}}_{\mathtt{i}\to\mathtt{f}}\right] &= \frac{2\pi}{\hbar}\delta(E_{\mathtt{i}} - E_{\mathtt{f}}) \\ &\times \begin{bmatrix} |T^{[1]}_{\mathtt{i}\to\mathtt{f}}|^2 + |T^{[1,1]}_{\mathtt{i}\to\mathtt{f}}|^2 + |T^{[2]}_{\mathtt{i}\to\mathtt{f}}|^2 & ; \\ 2\mathfrak{Re}\left\{(T^{[1,1]}_{\mathtt{i}\to\mathtt{f}})^* T^{[2]}_{\mathtt{i}\to\mathtt{f}}\right\} & ; \\ 2\mathfrak{Re}\left\{(T^{[1,2]}_{\mathtt{i}\to\mathtt{f}})^* T^{[1]}_{\mathtt{i}\to\mathtt{f}} + (T^{[1,1,1]}_{\mathtt{i}\to\mathtt{f}})^* T^{[1]}_{\mathtt{i}\to\mathtt{f}}\right\} \end{bmatrix}.\end{aligned} \tag{3.23}$$

This decomposition into three terms is discussed in Sec. 3.3.4.3.

3.3.3.2 Collision matrix elements

Following Eq. (3.9), the scattering rates $\Gamma_{\mathtt{i}\to\mathtt{f}}$ give access to the collision integral, i.e. to $M_{n\mathbf{k},n'\mathbf{k}'}$ and $D_{n\mathbf{k}}$. We decompose the latter as $D_{n\mathbf{k}} = D^{(1)}_{n\mathbf{k}} + D^{(2)}_{n\mathbf{k}} + \breve{D}_{n\mathbf{k}}$, where $D^{(1)}$ and $D^{(2)}$ are obtained in our perturbative expansion at orders λ^2 and λ^4, respectively, and $\breve{D}_{n\mathbf{k}}$ encompasses contributions due to other scattering

processes as well as higher-order terms of the expansion. In the following, we also use the "$[l_i];[l'_j]$" superscripts to denote a term obtained from the product of $T^{[l_i]}_{\mathtt{i}\to\mathtt{f}}$ and $T^{[l'_j]}_{\mathtt{i}\to\mathtt{f}}$ within $|T_{\mathtt{i}\to\mathtt{f}}|^2$. For instance, at order λ^2, we have $D^{(1)}_{n\mathbf{k}} = D^{[1];[1]}_{n\mathbf{k}}$; details of the derivation are given in Appendix 3.C.2. At order λ^4, the diagonal and off-diagonal contributions to the collision integral take the forms

$$D^{(2)}_{n\mathbf{k}} = -\frac{1}{N_{\mathrm{uc}}} \sum_{n'\mathbf{k}'} \sum_{qq'} q \left(N^{\mathrm{eq}}_{n'\mathbf{k}'} + \tfrac{q'+1}{2}\right) \left[\mathfrak{W}^{qq'}_{n\mathbf{k}n'\mathbf{k}'}\right], \tag{3.24}$$

and

$$M_{n\mathbf{k}n'\mathbf{k}'} = \frac{1}{N_{\mathrm{uc}}} \sum_{q,q'=\pm} q \left(N^{\mathrm{eq}}_{n\mathbf{k}} + \tfrac{q+1}{2}\right) \left[\mathfrak{W}^{qq'}_{n\mathbf{k}n'\mathbf{k}'}\right], \tag{3.25}$$

respectively, where $\mathfrak{W}^{qq'}_{n\mathbf{k},n'\mathbf{k}'}$ is an off-diagonal scattering rate which involves two different phonon states $|n\mathbf{k}\rangle$ and $|n'\mathbf{k}'\rangle$. More precisely, $\mathfrak{W}^{+,+}$ (resp. $\mathfrak{W}^{-,-}$) corresponds to scattering processes where two phonons are emitted (resp. absorbed), and $\mathfrak{W}^{+,-}, \mathfrak{W}^{-,+}$ to processes where one phonon is emitted and one is absorbed. $D_{n\mathbf{k}}$ is the diagonal scattering rate, i.e. it is associated with variations in $\delta\overline{N}_{n\mathbf{k}}$ only.

We will now decompose the $\mathfrak{W}^{qq'}_{n\mathbf{k},n'\mathbf{k}'}$ scattering rates into

$$\mathfrak{W}^{qq'}_{n\mathbf{k},n'\mathbf{k}'} = \mathfrak{W}^{\oplus,qq'}_{n\mathbf{k}n'\mathbf{k}'} + \mathfrak{W}^{\ominus,qq'}_{n\mathbf{k}n'\mathbf{k}'}, \tag{3.26}$$

where $\mathfrak{W}^{\oplus/\ominus,qq'}_{n\mathbf{k},n'\mathbf{k}'}$ satisfy detailed ($\sigma = 1$) or "anti-detailed" ($\sigma = -1$) balance equations

$$\mathfrak{W}^{\sigma,qq'}_{n\mathbf{k}n'\mathbf{k}'} = \sigma\ e^{-\beta(q\omega_{n\mathbf{k}} + q'\omega_{n'\mathbf{k}'})}\ \mathfrak{W}^{\sigma,-q-q'}_{n\mathbf{k}n'\mathbf{k}'}, \quad \sigma = \pm \text{ or } \oplus, \ominus. \tag{3.27}$$

Physically, Eq. (3.27) expresses "microscopic" thermodynamic equilibrium between the process which takes $\{N_{n\mathbf{k}} \to N_{n\mathbf{k}} + q, N_{n'\mathbf{k}'} \to N_{n'\mathbf{k}'} + q'\}$ to the "conjugate" process taking $\{N_{n\mathbf{k}} \to N_{n\mathbf{k}} - q, N_{n'\mathbf{k}'} \to N_{n'\mathbf{k}'} - q'\}$, with $q, q' = \pm 1$, leaving $N_{n''\mathbf{k}''}$ unchanged for $n''\mathbf{k}'' \notin \{n\mathbf{k}, n'\mathbf{k}'\}$. Note that this is different from time-reversal symmetry which provides a relation between the processes acting on $\{|n_l, \mathbf{k}_l\rangle\}$ phonons to the *same* processes acting on the $\{|n_l, -\mathbf{k}_l\rangle\}$ phonons.

Moreover, since, by construction, the two-phonon scattering rates satisfy

$$\mathfrak{W}^{\sigma,qq'}_{n\mathbf{k}n'\mathbf{k}'} = \mathfrak{W}^{\sigma,q'q}_{n'\mathbf{k}'n\mathbf{k}}, \tag{3.28}$$

the following relations also hold:

$$\mathfrak{W}^{\sigma,+-}_{n'\mathbf{k}'n\mathbf{k}} = \sigma\, e^{\beta(\omega_{n\mathbf{k}} - \omega'_{n'\mathbf{k}})} \mathfrak{W}^{\sigma,+-}_{n\mathbf{k}n'\mathbf{k}'}. \tag{3.29}$$

Together, these imply that there are only four independent such scattering rates between the $|n, \mathbf{k}\rangle$ and $|n', \mathbf{k}'\rangle$ phonons, namely $\mathfrak{W}^{\sigma,++}_{n\mathbf{k},n'\mathbf{k}'}$ and $\mathfrak{W}^{\sigma,+-}_{n\mathbf{k},n'\mathbf{k}'}$ with $\sigma = \oplus, \ominus$.

As discussed at length, the first Born approximation alone does not lead to a nonzero thermal Hall effect, neither do those scattering rates which satisfy detailed balance as the latter imposes thermal equilibrium between "left" and

"right" scattering. We find the kernels $K^{L/H}$ defined in Eqs. (3.14,3.15) in terms of the $\mathfrak{W}$ scattering rates:

$$K^L_{n\mathbf{k}n'\mathbf{k}'} = \frac{e^{\beta\hbar\omega_{n\mathbf{k}}}}{D_{n\mathbf{k}}}\Bigg(\delta_{n,n'}\delta_{\mathbf{k},\mathbf{k}'} + \frac{e^{\beta\hbar\omega_{n'\mathbf{k}'}}}{2N_{\rm uc}D_{n'\mathbf{k}'}}\sum_{q=\pm} e^{\frac{q-1}{2}\beta\hbar\omega_{n'\mathbf{k}'}} \tag{3.30}$$
$$\times\left\{\mathfrak{W}^{\ominus,+,q}_{n\mathbf{k},n'\mathbf{k}'}\left(q\coth(\tfrac{\beta\hbar\omega_{n\mathbf{k}}}{2})+\coth(\tfrac{\beta\hbar\omega_{n'\mathbf{k}'}}{2})\right) - 2\,\mathfrak{W}^{\oplus,+,q}_{n\mathbf{k},n'\mathbf{k}'}\right\}\Bigg),$$

$$K^H_{n\mathbf{k}n'\mathbf{k}'} = \frac{e^{\beta\hbar\omega_{n\mathbf{k}}}e^{\beta\hbar\omega_{n'\mathbf{k}'}}}{2N_{\rm uc}D_{n\mathbf{k}}D_{n'\mathbf{k}'}}\sum_{q=\pm}\mathfrak{W}^{\ominus,+,q}_{n\mathbf{k},n'\mathbf{k}'} \tag{3.31}$$
$$\times e^{\frac{q-1}{2}\beta\hbar\omega_{n'\mathbf{k}'}}\left(\coth(\tfrac{\beta\hbar\omega_{n'\mathbf{k}'}}{2})-q\coth(\tfrac{\beta\hbar\omega_{n\mathbf{k}}}{2})\right).$$

Incorporating the expression for D in the denominators of $K^{L,H}$ provides an expansion up to $O(\lambda^4)$ of the latter. We recover, as mentioned before, that the terms in $\mathfrak{W}^{\oplus}$ do not contribute to K^H (they satisfy detailed-balance). The "anti-detailed-balance" relations satisfied by the $\mathfrak{W}^{\ominus}$ terms do not however prohibit their contribution to K^L. See Sec. 3.4.2 for a discussion. Inserting Eq. (3.31) into Eq. (3.13), and after some algebra, one obtains the result Eq. (3.5) for $\kappa_{\rm L,H}$.

3.3.4 The collision integral as correlation functions

3.3.4.1 Terms at $O(\lambda^2)$

The diagonal scattering rate $D^{(1)}_{n\mathbf{k}}$, obtained by inserting $T^{[1]}_{\mathtt{i}\to\mathtt{f}}$ into Eqs. (3.8-3.10), may now be cast into the form of a correlation function of Q operators. To do so, we first enforce the energy conservation $\delta(E_{\mathtt{f}}-E_{\mathtt{i}})$ by writing the latter as a time integral, i.e. use $\int_{-\infty}^{+\infty}\mathrm{d}t e^{i\omega t} = 2\pi\delta(\omega)$; we then identify $A(t) = e^{+iHt}Ae^{-iHt}$ and use the identity $1 = \sum_{f_s}|f_s\rangle\langle f_s|$. Taking the Qs in the initial state to be in thermal equilibrium $p_{i_s} = Z_s^{-1}e^{-\beta E_{i_s}}$, summing over $|i_s\rangle$, identifying $\langle A\rangle_\beta = Z^{-1}\mathrm{Tr}(e^{-\beta H}A)$, summing over final phononic states f_p and taking the average over initial phononic states i_p, we obtain

$$D^{(1)}_{n\mathbf{k}} = -\frac{1}{\hbar^2}\int dt e^{-i\omega_{n\mathbf{k}}t}\left\langle[Q_{n\mathbf{k}}(t),Q^\dagger_{n\mathbf{k}}(0)]\right\rangle_\beta. \tag{3.32}$$

We now apply the same method to higher orders of the perturbative expansion.

3.3.4.2 Terms at $O(\lambda^4)$

We use the following time integral representation for the denominators appearing at second and higher Born orders (using a regularized definition of the sign function, i.e. $\lim_{\eta\to0}\mathrm{sign}(t)e^{-\eta|t|}\to\mathrm{sign}(t)$),

$$\frac{1}{x\pm i\eta} = \mathrm{PP}\frac{1}{x}\mp i\pi\delta(x) \tag{3.33}$$
$$= \frac{1}{2i}\int_{-\infty}^{+\infty}\mathrm{d}t_1 e^{it_1x}\left(\mathrm{sign}(t_1)\pm1\right).$$

Using Eqs. (3.18) and Eq. (3.23), we find the explicit expressions for the semi-classical scattering rates as correlation functions of the Q operators,

$$\mathfrak{W}^{\oplus,[2];[2],qq'}_{n\mathbf{k}n'\mathbf{k}'} = \frac{2}{\hbar^4} \fint_t \left\langle Q^{-q,-q'}_{n\mathbf{k}n'\mathbf{k}'}(-t) Q^{q,q'}_{n\mathbf{k}n'\mathbf{k}'}(0) \right\rangle , \tag{3.34}$$

$$\mathfrak{W}^{\ominus,[1,1];[1,1],qq'}_{n\mathbf{k}n'\mathbf{k}'} = \frac{2}{\hbar^4} N_{\mathrm{uc}} \, \mathfrak{Re} \fint_{t,t_1,t_2} \Big\langle [\![Q^{-q}_{n\mathbf{k}}(-t-t_2), Q^{-q'}_{n'\mathbf{k}'}(-t+t_2)]\!] \times \{ Q^{q'}_{n'\mathbf{k}'}(-t_1), Q^{q}_{n\mathbf{k}}(t_1) \} \Big\rangle , \tag{3.35}$$

$$\mathfrak{W}^{\oplus,[1,1];[1,1],qq'}_{n\mathbf{k}n'\mathbf{k}'} = \frac{1}{\hbar^4} N_{\mathrm{uc}} \fint_{t,t_1,t_2} \langle \{\cdot,\cdot\}\{\cdot,\cdot\} - [\![\cdot,\cdot]\!][\![\cdot,\cdot]\!] \rangle , \tag{3.36}$$

where we use the shorthand notation

$$[\![A(t_a), B(t_b)]\!] = \mathrm{sign}(t_b - t_a)[A(t_a), B(t_b)], \tag{3.37}$$

and $\fint_{t,\{t_j\}}$, $j = 1,..,l$, denotes the set of $1+l$ Fourier transforms evaluated once at $\Sigma^{n'\mathbf{k}'q'}_{n\mathbf{k}q} = q\omega_{n\mathbf{k}} + q'\omega_{n'\mathbf{k}'}$ and l times at $\Delta^{n'\mathbf{k}'q'}_{n\mathbf{k}q} = q\omega_{n\mathbf{k}} - q'\omega_{n'\mathbf{k}'}$, i.e. $\fint_{t,\{t_j\}} = \int \mathrm{d}t \mathrm{d}t_1 .. \mathrm{d}t_l e^{i\Sigma^{n'\mathbf{k}'q'}_{n\mathbf{k}q} t} e^{i\Delta^{n'\mathbf{k}'q'}_{n\mathbf{k}q}(t_1+..+t_l)}$. The symbols $\cdot$ must be replaced by the same set of operators as the expression from the above. The commutators and anticommutators ultimately capture antisymmetrization and symmetrization over the $n\mathbf{k}q \leftrightarrow n'\mathbf{k}'q'$ indices. We provide expressions for $\mathfrak{W}^{\ominus,[1,1];[2],qq'}_{n\mathbf{k}n'\mathbf{k}'}$, $\mathfrak{W}^{\oplus,[1,1];[2],qq'}_{n\mathbf{k}n'\mathbf{k}'}$, $\mathfrak{W}^{[1,2];[1],qq'}_{n\mathbf{k}n'\mathbf{k}'}$ and $\mathfrak{W}^{[1,1,1];[1],qq'}_{n\mathbf{k}n'\mathbf{k}'}$ in Appendices 3.C.4.4,3.C.5.

3.3.4.3 Scattering channels and conserving approximation

The above terms capture all contributions to the collision integral arising from the Born expansion of the transition amplitude, up to perturbative order λ^4. This gives, correspondingly, physical processes in the collision integral which contribute up to $O(\lambda^4)$.

In Eq. (3.22), while $\Gamma^{\mathtt{SC}}_{\mathtt{i}\to\mathtt{f}}$ and $\Gamma^{\mathtt{Q2}}_{\mathtt{i}\to\mathtt{f}}$ are "two-phonon" terms, the contribution from $\Gamma^{\mathtt{Q1}}_{\mathtt{i}\to\mathtt{f}}$ is a "one-phonon" term, i.e. one where the initial $\mathtt{i}$ and final $\mathtt{f}$ states differ by only one phonon $|n\mathbf{k}\rangle$. Physically, this contributes to processes which create or annihilate a single phonon, in contrast with the $O(\lambda^4)$ processes described so far, which create/annihilate two phonons with different quantum numbers. Because the single phonon process is physically distinct from the two-phonon ones, we expect that it is independent from the latter in the sense that the set of all the $O(\lambda^4)$ single-phonon processes satisfies *independently* all physical constraints such as symmetries and conservation laws. Hence omitting these contributions is a "conserving approximation" in the traditional sense [Baym and Kadanoff, 1961], and we will proceed with this omission for the most part in the following. We however include formal expressions for these terms in the appendices.

The remaining contributions in Eq. (3.22) are "two-phonon" terms, i.e. terms in which the initial $\mathtt{i}$ and final $\mathtt{f}$ states differ by two phonons $|n\mathbf{k}\rangle, |n'\mathbf{k}'\rangle$. The

two-phonon, $O(\lambda^4)$, contributions to the $\mathfrak{W}$ scattering rates thus read

$$\mathfrak{W}^{\ominus,qq'}_{n\mathbf{k},n'\mathbf{k}'} = \mathfrak{W}^{\ominus,[1,1];[2],qq'}_{n\mathbf{k},n'\mathbf{k}'} + \mathfrak{W}^{\ominus,[1,1];[1,1],qq'}_{n\mathbf{k},n'\mathbf{k}'}, \tag{3.38}$$

$$\mathfrak{W}^{\oplus,qq'}_{n\mathbf{k},n'\mathbf{k}'} = \mathfrak{W}^{\oplus,[2];[2],qq'}_{n\mathbf{k},n'\mathbf{k}'} + \mathfrak{W}^{\oplus,[1,1];[2],qq'}_{n\mathbf{k},n'\mathbf{k}'} + \mathfrak{W}^{\oplus,[1,1];[1,1],qq'}_{n\mathbf{k},n'\mathbf{k}'}. \tag{3.39}$$

Another physical distinction between the contributions in Eq. (3.22) can be made according to the "quantum" or semiclassical, nature of the terms. The one-phonon $\Gamma^{\mathtt{Q1}}_{\mathtt{i}\to\mathtt{f}}$ and two-phonon $\Gamma^{\mathtt{Q2}}_{\mathtt{i}\to\mathtt{f}}$ terms in Eq. (3.22) are "quantum" in the sense that the physical process corresponding to each contribution therein is an interference term between *distinct* scattering channels. In particular, in a "quantum" term, the number of scattering events in the two channels are different. On the contrary, each contribution in $\Gamma^{\mathtt{SC}}_{\mathtt{i}\to\mathtt{f}}$ is the probability amplitude of one given scattering channel, corresponding physically to the probability amplitude of a given scattering process, and in this respect is truly semiclassical. As a semiclassical approximation, we will neglect "quantum" contributions in the following; formal expressions for these terms are nonetheless included in the appendices. The only "semiclassical" contributions, up to $O(\lambda^4)$, to the collision integral are from the scattering rates shown in Eq. (3.34).

Upon applying our results to the case of a staggered antiferromagnet in Sec. 3.5, we focus on the lowest-order contributions to $K^L_{n\mathbf{k},n'\mathbf{k}'}$ and $K^H_{n\mathbf{k},n'\mathbf{k}'}$, which come from $D^{(1)}_{n\mathbf{k}}$ and $\mathfrak{W}^{\ominus,qq'}_{n\mathbf{k},n'\mathbf{k}'}$, respectively. Therefore, in Sec. 3.5, we consider only the lowest-order semiclassical contributions $D_{n\mathbf{k}} \approx D^{(1)}_{n\mathbf{k}} + \breve{D}_{n\mathbf{k}}$ and $\mathfrak{W}^{\ominus,qq'}_{n\mathbf{k},n'\mathbf{k}'} \approx \mathfrak{W}^{\ominus,[1,1];[1,1],qq'}_{n\mathbf{k},n'\mathbf{k}'}$.

3.3.4.4 Physical interpretation

To leading order, the longitudinal conductivity is controlled by the diagonal scattering rate, whose main contribution occurs at order λ^2. The latter is given as the first term in Eq. (3.2), and is shown again in Eq. (3.32). It is related to the Fourier transform of the commutator of two $Q_{n\mathbf{k}}$ operators at unequal times. The commutator structure identifies the phonon scattering rate $D^{(1)}_{n\mathbf{k}}$ with the spectral function of the $Q_{n\mathbf{k}}$ field at energy $\omega_{n\mathbf{k}}$, i.e. it captures the proportion of the energy density contained in the $Q_{n\mathbf{k}}$ field located at $\omega_{n\mathbf{k}}$, as expected from (lowest-order) linear response [Bruus and Flensberg, 2004, Gangadharaiah et al., 2010].

As mentioned above, the first Born order transition matrices are hermitian. At second Born's order, the advanced/retarded Green's function, $1/(E_{\mathtt{i}/\mathtt{f}} - E_{\mathtt{m}} \pm i\eta)$, appearing in $T_{\mathtt{i}\mapsto\mathtt{f}}$, splits into on-shell and off-shell contributions, so that the scattering rate $\propto |T_{\mathtt{i}\mapsto\mathtt{f}}|^2$ then involves the product of two on-shell or two-offshell contributions, as well as the products of one on-shell and one off-shell one. Because of complex conjugation of one term upon taking the square modulus of the T matrix, the scattering rates which involve either two on-shell or two off-shell contributions are blind to the sign of $\pm i\eta$, i.e. to the advanced or retarded nature of the process, and enforce a detailed-balance relation, Eq. (3.27) with $\sigma = \oplus$. Therefore, the only scattering rates which can contribute to the Hall conductivity are those involving one on-shell (imaginary part) and one off-shell (real part)

scattering event, which translates here into the product of a commutator and an anticommutator, Eq. (3.35).

3.4 Relations and symmetries

In this section, we explore in more detail some physical relations verified by the scattering rates defined above, and their possible consequences on the longitudinal and Hall conductivities.

3.4.1 Time-reversal symmetry: reversal of the momenta

Q operators	$\widehat{Q^q_{n\mathbf{k}}} = Q^q_{n,-\mathbf{k}}$
	$\widehat{Q^{qq'}_{n\mathbf{k},n'\mathbf{k}'}} = Q^{qq'}_{n-\mathbf{k},n'-\mathbf{k}'}$
scattering rates	$D^{(1)}_{n,\mathbf{k}} = D^{(1)}_{n,-\mathbf{k}}$
	$\mathfrak{W}^{\sigma,qq'}_{n\mathbf{k},n'\mathbf{k}'} = \sigma\,\mathfrak{W}^{\sigma,qq'}_{n-\mathbf{k},n'-\mathbf{k}'}$
conjugate process	$\frac{\mathfrak{W}^\sigma(\mathrm{mr}[S])}{\mathfrak{W}^\sigma(S)} = e^{-\delta E^{(S)}_{s\to p}}\frac{\mathfrak{W}^\sigma(\mathrm{pc}[S])}{\mathfrak{W}^\sigma(S)} = \sigma$
kernels	$K^H_{n\mathbf{k},n'\mathbf{k}'} = -K^H_{n-\mathbf{k},n'-\mathbf{k}'}$
conductivities	$\boldsymbol{\kappa}_H = \mathbf{0}$

Table 3.4.1: Relations which hold true in the presence of time-reversal *symmetry*. The phonon operator relation $\widehat{a^q_{n\mathbf{k}}} = a^q_{n,-\mathbf{k}}$ holds true even when no time-reversal symmetry is present. See text for definitions and justifications.

We investigate the implications of time-reversal (TR) invariance on our results. In particular, we check explicitly that the Hall conductivity vanishes in a TR-symmetric system. It is important to note that, in a time-reversal invariant system, the scattering rates are a priori not time-reversal invariant themselves.

We denote with $\widehat{Q}$ and $|\widehat{\mathtt{n}}\rangle$ the time-reversed of operator Q and of state $|\mathtt{n}\rangle$, respectively. Then, because of the antiunitarity of the time-reversal operator, for any states $\mathtt{n},\mathtt{m}$ and any operator Q, we have $\langle\widehat{\mathtt{n}}|Q^\dagger|\widehat{\mathtt{m}}\rangle = \langle\mathtt{m}|\widehat{Q}|\mathtt{n}\rangle$. Moreover, it is possible to choose a polarization index n invariant under TR, whence $\widehat{a^q_{n\mathbf{k}}} = a^q_{n,-\mathbf{k}}$.

Let us now consider what happens in a time-reversal-invariant system. In that case, the hamiltonian $H'_{[1]} = \sum_{n\mathbf{k}q} Q^q_{n\mathbf{k}} a^q_{n\mathbf{k}}$ must be TR-invariant, so that $\widehat{Q^q_{n\mathbf{k}}} = Q^q_{n,-\mathbf{k}}$. Similarly, TR-invariance of $H'_{[2]}$ (defined in Eq. (3.16)) entails $\widehat{Q^{qq'}_{n\mathbf{k},n'\mathbf{k}'}} = Q^{qq'}_{n-\mathbf{k},n'-\mathbf{k}'}$.

3.4.1.1 Consequences for the scattering rates.

Following the same steps as those sketched in Sec. 3.3.4.1, and using the fact that $E_{\widehat{\mathtt{m}}} = E_{\mathtt{m}}$ for any state $\mathtt{m}$ of a TR-symmetric system, we can show explicitly that,

in a time-reversal-invariant system, the following relations for the scattering rates exist:

$$D^{(1)}_{n,\mathbf{k}} = D^{(1)}_{n,-\mathbf{k}} \tag{3.40}$$

$$\mathfrak{W}^{\sigma,qq'}_{n\mathbf{k},n'\mathbf{k}'} = \sigma\,\mathfrak{W}^{\sigma,qq'}_{n-\mathbf{k},n'-\mathbf{k}'}. \tag{3.41}$$

The σ sign in the second relation can be understood as arising from two facts: *(1)* schematically, $\mathfrak{W}^{\sigma} \sim \frac{1}{E_{\mathtt{f}}-E_{\mathtt{m}}+i\eta}\frac{1}{E_{\mathtt{i}}-E_{\mathtt{m}}-i\eta} + \sigma\,\mathrm{h.c.}$ —which is reflected in the fact that $\mathfrak{W}^{\oplus}$ (resp. $\mathfrak{W}^{\ominus}$) expressed as an integral, Eqs. (3.34–3.36), contains an even (resp. odd) number of sign functions— and *(2)* an effect of time-reversal on the T-matrix is to exchange denominators $\frac{1}{E_{\mathtt{f}}-E_{\mathtt{m}}+i\eta} \to \frac{1}{E_{\widehat{\mathtt{f}}}-E_{\widehat{\mathtt{m}}}-i\eta}$ (see Sec. 3.3.4.4 for an interpretation of the $+i\eta$ regularization).

3.4.1.2 Relation to detailed balance.

The decomposition of the scattering rate $\mathfrak{W}^{qq'}_{n\mathbf{k},n'\mathbf{k}'} = \sum_{\sigma}\mathfrak{W}^{\sigma,qq'}_{n\mathbf{k},n'\mathbf{k}'}$ into odd and even terms under the "conjugation" (in the sense of detailed balance, i.e. thermodynamic equilibrium) of the associated scattering processes, is also that of its decomposition into terms, odd and even under the inversion of momentum, in the presence of time-reversal symmetry. Indeed, if a scattering process $S = \left(\begin{smallmatrix} q\cdot n\mathbf{k} \\ \longrightarrow \\ q'\cdot n'\mathbf{k}' \end{smallmatrix}\right)$ transfers an energy $\delta E^{(S)}_{s\to p} = q\omega_{n\mathbf{k}} + q'\omega_{n'\mathbf{k}'}$ to the phonon system, (anti-)detailed balance with the "conjugate process" $\mathrm{pc}[S] = \left(\begin{smallmatrix} -q\cdot n\mathbf{k} \\ \longrightarrow \\ -q'\cdot n'\mathbf{k}' \end{smallmatrix}\right)$ reads $\mathfrak{W}^{\sigma}(\mathrm{pc}[S]) = \sigma e^{\delta E^{(S)}_{s\to p}}\mathfrak{W}^{\sigma}(S)$. Meanwhile, in the presence of time-reversal symmetry, the momentum-reversal symmetry reads $\mathfrak{W}^{\sigma}(\mathrm{mr}[S]) = \sigma\mathfrak{W}^{\sigma}(S)$, for the "momentum-reversed" process $\mathrm{mr}[S] = \left(\begin{smallmatrix} q\cdot n-\mathbf{k} \\ \longrightarrow \\ q'\cdot n'-\mathbf{k}' \end{smallmatrix}\right)$. In other words, in a time-reversal invariant system, the scattering rate associated with the process "conjugate" of a given process S coincides (up to a Boltzmann weight) with that of its momentum-reversed one:

$$\frac{\mathfrak{W}^{\sigma}(\mathrm{mr}[S])}{\mathfrak{W}^{\sigma}(S)} = e^{-\delta E^{(S)}_{s\to p}}\frac{\mathfrak{W}^{\sigma}(\mathrm{pc}[S])}{\mathfrak{W}^{\sigma}(S)} = \sigma. \tag{3.42}$$

Hence, while σ was defined as signature of the behavior of the scattering rates under "process conjugation," it is *also* that of momentum reversal in a time-reversal invariant system. [1]

3.4.1.3 Consequences for the kernels.

How is this reflected in the kernels K^L, K^H? Because the relation $\boldsymbol{v}_{n\mathbf{k}} = \boldsymbol{\nabla}_{\mathbf{k}}\omega_{n\mathbf{k}} = -\boldsymbol{v}_{n,-\mathbf{k}}$ holds, only that component of $K^{L/H}$ which is even upon reversal of the momenta, $\mathbf{k}^{(\prime)} \leftrightarrow -\mathbf{k}^{(\prime)}$, has a non-vanishing contribution to the sum Eq. (3.13). A first consequence of this is that, in a TR-invariant system, the identity

$$K^H_{n\mathbf{k},n'\mathbf{k}'} = -K^H_{n-\mathbf{k},n'-\mathbf{k}'} \tag{3.43}$$

[1] Notice, however, that this coincidence does not survive the breaking of time reversal symmetry.

entails $\boldsymbol{\kappa}_H = \mathbf{0}$ – as per Onsager's reciprocity relations stating that $\boldsymbol{\kappa}_H$ is TR-odd. Note that K^L in Eq. (3.30) involves both $\mathfrak{W}^{\ominus}$ and $\mathfrak{W}^{\oplus}$. Therefore, there is no analog to Eq. (3.43) for K^L. However, in a TR-invariant system, the $\mathfrak{W}^{\ominus}$ term in K^L does not contribute to κ_L – this is consistent with the Onsager-Casimir relations which state that κ_L is TR-even.

This indeed reflects the previous discussion as follows: when time reversal is preserved, TR-even κ_L gets contributions solely from "detailed-balance-even" and TR-even $\mathfrak{W}^{\oplus}$. On the other hand TR-odd $\boldsymbol{\kappa}_H$ gets contributions solely from "detailed-balance-odd" and TR-odd $\mathfrak{W}^{\ominus}$. Since the system is actually TR-even, $\boldsymbol{\kappa}_H$ vanishes.

3.4.2 Point-group symmetries

Here we provide some sufficient (but non-necessary) conditions on $K^H_{n\mathbf{k}n'\mathbf{k}'}$ under which the Hall conductivity vanishes.

3.4.2.1 Curie relations

From Fourier's law $j^\mu = -\kappa^{\mu\nu}\nabla_\nu T$, the Curie and Onsager relations provide general constraints on the $\kappa^{\mu\nu}$ coefficients, and in turn on its Hall component $\kappa_H^{\mu\nu}$. In Table 3.4.2, we look at the $D_{4h} = D_4 \times \mathbb{Z}_2$ point group—the largest tetragonal point group— with the associated axes aligned with the orthogonal basis (μ, ν, ρ) ($\mu\nu$ is the basal plane and ρ the transverse direction). We can see that if the system is invariant under any one of the transformations $g \in D_{4h}$ which are odd under the A_{2g} representation (i.e. C_2', C_2'', σ_v, σ_d), the Hall conductivity must vanish.

3.4.2.2 Symmetry relations on K^H

We now turn to relations specific to the scattering situation, i.e. we analyze under which conditions on $K^H_{n\mathbf{k}n'\mathbf{k}'}$ it befalls that $\kappa_H^{\mu\nu} = 0$. We start with the expression of $\kappa_H^{\mu\nu}$ as a momentum integral, Eq. (3.13), i.e. $\kappa_H^{\mu\nu} \propto \sum_{n\mathbf{k}n'\mathbf{k}'} J^\mu_{n\mathbf{k}} J^\nu_{n'\mathbf{k}'} K^H_{n\mathbf{k}n'\mathbf{k}'}$ and recall $J^\mu_{n\mathbf{k}} = N^{\mathrm{eq}}_{n\mathbf{k}} \omega_{n\mathbf{k}} \partial_{k^\mu} \omega_{n\mathbf{k}}$.

If the *phonon* system is invariant under a unitary transformation g, then $\omega_{n\mathbf{k}}$ is also invariant under this transformation. In turn only μ in $J^\mu_{n\mathbf{k}}$ transforms nontrivially under g. Therefore:

- *If* the phonon system is invariant under an operation $g \in D_{4h}$ which leaves the μ, ν axes invariant, i.e. $g = C_2, C_2', \mathrm{inv}, \sigma_h, \sigma_v$, and *if* one of the two following conditions, *(a)* under g the $\mu\nu$ product is even (i.e. $g = C_2, \mathrm{inv}, \sigma_h$) and $K^H_{n\mathbf{k}n'\mathbf{k}'}$ is odd, *(b)* under g the $\mu\nu$ product is odd (i.e. $g = C_2', \sigma_v$) and $K^H_{n\mathbf{k}n'\mathbf{k}'}$ is even, is satisfied, *then* it follows that $\kappa^{\mu\nu}_{\mathrm{H}} = 0$.
- Besides, recalling that by construction $K^H_{n\mathbf{k}n'\mathbf{k}'} = -K^H_{n'\mathbf{k}'n\mathbf{k}}$, *if* the system is invariant under an operation $g \in D_{4h}$ which exchanges the μ, ν axes, i.e. $g = C_4, C_2'', S_4, \sigma_d$, and *if* one of the two following conditions, *(c)* under g the $\mu\nu$ product is even (i.e. $g = C_2'', \sigma_d$) and $K^H_{n\mathbf{k}n'\mathbf{k}'}$ is even, *(d)* under g

D_{4h}	Id	C_4	C_2	C_2'	C_2''	inv	S_4	σ_h	σ_v	σ_d
A_{2g}	1	1	1	-1	-1	1	1	1	-1	-1
μ	μ	ν	$-\mu$	$\pm\mu$	$\pm\nu$	$-\mu$	ν	μ	$\pm\mu$	$\pm\nu$
ν	ν	$-\mu$	$-\nu$	$\mp\nu$	$\pm\mu$	$-\nu$	$-\mu$	ν	$\mp\nu$	$\pm\mu$
ρ	ρ	ρ	ρ	$-\rho$	$-\rho$	$-\rho$	$-\rho$	$-\rho$	ρ	ρ
$\kappa^{\mu\nu}$	$\kappa^{\mu\nu}$	$-\kappa^{\nu\mu}$	$\kappa^{\mu\nu}$	$-\kappa^{\mu\nu}$	$\kappa^{\nu\mu}$	$\kappa^{\mu\nu}$	$-\kappa^{\nu\mu}$	$\kappa^{\mu\nu}$	$-\kappa^{\mu\nu}$	$\kappa^{\nu\mu}$
$\kappa_H^{\mu\nu}$	$\kappa_H^{\mu\nu}$	$\kappa_H^{\mu\nu}$	$\kappa_H^{\mu\nu}$	$-\kappa_H^{\mu\nu}$	$-\kappa_H^{\mu\nu}$	$\kappa_H^{\mu\nu}$	$\kappa_H^{\mu\nu}$	$\kappa_H^{\mu\nu}$	$-\kappa_H^{\mu\nu}$	$-\kappa_H^{\mu\nu}$
cat	*(a)*	*(d)*	*(a)*	*(b)*	*(c)*	*(a)*	*(d)*	*(a)*	*(b)*	*(c)*

Table 3.4.2: Elements of the D_{4h} point group aligned along the (μ, ν, ρ) basis (with $\mu\nu$ the basal plane), their characters in the A_{2g} irrep (also labeled Γ_2^+), and transformations of $\mu, \nu, \rho, \kappa^{\mu\nu}, \kappa_H^{\mu\nu}$. The lines for $\kappa^{\mu\nu}$ and $\kappa_H^{\mu\nu}$ hold true when the system is invariant under the corresponding D_{4h} operation (aligned with the $\mu\nu\rho$ basis). The last line is the "category" (cat) to which the operation belongs, as defined in Sec. 3.4.2.2. Here Id is the identity; C_4 is the $\pi/2$ rotation around the ρ axis; C_2, C_2' and C_2'' are π rotations around the ρ axis, μ or ν axes, and in-plane directions bisecting the μ, ν axes, respectively; inv is inversion, S_4 are $\pi/2$ rotations around the ρ axis followed by a reflection through the basal $\mu\nu$ plane; σ_h, σ_v and σ_d are reflections through the $\mu\nu$ plane, through a plane containing μ or ν and the ρ direction, and through a plane containing the ρ direction and one bissecting the μ, ν directions, respectively.

the $\mu\nu$ product is odd (i.e. $g = C_4, S_4$) and $K^H_{n\mathbf{k}n'\mathbf{k}'}$ is odd, is satisfied, *then* it follows that $\kappa^{\mu\nu}_{\mathrm{H}} = 0$.

In terms of the behavior of $K^H_{n\mathbf{k}n'\mathbf{k}'}$, this analysis reduces to: *if* $g \in D_{4h}$ is a symmetry of the phonon system, and *if* $g : K^H_{n\mathbf{k}n'\mathbf{k}'} \mapsto -\chi_{A_{2g}}(g) K^H_{n\mathbf{k}n'\mathbf{k}'}$, where $\chi_{A_{2g}}(g)$ is the character of g in the A_{2g} representation of the D_{4h} point group, *then* $\kappa^{\mu\nu}_H = 0$. We emphasize that this analysis holds *if* the transformation g is a symmetry of the phonon system, and whether or not g is a symmetry of the whole system. For example, we will show explicitly in Sec. 3.5.3.4 that there are cases where, under TR or σ_d the system is not invariant, but the kernel $K^H_{n\mathbf{k},n'\mathbf{k}'}$ and the phonon system are, and so $\kappa_H = 0$.

Finally, note that the above analysis goes beyond the general predictions from Onsager, which tell us *that* κ_H vanishes in the presence of some symmetries of the *whole* system, namely C_2', C_2'', σ_v or σ_d (as well as time-reversal discussed in the previous subsection). Here, not only do we establish relations for the other symmetries in D_{4h} (as symmetries of the *phonon subsystem only*), we also show *in which way* κ_H vanishes, by inspecting the behavior of the kernels $K^H_{n\mathbf{k},n'\mathbf{k}'}$ under those symmetry transformations. In turn, this may for example allow to gather information about the *system*— about $K^H_{n\mathbf{k},n'\mathbf{k}'}$—from the (non-)cancellation of κ_H.

3.5 Application to an ordered magnet

We now turn to an application of these general results. There, we keep only the lowest-order terms in the expressions derived above, as described in Sec. 3.3.4.4. We consider an

ordered magnetic system, which we take to be a spin-orbit coupled Néel antiferromagnet with tetragonal symmetry. For concreteness, we treat the magnetism as purely two-dimensional, i.e. the full spin+phonon system is described by a stack of two dimensional antiferromagnets embedded into the three-dimension solid, so that in particular, we take, when going from the lattice to the continuum limit

$$\sum_{\mathbf{r}} \to \frac{1}{\mathfrak{a}^2} \sum_z \int d^2x, \quad \sum_{\mathbf{k}} \to \frac{\mathfrak{a}^2}{(2\pi)^2} \sum_{k_z} \int d^2k, \tag{3.44}$$

where $\mathfrak{a}$ is the in-plane lattice spacing.

3.5.1 Magnon dynamics

3.5.1.1 Low-energy field-theoretical description

We consider a Néel antiferromagnet with a two-site magnetic unit cell, more precisely a bipartite lattice of spins such that the classical ground state is ordered in an antiferromagnetic configuration, with a local moment μ_0 oriented in the direction $\mathbf{n}$, i.e. $\mathbf{n}$ is the Néel vector which has unit length in the ordered state at zero field. Within standard spin-wave theory, $\mu_0 = S$ with S the spin value. For concreteness, we will choose the ordering axis at zero field to be aligned along

the $\hat{\mathbf{u}}_x$ axis (the set $(\hat{\mathbf{u}}_x, \hat{\mathbf{u}}_y, \hat{\mathbf{u}}_z)$ is an orthonormal cartesian basis)—the results of this subsection hold regardless of this choice.

A general low energy spin configuration is described by two continuum fields: the aforementioned Néel vector $\mathbf{n}(\mathbf{r})$ *and* a uniform magnetization *density* $\mathbf{m}(\mathbf{r})$, such that

$$\mathbf{S}_\mathbf{r} = (-1)^\mathbf{r} \mu_0 \mathbf{n}(\mathbf{r}) + \mathfrak{a}^2 \mathbf{m}(\mathbf{r}). \tag{3.45}$$

where $(-1)^\mathbf{r}$ is a sign which alternates between neighboring sites (recall we are considering a Néel antiferromagnet), and both continuum fields are assumed to be slowly-varying relative to the lattice spacing. Here $\mathfrak{a}$ is the 2d lattice spacing. We will assume the non-linear sigma model constraint that the spin length is fixed to μ_0, which implies that

$$|\mathbf{n}|^2 + \frac{\mathfrak{a}^4}{\mu_0^2} |\mathbf{m}|^2 = 1, \qquad \mathbf{m} \cdot \mathbf{n} = 0. \tag{3.46}$$

The spin wave expansion consists of expanding these fields around the zero field ordered state, i.e. $\mathbf{n}_\text{ord} = \hat{\mathbf{u}}_x, \mathbf{m}_\text{ord} = \mathbf{0}$. To linear order around this state, we take $\mathbf{n} = \hat{\mathbf{u}}_x + \boldsymbol{n}$ and $\mathbf{m} = \boldsymbol{m}$, where $n_x = m_x = 0$, leaving the remaining degrees of freedom n_y, n_z, m_y, m_z. In terms of the spins, this gives

$$\mathbf{S}_\mathbf{r} = (-1)^\mathbf{r} \mu_0 \hat{\mathbf{u}}_x + \sum_{a=y,z} ((-1)^\mathbf{r} \mu_0 n_a(\mathbf{r}) + \mathfrak{a}^2 m_a(\mathbf{r})) \hat{\mathbf{u}}_a. \tag{3.47}$$

Because the local moment along the $\hat{\mathbf{u}}_x$ axis is non-zero, the low energy fields satisfy the commutation relations $[m_y(\mathbf{r}), n_z(\mathbf{r}')] = -[m_z(\mathbf{r}), n_y(\mathbf{r}')] = -i\delta(\mathbf{r} - \mathbf{r}')$. The low energy continuum Hamiltonian density for these fields is

$$\begin{aligned} \mathcal{H}_\text{NLS} &= \frac{\rho}{2} \left(|\underline{\boldsymbol{\nabla}} n_y|^2 + |\underline{\boldsymbol{\nabla}} n_z|^2 \right) \\ &\quad + \frac{1}{2\chi} (m_y^2 + m_z^2) + \sum_{a,b=y,z} \frac{\Gamma_{ab}}{2} n_a n_b, \end{aligned} \tag{3.48}$$

where ρ is the spin stiffness constant, χ is the spin susceptibility, $\underline{\boldsymbol{\nabla}} = (\partial_x, \partial_y)$ denotes the in-plane gradient, and the Γ_{ab} are anisotropy coefficients which open a small spin wave gap (see App. 3.F.3). For an approximately Heisenberg system with isotropic exchange constant J, we have within spin wave theory that $\chi^{-1} \approx 4J\mathfrak{a}^2$, $\rho \approx 2J\mu_0^2$, while Γ_{ab} are determined by exchange anisotropies. The choice to normalize $\boldsymbol{m}$ as a density while keeping $\boldsymbol{n}$ dimensionless ensures that $m_{y,z}$ fields are just the canonical momenta conjugate to the $n_{z,y}$ fields, and hence Eq. (3.48) is just a Hamiltonian density of two free scalar boson fields.

The above description is appropriate to describe the ordered phase of the antiferromagnet, for any value of the spin, provided temperature is low compared to the Néel temperature and any applied magnetic fields are small compared to the saturation field. These conditions are well-satisfied in practice in experiments on many antiferromagnets. Specifically we will be interested in the case with an applied magnetic field perpendicular to the axis of the Néel vector (e.g. along z or y, given the choice in Eq. (3.47)). In general the field induces a non-zero uniform magnetization along its direction, e.g. for a z-axis field $\langle m_z \rangle \neq 0$. Such a "spin flop" configuration is favorable for an antiferromagnet in a field.

3.5.1.2 Symmetry considerations

Two symmetries clarify the calculations and provide physical insight. The first is the macroscopic time-reversal symmetry of the zero field state, which is what makes it an *anti*-ferromagnet. Specifically, the system in zero field is invariant under the combination of time-reversal symmetry TR and a translation T. Under this operation, we see that the continuum fields transform according to

$$\mathcal{T} = \mathrm{TR} \times T : \quad m \to -m, \quad n \to n. \tag{3.49}$$

The presence of a staggered magnetization (with any orientation) does not break this symmetry, but a uniform magnetization does. Note that the *effective* quadratic low energy Hamiltonian, Eq. (3.48), is invariant under this symmetry. This is true even at non-zero fields, because the low energy Hamiltonian is quadratic. Thus effects of time-reversal symmetry breaking will become evident in terms beyond this form, notably in anharmonic corrections, and in the spin-lattice coupling itself. Specifically, we see that time-reversal symmetry will be effectively broken only by terms involving an odd number of powers of the m_a fields.

The second important symmetry is one which may be preserved not only by the underlying exchange Hamiltonian and crystal structure, but *also* by the applied field and the spontaneous ordered moments. In particular, the latter breaks the original translational symmetry of the square lattice by a single lattice spacing. However, a symmetry may be retained under such a simultaneous translation composed with a C_2 spin rotation around the field axis. In the presence of spin-orbit coupling, generically the spin rotation must be accompanied by a spatial rotation, and the full combined operation is in fact nothing but a C_2 rotation about an axis passing through the mid-point of a bond of the square lattice. This of course requires the C_2 rotation in question to be part of the lattice point group. In our problem, this is true when the field is along z or y (but not for a general orientation in the yz plane).

This odd symmetry is important for simplifying the magnon interactions. In particular, if the field axis is along z, then we see that m_z and n_y are both even under this operation, while m_y and n_z are odd under it (and vice versa if the field is along y). Note that the fields within a canonically conjugate pair transform the same way under this symmetry. We take advantage of these facts in the following. In particular, only $\Gamma_0 = \Gamma_{yy}$ and $\Gamma_1 = \Gamma_{zz}$ do not vanish a priori, which ensures that the two valleys ($\ell = 0, 1$) are exactly decoupled.

3.5.1.3 External magnetic field

At the lowest order, an applied external magnetic field $\mathbf{h}$ couples solely to the $\boldsymbol{m}$ field; this is already taken into account in Eq. (3.48) where the $\boldsymbol{m}$ fields can acquire a (static) nonzero expectation value due to the spin alignment with the field.

Meanwhile, at higher orders the magnetic field also couples to the $\boldsymbol{n}$ field; the main contribution comes from the square, isotropic coupling $(\boldsymbol{n} \cdot \mathbf{h})^2$. Due to the C_2 symmetry around the field axis (y or z), and since first-order terms of the

form $h_a n_b$ are forbidden by translational symmetry, this results in an additional term

$$\mathcal{H}_{\text{field}} = \frac{\chi}{2} \sum_{a=y,z} h_a^2 n_a^2. \tag{3.50}$$

Note this form is valid only when the field is along the y or z axis, not at other angles in the $y-z$ plane (which would violate the C_2 symmetry). The prefactor $\chi/2$ is fixed to match the results obtained from microscopic calculations in Ref. [Benfatto and Silva Neto, 2006], and we provide an alternative derivation in App. 3.F.3 as well as a more detailed derivation of the full form of the gap from a microscopic XXZ exchange model plus a Zeeman coupling to the field in App. 3.F.3.

3.5.1.4 Diagonalization

We proceed to diagonalize Eq. (3.48), supplemented by Eq. (3.50) following the discussion in Sec. 3.5.1.3, by introducing creation and annihilation operators in the standard way for free fields. We use the Fourier convention $\phi_{\mathbf{k}} = \frac{1}{\sqrt{V}} \int d\mathbf{x} \phi(\mathbf{x}) e^{-i\mathbf{k}\cdot\mathbf{x}}$ for any continuum field ϕ, where V is the volume of the system. Then

$$m_{\mathbf{k}}^y = \sqrt{\frac{\chi\Omega_{\mathbf{k},0}}{2}} \left(b_{-\mathbf{k},0} + b_{\mathbf{k},0}^\dagger \right), \tag{3.51}$$

$$n_{\mathbf{k}}^z = i \frac{1}{\sqrt{2\chi\Omega_{\mathbf{k},0}}} \left(b_{-\mathbf{k},0} - b_{\mathbf{k},0}^\dagger \right), \tag{3.52}$$

$$m_{\mathbf{k}}^z = \sqrt{\frac{\chi\Omega_{\mathbf{k},1}}{2}} \left(b_{-\mathbf{k},1} + b_{\mathbf{k},1}^\dagger \right), \tag{3.53}$$

$$n_{\mathbf{k}}^y = -i \frac{1}{\sqrt{2\chi\Omega_{\mathbf{k},1}}} \left(b_{-\mathbf{k},1} - b_{\mathbf{k},1}^\dagger \right), \tag{3.54}$$

where

$$\Omega_{\mathbf{k},\ell} = \sqrt{v_{\text{m}}^2 \underline{\mathbf{k}}^2 + \Delta_\ell^2}, \tag{3.55}$$

with $v_{\text{m}} = \sqrt{\rho/\chi}$. The magnon gaps depend on the applied (transverse) magnetic field in the form

$$\Delta_\ell = \sqrt{\Gamma_\ell/\chi + h_\ell^2}, \tag{3.56}$$

with valley index $\ell = 0, 1$ and where we set $h_0 = h_y$ and $h_1 = h_z$. This reflects the explicit breaking of $O(3)$ rotational symmetry of the order parameter $\boldsymbol{n}$ by the transverse field. With these definitions, we obtain

$$H_{\text{NLS}} + H_{\text{field}} = \sum_\ell \sum_{\mathbf{k}} \Omega_{\mathbf{k},\ell} b_{\mathbf{k},\ell}^\dagger b_{\mathbf{k},\ell}. \tag{3.57}$$

The $b, b^\dagger$ fields with index $\ell = 0$ have opposite C_2 eigenvalue to those with $\ell = 1$. This guarantees that all terms preserving C_2 symmetry must conserve the two boson flavors modulo 2.

3.5.2 Formal couplings

3.5.2.1 Definitions

In general we can expand the operator $Q_{n\mathbf{k}}$, which couples to a single phonon, in powers of the magnon operators,

$$Q^q_{n\mathbf{k}} = \sum_{\ell,q_1,z} \mathcal{A}^{n,\ell|q_1 q}_{\mathbf{k}}\, e^{ik_z z} b^{q_1}_{\ell,\mathbf{k},z} \tag{3.58}$$

$$+ \frac{1}{\sqrt{N_{\mathrm{uc}}}} \sum_{\substack{\mathbf{p},\ell,\ell' \\ q_1,q_2,z}} \mathcal{B}^{n,\ell_1,\ell_2|q_1 q_2 q}_{\mathbf{k};\mathbf{p}}\; e^{ik_z z} b^{q_1}_{\ell_1,\mathbf{p}+\frac{q}{2}\mathbf{k},z} b^{q_2}_{\ell_2,-\mathbf{p}+\frac{q}{2}\mathbf{k},z}. \tag{3.59}$$

Note that while the phonons are three-dimensional excitations, and hence have a three-dimensional momentum $\mathbf{k}$, the spin operators (and hence magnons) only have two dimensional momenta. We will make use of the following: $\mathbf{k} = \underline{\mathbf{k}} + k_z \hat{\mathbf{u}}_z$, where $\underline{\mathbf{k}}$ is the projection of $\mathbf{k}$ onto the $k_z = 0$ plane and $\hat{\mathbf{u}}_z$ is the unit vector along z. A phonon is coupled to the sum of spin operators in all layers—we have here introduced the explicit label z for the layer. Because the spins in different layers are completely uncorrelated, there are however no cross-terms involving b operators from different layers, and in correlation functions the sums over z will collapse to independent correlators within each layer, which are all identical to one another. When possible, we will therefore take $z = 0$ and suppress this index.

The naïve leading term in Eq. (3.58) is the single magnon one $\mathcal{A}$, linear in $b_{\ell,\mathbf{k}}$ and $b^\dagger_{\ell,\mathbf{k}}$ operators (notations defined below). This results in a quadratic mixing term in the Hamiltonian, hybridizing phonons and magnons. Being quadratic, it is trivially diagonalized, and has been considered by several authors. Generally, such coupling has little effect except when it is resonant, i.e. near a crossing point of the decoupled magnon and phonon bands. Since such a crossing is highly constrained by momentum and energy matching, it occurs in a narrow region of phase space, if at all, and is likely to be unimportant for transport. It in any case does not give rise to scattering, the focus of this work. We therefore henceforth neglect the $\mathcal{A}$ contribution.

Non-trivial scattering processes arise from the second order term in the magnon field expansion of $Q_{n\mathbf{k}}$, parametrized by $\mathcal{B}$. Here as elsewhere we introduce particle-hole indices $q_1, q_2 \in +, -$, such that in particular

$$b^+_{\ell,\mathbf{p},z} = b^\dagger_{\ell,\mathbf{p},z}, \qquad\qquad b^-_{\ell,\mathbf{p},z} = b_{\ell,-\mathbf{p},z}. \tag{3.60}$$

Note the minus sign in the momentum in the second relation. This means generally that

$$\left(b^q_{\ell,\mathbf{p},z}\right)^\dagger = b^{-q}_{\ell,-\mathbf{p},z}. \tag{3.61}$$

To make the coefficients unambiguous, we choose the symmetrized form

$$\mathcal{B}^{n,\ell_1,\ell_2|q_1 q_2 q}_{\mathbf{k};\mathbf{p}} = \mathcal{B}^{n,\ell_2,\ell_1|q_2 q_1 q}_{\mathbf{k};-\mathbf{p}}. \tag{3.62}$$

Demanding that $Q^{+}_{n\mathbf{k}} = (Q^{-}_{n\mathbf{k}})^{\dagger}$ implies that

$$\mathcal{B}^{n,\ell_1,\ell_2|q_1 q_2+}_{\mathbf{k};\mathbf{p}} = \left(\mathcal{B}^{n,\ell_2,\ell_1|-q_2-q_1-}_{\mathbf{k};\mathbf{p}}\right)^{*}. \tag{3.63}$$

If the phonon mode n which $Q^{q}_{n\mathbf{k}}$ is coupled to is C_2 invariant, then only terms with $\ell_1 = \ell_2$ are non-zero. In Sec. 3.5.3.1, we will introduce a concrete and general model of spin-lattice couplings, and see that within this model, almost all interactions obey this selection rule. In particular, off-diagonal terms with $\ell_1 \neq \ell_2$ arise only from the $\Lambda^{(\xi)}_{6,7}$ couplings defined in Eq. (3.74), which are furthermore smaller in magnitude than other couplings as they are related to magnetic anisotropy.

3.5.2.2 Diagonal scattering rate

Contributions to the first-order longitudinal scattering rate, Eq. (3.2) or Eq. (3.24), can be computed exactly using Wick's theorem. To do so we use the free particle two point function, which in the notation of Eq. (3.60) is

$$\begin{aligned}\left\langle b^{q_1}_{\ell_1,\mathbf{p}_1,z_1}(t_1) b^{q_2}_{\ell_2,\mathbf{p}_2,z_2}(t_2)\right\rangle = \quad & \delta_{\ell_1,\ell_2}\delta_{z_1,z_2}\delta_{q_1,-q_2}\delta_{\mathbf{p}_1+\mathbf{p}_2,\mathbf{0}} \\ & \times f_{q_2}(\Omega_{\ell_1,\mathbf{p}_1}) e^{-iq_2\Omega_{\ell_2,\mathbf{p}_2}(t_1-t_2)},\end{aligned} \tag{3.64}$$

where $f_q(\Omega) = (1+q)/2 + n_{\mathrm{B}}(\Omega)$, where $n_{\mathrm{B}}(\Omega)$ is the Bose distribution. One obtains two contributions, $D^{(1)}_{n\mathbf{k}} = \sum_{s=\pm} D^{(1)|s}_{n\mathbf{k}}$, where $D^{(1)|+}$ corresponds to the emission of two magons and $D^{(1)|-}$ corresponds to the scattering of a magnon from one state to another:

$$\begin{aligned}D^{(1)|+}_{n\mathbf{k}} \quad &= \frac{2\pi}{\hbar^2}\frac{1}{N^{\mathrm{2d}}_{\mathrm{uc}}}\sum_{\mathbf{p},\ell,\ell'} \frac{\sinh(\frac{\beta}{2}\hbar\omega_{n\mathbf{k}})}{\sinh(\frac{\beta}{2}\hbar\Omega_{\ell,\mathbf{p}-\frac{\mathbf{k}}{2}})\sinh(\frac{\beta}{2}\hbar\Omega_{\ell',-\mathbf{p}-\frac{\mathbf{k}}{2}})} \\ &\quad \times\delta(\omega_{n\mathbf{k}} - \Omega_{\ell,\mathbf{p}-\frac{\mathbf{k}}{2}} - \Omega_{\ell',-\mathbf{p}-\frac{\mathbf{k}}{2}}) \left|\mathcal{B}^{n,\ell,\ell'|++-}_{\mathbf{k};\mathbf{p}}\right|^2,\end{aligned} \tag{3.65}$$

and

$$\begin{aligned}D^{(1)|-}_{n\mathbf{k}} \quad &= \frac{4\pi}{\hbar^2}\frac{1}{N^{\mathrm{2d}}_{\mathrm{uc}}}\sum_{\mathbf{p},\ell,\ell'} \frac{\sinh(\frac{\beta}{2}\hbar\omega_{n\mathbf{k}})}{\sinh(\frac{\beta}{2}\hbar\Omega_{\ell,\mathbf{p}-\frac{\mathbf{k}}{2}})\sinh(\frac{\beta}{2}\hbar\Omega_{\ell',\mathbf{p}+\frac{\mathbf{k}}{2}})} \\ &\quad \times\delta(\omega_{n\mathbf{k}} - \Omega_{\ell,\mathbf{p}-\frac{\mathbf{k}}{2}} + \Omega_{\ell',\mathbf{p}+\frac{\mathbf{k}}{2}}) \left|\mathcal{B}^{n,\ell,\ell'|+--}_{\mathbf{k};\mathbf{p}}\right|^2.\end{aligned} \tag{3.66}$$

Note that the prefactor involves just the number of two-dimensional unit cells in a single layer, $N^{\mathrm{2d}}_{\mathrm{uc}} = N_{\mathrm{uc}}/N_{\mathrm{layers}}$, which results because a single sum over z gives a factor of the number of layers N_{layers}, converting the N_{uc} to $N^{\mathrm{2d}}_{\mathrm{uc}}$. One can compare the expressions in Eq. (3.65) and Eq. (3.66), and observe a difference of a factor 2 in the prefactor, the sign of the second Ω frequency in the delta function, and that of the second to last index in $\mathcal{B}$. The squared modulus $|\cdots|^2$ can be traced back to Fermi's golden rule, and the thermal $\sinh(\cdots)$ factors, which originate from Bose factors, fall off exponentially at large momenta. Energy conservation imposed by the delta functions strongly constrain these scattering

rates. Specifically, if all magnons have the same velocity $v_{\rm m}$ and the phonons have an isotropic velocity $v_{\rm ph}$, then we find that

$$\mathrm{supp}\left(D^{(1)|+}_{n\mathbf{k}}\right) \subseteq \left\{(\underline{\mathbf{k}}, k_z)\middle|(v_{\rm ph}^2 - v_{\rm m}^2)|\underline{\mathbf{k}}|^2 + v_{\rm ph}^2 k_z^2 > 4\Delta^2\right\}, \tag{3.67}$$

$$\mathrm{supp}\left(D^{(1)|-}_{n\mathbf{k}}\right) \subseteq \left\{(\underline{\mathbf{k}}, k_z)\middle|(v_{\rm ph}^2 - v_{\rm m}^2)|\underline{\mathbf{k}}|^2 + v_{\rm ph}^2 k_z^2 < 0\right\}, \tag{3.68}$$

where $\Delta = \min(\Delta_0, \Delta_1)$ and $\mathrm{supp}(D)$ is the support of D. It follows that if $v_{\rm m} > v_{\rm ph}$, $D^{(1)|+}_{n\mathbf{k}}$ is non-zero in two regions of large $|k_z|$ bounded by hyperboloid surfaces tangent to the $\left\{\frac{k_z}{|\underline{\mathbf{k}}|} = \frac{\sqrt{v_{\rm m}^2 - v_{\rm ph}^2}}{v_{\rm ph}}\right\}$ cone, while $D^{(1)|-}_{n\mathbf{k}}$ is non-zero in the region outside the said cone, containing large $|\underline{\mathbf{k}}|$. The two regions are mutually exclusive, i.e. for any given $\mathbf{k}$ at most one of the two rates is non-zero. For $v_{\rm m} < v_{\rm ph}$, the constraints are even stronger, and $D^{(1)|-}_{n\mathbf{k}} = 0$ strictly vanishes, while $D^{(1)|+}_{n\mathbf{k}}$ is non-zero within an ellipsoid region containing $\mathbf{k} = \mathbf{0}$. The first and second scenarios are realized in La_2CuO_4 [Bazhenov et al., 1996], and in, e.g., $FeCl_2$ [Laurence and Petitgrand, 1973], respectively.

3.5.2.3 Off-diagonal scattering rate

Expanding each Q operator in terms of magnon operators in the four-point correlations, i.e. plugging in Eq. (3.58) into Eqs. (3.34), one can obtain the Hall scattering rate using Wick's theorem. We find

$$\begin{aligned}
\mathfrak{W}^{\ominus,qq'}_{n\mathbf{k},n'\mathbf{k}'} = \frac{64\pi^2}{\hbar^4}\frac{1}{N_{\rm uc}^{2d}} \sum_{\mathbf{p}} \sum_{\{\ell_i,q_i\}} \mathfrak{D}^{nn'|q_1q_2q_3,\ell_1\ell_2\ell_3}_{q\mathbf{k}q'\mathbf{k}',\mathbf{p}}\ \mathfrak{F}^{q_1q_2q_4,\ell_1\ell_2\ell_3}_{q\mathbf{k}q'\mathbf{k}',\mathbf{p}} \\
\mathfrak{Im}\Bigg\{ \mathcal{B}^{n\ell_2\ell_3|q_2q_3q}_{\mathbf{k},\mathbf{p}+\frac{1}{2}q\mathbf{k}+q'\mathbf{k}'} \mathcal{B}^{n'\ell_3\ell_1|-q_3q_1q'}_{\mathbf{k}',\mathbf{p}+\frac{1}{2}q'\mathbf{k}'} \\
\times \mathrm{PP}\Big[\frac{\mathcal{B}^{n\ell_1\ell_4|-q_1q_4-q}_{\mathbf{k},\mathbf{p}+\frac{1}{2}q\mathbf{k}} \mathcal{B}^{n'\ell_4\ell_2|-q_4-q_2-q'}_{\mathbf{k}',\mathbf{p}+q\mathbf{k}+\frac{1}{2}q'\mathbf{k}'}}{\Delta^{qq'}_{n\mathbf{k}n'\mathbf{k}'} + q_1\Omega^{\ell_1,-q_1}_{\mathbf{p}} - q_2\Omega^{\ell_2,q_2}_{\mathbf{p}+q\mathbf{k}+q'\mathbf{k}'} - 2q_4\Omega^{\ell_4,-q_4}_{\mathbf{p}+q\mathbf{k}}} \\
+ \frac{\mathcal{B}^{n'\ell_1\ell_4|-q_1-q_4-q'}_{\mathbf{k}',\mathbf{p}+\frac{1}{2}q'\mathbf{k}'} \mathcal{B}^{n\ell_4\ell_2|q_4-q_2-q}_{\mathbf{k},\mathbf{p}+\frac{1}{2}q\mathbf{k}+q'\mathbf{k}'}}{\Delta^{qq'}_{n\mathbf{k}n'\mathbf{k}'} - q_1\Omega^{\ell_1,-q_1}_{\mathbf{p}} + q_2\Omega^{\ell_2,q_2}_{\mathbf{p}+q\mathbf{k}+q'\mathbf{k}'} - 2q_4\Omega^{\ell_4,q_4}_{\mathbf{p}+q'\mathbf{k}'}} \Big] \Bigg\},
\end{aligned} \tag{3.69}$$

where we defined $\Omega^{\ell,q}_{\mathbf{p}} = \Omega_{\ell,q\mathbf{p}}$, and the product of delta functions $\mathfrak{D}$ and 'thermal factor' $\mathfrak{F}$

$$\begin{aligned}
\mathfrak{D}^{nn'|q_1q_2q_3,\ell_1\ell_2\ell_3}_{q\mathbf{k}q'\mathbf{k}',\mathbf{p}} = \delta\left(\Sigma^{qq'}_{n\mathbf{k}n'\mathbf{k}'} + q_1\Omega^{\ell_1,-q_1}_{\mathbf{p}} + q_2\Omega^{\ell_2,q_2}_{\mathbf{p}+q\mathbf{k}+q'\mathbf{k}'}\right) \\
\delta\left(\Delta^{qq'}_{n\mathbf{k}n'\mathbf{k}'} + 2q_3\Omega^{\ell_3,-q_3}_{\mathbf{p}+q'\mathbf{k}'} - q_1\Omega^{\ell_1,-q_1}_{\mathbf{p}} + q_2\Omega^{\ell_2,q_2}_{\mathbf{p}+q\mathbf{k}+q'\mathbf{k}'}\right),
\end{aligned} \tag{3.70}$$

$$\begin{aligned}
\mathfrak{F}^{q_1q_2q_4,\ell_1\ell_2\ell_3}_{q\mathbf{k}q'\mathbf{k}',\mathbf{p}} = q_4\left(2n_{\rm B}(\Omega^{\ell_3,-q_3}_{\mathbf{p}+q'\mathbf{k}'}) + 1\right) \\
\left(2n_{\rm B}(\Omega^{\ell_1,-q_1}_{\mathbf{p}}) + q_1 + 1\right)\left(2n_{\rm B}(\Omega^{\ell_2,q_2}_{\mathbf{p}+q\mathbf{k}+q'\mathbf{k}'}) + q_2 + 1\right),
\end{aligned} \tag{3.71}$$

and $\Sigma^{q,q'}_{n\mathbf{k}n'\mathbf{k}'} = q\omega_{n\mathbf{k}} + q'\omega_{n'\mathbf{k}'}$, $\Delta^{q,q'}_{n\mathbf{k}n'\mathbf{k}'} = q\omega_{n\mathbf{k}} - q'\omega_{n'\mathbf{k}'}$. Note that while we described and will use below a continuum formulation of the spin wave theory in Sec. 3.5.1, the result in Eq. (3.69) is actually valid at the lattice level, i.e. when the full periodic band structure of the magnons is included, as it relies only upon the canonical commutation relations of the magnon operators, and their dispersions and couplings are taken completely arbitrary at this stage. Therefore this formula could be applied directly in many other circumstances.

We may understand the terms in Eq. (3.69) as follows: the second energy conservation delta function comes from Fermi's golden rule; the first delta function, and the denominator in the third line, come from $\frac{1}{E_{\mathtt{i}}-E_{\mathtt{n}}+i\eta} = \mathrm{PP}\frac{1}{E_{\mathtt{i}}-E_{\mathtt{n}}} - i\pi\delta(E_{\mathtt{i}} - E_{\mathtt{n}})$; while the Bose factors appear when evaluating the thermal averages of magnon population numbers, and their product falls off exponentially at large momenta. $\mathfrak{W}^{\ominus,qq'}_{n\mathbf{k}n'\mathbf{k}'}$ may display divergences when the denominator vanishes. One can explicitly check that the detailed balance relation, Eq. (3.27), holds, using the properties of the $\mathcal{B}$ coefficients, as well as $\mathfrak{W}^{\ominus,qq'}_{n\mathbf{k},n'\mathbf{k}'} = \mathfrak{W}^{\ominus,q'q}_{n'\mathbf{k}',n\mathbf{k}}$.

3.5.3 Phenomenological coupling Hamiltonian

We now propose a symmetry-based phonon-magnon coupling Hamiltonian, Eq. (3.73), for the low-temperature ordered phase of a Néel antiferromagnet on lattice made of layers of square lattices, and, as above, we consider the layers to be *magnetically* decoupled. Moreover, for concreteness, we take the classical ground state to be Néel antiferromagnetic along the $\hat{\mathbf{u}}_x$ axis, so that all the point-group symmetries of the crystal are preserved by the magnetic structure, up to a translation of half a magnetic unit cell. [2]

3.5.3.1 Interaction Hamiltonian density

We consider the most general coupling between *(1)* the strain tensor, $\mathcal{E}^{\alpha\beta} = \frac{1}{2}(\partial^\alpha u^\beta + \partial^\beta u^\alpha)$, where $\boldsymbol{u}$ is the lattice displacement field, and *(2)* spin bilinears in terms of the $\mathbf{m}, \mathbf{n}$ fields, allowed by the symmetries of our tetragonal crystal in its paramagnetic phase, which has the largest symmetry group provided by the crystal structure (generated by mirror symmetries $\mathcal{S}_x, \mathcal{S}_y, \mathcal{S}_z$, fourfold rotational symmetry $\mathcal{C}_4^{xy}$, translation and time-reversal). Since we treat the magnetism as two dimensional, the coupling Hamiltonian is a sum over layers and an integral over two dimensional space,

$$H'_{\mathrm{tetra}} = \sum_z \int d^2\mathbf{x}\, \mathcal{H}'_{\mathrm{tetra}}(\mathbf{r}). \tag{3.72}$$

We use $\mathbf{r} = (\mathbf{x}, z)$ to denote the three-dimensional coordinate. The corresponding local hamiltonian density reads, with all fields expressed in real space:

$$\mathcal{H}'_{\mathrm{tetra}}(\mathbf{r}) = \sum_{\substack{\alpha,\beta \\ a,b=x,y,z}} \mathcal{E}^{\alpha\beta}_{\mathbf{r}} \left(\Lambda^{(\mathrm{n}),\alpha\beta}_{ab} \mathrm{n}_a \mathrm{n}_b + \frac{\Lambda^{(\mathrm{m}),\alpha\beta}_{ab}}{n_0^2} \mathrm{m}_a \mathrm{m}_b \right) \Bigg|_{\mathbf{x},z}, \tag{3.73}$$

[2] In the absence of a magnetic field, and an "alternating" Dzyaloshinskii-Moriya (DM) interaction which we do not consider here.

where $n_0 = \mu_0/\mathfrak{a}^2$ is the ordered moment density. Here each $\Lambda^{(\xi)}$ tensor, which we define to be symmetric in both ab and $\alpha\beta$ variables, has seven independent coefficients, which we call

$$\begin{aligned}
\Lambda_1^{(\xi)} &= \Lambda_{xx}^{(\xi),xx} = \Lambda_{yy}^{(\xi),yy}, \\
\Lambda_2^{(\xi)} &= \Lambda_{yy}^{(\xi),xx} = \Lambda_{xx}^{(\xi),yy}, \\
\Lambda_3^{(\xi)} &= \Lambda_{zz}^{(\xi),xx} = \Lambda_{zz}^{(\xi),yy}, \\
\Lambda_4^{(\xi)} &= \Lambda_{xx}^{(\xi),zz} = \Lambda_{yy}^{(\xi),zz}, \\
\Lambda_5^{(\xi)} &= \Lambda_{zz}^{(\xi),zz}, \\
\Lambda_6^{(\xi)} &= \Lambda_{xy}^{(\xi),xy} = \Lambda_{xy}^{(\xi),yx} = \Lambda_{yx}^{(\xi),yx} = \Lambda_{yx}^{(\xi),xy}, \\
\Lambda_7^{(\xi)} &= \Lambda_{xz}^{(\xi),xz} = \Lambda_{xz}^{(\xi),zx} = \Lambda_{zx}^{(\xi),zx} = \Lambda_{zx}^{(\xi),xz}, \\
&= \Lambda_{yz}^{(\xi),yz} = \Lambda_{yz}^{(\xi),zy} = \Lambda_{zy}^{(\xi),zy} = \Lambda_{zy}^{(\xi),yz},
\end{aligned} \tag{3.74}$$

and all other $\Lambda_{ab}^{(\xi),\alpha\beta}$ are zero. In Appendix 3.F.1, we provide a microscopic derivation of these $\Lambda_{ab}^{(\xi),\alpha\beta}$ coefficients in terms of $\eta^\beta \partial_{\eta^\alpha} J^{ab}|_{\boldsymbol{\eta}}$, i.e. in terms of the spatial derivatives of the magnetic exhange $J^{\alpha\beta}$. Within this microscopic approach $\Lambda_{6,7}^{(\xi)}$ are related to the spatial derivatives of symmetric off-diagonal exchange J^{xy}, J^{xz}, J^{yz}, while $\Lambda_{1,2}^{(\xi)} - \Lambda_3^{(\xi)}$ and $\Lambda_4^{(\xi)} - \Lambda_5^{(\xi)}$ are associated with the spatial derivatives of XXZ exchange anisotropy $J^{xx,yy} - J^{zz}$. Finally, note that in Eq. (3.73) bilinears of the $\mathrm{m}_a \mathrm{n}_b$ kind, arising from e.g. alternating DM interactions J_{ij}^D i.e. such that $J^D_{\mathbf{r},\mathbf{r}+\hat{\mathbf{u}}_a} = -J^D_{\mathbf{r}-\hat{\mathbf{u}}_a,\mathbf{r}}$ with $a = x, y$, could also contribute to the thermal Hall conductivity [Zhang et al., 2019], but are not allowed in the single-site (paramagnetic) Bravais lattice we consider here.

3.5.3.2 Expansion

We now carry out an expansion of the $\mathbf{m}, \mathbf{n}$ fields in two steps. First we expand around the *zero-field*, *zero-net-magnetization* Néel-ordered configuration ($\mathbf{n}_{\mathrm{ord}} = \hat{\mathbf{u}}_x, \mathbf{m}_{\mathrm{ord}} = \mathbf{0}$), assuming deviations are small and satisfy Eq. (3.46). One thereby expresses n_x and m_x in terms of the free fields $\mathsf{m}_{y/z}, \mathsf{n}_{y/z}$ as, in real space:

$$\mathrm{n}_x = 1 - \frac{1}{2} \sum_{b=y,z} \left(\mathsf{n}_b^2 + \frac{1}{n_0^2} \mathsf{m}_b^2 \right), \tag{3.75}$$

$$\mathrm{m}_x = - \sum_{b=y,z} \mathsf{m}_b \mathsf{n}_b, \tag{3.76}$$

which are correct to second order in the free fields (this constitutes a non-linear correction to Eq. (3.47)). In a second step, we include a net magnetization and expand $\vec{\mathsf{m}}$ around it, i.e. write $\mathsf{m}^\alpha = m_0^\alpha + m^\alpha$ where m_0^α is the sum of both a possible spontaneous magnetization and response to the external magnetic field. This two-step expansion physically assumes $m \ll m_0 \ll n_0$. Using these forms in Eq. (3.73), we obtain the spin-lattice coupling to second order in the free field fluctuations:

$$\mathcal{H}'_{\mathrm{tetra}}(\mathbf{r}) \approx \sum_{\alpha\beta} \mathcal{E}_{\mathbf{r}}^{\alpha\beta} \sum_{a,b=y,z} \sum_{\xi,\xi'=0,1} \lambda_{ab;\xi\xi'}^{\alpha\beta} n_0^{-\xi-\xi'} \eta_{a\xi\mathbf{r}} \eta_{b\xi'\mathbf{r}}, \tag{3.77}$$

where $\eta_{a0} = n_a$ and $\eta_{a1} = m_a$ and with

$$\lambda^{\alpha\beta}_{ab;\xi\xi} = \Lambda^{(\xi),\alpha\beta}_{ab} - \delta_{ab}\Lambda^{(0),\alpha\beta}_{xx}, \tag{3.78}$$

$$\lambda^{\alpha\beta}_{ab;01} = \lambda^{\alpha\beta}_{ba;10} = \frac{-1}{n_0}\left[m^a_0\Lambda^{(1),\alpha\beta}_{bx} + \delta_{ab}m^{\overline{a}}_0\Lambda^{(1),\alpha\beta}_{\overline{a}x} + m^b_0\Lambda^{(0),\alpha\beta}_{ax}\right], \tag{3.79}$$

where $\overline{y} = z$, $\overline{z} = y$ and we have associated $\xi = \mathrm{n} \Leftrightarrow \xi = 0$ and $\xi = \mathrm{m} \Leftrightarrow \xi = 1$ in $\Lambda^{(\xi)}$.

These relations are satisfied for any $\Lambda^{(\xi),\alpha\beta}_{ab}$ in Eq. (3.73) (i.e. not necessarily satisfying the constraints Eq. (3.74)), but do assume a Néel moment along the x direction, and a net moment in the yz plane. Note that, while the bare (not linearized) interactions in Eq. (3.73) did not couple the n_a and m_b fields, such a coupling is present in the linearized $\lambda_{ab;01}$ coefficient (i.e. that coupling n_a and m_b). We can see immediately from Eq. (3.78) that this coupling vanishes in the absence of "anisotropic" couplings $\Lambda^{(\xi)}_{6,7}$. Importantly, it also vanishes in the absence of any uniform magnetization. This is a consequence of macroscopic time-reversal symmetry, Eq. (3.49). Conversely, $\lambda_{ab;01}$ is the *only* term in our low energy description of the coupled spin-lattice system which is odd under this effective time-reversal symmetry. Consequently, time-reversal odd effects like skew scattering *must* involve at least one factor of this coupling. This will appear explicitly at the end of the next subsection.

3.5.3.3 In terms of the eigenbosons, $b, b^\dagger$

We now seek to identify the $\mathcal{B}$ coefficients as defined in Eq. (3.58) (with the convention Eq. (3.60)). To do so, we use the Eq. (3.51) representation of the m_a, n_a fields in terms of the b bosons, which diagonalize the pure magnetic Hamiltonian, and plug in their expressions into Eq. (3.77). This involves a unitary transformation which can be defined as (using $a = 1 \Leftrightarrow a = y$ and $a = 2 \Leftrightarrow a = z$)

$$\eta_{a\xi\mathbf{r}} = \sum_{\mathbf{p}}\sum_{\ell=0,1}\sum_{q=\pm} U_{a\xi\ell q}(\mathbf{p})b^q_{\ell\mathbf{p}}e^{i\mathbf{p}\cdot\mathbf{r}}, \tag{3.80}$$

with

$$U_{a\xi\ell q}(\mathbf{p}) = -\delta_{a-1,\ell-\overline{\xi} \bmod 2}F_{\xi q\ell}(\mathbf{p}), \tag{3.81}$$

$$F_{\xi q\ell}(\mathbf{p}) = (iq)^{\overline{\xi}}(-1)^{\overline{\xi}\ell}(\chi\Omega_{\ell\mathbf{p}})^{\xi-\frac{1}{2}}. \tag{3.82}$$

We defined $\overline{\xi} = 1 - \xi$, i.e. $\overline{0} = 1, \overline{1} = 0$, and $\widetilde{\xi} = 2\xi - 1$, i.e. $\widetilde{0} = -1, \widetilde{1} = 1$. We also used relation for the valley $\ell = \delta_{a-1,\xi}$, and conversely $a = 1 + \widetilde{\xi}\ell + \overline{\xi}$. Now inserting this expression into Eq. (3.77), and collapsing the a, b sums, we obtain

$$\begin{aligned}\mathcal{H}'_{\mathrm{tetra}} = \sum_{\alpha\beta}\sum_{\mathbf{p}_1,\mathbf{p}_2}\mathcal{E}^{\alpha\beta}_{\mathbf{r}}\sum_{q_1q_2}\sum_{\ell_1\ell_2=0,1}\sum_{\xi\xi'=0,1} n_0^{-\xi-\xi'}\lambda^{\alpha\beta}_{\ell_1-\bar{\xi},\ell_2-\bar{\xi}';\xi\xi'} \\ F_{\xi q_1\ell_1}(\mathbf{p}_1)F_{\xi' q_2\ell_2}(\mathbf{p}_2)b^{q_1}_{\ell_1\mathbf{p}_1}b^{q_2}_{\ell_2\mathbf{p}_2}e^{i(\mathbf{p}_1+\mathbf{p}_2)\cdot\mathbf{r}}.\end{aligned} \tag{3.83}$$

We similarly express the local strain in terms of its constituent Fourier modes, which are proportional to the phonon creation/annihilation operators,

as discussed in detail in Appendix 3.A. Putting in these two ingredients, some algebra (shown also in Appendix 3.A) finally yields, if we define $\hat{\lambda}^{\ell\ell';\alpha\beta}_{\xi\xi'} = \lambda^{\alpha\beta}_{\ell-\bar{\xi} \bmod 2,\ell'-\bar{\xi}' \bmod 2;\xi\xi'}$,

$$\mathcal{B}^{n,\ell_1\ell_2|q_1q_2q}_{\mathbf{k};\mathbf{p}} = \frac{iq}{2\sqrt{2M_{\rm uc}}} \sum_{\xi\xi'} n_0^{-\xi-\xi'} \mathcal{L}^{q,\ell_1,\ell_2}_{n\mathbf{k};\xi,\xi'} F_{\xi q_1\ell_1}\left(\mathbf{p}+\frac{q}{2}\mathbf{k}\right) F_{\xi' q_2\ell_2}\left(-\mathbf{p}+\frac{q}{2}\mathbf{k}\right) \tag{3.84}$$

where

$$\mathcal{L}^{q,\ell_1,\ell_2}_{n\mathbf{k};\xi,\xi'} = \sum_{\alpha,\beta=x,y,z} \hat{\lambda}^{\ell_1\ell_2;\alpha\beta}_{\xi\xi'} \frac{k^\alpha (\varepsilon^\beta_{n\mathbf{k}})^q + k^\beta (\varepsilon^\alpha_{n\mathbf{k}})^q}{\sqrt{\omega_{n\mathbf{k}}}}. \tag{3.85}$$

Eq. (3.84) may now be inserted into Eq. (3.69). Note that $i^{\bar{\xi}}$ in F plays an important role as discussed in Sec. 3.5.3.4.

Finally, note that the only coefficients $\lambda_{ab,\xi\xi'}$ which contribute to $\mathcal{B}^{\ell_1\ell_2}$ *with* $\ell_1 \neq \ell_2$ (i.e. to "intervalley hopping" recalling $\mathcal{B}^{\ell_1\ell_2}$ is the coefficient of $b^{q_1}_{\ell_1} b^{q_2}_{\ell_2}$ in Q^q) are those which satisfy $\delta_{ab} + \delta_{\xi\xi'} = 1$—see App. 3.F.2 for details. Such coefficients involve only the $\Lambda^{(\xi)}_{6,7}$ couplings, which are typically much smaller than $\Lambda^{(\xi)}_{1..5}$. Therefore a good approximation is to consider only those contributions to the scattering rates Eqs. (3.65,3.66,3.69) with the smallest possible number of intervalley hoppings. Now, the forms $D^{(1)} \sim \mathcal{B}^{\ell_1\ell_2}\mathcal{B}^{\ell_2\ell_1}$ and $\mathfrak{W}^{\ominus} \sim \mathcal{B}^{\ell_1\ell_2}\mathcal{B}^{\ell_2\ell_3}\mathcal{B}^{\ell_3\ell_4}\mathcal{B}^{\ell_4\ell_1}$ impose that intervalley hopping can only happen an even number of times in $D^{(1)}$ and $\mathfrak{W}^{\ominus}$. Because $D^{(1)}_{n\mathbf{k}}$ is a priori nonzero even when $\Lambda_{6,7} = 0$, we discard the subdominant, of order $\left(\frac{\Lambda_{6,7}}{\Lambda_{1..5}}\right)^2$, contributions from $\ell_1 \neq \ell_2$ upon calculating $D^{(1)}_{n\mathbf{k}}$. On the other hand, a nonzero

$$\mathfrak{W}^{\ominus,\mathrm{eff},qq'}_{n\mathbf{k},n'\mathbf{k}'} := \frac{1}{2}\left(\mathfrak{W}^{\ominus,qq'}_{n\mathbf{k},n'\mathbf{k}'} + \mathfrak{W}^{\ominus,qq'}_{n-\mathbf{k},n'-\mathbf{k}'}\right) \tag{3.86}$$

requires either (or both) nonzero $\Lambda_{6,7}$. The first nonzero term with $\ell_1 = \ell_2 = \ell_3 = \ell_4$ in turn occurs at order $\left(\frac{\Lambda_{6,7}}{\Lambda_{1..5}}\right)^1$, and therefore corrections due to $\ell_i \neq \ell_j$ are another order $\left(\frac{\Lambda_{6,7}}{\Lambda_{1..5}}\right)^1$ smaller for $\mathfrak{W}^{\ominus,\mathrm{eff},qq'}_{n\mathbf{k},n'\mathbf{k}'}$. We use this approximation in what follows, i.e. in Secs. 3.5.4 and 3.5.6.

3.5.3.4 Effective breaking of symmetries

(i) Time reversal. We now briefly comment on the relation between the "effective" time-reversal of the spin system $\mathcal{T}$ and the transport properties of the phonon system. Indeed, it is obvious from Eqs. (3.65) and Eq. (3.69) that if all the $\mathcal{B}$ coefficients satisfy

$$\mathcal{B}^{n,\ell_1\ell_2|q_1q_2q}_{-\mathbf{k};-\mathbf{p}} \stackrel{?}{=} \left(\mathcal{B}^{n,\ell_1\ell_2|q_1q_2q}_{\mathbf{k};\mathbf{p}}\right)^*, \tag{3.87}$$

then $D^{(1)}_{n-\mathbf{k}} = D^{(1)}_{n\mathbf{k}}$ and $\mathfrak{W}^{\ominus,qq'}_{n-\mathbf{k},n'-\mathbf{k}'} = -\mathfrak{W}^{\ominus,qq'}_{n\mathbf{k},n'\mathbf{k}'}$, i.e. the phonon collision integral is effectively time-reversal symmetry preserving, as discussed in Sec. 3.4.1.

Therefore, no phonon Hall effect follows if the spin-phonon coupling satisfies Eq. (3.87).

Which terms in Eq. (3.77) are compatible with an effective time-reversal symmetry breaking? By direct inspection of Eq. (3.85), one finds that $i\mathcal{L}^{q,\ell_1,\ell_2}_{n-\mathbf{k};\xi,\xi'} = \left(i\mathcal{L}^{q,\ell_1,\ell_2}_{n\mathbf{k};\xi,\xi'}\right)^*$. Thus, only those terms in Eq. (3.84) with $i^{\overline{\xi}+\overline{\xi}'} = i$ may satisfy $\mathcal{B}^{n,\ell_1\ell_2|q_1q_2q}_{-\mathbf{k};-\mathbf{p}} \neq \left(\mathcal{B}^{n,\ell_1\ell_2|q_1q_2q}_{\mathbf{k};\mathbf{p}}\right)^*$. All others are such that $\mathcal{B}^{n,\ell_1\ell_2|q_1q_2q}_{-\mathbf{k};-\mathbf{p}} = \left(\mathcal{B}^{n,\ell_1\ell_2|q_1q_2q}_{\mathbf{k};\mathbf{p}}\right)^*$.

The breaking of effective time-reversal in the phonon system thus relies upon the presence of spin-phonon couplings where $\xi' = \overline{\xi}$, i.e. $\lambda_{ab,01}$ and $\lambda_{ab,10}$ (henceforth denoted "λ_{nm}") coefficients; this is consistent with the argument in Sec. 3.5.3.2, based on macroscopic time-reversal $\mathcal{T}$, Eq. (3.49). Morevoer, going back to Sec. 3.4.2.2, we see that if $\boldsymbol{m}_0 \neq \mathbf{0}$ but $\Lambda^{(\xi)}_6 = 0 = \Lambda^{(\xi)}_7$, then the kernel $K^H_{n\mathbf{k},n'\mathbf{k}'}$ is invariant under momentum reversal; and so $\kappa_H = 0$, even though the system breaks $\mathcal{T}$.

(ii) σ_d **operation.** Here we briefly study the σ_d operation, i.e. a mirror transformation through the plane containing the $\hat{z}$ and $\frac{\hat{x}+\hat{y}}{\sqrt{2}}$ directions. The system, having antiferromagnetic ordering along the x axis as well as possibly $m^y_0 \neq 0$, explicitly breaks this symmetry. However, if $\Lambda^{(\xi)}_1 = \Lambda^{(\xi)}_2$ and $\Lambda^{(\xi)}_7 = 0$, then σ_d is preserved at the level of the kernel $K^H_{n\mathbf{k},n'\mathbf{k}'}$, whence $\kappa_H = 0$. This illustrates the importance of knowing the action of D_{4h} operations upon the *kernels* $K^H_{n\mathbf{k},n'\mathbf{k}'}$, because some symmetries which are explicitly broken globally might fail to be effectively broken in phonon scattering.

3.5.4 Solutions of the delta functions

Each contribution to the scattering rate involves a momentum integral over an integrand which contains either a single delta function or a product of two delta functions. These express energy conservation constraints, which must be solved to carry out the integration. The argument of each delta function, which must be set to zero, is of the form

$$\varpi - \Omega_{\ell,\mathbf{p}} - s\Omega_{\ell,\mathbf{p}-\mathbf{k}} = 0, \tag{3.88}$$

where $s = \pm 1$. Using the continuum form of the magnon dispersion, $\Omega_{\ell,\mathbf{p}} = \sqrt{v_{\rm m}^2|\underline{\mathbf{p}}|^2 + \Delta_\ell^2} = v_{\rm m}\sqrt{|\underline{\mathbf{p}}|^2 + \delta_\ell^2} = v_{\rm m}\hat{\Omega}_{\ell,\mathbf{p}}$, where $\delta_\ell = \Delta_\ell/v_{\rm m}$, we can rewrite this as

$$\sqrt{|\underline{\mathbf{p}}|^2 + \delta_\ell^2} + s\sqrt{|\underline{\mathbf{p}} - \underline{\mathbf{k}}|^2 + \delta_\ell^2} = a, \tag{3.89}$$

where $a = \varpi/v_{\rm m}$ and $s = \pm 1$.

The existence and type of solutions depend on the value of $a^2 - \underline{k}^2$, where $\underline{k}^2 = k_x^2 + k_y^2$. When they exist, the solutions are conics, as is summarized in Table 3.5.1.

It is then best to introduce coordinates $p_\parallel, p_\perp$ which are along the principal axes of the hyperbola/ellipse:

$$\underline{\mathbf{p}} = p_\parallel \widehat{\underline{\mathbf{k}}} + p_\perp \hat{\mathbf{z}} \times \widehat{\underline{\mathbf{k}}}, \tag{3.90}$$

	$a^2-\underline{k}^2<0$	$0<a^2-\underline{k}^2<4\delta_\ell^2$	$4\delta_\ell^2<a^2-\underline{k}^2$
$s=+$	no solutions	no solutions	ellipse
$s=-$	half-hyperbola	no solutions	no solutions

Table 3.5.1: Solutions to a single delta function of the form $\delta(\varpi-\Omega_{\ell,\mathbf{p}}-s\Omega_{\ell,\mathbf{p}-\mathbf{k}})$, with $s=\pm1$, as a function of the value of a^2-k^2, where $a=\varpi/v_\mathrm{m}$, $\underline{k}^2=k_x^2+k_y^2$, and $\Omega_{\ell,\mathbf{p}}=v_\mathrm{m}\sqrt{\underline{p}^2+\delta_\ell^2}$. The necessary existence conditions described in this Table are captured by the equation $s(a^2-\underline{k}^2)>4\delta_\ell^2(s+1)/2$.

where we define $\widehat{\underline{\mathbf{k}}}=(k_x\hat{\mathbf{x}}+k_y\hat{\mathbf{y}})/\underline{k}$ (note the denominator $\underline{k}$ which differs from k when $k_z\neq0$), and we can define the major $\bar{a}$ and minor $\bar{b}$ semi-axes, or conversely, of the conics:

$$\bar{a}=\frac{|a|}{2}\sqrt{1-\frac{4\delta_\ell^2}{a^2-\underline{k}^2}},\quad \bar{b}=\frac{1}{2}\sqrt{|a^2-\underline{k}^2-\delta_\ell^2|}. \tag{3.91}$$

An immediate consequence is that, in the case of the ellipse $-\bar{a}\leq p_\parallel-\frac{k}{2}\leq\bar{a}$ and $-\bar{b}\leq p_\perp\leq\bar{b}$, while in the case of the half-hyperbola: $p_\parallel\geq\frac{k}{2}+\bar{a}$.

Both Eq. (3.89) and a pair of such equations may be solved analytically, but the solutions are analytically complicated. We provide their details in Appendix 3.E.1, and give here only the final results.

3.5.4.1 Diagonal scattering rate

We have, in particular, the following compact form for $D_{n\mathbf{k}}^{(1)|s}$, with $s=\pm$,

$$\begin{aligned}D_{n\mathbf{k}}^{(1)|s} &= \frac{(3-s)\pi\mathfrak{a}^2}{(2\pi)^2\hbar^2}\sum_{\ell,\ell'}\int d^2\mathbf{p}\,\frac{\sinh(\frac{\beta}{2}\hbar\omega_{n\mathbf{k}})}{\sinh(\frac{\beta}{2}\hbar\Omega_{\ell,\mathbf{p}})\sinh(\frac{\beta}{2}\hbar\Omega_{\ell',\mathbf{p}-\mathbf{k}})}\\ &\quad\times\delta(\omega_{n\mathbf{k}}-\Omega_{\ell,\mathbf{p}}-s\Omega_{\ell',\mathbf{p}-\mathbf{k}})\left|\mathcal{B}^{n,\ell,\ell'|+s-}_{\mathbf{k};-\mathbf{p}+\frac{\mathbf{k}}{2}}\right|^2,\end{aligned} \tag{3.92}$$

where we converted the *two-dimensional* momentum sum to an integral using $\sum_{\mathbf{p}}\to N_\mathrm{uc}^\mathrm{2d}\mathfrak{a}^2\int\frac{d^2\mathbf{p}}{(2\pi)^2}$, where $N_\mathrm{uc}^\mathrm{2d}\mathfrak{a}^2$ is the area of the sample in the xy plane.

From now on, in this paragraph and the following, we make use of the approximation $\mathcal{B}^{\ell\neq\ell'}\to0$, as explained previously. Then, collapsing the delta function (to avoid clutter, we identify $y=p_\perp$):

$$\begin{aligned}D_{n\mathbf{k}}^{(1)|s} &= \frac{(3-s)\mathfrak{a}^2\sinh(\frac{\beta}{2}\hbar\omega_{n\mathbf{k}})}{4\pi v_\mathrm{m}\hbar^2}\\ &\quad\times\int_{-\infty}^{+\infty}\mathrm{d}y\sum_\eta \mathrm{f}_\eta^s(y)J_\eta^s(y)\sum_\ell\frac{\left|\mathcal{B}^{n,\ell,\ell|+s-}_{\mathbf{k};-\mathbf{p}_{\ell,\mathbf{k}}^{(\eta)}(y)+\frac{\mathbf{k}}{2}}\right|^2}{\sinh(\frac{\beta}{2}\hbar\Omega_{\ell,\mathbf{p}_{\ell,\mathbf{k}}^{(\eta)}(y)})\sinh(\frac{\beta}{2}\hbar\Omega_{\ell,\mathbf{p}_{\ell,\mathbf{k}}^{(\eta)}(y)-\mathbf{k}})},\end{aligned} \tag{3.93}$$

where

$$\begin{cases} \mathrm{f}_\eta^{s=1}(y) = \Theta(\bar{b} - |y|)\,\Theta(a^2 - \underline{k}^2 - 4\delta_\ell^2) \\ \mathrm{f}_\eta^{s=-1}(y) = \delta_{\eta,1}\,\Theta(\underline{k}^2 - a^2) \end{cases}, \tag{3.94}$$

where $a = \omega_{n\mathbf{k}}/v_\mathrm{m}$, $\eta = \pm 1$ and

$$J_D^s(y) = \left| \sum_{r=\pm} \frac{s^{(r-1)/2} r c_r(y)}{\sqrt{c_r(y)^2 + y^2 + \delta_\ell^2}} \right|^{-1}, \tag{3.95}$$

with

$$c_\eta(y) = \frac{1}{2}\left(\underline{k} + \eta\, a \sqrt{1 - 4\frac{\delta_\ell^2 + y^2}{a^2 - \underline{k}^2}} \right), \tag{3.96}$$

and

$$\mathbf{p}_{\ell,\mathbf{k}}^{(\eta)}(y) = c_\eta(y)\widehat{\underline{\mathbf{k}}} + y\hat{\mathbf{z}} \times \widehat{\underline{\mathbf{k}}}, \tag{3.97}$$

i.e. we identified $p_\parallel$ and $p_\perp$ in Eq. (3.90) with $c_\eta(y)$ and y, respectively. At this point it may be comforting to check dimensions. Noting that y has dimensions of momentum, i.e. inverse length, and $\mathcal{B}$ has dimensions of energy, i.e. inverse time, one can indeed see that D in Eq. (3.93) has proper dimensions of a rate.

3.5.4.2 Off-diagonal scattering rate

In this case, we must solve a *pair* of conic equations simultaneously, which takes the form:

$$\begin{cases} \varpi_1 - \Omega_{\ell,\mathbf{p}} - s_1 \Omega_{\ell,\mathbf{p}-\mathbf{k}_1} = 0 \\ \varpi_2 - \Omega_{\ell,\mathbf{p}} - s_2 \Omega_{\ell,\mathbf{p}-\mathbf{k}_2} = 0, \end{cases} \tag{3.98}$$

i.e.

$$\begin{cases} \sqrt{|\underline{\mathbf{p}}|^2 + \delta_\ell^2} + s_1 \sqrt{|\underline{\mathbf{p}} - \underline{\mathbf{k}}_1|^2 + \delta_\ell^2} = a_1 \\ \sqrt{|\underline{\mathbf{p}}|^2 + \delta_\ell^2} + s_2 \sqrt{|\underline{\mathbf{p}} - \underline{\mathbf{k}}_2|^2 + \delta_\ell^2} = a_2, \end{cases} \tag{3.99}$$

where $a_i = \varpi_i/v_\mathrm{m}$. Indeed, the integrals which occur in the second order scattering rates involve pairs of delta functions, whose arguments are of the form considered above, with in Eq. (3.98), $\varpi_1 = -q_1 \Sigma^{qq'}_{n\mathbf{k}n'\mathbf{k}'}$, $\varpi_2 = -q_1 q' \omega_{n'\mathbf{k}'}$, $s_1 = q_1 q_2$, $s_2 = -q_1 q_3$, $\mathbf{k}_1 = -q\mathbf{k} - q'\mathbf{k}'$, $\mathbf{k}_2 = -q'\mathbf{k}'$, $\delta_\ell = \Delta_\ell/v_\mathrm{m}$. In this case, each of the two delta function constraints defines a half-hyperbola or an ellipse in the $\mathbf{p}$ plane, and the integrand is confined to the intersections of these two curves. Consequently, the integral will be collapsed to a discrete set of points. It is straightforward to see geometrically that the intersection of two curves of these types is, except for the degenerate cases in which the two curves are identical, a set of at most four points. The two simultaneous equations can be solved analytically, but the solutions are algebraically complicated and we give here only the results and leave details to the Appendices.

Collapsing the delta functions as explained in Appendix 3.E.1, we can write:

$$\mathfrak{W}^{\ominus,qq'}_{n\mathbf{k},n'\mathbf{k}'} = \frac{4\mathfrak{a}^2}{v_{\mathrm{m}}^3\hbar^4}\sum_j\sum_{\ell,\{q_i\}} J_{\mathfrak{W}}(\mathbf{p}_j)\hat{\mathcal{F}}^{\ell,\ell,\ell|q_4,q_1,q_2}_{\mathbf{p}_j,q\mathbf{k},q'\mathbf{k}'} \tag{3.100}$$

$$\times\mathfrak{Im}\Bigg\{\mathcal{B}^{n\ell\ell|q_2q_3q}_{\mathbf{k},\mathbf{p}_j+\frac{1}{2}q\mathbf{k}+q'\mathbf{k}'}\mathcal{B}^{n'\ell\ell|-q_3q_1q'}_{\mathbf{k}',\mathbf{p}_j+\frac{1}{2}q'\mathbf{k}'}$$

$$\times\mathrm{PP}\left[\frac{\mathcal{B}^{n\ell\ell|-q_1q_4-q}_{\mathbf{k},\mathbf{p}_j+\frac{1}{2}q\mathbf{k}}\mathcal{B}^{n'\ell\ell|-q_4-q_2-q'}_{\mathbf{k}',\mathbf{p}_j+q\mathbf{k}+\frac{1}{2}q'\mathbf{k}'}}{\frac{q_1q\omega_{n\mathbf{k}}}{v_{\mathrm{m}}}+\hat{\Omega}_{\ell,\mathbf{p}_j}-q_1q_4\hat{\Omega}_{\ell,\mathbf{p}_j+q\mathbf{k}}}+\frac{\mathcal{B}^{n'\ell\ell|-q_1-q_4-q'}_{\mathbf{k}',\mathbf{p}_j+\frac{1}{2}q'\mathbf{k}'}\mathcal{B}^{n\ell\ell|q_4-q_2-q}_{\mathbf{k},\mathbf{p}_j+q'\mathbf{k}'+\frac{1}{2}q\mathbf{k}}}{\frac{q_1q'\omega_{n'\mathbf{k}'}}{v_{\mathrm{m}}}+\hat{\Omega}_{\ell,\mathbf{p}_j}+q_1q_4\hat{\Omega}_{\ell,\mathbf{p}_j+q'\mathbf{k}'}}\right]\Bigg\},$$

where $\hat{\Omega}=\Omega/v_{\mathrm{m}}$, and

$$\begin{aligned}\hat{\mathcal{F}}^{\ell_3,\ell_1,\ell_2|q_4,q_1,q_2}_{\mathbf{p},q\mathbf{k},q'\mathbf{k}'} &= q_1q_4\left(2n_{\mathrm{B}}(\Omega_{\ell_3,\mathbf{p}+q'\mathbf{k}'})+1\right)\left(2n_{\mathrm{B}}(\Omega_{\ell_1,\mathbf{p}})+q_1+1\right)\\ &\quad\times\left(2n_{\mathrm{B}}(\Omega_{\ell_2,\mathbf{p}+q\mathbf{k}+q'\mathbf{k}'})+q_2+1\right)\end{aligned} \tag{3.101}$$

is a product of thermal factors and where, when they exist, the solutions, $j=0,..,3$ take the form

$$\mathbf{p}_j = t_{\lfloor j/2\rfloor}\mathbf{v}_{\lfloor j/2\rfloor}+u^{(\widetilde{j\,[2]})}_{\lfloor j/2\rfloor}\mathbf{w}_{\lfloor j/2\rfloor}, \tag{3.102}$$

where, for $i=0,1$ $\mathbf{v}_i=a_2\underline{\mathbf{k}}_1+(-1)^ia_1\underline{\mathbf{k}}_2$, $\mathbf{w}_i=\hat{\mathbf{z}}\times\mathbf{v}_i$ (note that $\mathbf{v}_i=\underline{\mathbf{v}}_i$, $\mathbf{w}_i=\underline{\mathbf{w}}_i$ and $\mathbf{p}_j=\underline{\mathbf{p}}_j$ are all in-plane vectors), t_i and $u_i^{(\pm)}$ are given in Appendix 3.E.1 (also recall we defined $\widetilde{0}=-1$, $\widetilde{1}=1$, $x\,[2]$ is x mod 2, and $\lfloor x\rfloor$ denotes the floor of x), and

$$J_{\mathfrak{W}}(\mathbf{p}_j)=\left|s_1\frac{\underline{\mathbf{k}}_1\wedge\underline{\mathbf{p}}_j}{\hat{\Omega}_{\ell,\mathbf{p}_j}\hat{\Omega}_{\ell,\mathbf{p}_j-\mathbf{k}_1}}+s_2\frac{\underline{\mathbf{p}}_j\wedge\underline{\mathbf{k}}_2}{\hat{\Omega}_{\ell,\mathbf{p}_j}\hat{\Omega}_{\ell,\mathbf{p}_j-\mathbf{k}_2}}+s_1s_2\frac{-\underline{\mathbf{k}}_1\wedge\underline{\mathbf{k}}_2+\underline{\mathbf{p}}_j\wedge\underline{\mathbf{k}}_2-\underline{\mathbf{p}}_j\wedge\underline{\mathbf{k}}_1}{\hat{\Omega}_{\ell,\mathbf{p}_j-\mathbf{k}_1}\hat{\Omega}_{\ell,\mathbf{p}_j-\mathbf{k}_2}}\right|^{-1}, \tag{3.103}$$

where $\underline{\mathbf{V}}_1\wedge\underline{\mathbf{V}}_2=V_1^xV_2^y-V_2^yV_1^x$ for any in-plane vectors $\underline{\mathbf{V}}_{1,2}$. Coefficients $t_{0,1}$ are always well defined, but *for each* i, $u_i^{(\pm)}$ are the solutions to a quadratic equation which has zero, one or two solutions, whether the discriminant $\mathsf{d}_{u,i}$ thereof is negative, zero, or positive.

Necessary (but not sufficient) conditions of existence of solutions are: *(i)* the existence of *both* conics, cf. Table 3.5.1, *(ii)* $\mathsf{d}_{u,0}\geq 0$ and/or $\mathsf{d}_{u,1}\geq 0$, *(iii)* when s_1 and/or s_2 is negative, the $\mathbf{p}_j$ must lie on the $\eta_{1,2}=1$ branch of the 1 and/or 2 hyperbola. Even with these constraints, spurious solutions exist, so that one must check that the solutions Eq. (3.102) also satisfy the equations for the given values of $a_1,a_2,\underline{\mathbf{k}}_1,\underline{\mathbf{k}}_2,q,q',q_i$.

3.5.5 Scaling and orders of magnitude

In this subsection, we discuss the temperature dependence and magnitude of the magnonic contributions to the different phonon scattering rates, which determine the phonon thermal conductivity and thermal diffusivity tensors. Since we consider a low-energy continuum theory (without a momentum cutoff) in which

the dispersion of the phonons is linear, these hold only in the low-temperature limit, i.e. for $T \ll \hbar v_{\rm ph}/(\mathfrak{a} k_{\rm B})$. Similarly, we consider the low-energy dispersion of magnons, so our results are valid for $T \ll \hbar v_{\rm m}/(\mathfrak{a} k_{\rm B}) \sim J/k_{\rm B}$. In Table 3.5.2, we summarize some of the relations derived in this section.

quantity	τ^{-1}	$\kappa_{\rm L}$	$\mathfrak{W}^{\ominus}$	$\tau_{\rm skew}^{-1}$	$\varrho_{\rm H}$
T-scaling	T^{d+2x}	T^{3-d-2x}	T^{d-1+3x}	T^{d+2+3x}	T^{d-1+3x}
Eq. ref	(3.105)	(3.106)	(3.109)	(3.110)	(3.115)

Table 3.5.2: Scaling relations derived in Sec. 3.5.5 and the corresponding equation number where they appear. Note that these were obtained within a low-energy approach which omit in particular larger-k deviations away from the acoustic phonon linear dispersion limit and other higher-T effects such as Umklapp [Tritt, 2004].

3.5.5.1 Longitudinal scattering rate: Role of anisotropies and scaling exponent

First we consider the leading magnonic contributions to the longitudinal scattering rate, $D^{(1)}_{n\mathbf{k}}$. The typical magnitude of this quantity for $|\mathbf{k}| \sim k_B T/v_{\rm ph}$ sets the basic rate $1/\tau$. This rate has been studied previously in classic work on the phonon-magnon coupling in antiferromagnets. Reference [Cottam, 1974] finds that $1/\tau \sim T^5$ (for the moment we give only the T dependence under the above condition, and do not give the prefactor), for a model of exchange-striction in a Heisenberg antiferromagnet in three dimensions. This should be recovered from our formalism.

A general estimate can be obtained from Eqs. (3.65,3.66). To evaluate it requires, in addition to the dispersion relations, the phonon-magnon couplings $\mathcal{B}$, which are given in Eq. (3.84). At the level of temperature scaling for typical thermal momenta, for temperatures well above the magnon gap, $v_{\rm m} k \gg \Delta$, we may replace $k \sim k_B T/v_{\rm ph}$, $\omega \sim v_{\rm ph} k \sim k_B T$ and $\Omega \sim k_B T$ (the latter is true if the ratio between $v_{\rm m}$ and $v_{\rm ph}$ is order one). Noting that $\tilde{\xi}$ and $\tilde{\xi}'$ in Eq. (3.84) equal ± 1, we see that a general phonon-magnon coupling is a sum of three contributions,

$$\mathcal{B} \sim \left(\frac{k_B T}{M v_{\rm ph}^2}\right)^{\frac{1}{2}} n_0^{-1} \left(\lambda_{mm} \frac{\chi k_B T}{n_0} + \lambda_{mn} + \lambda_{nn} \frac{n_0}{\chi k_B T}\right). \tag{3.104}$$

Here, as above, we label generic Néel-Néel vector couplings $\lambda_{nn} \equiv \lambda_{ab,00}$, net magnetization-magnetization couplings $\lambda_{mm} \equiv \lambda_{ab,11}$ and "cross" Néel-magnetization couplings $\lambda_{mn} \equiv \lambda_{ab,10}$.

Depending upon which of these terms is dominant, the temperature dependence of $\mathcal{B} \sim T^{1/2+x}$, with $x = -1, 0, 1$ corresponding to the λ_{nn}, λ_{mn} and λ_{mm} terms, respectively. We can then estimate the scattering rate by converting

the momentum sum over $\mathbf{p}$ to a d-dimensional integral (d is the spin-exchange dimensionality) and recalling $|p| \sim T$. We see therefore that

$$\frac{1}{\tau} \sim T^{d-1}|\mathcal{B}|^2 \sim T^{d+2x}. \tag{3.105}$$

A priori, the dominant contributions would arise from terms with $x = -1$, which have the smallest power of temperature, which would give $1/\tau \sim_? T^{d-2} \sim T$ in $d = 3$ dimensions. This *does not* agree with Ref. [Cottam, 1974]. Instead, one notices that what one might expect to be the subdominant contribution from $x = +1$, which gives $1/\tau \sim T^{d+2}$ in general dimensions, does agree with the classic theory for $d = 3$.

Why is this the case? The resolution lies in the fact that Ref. [Cottam, 1974] assumes isotropic Heisenberg interactions, and is carried out in zero magnetic field. As a consequence, the Hamiltonian has SU(2) symmetry, and Goldstone's theorem protects the gaplessness of the magnon modes *even in the presence of strain*. In particular, because even an arbitrarily strained lattice must preserve the gapless magnons in this case, the spin-lattice coupling, Eq. (3.73) must be spin-rotationally invariant, and moreover its quadratic expansion, Eq. (3.77), must vanish for a magnon configuration which is a small rotation of the Néel order, which corresponds to either n_y or n_z non-zero and spatially constant. This means that the non-zero terms in Eq. (3.77) involve only $\xi, \xi' = m$ and not n (in a treatment including higher order terms, spatial gradients ∇n would appear, but these scale in the same manner as m). One can indeed check in Eq. (3.78) that when the interactions $\Lambda_{ab}^{(\mathrm{m/n}),\alpha\beta}$ are isotropic ($\propto \delta_{ab}$), λ_{nn} vanishes, and λ_{mn} vanishes at zero field when the uniform magnetization $m_0^a = 0$. Taking the λ_{mm} contribution in Eq. (3.104) gives $x = +1$ in Eq. (3.105) as needed for agreement with earlier work.

What is the physics of the different values of x? We see that stronger effects (smaller powers of temperature) arise from coupling to n than to m. This is a fundamental property of antiferromagnets: fluctuations of the order parameter n are stronger and more long-ranged than those of the uniform magnetization m, which is naturally suppressed when antiferromagnetic interactions dominate. Thus larger effects would be expected from coupling of strain to the staggered magnetization than to the uniform one, as the formula indeed shows.

How is this reflected in $\kappa_L(T)$? The last step from the scattering time τ to the longitudinal conductivity κ_L is a standard one [Tritt, 2004, Carruthers, 1961]. The sum over phonon momentum $\mathbf{k}$ in Eq. (3.3) is converted to a three-dimensional integral (the *magnon* momentum integral was d-dimensional, with $d = 2$ in the case of a layered antiferromagnet).

For temperatures $k_B T \gg \Delta$, the scaling for the temperature dependence of the longitudinal conductivity is

$$\kappa_L \sim T^{3-d-2x}. \tag{3.106}$$

As can be seen from Eq. (3.104), a crossover between the low-temperature

$x = -1$ and the high-temperature $x = +1$ behaviors occurs at $T^\star_\lambda$,

$$k_B T^\star_\lambda \sim \frac{n_0}{\chi}\sqrt{\frac{\lambda_{nn}}{\lambda_{mm}}}. \tag{3.107}$$

Eq. (3.107) assumes that the intermediate behavior $x = 0$, due to the λ_{mn} coupling which is proportional to both anisotropic exchanges and the net magnetization, is negligible; this is consistent with our numerical results shown in Sec. 3.5.6.4. The above results, Eqs. (3.106,3.107), also assume that $D^{(1)}_{n\mathbf{k}}$ is the dominant scattering rate contributing to the longitudinal inverse scattering time $D_{n\mathbf{k}}$. (The role of $\breve{D}_{n\mathbf{k}}$ is considered in more detail in Sec. 3.5.6.4.) However, many more scattering processes, such as boundary or impurity scattering, which in Eq. (3.2) are encompassed as $\breve{D}_{n\mathbf{k}}$, ontribute (through Matthiessen's rule) to the phonon relaxation. Thus, κ_L should be considered a probe of the *full* $D_{n\mathbf{k}}$.

3.5.5.2 Longitudinal scattering rate: Role of the gap and magnetic field dependence

Since we have seen that the assumption of isotropic interactions suppresses the coupling to the staggered magnetization, this discussion suggests that breaking of spin-rotation symmetry should greatly enhance phonon scattering. While this may indeed be the case, we should note a subtlety: although spin anisotropy indeed allows such coupling, it also allows the formation of a magnon gap — enlarged by the presence of an external magnetic field, $\Delta_\ell = \sqrt{\Gamma_\ell/\chi + h_\ell^2}$. Which behavior should be expected from the combination of these two effects?

Regardless of the form of coupling (scaling exponent x), if $k_B T \ll \Delta$, magnon-phonon scattering will become energetically unavailable. More precisely, $D^{(1)|+}$, corresponding to the process whereby a phonon excites two magnons, is exponentially suppressed due to the required rest energy 2Δ, while $D^{(1)|-}$, corresponding to the process whereby a phonon scatters a magnon, is exponentially suppressed due to the exponential decrease of all magnon populations at temperatures below the gap. Therefore $D^{(1)}$ as a whole is exponentially suppressed if $k_B T \ll \Delta$; We check this behavior numerically in Sec. 3.5.6.6.

Thus, a crossover in the behavior of $\kappa_L(T)$ occurs at temperature $T^\star_\Delta \sim \Delta/k_B$. Below $T^\star_\Delta$, the phonon thermal conductivity is mostly due to *other* scattering effects, which are captured by $\breve{D}_{n\mathbf{k}}$ in this work. For constant $\breve{D}_{n\mathbf{k}}$, this yields $\kappa_L \sim T^3$. Above $T^\star_\Delta$, phonon-magnon scattering becomes available, and is enhanced by anisotropic coupling; provided this is the dominant effect, the resulting thermal conductivity behavior is $\kappa_L \sim T^{3-d-2x}$ with $x = -1$ which, for $d = 2$ (two-dimensional magnons), is the *same power* of temperature as that obtained with only constant $\breve{D}_{n\mathbf{k}}$. However, the proportionality constant is larger with phonon-magnon scattering than without, which, for sufficiently strong anisotropic couplings (i.e. sufficiently large λ_{nn}), may lead to a "bump" in $\kappa_L(T)$, as we indeed numerically see in Sec. 3.5.6.4.

Remarkably, this effect depends on the external magnetic field through the width of the magnon gap (recall the latter is field dependent), and may be an important feature of $\kappa_L(\mathbf{h}, T) - \kappa_L(\mathbf{0}, T)$. For the sake of completeness, we note that

types of dependences on the magnetic field may arise at temperatures where the scaling exponent $x = 0$ plays a role, because the λ_{mn} coupling depends explicitly on the net magnetization m_0 in (see Eq. (3.78)). It is however not clear how this contribution could become non-negligible in any range of temperatures, and the gap dependence $\Delta(\mathbf{h})$ is arguably the main culprit as regards the dependence on $\mathbf{h}$ of the longitudinal conductivity.

3.5.5.3 Transverse scattering: scaling exponent

We can now apply similar reasoning to the transverse/Hall scattering rate $\mathfrak{W}^{\ominus}$ from Eq. (3.69). Obviously if temperature is sufficiently low, i.e. below magnon gaps, the result will be exponentially suppressed. Of greater interest is the energy regime above the magnon gaps, in which we may assume acoustic linearly dispersing magnons (and phonons). We proceed by counting the obvious factors of momentum and energy, and by assuming the relevant momentum scales are set by dimensional analysis, i.e. $\mathbf{k}, \mathbf{k}' \sim k_B T / v_{\mathrm{m}}$ etc. Inspection of Eq. (3.69) shows one sum over magnon momentum $\mathbf{p}$, which converts to an integration in the thermodynamic limit, two energy delta functions, and one energy denominator, which, using the aforementioned momentum scaling implies that

$$\mathfrak{W}^{\ominus} \sim T^{d-3} \mathcal{B}^4. \tag{3.108}$$

Here we considered the *magnon* momentum integration as d-dimensional, as in the previous discussion of longitudinal scattering rates.

Now to proceed we must estimate the contribution of the four $\mathcal{B}$ factors. To do so, we need to consider the effective time-reversal symmetry $\mathcal{T}$. This symmetry must be broken to obtain a non-zero effective skew-cattering rate, $\mathfrak{W}^{\ominus,\mathrm{eff},qq'}_{n\mathbf{k},n'\mathbf{k}'}$, which in particular is odd under $\mathcal{T}$. As discussed in Secs. 3.5.3.2 and 3.5.3.3, under $\mathcal{T}$ the λ_{mm} and λ_{nn} couplings are even while only the λ_{mn} couplings are odd; therefore $\mathfrak{W}^{\ominus,\mathrm{eff}}$ must contain an odd number of factors of λ_{mn}. Furthermore, in the low field regime we consider here, $\mathcal{T}$ symmetry breaking happens through the development of a small uniform magnetization, hence $\lambda_{mn} \propto m_0$, which in turn is linearly proportional to the applied field (see Eq. (3.78)). Consequently, to obtain the linear-in-field Hall scattering rate, we should keep just one (and not three, the other available odd number) factors of λ_{mn}. Therefore, we may use Eq. (3.104) to estimate

$$\mathfrak{W}^{\ominus,\mathrm{eff}} \sim T^{d-1} \lambda_{mn} \left(\lambda_{mm} T + \lambda_{nn} T^{-1} \right)^3 \sim T^{d-1+3x}. \tag{3.109}$$

Here, as in Sec. 3.5.5.1, $x = +1$ obtains in a large parameter region where $\frac{\lambda_{mm}}{\lambda_{nn}} \ll \left(\frac{n_0}{\chi k_B T} \right)^2$, while $x = -1$ results if λ_{nn} is non-zero and dominant in a low-temperature regime where the magnon gap remains negligible.

It is by no means clear *how* the latter regime would be achieved, and if we assume that the $x = +1$ case dominates, then it is interesting to see that $\mathfrak{W}^{\ominus,\mathrm{eff}}$ in Eq. (3.109) scales like T^{d+2}, which is the *same power* of temperature as the magnon contribution to the longitudinal scattering rate in Eq. (3.105).

This scaling is a bit surprising, as we should expect that the transverse is smaller than the longitudinal scattering, since it comes from a higher order term.

To resolve this, we should consider more carefully the relationship of $\mathfrak{W}^{\ominus,\text{eff}}$ to a "skew scattering rate". In particular, one should note that $\mathfrak{W}^{\ominus,\text{eff}}_{n\mathbf{k}n\mathbf{k}'}$ enters the collision term via a *sum* over $\mathbf{k}'$, which converts to an integral over $\mathbf{k}'$ in the thermodynamic limit. Therefore the measure of this integral, which is expected to be dominated by $|\mathbf{k}'| \sim k_B T/v_\text{m}, k_B T/v_\text{ph}$, contributes an additional factor of T^3 (since phonons are always three-dimensional). Thus it would be more correct to estimate the skew scattering rate as

$$\frac{1}{\tau_\text{skew}} \sim T^3 \mathfrak{W}^{\ominus,\text{eff}} \sim T^{d+2+3x}. \tag{3.110}$$

For $x = 1$ and $d = 2$, this scales as T^7 which is indeed small compared to the T^4 predicted in the same regime for the longitudinal scattering.

Additionally, we highlight in Sec. 3.5.6.7, through numerical evaluations, the strong momentum-orientation dependence of $\mathfrak{W}^{\ominus}$.

3.5.5.4 Transverse scattering: thermal Hall resistivity

We would like to emphasize that within any scattering mechanism of phonon thermal Hall effect, the skew scattering rate is a more fundamental measure of chirality of the phonons than the thermal Hall *conductivity*. This is because the Hall conductivity inevitably involves the combination of the skew and longitudinal scattering rates (in the form τ^2/τ_skew), and the longitudinal scattering rate of phonons has many other contributions that do not probe chirality, and may have complex dependence on temperature and other parameters that obscure the skew scattering. The scaling of the temperature dependence of $1/\tau_\text{skew}$ given above is a much more reliable prediction than any corresponding one made for κ_H for this reason, and we do not quote the latter here. Instead, to extract the skew scattering rate, one should look at the thermal Hall *resistivity*, ϱ_H, which is simply proportional to $1/\tau_\text{skew}$, at least in the simplest view where the angle-dependence of the longitudinal scattering does not spoil its cancellation.

We define the thermal Hall resistivity tensor as usual by the matrix inverse, $\boldsymbol{\varrho} = \boldsymbol{\kappa}^{-1}$. In particular, considering the simplest case of isotropic $\kappa^{\mu\mu} \to \kappa_L$ and $\kappa_L \gg \kappa^{\mu\neq\nu}$, one thus has

$$\varrho_H^{\mu\nu} = \frac{\varrho_{\mu\nu} - \varrho_{\nu\mu}}{2} \approx \frac{-\kappa_{\mu\nu} + \kappa_{\nu\mu}}{2\kappa_L^2} = -\frac{\kappa_H^{\mu\nu}}{\kappa_L^2}. \tag{3.111}$$

The quantity $\varrho_H^{\mu\nu}$ is independent of the scale of the longitudinal scattering, in the sense that under a rescaling $D_{n\mathbf{k}} \to \zeta D_{n\mathbf{k}}$, then $\varrho_H^{\mu\nu}$ is unchanged (see indeed Eqs. (3.3,3.5) for an explicit check at leading perturbative order).

As explained before, let us further assume that $D_{n\mathbf{k}} = 1/\tau$ is $(n, \mathbf{k})$—independent, e.g. as if the case if dominated by some extrinsic effects. In that case, we can extract the longitudinal dependence from the transverse conductivity kernel, and redefine $\tilde{K}^H_{n\mathbf{k}n'\mathbf{k}'} = \tau^{-2} K^H_{n\mathbf{k}n'\mathbf{k}'}$ which is now independent of the longitudinal scattering rate τ^{-1}. Besides, to leading order one has simply $K^L_{n\mathbf{k}n'\mathbf{k}'} = \tau e^{\beta\hbar\omega_{n\mathbf{k}}} \delta_{nn'} \delta_{\mathbf{k}\mathbf{k}'}$, from which, assuming $\omega_{n\mathbf{k}} = v_\text{ph}|\mathbf{k}|$ and $N^\text{eq} = n_B$,

we have simply

$$\kappa_L = \tau \frac{\hbar^2}{k_B T^2} \frac{1}{V} \sum_{n\mathbf{k}} e^{\beta\hbar\omega_{n\mathbf{k}}} \left(J^\alpha_{n\mathbf{k}}\right)^2 = \tau c_v \frac{v_{\mathrm{ph}}^2}{3}, \tag{3.112}$$

where by construction the result does not depend on the chosen direction α of the current (for instance $\alpha = x, y, z$). This is the well-known relation between the thermal conductivity κ_L and the thermal capacity

$$c_v = \frac{\partial}{\partial T} \left[\frac{1}{V} \sum_{n\mathbf{k}} N^{\mathrm{eq}}_{n\mathbf{k}} \hbar\omega_{n\mathbf{k}} \right] = k_B \frac{2\pi^2}{5} \left(\frac{k_B T}{\hbar v_{\mathrm{ph}}} \right)^3 \tag{3.113}$$

of the phonon gas. Consequently, Eq. (3.111) evaluates to

$$\varrho_H^{\mu\nu} = -k_B^{-1} \left(\frac{15 v_{\mathrm{ph}}}{2\pi^2} \right)^2 \left(\frac{\hbar}{k_B T} \right)^8 \frac{V}{(2\pi)^6} \sum_{n\mathbf{k}n'\mathbf{k}'} J^\mu_{n\mathbf{k}} \tilde{K}^H_{n\mathbf{k}n'\mathbf{k}'} J^\nu_{n'\mathbf{k}'}. \tag{3.114}$$

This expression does not depend on τ, which justifies studying ϱ_H instead of κ_H. From it and Eq. (3.31), one can readily derive the scaling relation

$$\varrho_H \sim \mathfrak{W}^{\ominus,\mathrm{eff}} \sim T^{d-1+3x}, \tag{3.115}$$

which we check numerically in Sec. 3.5.6.5.

3.5.5.5 Detailed scaling analysis of the longitudinal conductivity

The scaling with temperature described above, obtained by replacing every momentum scale $\hbar v_{\mathrm{m,ph}} k$, $\hbar v_{\mathrm{m,ph}} \underline{k}$, $\hbar v_{\mathrm{m,ph}} p$ by that of the temperature, $k_{\mathrm{B}} T$, are expected to be valid for $\gamma = v_{\mathrm{m}}/v_{\mathrm{ph}}$ of "order one". Here we investigate more carefully the dependence of these quantities on γ when the latter becomes large. Surprisingly, we show below that the prediction of Eq. (3.106) for the high temperature scaling of κ_L breaks down already for $\gamma > 3$, giving way to a continuously variable power law exponent. For the thermal Hall resistivity, we find that the temperature exponent, Eq. (3.115), remains independent of the velocity ratio.

To obtain these results, we analyze the full integral expressions directly, distinguishing momentum and temperature dependencies. Various technical details are provided in Appendix 3.E.4.

To analyze κ_L, we start by writing the expression for the diagonal scattering rate, Eq. (3.93), in dimensionless form, in terms of a scaling parameter $\varkappa$ and dimensionless variable $\tilde{y}$,

$$\varkappa = \frac{\hbar v_{\mathrm{ph}} k}{k_{\mathrm{B}} T}, \quad \tilde{y} = y/k. \tag{3.116}$$

We assume the relevant momentum and energy scales are large compared to any gaps, $\delta_\ell \ll k, k_B T/v_{\mathrm{m}}$, and therefore in the following set $\delta_\ell \to 0$. Then we can

obtain scaling forms,

$$\begin{aligned} c_\eta(y) &= k\,\tilde{c}_\eta(\tilde{y}), && (3.117)\\ \Omega_{\ell,\mathbf{p}^{(\eta)}_{\ell,\mathbf{k}}(y)}, \Omega_{\ell,\mathbf{p}^{(\eta)}_{\ell,\mathbf{k}}(y)-\mathbf{k}} &= v_{\rm m}\,k\,\tilde{\Omega}^{\pm\eta}_\ell(\tilde{y}), && (3.118)\\ \mathcal{B}^{n,\ell,\ell|+s-}_{\mathbf{k};-\mathbf{p}+\mathbf{k}/2} &= k^{3/2}\,\tilde{\mathcal{B}}_{mm}(\tilde{y}) + k^{1/2}\,\tilde{\mathcal{B}}_{mn}(\tilde{y}) + k^{-1/2}\,\tilde{\mathcal{B}}_{nn}(\tilde{y}), \end{aligned}$$

and the precise functional forms of $\tilde{c}_\eta(\tilde{y})$, $\tilde{\Omega}^{\pm\eta}_\ell(\tilde{y})$ and $\tilde{\mathcal{B}}_{\xi\xi'}$ are given in Appendix 3.E.4, Eqs. (3.261-3.269). We find, after making the change of variables in the integral of Eq. (3.93) from y to $\tilde{y}$,

$$D^{(s)}_{n\mathbf{k}}(T) = \sum_{x=-1}^{1} k^{2+2x} \mathrm{F}^{(s)}_x(\varkappa,\gamma,\theta), \tag{3.119}$$

where the scaling functions $\mathrm{F}^{(s)}_x(\varkappa,\gamma,\theta)$ are

$$\begin{aligned} \mathrm{F}^{(s)}_x(\varkappa,\gamma,\theta) \quad &= \frac{(3-s)\mathfrak{a}^2\sinh(\varkappa/2)}{4\pi v_{\rm m}\hbar^2}\int_{-\infty}^{+\infty}\mathrm{d}\tilde{y}\sum_\eta \tilde{\mathrm{f}}^s_\eta(\tilde{y})\tilde{J}^s_D(\tilde{y})\\ &\times\sum_\ell \frac{\tilde{\mathcal{C}}_x(\tilde{y})}{\sinh(\frac{\gamma\varkappa}{2}\tilde{\Omega}^{+\eta}_\ell(\tilde{y}))\sinh(\frac{\gamma\varkappa}{2}\tilde{\Omega}^{-\eta}_\ell(\tilde{y}))}. \end{aligned} \tag{3.120}$$

Here $\tilde{\mathcal{C}}_x(\tilde{y})$ are quadratic combinations of the original $\tilde{\mathcal{B}}_{mm}, \tilde{\mathcal{B}}_{mn}$, and $\tilde{\mathcal{B}}_{nn}$ coefficients given in Appendix 3.E.4. Eq. (3.119) agrees with the scaling behavior given in Eq. (3.105) (with $d = 2$). In Appendix 3.E.4 we derive the behavior of the scaling functions $\mathrm{F}^{(s)}_x$ at small and large $\varkappa$, which will be useful in the following.

The scaling form of the scattering rate is input to the thermal conductivity. To see the implication, we presume for simplicity the total scattering rate $D_{n\mathbf{k}} = \sum_s D^{(s)}_{n\mathbf{k}} + \breve{D}$ is dominated by a single value of x . We note in passing that when the gaps are zero, only one value of s contributes here: $s = -1$ for $\gamma > 1$ (the case of most interest), and $s = 1$ for $\gamma < 1$. Then

$$D_{n\mathbf{k}} = \left(\frac{k_{\rm B}T}{\hbar v_{\rm ph}}\right)^{2+2x}\left(\varkappa^{2+2x}\mathrm{F}_x(\varkappa) + \breve{D}(T)\right). \tag{3.121}$$

Here we defined $\breve{D}(T) = \left(\frac{\hbar v_{\rm ph}}{k_{\rm B}T}\right)^{2+2x}\breve{D}$, which is temperature-dependent. In particular for $x = 0, 1$, it becomes very small at high temperature. Inserting this into Eq. (3.3), turning the sum over $\mathbf{k}$ into an integral, and using spherical coordinates, we obtain

$$\begin{aligned} \kappa^{\mu\mu}_{\rm L} \quad &\sim \quad \frac{k_{\rm B}}{\hbar^2}\left(\frac{\hbar v_{\rm ph}}{k_{\rm B}T}\right)^{2x-1} && (3.122)\\ &\int_0^{+\infty}\mathrm{d}\varkappa\int_0^{\pi}\mathrm{d}\theta\int_0^{2\pi}\mathrm{d}\phi\frac{\hat{k}^\mu\hat{k}^\mu\sin\theta\varkappa^4\sinh^{-2}(\varkappa/2)}{\varkappa^{2x+2}\mathrm{F}_x(\varkappa,\gamma,\theta)+\breve{D}(T)}. \end{aligned}$$

Now we are in a position to investigate the temperature dependence of the conductivity. To simplify the discussion, we restrict the remainder of this section

to the case $x = 1$, since F_1 is the largest contribution when spin-orbit coupling is weak, and is also enhanced at high temperature. First consider the low temperature limit. Then $\check{D}(T)$ becomes large at low T, and we can simply replace the denominator of the integrand in Eq. (3.122) by $\check{D}(T)$. This is just the extrinsic limit in which the constant $\check{D}$ scattering dominates and one recovers the T^3 dependence of the thermal conductivity arising from the phonon heat capacity.

Next we turn to the higher temperature limit. There, the parameter $\check{D}(T)$ becomes small, and might naïvely be neglected. Dropping this term in Eq. (3.122), the sole remaining temperature dependence is in the prefactor, and agrees with what was found earlier in Eq. (3.106) (for $d = 2$). This procedure is valid provided the integral in Eq. (3.122) converges for $\check{D}(T) = 0$. To check this, we must consider the potential divergences at small and large $\varkappa$. At small $\varkappa$, the integrand behaves like $1/(\varkappa^2 \mathrm{F}_1(\varkappa))$. As shown in Sec. 3.E.4, $F_1(\varkappa)$ grows as small $\varkappa$ (see Eq. (3.273)), ensuring there is no divergence. The large $\varkappa$ limit is more problematic. This is because although the $\sinh^{-2}(\varkappa/2)$ factor decays exponentially, the factor F_x in the denominator also decays exponentially. Specifically, we show in Sec. 3.E.4 that Eq. (3.120) implies

$$\mathrm{F}_x(\varkappa, \gamma, \theta) \underset{\varkappa \gg 1}{\sim} \bar{\mathrm{F}}(\gamma, \theta) e^{-\alpha(\gamma,\theta)\varkappa}, \tag{3.123}$$

where the function $\alpha(\gamma, \theta) = \frac{1}{2}(\gamma|\sin\theta| - 1)$ (see Eq. (3.271)), and $\bar{\mathrm{F}}(\gamma, \theta)$ a constant. This implies an exponential *growth* of $1/\mathrm{F}_x$ with $\varkappa$ when $\check{D}$ is neglected. For $\gamma > 3$, the integral becomes divergent for $\check{D} = 0$, and the naïve scaling fails.

To see what happens for $\gamma > 3$, we deduce from the above discussion that the integral in Eq. (3.122) becomes dominated in this case by large $\kappa \gg 1$. Then we approximate $\sinh \frac{\varkappa}{2} \sim e^{\varkappa/2}$, and use the asymptotic form of F_x in Eq. (3.123). We must then distinguish two cases. If $\alpha < 1$, the $\varkappa$ integral converges, even for $\check{D}(T) \to 0$, and we obtain, in the latter limit, $\kappa_{\mathrm{L}} \sim T^{-1}$. When $\alpha > 1$, we must be more careful. Successively performing the changes of variables $u = e^{-\varkappa}$, $u = v\check{D}(T)^{\alpha(\gamma,\theta)^{-1}}$ and $v = w[-\alpha(\gamma, \theta)^{-1} \ln \check{D}(T)]^{-\alpha(\gamma,\theta)^{-1}}$, and a saddle-point procedure assuming $\alpha > 1$, we arrive at (see Appendix 3.E.4)

$$\kappa_{\mathrm{L}} \sim \frac{1}{T} \check{D}(T)^{\alpha_0^{-1}-1} \left(-\alpha_0^{-1} \ln \check{D}(T)\right)^{4-\alpha_0^{-1}} I_0(\gamma) \tag{3.124}$$

where $\alpha_0(\gamma) = \alpha(\gamma, 0) = (\gamma - 1)/2 > 1$, $I_0(\gamma) = \int_0^{+\infty} \mathrm{d}w \frac{1}{w^{\alpha_0 F_0(\gamma,0)+1}}$. This entails, up to logarithmic corrections,

$$\kappa_{\mathrm{L}} \sim \begin{cases} T^{-1} & \text{for } \gamma < 3 \\ T^{3-8(\gamma-1)^{-1}} & \text{for } \gamma > 3 \end{cases}. \tag{3.125}$$

We see that the $1/T$ high-temperature behavior of κ_{L} changes for $\gamma > 3$ to a power law with an exponent that continuously depends upon γ, and even changes sign: for $\gamma > 11/3$, the conductivity *increases* with increasing temperature at high T. We indeed recover this nontrivial feature numerically, see Fig. 3.5.3.

Note that this behavior is all obtained within the linearized phonon and magnon models, and thus eventually changes when the temperature exceeds for example the Debye energy.

3.5.6 Numerical results

3.5.6.1 Implementation

Details about the numerical implementation are given in Appendix 3.E.3. In short, we use C together with *(i)* the Cubature library to perform the one-dimensional momentum integrals (appearing in the definitions of $D^{(1)|s}_{n\mathbf{k}}$, Eq. (3.93)), *(ii)* the Cuba library [Hahn, 2005] to perform multi-dimensional integrals (in $\kappa^{\mu\mu}_L$, Eq. (3.3), and in $\varrho^{\mu\nu}_H$, Eq. (3.114)).

3.5.6.2 Choice of parameters

(i) Polarization vectors In Eq. (3.85), $\mathcal{L}$ is the trace over the product of the coupling matrix $\boldsymbol{\lambda}$, with matrix elements $\lambda^{\alpha\beta}$, and that, $\boldsymbol{\mathcal{S}}$, which determines the structure of the strain tensor and has matrix elements

$$\mathcal{S}^{q;\alpha\beta}_{n\mathbf{k}} = \frac{k^\alpha(\varepsilon^\beta_{n\mathbf{k}})^q + k^\beta(\varepsilon^\alpha_{n\mathbf{k}})^q}{\sqrt{\omega_{n\mathbf{k}}}}. \tag{3.126}$$

Values of $(n,\mathbf{k})$ such that this factor vanishes correspond to phonons which are not coupled to the magnons, and whose longitudinal conductivity is solely driven by $\breve{D}_{n\mathbf{k}}$, i.e. other scattering effects. While this may indeed happen in practice, to highlight the effects of phonon-magnon scattering we choose a basis of polarization vectors $(\boldsymbol{\varepsilon}_{0,\mathbf{k}}, \boldsymbol{\varepsilon}_{1,\mathbf{k}}, \boldsymbol{\varepsilon}_{2,\mathbf{k}})$ such that this is never the case (at least for $\alpha = \beta$, as with $\Lambda_{1..5}$ which are much larger than $\Lambda_{6,7}$).

These polarization vectors enforce $\boldsymbol{\varepsilon}_{n,-\mathbf{k}} = \boldsymbol{\varepsilon}^*_{n\mathbf{k}} = -\boldsymbol{\varepsilon}_{n\mathbf{k}}$ (so that $\mathcal{S}^{q;\alpha\beta}_{n,-\mathbf{k}} = \mathcal{S}^{q;\alpha\beta}_{n\mathbf{k}} = -\mathcal{S}^{-q;\alpha\beta}_{n\mathbf{k}}$) as well as the tetragonal symmetry of the crystal, as required by the general theory of elasticity [Maradudin and Vosko, 1968]; explicit expressions are given in App. 3.E.2.2.

(ii) Extrinsic phonon scattering rate For similar reasons, the extrinsic phonon scattering rate is taken to be $\breve{D}_{n\mathbf{k}} \to \gamma_{\text{ext}}$, a constant independent of $(n,\mathbf{k})$ and small compared with the typical $D_{n\mathbf{k}}$ as soon as $T > T^\star_\Delta$ (see Sec. 3.5.5.2). In very clean monocrystals and in the absence of any other phonon scattering events, $\gamma_{\text{ext}} \sim v_{\text{ph}}/L$ reduces to the rate at which phonons bounce off the boundaries of the sample (of size L).

(iii) Phonon dispersion The phonon dispersion relation is chosen linear, n-independent and isotropic, $\omega_{n\mathbf{k}} = v_{\text{ph}}|\mathbf{k}|$, so that the different regimes of scaling exponents x appear clearly.

3.5.6.3 Units and numerical values

We express our numerical results in units where $\hbar^{\text{code}} = 1$, $k_B^{\text{code}} = 1$, $v_{\text{ph}}^{\text{code}} = 1$ and with unit lattice spacing $\mathfrak{a}^{\text{code}}$. Then, the mass of the unit cell M_{uc} is expressed in units of $M_0 = \frac{\hbar}{v_{\text{ph}}\mathfrak{a}}$ and is typically large—of the order $M_{\text{uc}} \sim 10^4 M_0$. T is expressed in units of $T_0 = \frac{\hbar v_{\text{ph}}}{\mathfrak{a}k_B}$ and should verify $T/T_0 \lesssim 1$ so that the

assumption of linearly dispersing phonons is correct. Correspondingly, we can define an energy $\epsilon_0 = k_B T_0$, and the isotropic part of the exchange J is expressed in units of ϵ_0.

The magnon velocity is fixed according to linear spin wave theory, which gives $v_m = 2\sqrt{d}JS\mathfrak{a}/\hbar$, with J the isotropic magnetic exchange constant. We take $d = 2$ and $S = 1/2$; moreover, it is known that for $S = 1/2$ there is a renormalization factor $Z \approx 1.2$ enhancing the velocity, so that $v_m/v_{ph} = \sqrt{2}ZJ/\epsilon_0 \approx 1.7J/\epsilon_0$ in our units. Since, for isotropic exchange, $\chi = \frac{1}{4\mathfrak{a}^2 J}$, we also take $\chi^{-1}_{\text{code}} = 4(J/\epsilon_0)$.

Spin-phonon couplings $\Lambda_{1..7}$ are expressed in units of $\epsilon_0/\mathfrak{a} = \hbar v_{ph}/\mathfrak{a}^2$. We describe a possible microscopic mechanism for spin-strain coupling in App. 3.F.1, where we show that $\Lambda_{1..5}$ typically arise as derivatives of the isotropic magnetic exchange constants. Since the latter ultimately arises from the overlap of atomic wavefunctions, which vary over distances of the order a_B the Bohr radius, we expect $\Lambda_{1..5} \sim J/a_B$. Meanwhile $\Lambda_{6,7}$ come from anisotropic exchanges and are thus expected to be considerably smaller.

Since the differences $\Lambda^{(\xi)}_{1,2} - \Lambda^{(\xi)}_3$ and $\Lambda^{(\xi)}_4 - \Lambda^{(\xi)}_5$ are due to anisotropic exchanges, they are chosen a fraction of a $\Lambda^{(\xi)}_{1..5}$. Since these magnetoelastic couplings typically arise as derivatives of magnetic exchange, we also take $\Lambda^{(m)}_i \approx -\Lambda^{(n)}_i$ for $i = 1..7$; see App. 3.F.1 for a detailed derivation.

Scattering rates $D_{n\mathbf{k}}$ and γ_{ext} are expressed in units of $\gamma_0 = v_{ph}/\mathfrak{a}$, and we assume γ_{ext} to be small, of the order of $1/L$ with L the size of the sample—typically $\gamma_{ext} \sim 10^{-7} v_{ph}/\mathfrak{a}$. Finally, thermal conductivities are expressed in units of $\kappa_0 = k_B v_{ph}/\mathfrak{a}^2$.

For numerical calculations, we kept most dimensionless materials parameters (e.g. the ratio of v_m and v_{ph}) fixed and constant, with the values given in Table 3.5.4. Those parameters for which we explore a given range of values are given in the captions of the figures in the following subsections. The fixed values are loosely inspired by Copper Deuteroformate Tetradeuterate (CFTD), a square lattice S=1/2 antiferromagnet which has been intensively studied via neutron scattering [Christensen et al., 2007, Dalla Piazza et al., 2015, Rønnow et al., 2001] due to its convenient scale of exchange which suits such measurements. For our purposes, CFTD has the desirable attribute that the magnon and phonon velocities are comparable (based on an estimate of the sound velocity from the corresponding hydrate [Kameyama et al., 1973]), which creates a significant phase space for magnon-phonon scattering. By contrast, in La_2CuO_4, v_m is much larger than v_{ph}.

v_0	$\mathfrak{a}_0$	γ_0	M_0	T_0	ϵ_0	χ_0^{-1}	Λ_0	κ_0
v_{ph}	$\mathfrak{a}$	$\frac{v_{ph}}{\mathfrak{a}}$	$\frac{\hbar}{v_{ph}\mathfrak{a}}$	$\frac{\hbar v_{ph}}{\mathfrak{a} k_B}$	$k_B T_0$	$\epsilon_0 \mathfrak{a}^2$	$\frac{\epsilon_0}{\mathfrak{a}}$	$\frac{k_B v_{ph}}{\mathfrak{a}^2}$

Table 3.5.3: Table of units of velocity v_0, distance $\mathfrak{a}_0$, rate γ_0, mass M_0, temperature T_0, energy ϵ_0, inverse susceptibility χ_0^{-1}, coupling Λ_0 and thermal conductivity κ_0 used in Table 3.5.4.

$v_{\rm m}$	$v_{\rm ph}$	χ^{-1}	n_0	$\mathfrak{a}$	$M_{\rm uc}$	m_0^x	m_0^y	m_0^z	Δ_0	Δ_1
υ	1.0	2.08υ	1/2	1.0	$8 \cdot 10^3$	0	0.0 0.05	0.05 0.0	0.2	0.04

ξ	$\Lambda_1^{(\xi)}$	$\Lambda_2^{(\xi)}$	$\Lambda_3^{(\xi)}$	$\Lambda_4^{(\xi)}$	$\Lambda_5^{(\xi)}$	$\Lambda_6^{(\xi)}$	$\Lambda_7^{(\xi)}$
n = 0	4.8υ	4.0υ	5.6υ	4.0υ	4.8υ	0.24υ	0.32υ
m = 1	-4.0υ	-4.8υ	-5.6υ	-4.8υ	-4.0υ	-0.32υ	-0.24υ

Table 3.5.4: Numerical values of the fixed parameters used in all numerical evaluations, expressed in the units given in Table 3.5.3. The upper and lower entries for m_0^y and m_0^z correspond to the two cases for calculating ϱ_H^{xy} and ϱ_H^{xz}, respectively. $\upsilon = \gamma = v_{\rm m}/v_{\rm ph}$ is a dimensionless multiplier used to reproduce the effect of a varying magnetic exchange scale, which mainly impacts $v_{\rm m}, \chi, \Lambda_i^{\xi}$. In the plots, we use the values $\upsilon = 2.5, 5, 10$.

Finally, note that the following scaling relations for κ_L,

$$\kappa_L\left(\{\Lambda^{(\xi)}_{1,..,7}\}, \gamma_{\rm ext}\right) = \zeta_0^2\ \kappa_L\left(\{\zeta_0\Lambda^{(\xi)}_{1,..,7}\}, \zeta_0^2\gamma_{\rm ext}\right), \tag{3.127}$$

and for ϱ_H,

$$\begin{aligned}\varrho_H&\left(\{\Lambda^{(\xi)}_{1,..,5}\}, \{\Lambda^{(\xi)}_{6,7}\}, m_0^{y,z}\right)\\ &= \zeta_1^{-3}\zeta_2^{-1}\zeta_3^{-1}\varrho_H\left(\{\zeta_1\Lambda^{(\xi)}_{1,..,5}\}, \{\zeta_2\Lambda^{(\xi)}_{6,7}\}, \zeta_3 m_0^{y,z}\right)\\ &\quad + O\left((m_0^{y,z})^3(\Lambda^{(\xi)}_{6,7})^3\right),\end{aligned} \tag{3.128}$$

hold for any rescaling factors $\zeta_{0,..,3}$. Eqs. (3.127,3.128) make it possible to extrapolate results from our calculations for values of the parameters which are not explicitly explored in Table 3.5.4 and Figs. 3.5.5(a), 3.5.5(b), 2.3(a), and 2.3(b).

3.5.6.4 Results for κ_L

Numerical results for $\kappa_L(T)$ are displayed in Figs. 3.5.1, 3.5.2 at fixed $\upsilon = \gamma = v_{\rm m}/v_{\rm ph} = 2.5$.

Fig. 2.3(a) shows plots of $\kappa_L(T)$ for several values of the extrinsic scattering $\gamma_{\rm ext}$ fixed $\upsilon = \gamma = v_{\rm m}/v_{\rm ph} = 2.5$. This figure exhibits all the behaviors described in Secs. 3.5.5.1, 3.5.5.2, with the extra feature that here there are two crossovers temperatures, $T^\star_{\Delta,0}$ and $T^\star_{\Delta,1}$ defined by the two different magnon gaps Δ_0, Δ_1 whose values we give in Tab. 3.5.4. These are more clearly visible in Fig. 2.3(b), where we show $\kappa_L(T)$ in a small window of low temperatures and for smaller values of $\gamma_{\rm ext}$.

Four scaling regimes can then be identified:

(i) For $T \lesssim T^\star_{\Delta,1}$, only extrinsic scattering contributes to the full phonon scattering rate, and $\kappa_L \propto T^3/\gamma_{\rm ext}$.

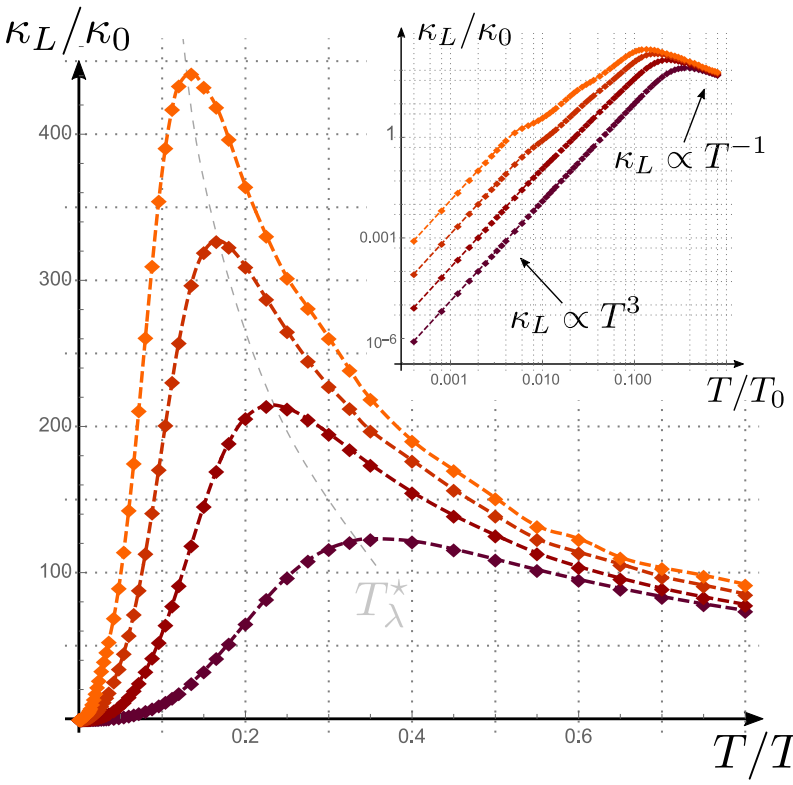

Figure 3.5.1: Longitudinal thermal conductivity κ_L (in units of $\kappa_0 = k_B v_{ph}/\mathfrak{a}^2$) with respect to temperature T (in units of $T_0 = \hbar v_{ph}/(\mathfrak{a} k_B)$), for four different values of γ_{ext}. $\gamma_{ext} = 1 \cdot 10^{-z}(v_{ph}/\mathfrak{a}), z \in [\![4, 7]\!]$, from darker ($z = 4$) to lighter ($z = 7$) shade. The dashed gray line indicates the evolution of the crossover temperature $T^\star_\lambda$ as a function of γ_{ext}. Inset: log-log plot; the scaling behaviors are consistent with the analysis presented in the text. The inset is reproduced in App. 3.G.

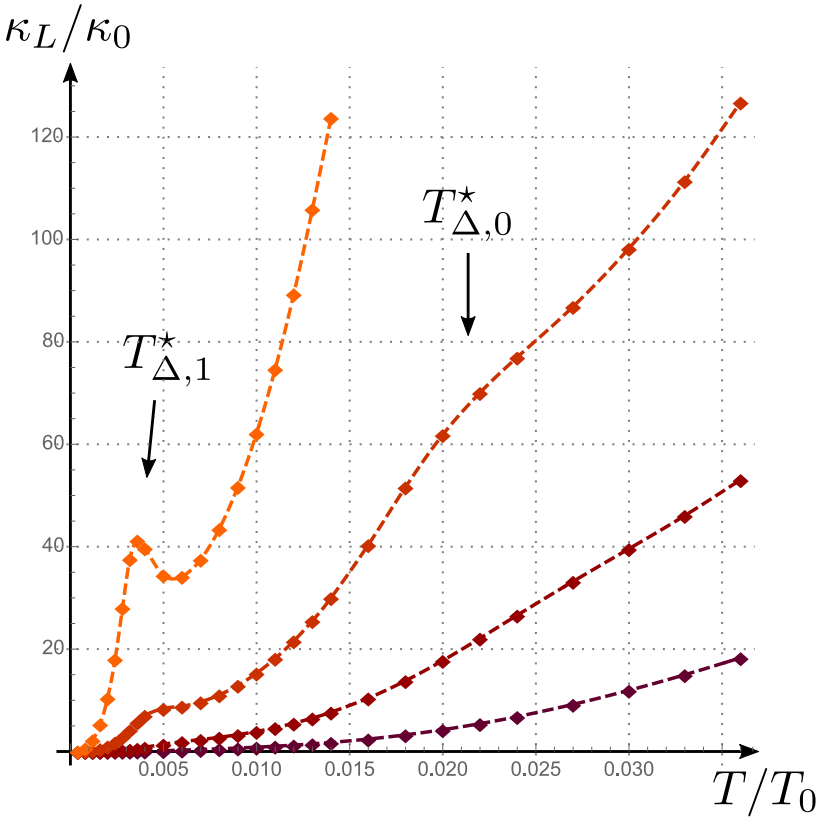

Figure 3.5.2: Longitudinal thermal conductivity κ_L (in units of $\kappa_0 = k_B v_{ph}/\mathfrak{a}^2$) with respect to temperature T (in units of $T_0 = \hbar v_{ph}/(\mathfrak{a} k_B)$), for four different values of γ_{ext}. $\gamma_{ext} = 1 \cdot 10^{-z}(v_{ph}/\mathfrak{a}), z \in [\![6, 9]\!]$, from darker ($z = 6$) to lighter ($z = 9$) shade. The two crossover temperatures $T^\star_{\Delta,1}$ and $T^\star_{\Delta,0}$ are defined in the text up to a prefactor; here we identify the corresponding features in κ_L but do not indicate specific values of T. See App. 3.G for a log-log plot.

(ii) For $T^\star_{\Delta,1} \lesssim T \lesssim T^\star_{\Delta,0}$, both the extrinsic and the $x = -1$ phonon-magnon (only in the $\ell = 1$ valley) scattering rates contribute with the same scaling exponent, yielding $\kappa_L \propto T^3$ with a smaller proportionality coefficient than in the first regime.

(iii) For $T^\star_{\Delta,0} \lesssim T \lesssim T^\star_\lambda$, both the extrinsic and the $x = -1$ phonon-magnon (now in both valleys) scattering rates contribute with the same scaling exponent, yielding $\kappa_L \propto T^3$ with yet a smaller proportionality coefficient.

(iv) For $T > T^\star_\lambda$, the $x = +1$ phonon-magnon scattering rate is dominant and yields $\kappa_L \propto T^{-1}$. Note that $T^\star_\lambda$ is defined in Eq. (3.107) in the $\breve{D}_{n\mathbf{k}} = 0$ case; here by $T^\star_\lambda$ we mean the more general crossover temperature in the presence of a finite $\breve{D}_{n\mathbf{k}} = \gamma_{\rm ext}$.

The exponents quoted above are found with very good accuracy from a log-log scale plot (see inset of Fig. 2.3(a) and Appendices), regardless of the value of $\gamma_{\rm ext}$; in that sense these exponents are universal. The influence of (non-universal) $\gamma_{\rm ext}$ on the results of Fig. 2.3(a) is essentially threefold:

- Since the full phonon scattering rate is $D_{n\mathbf{k}} = \gamma_{\rm ext} + D^{(1)}_{n\mathbf{k}}$, unsurprisingly $\kappa_L(T)$ is always a decreasing function of $\gamma_{\rm ext}$.
- The "bumps" at $T \sim T^\star_{\Delta,\ell}$ come from the fact that the $x = -1$ phonon-magnon scattering rate is much larger than $\gamma_{\rm ext}$ as soon as the gap permits this scattering process; therefore, for large enough $\gamma_{\rm ext}$, this feature disappears. More precisely, one should compare $\gamma_{\rm ext}$ with $D_{nn,\ell} := \eta^2 f^2 \Delta_\ell / M_{\rm uc}$, where the dimensionless parameters η, f are defined by $\lambda_{nn} \simeq \eta \lambda_{mm}$ and $\Lambda_{1..5} \simeq fJ/\mathfrak{a}$. The first bump is noticeable iff $\gamma_{\rm ext} \lesssim D_{nn,1}$, and the second bump is noticeable iff $\max(\gamma_{\rm ext}, D_{nn,1}) \lesssim D_{nn,0}$.
- Since $\gamma_{\rm ext}$ and the λ_{nn} coupling lead to the same scaling exponent, the $T \sim T^\star_\lambda$ crossover results from a competition between λ_{mm} on the one hand and $(\gamma_{\rm ext}, \lambda_{nn})$ on the other; thus the larger $\gamma_{\rm ext}$, the greater the dependence of $T^\star_\lambda$ on $\gamma_{\rm ext}$, and $T^\star_\lambda(\gamma_{\rm ext})$ is an increasing function of $\gamma_{\rm ext}$.

Finally, Fig. 3.5.3 shows plots of $\kappa_L(T)$ for several values of the velocity ratio $v_{\rm m}/v_{\rm ph} = \gamma = \upsilon$ at fixed $\gamma_{\rm ext} = 10^{-6}$. In particular, we recover, at $T \gg T^\star_\lambda$, the particularly non-trivial behavior described in Sec. 3.5.5.5; namely that for all γ values greater than $\gamma = 3$ the high-temperature behavior of $\kappa_{\rm L}$ goes like $T^{3-8(\gamma-1)^{-1}}$ (Eq. (3.125)) and the exponent indeed changes signs at $\gamma = 11/3$, i.e. the conductivity *increases* with increasing temperature for $\gamma > 11/3$.

3.5.6.5 Results for ϱ_H

We evaluated numerically $\varrho_H^{\mu\nu}$ for both $\mu\nu = xy$ and xz, in both cases with a net magnetization $\boldsymbol{m}_0$ oriented along ρ, the axis perpendicular to the Hall plane $\mu\nu$. Results are presented in Fig. 3.5.4. Here the dashed straight lines on the double logarithmic scale indicate the expected T^4 scaling.

This behavior is consistent with the arguments given in Sec. 3.5.5.4, especially Eq. (3.115), with $d = 2$-dimensional magnons and scaling exponent $x = +1$, corresponding to the temperature regime where isotropic exchange dominates over the phonon-magnon coupling. We expect from Eq. (3.109) that deviations from this scaling behavior would be observed at lower temperatures, not investigated here.

We emphasize that the numerical values of ϱ_H^{xy} and ϱ_H^{zx} are of the same order of magnitude. This is remarkable in a layered system which has entirely different magnon dynamics in the xy and xz planes, in this case where magnons are explicitly two-dimensional, carrying energy only within xy layers. It can be understood from the fact that here *phonons* are isotropic, carrying energy in all three directions, and that *including* $\mathcal{T}$-odd scattering exists in all directions, therefore allowing a Hall effect in both the xy and xz directions.

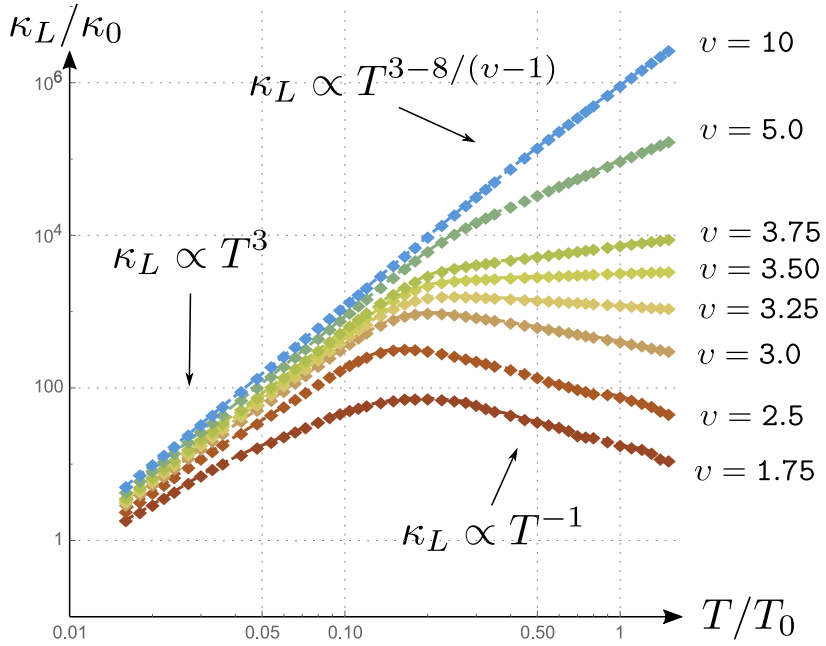

Figure 3.5.3: Dependence upon $\upsilon = v_{\rm m}/v_{\rm ph}$ of the longitudinal conductivity as a function of temperature, in log-log scale, for $\gamma_{\rm ext} = 10^{-6}$. We highlight the change of scaling behaviors for $T > T_\lambda^\star$ at $v_{\rm m}/v_{\rm ph} = 3$, above which the temperature scaling exponent of $\kappa_{\rm L}$ is a continuous function of $v_{\rm m}/v_{\rm ph}$, see Eq. (3.125).

Numerically evaluating the dependence on $v_{\rm m}/v_{\rm ph} = \gamma$ of $\varrho_{\rm H}$, we find that $|\varrho_H^{xy}/\varrho_H^{xz}| < 1$ for all the values of γ studied, and that the prefactors of $\varrho_H^{xy}, \varrho_H^{xz}$ are rapidly suppressed for large γ, as shown in Fig. 3.5.4. From a simple analysis, we expect $|\varrho_H^{xy}/\varrho_H^{xz}| \propto 1/\gamma$ for large γ. The reason for the overall suppression of the Hall resistivity with increasing γ is also clearly due to the diminishing phase space for scattering, but we have not obtained the exact dependence analytically.

Finally, we note that for our *choice* of antiferromagnetic order along the $\hat{x}$-axis in this model and within linearized spin-wave theory, $\varrho_H^{yz} = 0$.

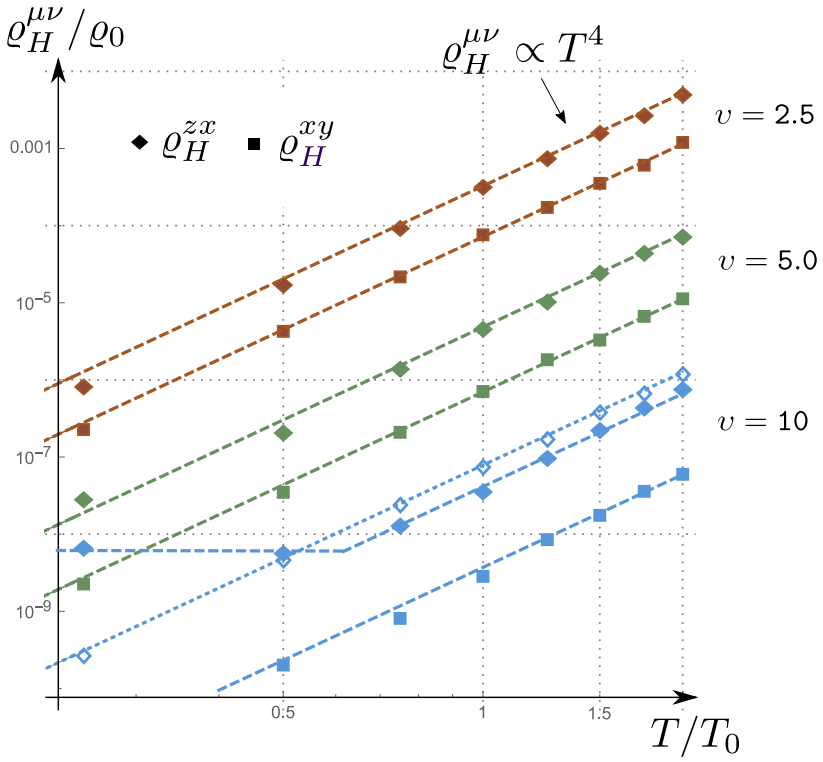

Figure 3.5.4: Hall resistivities $\varrho_{\rm H}^{xy}(T)/\varrho_0$ and $\varrho_{\rm H}^{xz}(T)/\varrho_0$ for three values of $v_{\rm m}/v_{\rm ph}$. The low temperature saturation of $\varrho_{\rm H}^{xz}(T)/\varrho_0$ observed for $v = 10$ is due to the non-negligible contributions of the λ_{nn} term in that range. This is confirmed by the data shown in empty blue diamonds, which is the result of calculations at the same value of $v_{\rm m}/v_{\rm ph} = 10$ and approximately the same coupling constants as the full blue diamonds, except that $\lambda_{nn} = 0$ there (the values of λ_{mm} are also slightly different but, importantly, the values of λ_{mn} are unchanged).

3.5.6.6 Results for $D_{n\mathbf{k}}$

Fig. 3.5.5(a) shows the angular dependence of $D_{n\mathbf{k}}$. Throughout this section, we use $\underline{\mathbf{k}} = \underline{k}(\cos\phi\hat{\mathbf{u}}_x + \sin\phi\hat{\mathbf{u}}_y)$, with $\phi \in [0, 2\pi[$, and $k_z = k\cos\theta$ with $\theta \in [0, \pi]$. Note that, in turn, $\underline{k}^2 = k^2 \sin^2\theta$. Also, since all the results are invariant under $k_z \to -k_z$ i.e. $\theta \to \pi - \theta$, we plot results for $\theta \in [0, \pi/2]$ only.

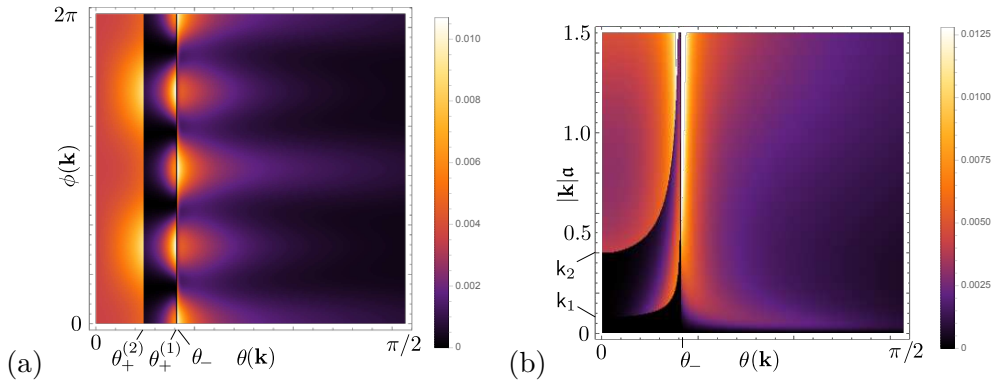

Figure 3.5.5: Diagonal scattering rate $D^{(1)}_{n\mathbf{k}}/\gamma_0$ at fixed temperature $T = 0.5T_0$ and in polarization $n = 0$. (a) as a function of $\theta(\mathbf{k}) = \arccos(k_z/|\mathbf{k}|) \in [0, \pi/2]$ (horizontal axis) and $\phi(\mathbf{k}) = \mathrm{Arg}(k_x + \mathrm{i}k_y) \in [0, 2\pi]$ (vertical axis) for fixed $|\mathbf{k}| = 0.5/\mathfrak{a}$. (b) as a function of $\theta(\mathbf{k}) = \arccos(k_z/|\mathbf{k}|) \in [0, \pi/2]$ (horizontal axis) and $|\mathbf{k}|\mathfrak{a}$ (vertical axis) for fixed $\phi(\mathbf{k}) = 0$. Other parameter values are explored in App. 3.G.

(i) In-plane $\phi(\mathbf{k})$ angular dependence. We see from Fig. 3.5.5(a) that phonon-magnon scattering is typically larger for values of $\phi(\mathbf{k})$ associated with high-symmetry axes of the system, i.e. $\phi = 0 \bmod[\pi/2]$. This is inherited from the structure of $\mathcal{L} = \mathrm{Tr}[\boldsymbol{\lambda}^T \boldsymbol{\mathcal{S}}]$ in Eq. (3.85), which enters the magnetoelastic coupling, Eq. (3.73). The latter is by definition invariant under all symmetries of the crystal, so that components of the strain tensor couple to functions of the magnetization fields $\boldsymbol{m}, \boldsymbol{n}$ with the same symmetries.

Now, while the symmetry group of the crystal structure is tetragonal, the C_4 symmetry is spontaneously broken by the antiferromagnetic order along the x axis, while the C_2 and mirror symmetries are preserved when the magnetic field is along the z axis. More precisely, *how* does the C_4 symmetry (as acting on the α, β indices) break? Since the $\boldsymbol{\mathcal{S}}$ factor in Eq. (3.85) has the same structure as the strain tensor itself, it preserves C_4; therefore the latter can only be broken in the $\boldsymbol{\lambda}$ factor. Let us focus on the $\lambda_{mm}, \lambda_{nn}$ cases, since these coefficients can be nonzero in the absence of a net magnetization m_0. A broken C_4 symmetry then means that $0 \neq \lambda'_{\xi,a} := \lambda^{xx}_{aa;\xi\xi} - \lambda^{yy}_{aa;\xi\xi}$. By inspection of Eqs. (3.74) and (3.78), one sees that there are two ways the latter can be nonzero: *(1)* in the ($\xi = \mathrm{n}$) channel, $\lambda'_{\mathrm{n},a}$ is proportional to anisotropic exchanges; and *(2)* in the ($\xi = \mathrm{m}$) channel, $\lambda'_{\mathrm{m},a}$ contains both isotropic and anisotropic exchange constants, and is consequently much larger than $\lambda'_{\mathrm{n},a}$. From this analysis, it follows that the

deviation from C_4 symmetry as captured in $D^{(1)}_{n\mathbf{k}}$ by $\lambda'_{\xi,a}$ is largest for values of $|\mathbf{k}|$ where the λ_{mm} contributions dominate over the λ_{nn} ones, i.e. at large $|\mathbf{k}|$ (recall Eq. (3.104)). One can check that this is indeed the case, as is shown in Appendix 3.G.

(ii) Out-of-plane $\theta(\mathbf{k})$ angular dependence. The out-of-plane angular dependence illustrates quite clearly the dynamical constraints satisfied by $D_{n\mathbf{k}}$, as outlined in Sec. 3.5.2.2. By inspection of Eq. (3.67), we define

$$\theta_- = \arctan\left(v_{\rm ph}^{-1}\sqrt{v_{\rm ph}^2 - v_{\rm m}^2}\right), \tag{3.129}$$

$$\theta_+^{(1)}(|\mathbf{k}|) = \arcsin\left(v_{\rm m}^{-1}\sqrt{v_{\rm ph}^2 - 4\Delta'/|\mathbf{k}|^2}\right), \tag{3.130}$$

$$\theta_+^{(2)}(|\mathbf{k}|) = \arcsin\left(v_{\rm m}^{-1}\sqrt{v_{\rm ph}^2 - 4\Delta/|\mathbf{k}|^2}\right), \tag{3.131}$$

where $\Delta' = \max(\Delta_0, \Delta_1)$. Note that outside the domain of definition of $\sqrt{\dots}$, by continuity one fixes $\theta_+^{(1,2)} := 0$. The figure Fig. 3.5.5(a) can then be divided in four areas as follows:

- The vertical black band at angles $\theta(\mathbf{k}) \in [\theta_+^{(1)}(|\mathbf{k}|), \theta_-]$ corresponds to values of $(k_z, |\underline{\mathbf{k}}|)$ such that energy and momentum conservation cannot be satisfied simultaneously because of the magnon gap Δ; therefore $D^+_{n\mathbf{k}} = 0 = D^-_{n\mathbf{k}}$.
- For angles $\theta(\mathbf{k}) > \theta_-$, scattering of the "ph+m $\to$ m" type becomes possible, i.e. $D^- > 0$. Meanwhile, following Eq. (3.67), $D^+ = 0$.
- Conversely, for $\theta(\mathbf{k}) < \theta_+^{(2)}(|\mathbf{k}|)$, scattering of the "ph $\to$ m+m" type becomes possible, i.e. $D^+ > 0$, while $D^- = 0$.
- For $\theta \in [\theta_+^{(2)}, \theta_+^{(1)}]$, scattering of the "ph $\to$ m+m" type is possible only in the valley with the smallest gap, while in the other no scattering can happen; therefore, in that region $D^+ > 0$ but its value drops (without vanishing a priori) at the interface $\theta(\mathbf{k}) = \theta_+^{(2)}(|\mathbf{k}|)$.

(iii) Dependence on $|\mathbf{k}|$. In Fig. 3.5.5(b), we show the dependence of $D_{n\mathbf{k}}$ as a function of the norm $|\mathbf{k}|$ and the out-of-plane angle θ. This plot displays divergences near the singular lines $\theta_+^{(1,2)}, \theta_-$, which can be attributed to the thresholds for magnon scattering just above the gaps.

The angular width $\delta\theta(\mathbf{k})$ of the two black and darker regions bounded from the right by θ_-, where scattering is forbidden in at least one of the two valleys, varies with $|\mathbf{k}|$. From Eq. (3.67), we see that this width scales like $\delta\theta \sim (\Delta_\ell / v_{\rm ph}|\mathbf{k}|)^2$. These regions extend down to $|\mathbf{k}| = 0$, reflecting the fact that phonons with too little energy are unable to excite magnon pairs. The momentum magnitude thresholds for the excitation of magnon pairs are naturally given by $\mathsf{k}_1 = 2\Delta/v_{\rm ph}$ and $\mathsf{k}_2 = 2\Delta'/v_{\rm ph}$.

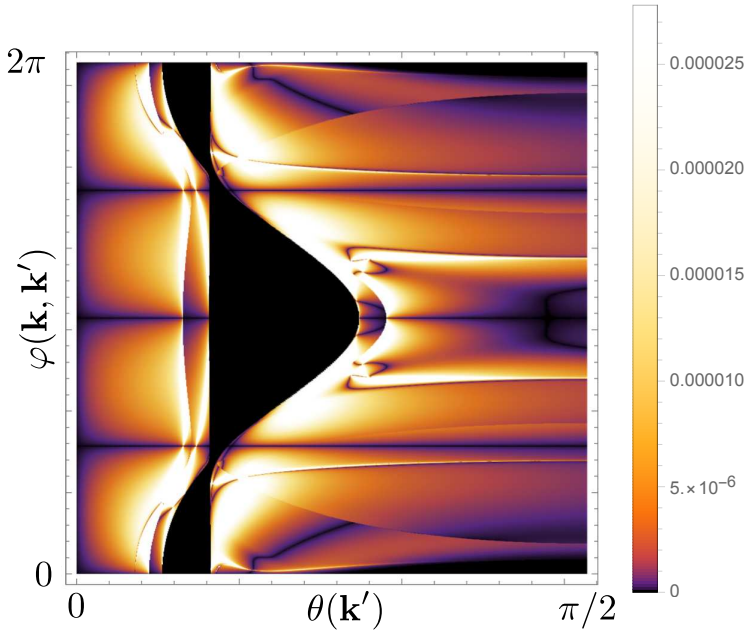

Figure 3.5.6: Skew-scattering rate $\mathfrak{W}^{\ominus,--}_{n\mathbf{k}n'\mathbf{k}'}/\gamma_0$ as a function of $\theta(\mathbf{k}') \in [0, \pi/2]$ (horizontal axis) and $\varphi(\mathbf{k}, \mathbf{k}') = \phi(\mathbf{k}') - \phi(\mathbf{k})$ (vertical axis) for fixed $|\mathbf{k}'| = 0.8/\mathfrak{a}$, $k_x = 0$, $k_y = 0.2/\mathfrak{a}$, $k_z = 0.1/\mathfrak{a}$, $\boldsymbol{m}_0 = 0.05\,\hat{\boldsymbol{z}}$ and temperature $T = 0.5\,T_0$. Other parameter values are explored in App. 3.G. Note that the colorbar is not scaled linearly.

3.5.6.7 Results for $\mathfrak{W}^{\ominus}_{n\mathbf{k}n'\mathbf{k}'}$

Although the angular dependences of the $\mathfrak{W}^{\ominus,qq'}_{n\mathbf{k}n'\mathbf{k}'}$ skew-scattering rates are more intricate than those of $D_{n\mathbf{k}}$, a few general remarks can be made. In particular, in Fig. 3.5.6, where we plot $\mathfrak{W}^{\ominus,-+}$ as a function of θ and φ at fixed $|\mathbf{k}'| = 0.8/\mathfrak{a}$, $k_x = 0.2/\mathfrak{a}$, $k_y = 0$, $k_z = 0.1/\mathfrak{a}$ (and temperature $T = 0.5T_0$), we have:

- Although $k_z \neq 0$, we can still take advantage of the $k'_z \leftrightarrow -k'_z$ symmetry, and it is sufficient to consider $\theta(\mathbf{k}') \in [0, \pi/2]$. This comes from the fact that, for purely planar magnons, the phonon momenta k_z, k'_z are not coupled. Meanwhile there is a priori no $\varphi(\mathbf{k}, \mathbf{k}') \leftrightarrow -\varphi(\mathbf{k}, \mathbf{k}')$ symmetry except when $\underline{\mathbf{k}}$ is along one of the high-symmetry axes of the crystal, as is the case here (cf. $k_y = 0$).

- The vertical black line at $\theta(\mathbf{k}') = \theta_-$ can still be identified, and corresponds to magnons being gapped as in $D^{(1)}_{n\mathbf{k}}$. However, in $\mathfrak{W}^{\ominus}$, the width and position of the gapped (black) zone now depend also on $\varphi(\mathbf{k}, \mathbf{k}')$, due to the second energy conservation constraint in $\mathfrak{W}^{\ominus}$ (a feature absent in $D^{(1)}$ where there is only one energy constraint).

- In Appendix 3.G, we explore other orientations of in-plane (k_x, k_y), and show that the features of $\mathfrak{W}^{\ominus,qq'}_{n\mathbf{k}n'\mathbf{k}'}$ quoted above still hold. This is consistent with the above observations being consequences of the energy conservation constraints, which depend only of the *relative* angle $\phi(\mathbf{k}) - \phi(\mathbf{k}')$ since both phonon and magnon dispersions are isotropic in the xy plane.

- In Fig. 3.5.6, $\mathfrak{W}^{\ominus,-+}_{n\mathbf{k}n'\mathbf{k}'}$ also seems to vanish along certain special lines, especially those located at $\varphi(\mathbf{k}, \mathbf{k}') = 0, \pi/2, \pi, 3\pi/2, 2\pi$. These features are *not* independent of the orientation $\phi(\mathbf{k})$; in fact they are salient features of the in-plane momenta being along the high-symmetry axes of the crystal. Thus, they do not result from energy conservation constraints, but from subtle effects in the structure of Eq. (3.69).

Finally, we point out that the values of $\mathfrak{W}^{\ominus}$ in Fig. 3.5.6 are small compared to the values of $D^{(1)}$ obtained for similar values of momenta. This can be understood from the combination of *(1)* the anti-detailed-balance structure of $\mathfrak{W}^{\ominus}$, from which it follows that $\mathfrak{W}^{\ominus,qq'}_{n\mathbf{k},n'\mathbf{k}'} + \mathfrak{W}^{\ominus,qq'}_{n-\mathbf{k},n'-\mathbf{k}'} = O(\boldsymbol{m}_0)$ as shown in Sec. 3.4.1, and *(2)* the C_2 symmetry of the system around the $\hat{z}$ axis, which (since for planar magnons $k_z \leftrightarrow -k_z$ is a symmetry) entails $\mathfrak{W}^{\ominus,qq'}_{n\mathbf{k},n'\mathbf{k}'} = \mathfrak{W}^{\ominus,qq'}_{n-\mathbf{k},n'-\mathbf{k}'}$. Thus $\mathfrak{W}^{\ominus,qq'}_{n\mathbf{k},n'\mathbf{k}'} = O(\boldsymbol{m}_0)$ itself. This, together with the analysis given in Sec. 3.5.3.4 showing that terms which are odd in $\boldsymbol{m}_0$ are also proportional to anisotropic couplings, implies that $\mathfrak{W}^{\ominus,qq'}_{n\mathbf{k},n'\mathbf{k}'}$ is indeed typically much smaller than $D^{(1)}_{n\mathbf{k}}$.

3.5.7 Discussion of the results in absolute scales

Here we discuss the absolute scales of κ_L, ϱ_H and κ_H we obtain using the parameter values from Table 3.5.4 and those in the figure captions. First it is

instructive to estimate the basic scales for thermal conductivity and temperature derived from phonons, which define the scales for our numerical plots. Using the phonon velocity for CFTD, $v_{\mathrm{ph}}^{\mathrm{CFTD}} = 4 \cdot 10^3$ m·s^{-1} and its in-plane lattice parameter $\mathfrak{a}^{\mathrm{CFTD}} = 5.7 \cdot 10^{-10}$ m, we find (see Table 3.5.3),

- $\kappa_0^{\mathrm{CFTD}} = 0.17$ W·K^{-1}·m^{-1},
- $T_0^{\mathrm{CFTD}} = 54$ K,
- $\gamma_0 = 7.0 \cdot 10^{12}$ Hz.

Note that these scales do not vary greatly for many materials. For example, in La_2CuO_4, we find $\kappa_0^{\mathrm{LCO}} = 0.38$ W·K^{-1}·m^{-1} and $T_0^{\mathrm{LCO}} = 80$ K. Importantly, the scale κ_0 is order one in SI units, which allows a roughly direct comparison with most data.

Next we can use the actual computed values to see what this mechanism predicts for the "test" material CFTD. We have at $T \approx 0.5T_0 \approx 27$ K,

- $\kappa_L^{\mathrm{CFTD}} \approx 125\kappa_0 \approx 22$ W·K^{-1}·m^{-1} for any of the γ_{ext} values presented in Fig. 2.3(a),
- for $\gamma_{\mathrm{ext}} = 10^{-4}\gamma_0 = 7.0 \cdot 10^8$ Hz, $T_\lambda^{\star,\mathrm{CFTD}} \approx 0.3T_0 \approx 16$ K,
- for $\gamma_{\mathrm{ext}} = 10^{-7}\gamma_0 = 7.0 \cdot 10^5$ Hz, $T_\lambda^{\star,\mathrm{CFTD}} \approx 0.1T_0 \approx 5.4$ K,
- $\varrho_H^{\mathrm{CFTD}} \approx 2 \cdot 10^{-5}\varrho_0 \approx 1.2 \cdot 10^{-4}$ K·m·W^{-1},
- $|\theta_H^{\mathrm{CFTD}}| \approx 2.6 \cdot 10^{-3}$,
- $|\kappa_H^{\mathrm{CFTD}}| \approx 5.8 \cdot 10^{-2}$ W·K^{-1}·m^{-1}.

Note that κ_L, κ_H and θ_H all depend on the choice of values for γ_{ext}.

3.6 Conclusions

3.6.1 Summary of results and method

In this paper, we studied the problem of scattering of phonons due to a weak *intrinsic* (i.e. without disorder) coupling to a fluctuating field Q, which is itself a quantum mechanical degree of freedom. Using the T-matrix formalism, we derived the scattering rates of phonons up to fourth order in coupling. The result is expressed generally, without any assumptions on the nature of the fluctuating field (i.e. it can be highly non-Gaussian), in terms of correlation functions of Q. Using these scattering rates in the Boltzmann equation leads to general expressions for the thermal conductivity tensor, and, when symmetry allows, a non-vanishing thermal Hall effect. A central result is that the skew scattering of phonons (which we define sharply as a scattering component which obeys an *anti*-detailed balance relation), and hence the thermal Hall conductivity, is proportional to a four-point correlation function of Q, which we give explicitly.

We highlight throughout the various constraints due to symmetry (both exact and approximate), unitarity, and thermal equilibrium.

As an illustration of the method, we applied these results to the case where the fluctuating field Q arises from spin wave (magnon) excitations of an ordered two-sublattice antiferromagnet. We model the latter via standard spin wave theory, for which phase space constraints imply that the dominant contribution arises from bilinears in the creation/annihilation operators of the spin waves. We obtain a general formula for the second order and fourth order scattering rates in terms of the dispersion of phonons and magnons, and the spin-lattice coupling constants. To obtain concrete results, we focus in particular on the limit in which the relevant magnons are acoustic, and we assume tetragonal symmetry and two-dimensionality of the magnons (but we retain the three dimensionality of the phonons). Under these assumptions we obtain all the (seven) symmetry-allowed spin-lattice coupling interactions, and calculate the second order and fourth order scattering rates, and thereby the thermal conductivity, including a phenomenological parallel scattering rate of phonons due to other mechanisms, e.g. boundary and impurity scattering. The final formulae are evaluated via numerical integration for representative model parameters. We observe a number of distinct scattering regimes, which we identify with features in the longitudinal thermal conductivity. We obtain a non-vanishing thermal Hall effect, in agreement with general symmetry arguments. Please see Sec. 3.5 for details.

3.6.2 Relation to other work

While we are not aware of any general results on the intrinsic phonon Hall conductivity due to scattering, there are a number of complementary theoretical papers as well as some prior work which overlap a small part of our results. The specific problem of phonons scattering from magnons was studied long ago to the leading second order in the coupling by Cottam [Cottam, 1974]. That work, which assumed the isotropic SU(2) invariant limit, agrees with our calculations when these assumptions are imposed. The complementary mechanism of intrinsic phonon Hall effect due to phonon Berry curvature was studied by many authors [Qin et al., 2012, Saito et al., 2019, Zhang et al., 2010, Zhang et al., 2021b], including how the phonon Berry curvature is induced by spin-lattice coupling in Ref. [Ye et al., 2021]. The majority of recent theoretical work has concentrated on *extrinsic* effects due to scattering of phonons by defects [Sun et al., 2021, Guo and Sachdev, 2021, Guo et al., 2022, Flebus and MacDonald, 2021]. The pioneering paper of Mori *et al.* [Mori et al., 2014] in particular recognized the importance of higher order contributions to scattering for the Hall effect, and is in some ways a predecessor to our work.

3.6.3 General observations

While often times scattering is regarded as a process which destroys coherence and suppresses interesting dynamical phenomena, our work reveals that higher order scattering probes highly non-trivial structure of correlations. Due to the

constraints of detailed balance, the skew scattering, appropriately defined, contains only contributions of $O(Q^4)$ and no terms of lower order in Q, and so can in principle directly reveal subtle structures in the quantum correlations, without a need for subtraction. Measurements of such skew scattering of phonons—which *a priori* include but are not limited to the thermal Hall effect—might therefore be considered a probe of the quantum material hosting those phonons. Taking advantage of this potential opportunity is a challenge to experiment, as well as to theory, which should interpret the results and predict systems to maximize the effects.

We would like to comment on the analysis of thermal Hall effect experiments in quantum materials. As is well-known, thermal Hall conductivity is generally a small effect. In particular, the dimensionless measure of the Hall angle, $\theta_H = \tan^{-1}(\kappa_{\rm H}^{xy}/\kappa^{xx})$ is always much less than $\pi/2$ by two or more orders of magnitude, even in systems where thermal Hall effect is lauded as "huge". (An actually large thermal Hall angle ($\theta_H = O(1)$) is obtained only the quantum thermal Hall regime when phonons are ballistic and edge states dominate over the bulk phonon contributions, which is extraordinarily difficult to achieve.) For small θ_H, the skew scattering contributions are perturbative to the thermal conductivity, i.e. proportional to the latter rate $1/\tau_{\rm skew}$. Dimensional reasoning implies that therefore $\kappa_H \sim \tau^2/\tau_{\rm skew}$, where τ is the standard, non-skew scattering time. This means that the thermal Hall *conductivity* has a very strong dependence on τ, which is often sample-dependent and of course grows with sample quality, implying that the thermal Hall conductivity is larger in cleaner samples.

This dependence also means that κ_H itself, as well as the dimensionless Hall angle $\theta_H \sim \kappa_H/\kappa_L$ depend not only on the skew scattering but also the ordinary scattering. Since the latter receives contributions from many different mechanisms, which may themselves have strong temperature and field dependence, neither κ_H itself nor κ_H/κ_L are ideal quantities to examine to probe the physics of skew scattering. Instead, we suggest that the thermal Hall *resistivity*, $\varrho_H \equiv -\kappa_H/\kappa_L^2$, is the quantity which is most easily interpreted physically. This quantity is independent of the non-skew scattering, at least when the latter is largely momentum-independent, and is always independent of the overall scale of non-skew scattering. The temperature and field dependence of ϱ_H is generally expected to be simpler than that of the other quantities, at least when phonon skew scattering is the dominant mechanism for the Hall effect. This expectation is true not only when the skew scattering is intrinsic, as studied here, but also for extrinsic skew scattering due to defects.

3.6.4 Future directions

Our general formalism can be applied very broadly. In particular, because it does not require any assumptions on the nature of the Q correlations, it may be applied directly to exotic states, to quantum or classical critical points, or to situations in which the Q field is a composite operator. We will present an application to a spinon Fermi surface spin liquid in an upcoming paper. Apart from other specific applications which may be easily imagined, it would also be interesting

to explore further how general properties of four-point correlations of Q may be detected via phonon skew scattering. In particular, the correlations which enter the scattering rates are not obviously time-ordered, and we wonder if these might contain some information on many-body chaos (Ref. [Swingle, 2018]).

Despite the generality of our formulation, it is still specialized in several ways. We consider only scattering contributions to the phonon Boltzmann equation. In general the interactions with fields Q will both induce scattering and modify the dynamics of the phonons in a non-dissipative way, e.g. induce phonon Berry phases [Ye et al., 2021]. While we believe it is usually the case that scattering is dominant, a more complete treatment including both effects would be of interest. Furthermore, in this paper we fully "integrate out" the electronic degrees of freedom, and follow the distribution function of the phonons only. More generally, there are coupled modes of phonons and electronic states, and one can consider the distributions for these coupled modes. One expects such effects are important largely when there are resonances between phonons and electronic excitations. All these problems could be addressed via a Keldysh treatment of coupled quantum kinetic equations, which is an interesting subject for future work.

Appendix

3.A Strain tensor

In Sec. 3.5.3 we employ a continuum model of the spin-phonon system. The phonons themselves correspondingly derive from the theory of continuum elasticity, which has the Hamiltonian density

$$\mathcal{H}_{\text{el}} = \frac{1}{2\rho}\Pi_\mu^2 + \frac{1}{2}C_{\alpha\beta\gamma\delta}\mathcal{E}^{\alpha\beta}\mathcal{E}^{\gamma\delta}. \tag{3.132}$$

Within this appendix, ρ is the mass density (we will take $\rho V = M_{\text{uc}}N_{\text{uc}}$) and $C_{\alpha\beta\gamma\delta}$ is a rank four tensor of elastic constants, which can be taken to satisfy $C_{\alpha\beta\gamma\delta} = C_{\beta\alpha\gamma\delta} = C_{\alpha\beta\delta\gamma} = C_{\gamma\delta\alpha\beta}$. The canonical variables of this classical field theory are the displacement field u_μ and its canonically conjugate momentum Π_μ. Due to translational and rotational symmetry, the Hookian potential energy is expressed solely through the strain tensor,

$$\mathcal{E}^{\alpha\beta}(\mathbf{R}) = \frac{1}{2}\left(\partial_\alpha u_\beta + \partial_\beta u_\alpha\right). \tag{3.133}$$

By construction the strain is a symmetric tensor in its two indices, i.e. $\mathcal{E}^T = \mathcal{E}$. Define the Fourier transforms

$$u_\mu(\mathbf{x}) = \frac{1}{\sqrt{V}}\sum_{\mathbf{k}} e^{i\mathbf{k}\cdot\mathbf{x}}u_{\mu,\mathbf{k}}, \qquad \Pi_\mu(\mathbf{x}) = \frac{1}{\sqrt{V}}\sum_{\mathbf{k}} e^{i\mathbf{k}\cdot\mathbf{x}}\Pi_{\mu,\mathbf{k}}. \tag{3.134}$$

Here since $u_\mu(\mathbf{x})$ and $\Pi_\mu(\mathbf{x})$ are real fields, we have $u_{n,-\mathbf{k}} = u_{n\mathbf{k}}^*$ and $\Pi_{n,-\mathbf{k}} = \Pi_{n\mathbf{k}}^*$. The Fourier space fields satisfy the commutation relations

$$\left[\Pi_{\mu,\mathbf{k}}, u_{\nu,\mathbf{k}'}\right] = i\delta_{\mu\nu}\delta_{\mathbf{k}+\mathbf{k}',\mathbf{0}}. \tag{3.135}$$

We obtain

$$H_{\text{el}} = \sum_{\mathbf{k}}\left\{\frac{1}{2\rho}\Pi_{\mu,-\mathbf{k}}\Pi_{\mu,\mathbf{k}} + \frac{1}{2}\mathcal{K}_{\alpha\beta}(\mathbf{k})u_{\alpha,-\mathbf{k}}u_{\beta,\mathbf{k}}\right\}, \tag{3.136}$$

with

$$\mathcal{K}_{\alpha\beta}(\mathbf{k}) = C_{\alpha\gamma\beta\delta}k_\gamma k_\delta. \tag{3.137}$$

The matrix $\mathcal{K}_{\alpha\beta}$ is by construction real and symmetric, and hence has real eigenvalues $\mathcal{K}_n$, which additionally must be positive for stability. We define the eigenvalues and eigenvectors ε_n^α via

$$\mathcal{K}_{\alpha\beta}(\mathbf{k})\varepsilon_n^\beta(\mathbf{k}) = \mathcal{K}_n(\mathbf{k})\varepsilon_n^\alpha(\mathbf{k}), \tag{3.138}$$

with $\varepsilon_n^\alpha(-\mathbf{k}) = (\varepsilon_n^\alpha(\mathbf{k}))^*$ and the standard normalization $\sum_\alpha(\varepsilon_n^\alpha(\mathbf{k}))^*\varepsilon_{n'}^\alpha(\mathbf{k}) = \delta_{nn'}$. Now we make the change of basis

$$u_{\mu\mathbf{k}} = \sum_n \varepsilon_n^\mu(\mathbf{k})u_{n\mathbf{k}}, \qquad \Pi_{\mu\mathbf{k}} = \sum_n \varepsilon_n^\mu(\mathbf{k})\Pi_{n\mathbf{k}}, \tag{3.139}$$

which gives

$$[\Pi_{n\mathbf{k}}, u_{n'\mathbf{k}'}] = i\delta_{nn'}\delta_{\mathbf{k}+\mathbf{k}',\mathbf{0}}, \tag{3.140}$$

and

$$H_{\text{el}} = \sum_{n,\mathbf{k}} \left\{ \frac{1}{2\rho}\Pi_{n,-\mathbf{k}}\Pi_{n,\mathbf{k}} + \frac{1}{2}\mathcal{K}_n(\mathbf{k})u_{n,-\mathbf{k}}u_{n,\mathbf{k}} \right\}. \tag{3.141}$$

Now we can finally define creation/annihilation operators

$$\begin{aligned} u_{n\mathbf{k}} &= \frac{1}{\sqrt{2}}\frac{1}{(\rho\mathcal{K}_n)^{1/4}}(a_{n\mathbf{k}} + a_{n,-\mathbf{k}}^\dagger), \\ \Pi_{n\mathbf{k}} &= i\frac{1}{\sqrt{2}}(\rho\mathcal{K}_n)^{1/4}(a_{n\mathbf{k}} - a_{n,-\mathbf{k}}^\dagger), \end{aligned} \tag{3.142}$$

with canonical boson operators

$$\left[a_{n\mathbf{k}}, a_{n'\mathbf{k}'}^\dagger\right] = \delta_{nn'}\delta_{\mathbf{k},\mathbf{k}'}, \tag{3.143}$$

and the Hamiltonian

$$H_{\text{el}} = \sum_{n\mathbf{k}} \omega_{n\mathbf{k}} a_{n\mathbf{k}}^\dagger a_{n\mathbf{k}}, \tag{3.144}$$

and

$$\omega_{n\mathbf{k}} = \sqrt{\frac{\mathcal{K}_n(\mathbf{k})}{\rho}}. \tag{3.145}$$

Having finally arrived at the canonical phonon operators, we recombine the several steps of the above procedure to obtain the expression for the displacement field,

$$u_\mu(\mathbf{x}) = \frac{1}{\sqrt{V}}\sum_{n\mathbf{k}} \frac{1}{\sqrt{2\rho\omega_{n\mathbf{k}}}} \left(a_{n\mathbf{k}} + a_{n,-\mathbf{k}}^\dagger\right) \varepsilon_{n\mathbf{k}}^\mu e^{i\mathbf{k}\cdot\mathbf{x}}. \tag{3.146}$$

Now we can use the definition in Eq. (3.75) of the strain to obtain

$$\mathcal{E}^{\mu\nu}(\mathbf{x}) = \tag{3.147}$$

$$\frac{1}{\sqrt{V}}\sum_{n\mathbf{k}} \frac{1}{\sqrt{2\rho\omega_{n\mathbf{k}}}} \left(a_{n\mathbf{k}} + a_{n,-\mathbf{k}}^\dagger\right) \frac{i}{2}\left(k^\mu\varepsilon_{n\mathbf{k}}^\nu + k^\nu\varepsilon_{n\mathbf{k}}^\mu\right) e^{i\mathbf{k}\cdot\mathbf{x}}. \tag{3.148}$$

Now let us consider the coupling of the strain to the continuum spin fluctuations, Eq. (3.77) of the main text. The full spin-lattice coupling in three dimensions is written as

$$H'_{\text{s-l}} = \sum_z \int dxdy\, \mathcal{E}^{\alpha\beta}(\mathbf{x}) \lambda^{\alpha\beta}_{ab;\xi\xi'} n_0^{-\xi-\xi'} \eta_{a\xi\mathbf{x}} \eta_{b\xi'\mathbf{x}}. \tag{3.149}$$

Note the sum over discrete 2d layers. We now insert the Fourier expansion of the strain from Eq. (3.147) and the corresponding Fourier expansion of the magnetic fluctuations, which we repeat here:

$$\eta_{a\xi\mathbf{x}} = \frac{1}{\sqrt{A_{2d}}} \sum_{\underline{\mathbf{q}}} \eta_{a\xi\underline{\mathbf{q}},z} e^{i\underline{\mathbf{q}}\cdot\underline{\mathbf{x}}}. \tag{3.150}$$

In this equation, and in the rest of this section, we are careful to denote two-dimensional vectors with an underline. Since magnetic fluctuations in different layers are taken as independent, we do not introduce a z-component of the wavevector for the magnons, and simply leave z explicitly as a layer index for these fields. Note also the prefactor Eq. (3.150) therefore involves the square root of the two dimensional area of a single plane, A_{2d}.

With this in mind, we obtain from Eq. (3.149)

$$\begin{aligned} H'_{\text{s-l}} = \frac{1}{\sqrt{V}} \sum_z \sum_{\mathbf{k},\underline{\mathbf{p}}} \lambda^{\mu\nu}_{ab;\xi\xi'} n_0^{-\xi-\xi'} \frac{1}{\sqrt{2\rho\omega_{n\mathbf{k}}}} e^{ik_z z} \\ \times \frac{i}{2} \left(k^\mu \varepsilon^\nu_{n\mathbf{k}} + k^\nu \varepsilon^\mu_{n\mathbf{k}}\right) \left(a_{n\mathbf{k}} + a^\dagger_{n,-\mathbf{k}}\right) \eta_{a\xi,\underline{\mathbf{p}}-\frac{1}{2}\underline{\mathbf{k}},z} \eta_{b\xi',-\underline{\mathbf{p}}-\frac{1}{2}\underline{\mathbf{k}},z}. \end{aligned} \tag{3.151}$$

From here we can see that

$$\begin{aligned} Q_{n\mathbf{k}} = \frac{i}{2\sqrt{V}} \frac{\left(k^\mu \varepsilon^\nu_{n\mathbf{k}} + k^\nu \varepsilon^\mu_{n\mathbf{k}}\right)}{\sqrt{2\rho\omega_{n\mathbf{k}}}} \sum_{\xi\xi',ab} \lambda^{\mu\nu}_{ab;\xi\xi'} n_0^{-\xi-\xi'} \\ \times \sum_z \sum_{\underline{\mathbf{p}}} e^{ik_z z} \eta_{a\xi,\underline{\mathbf{p}}-\frac{1}{2}\underline{\mathbf{k}},z} \eta_{b\xi',-\underline{\mathbf{p}}-\frac{1}{2}\underline{\mathbf{k}},z}. \end{aligned} \tag{3.152}$$

Next we use Eq. (3.80) to express this in terms of canonical bosons:

$$\begin{aligned} Q_{n\mathbf{k}} = \frac{i\left(k^\mu \varepsilon^\nu_{n\mathbf{k}} + k^\nu \varepsilon^\mu_{n\mathbf{k}}\right)}{4\sqrt{2V\rho\,\omega_{n\mathbf{k}}}} \sum_z \sum_{\underline{\mathbf{p}}} \sum_{qq'} \sum_{\xi\xi' ab} \lambda^{\mu\nu}_{ab;\xi\xi'} n_0^{-\xi-\xi'} \\ \times e^{ik_z z} (-1)^{\bar{\xi}(\delta_{a-1,\xi}+\frac{1+q}{2})+\bar{\xi}'(\delta_{b-1,\xi'}+\frac{1+q'}{2})} i^{\bar{\xi}+\bar{\xi}'} \\ \times (\chi\Omega_{\delta_{a-1,\xi},\mathbf{p}-\frac{1}{2}\mathbf{k}})^{\tilde{\xi}/2} (\chi\Omega_{\delta_{b-1,\xi'},-\mathbf{p}-\frac{1}{2}\mathbf{k}})^{\tilde{\xi}'/2} b^q_{\mathbf{p}-\frac{1}{2}\mathbf{k},\delta_{a-1,\xi},z} b^{q'}_{-\mathbf{p}-\frac{1}{2}\mathbf{k},\delta_{b-1,\xi'},z}. \end{aligned} \tag{3.153}$$

We now define $\ell_1 = \delta_{a-1,\xi} = 0, 1$ and $\ell_2 = \delta_{b-1,\xi'}$, which is inverted by $a = 1 + \tilde{\xi}\ell_1 + \bar{\xi}$ and $b = 1 + \tilde{\xi}'\ell_2 + \bar{\xi}'$. This gives

$$\begin{aligned} Q_{n\mathbf{k}} = \frac{i\left(k^\mu \varepsilon^\nu_{n\mathbf{k}} + k^\nu \varepsilon^\mu_{n\mathbf{k}}\right)}{4\sqrt{2V\rho\,\omega_{n\mathbf{k}}}} \sum_z \sum_{\underline{\mathbf{p}}} \sum_{qq'} \sum_{\xi\xi'\ell_1\ell_2} \lambda^{\mu\nu}_{\tilde{\xi}\ell_1+\bar{\xi}+1,\tilde{\xi}'\ell_2+\bar{\xi}'+1;\xi,\xi'} n_0^{-\xi-\xi'} \\ \times e^{ik_z z} (-1)^{\bar{\xi}(\ell_1+\frac{1+q}{2})+\bar{\xi}'(\ell_2+\frac{1+q'}{2})} i^{\bar{\xi}+\bar{\xi}'} \\ \times (\chi\Omega_{\ell_1,\mathbf{p}-\frac{1}{2}\mathbf{k}})^{\tilde{\xi}/2} (\chi\Omega_{\ell_2,-\mathbf{p}-\frac{1}{2}\mathbf{k}})^{\tilde{\xi}'/2} b^q_{\mathbf{p}-\frac{1}{2}\mathbf{k},\ell_1,z} b^{q'}_{-\mathbf{p}-\frac{1}{2}\mathbf{k},\ell_2,z}. \end{aligned} \tag{3.154}$$

From here, we recognize that $Q_{n\mathbf{k}} = Q^-_{n\mathbf{k}}$ in Eq. (3.58), and thereby extract $\mathcal{B}$. We use $V\rho = N_{\rm uc}M_{\rm uc}$.

3.B General hydrodynamics of phonons

Our goal is to derive the thermal current carried by the phonons,

$$j^\mu = \frac{1}{V}\sum_{n\mathbf{k}} \overline{N}_{n\mathbf{k}} v^\mu_{n\mathbf{k}} \omega_{n\mathbf{k}}, \tag{3.155}$$

in order to extract the thermal conductivity tensor. This requires knowledge of the average phonon populations $\overline{N}_{n\mathbf{k}}$, which, in the presence of a gradient of temperature, differ from their equilibrium values. These populations can be obtained by solving Boltzmann's equation

$$\partial_t \overline{N}_{n\mathbf{k}} + \boldsymbol{v}_{n\mathbf{k}} \cdot \boldsymbol{\nabla}_{\mathbf{r}} \overline{N}_{n\mathbf{k}} = \mathcal{C}_{n\mathbf{k}}[\{\overline{N}_{n'\mathbf{k}'}\}], \tag{3.156}$$

where the collision integral $\mathcal{C}_{n\mathbf{k}}[\{\overline{N}_{n'\mathbf{k}'}\}]$ depends on the populations in *all* $(n', \mathbf{k}')$ states. To solve this equation, we expand the out-of-equilibrium populations around their equilibrium value as $\overline{N}_{n\mathbf{k}} = N^{\rm eq}_{n\mathbf{k}} + \delta\overline{N}_{n\mathbf{k}}$. Within linear response, the perturbations can be considered small and we may expand the collision integral

$$\mathcal{C}_{n\mathbf{k}}[\{\overline{N}_{n'\mathbf{k}'}\}] = O_{n\mathbf{k}} + \sum_{n'\mathbf{k}'} C_{n\mathbf{k}n'\mathbf{k}'} \delta\overline{N}_{n'\mathbf{k}'} + O(\delta\overline{N}^2), \tag{3.157}$$

around its value $O_{n\mathbf{k}}$ in equilibrium. Since the thermal current must vanish in equilibrium, $O_{n\mathbf{k}}$ must be zero (we go back to this statement in Sec. 3.C.2.3). In Eq. (3.157), the "collision matrix" $C_{n\mathbf{k}n'\mathbf{k}'}$ is defined as the first-order Taylor coefficient, and one neglects the quadratic order in the perturbation. Formally inverting the collision matrix in the stationary Boltzmann equation (i.e. Eq. (3.155) with $\partial_t \overline{N} = 0$) leads to

$$\delta\overline{N}_{n\mathbf{k}} = C^{-1}_{n\mathbf{k}n'\mathbf{k}'} \frac{\omega_{n'\mathbf{k}'}}{k_B T^2} (N^{\rm eq}_{n'\mathbf{k}'})^2 v^\nu_{n'\mathbf{k}'} \partial_\nu T. \tag{3.158}$$

From Eq. (3.158) and Fourier's law, we can identify the components of the thermal conductivity tensor:

$$\begin{aligned} \frac{\kappa^{\mu\nu} \pm \kappa^{\nu\mu}}{2} \;=\; & -\frac{1}{2k_B T^2}\frac{1}{V}\sum_{n\mathbf{k}n'\mathbf{k}'} \omega_{n\mathbf{k}}\omega_{n'\mathbf{k}'} v^\mu_{n\mathbf{k}} v^\nu_{n'\mathbf{k}'} \\ & \cdot \left(C^{-1}_{n\mathbf{k},n'\mathbf{k}'} \, e^{\beta\omega_{n'\mathbf{k}'}} (N^{\rm eq}_{n'\mathbf{k}'})^2 \pm (n\mathbf{k} \leftrightarrow n'\mathbf{k}') \right). \end{aligned} \tag{3.159}$$

This expression shows that a nonzero phonon Hall conductivity requires the factor in the second line to be nonzero, which is equivalent to

$$C_{n\mathbf{k},n'\mathbf{k}'} \, e^{\beta\omega_{n'\mathbf{k}'}} (N^{\rm eq}_{n'\mathbf{k}'})^2 \neq C_{n'\mathbf{k}',n\mathbf{k}} \, e^{\beta\omega_{n\mathbf{k}}} (N^{\rm eq}_{n\mathbf{k}})^2, \tag{3.160}$$

where the constraint is now on $C_{n\mathbf{k},n'\mathbf{k}'}$ instead of its inverse. In other words, only the antisymmetric in $n\mathbf{k} \leftrightarrow n'\mathbf{k}'$ part of $C_{n\mathbf{k},n'\mathbf{k}'} \, e^{\beta\omega_{n'\mathbf{k}'}} (N^{\rm eq}_{n'\mathbf{k}'})^2$ contributes to the Hall conductivity.

In order to proceed further analytically, and invert the scattering matrix, we the separate diagonal from the off-diagonal parts in $C_{n\mathbf{k}n'\mathbf{k}'} = -\delta_{nn'}\delta_{\mathbf{k},\mathbf{k}'}D_{n\mathbf{k}} + M_{n\mathbf{k}n'\mathbf{k}'}$, and assume that $D_{n\mathbf{k}} \gg \sum_{n'\mathbf{k}'} M_{n\mathbf{k}n'\mathbf{k}'}$. This ought to be the case whenever the interactions are small, and/or if other damping processes are large. Then, $C^{-1}_{n\mathbf{k}n'\mathbf{k}'} \approx -\delta_{nn'}\delta_{\mathbf{k},\mathbf{k}'}D^{-1}_{n\mathbf{k}} - M_{n\mathbf{k}n'\mathbf{k}'}D^{-1}_{n\mathbf{k}}D^{-1}_{n'\mathbf{k}'}$. The antisymmetry in $n\mathbf{k} \leftrightarrow n'\mathbf{k}'$ condition for the Hall conductivity mentioned above leads to the fact that the diagonal term contributes to the longitudinal conductivity, but not to the Hall part, and translates into

$$\begin{aligned}\frac{\kappa^{\mu\nu} - \kappa^{\nu\mu}}{2} \quad =: \quad & \frac{1}{2k_BT^2}\frac{1}{V}\sum_{n\mathbf{k}n'\mathbf{k}'} \frac{\omega_{n\mathbf{k}}v^{\mu}_{n\mathbf{k}}}{D_{n\mathbf{k}}}\frac{\omega_{n'\mathbf{k}'}v^{\nu}_{n'\mathbf{k}'}}{D_{n'\mathbf{k}'}} \\ & \cdot \left[M_{n\mathbf{k},n'\mathbf{k}'}\, e^{\beta\omega_{n'\mathbf{k}'}}(N^{\mathrm{eq}}_{n'\mathbf{k}'})^2 - (n\mathbf{k} \leftrightarrow n'\mathbf{k}')\right].\end{aligned} \tag{3.161}$$

The longitudinal conductivity is

$$\begin{aligned}\kappa^{\mu\mu} \quad = \quad & \frac{1}{k_BT^2}\frac{1}{V}\sum_{n\mathbf{k}n'\mathbf{k}'} \omega_{n\mathbf{k}}\omega_{n'\mathbf{k}'}v^{\mu}_{n\mathbf{k}}v^{\mu}_{n'\mathbf{k}'} \\ & \cdot \left[\frac{\delta_{nn'}\delta_{\mathbf{k},\mathbf{k}'}}{D_{n\mathbf{k}}} + \frac{M_{n\mathbf{k},n'\mathbf{k}'}}{D_{n\mathbf{k}}D_{n'\mathbf{k}'}}\right] e^{\beta\omega_{n'\mathbf{k}'}}(N^{\mathrm{eq}}_{n'\mathbf{k}'})^2.\end{aligned} \tag{3.162}$$

Note that we will include all other (diagonal) scattering processes not taken into account here (e.g. boundary scattering, scattering by impurities, phonon-phonon sccattering etc.) by adding a phenomenological relaxation rate $\breve{D}_{n\mathbf{k}}$ to the diagonal of the scattering matrix.

3.C From interaction terms to the collision integral

3.C.1 General method and definitions

We now aim at deriving an expression for the collision integral of Boltzmann's equation using kinetic theory methods. The probability for the system to be found in a given quantum state $|\mathtt{i}\rangle = |i_p\rangle|i_s\rangle$ is governed by the master equation

$$\partial_t p_{i_p i_s} = \sum_{f_p f_s} \left[\Gamma_{f_p f_s \to i_p i_s}\, p_{f_p f_s} - \Gamma_{i_p i_s \to f_p f_s}\, p_{i_p i_s}\right], \tag{3.163}$$

where we will compute the transition rates $\Gamma_{i_p i_s \to f_p f_s}$ using scattering theory. The probability of a phonon state $|i_p\rangle$ is then obtained by summing over all possible spin configurations of the system, $p_{i_p} = \sum_{i_s} p_{i_p i_s}$. Assuming the phonon and spin probabilities are independent, i.e. $p_{i_p i_s} = p_{i_p}p_{i_s}$, and defining the transition rates $\Gamma_{f_p \to i_p} = \sum_{i_s f_s} \Gamma_{f_p f_s \to i_p i_s}\, p_{f_s}$ between phonon states only, we obtain the master equation for the probabilities of phonon states. We may in turn express the collision integral in the RHS of Boltzmann's equation, which is given by the time evolution of the populations in each phonon state $|i_p\rangle$ through the definition $\mathcal{C}_{n\mathbf{k}}[\{\overline{N}_{n'\mathbf{k}'}\}] = \sum_{i_p} N_{n\mathbf{k}}(i_p)\, \partial_t p_{i_p}$, in terms of transition rates between phonon states:

$$\mathcal{C}_{n\mathbf{k}}[\{\overline{N}_{n'\mathbf{k}'}\}] = \sum_{i_p, f_p} \Gamma_{i_p \to f_p}\left(N_{n\mathbf{k}}(f_p) - N_{n\mathbf{k}}(i_p)\right) p_{i_p}, \tag{3.164}$$

where $N_{n\mathbf{k}}(i_p) = \langle i_p | a^\dagger_{n\mathbf{k}} a_{n\mathbf{k}} | i_p \rangle$ is the number of $(n, \mathbf{k})$ phonons in the $|i_p\rangle$ state and $\overline{N}_{n\mathbf{k}} = \sum_{i_p} N_{n\mathbf{k}}(i_p) p_{i_p}$ is the average population. The only phonon states involved in the sums are those whose populations of $(n, \mathbf{k})$ phonons are different. Now, in order to obtain the scattering rates between spin-phonon states, we use Fermi's golden rule

$$\Gamma_{i_p i_s \to f_p f_s} = 2\pi \ |T_{i_s i_p \to f_s f_p}|^2 \ \delta(E_{i_p i_s} - E_{f_p f_s}), \tag{3.165}$$

where the factor $N_{\rm uc}$ ensures that $\Gamma_{i_p i_s \to f_p f_s}$ is a finite quantity in the thermodynamic limit, consistent with the choice of H' as a hamiltonian *density*. We use Born's expansion of the scattering matrix

$$\begin{aligned} T_{i_s i_p \to f_s f_p} &= \langle f_s f_p | H' | i_s i_p \rangle \\ &\quad + \sum_{n_s n_p} \frac{\langle f_s f_p | H' | n_s n_p \rangle \langle n_s n_p | H' | i_s i_p \rangle}{E_{i_s i_p} - E_{n_s n_p} + i\eta} + \cdots , \end{aligned} \tag{3.166}$$

where H' is the (perturbative) interaction hamiltonian between the phonons and the Q fields, and the $\eta \to 0^+$ appearing in the denominator of the second-order term ensures causality, which will prove crucial in the following.

To describe the interaction between phonon and spin degrees of freedom, we introduce general coupling terms between phonon creation-annihilation operators $a^{(\dagger)}_{n\mathbf{k}}$ and general, for now unspecified, fields $Q^{\{q_j\}}_{\{n_j \mathbf{k}_j\}}$ which depend on the spin structure: denoting $a^+_{n\mathbf{k}} \equiv a^\dagger_{n\mathbf{k}}$ and $a^-_{n\mathbf{k}} \equiv a_{n\mathbf{k}}$, and similarly for the Q operators, $Q^+_{\{n_i \mathbf{k}_i\}} \equiv Q^\dagger_{\{n_i \mathbf{k}_i\}}$ and $Q^-_{\{n_i \mathbf{k}_i\}} \equiv Q_{\{n_i \mathbf{k}_i\}}$, we write the couplings

$$H'_{[1]} = \sum_{n\mathbf{k}} \sum_{q=\pm} a^q_{n\mathbf{k}} Q^q_{n\mathbf{k}} \tag{3.167}$$

$$H'_{[2]} = \frac{1}{\sqrt{N_{\rm uc}}} \sum_{n\mathbf{k}, n'\mathbf{k}'} \sum_{q,q'=\pm} a^q_{n\mathbf{k}} a^{q'}_{n'\mathbf{k}'} Q^{qq'}_{n\mathbf{k}n'\mathbf{k}'}, \tag{3.168}$$

where $Q^{qq'}_{n\mathbf{k}n'\mathbf{k}'} = Q^{q'q}_{n'\mathbf{k}'n\mathbf{k}} = (Q^{-q-q'}_{n\mathbf{k}n'\mathbf{k}'})^\dagger$ ensures the hermiticity of $H'_{[2]}$. Here and throughout the manuscript, a square bracket index, e.g. $[p]$ denotes the number of interacting phonons.

By definition the term $H'_{[p]}$ involves p phonon creation-annihilation operators, and as such typically arises from microscopic models as the pth spatial derivative of orbital overlaps. Consequently, we assume $H'_{[2]}$ to be of the same order of magnitude as the square of $H'_{[1]}$, that is to say, $Q^q_{n\mathbf{k}} \sim \lambda$, $Q^{qq'}_{n\mathbf{k}n'\mathbf{k}'} \sim \lambda^2$ with λ a small parameter. In this paper, we keep only the first two terms of the expansion (i.e. we take $H' = H'_{[1]} + H'_{[2]}$).

3.C.2 Computation at first Born order

In this subsection we consider only the first term of Born's expansion. The transition rates associated with $H' = H'_{[1]} + H'_{[2]}$ at this order are simply the matrix elements:

$$T^{[1]}_{\mathtt{i}\to\mathtt{f}} = \sum_{n\mathbf{k}q} \sqrt{N^i_{\mathbf{k},n} + \tfrac{q+1}{2}} \ \langle f_s | Q^q_{n\mathbf{k}} | i_s \rangle \ \mathbb{I}(i_p \xrightarrow{q \cdot n\mathbf{k}} f_p), \tag{3.169}$$

$$T^{[2]}_{\mathtt{i}\to\mathtt{f}} = \frac{1}{\sqrt{N_{\rm uc}}} \sum_{n\mathbf{k},n'\mathbf{k}'} \sum_{qq'} \sqrt{N^i_{n\mathbf{k}} + \tfrac{q+1}{2}} \sqrt{N^i_{n'\mathbf{k}'} + \tfrac{q'+1}{2}} \cdot \langle f_s | Q^{qq'}_{n\mathbf{k}n'\mathbf{k}'} | i_s \rangle \; \mathbb{I}(i_p \xrightarrow[q'\cdot n'\mathbf{k}']{q\cdot n\mathbf{k}} f_p), \tag{3.170}$$

where $\mathbb{I}(i_p \xrightarrow{q\cdot n\mathbf{k}} f_p)$ means that the only difference between $|i_p\rangle$ and $|f_p\rangle$ is that there is $q = \pm 1$ more phonon of species $(n, \mathbf{k})$ in the final state. Note that the cases where $n\mathbf{k} = n'\mathbf{k}'$ require a formal correction. However, at any given order in the λ expansion, such terms are smaller than all others by a factor $1/N_{\rm uc}$, where $N_{\rm uc}$ is the number of unit cells, and therefore vanish in the thermodynamic limit. In this article we thus take $\sum_{n\mathbf{k},n'\mathbf{k}'}$ and $\sum_{n\mathbf{k}\neq n'\mathbf{k}'}$ exchangeably, unless we specify otherwise.

We then compute the squared matrix element.

"Cross terms" such as $\langle \mathtt{i}|H'_{[2]}|\mathtt{f}\rangle\langle \mathtt{f}|H'_{[1]}|\mathtt{i}\rangle$ (which are of order λ^3) vanish because $\langle i_p|\widehat{A}|i_p\rangle = 0$ for any operator $\widehat{A}$ containing an odd number of phonon creation-annihilation operators. At order λ^2, there thus remains only $\langle \mathtt{i}|H'_{[1]}|\mathtt{f}\rangle\langle \mathtt{f}|H'_{[1]}|\mathtt{i}\rangle$, and at order λ^4, only $\langle \mathtt{i}|H'_{[2]}|\mathtt{f}\rangle\langle \mathtt{f}|H'_{[2]}|\mathtt{i}\rangle$.

3.C.2.1 Terms at $O(\lambda^2)$

At order λ^2, we have therefore

$$\left|T^{[1]}_{\mathtt{i}\to\mathtt{f}}\right|^2 = \sum_{n\mathbf{k}q} \left(N^i_{\mathbf{k},n} + \tfrac{q+1}{2}\right) \; \mathbb{I}(i_p \xrightarrow{q\cdot n\mathbf{k}} f_p) \langle i_s|Q^{-q}_{n\mathbf{k}}|f_s\rangle\langle f_s|Q^{q}_{n\mathbf{k}}|i_s\rangle. \tag{3.171}$$

We then enforce the energy conservation $\delta(E_{\mathtt{f}} - E_{\mathtt{i}}) = \delta(q\omega_{n\mathbf{k}} + E_{f_s} - E_{i_s})$ by writing the latter as a time integral, i.e. $\int_{-\infty}^{+\infty} \mathrm{d}t e^{i\omega t} = 2\pi\delta(\omega)$, identify $A(t) = e^{+iHt}Ae^{-iHt}$, use the identity $1 = \sum_{f_s} |f_s\rangle\langle f_s|$, and take the spins in the initial state to be in thermal equilibrium $p_{i_s} = Z^{-1}e^{-\beta E_{i_s}}$. Finally summing over $|i_s\rangle$ and identifying $\langle A\rangle_\beta = Z^{-1}\mathrm{Tr}(e^{-\beta H}A)$, we find

$$\begin{aligned} W^{[1];[1]}_{n\mathbf{k}q} &= 2\pi \sum\nolimits_{f_s,i_s} \langle i_s|Q^{-q}_{n\mathbf{k}}|f_s\rangle\langle f_s|Q^{q}_{n\mathbf{k}}|i_s\rangle p_{i_s} \times \delta(q\omega_{n\mathbf{k}} + E_{f_s} - E_{i_s}) \\ &= \int_{-\infty}^{\infty} \mathrm{d}t \, e^{-iq\omega_{n\mathbf{k}}t} \left\langle Q^{-q}_{n\mathbf{k}}(t) \; Q^{q}_{n\mathbf{k}}(0)\right\rangle_\beta . \end{aligned} \tag{3.172}$$

Note that this calculation, in a time-reversal symmetric system, leads to the extra symmetry $W^{[1];[1]}_{n\mathbf{k}q} = W^{[1];[1]}_{n-\mathbf{k}q}$.

The scattering rate between phonon states, for the one-phonon interaction term at first Born's order, then reads

$$\Gamma^{[1];[1]}_{i_p\to f_p} = \sum_{n\mathbf{k}q} \left(N^i_{n\mathbf{k}} + \tfrac{q+1}{2}\right) W^{[1];[1]}_{n\mathbf{k}q} \; \mathbb{I}(i_p \xrightarrow{q\cdot n\mathbf{k}} f_p). \tag{3.173}$$

To arrive at the collision integral, the final step involves summing over final phononic states f_p and taking the average over initial phononic states i_p. We

find, the contributions to $\mathcal{C}$ at order λ^2 to be:

$$O^{[1];[1]}_{n\mathbf{k}} = \sum_{q=\pm} q\, W^{[1];[1]}_{n,\mathbf{k},q} \left(N^{\rm eq}_{n,\mathbf{k}} + \tfrac{q+1}{2}\right), \tag{3.174}$$

$$-D^{[1];[1]}_{n\mathbf{k}} = \sum_{q=\pm} q\, W^{[1];[1]}_{n,\mathbf{k},q}. \tag{3.175}$$

We will address the constant term $O^{[1];[1]}_{n\mathbf{k}}$ (expected to be zero) in more detail in Sec. 3.C.2.3. The collision matrix is clearly diagonal, i.e. $M^{[1];[1]}_{n\mathbf{k},n'\mathbf{k}'} = 0$. Therefore this λ^2 contribution to $\mathcal{C}$ may contribute to the longitudinal conductivity, but not to the Hall conductivity.

3.C.2.2 Terms at $O(\lambda^4)$

We address the $O(\lambda^4)$ term in a similar fashion. There, the energy conservation reads $\delta(E_{\mathtt{f}} - E_{\mathtt{i}}) = \delta(q\omega_{n\mathbf{k}} + q'\omega_{n'\mathbf{k}'} + E_{f_s} - E_{i_s})$, and we find

$$\begin{aligned}\Gamma^{[2];[2]}_{i_p\to f_p} &= \frac{1}{2N_{\rm uc}} \sum_{n\mathbf{k},n'\mathbf{k}'} \sum_{q,q'=\pm} W^{[2];[2]}_{n\mathbf{k}q,n'\mathbf{k}'q'}\, \mathbb{I}(i_p \xrightarrow[q'\cdot n'\mathbf{k}']{q\cdot n\mathbf{k}} f_p) \\ &\quad \cdot \left(N^i_{n\mathbf{k}} + \tfrac{q+1}{2}\right)\left(N^i_{n'\mathbf{k}'} + \tfrac{q'+1}{2}\right),\end{aligned} \tag{3.176}$$

where

$$W^{[2];[2]}_{n\mathbf{k}q,n'\mathbf{k}'q'} = 2\int_{-\infty}^{+\infty} {\rm d}t\; e^{-i(q\omega_{n\mathbf{k}} + q'\omega_{n'\mathbf{k}'})t} \times \left\langle Q^{-q-q'}_{n\mathbf{k}n'\mathbf{k}'}(t)\; Q^{qq'}_{n\mathbf{k}n'\mathbf{k}'}(0)\right\rangle_\beta, \tag{3.177}$$

and $W^{[2];[2]}_{n\mathbf{k}q,n'\mathbf{k}'q'} = W^{[2];[2]}_{n'\mathbf{k}'q',n\mathbf{k}q}$, by definition. The resulting collision integral, up to linear order in the perturbed populations $\delta\overline{N}$ contains the following contributions:

$$O^{[2];[2]}_{n\mathbf{k}} = \frac{1}{N_{\rm uc}} \sum_{n'\mathbf{k}'} \sum_{q,q'=\pm} q W^{[2];[2]}_{n\mathbf{k}q,n'\mathbf{k}'q'} \cdot \left(N^{\rm eq}_{n\mathbf{k}} + \tfrac{q+1}{2}\right)\left(N^{\rm eq}_{n'\mathbf{k}'} + \tfrac{q'+1}{2}\right), \tag{3.178}$$

$$-D^{[2];[2]}_{n\mathbf{k}} = \frac{1}{N_{\rm uc}} \sum_{n'\mathbf{k}'} \sum_{q,q'=\pm} q\, \left(N^{\rm eq}_{n'\mathbf{k}'} + \tfrac{q'+1}{2}\right) W^{[2];[2]}_{n\mathbf{k}q,n'\mathbf{k}'q'}, \tag{3.179}$$

$$M^{[2];[2]}_{n\mathbf{k},n'\mathbf{k}'} = \frac{1}{N_{\rm uc}} \sum_{q,q'=\pm} q\, \left(N^{\rm eq}_{n\mathbf{k}} + \tfrac{q+1}{2}\right)\, W^{[2];[2]}_{n\mathbf{k}q,n'\mathbf{k}'q'}. \tag{3.180}$$

As above, we will address the constant term in Sec. 3.C.2.3. The diagonal contribution is of order λ^4, and we therefore expect it to be subdominant compared with the λ^2 contribution from the previous section. Finally, the off-diagonal contribution is nonzero. However, we will show that its contribution to $C_{n\mathbf{k},n'\mathbf{k}'}\, e^{\beta\omega_{n'\mathbf{k}'}} (N^{\rm eq}_{n'\mathbf{k}'})^2$ is purely symmetric under $n\mathbf{k} \leftrightarrow n'\mathbf{k}'$ and therefore contributes only to the symmetric off-diagonal conductivity but not to the Hall one − see Eq. (3.160).

3.C.2.3 Detailed balance

First, we notice that a change of variables $i_s \leftrightarrow f_s$ in Eq. (3.172) leads to the detailed-balance relation

$$W^{[1];[1]}_{n\mathbf{k},q} = W^{[1];[1]}_{n\mathbf{k},-q} e^{-q\beta\omega_{n\mathbf{k}}}. \tag{3.181}$$

An immediate consequence is that $O^{[1];[1]}_{n\mathbf{k}} = 0$ if we take the equilibrium phonon population $N^{\mathrm{eq}}_{n\mathbf{k}}$ to be Bose-Einstein's distribution, as was physically required. Similarly, for the two-phonon interactions at first order, we find the detailed-balance relation

$$W^{[2];[2]}_{n\mathbf{k}q,n'\mathbf{k}'q'} = e^{-\beta(q\omega_{n\mathbf{k}}+q'\omega_{n'\mathbf{k}'})} W^{[2];[2]}_{n\mathbf{k}-q,n'\mathbf{k}'-q'}. \tag{3.182}$$

Again, taking $N^{\mathrm{eq}}_{n\mathbf{k}}$ to be Bose-Einstein's distribution implies $O^{[2];[2]}_{n\mathbf{k}} = 0$. Moreover, the detailed-balance relation also implies

$$M^{[2];[2]}_{n\mathbf{k},n'\mathbf{k}'} e^{\beta\omega_{n'\mathbf{k}'}} (N^{\mathrm{eq}}_{n'\mathbf{k}'})^2 = (n\mathbf{k} \leftrightarrow n'\mathbf{k}'), \tag{3.183}$$

i.e. there are no antisymmetric contributions, and hence no thermal Hall effect at first Born's order. While we proved this explicitly for the one-phonon and two-phonon cases, this is true in general (along with $O_{n\mathbf{k}} = 0$) for any number of phonon creation-annihilation operators at first order in Born's expansion (see Sec. 3.D.2.3).

3.C.2.4 Extra structure

Independently, by writing

$$Q^{-q}_{n\mathbf{k}}(t) Q^{q}_{n\mathbf{k}}(0) = \frac{1}{2}[Q^{-q}_{n\mathbf{k}}(t), Q^{q}_{n\mathbf{k}}(0)] + \frac{1}{2}\{Q^{-q}_{n\mathbf{k}}(t), Q^{q}_{n\mathbf{k}}(0)\} \tag{3.184}$$

it is straightforward to show that only the commutator term contributes to $W^{[1](1)}_{n,\mathbf{k},q} - W^{[1](1)}_{n,\mathbf{k},-q}$. In turn, the final expression for the diagonal of the collision matrix Eq. (3.174) takes the form of the spectral function:

$$D^{[1];[1]}_{n\mathbf{k}} = -\int_{-\infty}^{+\infty} \mathrm{d}t e^{-i\omega_{n\mathbf{k}}t} \left\langle [Q^{-}_{n\mathbf{k}}(t), Q^{+}_{n\mathbf{k}}(0)] \right\rangle_{\beta}. \tag{3.185}$$

In the two-phonon case, a commutator structure does not naturally appear, so that one is left with

$$\begin{aligned} D^{[2];[2]}_{n\mathbf{k}} \;=\; & -\frac{2}{N_{\mathrm{uc}}} \sum_{n'\mathbf{k}'} \sum_{q,q'=\pm} q \left(N^{\mathrm{eq}}_{n'\mathbf{k}'} + \tfrac{q'+1}{2} \right) \\ & \times \int_{\mathbb{R}} \mathrm{d}t \; e^{-i(q\omega_{n\mathbf{k}}+q'\omega_{n'\mathbf{k}'})t} \left\langle Q^{-q-q'}_{n\mathbf{k}n'\mathbf{k}'}(t) Q^{qq'}_{n\mathbf{k}n'\mathbf{k}'}(0) \right\rangle_{\beta}, \end{aligned} \tag{3.186}$$

at order λ^4 and first Born's order.

3.C.3 Energy shift of the phonons

We now address the constant term $O_{n\mathbf{k}}$ appearing in the collision integral, which must vanish because there is no current in equilibrium. Its cancellation is equivalent to a redefinition of the energies of the phonons, due to their interaction with the Q degrees of freedom. This energy shift corresponds to the real part of the associated self-energy. Consequently, the equilibrium phonon populations $N^{\mathrm{eq}}_{n'\mathbf{k}'}$ are a priori not equal to $N^{\mathrm{BE}}_{n'\mathbf{k}'}$, the Bose-Einstein populations for the *unperturbed* phonon energies.

In this subsection, we show that the energy shift, although a priori nonzero, does not alter the results which we obtained for the thermal conductivities, up to the order λ^4 in our perturbative expansion. To understand this, we decompose

$$O_{n\mathbf{k}}[N^{\mathrm{eq}}_{n'\mathbf{k}'}] = O^{(1)}_{n\mathbf{k}}[N^{\mathrm{eq}}_{n'\mathbf{k}'}] + O^{(2)}_{n\mathbf{k}}[N^{\mathrm{eq}}_{n'\mathbf{k}'}] + \mathcal{O}(\lambda^6) \tag{3.187}$$

where, as for $D_{n\mathbf{k}}$ elsewhere in this paper, the upper index $O^{(p)}$ indicates a term of order λ^{2p}.

We have shown in Sec. 3.C.2.3 that $O^{(1)}_{n\mathbf{k}}[N^{\mathrm{BE}}_{n'\mathbf{k}'}] = 0$. However, $O^{(2)}_{n\mathbf{k}}[N^{\mathrm{BE}}_{n'\mathbf{k}'}] \neq 0$ a priori, so that an energy shift is actually required to cancel the equilibrium current. We thus consider the *physical requirement*, $O_{n\mathbf{k}}[N^{\mathrm{eq}}_{n'\mathbf{k}'}] = 0$, to be an equation on the unknown $N^{\mathrm{eq}}_{n'\mathbf{k}'}$.

Now expanding $N^{\mathrm{eq}}_{n'\mathbf{k}'} = N^{\mathrm{BE}}_{n'\mathbf{k}'} + \delta N^{\mathrm{eq}}_{n'\mathbf{k}'}$ (with $\delta N^{\mathrm{eq}}_{n'\mathbf{k}'}$ at least of order λ^2), this equation becomes

$$0 = O^{(1)}_{n\mathbf{k}}[N^{\mathrm{BE}}_{n''\mathbf{k}''}] + \sum_{n'\mathbf{k}'} \delta N^{\mathrm{eq}}_{n'\mathbf{k}'} \partial_{N^{\mathrm{eq}}_{n'\mathbf{k}'}} O^{(1)}_{n\mathbf{k}}[N^{\mathrm{BE}}_{n''\mathbf{k}''}] + O^{(2)}_{n\mathbf{k}}[N^{\mathrm{BE}}_{n''\mathbf{k}''}] + \mathcal{O}(\lambda^6) \tag{3.188}$$

At order λ^2, one recovers $O^{(1)}_{n\mathbf{k}}[N^{\mathrm{BE}}_{n'\mathbf{k}'}] = 0$, as is required by detailed balance (see Sec. 3.D.2.2).

At order λ^4, formally inverting this linear equation, one obtains

$$\delta N^{\mathrm{eq}}_{n\mathbf{k}} = -\sum_{n'\mathbf{k}'} \left(\partial_{N^{\mathrm{eq}}_{n_j\mathbf{k}_j}} O^{(1)}_{n_i\mathbf{k}_i}[N^{\mathrm{BE}}_{n''\mathbf{k}''}] \right)^{-1} \Big|_{n\mathbf{k},n'\mathbf{k}'} \times O^{(2)}_{n'\mathbf{k}'}[N^{\mathrm{BE}}_{n''\mathbf{k}''}] \quad + \mathcal{O}(\lambda^4). \tag{3.189}$$

This correction Eq. (3.17) to the phonon equilibrium populations is of order λ^2.

This ensures that using the approximate populations $N^{\mathrm{eq}}_{n'\mathbf{k}'} = N^{\mathrm{BE}}_{n'\mathbf{k}'}$ leads to a correct estimation of $D^{(1)}_{n\mathbf{k}}$ the lowest-order contribution to $D_{n\mathbf{k}}$, of order λ^2. However, the next-order contribution $D^{(2)}_{n\mathbf{k}} \sim \lambda^4$ can only be estimated correctly if one adds to it the correction that $\delta N^{\mathrm{eq}}_{n\mathbf{k}}$ brings to $D^{(1)}_{n\mathbf{k}}$. Similarly, using the approximate populations $N^{\mathrm{eq}}_{n'\mathbf{k}'} = N^{\mathrm{BE}}_{n'\mathbf{k}'}$ leads to a correct estimation of the lowest-order contribution, of order λ^4, to $M_{n\mathbf{k}n'\mathbf{k}'}$ as expressed in the main text. Corrections of order λ^6, not considered in the present work, would require that the population corrections $\delta N^{\mathrm{eq}}_{n\mathbf{k}}$ be taken into account.

3.C.4 Computation at second Born order

As discussed at length, the first Born approximation alone does not lead to a nonzero thermal Hall effect. Here we compute that which appears when the Born

expansion is taken up to the second Born order. More precisely, we consider all possible terms up to second Born order that lead to an off-diagonal scattering rate of order at most λ^4. This includes terms like $\langle \mathtt{f}|H'_{[1]}|\mathtt{n}\rangle\langle \mathtt{n}|H'_{[1]}|\mathtt{i}\rangle$ as well as $\langle \mathtt{f}|H'_{[1]}|\mathtt{n}\rangle\langle \mathtt{n}|H'_{[2]}|\mathtt{i}\rangle$, but not $\langle \mathtt{i}|H'_{[2]}|\mathtt{n}\rangle\langle \mathtt{n}|H'_{[2]}|\mathtt{i}\rangle$ since this term is already of order λ^4 (thus contributes to $|T_{\mathtt{i}\to\mathtt{f}}|^2$ at order λ^5 at least).

3.C.4.1 Term with one-phonon interactions only

The first of these terms reads

$$\begin{aligned} T^{[1,1]}_{\mathtt{i}\to\mathtt{f}} &= \sum_{n\mathbf{k},n'\mathbf{k}'} \sum_{q,q'=\pm} \sqrt{N^i_{n\mathbf{k}} + \tfrac{1+q}{2}}\sqrt{N^f_{n'\mathbf{k}'} + \tfrac{1-q'}{2}} \\ &\quad \cdot \sum_{m_s} \frac{\langle f_s|Q^{q'}_{n'\mathbf{k}'}|m_s\rangle\langle m_s|Q^{q}_{n\mathbf{k}}|i_s\rangle}{E_{i_s} - E_{m_s} - q\omega_{\mathbf{k},n} + i\eta}\ \mathbb{I}(i_p \xrightarrow[q'\cdot n'\mathbf{k}']{q\cdot n\mathbf{k}} f_p), \end{aligned} \tag{3.190}$$

where the upper index indicates that within Born's expansion, $T^{[i,j]} \sim \frac{\langle f|H'_{[j]}|m\rangle\langle m|H'_{[i]}|i\rangle}{E_i - E_m + i\eta}$.

The squared T-matrix elements now include cross-terms between the first and second orders of Born's expansion (although we keep only terms of order λ^4 at most). Here we give details of the calculation of one term, the square of Eq. (3.190), $\left|T^{[1,1]}_{\mathtt{i}\to\mathtt{f}}\right|^2$.

In the numerator, the matrix elements of the Q operators can combine themselves in two different ways, which we denote in the following as

$$\text{(a)}: \qquad \langle i_s|Q^{q}_{n\mathbf{k}}|m_s\rangle\langle m_s|Q^{q'}_{n'\mathbf{k}'}|f_s\rangle\langle f_s|Q^{-q'}_{n'\mathbf{k}'}|m'_s\rangle\langle m'_s|Q^{-q}_{n\mathbf{k}}|i_s\rangle \tag{3.191}$$

$$\text{(b)}: \qquad \langle i_s|Q^{q}_{n\mathbf{k}}|m_s\rangle\langle m_s|Q^{q'}_{n'\mathbf{k}'}|f_s\rangle\langle f_s|Q^{-q}_{n\mathbf{k}}|m'_s\rangle\langle m'_s|Q^{-q'}_{n'\mathbf{k}'}|i_s\rangle. \tag{3.192}$$

We use the following time integral representation of each of the denominators (using a regularized definition of the sign function),

$$\begin{aligned} \frac{1}{x \pm i\eta} &= \mathrm{PP}\frac{1}{x} \mp i\pi\delta(x) \qquad (3.193)\\ &= \frac{1}{2i}\int_{-\infty}^{+\infty} \mathrm{d}t_1 e^{it_1 x}\mathrm{sign}(t_1) \pm \frac{1}{2i}\int_{-\infty}^{+\infty} \mathrm{d}t_1 e^{it_1 x}. \end{aligned}$$

and a introduce a third time integral to enforce the energy conservation $E_{\mathtt{f}} - E_{\mathtt{i}} = q'\omega_{n'\mathbf{k}'} + q\omega_{n\mathbf{k}} + E_{f_s} - E_{i_s}$. The product of the denominators (cf. Eq. (3.193)) leads to four terms, which can be labeled by two signs $s, s' = \pm$, and we define, for convenience,

$$\Theta_{ss'}(t_1,t_2) := [-\mathrm{sign}(t_1)]^{\frac{1-s}{2}}\,[\mathrm{sign}(t_2)]^{\frac{1-s'}{2}}\,. \tag{3.194}$$

Then, the transition rate coming from this part of the total squared matrix element can be written as a sum of eight terms:

$$\begin{aligned} \Gamma^{[1,1];[1,1]}_{i_p\to f_p} &= \sum_{n\mathbf{k},n'\mathbf{k}'} \sum_{q,q'} \left(N^i_{n\mathbf{k}} + \tfrac{q+1}{2}\right)\left(N^i_{n'\mathbf{k}'} + \tfrac{q'+1}{2}\right) \qquad (3.195)\\ &\quad \cdot \sum_{s,s'=\pm}\sum_{i=a,b} W^{[1,1];[1,1],(i),ss'}_{n\mathbf{k}q,n'\mathbf{k}'q'}\ \mathbb{I}(i_p \xrightarrow[q'\cdot n'\mathbf{k}']{q\cdot n\mathbf{k}} f_p), \end{aligned}$$

where we defined (notice the order of the first two operators in the correlator and the sign $t_1 \pm t_2$ in the exponential):

$$W^{[1,1];[1,1],(a),ss'}_{n\mathbf{k}q,n'\mathbf{k}'q'} = \int \mathrm{d}t\mathrm{d}t_1\mathrm{d}t_2\Theta_{ss'}(t_1,t_2)e^{i(q\omega_{n\mathbf{k}}+q'\omega_{n'\mathbf{k}'})t}e^{i(t_1+t_2)(q\omega_{n\mathbf{k}}-q'\omega_{n'\mathbf{k}'})} \cdot \left\langle Q^{-q}_{n\mathbf{k}}(-t-t_2)Q^{-q'}_{n'\mathbf{k}'}(-t+t_2)Q^{q'}_{n'\mathbf{k}'}(-t_1)Q^{q}_{n\mathbf{k}}(+t_1)\right\rangle_\beta, \quad (3.196)$$

$$W^{[1,1];[1,1],(b),ss'}_{n\mathbf{k}q,n'\mathbf{k}'q'} = \int \mathrm{d}t\mathrm{d}t_1\mathrm{d}t_2\Theta_{ss'}(t_1,t_2)e^{i(q\omega_{n\mathbf{k}}+q'\omega_{n'\mathbf{k}'})t}e^{i(t_1-t_2)(q\omega_{n\mathbf{k}}-q'\omega_{n'\mathbf{k}'})} \cdot \left\langle Q^{-q'}_{n'\mathbf{k}'}(-t-t_2)Q^{-q}_{n\mathbf{k}}(-t+t_2)Q^{q'}_{n'\mathbf{k}'}(-t_1)Q^{q}_{n\mathbf{k}}(+t_1)\right\rangle_\beta. \quad (3.197)$$

We will investigate the symmetries of these terms in Sec. 3.C.4.3, and show that only some combinations contribute to the thermal Hall conductivity. In fact the eight terms from Eq. (3.195) can be rewritten as products of (anti-)commutators. Meanwhile, defining the symmetrized in $(n\mathbf{k}q \leftrightarrow n'\mathbf{k}'q')$ collision rate,

$$\mathcal{W}^{[1,1];[1,1],ss'}_{n\mathbf{k}q,n'\mathbf{k}'q'} = \sum_{i=a,b} W^{[1,1];[1,1],(i),ss'}_{n\mathbf{k}q,n'\mathbf{k}'q'} + (n\mathbf{k}q \leftrightarrow n'\mathbf{k}'q'), \quad (3.198)$$

we obtain components of the part of the collision matrix due to $\left|T^{[1,1]}_{\mathtt{i}\to\mathtt{f}}\right|^2$:

$$O^{[1,1];[1,1]}_{n,\mathbf{k}} = \sum_{n'\mathbf{k}'}\sum_{q,q'} q \sum_{s,s'} \mathcal{W}^{[1,1];[1,1],ss'}_{n\mathbf{k}q,n'\mathbf{k}'q'} \left(N^{\mathrm{eq}}_{n,\mathbf{k}} + \tfrac{q+1}{2}\right)\left(N^{\mathrm{eq}}_{n'\mathbf{k}'} + \tfrac{q'+1}{2}\right), \quad (3.199)$$

$$-D^{[1,1];[1,1]}_{n,\mathbf{k}} = \sum_{n'\mathbf{k}'}\sum_{q,q'} q \left(N^{\mathrm{eq}}_{n',\mathbf{k}'} + \tfrac{q'+1}{2}\right)\sum_{s,s'} \mathcal{W}^{[1](2),ss'}_{n\mathbf{k}q,n'\mathbf{k}'q'}, \quad (3.200)$$

$$M^{[1,1];[1,1]}_{n\mathbf{k},n'\mathbf{k}'} = \sum_{q,q'} q \left(N^{\mathrm{eq}}_{n,\mathbf{k}} + \tfrac{q+1}{2}\right)\sum_{s,s'} \mathcal{W}^{[1](2),ss'}_{n\mathbf{k}q,n'\mathbf{k}'q'}. \quad (3.201)$$

3.C.4.2 Commutators and anticommutators

In what follows, we write $[\![A,B]\!]_\pm = AB \pm BA$.

Upon replacing $Q^{-q}_{n\mathbf{k}}(-t-t_2)Q^{-q'}_{n'\mathbf{k}'}(-t+t_2)$ by

$$Q^{-q}_{n\mathbf{k}}(-t-t_2)Q^{-q'}_{n'\mathbf{k}'}(-t+t_2) - [\![Q^{-q}_{n\mathbf{k}}(-t-t_2), Q^{-q'}_{n'\mathbf{k}'}(-t+t_2)]\!]_{s'}$$

in the definition of $W^{[1,1];[1,1],(a),ss'}_{n\mathbf{k}q,n'\mathbf{k}'q'}$ hereabove, (after changing $t_2 \leftrightarrow -t_2$ if $s' = -$) one obtains $-W^{[1,1];[1,1],(b),ss'}_{n\mathbf{k}q,n'\mathbf{k}'q'}$. Therefore,

$$\begin{aligned} & W^{[1,1];[1,1],(a),ss'}_{n\mathbf{k}q,n'\mathbf{k}'q'} + W^{[1,1];[1,1],(b),ss'}_{n\mathbf{k}q,n'\mathbf{k}'q'} \quad (3.202)\\ = & \int \mathrm{d}t\mathrm{d}t_1\mathrm{d}t_2\Theta_{ss'}(t_1,t_2)e^{i(q\omega_{n\mathbf{k}}+q'\omega_{n'\mathbf{k}'})t}e^{i(t_1+t_2)(q\omega_{n\mathbf{k}}-q'\omega_{n'\mathbf{k}'})} \\ & \cdot \left\langle [\![Q^{-q}_{n\mathbf{k}}(-t-t_2), Q^{-q'}_{n'\mathbf{k}'}(-t+t_2)]\!]_{s'} Q^{q'}_{n'\mathbf{k}'}(-t_1)Q^{q}_{n\mathbf{k}}(+t_1)\right\rangle_\beta. \end{aligned}$$

Similarly, upon replacing $Q^{q'}_{n'\mathbf{k}'}(-t_1)Q^{q}_{n\mathbf{k}}(t_1)$ by

$$Q^{q'}_{n'\mathbf{k}'}(-t_1), Q^{q}_{n\mathbf{k}}(t_1) - [\![Q^{q'}_{n'\mathbf{k}'}(-t_1), Q^{q}_{n\mathbf{k}}(t_1)]\!]_s$$

into $W^{[1,1];[1,1],(a),ss'}_{n\mathbf{k}q,n'\mathbf{k}'q'} + W^{[1,1];[1,1],(b),ss'}_{n\mathbf{k}q,n'\mathbf{k}'q'}$ i.e. Eq.(3.202), (after changing $t_1 \leftrightarrow -t_1$ if $s = -$) one obtains $-W^{[1,1];[1,1],(b),ss'}_{n'\mathbf{k}'q',n\mathbf{k}q} - W^{[1,1];[1,1],(a),ss'}_{n'\mathbf{k}'q',n\mathbf{k}q}$.

Therefore, the only nonzero contribution to $W^{[1,1];[1,1],(a),ss'}_{n\mathbf{k}q,n'\mathbf{k}'q'} + W^{[1,1];[1,1],(b),ss'}_{n'\mathbf{k}'q',n\mathbf{k}q} + (n\mathbf{k}q \leftrightarrow n'\mathbf{k}'q')$, i.e. Eq. (3.198), takes the form

$$\begin{aligned}\mathcal{W}^{[1,1];[1,1],ss'}_{n\mathbf{k}q,n'\mathbf{k}'q'} &= \int \mathrm{d}t\mathrm{d}t_1\mathrm{d}t_2\Theta_{ss'}(t_1,t_2)e^{i(q\omega_{nk}+q'\omega_{n'k'})t}e^{i(t_1+t_2)(q\omega_{nk}-q'\omega_{n'k'})} \\ &\quad\cdot\left\langle [\![Q^{-q}_{n\mathbf{k}}(-t-t_2),Q^{-q'}_{n'\mathbf{k}'}(-t+t_2)]\!]_{s'}[\![Q^{q'}_{n'\mathbf{k}'}(-t_1),Q^{q}_{n\mathbf{k}}(+t_1)]\!]_{s}\right\rangle_{\beta},\end{aligned} \tag{3.203}$$

where $s, s' = +$ corresponds to an energy conservation constraint, i.e. to on-shell scattering event, while $s, s' = -$ corresponds to a $\mathrm{PP}(E_{\mathtt{i}} - E_{\mathtt{n}})^{-1}$ term, i.e. off-shell scattering (with $\mathtt{i}, \mathtt{n}, \mathtt{f}$ the initial, intermediate, and final states in the second-order process).

Note that, in a time-reversal symmetric system, these satisfy the symmetry

$$\mathcal{W}^{[1,1];[1,1],ss'}_{n\mathbf{k}q,n'\mathbf{k}'q'} = ss'\mathcal{W}^{[1,1];[1,1],s's}_{n-\mathbf{k}q,n'-\mathbf{k}'q'}, \tag{3.204}$$

reflecting the role of $\pm i\eta$ in the denominators in terms of causality.

3.C.4.3 Detailed balance

Using the method of the previous subsection Sec. 3.C.2.3, we show the following ("anti-")detailed-balance relations

$$W^{[1,1];[1,1],(a),ss'}_{n\mathbf{k}q,n'\mathbf{k}'q'} = ss'\ W^{[1,1];[1,1],(a),s's}_{n'\mathbf{k}'-q',n\mathbf{k}-q}e^{-\beta(q\omega_{\mathbf{k}}+q'\omega_{\mathbf{k}'})}, \tag{3.205}$$

$$W^{[1,1];[1,1],(b),ss'}_{n\mathbf{k}q,n'\mathbf{k}'q'} = ss'\ W^{[1,1];[1,1],(b),s's}_{n\mathbf{k}-q,n'\mathbf{k}'-q'}e^{-\beta(q\omega_{\mathbf{k}}+q'\omega_{\mathbf{k}'})}. \tag{3.206}$$

From this, the same holds for the symmetrized in $n\mathbf{k}q \leftrightarrow n'\mathbf{k}'q'$ scattering rate:

$$\mathcal{W}^{[1,1];[1,1],ss'}_{n\mathbf{k}q,n'\mathbf{k}'q'} = ss'\ e^{-\beta(q\omega_{\mathbf{k}}+q'\omega_{\mathbf{k}'})}\mathcal{W}^{[1,1];[1,1],ss'}_{n\mathbf{k}-q,n'\mathbf{k}'-q'}. \tag{3.207}$$

We now identify

$$\mathfrak{W}^{\ominus,[1,1];[1,1],qq'}_{n\mathbf{k},n'\mathbf{k}'} = N_{\mathrm{uc}}\sum_{s=\pm}\mathcal{W}^{[1,1];[1,1],s,-s}_{n\mathbf{k}q,n'\mathbf{k}'q'}, \tag{3.208}$$

$$\mathfrak{W}^{\oplus,[1,1];[1,1],qq'}_{n\mathbf{k},n'\mathbf{k}'} = N_{\mathrm{uc}}\sum_{s=\pm}\mathcal{W}^{[1,1];[1,1],ss}_{n\mathbf{k}q,n'\mathbf{k}'q'}, \tag{3.209}$$

complete expressions of which are given in the main text.

By construction, these enforce

$$\mathfrak{W}^{\sigma,[1,1];[1,1],qq'}_{n\mathbf{k},n'\mathbf{k}'} = \sigma\ e^{-\beta(q\omega_{\mathbf{k}}+q'\omega_{\mathbf{k}'})}\mathfrak{W}^{\sigma,[1,1];[1,1],-q-q'}_{n\mathbf{k},n'\mathbf{k}'}, \tag{3.210}$$

where $\sigma = \oplus$ (resp. $\sigma = \ominus$) indicates that $\mathfrak{W}$ enforces detailed balance (resp. "anti-detailed balance").

3.C.4.4 All contributions

As mentioned at the beginning of this subsection, other terms of order λ^4 contribute to the thermal conductivity at second Born's order. In the following, we use the shorthand $[\![A(-t),B(t')]\!] = \mathrm{sign}(t+t')[A(-t),B(t')]$ and $\fint_{t,\{t_j\}}$ (resp. $\fint'_{t,\{t_j\}}$), $j=1,..,l$, denotes the set of $1+l$ inverse Fourier transforms evaluated once at $\Sigma^{n'\mathbf{k}'q'}_{n\mathbf{k}q} = q\omega_{n\mathbf{k}} + q'\omega_{n'\mathbf{k}'}$ and l times at $\Delta^{n'\mathbf{k}'q'}_{n\mathbf{k}q} = q\omega_{n\mathbf{k}} - q'\omega_{n'\mathbf{k}'}$, i.e. $\fint_{t,\{t_j\}} = \int \mathrm{d}t\mathrm{d}t_1..\mathrm{d}t_l e^{i\Sigma^{n'\mathbf{k}'q'}_{n\mathbf{k}q}t} e^{i\Delta^{n'\mathbf{k}'q'}_{n\mathbf{k}q}(t_1+..+t_l)}$, (resp. once at $q\omega_{n\mathbf{k}}$ and l times at $q'\omega_{n'\mathbf{k}'}$, i.e. $\fint'_{t,\{t_j\}} = \int \mathrm{d}t\mathrm{d}t_1..\mathrm{d}t_l e^{iq\omega_{n\mathbf{k}}t} e^{iq'\omega_{n'\mathbf{k}'}(t_1+..+t_l)}$).

One contribution comes from the "cross-term" $2\mathfrak{Re}\{(T^{[2]}_{\mathtt{i}\to\mathtt{f}})^* T^{[1,1]}_{\mathtt{i}\to\mathtt{f}}\}$, which contributes to the scattering rates in the form of

$$\mathfrak{W}^{\ominus,[1,1];[2],qq'}_{n\mathbf{k}n'\mathbf{k}'} = \frac{2N_{\mathrm{uc}}^{1/2}}{\hbar^4}\,\mathfrak{Im}\fint_{t,t_1}\left\langle Q^{-q,-q'}_{n\mathbf{k}n'\mathbf{k}'}(-t)\{Q^{q'}_{n'\mathbf{k}'}(-t_1),Q^{q}_{n\mathbf{k}}(t_1)\}\right\rangle \tag{3.211}$$

$$\mathfrak{W}^{\oplus,[1,1];[2],qq'}_{n\mathbf{k}n'\mathbf{k}'} = -\frac{2N_{\mathrm{uc}}^{1/2}}{\hbar^4}\,\mathfrak{Im}\fint_{t,t_1}\left\langle Q^{-q,-q'}_{n\mathbf{k}n'\mathbf{k}'}(-t)[\![Q^{q'}_{n'\mathbf{k}'}(-t_1),Q^{q}_{n\mathbf{k}}(t_1)]\!]\right\rangle. \tag{3.212}$$

The last contribution comes from considering the second Born's order matrix element

$$\begin{aligned} T^{[2,1]}_{\mathtt{i}\to\mathtt{f}} \;=\; & \frac{1}{\sqrt{N_{\mathrm{uc}}}}\sum_{n\mathbf{k},n'\mathbf{k}'}\sum_{q,q'=\pm}\left(N^i_{n'\mathbf{k}'}+\tfrac{1+q'}{2}\right)\sqrt{N^i_{n\mathbf{k}}+\tfrac{1+q}{2}}\;\mathbb{I}(\mathtt{i}_p \xrightarrow{q\cdot n\mathbf{k}} \mathtt{f}_p) \\ & \sum_{\mathtt{m}_s}\left\{\frac{\langle\mathtt{f}_s|Q^{-q'}_{n'\mathbf{k}'}|\mathtt{m}_s\rangle\langle\mathtt{m}_s|Q^{qq'}_{n\mathbf{k},n'\mathbf{k}'}|\mathtt{i}_s\rangle}{E_{\mathtt{f}_s}-E_{\mathtt{m}_s}-q'\omega_{n'\mathbf{k}'}+i\eta}+\frac{\langle\mathtt{f}_s|Q^{qq'}_{n\mathbf{k},n'\mathbf{k}'}|\mathtt{m}_s\rangle\langle\mathtt{m}_s|Q^{-q'}_{n'\mathbf{k}'}|\mathtt{i}_s\rangle}{E_{\mathtt{i}_s}-E_{\mathtt{m}_s}+q'\omega_{n'\mathbf{k}'}+i\eta}\right\}, \end{aligned} \tag{3.213}$$

which contains two-phonon operators, of order λ^2. At order λ^4, it is thus involved in the "cross-term" $2\,\mathfrak{Re}\{(T^{[1]}_{\mathtt{i}\to\mathtt{f}})^* T^{[2,1]}_{\mathtt{i}\to\mathtt{f}}\}$, which contributes to scattering rates in the form of $\mathfrak{W}^{[2,1];[1],qq'}_{n\mathbf{k}n'\mathbf{k}'} = \sum_{s=\pm}\mathfrak{W}^{[2,1];[1],qq'}_{n\mathbf{k}n'\mathbf{k}'|s}$, where

$$\mathfrak{W}^{[2,1];[1],qq'}_{n\mathbf{k}n'\mathbf{k}'|s} = \frac{N_{\mathrm{uc}}^{1/2}}{\hbar^4}\mathfrak{Im}\fint'_{t,t_1}\left\langle Q^{-q}_{n\mathbf{k}}(-t)[\mathrm{sign}(t_1)]^{\frac{1-s}{2}}[\![Q^{-q'}_{n'\mathbf{k}'}(-t_1),Q^{qq'}_{n\mathbf{k}n'\mathbf{k}'}(0)]\!]_s\right\rangle, \tag{3.214}$$

and we recall the shorthand $[\![A,B]\!]_\pm = AB \pm BA$.

The first two terms enforce the usual, "two-phonon", (anti-)detailed balance relations

$$\mathfrak{W}^{\sigma,[2];[1,1],qq'}_{n\mathbf{k}q,n'\mathbf{k}'q'} = \sigma\; e^{-\beta(q\omega_{\mathbf{k}}+q'\omega_{\mathbf{k}'})}\mathfrak{W}^{\sigma,[2];[1,1],qq'}_{n\mathbf{k}q,n'\mathbf{k}'q'}, \tag{3.215}$$

with $\sigma=\oplus,\ominus$. Meanwhile, the last term satisfies "one-phonon" (anti-)detailed balance,

$$\mathfrak{W}^{[2,1];[1],qq'}_{n\mathbf{k},n'\mathbf{k}'|s} = s\,e^{-q\beta\omega_{n\mathbf{k}}}\mathfrak{W}^{[2,1];[1],-q-q'}_{n\mathbf{k},n'\mathbf{k}'|s}, \tag{3.216}$$

where we used a different notation ($s=\pm$ as a lower index) to emphasize the difference with the other terms derived hereabove.

3.C.5 Computation at third Born's order

The only third-order element of $T_{\mathtt{i}\mapsto\mathtt{f}}$ which can appear in a term of order λ^4 in $|T_{\mathtt{i}\mapsto\mathtt{f}}|^2$ is

$$\begin{aligned}T^{[1,1,1]}_{\mathtt{i}\to\mathtt{f}} = &\sum_{n\mathbf{k}q,n'\mathbf{k}'q'} \sqrt{N^i_{n\mathbf{k}} + \tfrac{1+q}{2}}\left(N^i_{n'\mathbf{k}'} + \tfrac{1+q'}{2}\right)\ \mathbb{I}(i_p \xrightarrow{q\cdot n\mathbf{k}} f_p)\\ &\times \sum_{m_s,m'_s}\left\{\frac{\langle f_s|Q^{-q'}_{n'\mathbf{k}'}|m'_s\rangle\langle m'_s|Q^{q'}_{n'\mathbf{k}'}|m_s\rangle\langle m_s|Q^{q}_{n\mathbf{k}}|i_s\rangle}{(E_{i_s}-E_{m_s}-q\omega_{n\mathbf{k}}+i\eta)(E_{f_s}-E_{m'_s}-q'\omega_{n'\mathbf{k}'}+i\eta)}\right.\\ &\quad+\frac{\langle f_s|Q^{-q'}_{n'\mathbf{k}'}|m'_s\rangle\langle m'_s|Q^{q}_{n\mathbf{k}}|m_s\rangle\langle m_s|Q^{q'}_{n'\mathbf{k}'}|i_s\rangle}{(E_{i_s}-E_{m_s}-q'\omega_{n'\mathbf{k}'}+i\eta)(E_{f_s}-E_{m'_s}-q'\omega_{n'\mathbf{k}'}+i\eta)}\\ &\quad\left.+\frac{\langle f_s|Q^{q}_{n\mathbf{k}}|m'_s\rangle\langle m'_s|Q^{-q'}_{n'\mathbf{k}'}|m_s\rangle\langle m_s|Q^{q'}_{n'\mathbf{k}'}|i_s\rangle}{(E_{i_s}-E_{m_s}-q'\omega_{n'\mathbf{k}'}+i\eta)(E_{f_s}-E_{m'_s}+q\omega_{n\mathbf{k}}+i\eta)}\right\},\end{aligned} \tag{3.217}$$

which is involved in the scattering rate

$$\mathfrak{W}^{[1,1,1];[1],qq'}_{n\mathbf{k}n'\mathbf{k}'} = 2\mathfrak{Re}\left[(T^{[1,1,1]}_{\mathtt{i}\to\mathtt{f}})^* T^{[1]}_{\mathtt{i}\to\mathtt{f}}\right] = \sum_{s,s'=\pm}\mathfrak{W}^{[1,1,1];[1],qq'}_{n\mathbf{k}n'\mathbf{k}'|ss'}, \tag{3.218}$$

where we denote

$$\mathfrak{W}^{[1,1,1];[1],qq'}_{n\mathbf{k}n'\mathbf{k}'|ss'} = \frac{-1}{2\hbar^4}\mathfrak{Re}\fint'_{t,t_1,t_2}\left\langle Q^{-q}_{n\mathbf{k}}(-t)\ \left(Q^{-q'}_{n'\mathbf{k}'}(-t_1),\, Q^{q}_{n\mathbf{k}}(0),\, Q^{q'}_{n'\mathbf{k}'}(t_2)\right)_{s,s'}\right\rangle, \tag{3.219}$$

$$\begin{aligned}\Big(A(t),B(t'),C(t'')\Big)_{s,s'} = &\,[\mathrm{sign}(t-t')]^{\frac{1-s}{2}}[\mathrm{sign}(t'-t'')]^{\frac{1-s'}{2}}\\ &\times\Big(A(t)B(t')C(t'')+sB(t')A(t)C(t'')+s'A(t)C(t'')B(t')\Big).\end{aligned}$$

This term enforces an unusual version of (anti-)detailed balance, namely

$$\mathfrak{W}^{[1,1,1];[1],qq'}_{n\mathbf{k}n'\mathbf{k}'|ss'} = ss'e^{-q\beta\omega_{n\mathbf{k}}}\mathfrak{W}^{[1,1,1];[1],-q,q'}_{n\mathbf{k}n'\mathbf{k}'|ss'}, \tag{3.220}$$

where the index q' remains inchanged.

3.D Generalizations

3.D.1 Generalized model and higher perturbative orders

To describe the interaction between phonon and another degree of freedom, we introduce general coupling terms between phonon annihilation (creation) operators $a^{(\dagger)}_{n\mathbf{k}}$ and general, for now unspecified, fields $Q^{\{q_j\}}_{\{n_j,\mathbf{k}_j\}}$ which are operators acting in their own Hilbert space, i.e. we write $H' = \sum_l H'_{[l]}$, with

$$H'_{[l]} = \frac{1}{\sqrt{N^l_{\mathrm{uc}}}}\sum_{\{n_i\mathbf{k}_i\}}\sum_{\{q_i=\pm\}}\Big(\prod_{j=1}^m a^{q_j}_{n_j\mathbf{k}_j}\Big)Q^{\{q_j\}}_{\{n_j\mathbf{k}_j\}}. \tag{3.221}$$

In this expression, m is the number of phonon creation-annihilation operators coupled to $Q^{\{q_j\}_{i=1..l}}_{\{n_j\mathbf{k}_j\}_{i=1..l}}$. In terms of the perturbative expansion introduced in the main text and the other appendices, this means $Q^{\{q_j\}_{i=1..l}}_{\{n_j\mathbf{k}_j\}_{i=1..l}} \sim \lambda^l$; note that since the perturbative expansion is considered (formally) up to *infinite* order in this appendix, we make this specification only for the sake of clarity. To avoid ambiguities, we assume that all the $n_j\mathbf{k}_j$ indices involved in a given term of $H'_{[l]}$ are distinct; this is correct in the thermodynamic limit. Note also that, for the sake of clarity in the following developments, the normalization factors of $N_{\rm uc}$ are not defined following the same convention as in the rest of the paper.

In what follows, we take special notations for the first two indices: $n_1\mathbf{k}_1 \equiv n\mathbf{k}$, $n_2\mathbf{k}_2 \equiv n'\mathbf{k}'$. Using the model Eq. (3.72) and following the general procedure described in Sec. 3.C and in the main text, one can then (at least formally) derive the collision integral which always takes the form

$$\mathcal{C}_{n\mathbf{k}} = \sum_{p=1}^{\infty} \frac{1}{N_{\rm uc}^p} \sum_{\{n_i\mathbf{k}_i\}_{i=2,..,p}} \sum_{\{q_i\}_{i=1,..,p}} q_1 \times \left[\prod_{i=1}^{p} \left(\overline{N}_{n_i\mathbf{k}_i} + \tfrac{q_i+1}{2}\right)\right] W^{(p),\{q_i\}}_{\{n_i\mathbf{k}_i\}}, \quad (3.222)$$

where the index (p) denotes a term of order λ^{2p}. The scattering rate $W^{(p),\{q_i\}}_{\{n_i\mathbf{k}_i\}} = W^{(p),\{q_i\}_{i=1,..,p}}_{\{n_i\mathbf{k}_i\}_{i=1,..,p}}$ is the sum of all the scattering rates of the $[l_1,..,l_m];[l'_1,..,l'_{m'}]$ kind (according to the nomenclature introduced in the main text) such that $\sum_{i=1}^{m} l_i + \sum_{j=1}^{m'} l'_j = 2p$. In terms of physical process, each of these terms corresponds to the interference between two scattering channels, $[l_1,..,l_m]$ and $[l'_1,..,l'_{m'}]$, such that in all, $2p$ phonon creations or annihilations occur between the initial `i` and final `f` states. Note that in the present paper, we compute explicitly this expansion up to $p = 2$.

We then expand the phonon average populations as $\overline{N}_{n_i\mathbf{k}_i} = N^{\rm eq}_{n_i\mathbf{k}_i} + \delta\overline{N}_{n_i\mathbf{k}_i}$. Following Eq.(3.11), the diagonal scattering rate is obtained as $D_{n\mathbf{k}} = -\partial_{\overline{N}_{n\mathbf{k}}} \mathcal{C}_{n\mathbf{k}}\Big|_{\overline{N}=N^{\rm eq}}$. It can be decomposed as $D_{n\mathbf{k}} = \sum_{p=1}^{\infty} D^{(p)}_{n\mathbf{k}}$, where

$$D^{(p)}_{n\mathbf{k}} = \frac{-1}{N_{\rm uc}^p} \sum_{\{n_i\mathbf{k}_i\}_{i=2,..,p}} \sum_{\{q_i\}_{i=1,..,p}} q_1 \times \left[\prod_{i=2}^{p} \left(N^{\rm eq}_{n_i\mathbf{k}_i} + \tfrac{q_i+1}{2}\right)\right] W^{(p),\{q_i\}}_{\{n_i\mathbf{k}_i\}}. \quad (3.223)$$

Similarly, the off-diagonal scattering rate is obtained as $M_{n\mathbf{k},n'\mathbf{k}'} = \partial_{\overline{N}_{n'\mathbf{k}'}} \mathcal{C}_{n\mathbf{k}}\Big|_{\overline{N}=N^{\rm eq}}$. It can be decomposed as $M_{n\mathbf{k},n'\mathbf{k}'} = \sum_{p=2}^{\infty} M^{(p)}_{n\mathbf{k},n'\mathbf{k}'}$, where

$$M^{(p)}_{n\mathbf{k}n'\mathbf{k}'} = \frac{1}{N_{\rm uc}^p} \sum_{\{n_i\mathbf{k}_i\}_{i=3,..,p}} \sum_{\{q_i\}_{i=1,..,p}} q_1 \times \left(N^{\rm eq}_{n\mathbf{k}} + \tfrac{q_1+1}{2}\right) \left[\prod_{i=3}^{p} \left(N^{\rm eq}_{n_i\mathbf{k}_i} + \tfrac{q_i+1}{2}\right)\right] W^{(p),\{q_i\}}_{\{n_i\mathbf{k}_i\}}. \quad (3.224)$$

Like in the equations for $p = 1, 2$ derived explicitly in Appendix 3.C, q_1 always factorizes in the collision integral, as the change in number of $n\mathbf{k}$ phonons due to the scattering event.

3.D.2 Special properties of first Born's order

3.D.2.1 Definitions and basic results

At first order of the Born expansion, all contributions to the collision integral are "semiclassical", in the sense defined in Sec. 3.3.4.3; i.e. an operator $Q^{q_1,..,q_l}_{n_1\mathbf{k}_1,..,n_l\mathbf{k}_l}$ does only appear in the collision integral as $|Q^{q_1,..,q_l}_{n_1\mathbf{k}_1,..,n_l\mathbf{k}_l}|^2$.

To make this statement more precise, we rewrite

$$H'_{[l]} = \frac{1}{\sqrt{N^l_{\rm uc}}} \sum_{r=0}^{l} \sum_{\{n_i\mathbf{k}_i\}_{i=1..l}} \Big(\prod_{j=1}^{r} a^+_{n_j\mathbf{k}_j} \Big) \Big(\prod_{j=r+1}^{l} a^-_{n_j\mathbf{k}_j} \Big) \times \frac{1}{\sqrt{r!(l-r)!}} Q^{+,..,+|-,..,-}_{n_1\mathbf{k}_1..n_r\mathbf{k}_r|n_{r+1}\mathbf{k}_{r+1}..n_l\mathbf{k}_l}, \tag{3.225}$$

where the upper indices of Q are r times '+' and $l-r$ times '−', and Q is by definition symmetric under permutation of its lower indices in the two blocks $\{n_i\mathbf{k}_i\}_{i=1,..,r}$ and $\{n_i\mathbf{k}_i\}_{i=r+1,..,l}$ separately. Hermiticity is guaranteed by $Q^{+,..,+|-,..,-}_{n_1\mathbf{k}_1..n_r\mathbf{k}_r|n_{r+1}\mathbf{k}_{r+1}..n_l\mathbf{k}_l} = (Q^{+,..,+|-,..,-}_{n_{r+1}\mathbf{k}_{r+1}..n_l\mathbf{k}_l|n_1\mathbf{k}_1..n_r\mathbf{k}_r})^\dagger$. Note that at first Born's order, distinct scattering channels $[l]$ and $[l']$ do not interfere for $l \neq l'$; one can thus study independently the contribution of each $H'_{[l]}$ to the collision integral.

The contribution to the squared T-matrix obtained from $H'_{[l]}$ at first Born's order is

$$\Big|T^{[l]}_{\mathtt{i}\to\mathtt{f}}\Big|^2 = \frac{1}{N^l_{\rm uc}} \sum_{r=0}^{l} \frac{1}{r!(l-r)!} \sum_{\{n_i\mathbf{k}_i\}_{i=1..l}} \left[\prod_{j=1}^{r} (N^{\mathtt{i}}_{n_j\mathbf{k}_j} + 1) \right] \left[\prod_{j=r+1}^{l} (N^{\mathtt{i}}_{n_j\mathbf{k}_j}) \right] \times \mathbb{I}(i_p \xrightarrow[-\{n_j\mathbf{k}_j\}^l_{r+1}]{+\{n_j\mathbf{k}_j\}^r_1} f_p) \, \langle i_s|Q^{+,..,+|-,..,-}_{\{n_j\mathbf{k}_j\}^l_{r+1}|\{n_j\mathbf{k}_j\}^r_1}|f_s\rangle \langle f_s|Q^{+,..,+|-,..,-}_{\{n_j\mathbf{k}_j\}^r_1|\{n_j\mathbf{k}_j\}^l_{r+1}}|i_s\rangle, \tag{3.226}$$

Summing over all scattering channels, the first Born's order contribution to the collision integral is

$$\mathcal{C}^{\mathtt{1B}}_{n\mathbf{k}} = \sum_{l=1}^{\infty} \frac{1}{N^l_{\rm uc}} \sum_{r=0}^{l} \sum_{\{n_i\mathbf{k}_i\}_{i=1,..,l}} \prod_{j=1}^{r} (\overline{N}_{n_j\mathbf{k}_j} + 1) \prod_{j=r+1}^{l} (\overline{N}_{n_j\mathbf{k}_j}) \times \left(\frac{r\delta_{n,n_1}\delta_{\mathbf{k},\mathbf{k}_1}}{r!(l-r)!} - \frac{(l-r)\delta_{n,n_{r+1}}\delta_{\mathbf{k},\mathbf{k}_{r+1}}}{r!(l-r)!} \right) W^{[l];[l]}_{\{n_j\mathbf{k}_j\}^r_1|\{n_j\mathbf{k}_j\}^l_{r+1}}, \tag{3.227}$$

where

$$W^{[l];[l]}_{\{n_j\mathbf{k}_j\}^r_1|\{n_j\mathbf{k}_j\}^l_{r+1}} = \int \mathrm{d}t e^{-i\left(\sum_{j=1}^r \omega_{n_j\mathbf{k}_j} - \sum_{j=r+1}^l \omega_{n_j\mathbf{k}_j}\right)t} \left\langle Q^{+,..,+|-,..,-}_{\{n_j\mathbf{k}_j\}^l_{r+1}|\{n_j\mathbf{k}_j\}^r_1}(t) \, Q^{+,..,+|-,..,-}_{\{n_j\mathbf{k}_j\}^r_1|\{n_j\mathbf{k}_j\}^l_{r+1}} \right\rangle. \tag{3.228}$$

Following the same steps as in Sec. 3.C.2.3, it is easy to see that $W^{[l];[l]}_{\{n_j\mathbf{k}_j\}^r_1|\{n_j\mathbf{k}_j\}^l_{r+1}}$ *always* enforces detailed-balance, namely

$$W^{[l];[l]}_{\{n_j\mathbf{k}_j\}^r_1|\{n_j\mathbf{k}_j\}^l_{r+1}} = e^{-\beta\left(\sum_{j=1}^r \omega_{n_j\mathbf{k}_j} - \sum_{j=r+1}^l \omega_{n_j\mathbf{k}_j}\right)} \times W^{[l];[l]}_{\{n_j\mathbf{k}_j\}^l_{r+1}|\{n_j\mathbf{k}_j\}^r_1}. \tag{3.229}$$

We now prove two important properties of the collision integral, as obtained from first Born's order, which derive therefrom.

3.D.2.2 No equilibrium current

The equilibrium current is due to $O_{n\mathbf{k}} = \mathcal{C}_{n\mathbf{k}}[\overline{N}_{n'\mathbf{k}'} \mapsto N^{\mathrm{eq}}_{n'\mathbf{k}'}]$, the constant term in the collision integral.

In the present case, by performing a change of index $r \mapsto l - r$ in the second term of $(\cdots - \dots)$ in Eq. (3.227), and resorting to the detailed balance relation Eq. (3.229) and taking $N^{\mathrm{eq}}_{n'\mathbf{k}'} = \frac{1}{e^{\beta\omega_{n'\mathbf{k}'}}-1}$, one can easily show that

$$O^{\mathtt{1B}}_{n\mathbf{k}} = \mathcal{C}^{\mathtt{1B}}_{n\mathbf{k}}[\overline{N}_{n_j\mathbf{k}_j} \mapsto N^{\mathrm{eq}}_{n_j\mathbf{k}_j}] = 0. \tag{3.230}$$

This means that no shift of the phonons' energies is needed at first Born's order to guarantee cancellation of the equilibrium current.

3.D.2.3 No phonon Hall effect

The off-diagonal contribution to the collision matrix at first Born's order, $M^{\mathtt{1B}}_{n\mathbf{k},n'\mathbf{k}'} = \partial_{\overline{N}_{n'\mathbf{k}'}} \mathcal{C}^{\mathtt{1B}}_{n\mathbf{k}}$, reads

$$\begin{aligned} M^{\mathtt{1B}}_{n\mathbf{k},n'\mathbf{k}'} = \sum_{l=1}^{\infty} \frac{1}{N_{\mathrm{uc}}^{l}} \sum_{r=0}^{l} \sum_{\{n_i\mathbf{k}_i\}_{i=1,..,l}} \prod_{j=1}^{r} (N^{\mathrm{eq}}_{n_j\mathbf{k}_j} + 1) \prod_{j=r+1}^{l} (N^{\mathrm{eq}}_{n_j\mathbf{k}_j})\, W^{[l];[l]}_{\{n_j\mathbf{k}_j\}_1^r|\{n_j\mathbf{k}_j\}_{r+1}^l} \\ \times \frac{1}{r!(l-r)!} \Big(r\delta_{n,n_1}\delta_{\mathbf{k},\mathbf{k}_1}\Big((r-1)\delta_{n',n_2}\delta_{\mathbf{k}',\mathbf{k}_2} + (l-r)\delta_{n',n_{r+1}}\delta_{\mathbf{k}',\mathbf{k}_{r+1}}\Big) \\ -(l-r)\delta_{n,n_{r+1}}\delta_{\mathbf{k},\mathbf{k}_{r+1}}\Big(r\delta_{n',n_1}\delta_{\mathbf{k}',\mathbf{k}_1} + (l-r-1)\delta_{n',n_{r+2}}\delta_{\mathbf{k}',\mathbf{k}_{r+2}}\Big)\Big) . \end{aligned} \tag{3.231}$$

After some algebra, following essentially the same steps as outlined hereabove, it is possible to show that

$$M^{\mathtt{1B}}_{n\mathbf{k},n'\mathbf{k}'} e^{\beta\omega_{n'\mathbf{k}'}} (N^{\mathrm{eq}}_{n'\mathbf{k}'})^2 = M^{\mathtt{1B}}_{n'\mathbf{k}',n\mathbf{k}} e^{\beta\omega_{n\mathbf{k}}} (N^{\mathrm{eq}}_{n\mathbf{k}})^2. \tag{3.232}$$

This, as was illustrated several times in the main text and the appendices, entails that $M^{\mathtt{1B}}$ does not contribute to κ_{H} – see Eq. 3.160. We have thus shown that no contribution to the thermal Hall conductivity can possibly come from first Born's order, regardless of the number of phonon operators in the Hamiltonian and of the nature of the operators Q to which they are coupled.

3.E Application—further technical details

3.E.1 Solving the delta functions

In order to solve the two simulaneous delta functions, we use the following rewriting of $\mathfrak{W}^{\ominus}$,

$$
\begin{aligned}
\mathfrak{W}^{\ominus,qq'}_{n\mathbf{k},n'\mathbf{k}'} &= \frac{64\pi^2}{\hbar^4 N_{\rm uc}^{2d}} \sum_{\mathbf{p}} \sum_{\{\ell_i,q_i\}} \mathcal{F}^{\ell_3,\ell_1,\ell_2|q_4,q_1,q_2}_{\mathbf{p},q\mathbf{k},q'\mathbf{k}'} \mathfrak{Im}\Bigg\{ \mathcal{B}^{n\ell_2\ell_3|q_2q_3q}_{\mathbf{k},\mathbf{p}+\frac{1}{2}q\mathbf{k}+q'\mathbf{k}'} \mathcal{B}^{n'\ell_3\ell_1|-q_3q_1q'}_{\mathbf{k}',\mathbf{p}+\frac{1}{2}q'\mathbf{k}'} \\
&\quad \mathrm{PP}\left[\frac{\mathcal{B}^{n\ell_1\ell_4|-q_1q_4-q}_{\mathbf{k},\mathbf{p}+\frac{1}{2}q\mathbf{k}} \mathcal{B}^{n'\ell_4\ell_2|-q_4-q_2-q'}_{\mathbf{k}',\mathbf{p}+q\mathbf{k}+\frac{1}{2}q'\mathbf{k}'}}{2v_{\rm m}q_1\left(\frac{q_1q\omega_{n\mathbf{k}}}{v_{\rm m}} + \hat{\Omega}_{\ell_1,\mathbf{p}} - q_1q_4\hat{\Omega}_{\ell_4,\mathbf{p}+q\mathbf{k}}\right)} + (n,q,\mathbf{k},q_4) \leftrightarrow (n',q',\mathbf{k}',-q_4) \right] \Bigg\} \\
&\quad \delta\left(v_{\rm m}q_1 \left[\frac{q_1\Sigma^{qq'}_{n\mathbf{k}n'\mathbf{k}'}}{v_{\rm m}} + \hat{\Omega}_{\ell_1,\mathbf{p}} + q_1q_2\hat{\Omega}_{\ell_2,\mathbf{p}+q\mathbf{k}+q'\mathbf{k}'} \right] \right) \\
&\quad \delta\left(-2v_{\rm m}q_1 \left[\frac{q_1q'\omega_{n'\mathbf{k}'}}{v_{\rm m}} + \hat{\Omega}_{\ell_1,\mathbf{p}} - q_1q_3\hat{\Omega}_{\ell_3,\mathbf{p}+q'\mathbf{k}'} \right] \right), \qquad (3.233)
\end{aligned}
$$

where $\hat{\Omega}_{\ell,\mathbf{p}} = \Omega_{\ell,\mathbf{p}}/v_{\rm m}$ and

$$
\begin{aligned}
\mathcal{F}^{\ell_3,\ell_1,\ell_2|q_4,q_1,q_2}_{\mathbf{p},q\mathbf{k},q'\mathbf{k}'} &= q_4\left(2n_{\rm B}(\Omega_{\ell_3,\mathbf{p}+q'\mathbf{k}'})+1\right)\left(2n_{\rm B}(\Omega_{\ell_1,\mathbf{p}})+q_1+1\right) \\
&\quad \times \left(2n_{\rm B}(\Omega_{\ell_2,\mathbf{p}+q\mathbf{k}+q'\mathbf{k}'})+q_2+1\right) \qquad (3.234)
\end{aligned}
$$

is a product of thermal factors (note $\hat{\mathcal{F}} = q_1\mathcal{F}$, cf. Eq. (3.101)). Now collapsing the delta functions, we can write:

$$
\begin{aligned}
\mathfrak{W}^{\ominus,qq'}_{n\mathbf{k},n'\mathbf{k}'} &= \frac{8\pi^2}{\hbar^4 v_{\rm m}^2} \sum_{j} \sum_{\ell,\{q_i\}} \mathfrak{Im}\Bigg\{ \mathcal{B}^{n\ell\ell|q_2q_3q}_{\mathbf{k},\mathbf{p}_j+\frac{1}{2}q\mathbf{k}+q'\mathbf{k}'} \mathcal{B}^{n'\ell\ell|-q_3q_1q'}_{\mathbf{k}',\mathbf{p}_j+\frac{1}{2}q'\mathbf{k}'} \qquad (3.235) \\
&\times \mathrm{PP}\left[\frac{\mathcal{B}^{n\ell\ell|-q_1q_4-q}_{\mathbf{k},\mathbf{p}_j+\frac{1}{2}q\mathbf{k}} \mathcal{B}^{n'\ell\ell|-q_4-q_2-q'}_{\mathbf{k}',\mathbf{p}_j+q\mathbf{k}+\frac{1}{2}q'\mathbf{k}'}}{2v_{\rm m}q_1\left(\frac{q_1q\omega_{n\mathbf{k}}}{v_{\rm m}} + \hat{\Omega}_{\ell,\mathbf{p}_j} - q_1q_4\hat{\Omega}_{\ell,\mathbf{p}_j+q\mathbf{k}}\right)} \right. \\
&\qquad \left. + (n,q,\mathbf{k},q_4) \leftrightarrow (n',q',\mathbf{k}',-q_4) \right] \Bigg\} J_{\mathfrak{W}}(\mathbf{p}_j) \mathcal{F}^{\ell,\ell,\ell|q_4,q_1,q_2}_{\mathbf{p}_j,q\mathbf{k},q'\mathbf{k}'},
\end{aligned}
$$

where, when they exist, the solutions, $j = 0,..,3$ take the form (recall $\mathbf{v}_i = \underline{\mathbf{v}}_i$, $\mathbf{w}_i = \underline{\mathbf{w}}_i$, $\mathbf{p}_j = \underline{\mathbf{p}}_j$)

$$
\mathbf{p}_j = t_{\lfloor j/2 \rfloor}\mathbf{v}_{\lfloor j/2 \rfloor} + u^{(\widetilde{j\ [2]})}_{\lfloor j/2 \rfloor}\mathbf{w}_{\lfloor j/2 \rfloor}, \qquad (3.236)
$$

where, for $i = 0, 1$

$$
\begin{aligned}
\mathbf{v}_i &= a_2\underline{\mathbf{k}}_1 + (-1)^i a_1\underline{\mathbf{k}}_2, && (3.237)\\
\mathbf{w}_i &= \hat{\mathbf{z}} \times \mathbf{v}_i, && (3.238)\\
t_i &= \frac{a_2\underline{\mathbf{k}}_1^2 + (-1)^i a_1\underline{\mathbf{k}}_2^2 - a_1a_2(a_1 + (-1)^i a_2)}{2\mathbf{v}_i^2}, && (3.239)\\
u_i^{(\pm)} &= \frac{-B_i \pm \sqrt{B_i^2 - 4A_iC_i}}{2A_i}, && (3.240)\\
A_i &= 4a_{i+1}^2(\mathbf{v}_i^2 - (\underline{\mathbf{k}}_1 \wedge \underline{\mathbf{k}}_2)^2), && (3.241)\\
B_i &= (-1)^i 4a_{i+1}(\underline{\mathbf{k}}_1 \wedge \underline{\mathbf{k}}_2)(a_{i+1}^2 - \underline{\mathbf{k}}_{i+1}^2 + 2(\mathbf{v}_i \cdot \underline{\mathbf{k}}_{i+1})t_i), && (3.242)\\
C_i &= -\left(a_{i+1}(a_{i+1} - 2\delta_\ell) - \underline{\mathbf{k}}_{i+1}^2\right)\left(a_{i+1}(a_{i+1} + 2\delta_\ell) - \underline{\mathbf{k}}_{i+1}^2\right) && (3.243)\\
&\quad -4(a_{i+1}^2 - \underline{\mathbf{k}}_{i+1}^2)(\mathbf{v}_i \cdot \underline{\mathbf{k}}_{i+1})t_i + 4(a_{i+1}^2\mathbf{v}_i^2 - (\mathbf{v}_i \cdot \underline{\mathbf{k}}_{i+1})^2)t_i^2,
\end{aligned}
$$

and $J_{\mathfrak{W}}(\mathbf{p}_j)$ is given in the main text, Eq. (3.103).

3.E.2 Choice of polarization vectors

Below, we enumerate possible explicit choices for a basis of polarization vectors $(\boldsymbol{\varepsilon}_{0,\mathbf{k}}, \boldsymbol{\varepsilon}_{1,\mathbf{k}}, \boldsymbol{\varepsilon}_{2,\mathbf{k}})$. In the numerical calculations, we use choice 2.

3.E.2.1 Choice 1

A simple choice is that of momentum-independent polarization vectors, which can be, for example: $\boldsymbol{\varepsilon}_0(\mathbf{k}) = \hat{\mathbf{x}}$, $\boldsymbol{\varepsilon}_1(\mathbf{k}) = \hat{\mathbf{y}}$, $\boldsymbol{\varepsilon}_2(\mathbf{k}) = \hat{\mathbf{z}}$.

3.E.2.2 Choice 2

Below, we describe the choice of polarization vectors used in the numerical implementation. Its polarization vectors $\boldsymbol{\varepsilon}_{n,\mathbf{k}}$ form an orthonormal basis in which $\mathbf{k}$ points along the $[1,1,1]$ axis, so that $\mathbf{k} \cdot \boldsymbol{\varepsilon}_{n,\mathbf{k}} = \frac{|\mathbf{k}|}{\sqrt{3}}$ $\forall n$. This, as explained in the main text, ensures that the structure factor $\boldsymbol{\mathcal{S}}^{\alpha,\beta}$ does not vanish for $\alpha = \beta$, corresponding to the largest coupling constants $\Lambda_{1..5}$ (as opposed to anisotropic $\Lambda_{6,7}$ for which $\alpha \neq \beta$).

The starting point is the orthonormal basis made of three vectors $\mathbf{e}_n, n = 0,1,2$, defined as

$$\begin{cases} \mathbf{e}_0 = \frac{1}{\sqrt{3}} \left(\sqrt{2}\hat{\mathbf{x}} + \hat{\mathbf{z}}\right) \\ \mathbf{e}_1 = \frac{1}{\sqrt{6}} \left(-\hat{\mathbf{x}} + \sqrt{3}\hat{\mathbf{y}} + \sqrt{2}\hat{\mathbf{z}}\right) \\ \mathbf{e}_2 = \frac{1}{\sqrt{6}} \left(-\hat{\mathbf{x}} - \sqrt{3}\hat{\mathbf{y}} + \sqrt{2}\hat{\mathbf{z}}\right) \end{cases} ; \tag{3.244}$$

in this basis, $\hat{\mathbf{z}} = [1,1,1]$. To rotate the $\hat{\mathbf{z}}$ axis into $\hat{\mathbf{k}}$'s direction, we define the polar angles of $\hat{\mathbf{k}}$,

$$\theta = \arccos(k_z/|\mathbf{k}|), \tag{3.245}$$

$$\phi = \mathrm{Arg}(k_x + \mathrm{i}k_y), \tag{3.246}$$

so that a good choice for the three polarization vectors is

$$\boldsymbol{\varepsilon}_{n,\mathbf{k}} = \mathrm{i}\, R_{\hat{\mathbf{z}}}(\phi) \cdot R_{\hat{\mathbf{y}}}(\theta) \cdot \mathrm{diag}\left[\mathsf{s}(\mathbf{k}), 1, 1\right] \cdot \mathbf{e}_n \tag{3.247}$$

for $n = 0,1,2$. In the above, we defined $R_{\hat{\boldsymbol{\mu}}}(\gamma)$ to be the direct rotation matrix around the μ axis by an angle γ, and we used the "sign" function

$$\mathsf{s}(\mathbf{k}) = \begin{cases} +1 & \text{if} \quad \mathbf{k} \in \mathcal{D}_+ \\ -1 & \text{if} \quad \mathbf{k} \in \mathcal{D}_- \end{cases} \tag{3.248}$$

with respect to two domains $\mathcal{D}_\pm$, corresponding (up to unimportant details in a set of null measure contained in the $k_z = 0$ plane) to the "upper" ($k_z > 0$) and

"lower" ($k_z < 0$) halves of $\mathbb{R}^3$, and more precisely defined by

$$\mathcal{D}_+ = \Big\{\mathbf{k} \;\Big|\; k_z > 0 \text{ or } \big(k_z = 0 \text{ and } (k_y > 0 \text{ or } (k_y = 0 \text{ and } k_x > 0))\big)\Big\}, \tag{3.249}$$

$$\mathcal{D}_- = \Big\{\mathbf{k} \;\Big|\; k_z < 0 \text{ or } \big(k_z = 0 \text{ and } (k_y < 0 \text{ or } (k_y = 0 \text{ and } k_x < 0))\big)\Big\} \tag{3.250}$$

such that $\mathbb{R}^3 = \mathcal{D}_+ \cup \mathcal{D}_- \cup \{\mathbf{0}\}$. The role of this $\mathtt{s}(\mathbf{k})$ function is to help ensure that this choice of polarizations enforces $\boldsymbol{\varepsilon}_n(-\mathbf{k}) = \boldsymbol{\varepsilon}_n(\mathbf{k})^*$, as well as all the tetragonal symmetry group of the crystal. This last statement means that under a symmetry operation g belonging to D_{4h} the symmetry group of the crystal, they transform as

$$\boldsymbol{\varepsilon}_n(g \cdot \mathbf{k}) = \sum_{n'} c^g_{nn'}(\mathbf{k})\, g \cdot \boldsymbol{\varepsilon}_{n'}(\mathbf{k}), \tag{3.251}$$

where $g\cdot$ denotes the action of g on a vector, and most importantly the $c^g_{nn'}$ coefficient either is $\delta_{nn'}$ or exchanges the $n = 1$ and $n = 2$ polarizations, depending on whether $\mathbf{k}$ is in a high-symmetry position. Indeed $n = 1, 2$ are constructed degenerate (as eigenvectors of the dynamical matrix) at the high-symmetry planes and axes of the Brillouin zone. See Ref. [Maradudin and Vosko, 1968] for details and further discussion on the behavior of polarization vectors under symmetry operations.

3.E.2.3 Choice 3

One may also use the Hall-plane-dependent basis for the polarization vectors and label $\boldsymbol{\varepsilon}_{n\mathbf{k}}$, assuming $\mu\nu$ is the Hall plane, ρ is the direction transverse to the plane, and $\mu\nu\rho$ forms a direct orthonormal basis:

$$\boldsymbol{\varepsilon}_{0,\mathbf{k}} = i\mathbf{k}/|\mathbf{k}| \quad \text{(longitudinal)}, \tag{3.252}$$

$$\boldsymbol{\varepsilon}_{1,\mathbf{k}} = i\frac{\hat{\mathbf{u}}_\rho \times \mathbf{k}}{|\hat{\mathbf{u}}_\rho \times \mathbf{k}|} \quad \text{(transverse, in Hall plane)}, \tag{3.253}$$

$$\boldsymbol{\varepsilon}_{2,\mathbf{k}} = \boldsymbol{\varepsilon}_{0,\mathbf{k}} \times \boldsymbol{\varepsilon}_{1,\mathbf{k}} = \frac{k^\rho \mathbf{k} - \mathbf{k}^2 \hat{\mathbf{u}}_\rho}{|\mathbf{k}||\hat{\mathbf{u}}_\rho \times \mathbf{k}|} \quad \text{(transverse)}. \tag{3.254}$$

$$\tag{3.255}$$

Then, *if* $\alpha, \beta, \mu, \nu, \rho \in \{x, y, z\}$, we can write:

$$\mathcal{S}^{q;\alpha\beta}_{0\mathbf{k}} = \frac{1}{\sqrt{\omega_{0\mathbf{k}}}} \frac{2qi}{|\mathbf{k}|} k^\alpha k^\beta, \tag{3.256}$$

$$\mathcal{S}^{q;\alpha\beta}_{1\mathbf{k}} = \frac{1}{\sqrt{\omega_{1\mathbf{k}}}} \frac{qi}{|\hat{\mathbf{u}}_\rho \times \mathbf{k}|} \left(k^\mu (k^\alpha \delta_{\beta,\nu} + k^\beta \delta_{\alpha,\nu}) - k^\nu (k^\alpha \delta_{\beta,\mu} + k^\beta \delta_{\alpha,\mu})\right), \tag{3.257}$$

$$\mathcal{S}^{q;\alpha\beta}_{2\mathbf{k}} = \frac{1}{\sqrt{\omega_{2\mathbf{k}}}} \frac{-1}{|\mathbf{k}||\hat{\mathbf{u}}_\rho \times \mathbf{k}|} \left(\mathbf{k}^2 (k^\alpha \delta_{\beta,\rho} + k^\beta \delta_{\alpha,\rho}) - 2k^\alpha k^\beta k^\rho\right), \tag{3.258}$$

so that $\mathcal{L}_0 \propto \mathbf{k} \cdot \boldsymbol{\lambda} \cdot \mathbf{k}$, $\mathcal{L}_1 \propto [\mathbf{k} \times (\boldsymbol{\lambda} \cdot \mathbf{k})]^\rho$, $\mathcal{L}_2 \propto [\mathbf{k}^2 (\boldsymbol{\lambda} \cdot \mathbf{k}) - (\mathbf{k} \cdot \boldsymbol{\lambda} \cdot \mathbf{k})\mathbf{k}]^\rho$.

For this choice of polarization vectors, the phonon-magnon coupling constants can be decomposed in such a way that their behavior under $\mathcal{M}_\mu, \mathcal{M}_\rho$ and $\mathcal{M}_\nu, \mathcal{C}_4^{\mu\nu}$ becomes transparent, in other words under the basis harmonics of the group generated by the latter operations. Note that, because the magnetic space group of the system is a priori independent of the symmetries associated with the choice of Hall "geometry," the coefficients of the harmonics need not be independent. (*In the the square lattice case discussed here*, some of the symmetries of the system coincide with those of the Hall geometry, so that these coefficients are not entirely independent. Note that this causes additional constraints for the existence of a nonzero Hall effect.)

3.E.3 Numerical implementation

We define $\hat{\lambda}^{\ell_1,\ell_2;\alpha\beta}_{\xi,\xi'} = \lambda^{\alpha\beta}_{\bar{\xi}\ell_1+\bar{\xi}+1,\bar{\xi}'\ell_2+\bar{\xi}'+1;\xi\xi'}$, so that, in particular,

$$\begin{aligned}
\hat{\lambda}^{\ell_1,\ell_2;\alpha\beta}_{1,1} &= \lambda^{\alpha\beta}_{\ell_1+1,\ell_2+1;11}, \\
\hat{\lambda}^{\ell_1,\ell_2;\alpha\beta}_{0,0} &= \lambda^{\alpha\beta}_{\bar{\ell}_1+1,\bar{\ell}_2+1;00}, \\
\hat{\lambda}^{\ell_1,\ell_2;\alpha\beta}_{1,0} &= \lambda^{\alpha\beta}_{\ell_1+1,\bar{\ell}_2+1;10},
\end{aligned} \tag{3.259}$$

(note the bars) and

$$\mathcal{L}^{q,\ell_1,\ell_2}_{n\mathbf{k};\xi,\xi'} = \mathrm{Tr}\left[(\hat{\boldsymbol{\lambda}}^{\ell_1\ell_2}_{\xi\xi'})^T \cdot \boldsymbol{\mathcal{S}}^q_{n\mathbf{k}}\right] = \sum_{\alpha,\beta=x,y,z} \hat{\lambda}^{\ell_1,\ell_2;\alpha\beta}_{\xi,\xi'} \mathcal{S}^{q;\alpha\beta}_{n\mathbf{k}}. \tag{3.260}$$

Moreover, given *(i)* our choice of isotropic elasticity, *(ii)* a given Hall plane $\mu\nu$ and perpendicular Hall axis, ρ, *(iii)* $\ell_1 = \ell_2 = \ell$, $\hat{\lambda}$ is a function of $\Lambda^{\xi(')}_{1,..,7}$ contains 72 values, which can be parametrized by a single index $i = 0, .., 71$ through, e.g. $i = 36\xi + 18\xi' + 9\ell + 3\alpha + \beta$ if we identify (x, y, z) with $(0, 1, 2)$ for α and β, $\mathcal{S}$ is a complex function of $n, \rho, \mathbf{k}, q, \ell, \alpha, \beta$.

3.E.4 Details of the derivation of the general forms of the scaling relations

Here we give details about the results and calculations in Sec. 3.5.5.5.

3.E.4.1 Dimensionless functions

The functional forms of the scaling functions introduced in Eq. (3.117) are

$$\tilde{c}_\eta(\tilde{y}) = \frac{1}{2}\left(|\sin\theta| + \eta\gamma^{-1}X(\tilde{y})\right), \tag{3.261}$$

$$\tilde{\Omega}^{\pm\eta}_\ell(\tilde{y}) = \frac{1}{2}\sqrt{\sin^2\theta X^2(\tilde{y}) + \gamma^{-2} \pm 2\eta|\sin\theta|\gamma^{-1}X(\tilde{y})}, \tag{3.262}$$

with

$$X(\tilde{y}) = \sqrt{1 + 4\frac{\tilde{y}^2}{\sin^2\theta - \gamma^{-2}}}, \tag{3.263}$$

and

$$\tilde{\mathrm{f}}_\eta^{s=1}(\tilde{y}) = \Theta\left(\gamma^{-2} - \sin^2\theta - 4|\tilde{y}|^2\right), \tag{3.264}$$

$$\tilde{\mathrm{f}}_\eta^{s=-1}(\tilde{y}) = \delta_{\eta,1}\Theta\left(\sin^2\theta - \gamma^{-2}\right), \tag{3.265}$$

$$\tilde{J}_D^s(\tilde{y}) = \left|\sum_{r=\pm1} \frac{s^{(r-1)/2} r \tilde{c}_r(\tilde{y})}{\sqrt{\tilde{c}_r(\tilde{y})^2 + \tilde{y}^2}}\right|^{-1}. \tag{3.266}$$

Inserting the expressions for $\mathcal{L}$ and F into that of $\mathcal{B}$, we find

$$\begin{aligned}\mathcal{B}^{n,\ell\ell|+s-}_{\mathbf{k};-\mathbf{p}^{(\eta)}_{\ell,\mathbf{k}}(y)+\frac{\mathbf{k}}{2}} &= \frac{-i}{2\sqrt{2M_{\rm uc}}} \sum_{\xi\xi'} n_0^{-\xi-\xi'} \sum_{\alpha,\beta=x,y,z} \hat{\lambda}^{\ell\ell;\alpha\beta}_{\xi\xi'}\, i^{\bar{\xi}} (si)^{\bar{\xi}'} (-1)^{(\bar{\xi}+\bar{\xi}')\ell} \\ &\times \frac{k^\alpha \varepsilon^\beta_{n\mathbf{k}} + k^\beta \varepsilon^\alpha_{n\mathbf{k}}}{\sqrt{\omega_{n\mathbf{k}}}} (\chi\Omega_{\ell\mathbf{p}^{(\eta)}_{\ell\mathbf{k}}}(y))^{\xi-\frac{1}{2}} (\chi\Omega_{\ell\mathbf{p}^{(-\eta)}_{\ell\mathbf{k}}}(y))^{\xi'-\frac{1}{2}}\end{aligned} \tag{3.267}$$

because $F_{\xi q\ell}(-\mathbf{p}) = F_{\xi q\ell}(\mathbf{p})$. Then, for $\delta_\ell = 0$, and defining $\hat{k}^\alpha = (\hat{\mathbf{k}})_\alpha$, the $\tilde{\mathcal{B}}_{\xi\xi'}$ introduced in Eq. (3.117) are:

$$\tilde{\mathcal{B}}_{nn} = \frac{is\chi^{-1}v_{\rm m}^{-1}}{2\sqrt{2M_{\rm uc}v_{\rm ph}}} \sum_{\alpha,\beta=x,y,z} \hat{\lambda}^{\ell\ell;\alpha\beta}_{00} \left(\hat{k}^\alpha \varepsilon^\beta_{n\mathbf{k}} + \hat{k}^\beta \varepsilon^\alpha_{n\mathbf{k}}\right)(\tilde{\Omega}^\eta(\tilde{y})\tilde{\Omega}^{-\eta}(\tilde{y}))^{-\frac{1}{2}}, \tag{3.268}$$

$$\tilde{\mathcal{B}}_{mm} = \frac{-in_0^{-2}\chi v_{\rm m}}{2\sqrt{2M_{\rm uc}v_{\rm ph}}} \sum_{\alpha,\beta=x,y,z} \hat{\lambda}^{\ell\ell;\alpha\beta}_{11} \left(\hat{k}^\alpha \varepsilon^\beta_{n\mathbf{k}} + \hat{k}^\beta \varepsilon^\alpha_{n\mathbf{k}}\right)(\tilde{\Omega}^\eta(\tilde{y})\tilde{\Omega}^{-\eta}(\tilde{y}))^{\frac{1}{2}}, \tag{3.269}$$

$$\begin{aligned}\tilde{\mathcal{B}}_{mn} = \frac{(-1)^\ell n_0^{-1}}{2\sqrt{2M_{\rm uc}v_{\rm ph}}} &\sum_{\alpha,\beta=x,y,z} \left(\hat{k}^\alpha \varepsilon^\beta_{n\mathbf{k}} + \hat{k}^\beta \varepsilon^\alpha_{n\mathbf{k}}\right) \\ &\left[\hat{\lambda}^{\ell\ell;\alpha\beta}_{01} (\tilde{\Omega}^\eta(\tilde{y}))^{-\frac{1}{2}} (\tilde{\Omega}^{-\eta}(\tilde{y}))^{\frac{1}{2}} + s\, \hat{\lambda}^{\ell\ell;\alpha\beta}_{10} (\tilde{\Omega}^{(\eta)}(\tilde{y}))^{\frac{1}{2}} (\tilde{\Omega}^{(-\eta)}(\tilde{y}))^{-\frac{1}{2}}\right].\end{aligned} \tag{3.270}$$

3.E.4.2 Details of the behavior of the scaling function F

Here we derive the behavior of the scaling functions $\mathrm{F}_x(\varkappa,\gamma,\theta)$ defined in Eq. (3.120) at small and large $\varkappa$.

Let us first consider the large-$\varkappa$ limit. The hyperbolic sines in the denominator of the integrand grow exponentially in this limit (because the two $\tilde{\Omega}^{\pm\eta}_\ell(\tilde{y})$ functions cannot be simultaneously be made to vanish), so that they can be approximated by their leading exponential forms. An application of the saddle point method then shows that the integral is dominated by region around $\tilde{y} = 0$, and is exponentially suppressed for large $\varkappa$. For $\gamma|\sin\theta| > 1$, i.e. when the azimuthal angle of $\mathbf{k}$ is smaller than γ^{-1}, this suppression exceeds the exponential growth of the $\sinh\varkappa/2$ prefactor, and the scaling function decays exponentially:

$$\mathrm{F}_x(\varkappa, \gamma > |\sin\theta|^{-1}) \underset{\varkappa\gg1}{\sim} \exp\left[\frac{\varkappa}{2}(1 - \gamma|\sin\theta|)\right]. \tag{3.271}$$

For smaller angles where $\gamma|\sin\theta| < 1$, F does not decay exponentially in the large κ limit. Here Eq. (3.271) is correct to exponential accuracy, i.e. it is asymptotically correct for $\ln(\mathrm{F})$ at large $\varkappa$. To this accuracy, the asymptotics are independent of x.

Now consider the small $\varkappa$ limit. The naïve result for the scaling function is obtained by expanding both the hyperbolic sine in the numerator and the two in the denominator of the integrand around zero leads to

$$\mathrm{F}_x^{(s)}(\varkappa \ll 1, \gamma, \theta) \underset{?}{\sim} \frac{1}{\varkappa} \frac{(3-s)\mathfrak{a}^2}{2\pi v_{\mathrm{m}} \hbar^2 \gamma^2} \int_{-\infty}^{+\infty} \mathrm{d}\tilde{y} \sum_{\eta} \tilde{\mathrm{f}}_\eta^s(\tilde{y}) \tilde{J}_D^s(\tilde{y}) \sum_{\ell} \frac{\tilde{\mathcal{C}}_x(\tilde{y})}{\tilde{\Omega}_\ell^{+\eta}(\tilde{y}) \tilde{\Omega}_\ell^{-\eta}(\tilde{y})}. \tag{3.272}$$

This expression is correct provided the integral in the second line converges. The convergence is problematic only at large $\tilde{y}$ for the case $s = -1$ (in the case $s = 1$, the integral is confined by the $\tilde{\mathrm{f}}^{s=1}$ factor to a finite domain). In this limit the Jacobean $\tilde{J}^{s=-1}$ grows linearly in $\tilde{y}$ as does $\tilde{\Omega}$, while the factor $\tilde{\mathcal{C}}_x(\tilde{y})$ behaves as $\tilde{y}^{2x}$. As a result, the integral converges for the case $x = -1$ and the $1/\varkappa$ scaling is correct in this case. In the cases $x = 0, 1$, the integral is logarithmically and quadratically divergent at large $\tilde{y}$, respectively.

In the latter two cases, we must reconsider the naïve result in Eq. (3.272). The divergence in this equation is an artificial result because the hyperbolic sines in the original expression in Eq. (3.120) grow rapidly once $\tilde{\Omega} > \varkappa^{-1}$ and ensure convergence of the integral (i.e. the large $\tilde{y} > |\gamma\varkappa|^{-1}$ contribution is negligible). Proper behavior is restored for small $\varkappa$ by simply using the expanded form of Eq. (3.272) but only integrating up to an upper cutoff $|\tilde{y}| < |\varkappa\gamma|^{-1}$. This regulates the divergences and one obtains additional $\ln(1/\varkappa)$ and $\varkappa^{-2}$ factors multiplying the $1/\varkappa$ form for the cases $x = 0, 1$, respectively. Collecting the above results we see that

$$\mathrm{F}_x^{(-1)}(\varkappa) \underset{\varkappa \ll 1}{\sim} \begin{cases} \frac{1}{\varkappa^3} & x = 1 \\ \frac{\ln(1/\varkappa)}{\varkappa} & x = 0 \\ \frac{1}{\varkappa} & x = -1 \end{cases}. \tag{3.273}$$

This function is non-zero for $|\gamma \sin\theta| > 1$, while $F^{(+1)}$ is non-zero when $|\gamma \sin\theta| < 1$.

In the latter case, as mentioned above, the integral over $\tilde{y}$ always converges because the set of integration is an ellipse instead of a half-hyperbola. Therefore the naïve scaling is the correct one and the $\mathrm{F}_x^{(+1)}(\varkappa) \underset{\varkappa \ll 1}{\sim} 1/\varkappa$ behavior holds for all x.

3.F Application—further physical details

3.F.1 Microscopic derivation of the coupling constants

We consider the most general coupling between the strain tensor and bilinears of the $\mathbf{m}, \mathbf{n}$ fields, exhibiting all the symmetries allowed by the crystal symmetry group in the paramagnetic phase: the D_{4h} tetragonal point-group generated by mirror symmetries $\mathcal{S}_x, \mathcal{S}_y, \mathcal{S}_z$, fourfold rotational symmetry $\mathcal{C}_4^{xy}$; translations of

one unit cell —which forbids interactions of the $\mathrm{m}_a\mathrm{n}_b$ type; and time-reversal. The corresponding hamiltonian density reads:

$$\begin{aligned}\mathcal{H}'_{\rm tetra} &= \Lambda_1^{(\mathrm{m})}\Big(\mathrm{m}_x\mathrm{m}_x\mathcal{E}^{xx}+\mathrm{m}_y\mathrm{m}_y\mathcal{E}^{yy}\Big)+\Lambda_1^{(\mathrm{n})}\Big(\mathrm{n}_x\mathrm{n}_x\mathcal{E}^{xx}+\mathrm{n}_y\mathrm{n}_y\mathcal{E}^{yy}\Big)\\
&+\Lambda_5^{(\mathrm{m})}\mathrm{m}_z\mathrm{m}_z\mathcal{E}^{zz}+\Lambda_5^{(\mathrm{n})}\mathrm{n}_z\mathrm{n}_z\mathcal{E}^{zz}\\
&+\Lambda_2^{(\mathrm{m})}\Big(\mathrm{m}_x\mathrm{m}_x\mathcal{E}^{yy}+\mathrm{m}_y\mathrm{m}_y\mathcal{E}^{xx}\Big)+\Lambda_2^{(\mathrm{n})}\Big(\mathrm{n}_x\mathrm{n}_x\mathcal{E}^{yy}+\mathrm{n}_y\mathrm{n}_y\mathcal{E}^{xx}\Big)\\
&+\Big(\Lambda_3^{(\mathrm{m})}\mathrm{m}_z\mathrm{m}_z+\Lambda_3^{(\mathrm{n})}\mathrm{n}_z\mathrm{n}_z\Big)\Big(\mathcal{E}^{xx}+\mathcal{E}^{yy}\Big)\\
&+\Lambda_4^{(\mathrm{m})}\Big(\mathrm{m}_x\mathrm{m}_x+\mathrm{m}_y\mathrm{m}_y\Big)\mathcal{E}^{zz}+\Lambda_4^{(\mathrm{n})}\Big(\mathrm{n}_x\mathrm{n}_x+\mathrm{n}_y\mathrm{n}_y\Big)\mathcal{E}^{zz}\\
&+\Lambda_6^{(\mathrm{m})}\mathrm{m}_x\mathrm{m}_y\mathcal{E}^{xy}+\Lambda_6^{(\mathrm{n})}\mathrm{n}_x\mathrm{n}_y\mathcal{E}^{xy}+\Lambda_7^{(\mathrm{m})}\Big(\mathrm{m}_x\mathrm{m}_z\mathcal{E}^{xz}\\
&+\mathrm{m}_y\mathrm{m}_z\mathcal{E}^{yz}\Big)+\Lambda_7^{(\mathrm{n})}(\mathrm{n}_x\mathrm{n}_z\mathcal{E}^{xz}+\mathrm{n}_y\mathrm{n}_z\mathcal{E}^{yz})\end{aligned}\tag{3.274}$$

We now propose a microscopic origin to the $\Lambda_I^{(\xi)}$ coefficients appearing in it. We start from a generic spin exchange hamiltonian of the form

$$H_{\rm ex}=\sum_{\mathbf{R},\mathbf{R}'}\sum_{a,b}S^a_{\mathbf{R}}J^{ab}_{\mathbf{R}-\mathbf{R}'}S^b_{\mathbf{R}'},\tag{3.275}$$

where $\mathbf{R},\mathbf{R}'$ indicate the actual locations of the sites in the *distorted* lattice, and each sum spans the whole distorted lattice.

We then express $\mathbf{R}=\mathbf{r}+\boldsymbol{u}_{\mathbf{r}}$, where $\mathbf{r}$ belongs to the undistorted lattice and $\boldsymbol{u}_{\mathbf{r}}$ is the displacement field at site $\mathbf{r}$. Taylor-expanding the coefficients $J^{ab}_{\mathbf{R}-\mathbf{R}'}$ with respect to the displacement field (and identifying $S^a_{\mathbf{R}}=S^a_{\mathbf{r}}$), we thus obtain $H_{\rm ex}=H^0_{\rm ex}+H'_{\rm ex}+O(u^2)$, where $H^0_{\rm ex}=H_{\rm ex}|_{\mathbf{R},\mathbf{R}'\mapsto\mathbf{r},\mathbf{r}'}$ and

$$H'_{\rm ex}=\sum_{\mathbf{r},\mathbf{r}'}\sum_{ab,\nu}S^a_{\mathbf{r}}\left(u^\nu_{\mathbf{r}}-u^\nu_{\mathbf{r}'}\right)\partial_{\eta^\nu}J^{ab}_{\boldsymbol{\eta}}\Big|_{\boldsymbol{\eta}=\mathbf{r}-\mathbf{r}'}S^b_{\mathbf{r}'}.\tag{3.276}$$

Then, identifying $\mathcal{E}_{\alpha\beta}=\frac{1}{2}(\partial_\alpha u_\beta+\partial_\beta u_\alpha)$ the symmetric rank-2 elasticity tensor (i.e. strain tensor), we identify $H'_{\rm ex}=H'_{ss\varepsilon}+\ldots$, where

$$H'_{ss\varepsilon}=\frac{1}{2}\sum_{\mathbf{r},\boldsymbol{\eta}}S^a_{\mathbf{r}+\boldsymbol{\eta}}S^b_{\mathbf{r}}\left[\eta_\alpha\partial_{\eta^\beta}+\eta_\beta\partial_{\eta^\alpha}\right]J^{ab}\Big|_{\boldsymbol{\eta}}\mathcal{E}_{\alpha\beta}(\mathbf{r})+\ldots,\tag{3.277}$$

where $a,b=x,y,z$ is a spin axis index, $\alpha,\beta=x,y,z$ is a spatial index, and "$+\ldots$" encompasses terms featuring $\omega_{\alpha\beta}$ the anti-symmetric rank-2 elasticity tensor, as well as higher-order derivatives of the displacement field.

Finally, we take the particular case of a square lattice with tetragonal symmetry, and describe the spins in terms of m,n fields as in the main text, namely $\mathbf{S}_{\mathbf{r}}=(-1)^{\mathrm{r}}\mu_0\mathbf{n}(\mathbf{r})+\mathfrak{a}^2\mathbf{m}(\mathbf{r})$. We identify $H'_{ss\varepsilon}=\sum_{\mathbf{r}}\mathcal{H}'_{\rm tetra}(\mathbf{r})+\ldots$ where "$+\ldots$" is made of rapidly oscillating (time-reversal breaking) terms, and $\mathcal{H}'_{\rm tetra}$ is as displayed in Eq. (3.274), with identification

$$\Lambda^{(\mathrm{m}),\alpha\beta}_{ab} = \frac{1}{2}\sum_{\boldsymbol{\eta}}\left(\eta_\alpha\partial_\beta+\eta_\beta\partial_\alpha\right)J^{ab}\Big|_{\boldsymbol{\eta}},\tag{3.278}$$

$$\Lambda^{(\mathrm{n}),\alpha\beta}_{ab} = \frac{1}{2}\sum_{\boldsymbol{\eta}}e^{i\boldsymbol{\pi}\boldsymbol{\eta}}\left(\eta_\alpha\partial_\beta+\eta_\beta\partial_\alpha\right)J^{ab}\Big|_{\boldsymbol{\eta}},\tag{3.279}$$

where the sum over $\boldsymbol{\eta}$ spans the whole direct (two-dimensional square) lattice, and $\boldsymbol{\pi} = \left(\frac{\pi}{\mathfrak{a}}, \frac{\pi}{\mathfrak{a}}\right)$ with $\mathfrak{a}$ the square lattice parameter.

3.F.2 Contributions to intervalley couplings

In the main text, the n_a, m_a fields live in the valleys identified by:

$$\begin{aligned} \ell = 0: &\qquad n_y, m_z \\ \ell = 1: &\qquad n_z, m_y. \end{aligned} \tag{3.280}$$

Therefore, intervalley couplings are of the form $\lambda_{ab;\xi\xi'}$ with $\delta_{\xi\xi'} + \delta_{ab} = 1$. More explicitly, using Eq. (3.78), they are:

$$\lambda^{\alpha\beta}_{yz;00} = \Lambda^{(\mathrm{n}),\alpha\beta}_{yz}, \tag{3.281}$$

$$\lambda^{\alpha\beta}_{yz;11} = \Lambda^{(\mathrm{m}),\alpha\beta}_{yz}, \tag{3.282}$$

$$\lambda^{\alpha\beta}_{yy;01} = \frac{-1}{n_0}\left[m^y_0 \Lambda^{(\mathrm{m}),\alpha\beta}_{yx} + m^z_0 \Lambda^{(\mathrm{m}),\alpha\beta}_{zx} + m^y_0 \Lambda^{(\mathrm{n}),\alpha\beta}_{yx}\right], \tag{3.283}$$

$$\lambda^{\alpha\beta}_{zz;01} = \frac{-1}{n_0}\left[m^z_0 \Lambda^{(\mathrm{m}),\alpha\beta}_{zx} + m^y_0 \Lambda^{(\mathrm{m}),\alpha\beta}_{yx} + m^z_0 \Lambda^{(\mathrm{n}),\alpha\beta}_{zx}\right]. \tag{3.284}$$

Also recall from Eq. (3.74) that

$$\Lambda^{(\xi),xy}_{yx} = \Lambda^{(\xi),yx}_{yx} = \Lambda^{(\xi)}_6, \tag{3.285}$$

$$\Lambda^{(\xi),xz}_{zx} = \Lambda^{(\xi),zx}_{zx} = \Lambda^{(\xi),yz}_{yz} = \Lambda^{(\xi),zy}_{yz} = \Lambda^{(\xi)}_7, \tag{3.286}$$

and all other values of α, β yield 0 for this set of lower indices. From this, it is clear that the $\Lambda^{(\xi)}_7$ couplings always mix valleys, regardless of $\boldsymbol{m}_0$, and contribute a $\lambda_{yz;\xi\xi}$ term. This intervalley coupling is a small contribution which does not contribute to $\mathcal{T}$ breaking. Meanwhile, the $\mathcal{T}$-odd $\lambda_{yy;01}$ and $\lambda_{zz;01}$ intervalley couplings both contain contributions from both $\Lambda^{(\xi)}_7 m^z_0$ and $\Lambda^{(\xi)}_6 m^y_0$.

3.F.3 Derivation of the gaps from a sigma model

Here we provide a heuristic microscopic argument for expressing the gaps in terms of spin-spin couplings. We ignore spin-lattice coupling, and just consider corrections to the isotropic Heisenberg model. We assume the addition of a term of the XXZ anisotropy form:

$$H_{\mathrm{XXZ}} = gJ \sum_{\langle ij \rangle} \left(2S^z_i S^z_j - S^x_i S^x_j - S^y_i S^y_j\right). \tag{3.287}$$

This is to be added to the isotropic Heisenberg model, along with a Zeeman coupling to the transverse field.

Carrying out the long-wavelength expansion in terms of $\mathbf{m}$ and $\mathbf{n}$ fields, we obtain the corrected potential part (i.e. without gradient terms) of the nonlinear sigma-model Eq. (3.48):

$$\begin{aligned} \mathcal{H}^{g,h}_{\mathrm{NLS}} = \frac{1}{2\chi}|\mathbf{m}|^2 + 2gJ\mathfrak{a}^2\left(2\mathrm{m}_z^2 - \mathrm{m}_x^2 - \mathrm{m}_y^2\right) \\ - 2gJ\frac{\mu_0^2}{\mathfrak{a}^2}\left(2\mathrm{n}_z^2 - \mathrm{n}_x^2 - \mathrm{n}_y^2\right) - h_y \mathrm{m}_y - h_z \mathrm{m}_z. \end{aligned} \tag{3.288}$$

Note that the first term includes an m_x^2 term, which is absent in the quadratic expansion describing linear spin waves in the main text. Indeed this term is higher order in the small fluctuations around an x-ordered state when carrying out a zero field spin wave expansion, which was the case in the main text where the external field had already been integrated out to yield the $\mathrm{n}_a\mathrm{n}_b$ mass term. We also included an external uniform field which lies in the $y-z$ plane.

Expanding around the x-ordered state, using that $\mathrm{m}_x = -\mathsf{m}_y\mathsf{n}_y - \mathsf{m}_z\mathsf{n}_z$ and $\mathrm{n}_x = 1 - \frac{1}{2}(\mathsf{n}_y^2 + \mathsf{n}_z^2 + \frac{1}{n_0^2}(\mathsf{m}_y^2 + \mathsf{m}_z^2))$, yields

$$\begin{aligned}\mathcal{H}^{g,h}_{\mathrm{NLS}} = &\frac{1}{2\chi}\left(\mathsf{m}_y^2 + \mathsf{m}_z^2\right) + 2gJ\mathfrak{a}^2\left(2\mathsf{m}_z^2 - \mathsf{m}_y^2\right) - 2gJ\frac{\mu_0^2}{\mathfrak{a}^2}\left(2\mathsf{n}_z^2 - \mathsf{n}_y^2\right) - h_y\mathsf{m}_y - h_z\mathsf{m}_z \\ &+ \left(\frac{1}{2\chi} - 2gJ\mathfrak{a}^2\right)\left(\mathsf{m}_y^2\mathsf{n}_y^2 + \mathsf{m}_z^2\mathsf{n}_z^2 + 2\mathsf{m}_y\mathsf{m}_z\mathsf{n}_y\mathsf{n}_z\right) \\ &+ 2gJ\frac{\mu_0^2}{\mathfrak{a}^2}\left[1 - \frac{1}{2}(\mathsf{n}_y^2 + \mathsf{n}_z^2 + \frac{1}{n_0^2}(\mathsf{m}_y^2 + \mathsf{m}_z^2))\right]^2. \end{aligned} \tag{3.289}$$

Note that the first term on the second line is of the form $(\mathbf{m}_\perp \cdot \mathbf{n}_\perp)^2$, where the $\perp$ indicates the components of the vectors normal to the ordering direction. Since we in the next step shift the magnetization by its value induced by the field, this is proportional to $(\mathbf{h}\cdot\mathbf{n})^2$, as is postulated in the main text on symmetry grounds.

We now show this explicitly. We shift the definition $\mathsf{m}_a = m_a + \chi_a h_a$ for $a = y, z$, and expand the result to quadratic order in m, n. Here $\chi_z = (1/\chi + 4gJ\mathfrak{a}^2)^{-1}$ and $\chi_y = (1/\chi - 2gJ\mathfrak{a}^2)^{-1}$.

This gives

$$\begin{aligned}\mathcal{H}^{g,h}_{\mathrm{NLS}} = &\frac{1}{2\chi}\left(m_y^2 + m_z^2\right) + 2gJ\mathfrak{a}^2\left(2m_z^2 - m_y^2\right) - 2gJ\frac{\mu_0^2}{\mathfrak{a}^2}\left(2n_z^2 - n_y^2\right) \\ &+ \left(\frac{1}{2\chi} - 2gJ\mathfrak{a}^2\right)\left(\chi_y^2 h_y^2 n_y^2 + \chi_z^2 h_z^2 n_z^2 + 2\chi_y\chi_z h_y h_z n_y n_z\right) \\ &- 2gJ\frac{\mu_0^2}{\mathfrak{a}^2}\left[n_y^2 + n_z^2 + \cdots\right], \end{aligned} \tag{3.290}$$

where the '$\cdots$' in the last brackets account for terms higher order in field, magnetization fluctuations, etc.

The anisotropy coefficients, denoted by Γ_{ab} in the text, can now be extracted. The terms in $\mathcal{H}^{g,h}_{\mathrm{NLS}}$ which are quadratic in the n_y, n_z fields read

$$\begin{aligned}\mathcal{H}_{nn} = &\chi_y^2 h_y^2\left(\frac{1}{2\chi} - 2gJ\mathfrak{a}^2\right)n_y^2 + \left[\chi_z^2 h_z^2\left(\frac{1}{2\chi} - 2gJ\mathfrak{a}^2\right) - 6gJ\frac{\mu_0^2}{\mathfrak{a}^2}\right]n_z^2 \\ &+ 2\chi_y\chi_z h_y h_z\left(\frac{1}{2\chi} - 2gJ\mathfrak{a}^2\right)n_y n_z. \end{aligned} \tag{3.291}$$

Note that the two terms proportional to n_y^2 from the right-most contributions on each line of Eq. (3.290) above canceled. That means the the coefficient of n_y^2 in Eq. (3.291) vanishes if $h_y = 0$. This occurs because of Goldstone's theorem and the assumed XXZ form of the anisotropy: if the field is purely

along the z direction, XY symmetry of the Hamiltonian under rotations about the z axis is preserved, and this makes one of the spin wave modes remain gapless. Conversely, for a field along the y direction, and in the presence of anisotropy, both modes are generally gapped.

We can simplify the above expression if we assume $|g| \ll 1$, which means $\chi_y^{-1} \approx \chi_z^{-1} \approx \chi^{-1} = 4\mathfrak{a}^2 J$ and therefore $1/\chi \gg gJ\mathfrak{a}^2$; hence

$$\mathcal{H}_{nn} \approx \frac{\chi h_y^2}{2} n_y^2 + \left[\frac{\chi h_z^2}{2} - 6gJ\frac{\mu_0^2}{\mathfrak{a}^2}\right] n_z^2 + \chi h_y h_z n_y n_z. \tag{3.292}$$

The above shows that if h_z is small or zero, stability requires $g < 0$. This can be understood from the fact that, if the field is along y, then H_{XXZ} is the only term, in the pure spin hamiltonian, breaking explicitly the $O(2)$ symmetry in the $x - z$ plane. It should therefore favor antiferromagnetic alignment along the x axis, which is the initial assumption of this derivation. It also proves the $\frac{\chi}{2}$ prefactor used in the main text.

The coefficients in Eq. (3.292) give contributions to Γ_{yy}, Γ_{zz} and Γ_{yz}, respectively. In this Appendix, as opposed to the more general expressions given in the main text, we assume they are the only contribution.

Since taking the magnetic field purely along one of the two axes y, z guarantees that $\Gamma_{yz} = 0$, so that (as explained in the main text) the two magnon valleys are independent, let us assume that the field is along the y axis. Then one gap is $\Delta_1 = |h_y|$, the Zeeman energy associated with the field along y. The other gap gets contributions both from the anisotropy and the Zeeman energy associated with the field along z.

Note that the anisotropy-induced gap involves the square root of the anisotropy, i.e. $\Delta_0\big|_{h_z=0} = 4\sqrt{3|g|}J\mu_0$, which is not necessarily *very* small for reasonably small values of g.

3.G Application—Supplementary figures

Here we present further calculations of scattering rates and (diagonal) thermal conductivity for the model of Sec. 3.5, as supplemental figures.

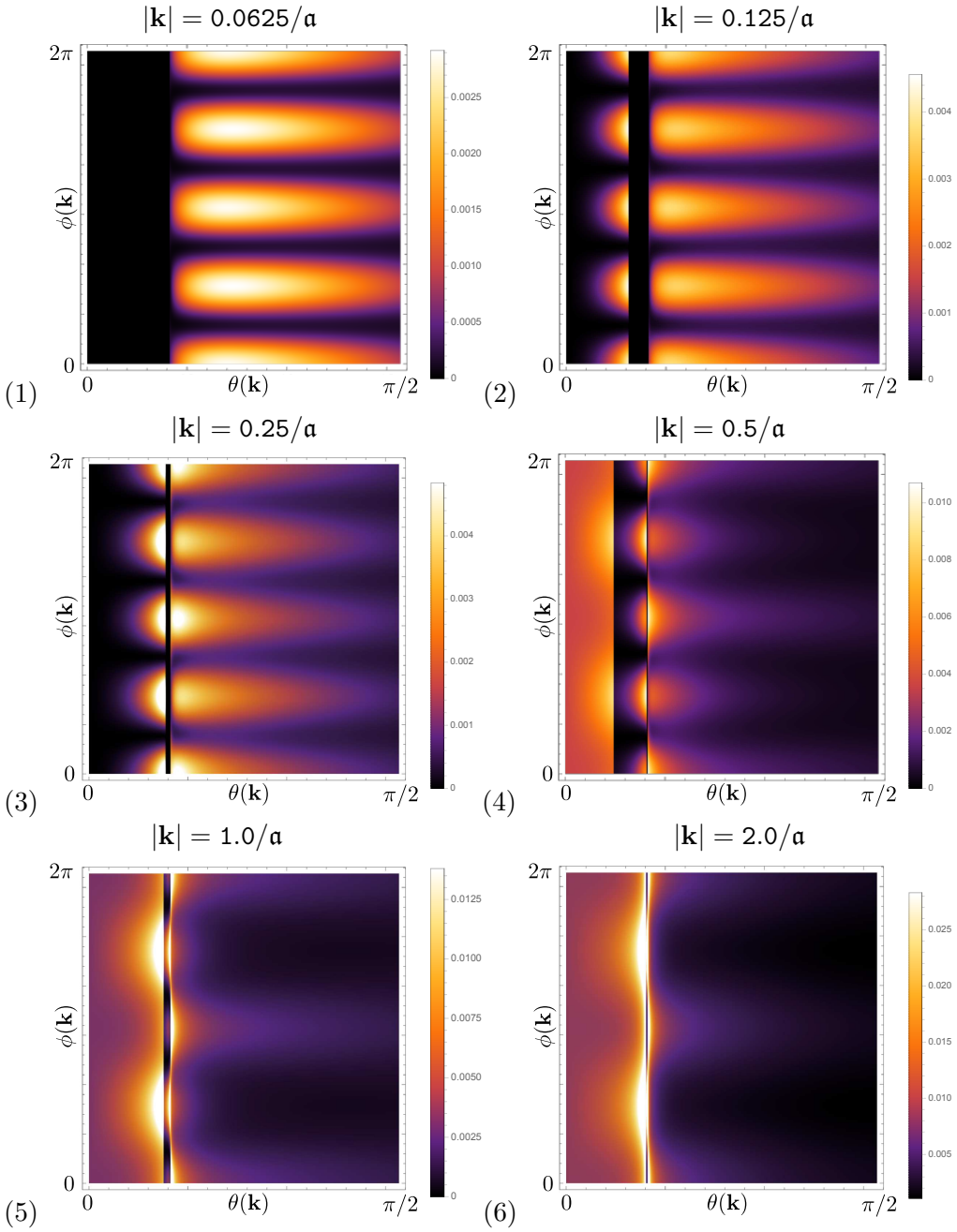

Figure 3.G.1: Diagonal scattering rate $D_{n\mathbf{k}}$ with respect to $\theta(\mathbf{k}) \in [0, \pi/2]$ (horizontal axis) and $\phi(\mathbf{k}) \in [0, 2\pi]$ (vertical axis) for fixed temperature $T = 0.5\,T_0$, polarization $n = 0$, and momentum (1) $|\mathbf{k}| = 0.0625/\mathfrak{a}$, (2) $|\mathbf{k}| = 0.125/\mathfrak{a}$, (3) $|\mathbf{k}| = 0.25/\mathfrak{a}$, (4) $|\mathbf{k}| = 0.5/\mathfrak{a}$, (5) $|\mathbf{k}| = 1.0/\mathfrak{a}$, (6) $|\mathbf{k}| = 2.0/\mathfrak{a}$. Color scales vary from figure to figure. Note that the C_4 symmetry is approximately preserved for small $|\mathbf{k}|$ but broken at large $|\mathbf{k}|$, as stated in the main text. Also note how scattering processes at $\theta(\mathbf{k}) < \theta_-$ become allowed for $\omega_{n\mathbf{k}} \geq 2\Delta, 2\Delta'$, then dominant at large $|\mathbf{k}|$.

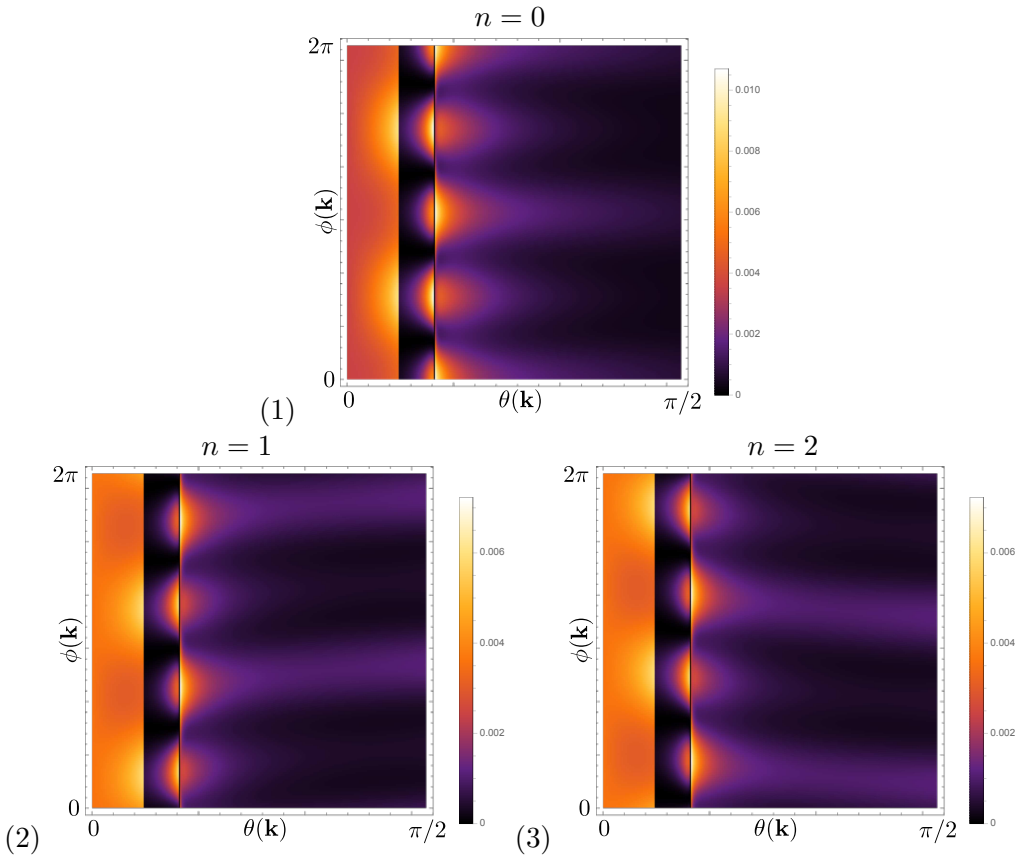

Figure 3.G.2: Diagonal scattering rate $D_{n\mathbf{k}}$ with respect to $\theta(\mathbf{k}) \in [0, \pi/2]$ (horizontal axis) and $\phi(\mathbf{k}) \in [0, 2\pi]$ (vertical axis) for fixed temperature $T = 0.5T_0$, momentum $|\mathbf{k}| = 0.5/\mathfrak{a}$, and polarizations (1) $n = 0$, (2) $n = 1$, (3) $n = 2$. Color scales are different in (1) and (2,3). Subfigure (1) is reproduced from the main text. Note that with our choice of polarization vectors $\boldsymbol{\varepsilon}_{n,\mathbf{k}}$, results for $n = 1$ and $n = 2$ are simply related by the mirror symmetry $\phi \mapsto \pi - \phi$.

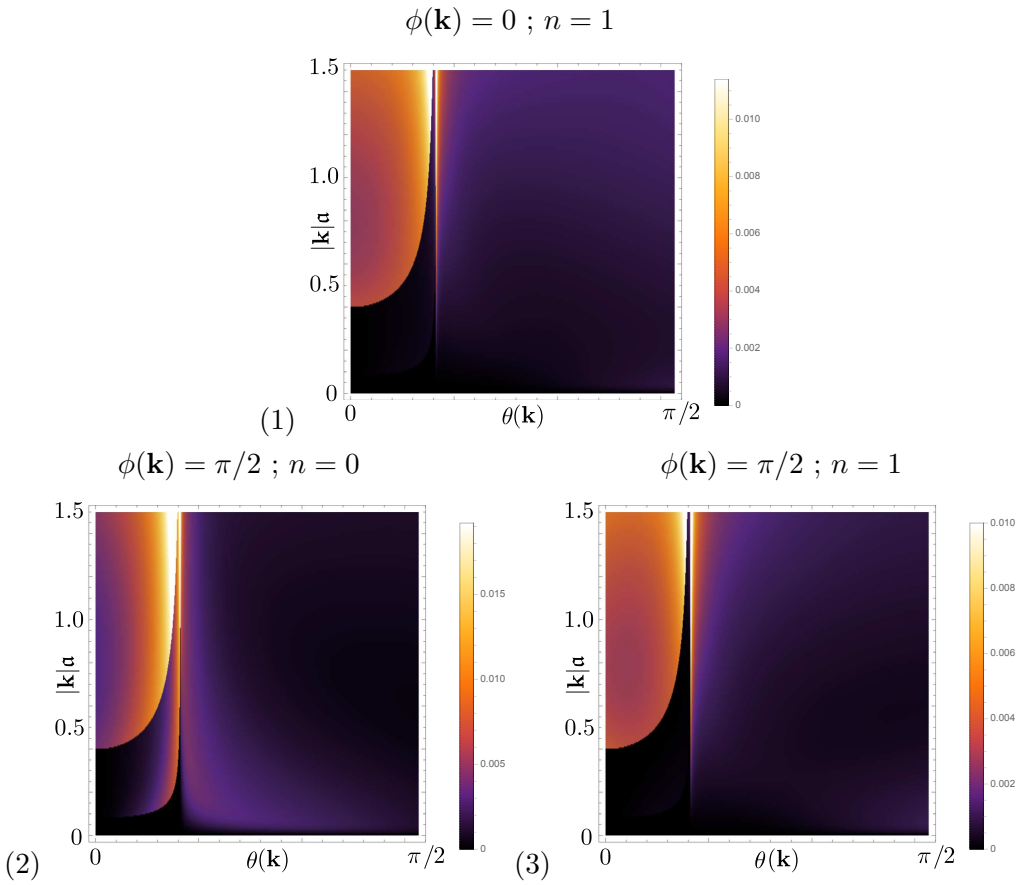

Figure 3.G.3: Diagonal scattering rate $D_{n\mathbf{k}}$ with respect to $\theta(\mathbf{k}) \in [0, \pi/2]$ (horizontal axis) and $|\mathbf{k}|\mathfrak{a}$ (vertical axis) for fixed temperature $T = 0.5T_0$ and (1) $\phi(\mathbf{k}) = 0$ and $n = 1$, (2) $\phi(\mathbf{k}) = \pi/2$ and $n = 0$, (3) $\phi(\mathbf{k}) = \pi/2$ and $n = 1$. Color scales are different for the three subfigures. The $\phi(\mathbf{k}) = 0$ and $n = 0$ case is displayed in the main text. Note that polarizations $n = 1$ and $n = 2$ yield the same results here. Note also that the general features are the same for polarizations $n = 1, 2$ as for $n = 0$: although the scattering rates of $n = 1, 2$ polarizations for energies $\omega_{n\mathbf{k}} \gtrsim 2\Delta$ are not as clearly visible as they are for $n = 0$, they are finite (of order 10^{-4} in our units) and are only *parametrically* smaller than those for the $n = 0$ polarization, due to purely geometrical factors ($\mathcal{S}^{q;\alpha\beta}_{n\mathbf{k}}$ in the main text).

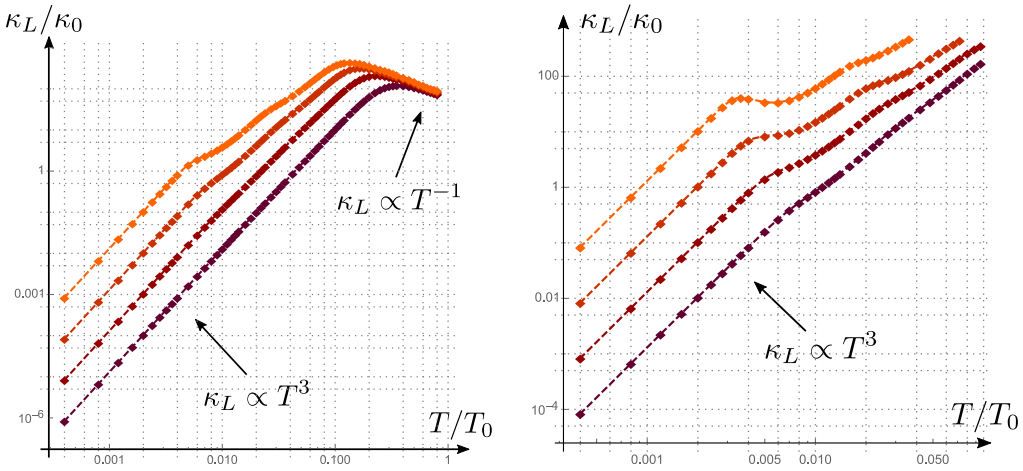

Figure 3.G.4: Longitudinal thermal conductivity κ_L with respect to temperature T, in log-log scale, *(left)* for four different values of $\gamma_{\text{ext}} = 1 \cdot 10^{-z}(v_{\text{ph}}/\mathfrak{a}), z \in [\![4, 7]\!]$, from darker ($z = 4$) to lighter ($z = 7$) shade, *(right)* for four different values $\gamma_{\text{ext}} = 1 \cdot 10^{-z}(v_{\text{ph}}/\mathfrak{a}), z \in [\![6, 9]\!]$, from darker ($z = 6$) to lighter ($z = 9$) shade. Note that the two "bumps" come from the competition between γ_{ext} and $D_{nn,\ell}$ for valley index $\ell = 0, 1$, as explained in the main text.

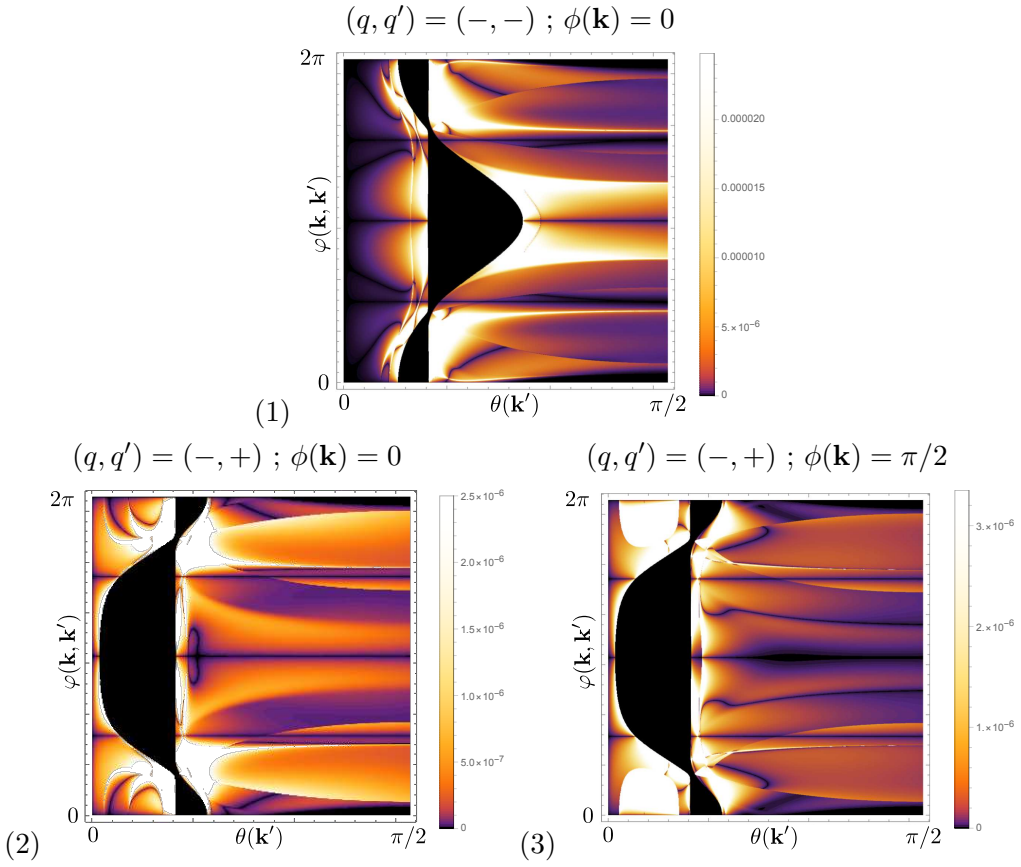

Figure 3.G.5: Skew-scattering rates (1) $\mathfrak{W}^{\ominus,--}_{n\mathbf{k}n'\mathbf{k}'}$ and (2,3) $\mathfrak{W}^{\ominus,-+}_{n\mathbf{k}n'\mathbf{k}'}$, with respect to $\theta(\mathbf{k}') \in [0,\pi/2]$ (horizontal axis) and $\varphi(\mathbf{k},\mathbf{k}') = \phi(\mathbf{k}') - \phi(\mathbf{k})$ (vertical axis), for fixed magnetization $\boldsymbol{m}_0 = 0.05\hat{\boldsymbol{z}}$, temperature $T = 0.5T_0$, momentum $|\mathbf{k}'| = 0.8/\mathfrak{a}$, $k_z = 0.1/\mathfrak{a}$, and (1,2) $k_x = 0.2/\mathfrak{a}$, $k_y = 0$, (3) $k_x = 0$, $k_y = 0.2/\mathfrak{a}$. The case $\mathfrak{W}^{\ominus,--}_{n\mathbf{k}n'\mathbf{k}'}, k_x = 0, k_y = 0.2/\mathfrak{a}$ is in the main text. The colorbars are different for each figure and not linearly scaled. Note that thanks to anti-detailed-balance, angular dependences of $\mathfrak{W}^{\ominus,++}_{n\mathbf{k}n'\mathbf{k}'}, \mathfrak{W}^{\ominus,+-}_{n\mathbf{k}n'\mathbf{k}'}$ are identical to those of $\mathfrak{W}^{\ominus,--}_{n\mathbf{k}n'\mathbf{k}'}, \mathfrak{W}^{\ominus,-+}_{n\mathbf{k}n'\mathbf{k}'}$, respectively, for an isotropic phonon dispersion.

Chapter 4

Phonon Thermal Hall Conductivity from Electronic Systems and Fermionic Quantum Spin Liquids

In this chapter, excerpts and figures are reprinted with permission from L. Mangeolle, L. Balents, L. Savary. The work presented here is still in progress. Upcoming copyright 2022 by the American Physical Society.

4.1 Introduction

In the previous two chapters, we studied in general terms the coupling of phonons $a_{n\mathbf{k}}$ to any other degree of freedom $Q_{n\mathbf{k}}$, and found that the phonon thermal conductivity is determined by correlation functions of this $Q_{n\mathbf{k}}$ field. Computing these correlation functions is a challenge, which must be taken up for each different degree of freedom coupled to the lattice (i.e. each instance of $Q_{n\mathbf{k}}$). We applied our results to the case of phonon-magnon coupling in Néel-ordered antiferromagnets. We showed in particular that a generic model for spin-lattice coupling, in the presence of both anisotropic magnetic exchange and an external magnetic field, enables a phonon Hall conductivity. This left open the question whether the presence of magnetic ordering, or any form of long-range spin correlations, is a necessary condition for the phonon Hall conductivity. Here, we consider the coupling of phonons to fermions. This includes electrons, as well as models for disordered magnets where the low-energy physics is described in terms of emergent neutral fermions. Our work addresses both Dirac cones and quadratic bands, with or without a Fermi surface.

4.2 Previous important results

Here, we recall a few important results from the previous chapters which we use in the present one.

The thermal conductivity of phonons $a_{n\mathbf{k}}$, where n is the polarization index and $\mathbf{k}$ is the momentum, exists through the couplings of the phonons to an other field $Q_{n\mathbf{k}}$ (note that here the phonon-field "coupling constant" is absorbed in Q) via the interaction hamiltonian density

$$H' = \sum_{n\mathbf{k}} \left(a^\dagger_{n\mathbf{k}} Q^\dagger_{n\mathbf{k}} + a_{n\mathbf{k}} Q_{n\mathbf{k}} \right). \tag{4.1}$$

The longitudinal (dissipative) part of the thermal conductivity, obtained from solving Boltzmann's equation for the phonons in a semiclassical treatment, is

$$\kappa_L^{\mu\nu} = \frac{\hbar^2}{k_B T^2} \frac{1}{V} \sum_{n\mathbf{k}} \frac{v^\mu_{n\mathbf{k}} \omega^2_{n\mathbf{k}} v^\nu_{n\mathbf{k}}}{4 D_{n\mathbf{k}} \sinh^2(\beta\hbar\omega_{n\mathbf{k}}/2)}, \tag{4.2}$$

for $\mu, \nu = x, y, z$, where V is the volume of the system, T the temperature, k_B Boltzmann's constant, $\beta = 1/(k_\mathrm{B}T)$, and $\omega_{n\mathbf{k}}$ and $\boldsymbol{v}_{n\mathbf{k}} = \boldsymbol{\nabla}_{\mathbf{k}} \omega_{n\mathbf{k}}$ are respectively the phonon frequency and velocity in mode $n\mathbf{k}$. It is controlled by the phonon scattering rate $D_{n\mathbf{k}} = D^{(1)}_{n\mathbf{k}} + \breve{D}_{n\mathbf{k}}$, where

$$D^{(1)}_{n\mathbf{k}} = -\frac{1}{\hbar^2} \int dt\, e^{-i\omega_{n\mathbf{k}} t} \left\langle [Q_{n\mathbf{k}}(t), Q^\dagger_{n\mathbf{k}}(0)] \right\rangle_\beta \tag{4.3}$$

is obtained at lowest order in perturbation theory in the strength of the coupling, with $\langle\cdot\rangle_\beta$ denoting thermal averaging, and $\breve{D}_{n\mathbf{k}}$ includes both higher order terms and contributions from other mechanisms such as scattering from impurities.

The thermal Hall (antisymmetric) conductivity at leading order in the coupling strength is expressed as

$$\kappa_H^{\mu\nu} = \frac{\hbar^2}{k_B T^2} \frac{1}{V} \sum_{n\mathbf{k}n'\mathbf{k}'} J^\mu_{n\mathbf{k}} \frac{e^{\beta\hbar\omega_{n\mathbf{k}}/2}}{2D_{n\mathbf{k}}} \left(\frac{1}{N_\mathrm{uc}} \sum_{q=\pm} \frac{\left(e^{\beta\hbar\omega_{n\mathbf{k}}} - e^{q\beta\hbar\omega_{n'\mathbf{k}'}}\right) \mathfrak{W}^{\ominus,+,q}_{n\mathbf{k},n'\mathbf{k}'}}{\sinh(\beta\hbar\omega_{n\mathbf{k}}/2)\sinh(\beta\hbar\omega_{n'\mathbf{k}'}/2)} \right) \frac{e^{\beta\hbar\omega_{n'\mathbf{k}'}/2}}{2D_{n'\mathbf{k}'}} J^\nu_{n'\mathbf{k}'}, \tag{4.4}$$

where $\mu, \nu = x, y, z$ and we defined the phonon current $J^\mu_{n\mathbf{k}} = N^\mathrm{eq}_{n\mathbf{k}}\, \omega_{n\mathbf{k}} v^\mu_{n\mathbf{k}}$, and $N^\mathrm{eq}_{n\mathbf{k}}$ is the number of phonons in mode $n\mathbf{k}$ in thermal equilibrium. It features the "skew-scattering" rate

$$\begin{aligned} \mathfrak{W}^{\ominus,qq'}_{n\mathbf{k},n'\mathbf{k}'} \;=\; & \frac{2N_\mathrm{uc}}{\hbar^4} \mathfrak{Re} \Big\{ \int \mathrm{d}t \mathrm{d}t_1 \mathrm{d}t_2 \mathrm{sign}(t_1) e^{i(q\omega_{n\mathbf{k}} + q'\omega_{n'\mathbf{k}'})t} e^{i(t_1+t_2)(q\omega_{n\mathbf{k}} - q'\omega_{n'\mathbf{k}'})} \\ & \left\langle \left[Q^{-q}_{n\mathbf{k}}(-t-t_1), Q^{-q'}_{n'\mathbf{k}'}(-t+t_1) \right] \left\{ Q^{q'}_{n'\mathbf{k}'}(-t_2), Q^{q}_{n\mathbf{k}}(+t_2) \right\} \right\rangle_\beta \Big\} \end{aligned} \tag{4.5}$$

where the exponent q identifies $Q^+ \equiv Q^\dagger, Q^- \equiv Q$. As a result of close-to-equilibrium thermodynamics, $\mathfrak{W}^\ominus$ satisfies "anti-detailed-balance"

$$\mathfrak{W}^{\ominus,qq'}_{n\mathbf{k}n'\mathbf{k}'} = -e^{-\beta(q\omega_{n\mathbf{k}} + q'\omega_{n'\mathbf{k}'})}\, \mathfrak{W}^{\ominus,-q-q'}_{n\mathbf{k}n'\mathbf{k}'}, \tag{4.6}$$

which in fact defines the specific form of the skew-scattering rate which appears in the thermal Hall conductivity and resistivity.

As mentioned above, in what follows, we consider $Q_{n\mathbf{k}}$ to be a fermion bilinear, for several species of fermions, in different contexts. In the last section we will also make a brief detour whereby $Q_{n\mathbf{k}}$ will be an electric field.

4.3 General results for fermions

We now consider the most general, *translationally-invariant*, coupling between one phonon operator and a fermion number-conserving bilinear, deriving from a local coupling to the strain tensor. We thus define $Q_{n\mathbf{k}}$, the field to which the phonon annihilation operator $a_{n\mathbf{k}}$ is coupled, as

$$Q_{n\mathbf{k}} = \sum_{\mathbf{p},\ell,\ell'} \mathcal{B}^{n,\ell,\ell'}_{\mathbf{k};\mathbf{p}} \; f^\dagger_{\ell,\mathbf{p}} f_{\ell',\mathbf{p}+\mathbf{k}}. \tag{4.7}$$

Here the coupling constant $\mathcal{B}^{n,\ell,\ell'}_{\mathbf{k};\mathbf{p}}$ is introduced phenomenologically, and a more specific expression will be derived in a particular case below. The fermion flavor index ℓ is kept general at this stage. We consider free fermions, with hamiltonian

$$H^0_f = \sum_{\ell,\mathbf{p}} \epsilon_{\ell,\mathbf{p}} f^\dagger_{\ell,\mathbf{p}} f_{\ell,\mathbf{p}}, \tag{4.8}$$

where $\epsilon_{\ell,\mathbf{p}}$ is the fermion's energy.

In order to obtain the diagonal scattering rate, we insert Eq. (4.7) into Eq. (4.3) and obtain, after straightforward algebra,

$$\begin{aligned} D^{(1)}_{n\mathbf{k}} = -\frac{2\pi}{\hbar} \sum_{\mathbf{p},\ell,\ell'} \; & \delta(\epsilon_{\ell,\mathbf{p}} - \epsilon_{\ell',\mathbf{p}+\mathbf{k}} - \omega_{n\mathbf{k}}) \\ \times \; & \left[n_{\mathrm{F}}(\epsilon_{\ell,\mathbf{p}}) - n_{\mathrm{F}}(\epsilon_{\ell',\mathbf{p}+\mathbf{k}}) \right] \; |\mathcal{B}^{n,\ell,\ell'}_{\mathbf{k};\mathbf{p}}|^2, \end{aligned} \tag{4.9}$$

where n_{F} is the Fermi distribution function. Note that when $\mathcal{B}^{n,\ell,\ell'}_{\mathbf{k};\mathbf{p}} = \delta_{\ell\ell'}$, Eq. (4.9) is the expression for the imaginary part of the density susceptibility (density-density correlations) of a fermion gas [Giuliani and Vignale, 2005]. We will evaluate Eq. (4.9) in specific models below, Eqs.(4.19,4.20).

We now turn to the skew scattering rate. By inserting Eq. (4.7) into Eq. (4.5), applying Wick's theorem, evaluating the time integrals, and after some algebra (see App. 4.A.2 for details), we find

$$\mathfrak{W}^{\ominus,qq'}_{n\mathbf{k},n'\mathbf{k}'} = \frac{(2\pi)^2}{\hbar^4} N_{\mathrm{uc}} \sum_{\mathbf{p},\{\ell_i\}} \mathcal{D}^{q,q',\{\ell_i\}}_{n\mathbf{k},n'\mathbf{k}'}(\mathbf{p}) \, \mathcal{N}^{q,q',\{\ell_i\}}_{n\mathbf{k},n'\mathbf{k}'}(\mathbf{p}) \, \mathcal{R}^{q,q',\{\ell_i\}}_{n\mathbf{k},n'\mathbf{k}'}(\mathbf{p}) \quad + (n\mathbf{k}q \leftrightarrow n'\mathbf{k}'q'), \tag{4.10}$$

where $\mathcal{D}^{q,q',\{\ell_i\}}_{n\mathbf{k},n'\mathbf{k}'}(\mathbf{p})$ is the product of two Dirac functions which enforce energy conservation,

$$\mathcal{D}^{q,q',\{\ell_i\}}_{n\mathbf{k},n'\mathbf{k}'}(\mathbf{p}) = \delta(\epsilon^{\ell_3}_{\mathbf{p}} - \epsilon^{\ell_2}_{\mathbf{p}+q'\mathbf{k}'} - q'\omega_{n'\mathbf{k}'}) \delta(q\omega_{n\mathbf{k}} + \epsilon^{\ell_1}_{\mathbf{p}+q\mathbf{k}+q'\mathbf{k}'} - \epsilon^{\ell_2}_{\mathbf{p}+q'\mathbf{k}'}), \tag{4.11}$$

$$\mathcal{N}^{q,q',\{\ell_i\}}_{n\mathbf{k},n'\mathbf{k}'}(\mathbf{p}) = n_F(\epsilon^{\ell_3}_{\mathbf{p}}) \left[2n_F(\epsilon^{\ell_2}_{\mathbf{p}+q'\mathbf{k}'}) - 1 \right] \left[1 - n_F(\epsilon^{\ell_1}_{\mathbf{p}+q\mathbf{k}+q'\mathbf{k}'}) \right], \tag{4.12}$$

and $\mathcal{R}^{q,q',\{\ell_i\}}_{n\mathbf{k},n'\mathbf{k}'}(\mathbf{p})$ is a factor whose structure is inherited from second-order perturbation theory, whose denominators are energy differences, namely

$$\mathcal{R}^{q,q',\{\ell_i\}}_{n\mathbf{k},n'\mathbf{k}'}(\mathbf{p}) = \left(\mathrm{PP}\frac{\mathfrak{Im}\left[\mathcal{K}^{0\ |\ q,q',\{\ell_i\}}_{n\mathbf{k},n'\mathbf{k}'}(\mathbf{p})\right]}{\epsilon^{\ell_4}_{\mathbf{p}+q\mathbf{k}} - \epsilon^{\ell_3}_{\mathbf{p}} + q\omega_{n\mathbf{k}}} + \mathrm{PP}\frac{\mathfrak{Im}\left[\mathcal{K}^{1\ |\ q,q',\{\ell_i\}}_{n\mathbf{k},n'\mathbf{k}'}(\mathbf{p})\right]}{\epsilon^{\ell_4}_{\mathbf{p}+q'\mathbf{k}'} - \epsilon^{\ell_3}_{\mathbf{p}} + q'\omega_{n'\mathbf{k}'}} \right), \quad (4.13)$$

and whose numerators are products of coupling constants,

$$\mathcal{K}^{\gamma\ |\ q,q',\{\ell_i\}}_{n\mathbf{k},n'\mathbf{k}'}(\mathbf{p}) = \mathcal{B}^{q|n,\ell_1,\ell_2}_{\mathbf{k};\mathbf{p}-\frac{1-q}{2}\mathbf{k}+q'\mathbf{k}'} \mathcal{B}^{q'|n',\ell_2,\ell_3}_{\mathbf{k}';\mathbf{p}-\frac{1-q'}{2}\mathbf{k}'} \quad (4.14)$$

$$\times \left[\delta_{\gamma,0}\ \mathcal{B}^{-q|n,\ell_3,\ell_4}_{\mathbf{k};\mathbf{p}-\frac{1-q}{2}\mathbf{k}} \mathcal{B}^{-q'|n',\ell_4,\ell_1}_{\mathbf{k}';\mathbf{p}-\frac{1-q'}{2}\mathbf{k}'+q\mathbf{k}} + \delta_{\gamma,1}\ \mathcal{B}^{-q'|n',\ell_3,\ell_4}_{\mathbf{k}';\mathbf{p}-\frac{1-q'}{2}\mathbf{k}'} \mathcal{B}^{-q|n,\ell_4,\ell_1}_{\mathbf{k};\mathbf{p}-\frac{1-q}{2}\mathbf{k}+q'\mathbf{k}'} \right]. \quad (4.15)$$

Here we defined $\mathcal{B}^{q|n,\ell,\ell'}_{\mathbf{k};\mathbf{p}}$ for $q = \pm$ as follows:

$$\mathcal{B}^{-|n,\ell,\ell'}_{\mathbf{k};\mathbf{p}} = \mathcal{B}^{n,\ell,\ell'}_{\mathbf{k};\mathbf{p}} \qquad ; \qquad \mathcal{B}^{+|n,\ell,\ell'}_{\mathbf{k};\mathbf{p}} = \left(\mathcal{B}^{n,\ell',\ell}_{\mathbf{k};\mathbf{p}}\right)^*. \quad (4.16)$$

Eq. (4.10), which expresses the skew-scattering rate, applies to *any* fermionic dispersion relation and regardless of their dependence on the ℓ index. In Appendix 4.A.3, we check explicitly that Eq. (4.10) satisfies anti-detailed balance, Eq. (4.6). Note also that Eq. (4.10) decomposes, as did the phonon-*magnon* scattering rate in the previous chapters, as a product $\mathfrak{W} \sim \mathcal{D}\mathcal{N}\mathcal{R}$. The differences with the magnon (boson) case lie in $\mathcal{N}$ which here includes *fermionic* population factors, and in $\mathcal{R}$, which is simpler in the fermionic case (here the q_i indices are absent) because phonons can only couple to $f^\dagger f$ operators (while $b^\dagger b^\dagger$ and bb combinations were allowed as well in the magnon case).

4.4 Application to Dirac and quadratic fermion dispersions (with or without a Fermi surface)

For the sake of clarity, in the main text, we present only applications to "simple" dispersion relations, namely Dirac and quadratic ones with or without Fermi surfaces. More precisely, we take the dispersion relation to be

$$\epsilon^{\text{Dirac 2d}}_{\ell,\mathbf{p}} = \sigma\, v_\nu\, |\mathbf{p} - \boldsymbol{\pi}_\nu| \ - \ \mu_{\nu,\alpha}, \quad (4.17)$$

$$\epsilon^{\text{Quad}}_{\ell,\mathbf{p}} = \frac{(\mathbf{p}-\boldsymbol{\pi}_0)^2}{2m_*} - \mu_\ell. \quad (4.18)$$

In Eq. (4.17), $\ell = (\nu, \sigma, \alpha)$, the Dirac cones are located at $\boldsymbol{\pi}_\nu$, and we take the two half-cones $\sigma = \pm$ to have the same velocity v_ν and to be independent of the extra index α. The momentum $\mathbf{p}$ in $\epsilon_{\ell,\mathbf{p}}$ is two-dimensional and assumed to be in a neighborhood of $\boldsymbol{\pi}_\nu$. Finally, $\mu_{\nu,\alpha}$ is a (spin- and valley-dependent) energy shift of the cone, responsible for the formation of a Fermi surface when it is nonzero. [1] In Eq. (4.18), $\mathbf{p}$ and $\boldsymbol{\pi}_0$ belong to the d-dimensional space

[1] We also consider that the Dirac cones are well separated, so that fermion scattering between different cones has a very small probability, namely $v_{\text{ph}}\delta\Pi \gg k_B T$ where $\delta\Pi = \min\{|\boldsymbol{\pi}_\nu - \boldsymbol{\pi}_{\nu'}|\ ,\ \nu \neq \nu'\}$. In what follows, we neglect such intervalley scatterings altogether by including a $\delta_{\nu,\nu'}$ factor in the solution of the energy conservation equations.

of fermionic momenta ($d = 2, 3$). This quadratic dispersion allows for analytic solutions for the longitudinal and skew scattering rates. [2] We present a more general model in Appendix 4.C.3. For each value of $\ell = \pm$, Eq. (4.18) describes a circular/spherical Fermi surface centered around a given point $\boldsymbol{\pi}_0$ in reciprocal space, and the mass m_* can be of any sign. This "low-energy" approximation of the dispersion relation by a second-order polynomial ought to yield an accurate description of phenomena occurring close to the Fermi surface if $k_B T \ll p_F^2/(2|m_*|)$, where the Fermi momentum $p_F = \sqrt{2|m_*|\mu_\ell}$ is a priori ℓ-dependent.

The diagonal scattering rate Eq. (4.9) involves an energy-conservation constraint in the form of a delta function which is nonzero when $\epsilon_{\ell,\mathbf{p}} - \epsilon_{\ell',\mathbf{p}+\mathbf{k}} - \omega_{n\mathbf{k}} = 0$. In the case of 2d Dirac fermions, the solution is a conic (see Chapter 3 and App. 4.C.1). In the case of quadratic fermions, the solution is a straight line ($d = 2$) or a plane ($d = 3$). Converting $\frac{1}{N_{\rm uc}} \sum_{\mathbf{p}} \longrightarrow V_{dD}^{\rm uc} \int \frac{\mathrm{d}^d \mathbf{p}}{(2\pi)^d}$, with $V_{dD}^{\rm uc}$ the volume of the d-dimensional unit cell,

$$
\begin{aligned}
D_{n\mathbf{k}}^{(1)\text{Dirac 2d}} &= -\frac{2\pi}{\hbar} \sum_{\ell,\ell'} \frac{\delta_{\nu,\nu'}}{v_\nu} \frac{V_{2D}^{\rm uc}}{(2\pi)^2} \int_{-\infty}^{+\infty} \mathrm{d}y \sum_{\eta} \, \mathrm{f}_{\nu,\eta}^{s}(y) \; J_\nu^s(y) \; \left| \mathcal{B}^{n,\ell,\ell'}_{\mathbf{k};\mathbf{p}_{\eta,\mathbf{k}}^{\ell,\ell'}(y)} \right|^2 \\
&\quad \times \left[n_{\rm F}(\epsilon_{\ell,\mathbf{p}_{\eta,\mathbf{k}}^{\ell,\ell'}(y)}) - n_{\rm F}(\epsilon_{\ell',\mathbf{p}_{\eta,\mathbf{k}}^{\ell,\ell'}(y)+\mathbf{k}}) \right], \qquad (4.19) \\
D_{n\mathbf{k}}^{(1)\text{Quad}} &= -\sum_{\ell,\ell'} V_{dD}^{\rm uc} \int_{(\underline{\mathbf{k}})_\perp} \frac{\mathrm{d}^{d-1}\mathbf{p}_\perp}{(2\pi)^{d-1}} \, \frac{|m_*|}{|\underline{\mathbf{k}}|} \left| \mathcal{B}^{n,\ell,\ell'}_{\mathbf{k};\boldsymbol{\pi}_0+\tilde{\mathbf{p}}_{n\mathbf{k}}^{\ell\ell'}+\mathbf{p}_\perp} \right|^2 \\
&\quad \times \left[n_{\rm F}(\epsilon_{\ell,\boldsymbol{\pi}_0+\tilde{\mathbf{p}}_{n\mathbf{k}}^{\ell\ell'}+\mathbf{p}_\perp}) - n_{\rm F}(\epsilon_{\ell',\boldsymbol{\pi}_0+\tilde{\mathbf{p}}_{n\mathbf{k}}^{\ell\ell'}+\mathbf{p}_\perp+\mathbf{k}}) \right]. \qquad (4.20)
\end{aligned}
$$

Hereabove, $\underline{\mathbf{k}}$ is the projection of $\mathbf{k}$ onto the space of fermionic momenta: thus for $d = 3$, $\underline{\mathbf{k}} = \mathbf{k}$ and for $d = 2$, $\underline{\mathbf{k}} = (k_x, k_y, 0)$. In Eq. (4.19), $s = -\sigma\sigma' = \pm$ and the η sum runs over $\eta = \pm$, the $\mathbf{p}_{\eta,\mathbf{k}}^{\ell,\ell'}(y) = c_\eta^{\ell,\ell'}(y)\, \hat{\mathbf{k}} + y\, \hat{\mathbf{z}} \times \hat{\mathbf{k}} + \boldsymbol{\pi}_\nu$ are the solutions to the energy conservation constraint in Eq. (4.9), which, when they exist, form a half-hyperbola or an ellipse parameterized by the variable y ($c_\eta^{\ell,\ell'}(y)$ is given in App. 4.C.1), $J_\nu^s(y)$ is the jacobian of the reparameterization (see Appendix) and solutions exist when $\mathrm{f}_{\nu,\eta}^+(y) \neq 0$ or $\mathrm{f}_{\nu,\eta}^-(y) \neq 0$, where $\begin{cases} \mathrm{f}_{\nu,\eta}^+(y) = \Theta(a^2 - \underline{\mathbf{k}}^2 - 4y^2) \\ \mathrm{f}_{\nu,\eta}^-(y) = \delta_{\eta,+}\, \Theta(\underline{\mathbf{k}}^2 - a^2) \end{cases}$, with $a = (\omega_{n\mathbf{k}} + \mu_{\nu,\alpha} - \mu_{\nu,\alpha'})/v_\nu$. In Eq. (4.20), $\tilde{\mathbf{p}}_{n\mathbf{k}}^{\ell\ell'} = \underline{\mathbf{k}} \left(-1/2 + m_* \left[\mu_{\ell'} - \mu_\ell - \omega_{n\mathbf{k}} \right] / |\underline{\mathbf{k}}|^2 \right)$ and the $(\underline{\mathbf{k}})_\perp$ integration is that over the $(d-1)$-dimensional field orthogonal to $\underline{\mathbf{k}}$.

The skew scattering rate in Eq. (4.10) involves two delta functions enforcing two energy conservation constraints. In the case of linearly dispersing fermions, the simultaneous solutions, when they exist, can be found analytically (see Chapter 3 and App. 4.C.1) and in turn the delta functions can be fully collapsed. In

[2] We note that the model Eq. (4.18) can be trivially generalized to a *collection* of circular Fermi surfaces with (fermion-like or hole-like) quadratic bands, provided that they are well separated in momentum space—namely, that $v_{\rm ph}\delta\Pi \gg k_B T$ where $\delta\Pi$ is the smallest distance between two Fermi surfaces.

the case of quadratic fermions, the solutions to the delta functions are given by $\mathbf{p} - \boldsymbol{\pi}_0 = \tilde{\mathbf{p}}^{\{\ell_i\}}_{n\mathbf{k},n'\mathbf{k}'} + \mathbf{p}_\perp$, for any $\mathbf{p}_\perp$ such that $\mathbf{p}_\perp \cdot \underline{\mathbf{k}}_1 = 0 = \mathbf{p}_\perp \cdot \underline{\mathbf{k}}_2$, where we define $\mathbf{k}_1 = q'\mathbf{k}'$ and $\mathbf{k}_2 = q\mathbf{k} + q'\mathbf{k}'$ and we provide an explicit expression for $\tilde{\mathbf{p}}^{\{\ell_i\}}_{n\mathbf{k},n'\mathbf{k}'}$ in App. 4.C.2. Then, recalling that $\mathcal{N}$ and $\mathcal{K}^{0,1}$ were defined in Eqs. (4.11-4.14),

$$\begin{aligned}
\mathfrak{W}^{\ominus,qq'\text{Dirac 2d}}_{n\mathbf{k},n'\mathbf{k}'} &= \pi^2 N_{\text{uc}} \sum_j \sum_{\{\ell_i\}} \left(\textstyle\prod_i \delta_{\nu_i,\nu}\right)\ V^{\text{uc}}_{2D}\, v_\nu^{-2} \qquad (4.21)\\
&\quad \times \mathcal{J}^{\{\ell_i\}}_{q\mathbf{k},q'\mathbf{k}'}(\mathbf{p}_j) \mathcal{N}^{q,q',\{\ell_i\}}_{n\mathbf{k},n'\mathbf{k}'}(\mathbf{p}_j)\ \mathcal{R}^{q,q',\{\ell_i\}}_{n\mathbf{k},n'\mathbf{k}'}(\mathbf{p}_j) + (n\mathbf{k}q \leftrightarrow n'\mathbf{k}'q'),\\
\mathfrak{W}^{\ominus,qq'\text{Quad}}_{n\mathbf{k},n'\mathbf{k}'} &= N_{\text{uc}} \sum_{\{\ell_i\}} V^{\text{uc}}_{dD} \int_{(\underline{\mathbf{k}}_1)_\perp \cap (\underline{\mathbf{k}}_2)_\perp} \frac{\mathrm{d}^{d-2}\mathbf{p}_\perp}{(2\pi)^{d-2}}\ \frac{m_*^2}{|\underline{\mathbf{k}}_1||\underline{\mathbf{k}}_2|}\left|\hat{\underline{\mathbf{k}}}_1 \times \hat{\underline{\mathbf{k}}}_2\right|^{-3}\ \mathcal{N}^{q,q',\{\ell_i\}}_{n\mathbf{k},n'\mathbf{k}'}(\mathbf{p})\\
&\quad \times \left(\text{PP}\frac{\mathfrak{Im}\left[\mathcal{K}^{0\ |\ q,q',\{\ell_i\}}_{n\mathbf{k},n'\mathbf{k}'}(\mathbf{p})\right]}{\sum_i (-1)^{i+1}\mu_{\ell_i} - qq'\underline{\mathbf{k}}\cdot\underline{\mathbf{k}}'/m_*} + \text{PP}\frac{\mathfrak{Im}\left[\mathcal{K}^{1\ |\ q,q',\{\ell_i\}}_{n\mathbf{k},n'\mathbf{k}'}(\mathbf{p})\right]}{\mu_{\ell_2} - \mu_{\ell_4}} \right)\\
&\quad + (n\mathbf{k}q \leftrightarrow n'\mathbf{k}'q'). \qquad (4.22)
\end{aligned}$$

In Eq. (4.21), we formally forbade intervalley coupling (as explained before) by adding an extra Kronecker delta $\prod_i \delta_{\nu_i,\nu}$ enforcing $\nu_1 = \nu_2 = \nu_3 = \nu_4 \to \nu$, and $\mathbf{p}_j$ for $j = 0,..,3$ are the solutions, *when they exist*, to the two energy conservation constraints in Eq. (4.11), and $\mathcal{J}^{\{\ell_i\}}_{q\mathbf{k},q'\mathbf{k}'}(\mathbf{p}_j)$ is a jacobian factor which appears when solving the energy constraints. We provide explicit expressions for both in App. 4.C.1. In Eq. (4.22), for clarity, we wrote $\mathbf{p} \leftarrow \boldsymbol{\pi}_0 + \tilde{\mathbf{p}}^{\{\ell_i\}}_{n\mathbf{k},n'\mathbf{k}'} + \mathbf{p}_\perp$, and for any vector $\mathbf{v}$ the unit vector $\hat{\mathbf{v}} = \mathbf{v}/|\mathbf{v}|$. The $(\underline{\mathbf{k}}_1)_\perp \cap (\underline{\mathbf{k}}_2)_\perp$ integration is that over the $(d-2)$-dimensional field of fermionic momenta orthogonal to both $\underline{\mathbf{k}}_1$ and $\underline{\mathbf{k}}_2$. For $d = 3$ this is an integral along the straight line with director $\underline{\mathbf{k}}_1 \times \underline{\mathbf{k}}_2$, and for $d = 2$ this reduces to replacing $\mathbf{p}_\perp \to \mathbf{0}$.

4.5 Fermionic spinons in a quantum spin liquid

Here we evaluate the thermal conductivity tensor in the case of emergent spinons from a spin model for a quantum spin liquid.

We start from a spin system with exchange interactions parametrized by $J^{ab}_{\mathbf{r},\mathbf{r}'}$ coupled to an external magnetic field $\boldsymbol{h}$ via the local g-tensor at site $\mathbf{r}$, $g^{ab}_{\{\mathbf{r}-\mathbf{r}''\}}$, i.e. we consider the Hamiltonian

$$H^0_S = \sum_{\mathbf{r},\mathbf{r}'} J^{ab}_{\mathbf{r},\mathbf{r}'} S^a_{\mathbf{r}} S^b_{\mathbf{r}'} - \sum_{\mathbf{r}} g^{ab}_{\{\mathbf{r}-\mathbf{r}''\}} h^a S^b_{\mathbf{r}}, \qquad (4.23)$$

where $a, b = x, y, z$ are the spin directions. Note that the g-tensor depends in principle on the positions $\mathbf{r}''$ of *all* the lattice sites because of crystal fields. In the main text, for clarity, we restrict the exchange matrix between two sites $\mathbf{r}, \mathbf{r}'$ to contain a Heisenberg and a Dzyaloshinskii-Moriya (DM) coupling of strengths $J^{\text{iso}}_{\mathbf{r},\mathbf{r}'}$ and $J^D_{\mathbf{r}'-\mathbf{r}}$, respectively, i.e.

$$J^{ab}_{\mathbf{r},\mathbf{r}'} = J^{\text{iso}}_{\mathbf{r},\mathbf{r}'}\delta_{ab} + \sum_{\boldsymbol{\eta}} \delta_{\mathbf{r}',\mathbf{r}+\boldsymbol{\eta}} (\hat{\mathbf{z}} \times \boldsymbol{\eta})^c J^D_{|\boldsymbol{\eta}|} \epsilon^{cab}, \qquad (4.24)$$

i.e. the DM vector is $\mathbf{D}_{\mathbf{r}'-\mathbf{r}} \perp (\mathbf{r}'-\mathbf{r})$. We then rewrite the spin operators using Abrikosov fermions, $\mathbf{S}_{\mathbf{r}} = \frac{1}{2}\sum_{\alpha\beta} \psi^\dagger_{\mathbf{r}\alpha}\boldsymbol{\sigma}_{\alpha\beta}\psi_{\mathbf{r}\beta}$ with spin indices $\alpha,\beta =\uparrow,\downarrow$ and a local constraint $\sum_\alpha \psi^\dagger_{\mathbf{r}\alpha}\psi_{\mathbf{r}\alpha} = 1 \quad \forall \mathbf{r}$. Finally, we perform a Hubbard-Stratonovich transformation in the channel where the mean-field boson expectation value $\chi^{\alpha\gamma}_{\mathbf{r},\mathbf{r}'} := \left\langle \psi^\dagger_{\mathbf{r}\alpha}\psi_{\mathbf{r}'\gamma}\right\rangle$ is nonzero (for a given gauge choice), and for concreteness take an ansatz of the following form:

$$\chi^{\beta'\beta}_{\mathbf{r}',\mathbf{r}} = (1-\delta_{\mathbf{r},\mathbf{r}'})\chi^0_{|\mathbf{r}'-\mathbf{r}|}\delta_{\beta\beta'} + \delta_{\mathbf{r},\mathbf{r}'}\chi^{\beta'\beta}_{\mathbf{r},\mathbf{r}}, \tag{4.25}$$

i.e., translationally invariant, and with a diagonal off-site contribution (the on-site term is not constrained at this stage). This procedure identifies $H^0_S \longrightarrow H^0_\psi$, where

$$H^0_\psi = \sum_{\mathbf{r},\mathbf{r}'} \psi^\dagger_{\mathbf{r},\alpha}\ \left(K^{\alpha\alpha'}_{\mathbf{r}-\mathbf{r}'} + \delta_{\mathbf{r},\mathbf{r}'}L^{\alpha\alpha'}_{\{\mathbf{r}-\mathbf{r}''\}}\right)\ \psi_{\mathbf{r}',\alpha'}, \tag{4.26}$$

where

$$\begin{aligned} K^{\alpha\beta}_{\boldsymbol{\eta}} &= J^0_{\boldsymbol{\eta}}\delta_{\alpha\beta} - i\alpha^{\mathrm{R}}_{\boldsymbol{\eta}}\ \hat{\mathbf{z}}\cdot(\boldsymbol{\eta}\times\boldsymbol{\sigma}_{\alpha\beta})\,, \\ L^{\alpha\beta}_{\{\mathbf{r}-\mathbf{r}''\}} &= \mathbf{h}_{\{\mathbf{r}-\mathbf{r}''\}}\cdot\boldsymbol{\sigma}_{\alpha\beta}, \end{aligned} \tag{4.27}$$

with

$$\begin{aligned} J^0_{\mathbf{r}-\mathbf{r}'} &= -\frac{1}{4}\chi^0_{|\mathbf{r}-\mathbf{r}'|}J^{\mathrm{iso}}_{\mathbf{r},\mathbf{r}'}, \\ \alpha^{\mathrm{R}}_{\mathbf{r}-\mathbf{r}'} &= -\frac{1}{4}\chi^0_{|\mathbf{r}-\mathbf{r}'|}J^D_{|\mathbf{r}-\mathbf{r}'|}, \\ \mathsf{h}^b_{\{\mathbf{r}-\mathbf{r}''\}} &= \frac{1}{4}\sum_{\mathbf{r}''} m^a_{\mathbf{r}''}J^{ab}_{\mathbf{r}'',\mathbf{r}} - \frac{1}{2}h^a g^{ab}_{\{\mathbf{r}-\mathbf{r}''\}}, \\ m^a_{\mathbf{r}} &= \left[\left(\textstyle\sum_{\mathbf{r}'}\boldsymbol{J}_{\mathbf{r},\mathbf{r}'}\right)^{-1}\right]_{ab} h^c g^{cb}_{\{\mathbf{r}-\mathbf{r}''\}}. \end{aligned} \tag{4.28}$$

Here $m^a_{\mathbf{r}}$ is the classical magnetization; it coincides with the mean-field value $m^a_{\mathbf{r}} = \sigma^a_{\alpha\beta}\chi^{\alpha\beta}_{\mathbf{r},\mathbf{r}}$, see App.4.G. Note, that the Dzyaloshinskii-Moriya interaction between spins manifests itself as a Rashba interaction between spinons: a nonzero $\alpha^{\mathrm{R}}_{\boldsymbol{\eta}}$ is allowed by spin-orbit coupling and the lack of inversion symmetry.

In momentum space, where $\psi_{\mathbf{r},\alpha} = \frac{1}{\sqrt{N_{\mathrm{uc}}}}\sum_{\mathbf{p}} e^{-i\mathbf{p}\mathbf{r}}\psi_{\mathbf{p},\alpha}$, the quadratic hamiltonian H^0_ψ is diagonalized by a unitary transformation of the fermion operators, $\psi_{\mathbf{p},\alpha} = \sum_\ell U^{\alpha\ell}_{\mathbf{p}} f_{\mathbf{p},\ell}$ so that $H^0_\psi \longrightarrow H^0_f$, as defined in Eq. (4.8). Technical details and the expression of $\boldsymbol{U}_{\mathbf{p}}$ are provided in App.4.E.

4.6 Phonon-fermion couplings

We now consider coupling this emergent fermion system to phonons as in the previous two chapters. As explained above, we consider a coupling term with parameters $\mathcal{B}$ from Eq. (4.7). Given our two-band system, $\mathcal{B}$ can be seen as a sum of Pauli matrices acting in this space, i.e. we define

$$\mathcal{B}^{n,\ell\ell'}_{\mathbf{k};\mathbf{p}} = (\mathsf{B}^0_{n,\mathbf{k};\mathbf{p}}\mathbb{1} + \vec{\mathsf{B}}_{n,\mathbf{k};\mathbf{p}}\cdot\vec{\sigma})_{\ell\ell'}, \tag{4.29}$$

where $\ell, \ell' = \pm$.

Before proceeding further with a symmetry analysis, we describe a possible microscopic magnetoelastic model from which the $\mathcal{B}^{n,\ell\ell'}_{\mathbf{k};\mathbf{p}}$ as in Eq. (4.29) can arise. Namely, we now consider the above model, Eq. (4.26), in a *distorted* lattice, by replacing all positions $\mathbf{r} \to \tilde{\mathbf{r}}$, with $\tilde{\mathbf{r}}$ the positions of the sites in the distorted lattice. The fermion hamiltonian then becomes $H^0_\psi \to H_\psi = H^0_\psi\big|_{\mathbf{r}\to\tilde{\mathbf{r}}}$. Then we Taylor-expand the couplings with respect to the displacement field $\boldsymbol{u}(\mathbf{r})$, i.e. $\tilde{\mathbf{r}} = \mathbf{r} + \boldsymbol{u}(\mathbf{r})$ where $\tilde{\mathbf{r}}$ belongs to the distorted lattice and $\mathbf{r}$ to the undistorted lattice. Then, $H_\psi = H^0_\psi + H'_\psi + \dots$ where "$+\dots$" accounts for terms at least quadratic in the displacement field, and the linear in $\boldsymbol{u}$ term, H'_ψ, is the interaction hamiltonian of the form aQ, with Q a fermion bilinear as in Eq. (4.7). It is convenient to define new fermion-phonon coupling terms $\widehat{\mathcal{B}}^{a;\ell\ell'}_{\boldsymbol{\eta};\mathbf{p};\mathbf{k}} \sim \left[\boldsymbol{U}^\dagger_{\mathbf{p}} \frac{\delta}{\delta u^a(\boldsymbol{\eta})}(\mathbf{K},\mathbf{L})\boldsymbol{U}_{\mathbf{p}+\mathbf{k}}\right]_{\ell,\ell'}$ (recall $\boldsymbol{U}$ diagonalizes the noninteracting fermion Hamiltonian) as along components of the polarization vectors $(\boldsymbol{\varepsilon})^a$. More precisely, $\widehat{\mathcal{B}}^{a;\ell\ell'}_{\boldsymbol{\eta};\mathbf{p};\mathbf{k}}$ is defined through

$$\mathcal{B}^{n,\ell\ell'}_{\mathbf{k};\mathbf{p}} = \sum_{a=x,y,z} \frac{\varepsilon^a_{n\mathbf{k}}}{\sqrt{2M_{\rm uc}N_{\rm uc}\omega_{n\mathbf{k}}}} \sum_{\boldsymbol{\eta}} (e^{i\mathbf{k}\boldsymbol{\eta}} - 1)\ \widehat{\mathcal{B}}^{a;\ell\ell'}_{\boldsymbol{\eta};\mathbf{p};\mathbf{k}}, \tag{4.30}$$

and contains all the information about the fermionic *wavefunctions* (as opposed to *dispersion*), and depends on the spatial derivatives of coupling tensors $\mathbf{K}, \mathbf{L}$. Indeed, $\frac{\delta}{\delta u^a(\boldsymbol{\eta})}$ denotes functional derivation with respect to the ath component of the displacement field at position $\boldsymbol{\eta}$. For later use, we parameterize $\widehat{\boldsymbol{\mathcal{B}}}^{a}_{\boldsymbol{\eta};\mathbf{p};\mathbf{k}}$ as

$$\begin{aligned}\widehat{\mathcal{B}}^{a;\ell\ell'}_{\boldsymbol{\eta};\mathbf{p};\mathbf{k}} \ :=\ & (U^\dagger_{\mathbf{p}})^{\ell\alpha}\Big[\textstyle\sum_{b=x,y}\sigma^b_{\alpha\alpha'}\left(e^{i\mathbf{p}\boldsymbol{\eta}}\mathsf{v}^b_{a,\boldsymbol{\eta}} + e^{-i\mathbf{k}\boldsymbol{\eta}}\mathsf{u}^b_{a,\boldsymbol{\eta}}\right) \\ & + e^{-i\mathbf{k}\boldsymbol{\eta}}\mathsf{u}^z_{a,\boldsymbol{\eta}}\sigma^z_{\alpha\alpha'} + e^{i\mathbf{p}\boldsymbol{\eta}}\mathsf{t}^0_{a,\boldsymbol{\eta}}\delta_{\alpha\alpha'}\Big](U_{\mathbf{p}+\mathbf{k}})^{\alpha'\ell'},\end{aligned} \tag{4.31}$$

where $\mathsf{t}^0, \mathsf{u}^{x,y}, \mathsf{v}^{x,y,z}$ are parameters.

Technical details and the full expression of $\widehat{\mathcal{B}}^{a;\ell\ell'}_{\boldsymbol{\eta};\mathbf{p};\mathbf{k}}$ (or, equivalently, of the parameters $\mathsf{t}^0, \mathsf{u}^{x,y}, \mathsf{v}^{x,y,z}$) can be found in Appendices 4.E,4.F. We moreover define $\widehat{\mathcal{B}}^{a,\ell\ell'}_{\boldsymbol{\eta};\mathbf{p};\mathbf{k}} = (B^0_{a,\boldsymbol{\eta};\mathbf{p};\mathbf{k}}\mathbb{1} + \vec{B}_{a,\boldsymbol{\eta};\mathbf{p};\mathbf{k}}\cdot\vec{\boldsymbol{\sigma}})_{\ell\ell'}$ (cf. Eq. (4.29)).

4.7 Anti-unitary symmetries and phonon thermal Hall effect

We now turn to an analysis of cases under which the thermal Hall effect vanishes. One can show (see App.4.B) that, if there exists a relation of the form

$$\mathcal{B}^{n,\ell,\ell'}_{\mathbf{k};\mathbf{p}} = \xi_{\ell,\ell'}\left(\mathcal{B}^{n,\tilde{\ell},\tilde{\ell}'}_{-\mathbf{k};-\mathbf{p}}\right)^*, \tag{4.32}$$

where $\ell \leftrightarrow \tilde{\ell}$ are in 1-to-1 correspondence and $\xi_{\ell,\ell'}$ is a coefficient satisfying the constraint $\xi_{\ell_1,\ell_2}\xi_{\ell_2,\ell_3}\xi_{\ell_3,\ell_4}\xi_{\ell_4,\ell_1} = 1 \quad \forall(\ell_1,\ell_2,\ell_3,\ell_4)$, then $\mathcal{K}^{0/1\ |\ q,q',\{\ell_i\}}_{n\mathbf{k},n'\mathbf{k}'}(\mathbf{p}) = \left(\mathcal{K}^{0/1\ |\ q,q',\{\tilde{\ell}_i\}}_{n-\mathbf{k},n'-\mathbf{k}'}(-\mathbf{p})\right)^*$. Formulated in terms of $\widehat{B}$ as a matrix, Eq. (4.32) is true

iff $\widehat{\boldsymbol{\mathcal{B}}}_{a,\boldsymbol{\eta};\mathbf{p};\mathbf{k}} + \widehat{\boldsymbol{\mathcal{B}}}_{a,\boldsymbol{\eta};-\mathbf{p};-\mathbf{k}}$ or $\widehat{\boldsymbol{\mathcal{B}}}_{a,\boldsymbol{\eta};\mathbf{p};\mathbf{k}} + \sigma^x \widehat{\boldsymbol{\mathcal{B}}}_{a,\boldsymbol{\eta};-\mathbf{p};-\mathbf{k}} \sigma^x$ have purely real diagonal components and purely real or purely imaginary off-diagonal components (in the $\ell, \ell' = \pm$ basis), see Table 4.7.1.

If, furthermore, the relation $\epsilon_{\ell,\mathbf{p}} = \epsilon_{\tilde{\ell},-\mathbf{p}}$ holds (i.e. if the noninteracting fermionic spectrum is symmetric under the reversal of momentum), by direct inspection of Eqs. (4.10-4.13) then $\mathfrak{W}^{\ominus,qq'}_{n\mathbf{k},n'\mathbf{k}'} + \mathfrak{W}^{\ominus,qq'}_{n-\mathbf{k},n'-\mathbf{k}'} = 0$. We showed in Chapter 2 that the latter leads to $\boldsymbol{\kappa}_H = \mathbf{0}$, and is a manifestation of (effectively) preserved time reversal symmetry (there, time-reversal combined with a translation is preserved).

We now ask whether there exists symmetries of the combined phonon-fermion system which imply realizations of Eq. (4.32) together with a fermionic spectrum symmetric under $\mathbf{p} \to -\mathbf{p}$. It is indeed the case provided that one can factorize $\xi_{\ell,\ell'} = \zeta_\ell \zeta_{\ell'}$ with $\zeta_{\ell^{(\prime)}} = \pm 1$ (which is true in all the specific cases we consider in App. 4.F.2, reported in Tab. 4.7.2), because $\omega_{n\mathbf{k}} = \omega_{n-\mathbf{k}}$ (always true because the pure phonon theory is time-reversal invariant and phonons do not directly couple to a magnetic field).

More precisely, the above is the case if and only if $H_0 + H' = H_{\rm tot} = \hat{\mathcal{T}} H_{\rm tot} \hat{\mathcal{T}}^{-1}$, where $H_0 = H_f^0 + \sum_{n\mathbf{k}} \omega_{n\mathbf{k}} a^\dagger_{n\mathbf{k}} a_{n\mathbf{k}}$, and the anti-unitary operator $\hat{\mathcal{T}} = \hat{\mathcal{U}}\hat{K}$ is the combination of complex conjugation $\hat{K}$ and the unitary operation

$$\hat{\mathcal{U}} : (a_{n\mathbf{k}}, f_{\ell,\mathbf{p}}) \mapsto (a_{n-\mathbf{k}}, \zeta_\ell f_{\tilde{\ell},-\mathbf{p}}). \tag{4.33}$$

$\tilde{\ell}$	$\xi_{\ell,\ell'}$	ξ^0	ξ^x	ξ^y	ξ^z	$\hat{\mathcal{U}}_f$	Cases
$\bar{\ell}$	$(-1)^{1+\delta_{\ell,\ell'}}$	$+$	$-$	$-$	$-$	$i\sigma^y$	(a)
$\bar{\ell}$	1	$+$	$+$	$+$	$-$	σ^x	(c)
ℓ	1	$+$	$+$	$-$	$+$	$\mathbb{1}$	(b),(d)
ℓ	$(-1)^{1+\delta_{\ell,\ell'}}$	$+$	$-$	$+$	$+$	σ^z	-

Table 4.7.1: Particular instances of relations Eq.(4.32), defined by columns 1 and 2. The corresponding ξ^μ (realizing $B^\mu_{a,\boldsymbol{\eta};\mathbf{p};\mathbf{k}} = \xi^\mu \left(B^\mu_{a,\boldsymbol{\eta};-\mathbf{p};-\mathbf{k}}\right)^*$, for $a = x, y, z$, $\mu = 0, x, y, z$) are displayed in columns 3 to 6. Column 7 identifies the corresponding unitary operator of the symmetry. Column 8 lists special cases where the symmetry is realized – see Table 4.7.2.

A summary of four particular cases is given in Table 4.7.1, where the corresponding symmetry operation on the fermions $\hat{\mathcal{U}}_f$ is defined by

$$\hat{\mathcal{U}} = (\hat{\mathcal{I}}_{\mathbf{k}} \circ \mathbb{1}_{\rm ph}) \otimes (\hat{\mathcal{I}}_{\mathbf{p}} \circ \hat{\mathcal{U}}_f), \tag{4.34}$$

i.e. the decomposition of $\hat{\mathcal{U}}$ between the phonon and fermion spaces. Here $\hat{\mathcal{I}}_{\mathbf{k}}$ and $\hat{\mathcal{I}}_{\mathbf{p}}$ reverse phonon and fermion momenta, respectively, and $\mathbb{1}_{\rm ph} : a_{n\mathbf{k}} \to a_{n\mathbf{k}}$ is the identity in phonon space.

Finally, in the case of our spinon Hamiltonian Eqs. (4.26-4.28) and microscopic magnetoelastic coupling given in App.4.E.2, we provide a number of conditions on the physical microscopic parameters α^{R}, h^a and $\mathsf{u}^b, \mathsf{v}^a$ (defined in the Appendix) under which $\boldsymbol{\kappa}_{\mathrm{H}} = \mathbf{0}$ in Table 4.7.2 (with the relation realized on the $B^{\mu}_{a,\boldsymbol{\eta};\mathbf{p};\mathbf{k}}$ in Table 4.7.1).

Case	$\mathsf{h}^{x,y}$	$\mathsf{u}^{x,y}_{\mu,\boldsymbol{\eta}}$	h^{z}	$\mathsf{u}^{z}_{\mu,\boldsymbol{\eta}}$	$\alpha^{\mathrm{R}}_{\boldsymbol{\eta}}$	$\mathsf{v}^{x,y}_{\mu,\boldsymbol{\eta}}$
(a)	0	0	0	0	–	–
(b)	–	0	–	0	0	0
(c)	–	–	0	0	0	0
(d)	0	0	–	–	0	0

Table 4.7.2: Summary of some particular cases, which all entail $\boldsymbol{\kappa}_{\mathrm{H}} = \mathbf{0}$. A "–" symbol indicates that the Hall conductivity vanishes regardless of the value of the corresponding parameter.

4.8 Phonon-photon coupling in a $U(1)$ spin liquid

For completeness, and although this chapter focuses mainly on fermionic systems, we also consider the coupling $H_{\mathcal{E}E}$ between the strain tensor $\boldsymbol{\mathcal{E}}$ and an emergent electric field:

$$H_{\mathcal{E}E} = \sum_{\mathbf{r}} \sum_{a,b,c} \lambda_{a;bc} \big[\partial_0 A_a(\tau,\mathbf{r}) - \partial_a A_0(\tau,\mathbf{r})\big] \mathcal{E}_{bc}(\tau,\mathbf{r}), \tag{4.35}$$

where $a,b,c \in \{x,y,z\}$, $\partial_0 = i\partial_\tau$, and $\lambda_{a;bc}$ is the coupling strength. The low-energy action of the electric field was derived in [Ioffe and Larkin, 1989] in terms of A_0 and $A_\perp$, the scalar and transverse components of the gauge field in Coulomb gauge, respectively. This theory has two parameters: $\chi = \frac{1}{24\pi m_s}$ the spinon gas diamagnetic susceptibility and $\gamma = \frac{2\overline{n}}{k_F}$ the Landau damping coefficient, with $\overline{n}$ the spinon density and m_s the spinon effective mass. Details of the model and our calculations are provided in appendix 4.H. The phonon-photon diagonal scattering rate is $D^{(1),A}_{n\mathbf{k}} = D^{(1),A^\perp}_{n\mathbf{k}} + D^{(1),A_0}_{n\mathbf{k}}$, where

$$D^{(1),A^\perp}_{n\mathbf{k}} = \frac{\gamma \omega^2_{n\mathbf{k}} M^{-1}_{\mathrm{uc}} |\underline{\mathbf{k}}|^{-3}}{\chi^2 |\underline{\mathbf{k}}|^4 + \gamma^2 \frac{\omega^2_{n\mathbf{k}}}{|\underline{\mathbf{k}}|^2}} \left| \sum_{a;b,c} \epsilon^{z a \overline{a}} k_a \lambda_{\overline{a};bc} \varepsilon^b_{n\mathbf{k}} k^c \right|^2, \tag{4.36}$$

$$D^{(1),A_0}_{n\mathbf{k}} = \frac{M^{-1}_{\mathrm{uc}} \omega^{-1}_{n\mathbf{k}}\ 2\pi/m_s}{\frac{v_F|\underline{\mathbf{k}}|}{\omega_{n\mathbf{k}}} + \frac{\omega_{n\mathbf{k}}}{v_F|\underline{\mathbf{k}}|}} \left| \sum_{a;b,c} k_a \lambda_{a;bc} \varepsilon^b_{n\mathbf{k}} k^c \right|^2, \tag{4.37}$$

$a \in \{x,y\}$, $a = x \Leftrightarrow \overline{a} = y$ and $b,c \in \{x,y,z\}$.

4.9 Further directions

4.9.1 Scaling relations

Our analysis of the scaling relations of $\kappa_{\mathrm{L}}(T), \varrho_{\mathrm{H}}(T)$ is still in progress. The interested reader may find them in Appendices 4.D and 4.I. Here I will just summarize our results for the temperature scalings of the phonons' longitudinal conductivity and thermal resistivity in a spin liquid with a Fermi surface of $d = 2$-dimensional spinons and an emergent electric field.

quantity	τ^{-1}	κ_{L}	$\mathfrak{W}^{\ominus}$	$\tau_{\mathrm{skew}}^{-1}$	ϱ_{H}
T-scaling	T^{δ}	$T^{3-\delta}$	$T^{\gamma+1-2\lambda}$	$T^{4-2\lambda+\gamma}$	$T^{\gamma+1-2\lambda}$
Eq. ref	(4.149)	(4.150)	(4.147)	(4.147)	(4.151)

Table 4.9.1: Scaling relations derived in Secs. 4.I.2, 4.I.3, 4.I.4 and the corresponding equation number where they appear. The exponents $\delta = 0, 1, 3$ and $\gamma, \lambda = 0, 1$ indicate which contribution dominates each scattering rate.

Our results are displayed in Table 4.9.1. The value of $\delta = 0, 1, 3$ indicates that the longitudinal resistivity is dominated by the scattering of phonons by sample boundaries, fermions, or the emergent electric field, respectively. The values of $\gamma = 0, 1$ and $\delta = 0, 1$ depend on the comparison between several parameters which depend on T, h, $\mathsf{u}^{x,y,z}$, $\mathsf{v}^{x,y}$, t^{0}, α^{R}, m_*, v_F. I do not reproduce the full discussion here.

4.9.2 Remark and outlook

This Chapter is still ongoing work. We want to investigate further the scaling relations of κ_{L} and ϱ_{H} with respect to temperature, as well as the dependence of ϱ_{H} on microscopic parameters.

Appendix

4.A Derivation of the scattering rates

4.A.1 Diagonal scattering rate

We apply the general formula Eq. (4.3) to the model Eq. (4.7), and using the formula

$$\begin{aligned}&\left\langle \left[f^\dagger_{\ell_1,\mathbf{p}_1}(t)\ f_{\ell'_1,\mathbf{p_1}+\mathbf{k}}(t),\ f^\dagger_{\ell'_2,\mathbf{p_2}+\mathbf{k}} f_{\ell_2,\mathbf{p}_2} \right] \right\rangle_\beta \\ &= \delta_{\mathbf{p}_1,\mathbf{p}_2}\delta_{\ell_1,\ell_2}\delta_{\ell'_1,\ell'_2} \times \quad e^{i\epsilon_{\ell_1,\mathbf{p}_1}t}\ e^{-i\epsilon_{\ell'_1,\mathbf{p}_1+\mathbf{k}}t}\ \left(n_F(\epsilon_{\ell_1,\mathbf{p}_1}) - n_F(\epsilon_{\ell'_1,\mathbf{p}_1+\mathbf{k}}) \right),\end{aligned} \tag{4.38}$$

then performing the time integration $\int \mathrm{d}t\, e^{it\Omega} = 2\pi\delta(\Omega)$, it is easy to derive the result for $D^{(1)}_{n\mathbf{k}}$, Eq. (4.9).

4.A.2 Skew-scattering rate

We apply the general formula Eq. (4.5) to the model Eq. (4.7), and using the useful formula

$$Q^q_{n\mathbf{k}} = \sum_{\mathbf{p},\ell,\ell'} \mathcal{B}^{q|n,\ell,\ell'}_{\mathbf{k};\mathbf{p}-\frac{1+q}{2}\mathbf{k}}\ f^\dagger_{\ell,\mathbf{p}} f_{\ell',\mathbf{p}-q\mathbf{k}}, \tag{4.39}$$

one arrives at the intermediate result

$$\begin{aligned}&\mathfrak{W}^{\ominus,qq'}_{n\mathbf{k},n'\mathbf{k}'} = \frac{2}{\hbar^4}\,\mathfrak{Re}\left\{ \int \mathrm{d}t\mathrm{d}t_1\mathrm{d}t_2 \mathrm{sign}(t_1) e^{i(q\omega_{n\mathbf{k}}+q'\omega_{n'\mathbf{k}'})t} e^{i(t_1+t_2)(q\omega_{n\mathbf{k}}-q'\omega_{n'\mathbf{k}'})} \right. \\ &\times \sum_{\{\mathbf{p}_i,\ell_i\ell'_i\}_{i=1..4}} \mathcal{B}^{-q|n,\ell_1,\ell'_1}_{\mathbf{k};\mathbf{p}_1-\frac{1-q}{2}\mathbf{k}} e^{-iq'\mathbf{p'_2}\boldsymbol{\eta}_2} \mathcal{B}^{-q'|n',\ell_2,\ell'_2}_{\mathbf{k}';\mathbf{p}_2-\frac{1-q'}{2}\mathbf{k}'} e^{iq'\mathbf{p'_4}\boldsymbol{\eta}_4} \mathcal{B}^{q'|n',\ell_4,\ell'_4}_{\mathbf{k}';\mathbf{p}_4-\frac{1+q'}{2}\mathbf{k}'} e^{iq'\mathbf{p'_3}\boldsymbol{\eta}_3} \mathcal{B}^{q|n,\ell_3,\ell'_3}_{\mathbf{k};\mathbf{p}_3-\frac{1+q}{2}\mathbf{k}} \\ &\times e^{i\left(\epsilon^{\ell_1}_{\mathbf{p}_1}-\epsilon^{\ell'_1}_{\mathbf{p}_1+q\mathbf{k}}\right)(-t-t_1)} e^{i\left(\epsilon^{\ell_2}_{\mathbf{p}_2}-\epsilon^{\ell'_2}_{\mathbf{p}_2+q'\mathbf{k}'}\right)(-t+t_1)} e^{i\left(\epsilon^{\ell_4}_{\mathbf{p}_4}-\epsilon^{\ell'_4}_{\mathbf{p}_4-q'\mathbf{k}'}\right)(-t_2)} e^{i\left(\epsilon^{\ell_3}_{\mathbf{p}_3}-\epsilon^{\ell'_3}_{\mathbf{p}_3-q\mathbf{k}}\right)(+t_2)} \\ &\times \left\langle \left[f^\dagger_{\mathbf{p}_1,\ell_1}\ f_{\mathbf{p}_1+q\mathbf{k},\ell'_1}, f^\dagger_{\mathbf{p}_2,\ell_2}\ f_{\mathbf{p}_2+q'\mathbf{k}',\ell'_2} \right] \left\{ f^\dagger_{\mathbf{p}_4,\ell_4}\ f_{\mathbf{p}_4-q'\mathbf{k}',\ell'_4}, f^\dagger_{\mathbf{p}_3,\ell_3}\ f_{\mathbf{p}_3-q\mathbf{k},\ell'_3} \right\} \right\rangle_\beta \Bigg\}.\end{aligned} \tag{4.40}$$

Then, we apply Wick's theorem:

$$
\begin{aligned}
& \left\langle \left[f^\dagger_{\mathbf{p}_1,\ell_1}\ f_{\mathbf{p}_1+q\mathbf{k},\ell'_1}, f^\dagger_{\mathbf{p}_2,\ell_2}\ f_{\mathbf{p}_2+q'\mathbf{k}',\ell'_2} \right] \left\{ f^\dagger_{\mathbf{p}_4,\ell_4}\ f_{\mathbf{p}_4-q'\mathbf{k}',\ell'_4}, f^\dagger_{\mathbf{p}_3,\ell_3}\ f_{\mathbf{p}_3-q\mathbf{k},\ell'_3} \right\} \right\rangle_\beta \\
= \ & -\delta_{\ell_1,\ell'_4}\delta_{\ell'_1,\ell_2}\delta_{\ell'_2,\ell_3}\delta_{\ell_4,\ell'_3}\ \delta_{\mathbf{p}_1,\mathbf{p}_4-q'\mathbf{k}'}\ \delta_{\mathbf{p}_1+q\mathbf{k},\mathbf{p}_2}\ \delta_{\mathbf{p}_2+q'\mathbf{k}',\mathbf{p}_3}\ \delta_{\mathbf{p}_4,\mathbf{p}_3-q\mathbf{k}} \\
& n_F(\epsilon_{\mathbf{p}_1,\ell_1})\left(2n_F(\epsilon_{\mathbf{p}_4,\ell_4})-1\right)\left(1-n_F(\epsilon_{\mathbf{p}_3,\ell_3})\right) \\
+ \ & \delta_{\ell'_2,\ell_1}\delta_{\ell_2,\ell'_3}\delta_{\ell_3,\ell'_4}\delta_{\ell'_1,\ell_4}\ \delta_{\mathbf{p}_2+q'\mathbf{k}',\mathbf{p}_1}\ \delta_{\mathbf{p}_2,\mathbf{p}_3-q\mathbf{k}}\ \delta_{\mathbf{p}_3,\mathbf{p}_4-q'\mathbf{k}'}\ \delta_{\mathbf{p}_1+q\mathbf{k},\mathbf{p}_4} \\
& n_F(\epsilon_{\mathbf{p}_2,\ell_2})\left(2n_F(\epsilon_{\mathbf{p}_3,\ell_3})-1\right)\left(1-n_F(\epsilon_{\mathbf{p}_4,\ell_4})\right) \\
- \ & \delta_{\ell_1,\ell'_3}\delta_{\ell'_1,\ell_2}\delta_{\ell_3,\ell'_4}\delta_{\ell'_2,\ell_4}\ \delta_{\mathbf{p}_1,\mathbf{p}_3-q\mathbf{k}}\ \delta_{\mathbf{p}_1+q\mathbf{k},\mathbf{p}_2}\ \delta_{\mathbf{p}_3,\mathbf{p}_4-q'\mathbf{k}'}\ \delta_{\mathbf{p}_2+q'\mathbf{k}',\mathbf{p}_4} \\
& n_F(\epsilon_{\mathbf{p}_1,\ell_1})\left(2n_F(\epsilon_{\mathbf{p}_3,\ell_3})-1\right)\left(1-n_F(\epsilon_{\mathbf{p}_4,\ell_4})\right) \\
+ \ & \delta_{\ell'_2,\ell_1}\delta_{\ell_2,\ell'_4}\delta_{\ell'_1,\ell_3}\delta_{\ell_4,\ell'_3}\ \delta_{\mathbf{p}_2+q'\mathbf{k}',\mathbf{p}_1}\ \delta_{\mathbf{p}_2,\mathbf{p}_4-q'\mathbf{k}'}\ \delta_{\mathbf{p}_1+q\mathbf{k},\mathbf{p}_3}\ \delta_{\mathbf{p}_4,\mathbf{p}_3-q\mathbf{k}} \\
& n_F(\epsilon_{\mathbf{p}_2,\ell_2})\left(2n_F(\epsilon_{\mathbf{p}_4,\ell_4})-1\right)\left(1-n_F(\epsilon_{\mathbf{p}_3,\ell_3})\right). \qquad (4.41)
\end{aligned}
$$

The first two lines correspond to the $\mathcal{K}^0$ term in Eq. (4.10), while the last two correspond to the $\mathcal{K}^1$ term. We can then compute the time integrals: we use $\int \mathrm{d}t\, e^{it\Omega} = 2\pi\delta(\Omega)$ and $\int \mathrm{d}t\, e^{it\Omega}\mathrm{sign}(t) = 2i\ \mathrm{PP}\frac{1}{\Omega}$, and finally $\delta(x)\delta(y) = 2\delta(x+y)\delta(x-y)$, yielding the result Eq.(4.10).

4.A.3 Anti-detailed-balance

We start from the definitions Eq. (4.14).

They verify the relations

$$\mathcal{K}^{0\ |\ q,q',\{\ell_1,\ell_2,\ell_3,\ell_4\}}_{n\mathbf{k},n'\mathbf{k}'}(\mathbf{p}) = \mathcal{K}^{0\ |\ -q,-q',\{\ell_3,\ell_4,\ell_1,\ell_2\}}_{n\mathbf{k},n'\mathbf{k}'}(\mathbf{p}+q\mathbf{k}+q'\mathbf{k}'), \qquad (4.42)$$

$$\mathcal{K}^{1\ |\ q,q',\{\ell_1,\ell_2,\ell_3,\ell_4\}}_{n\mathbf{k},n'\mathbf{k}'}(\mathbf{p}) = \mathcal{K}^{1\ |\ -q',-q,\{\ell_3,\ell_4,\ell_1,\ell_2\}}_{n'\mathbf{k}',n\mathbf{k}}(\mathbf{p}+q\mathbf{k}+q'\mathbf{k}'), \qquad (4.43)$$

and

$$\mathcal{K}^{0\ |\ q',q,\{\ell_1,\ell_4,\ell_3,\ell_2\}}_{n'\mathbf{k}',n\mathbf{k}}(\mathbf{p}) = \left[\mathcal{K}^{0\ |\ q,q',\{\ell_1,\ell_2,\ell_3,\ell_4\}}_{n\mathbf{k},n'\mathbf{k}'}(\mathbf{p})\right]^* \qquad (4.44)$$

$$\mathcal{K}^{1\ |\ q,q',\{\ell_1,\ell_4,\ell_3,\ell_2\}}_{n\mathbf{k},n'\mathbf{k}'}(\mathbf{p}) = \left[\mathcal{K}^{1\ |\ q,q',\{\ell_1,\ell_2,\ell_3,\ell_4\}}_{n\mathbf{k},n'\mathbf{k}'}(\mathbf{p})\right]^*. \qquad (4.45)$$

Note that the hereabove relations, Eqs. (4.42)-(4.45), do not resort to $Q^\dagger_{n\mathbf{k}} = Q_{n-\mathbf{k}}$, since anti-detailed-balance is a thermal equilibrium property of $\mathfrak{W}^\ominus$, embedded in its commutator/anticommutator structure Eq.(4.5), and which does not depend on the form of $Q_{n\mathbf{k}}$ at all.

Anti-detailed balance of the skew-scattering rate $\mathfrak{W}^\ominus$ can be checked in a few easy steps. It goes as follows. Start from $\mathfrak{W}^{\ominus,-q,-q'}_{n\mathbf{k}n'\mathbf{k}'}$ as defined in Eq. (4.10). Then perform the change of variables $\mathbf{p} \to \mathbf{p}+q\mathbf{k}+q'\mathbf{k}'$. Then use Eqs. (4.42), (4.43). Then use $n_F(E)\left[1-n_F(E')\right] = e^{-\beta(E-E')}\ n_F(E')\left[1-n_F(E)\right]$ along with the energy delta functions to extract the factor $e^{\beta(q\omega_{n\mathbf{k}}+q'\omega_{n'\mathbf{k}'})}$. Then use Eqs. (4.44), (4.45). Finally exchange $(n\mathbf{k}q \leftrightarrow n'\mathbf{k}'q')$. This concludes the proof of Eq. (4.6).

4.B Symmetry constraints and discussion

4.B.1 Remarks about the phonon-fermion coupling

We considered the most general, *translationally-invariant*, coupling between one phonon operator and a fermion number-conserving bilinear, deriving from a local

coupling to the strain tensor. $Q_{n\mathbf{k}}$, the field to which the phonon annihilation operator $a_{n\mathbf{k}}$ is coupled, was defined in Eq.(4.7).

Note that, contrarily to the case of a coupling between phonons and *bosonic* excitations, as was studied in the second part of Chapter 3 (Section V thereof), a term of the form $\mathcal{A}^{n,\ell}_{\mathbf{k}}\ f_{\ell,\mathbf{k}}{}^{(\dagger)}$ is not allowed in $Q_{n\mathbf{k}}$ since the latter must be a bosonic field, because it is coupled to $a_{n\mathbf{k}}$ in the hamiltonian. Such a term is also forbidden by the $U(1)$ gauge invariance of the fermions, whenever it exists. Indeed the latter entails number conservation. It also forbids "pairing" terms of the form $a^{(\dagger)}f^\dagger f^\dagger, a^{(\dagger)}ff$.

A few comments are in order. (i) Viewing the Fourier-transformed fermions $f_{\mathbf{r},\ell} = \frac{1}{\sqrt{N_{\rm uc}}}\sum_{\mathbf{p}} e^{-i\mathbf{pr}} f_{\mathbf{p},\ell}$ ($N_{\rm uc}$ is the number of unit cells) as local annihilation operators at site $\mathbf{r}$, and rewriting $\mathcal{B}^{n,\ell,\ell'}_{\mathbf{k};\mathbf{p}} = \sum_{\boldsymbol{\eta}} \mathtt{t}^{n,\ell,\ell'}_{\mathbf{k};\boldsymbol{\eta}} e^{i\mathbf{p}\boldsymbol{\eta}}$ where the sum over $\boldsymbol{\eta}$ spans the whole direct lattice, the $Q_{n\mathbf{k}}$ field then reads

$$Q_{n\mathbf{k}} = \sum_{\mathbf{r},\boldsymbol{\eta},\ell,\ell'} \mathtt{t}^{n,\ell,\ell'}_{\mathbf{k};\boldsymbol{\eta}} e^{i\mathbf{kr}}\ f^\dagger_{\mathbf{r}+\boldsymbol{\eta},\ell}\ f_{\mathbf{r},\ell'}, \tag{4.46}$$

and one can interpret $\mathtt{t}^{n,\ell,\ell'}_{\mathbf{k};\boldsymbol{\eta}}$ as a local hopping coefficient between sites distant by $\boldsymbol{\eta}$. (ii) In Eq. (4.7), $\ell \neq \ell'$ is a priori allowed, i.e. the interaction allows for "intervalley" or "inter-band" interactions. More generally, $\mathtt{t}^{n}_{\mathbf{k};\boldsymbol{\eta}}$ is not diagonal in the ℓ basis. In the case where $\ell = \uparrow,\downarrow$ is a spin-1/2 index, this means that the phonon-fermions couplings depend on the choice of quantization axis, i.e. that the $O(3)$ symmetry of spin rotation is a priori broken, as per spin-orbit coupling.

Before considering specific instances of $\mathcal{B}^{n,\ell,\ell'}_{\mathbf{k};\mathbf{p}}$, we nonetheless make one assumption about this otherwise completely general coefficient. We assume that $\mathcal{B}^{n,\ell,\ell'}_{\mathbf{k};\mathbf{p}}$ arises purely from a coupling between the fermions and the elastic *strain tensor*. In the strain tensor, $a_{n\mathbf{k}}$ and $a^\dagger_{n\mathbf{k}}$ do not appear independently, but always as the combination $(a^\dagger_{n\mathbf{k}} + a_{n-\mathbf{k}})$. In that case, without further loss of generality, we can choose $Q^\dagger_{n\mathbf{k}} = Q_{n-\mathbf{k}}$, which translates into the constraint $\mathcal{B}^{n,\ell,\ell'}_{\mathbf{k};\mathbf{p}} = \left(\mathcal{B}^{n,\ell',\ell}_{-\mathbf{k};\mathbf{p}+\mathbf{k}}\right)^*$. This relation will have strong implications on the existence of a nonzero thermal Hall effect, which requires the breaking of time reversal (see Sec. 4.F.2).

Note that in principle, other terms can occur, for example through the coupling of the fermions to the lattice *momentum* (see e.g. [Manenkov and Orbach, 1966, Abragam and Bleaney, 1970, Ioselevich and Capellmann, 1995]). In that case, the interaction Hamiltonian involves *two* phonon operators, and in turn should be expected to yield a smaller phonon Hall effect compared with that of single-phonon scattering [Kagan and Maksimov, 2008, Sheng et al., 2006].

4.B.2 General coupling : strain tensor to fermions

In the following, $\mu,\nu = x,y,z$ are spatial directions, and $\mathcal{E}_{\mu\nu}(\mathbf{r}) = \frac{1}{2}\left(\partial_\mu u_\nu + \partial_\nu u_\mu\right)\big|_{\mathbf{r}}$ is the strain tensor at position $\mathbf{r}$. The FT is defined as $\mathcal{E}_{\mu\nu}(\mathbf{r}) = \frac{1}{\sqrt{N_{\rm uc}}}\sum_{\mathbf{p}} \mathcal{E}_{\mu\nu}(\mathbf{p}) e^{i\mathbf{pr}}$.

Our starting point is a general translation-invariant local coupling between the strain tensor and number-preserving fermion bilinears:

$$H'_\psi = \sum_{\mathbf{r},\boldsymbol{\eta}} F_{\mu\nu}^{\ell_1\ell_2}(\boldsymbol{\eta}) \left(\mathcal{E}_{\mu\nu}(\mathbf{r}) + \mathcal{E}_{\mu\nu}(\mathbf{r}+\boldsymbol{\eta})\right) f^\dagger_{\ell_1,\mathbf{r}} f_{\ell_2,\mathbf{r}+\boldsymbol{\eta}} \tag{4.47}$$

$$= \sum_{\mathbf{p},\mathbf{k}} \mathcal{E}_{\mu\nu}(\mathbf{k}) \ \left(F_{\mu\nu}^{\ell_1\ell_2}(\mathbf{p}) + F_{\mu\nu}^{\ell_1\ell_2}(\mathbf{p}+\mathbf{k})\right) \ f^\dagger_{\ell_1,\mathbf{p}} f_{\ell_2,\mathbf{p}+\mathbf{k}}, \tag{4.48}$$

where $F_{\mu\nu}^{\ell_1\ell_2}(\boldsymbol{\eta})$ is a generic coupling constant, and the FT is defined as $F_{\mu\nu}^{\ell_1\ell_2}(\boldsymbol{\eta}) = \frac{1}{\sqrt{N_{\rm uc}}} \sum_{\mathbf{p}} F_{\mu\nu}^{\ell_1\ell_2}(\mathbf{p}) e^{i\mathbf{p}\boldsymbol{\eta}}$. The constraint of hermiticity requires $F_{\mu\nu}^{\ell_1\ell_2}(\boldsymbol{\eta}) = F_{\mu\nu}^{\ell_2\ell_1}(-\boldsymbol{\eta})^*$, or in other words $F_{\mu\nu}^{\ell_1\ell_2}(\mathbf{p}) = F_{\mu\nu}^{\ell_2\ell_1}(\mathbf{p})^*$.

Expanding the strain in terms of phonon operators as in App. 4.G above, the coupling hamiltonian can then be expressed as $H'_f = \sum_{n\mathbf{k}} Q_{n\mathbf{k}} a_{n\mathbf{k}} + \text{h.c.}$, in which $Q_{n\mathbf{k}}$ takes the form Eq. (4.46). The corresponding "hopping coefficient" is

$$\mathtt{t}_{n\mathbf{k}\boldsymbol{\eta}}^{\ell_1\ell_2} = \frac{i/2}{N_{\rm uc}} \sum_{\mathbf{p}} \frac{(k^\mu \varepsilon_{n\mathbf{k}}^\nu + k^\nu \varepsilon_{n\mathbf{k}}^\mu)}{\sqrt{2M\omega_{n\mathbf{k}}}} e^{i\mathbf{p}\boldsymbol{\eta}} (e^{i\mathbf{k}\boldsymbol{\eta}} + 1) F_{\mu\nu}^{\ell_1\ell_2}(\mathbf{p}), \tag{4.49}$$

in terms of which the hermiticity constraint reads $(\mathtt{t}_{n-\mathbf{k}-\boldsymbol{\eta}}^{\ell_2\ell_1})^* = e^{-i\mathbf{k}\boldsymbol{\eta}}\ \mathtt{t}_{n\mathbf{k}\boldsymbol{\eta}}^{\ell_1\ell_2}$. This is equivalent to the relation $\mathcal{B}^{n,\ell_1,\ell_2}_{\mathbf{k};\mathbf{p}} = \left(\mathcal{B}^{n,\ell_2,\ell_1}_{-\mathbf{k};\mathbf{p}+\mathbf{k}}\right)^*$ given in the main text, which is a consequence to the fermions' being coupled to the lattice *displacement* and not to the lattice *momentum*.

4.B.3 Time reversal operation

In this subsection, we assume that the fermion index ℓ is decomposed as $\ell = (\sigma, \alpha)$ where $\sigma = S, S-1, ..., -S+1, -S$ is a spin index (for any value of the local spin S carried by the fermions $f_{\ell,\mathbf{r}}$) and α encompasses any other time reversal invariant indices. Thus $\overline{\ell} = (-\sigma, \alpha)$ denotes the time reversed index.

The time-reversal operator is $\mathcal{T} = \mathcal{U}\hat{K}$ where $\hat{K}$ denotes complex conjugation and $\mathcal{U}$ is the unitary operator defined by $\mathcal{U}^{\ell_1\ell_2} = \delta_{\sigma_1,-\sigma_2}(-1)^{S-\sigma_1}$ (note that this choice is not unique and depends on the spin quantization axis). Thus $\mathcal{U}$ reverses spin within the σ space and acts trivially within the α space.

The time-reversed coupling constant is then

$$\mathcal{T} \cdot F_{\mu\nu}^{\ell_1\ell_2}(\boldsymbol{\eta}) \cdot \mathcal{T}^{-1} = (-1)^{\sigma_1+\sigma_2} [F_{\mu\nu}^{\bar{\ell}_1,\bar{\ell}_2}(\boldsymbol{\eta})]^*. \tag{4.50}$$

Equivalently, the time reversed hopping coefficient is $\widehat{\mathtt{t}_{n\mathbf{k}\boldsymbol{\eta}}^{\ell_1\ell_2}} = (-1)^{\sigma_1+\sigma_2} (\mathtt{t}_{n,-\mathbf{k},\boldsymbol{\eta}}^{\bar{\ell}_1,\bar{\ell}_2})^*$. The $S = \frac{1}{2}$ version of this identity is $\widehat{\mathtt{t}_{n\mathbf{k}\boldsymbol{\eta}}^{\ell_1\ell_2}} = -(-1)^{\delta_{\sigma_1,\sigma_2}} (\mathtt{t}_{n,-\mathbf{k},\boldsymbol{\eta}}^{\bar{\ell}_1,\bar{\ell}_2})^*$.

4.B.4 Identification of a *symmetry* of the model

We now ask if there exists a *symmetry* of the theory from which relations as those described above hold. In other words, what symmetries of the total Hamiltonian

$$H_{\rm tot} = \sum_{n\mathbf{k}} \omega_{n\mathbf{k}} a^\dagger_{n\mathbf{k}} a_{n\mathbf{k}} \ + \ \sum_{\ell,\mathbf{p}} \epsilon_{\ell,\mathbf{p}} f^\dagger_{\ell,\mathbf{p}} f_{\ell,\mathbf{p}}$$
$$+ \left(\sum_{n\mathbf{k}} \sum_{\mathbf{p},\ell,\ell'} \mathcal{B}^{n,\ell,\ell'}_{\mathbf{k};\mathbf{p}} a_{n\mathbf{k}} f^\dagger_{\ell,\mathbf{p}} f_{\ell',\mathbf{p}+\mathbf{k}} \quad + \text{h.c.} \right) \tag{4.51}$$

lead to Eq. (4.32) and $\epsilon_{\ell,\mathbf{p}} = \epsilon_{\tilde{\ell},-\mathbf{p}}$? Since $\omega_{n\mathbf{k}} = \omega_{n-\mathbf{k}}$ (which is always true because the pure phonon theory is time-reversal invariant), and provided that one can factorize $\xi_{\ell,\ell'} = \zeta_\ell \zeta_{\ell'}$ with $\zeta_{\ell^{(\prime)}} = \pm 1$ (which will be true in all the specific cases we consider in Sec. 4.F.2), Eq. (4.32) and $\epsilon_{\ell,\mathbf{p}} = \epsilon_{\tilde{\ell},-\mathbf{p}}$ are true if and only if $H_{\rm tot} = \hat{\mathcal{T}} H_{\rm tot} \hat{\mathcal{T}}^{-1}$, where the anti-unitary operator $\hat{\mathcal{T}} = \hat{\mathcal{U}}\hat{K}$ is the combination of complex conjugation $\hat{K}$ and the unitary operation

$$\hat{\mathcal{U}} : (a_{n\mathbf{k}}, f_{\ell,\mathbf{p}}) \mapsto (a_{n-\mathbf{k}}, \zeta_\ell f_{\tilde{\ell},-\mathbf{p}}). \tag{4.52}$$

This is discussed in particular cases in Sec. 4.F.2. Here we demonstrate generally the above statement. We write $H_{\rm tot} = H_a + H_f + H_{af}$ as in Eq. (4.51). Then,

$$H_a - \hat{\mathcal{T}} H_a \hat{\mathcal{T}}^{-1} = \sum_{n\mathbf{k}} \omega_{n\mathbf{k}} \left(a^\dagger_{n\mathbf{k}} a_{n\mathbf{k}} - a^\dagger_{n-\mathbf{k}} a_{n-\mathbf{k}} \right) = \sum_{n\mathbf{k}} \left(\omega_{n\mathbf{k}} - \omega_{n-\mathbf{k}} \right) a^\dagger_{n\mathbf{k}} a_{n\mathbf{k}}, \tag{4.53}$$

$$H_f - \hat{\mathcal{T}} H_f \hat{\mathcal{T}}^{-1} = \sum_{\ell,\mathbf{p}} \epsilon_{\ell,\mathbf{p}} \left(f^\dagger_{\ell,\mathbf{p}} f_{\ell,\mathbf{p}} - f^\dagger_{\tilde{\ell},-\mathbf{p}} f_{\tilde{\ell},-\mathbf{p}} \right) = \sum_{\ell,\mathbf{p}} \left(\epsilon_{\ell,\mathbf{p}} - \epsilon_{\tilde{\ell},-\mathbf{p}} \right) f^\dagger_{\ell,\mathbf{p}} f_{\ell,\mathbf{p}}, \tag{4.54}$$

$$\begin{aligned} H_{af} - \hat{\mathcal{T}} H_{af} \hat{\mathcal{T}}^{-1} &= \sum_{n\mathbf{k}} \sum_{\mathbf{p},\ell,\ell'} \Big(\mathcal{B}^{n,\ell,\ell'}_{\mathbf{k};\mathbf{p}} \; a_{n\mathbf{k}} f^\dagger_{\ell,\mathbf{p}} f_{\ell',\mathbf{p}+\mathbf{k}} \\ &\qquad - (\mathcal{B}^{n,\ell,\ell'}_{\mathbf{k};\mathbf{p}})^* \; \zeta_\ell \zeta_{\ell'} a_{n-\mathbf{k}} f^\dagger_{\tilde{\ell},-\mathbf{p}} f_{\tilde{\ell}',-\mathbf{p}-\mathbf{k}} \Big) \quad + \text{h.c.} \\ &= \sum_{n\mathbf{k}} \sum_{\mathbf{p},\ell,\ell'} \left(\mathcal{B}^{n,\ell,\ell'}_{\mathbf{k};\mathbf{p}} - \zeta_\ell \zeta_{\ell'} (\mathcal{B}^{n,\tilde{\ell},\tilde{\ell}'}_{-\mathbf{k};-\mathbf{p}})^* \right) a_{n\mathbf{k}} f^\dagger_{\ell,\mathbf{p}} f_{\ell',\mathbf{p}+\mathbf{k}} \quad + \text{h.c.}. \end{aligned} \tag{4.55}$$

Thus, $H_{\rm tot} - \hat{\mathcal{T}} H_{\rm tot} \hat{\mathcal{T}}^{-1} = 0$ if and only if the hereabove conditions (along with $\omega_{n\mathbf{k}} = \omega_{n-\mathbf{k}}$) hold. This proves the statement.

4.C Details about momentum-space integration

4.C.1 2D Dirac fermions

4.C.1.1 Diagonal scattering rate

The set of solutions, $\mathbf{p}^{\ell,\ell'}_{\eta,\mathbf{k}}(y) = c^{\ell,\ell'}_\eta(y)\,\hat{\mathbf{k}} + y\,\hat{\mathbf{z}} \times \hat{\mathbf{k}} + \boldsymbol{\pi}_\nu$, is a curve parameterized by one parameter y, where

$$c^{\ell,\ell'}_\eta(y) = \frac{1}{2} \left(|\underline{\mathbf{k}}| + \eta\, a \sqrt{1 - \frac{4y^2}{a^2 - \underline{\mathbf{k}}^2}} \right), \tag{4.56}$$

where $a = (\omega_{n\mathbf{k}} + \mu_{\nu,\alpha} - \mu_{\nu,\alpha'})/v_\nu$.

The jacobian of the transformation from the cartesian coordinates to coordinate y is

$$J^s_\nu(y) = \left| \sum_{r=\pm} \frac{s^{(r-1)/2} r c^{\ell,\ell'}_r(y)}{\sqrt{c^{\ell,\ell'}_r(y)^2 + y^2}} \right|^{-1}, \tag{4.57}$$

as we have already shown in Chapter 3.

4.C.1.2 Skew-scattering rate

The solutions are, for $j = 0, .., 3$,

$$\mathbf{p}_j = t_{\lfloor j/2 \rfloor} \mathbf{v}_{\lfloor j/2 \rfloor} + u^{(\widetilde{j\,[2]})}_{\lfloor j/2 \rfloor} \mathbf{w}_{\lfloor j/2 \rfloor} + \boldsymbol{\pi}_0. \tag{4.58}$$

In the above, $x\,[2]$ is x mod 2, $\lfloor x \rfloor$ denotes the floor of x, and for $i \in \{0, 1\}$, we note $\widetilde{i} = (-1)^{i+1}$ and define $\mathbf{v}_i = a_2 \underline{\mathbf{k}}_1 + (-1)^i a_1 \underline{\mathbf{k}}_2$, $\mathbf{w}_i = \hat{\mathbf{z}} \times \mathbf{v}_i$ where we use the shorthands $a_1 = \sigma_3(q\omega_{n\mathbf{k}} + q'\omega_{n'\mathbf{k}'} + \mu_{\nu,\alpha_3} - \mu_{\nu,\alpha_1})/v_\nu$, $a_2 = \sigma_3(q'\omega_{n'\mathbf{k}'} + \mu_{\nu,\alpha_3} - \mu_{\nu,\alpha_2})/v_\nu$, $\mathbf{k}_1 = -q\mathbf{k} - q'\mathbf{k}'$, $\mathbf{k}_2 = -q'\mathbf{k}'$.

Coefficients t_i and $u_i^{(\pm)}$ are:

$$t_i = \frac{a_2 \mathbf{k}_1^2 + (-1)^i a_1 \mathbf{k}_2^2 - a_1 a_2 (a_1 + (-1)^i a_2)}{2\mathbf{v}_i^2}, \tag{4.59}$$

$$u_i^{(\pm)} = \frac{-B_i \pm \sqrt{B_i^2 - 4A_i C_i}}{2A_i}, \tag{4.60}$$

with

$$\begin{aligned} A_i &= 4a_{i+1}^2 (\mathbf{v}_i^2 - (\underline{\mathbf{k}}_1 \wedge \underline{\mathbf{k}}_2)^2), \\ B_i &= (-1)^i 4a_{i+1} (\underline{\mathbf{k}}_1 \wedge \underline{\mathbf{k}}_2)(a_{i+1}^2 - \mathbf{k}_{i+1}^2 + 2(\mathbf{v}_i \cdot \mathbf{k}_{i+1}) t_i), \\ C_i &= -\left(a_{i+1}^2 - \mathbf{k}_{i+1}^2\right)^2 - 4(a_{i+1}^2 - \mathbf{k}_{i+1}^2)(\mathbf{v}_i \cdot \mathbf{k}_{i+1})\, t_i \\ &\quad + 4(a_{i+1}^2 \mathbf{v}_i^2 - (\mathbf{v}_i \cdot \mathbf{k}_{i+1})^2)\, t_i^2, \end{aligned} \tag{4.61}$$

where $\underline{\mathbf{V}}_1 \wedge \underline{\mathbf{V}}_2 = V_1^x V_2^y - V_2^y V_1^x$ for any in-plane vectors $\underline{\mathbf{V}}_{1,2}$.

Coefficients $t_{0,1}$ are always well defined, but for each $i \in \{0, 1\}$, $u_i^{(\pm)}$ are the solutions to a quadratic equation which has zero, one or two solutions, depending on whether its discriminant is negative, zero, or positive.

Finally, the jacobian appearing from the intersection of the energy conservation curves is

$$\begin{aligned} \mathcal{J}^{\{\ell_i\}}_{q\mathbf{k},q'\mathbf{k}'}(\mathbf{p}_j) = v_\nu^2 \times \Bigg| & s_1 \frac{\underline{\mathbf{k}}_1 \wedge \underline{\mathbf{p}}_j}{\epsilon_{\ell_3,\mathbf{p}_j} \epsilon_{\ell_1,\mathbf{p}_j - \mathbf{k}_1}} + s_2 \frac{\underline{\mathbf{p}}_j \wedge \underline{\mathbf{k}}_2}{\epsilon_{\ell_3,\mathbf{p}_j} \epsilon_{\ell_2,\mathbf{p}_j - \mathbf{k}_2}} \\ & + s_1 s_2 \frac{-\underline{\mathbf{k}}_1 \wedge \underline{\mathbf{k}}_2 + \underline{\mathbf{p}}_j \wedge \underline{\mathbf{k}}_2 - \underline{\mathbf{p}}_j \wedge \underline{\mathbf{k}}_1}{\epsilon_{\ell_1,\mathbf{p}_j - \mathbf{k}_1} \epsilon_{\ell_2,\mathbf{p}_j - \mathbf{k}_2}} \Bigg|^{-1}, \end{aligned} \tag{4.62}$$

where $s_1 = -\sigma_1\sigma_3$ and $s_2 = -\sigma_2\sigma_3$.

4.C.2 Quadratic dispersion in dD

4.C.2.1 Diagonal scattering rate

The solution to the energy conservation constraint is given by $\mathbf{p} = \boldsymbol{\pi}_0 + \tilde{\mathbf{p}}^{\ell\ell'}_{n\mathbf{k}} + \mathbf{p}_\perp$, where $\tilde{\mathbf{p}}^{\ell\ell'}_{n\mathbf{k}} = \underline{\mathbf{k}} \left(-1/2 + m_* \left[\mu_{\ell'} - \mu_\ell - \omega_{n\mathbf{k}}\right] / |\underline{\mathbf{k}}|^2\right)$ and $\mathbf{p}_\perp \cdot \underline{\mathbf{k}} = 0$ spans the whole

$(d-1)$-dimensional hyperplane orthogonal to $\underline{\mathbf{k}}$, which is the projection of $\mathbf{k}$ onto the d-dimensional space of fermionic momenta (thus for $d=3$, $\underline{\mathbf{k}}=\mathbf{k}$ and for $d=2$, $\underline{\mathbf{k}}=(k_x,k_y,0)$).

The delta distribution is

$$\delta(\epsilon_{\ell,\mathbf{p}}-\epsilon_{\ell',\mathbf{p}+\mathbf{k}}-\omega_{n\mathbf{k}})=\frac{|m_*|}{|\underline{\mathbf{k}}|}\delta^{(1)}\left([\mathbf{p}-\boldsymbol{\pi}_0]\cdot\hat{\underline{\mathbf{k}}}-|\tilde{\mathbf{p}}^{\ell\ell'}_{n\mathbf{k}}|\right), \tag{4.63}$$

where $\underline{\mathbf{k}}$ is the projection of $\mathbf{k}$ onto the d-dimensional space of fermion momenta (that is, the xy plane for $d=2$ or the whole space for $d=3$).

Therefore, the integral is converted as follows:

$$\begin{aligned} &2\pi\int\frac{\mathrm{d}^d\mathbf{p}}{(2\pi)^d}\delta(\epsilon_{\ell,\mathbf{p}}-\epsilon_{\ell',\mathbf{p}+\mathbf{k}}-\omega_{n\mathbf{k}})F(\mathbf{p}) \\ &\longrightarrow\quad\frac{|m_*|}{|\underline{\mathbf{k}}|}\int_{(\underline{\mathbf{k}})_\perp}\frac{\mathrm{d}^{d-1}\mathbf{p}_\perp}{(2\pi)^{d-1}}F(\boldsymbol{\pi}_0+\tilde{\mathbf{p}}^{\ell\ell'}_{n\mathbf{k}}+\mathbf{p}_\perp), \end{aligned} \tag{4.64}$$

where $(\underline{\mathbf{k}})_\perp$ is the $(d-1)$-dimensional set of fermionic momenta orthogonal to $\underline{\mathbf{k}}$, $F(\mathbf{p})$ denotes any function of $\mathbf{p}$, and $\tilde{\mathbf{p}}^{\ell\ell'}_{n\mathbf{k}}$ is given in the main text.

4.C.2.2 Skew-scattering rate

The solution in the $(\underline{\mathbf{k}}_1,\underline{\mathbf{k}}_2)$ plane to the two energy conservation delta distributions is

$$\tilde{\mathbf{p}}^{\{\ell_i\}}_{n\mathbf{k},n'\mathbf{k}'}=\underline{\mathbf{k}}_1F_1+\frac{\hat{\underline{\mathbf{k}}}_2-\left(\hat{\underline{\mathbf{k}}}_1\cdot\hat{\underline{\mathbf{k}}}_2\right)\hat{\underline{\mathbf{k}}}_1}{1-\left(\hat{\underline{\mathbf{k}}}_1\cdot\hat{\underline{\mathbf{k}}}_2\right)^2}\left(|\underline{\mathbf{k}}_2|F_2-|\underline{\mathbf{k}}_1|\left(\hat{\underline{\mathbf{k}}}_1\cdot\hat{\underline{\mathbf{k}}}_2\right)F_1\right), \tag{4.65}$$

where

$$\begin{aligned} F_1&=\left(1/2-m_*\left[\mu_{\ell_2}-\mu_{\ell_3}-q'\omega_{n'\mathbf{k}'}\right]/|\underline{\mathbf{k}}_1|^2\right), \\ F_2&=\left(1/2-m_*\left[\mu_{\ell_1}-\mu_{\ell_3}-q\omega_{n\mathbf{k}}-q'\omega_{n'\mathbf{k}'}\right]/|\underline{\mathbf{k}}_2|^2\right), \end{aligned} \tag{4.66}$$

where again $\mathbf{k}_1=-q\mathbf{k}-q'\mathbf{k}'$ and $\mathbf{k}_2=-q'\mathbf{k}'$.

Then the product of delta distributions is

$$\mathcal{D}^{q,q',\{\ell_i\}}_{n\mathbf{k},n'\mathbf{k}'}(\mathbf{p})=\delta(\epsilon^{\ell_3}_{\mathbf{p}}-\epsilon^{\ell_2}_{\mathbf{p}+q'\mathbf{k}'}-q'\omega_{n'\mathbf{k}'})\;\delta(q\omega_{n\mathbf{k}}+q'\omega_{n'\mathbf{k}'}-\epsilon^{\ell_3}_{\mathbf{p}}+\epsilon^{\ell_1}_{\mathbf{p}+q\mathbf{k}+q'\mathbf{k}'}) \tag{4.67}$$

$$\begin{aligned} &=\frac{m_*^2}{|\underline{\mathbf{k}}_1||\underline{\mathbf{k}}_2|}\left[1-(\hat{\underline{\mathbf{k}}}_1\cdot\hat{\underline{\mathbf{k}}}_2)^2\right]^{-1}\left|\hat{\underline{\mathbf{k}}}_1\times\hat{\underline{\mathbf{k}}}_2\right|^{-1} \\ &\times\delta^{(2)}(\mathcal{P}_{(\underline{\mathbf{k}}_1\times\underline{\mathbf{k}}_2)_\perp}[\mathbf{p}-\boldsymbol{\pi}_0]-\tilde{\mathbf{p}}^{\{\ell_i\}}_{n\mathbf{k},n'\mathbf{k}'}), \end{aligned} \tag{4.68}$$

where $\mathcal{P}_{(\underline{\mathbf{k}}_1\times\underline{\mathbf{k}}_2)_\perp}[.]$ is the projector onto $(\underline{\mathbf{k}}_1\times\underline{\mathbf{k}}_2)_\perp$, the $d-1$ dimensional space perpendicular to $\underline{\mathbf{k}}_1\times\underline{\mathbf{k}}_2$.

4.C.3 Generalization to a Fermi surface of any shape

4.C.3.1 Physical remark

It is possible to generalize the Hamiltonian Eq. (4.18) by adding:

- Rashba-like terms of the form $\alpha_{ij} p_j \hat{\sigma}_i$, where $\hat{\sigma}_i$, $i = x, y, z$ are the Pauli matrices acting in $\ell = \pm$ space, α_{ij} are real coefficients ;
- Zeeman-like terms of the form $h_i \hat{\sigma}_i$, where $\mathbf{h}$ represents an external magnetic field.

Such addenda lead to a correction to the (otherwise spin-independent) fermion energies,

$$\Delta\epsilon_{\mathbf{p}} = \pm \sqrt{\sum_i (\sum_j \alpha_{ij} p_j + h_i)^2}. \tag{4.69}$$

To leading perturbative order in $\alpha p_F / h \ll 1$, $\alpha_{ij} p_j \hat{\sigma}_i$ introduces Zeeman splitting of the Fermi surface (via the spin-dependent $\Delta\epsilon_{\mathbf{p}}$) which can be captured by a spin-dependent chemical potential $\mu_\ell = \ell |\mathbf{h}|$, already included in Eq. (4.18). An ℓ-dependent mass m_* or momentum $\boldsymbol{\pi}_0$ only occur at higher orders in $\alpha p_F / h \ll 1$. In the case of a circular Fermi surface considered hereabove, we thus considered implicitly the limit $\alpha p_F / h \ll 1$.

Much more generally, in the following, we reproduce the line of arguments given hereabove, Sec.4.C.2, for the case of a *completely general* Fermi surface of any shape in d dimensions.

4.C.3.2 Diagonal scattering rate

Again we write $\frac{1}{N_{\rm uc}} \sum_{\mathbf{p}} \longrightarrow V_{dD}^{\rm uc} \int \frac{\mathrm{d}^d \mathbf{p}}{(2\pi)^d}$, with $V_{dD}^{\rm uc}$ the "volume" of the d-dimensional unit cell.

The solution to the energy conservation constraint is denoted as $\mathbf{p} \in \Sigma_{n\mathbf{k}}^{\ell\ell'}$, where $\Sigma_{n\mathbf{k}}^{\ell\ell'}$ is a (possibly disconnected) $(d-1)$-dimensional surface contained in the d-dimensional space of fermionic momenta. Any fermionic momentum $\mathbf{p}$ thus decomposes as $\mathbf{p} = \mathcal{P}_{\Sigma_{n\mathbf{k}}^{\ell\ell'}}[\mathbf{p}] + p_\perp \mathbf{u}_{n\mathbf{k}}^{\ell\ell'}(\mathbf{p})$, where $\mathcal{P}_{\Sigma_{n\mathbf{k}}^{\ell\ell'}}[\cdot]$ is the orthogonal projection onto $\Sigma_{n\mathbf{k}}^{\ell\ell'}$ and $\mathbf{u}_{n\mathbf{k}}^{\ell\ell'}(\mathbf{p})$ is the unit vector orthogonal to $\Sigma_{n\mathbf{k}}^{\ell\ell'}$ at position $\mathcal{P}_{\Sigma_{n\mathbf{k}}^{\ell\ell'}}[\mathbf{p}]$.

The delta distribution thus reads

$$\delta(\epsilon_{\ell,\mathbf{p}} - \epsilon_{\ell',\mathbf{p}+\mathbf{k}} - \omega_{n\mathbf{k}}) = J_{n\mathbf{k}}^{\ell\ell'}(\mathcal{P}_{\Sigma_{n\mathbf{k}}^{\ell\ell'}}[\mathbf{p}])\ \delta^{(1)}(p_\perp)\,, \tag{4.70}$$

where $J_{n\mathbf{k}}^{\ell\ell'}$ is the jacobian of the coordinate change, namely

$$J_{n\mathbf{k}}^{\ell\ell'}(\mathbf{p}) = \left| \frac{\partial}{\partial \mathbf{p}} \left(\epsilon_{\ell,\mathbf{p}} - \epsilon_{\ell',\mathbf{p}+\mathbf{k}} \right) \cdot \mathbf{u}_{n\mathbf{k}}^{\ell\ell'}(\mathbf{p}) \right|^{-1}. \tag{4.71}$$

Therefore, for any function $F(\mathbf{p})$, the following integral rewriting holds:

$$2\pi \int \frac{\mathrm{d}^d\mathbf{p}}{(2\pi)^d}\delta(\epsilon_{\ell,\mathbf{p}} - \epsilon_{\ell',\mathbf{p}+\mathbf{k}} - \omega_{n\mathbf{k}})F(\mathbf{p}) \tag{4.72}$$
$$\longrightarrow \quad J^{\ell\ell'}_{n\mathbf{k}}(\mathcal{P}_{\Sigma^{\ell\ell'}_{n\mathbf{k}}}[\mathbf{p}]) \int_{\Sigma^{\ell\ell'}_{n\mathbf{k}}} \frac{\mathrm{d}^{d-1}\mathbf{p}_\Sigma}{(2\pi)^{d-1}} F(\mathbf{p}_\Sigma).$$

In particular, we find that

$$D^{(1)}_{n\mathbf{k}} = -\sum_{\ell,\ell'} V^{\mathrm{uc}}_{dD} \int_{\Sigma^{\ell\ell'}_{n\mathbf{k}}} \frac{\mathrm{d}^{d-1}\mathbf{p}_\Sigma}{(2\pi)^{d-1}} \left|\mathcal{B}^{n,\ell,\ell'}_{\mathbf{k};\mathbf{p}_\Sigma}\right|^2$$
$$\times J^{\ell\ell'}_{n\mathbf{k}}(\mathbf{p}_\Sigma) \left[n_{\mathrm{F}}(\epsilon_{\ell,\mathbf{p}_\Sigma}) - n_{\mathrm{F}}(\epsilon_{\ell',\mathbf{p}_\Sigma+\mathbf{k}})\right]. \tag{4.73}$$

4.C.3.3 Skew-scattering rate

The solution to the two energy conservation constraints is denoted as $\mathbf{p} \in \Sigma^{qq'\{\ell_i\}}_{n\mathbf{k}n'\mathbf{k}'}$, where $\Sigma^{qq'\{\ell_i\}}_{n\mathbf{k}n'\mathbf{k}'}$ is a $(d-2)$-dimensional set contained in the d-dimensional space of fermionic momenta, which may be disconnected or (for $d = 2$) a discrete collection of points.

Any fermionic momentum $\mathbf{p}$ thus decomposes as $\mathbf{p} = \mathcal{P}_{\Sigma^{qq'\{\ell_i\}}_{n\mathbf{k}n'\mathbf{k}'}}[\mathbf{p}] + \mathbf{p}_\perp$, where $\mathcal{P}_{\Sigma^{qq'\{\ell_i\}}_{n\mathbf{k}n'\mathbf{k}'}}[\cdot]$ is the orthogonal projection onto $\Sigma^{qq'\{\ell_i\}}_{n\mathbf{k}n'\mathbf{k}'}$, and $\mathbf{p}_\perp$ is defined by subtraction.

For a given point $\mathbf{p}_\Sigma \in \Sigma^{qq'\{\ell_i\}}_{n\mathbf{k}n'\mathbf{k}'}$, we also define $\Pi^{qq'\{\ell_i\}}_{n\mathbf{k}n'\mathbf{k}'}(\mathbf{p}_\Sigma)$ the plane of fermionic momenta locally orthogonal to $\Sigma^{qq'\{\ell_i\}}_{n\mathbf{k}n'\mathbf{k}'}$. For $d = 2$, $\Pi^{qq'\{\ell_i\}}_{n\mathbf{k}n'\mathbf{k}'}(\mathbf{p}_\Sigma)$ is simply the 2D space of fermionic momenta and is the same for all $\mathbf{p}_\Sigma$, while for $d = 3$, $\Sigma^{qq'\{\ell_i\}}_{n\mathbf{k}n'\mathbf{k}'}$ is a 1-dimensional curve embedded in $\mathbb{R}^3$ and $\Pi^{qq'\{\ell_i\}}_{n\mathbf{k}n'\mathbf{k}'}(\mathbf{p}_\Sigma)$ is the plane locally orthogonal to it at the point $\mathbf{p}_\Sigma$. A coordinate basis for this plane, $\mathbf{p}_\perp = p_1\mathbf{u}_1 + p_2\mathbf{u}_2$, can be defined globally for $d = 2$ (take $\mathbf{u}_x, \mathbf{u}_y$) but only locally for $d = 3$ (then $\mathbf{u}_{1,2}$ are functions of $\mathbf{p}_\Sigma$).

For a given such choice of basis, the product of delta distributions is

$$\mathcal{D}^{q,q',\{\ell_i\}}_{n\mathbf{k},n'\mathbf{k}'}(\mathbf{p}) = \delta(\epsilon^{\ell_3}_{\mathbf{p}} - \epsilon^{\ell_2}_{\mathbf{p}+q'\mathbf{k}'} - q'\omega_{n'\mathbf{k}'})\delta(q\omega_{n\mathbf{k}} + q'\omega_{n'\mathbf{k}'} - \epsilon^{\ell_3}_{\mathbf{p}} + \epsilon^{\ell_1}_{\mathbf{p}+q\mathbf{k}+q'\mathbf{k}'}) \tag{4.74}$$
$$= J^{qq'\{\ell_i\}}_{n\mathbf{k}n'\mathbf{k}'}(\mathcal{P}_{\Sigma^{qq'\{\ell_i\}}_{n\mathbf{k}n'\mathbf{k}'}}[\mathbf{p}])\ \delta^{(1)}(p_1)\ \delta^{(1)}(p_2), \tag{4.75}$$

and the jacobian of the coordinate transformation is

$$J^{qq'\{\ell_i\}}_{n\mathbf{k}n'\mathbf{k}'}(\mathbf{p}) = \left| \begin{array}{cc} \frac{\partial}{\partial p_1}\left(\epsilon^{\ell_3}_{\mathbf{p}} - \epsilon^{\ell_2}_{\mathbf{p}+q'\mathbf{k}'}\right)\Big|_{\mathbf{p}} & \frac{\partial}{\partial p_2}\left(\epsilon^{\ell_3}_{\mathbf{p}} - \epsilon^{\ell_2}_{\mathbf{p}+q'\mathbf{k}'}\right)\Big|_{\mathbf{p}} \\ \frac{\partial}{\partial p_1}\left(\epsilon^{\ell_1}_{\mathbf{p}+q\mathbf{k}+q'\mathbf{k}'} - \epsilon^{\ell_3}_{\mathbf{p}}\right)\Big|_{\mathbf{p}} & \frac{\partial}{\partial p_2}\left(\epsilon^{\ell_1}_{\mathbf{p}+q\mathbf{k}+q'\mathbf{k}'} - \epsilon^{\ell_3}_{\mathbf{p}}\right)\Big|_{\mathbf{p}} \end{array} \right|^{-1}, \tag{4.76}$$

where we emphasize that p_1 and p_2 are defined in a local basis which depends on $\mathcal{P}_{\Sigma^{qq'\{\ell_i\}}_{n\mathbf{k}n'\mathbf{k}'}}[\mathbf{p}]$.

The skew-scattering rate then reads

$$\mathfrak{W}^{\ominus,qq'}_{n\mathbf{k},n'\mathbf{k}'} = \sum_{\{\ell_i\}} V^{\rm uc}_{dD} \int_{\Sigma^{qq'\{\ell_i\}}_{n\mathbf{k}n'\mathbf{k}'}} \frac{\mathrm{d}^{d-2}\mathbf{p}_\Sigma}{(2\pi)^{d-2}}\; J^{qq'\{\ell_i\}}_{n\mathbf{k}n'\mathbf{k}'}(\mathbf{p}_\Sigma)\; \mathcal{N}^{q,q',\{\ell_i\}}_{n\mathbf{k},n'\mathbf{k}'}(\mathbf{p}_\Sigma)\; \mathcal{R}^{q,q',\{\ell_i\}}_{n\mathbf{k},n'\mathbf{k}'}(\mathbf{p}_\Sigma) + (n\mathbf{k}q \leftrightarrow n'\mathbf{k}'q'), \tag{4.77}$$

where the $\mathcal{N}$ and $\mathcal{R}$ functions were defined in the main text.

4.D Small momentum scaling behaviors

4.D.1 Linearly dispersing two-dimensional fermions

4.D.1.1 Diagonal scattering rate

The small-momentum scaling behavior, when $|\mathbf{k}| \sim |\mathbf{k}'| \sim k$, depends on the existence of a Fermi surface. Two cases must be distinguished.

(i) For $\mu_{\nu,\alpha} = 0$, i.e. when the Fermi surface reduces to a point.

- For $s = -$, the factor Δn_F is sizeable only for $|\mathbf{p}(y)| \sim k$ ($\lesssim k_B T$), namely $\Delta n_F \sim e^{-\beta O(y/k)}$. In the $T \to 0$ limit, the $\int \mathrm{d}y$ integral in Eq.(4.19) can be evaluated in the saddle-point approximation around $y = 0$, where $J^s_{\nu,\eta}(y) \approx \frac{1}{2}$, so that $D^{(1)}_{n\mathbf{k}} \sim k^1 |\mathcal{B}(k)|^2$.
- For $s = +$, the $\int \mathrm{d}y$ integral is over an ellipse with typical dimension $|\mathbf{p}(y)| \sim k$, and where $J^+_{\nu,\eta}(y) = O(1)$, therefore $D^{(1)}_{n\mathbf{k}} \sim k^1 |\mathcal{B}(k)|^2$.

(ii) For $|\mu_{\nu,\alpha}| \gg k_B T$, i.e. when there is a (circular) Fermi surface around each $\boldsymbol{\pi}_\nu$. Then only $s = -1$ contributions are significant. The factor $\Delta n_F \approx k v_\nu n'_F$ (where n'_F is the derivative of the Fermi function, namely $n'_F(x) = -\beta / \prod_{s=\pm}(e^{s\beta x} + 1) \underset{T\to 0}{\sim} -\beta\delta(\beta x)$) is sizeable only for $|\mathbf{p}(y)| \sim p_F \gg k$. Thus one can replace $\int \mathrm{d}y \Delta n_F g(y) \to k g(p_F)$ for any smooth function g. Besides, in this limit, $y/k \gg 1$, one finds $J^-_{\nu,\eta}(y) \sim y/k$. Therefore $D^{(1)}_{n\mathbf{k}} \sim k^0 |\mathcal{B}(k)|^2$.

4.D.1.2 Skew-scattering rate

Again, two cases must be distinguished.

(i) For $\mu_{\nu,\alpha} = 0$: the solutions of the energy conservation constraints, when they exist, are of order $|\mathbf{p}| \sim k$. For such values of $\mathbf{p}$ the jacobian scales like $\mathcal{J}(k) \sim k^0$. Thus $\mathfrak{W}^{\ominus,qq'}_{n\mathbf{k},n'\mathbf{k}'} \sim \mathcal{R}(k)$.

(ii) For $|\mu_{\nu,\alpha}| \gg k_B T$: the product of population factors $\mathcal{N}$ is sizeable only for solutions $\mathbf{p}$ close to the Fermi surface. Therefore:

- Decomposing $\mathbf{p} = \mathbf{p}_{\rm FS} + p_\perp \mathbf{u}_\perp$ where $\mathbf{p}_{\rm FS}$ belongs to the Fermi surface and $\mathbf{u}_\perp$ is locally orthogonal to it, we approximate $\mathcal{N}(\mathbf{p}) \approx \delta^{(1)}(p_\perp) \int \mathrm{d}p_\perp \mathcal{N}(\mathbf{p}_{\rm FS} + p_\perp \mathbf{u}_\perp)$. The integral is $O(\frac{k_B T}{v_F})$.

- Denoting by Σ the 5-dimensional surface in the space of $(\mathbf{k}, \mathbf{k}')$ defined by $p_\perp(\mathbf{k}, \mathbf{k}') = 0$, we have $\delta^{(1)}(p_\perp) \sim \frac{k}{p_F} \delta^{(1)}[(\mathbf{k}, \mathbf{k}') \in \Sigma]$.

- Finally, since $|\mathbf{p}| \sim p_F$ one has $\mathcal{J}(k) \sim (p_F/k)^2$. Therefore $\mathcal{N}(k)\mathcal{R}(k)\mathcal{J}(k) \to \frac{p_F}{k}\ \mathcal{R}(k) \times O(\frac{k_B T}{v_F}) \delta^{(1)}[(\mathbf{k}, \mathbf{k}') \in \Sigma]$.

- This, for $k \sim T$, entails the scaling $\mathfrak{W}^{\ominus, qq'}_{n\mathbf{k}, n'\mathbf{k}'} \sim k^{-1} \mathcal{R}(k)$.

(iii) Summary: we find $\mathfrak{W}^{\ominus}(k) \sim \mathcal{R}(k)$ when there is no Fermi surface, whereas $\mathfrak{W}^{\ominus}(k) \sim k^{-1}\mathcal{R}(k)$ when there is one. In both cases, as long as $|\mu_{\nu,\alpha} - \mu_{\nu,\alpha'}| \ll k_B T$ for all α, α', the energy denominators in $\mathcal{R}(k)$ are of order k^1, and therefore $\mathcal{R}(k) \sim k^{-1}\mathcal{K}(k)$.

4.D.2 Fermi surface of quadratic d-dimensional fermions

4.D.2.1 Diagonal scattering rate

Close to the Fermi surface we can linearize the fermionic dispersion relation, and assuming $\mu_\ell \ll p_F^2/m_*$, the population difference is $\Delta n_F \sim k v_F n'_F$. Thus, the small-momentum scaling with respect to $k \sim |\mathbf{k}|$ can be obtained following the same lines of reasoning as in App. 4.D.1.1. We find $D^{(1)}_{n\mathbf{k}} \sim |\mathcal{B}(k)|^2$. Note that this analysis does not rely on the particular shape of the dispersion relation, and it applies to any d-dimensional Fermi surface. In particular, it coincides with the scaling relation found in the case of 2D Dirac fermions with a one-dimensional (as opposed to point-like) Fermi surface.

4.D.2.2 Scaling of the denominators

If the band splitting $\delta\epsilon_{\ell_2,\ell_4} = \mu_{\ell_2} - \mu_{\ell_4}$ in Eq.(4.22) is much smaller than Γ_f, the typical inverse lifetime of a fermionic excitation (proportional to the imaginary part of the fermionic self-energy, governed by all interaction processes involving the fermions), then the second term in the bracket in Eq. (4.22) is negligible. Indeed, this corresponds to a regularization of "$\mathrm{PP}\frac{1}{0} = 0$", namely one has $\mathrm{PP}\frac{1}{\delta\epsilon_{\ell_2,\ell_4}} \to \frac{\delta\epsilon_{\ell_2,\ell_4}}{\delta\epsilon^2_{\ell_2,\ell_4} + \Gamma_f^2}$, which is negligible in comparison to the first term.

Two different regimes can then be identified, depending on the Zeeman splitting:

(i) Limit of large Zeeman splitting of the bands: $k^2/m_* \lesssim \Delta\mu = |\mu_\uparrow - \mu_\downarrow|$. The main contributions to $\mathcal{R}(k)$ come from the smallest energy denominators in the left-hand term of Eq. (4.22), corresponding to processes where $\sum_i (-1)^i \mu_{\ell_i} = 0$ – for instance when no spin flip occurs. Note that the right-hand term vanishes in that case, formally $\mathrm{PP}\frac{1}{0} \to 0$ (see also the remark about the Γ_f regularization hereabove). Then, it is easily shown that $\mathcal{R}(k) \sim k^{-2}\mathcal{K}(k)$. Therefore the small momentum scaling behavior of the skew-scattering rate is $\mathfrak{W}^{\ominus, qq'}_{n\mathbf{k}, n'\mathbf{k}'} \sim k^{-3}\mathcal{K}(k)$.

(ii) Limit of small Zeeman splitting of the bands: $k^2/m_* \gg \Delta\mu = |\mu_\uparrow - \mu_\downarrow|$. The main contributions to $\mathcal{R}(k)$ come from the smallest energy denominators in both terms of Eq. (4.22), which are of order $\Delta\mu$. In the right-hand term this requires $\delta\epsilon_{\ell_2,\ell_4} \gtrsim \Gamma_f$, as emphasized hereabove. In the left-hand term this requires $\mathbf{k}\cdot\mathbf{k}' = 0$. Then, it is easily shown that $\mathcal{R}(k) \sim \mathcal{K}(k)$. Therefore the small momentum scaling behavior of the skew-scattering rate is $\mathfrak{W}^{\ominus,qq'}_{n\mathbf{k},n'\mathbf{k}'} \sim k^{-1}\mathcal{K}(k)$.

4.D.2.3 Skew-scattering rate

The small-momentum scaling behavior, when $|\mathbf{k}| \sim |\mathbf{k}'| \sim k$, depends a priori on dimensionality. In $d = 3$, the integral over $\mathbf{p}$ along with the population factor $\mathcal{N} \sim kv_F n'_F$ scales obviously like k^1. Meanwhile, in $d = 2$, where the integral is reduced to a discrete sum, one can follow the same lines of reasoning as hereabove to show that $\mathcal{N} \sim k^1$ as well. This result, namely $\int \mathrm{d}^{d-2}\mathbf{p}_\perp \mathcal{N}(\mathbf{p}) \to O(k^1)$, is identical to that found hereabove, in case (2) with Dirac fermions. The subsequent skew-scattering rate, $\mathfrak{W}^{\ominus}(k) \sim k^{-1}\mathcal{R}(k)$, scales like that obtained for linearly dispersing fermions with a Fermi surface.

Above (Sec. 4.D.2.2) we investigate the scaling of $\mathcal{R}(k)$ as a function of k ($\sim k_BT/v_F$). Depending on the relative magnitudes of $(k_BT/v_F)^2/m_*$ and $\Delta\mu = |\mu_\uparrow - \mu_\downarrow|$, we find two different behaviors:

$$\mathcal{R}(k) \sim \begin{cases} \mathcal{K}(k) & \text{for } \Delta\mu \ll (k_BT/v_F)^2/m_* \\ k^{-2}\mathcal{K}(k) & \text{for } \Delta\mu \gg (k_BT/v_F)^2/m_* \end{cases}. \tag{4.78}$$

We write $\mathcal{R}(k) \sim k^{-2\lambda}$, where $\lambda = 0, 1$ labels the two behaviors; thus

$$\mathfrak{W}^{\ominus}(k) \sim k^{-1-2\lambda}\mathcal{K}(k). \tag{4.79}$$

We will resort to these results in Appendix 4.I.

4.E Details of the specific model

4.E.1 General method for the couplings

Starting from Eq. (4.26), we Taylor-expand the couplings with respect to the displacement field, $\tilde{\mathbf{r}} = \mathbf{r} + \boldsymbol{u}(\mathbf{r})$ where $\tilde{\mathbf{r}}$ belongs to the distorted lattice and $\mathbf{r}$ to the undistorted lattice and $\boldsymbol{u}(\mathbf{r})$ is the displacement field at site $\mathbf{r}$:

$$\begin{aligned} L^{\alpha\beta}_{\{\tilde{\mathbf{r}}-\tilde{\mathbf{r}}''\}} &\approx L^{\alpha\beta}_{\{\mathbf{r}-\mathbf{r}''\}} \\ &\quad - \sum_{\mathbf{r}'} \big(\boldsymbol{u}(\mathbf{r}) - \boldsymbol{u}(\mathbf{r}')\big) \cdot \frac{\delta}{\delta \boldsymbol{u}(\mathbf{r}')} \, L^{\alpha\beta}_{\{\tilde{\mathbf{r}}-\tilde{\mathbf{r}}''\}}\Big|_{\boldsymbol{u}=\mathbf{0}}, \end{aligned} \tag{4.80}$$

$$K^{\alpha\alpha'}_{\tilde{\mathbf{r}}-\tilde{\mathbf{r}}'} \approx K^{\alpha\alpha'}_{\mathbf{r}-\mathbf{r}'} + \big(\boldsymbol{u}(\mathbf{r}) - \boldsymbol{u}(\mathbf{r}')\big) \cdot \frac{\partial}{\partial \boldsymbol{\rho}} \, K^{\alpha\alpha'}_{\boldsymbol{\rho}}\Big|_{\boldsymbol{\rho}=\mathbf{r}-\mathbf{r}'}, \tag{4.81}$$

to the order $O(\boldsymbol{u})$. Thus $H_\psi = H^0_\psi + H'_\psi + \ldots$, where "$+\ldots$" accounts for terms of order $O(\boldsymbol{u}^2)$ at least, and

$$\begin{aligned} H'_\psi &= \sum_{\mathbf{r},\mathbf{r}',\mathbf{r}''} \psi^\dagger_{\alpha,\mathbf{r}} \left(\boldsymbol{u}(\mathbf{r}) - \boldsymbol{u}(\mathbf{r}'')\right) \psi_{\alpha',\mathbf{r}'} \\ &\quad \cdot \left(\delta_{\mathbf{r}',\mathbf{r}''} \frac{\partial}{\partial \boldsymbol{\rho}} \, K^{\alpha\alpha'}_{\boldsymbol{\rho}} \Big|_{\boldsymbol{\rho}=\mathbf{r}-\mathbf{r}'} - \delta_{\mathbf{r},\mathbf{r}'} \frac{\delta}{\delta \boldsymbol{u}(\mathbf{r}'')} \, L^{\alpha\alpha'}_{\{\boldsymbol{\eta}+\boldsymbol{u}\}} \Big|_{\boldsymbol{u}=\mathbf{0}} \right), \end{aligned} \tag{4.82}$$

where the set $\{\boldsymbol{\eta} + \boldsymbol{u}\}$ stands for $\{\mathbf{r} - \tilde{\mathbf{r}} + \boldsymbol{u}(\mathbf{r}) - \boldsymbol{u}(\tilde{\mathbf{r}}) \mid \tilde{\mathbf{r}}\}$.

Then, expanding the displacement field in terms of phonon operators,

$$\boldsymbol{u}(\mathbf{r}) = \frac{1}{\sqrt{N_{\rm uc}}} \sum_{n\mathbf{k}} \frac{e^{i\mathbf{k}\cdot\mathbf{r}} \, \boldsymbol{\varepsilon}_{n\mathbf{k}}}{\sqrt{2M_{\rm uc}\omega_{n\mathbf{k}}}} \left(a_{n\mathbf{k}} + a^\dagger_{n-\mathbf{k}}\right), \tag{4.83}$$

we obtain the spinon-phonon coupling $H'_\psi = \sum_{n\mathbf{k}} a_{n\mathbf{k}} Q_{n\mathbf{k}} + \text{h.c.}$, where we identified

$$\begin{aligned} Q_{n\mathbf{k}} = \sqrt{\frac{N_{\rm uc}^{-1}}{2M_{\rm uc}\omega_{n\mathbf{k}}}} \varepsilon^\mu_{n\mathbf{k}} \sum_{\mathbf{p},\boldsymbol{\eta}} \psi^\dagger_{\alpha,\mathbf{p}} \, \left(e^{i\mathbf{k}\cdot\boldsymbol{\eta}} - 1\right) \\ \times \left(e^{i\mathbf{p}\boldsymbol{\eta}} \, \frac{\partial}{\partial \boldsymbol{\rho}} K^{\alpha\beta}_{\boldsymbol{\rho}} \Big|_{\boldsymbol{\rho}=\boldsymbol{\eta}} + e^{-i\mathbf{k}\boldsymbol{\eta}} \, \frac{\delta}{\delta \boldsymbol{u}(\boldsymbol{\eta})} L^{\alpha\beta}_{\{\boldsymbol{\eta}'+\boldsymbol{u}(\boldsymbol{\eta}')\}} \Big|_{\boldsymbol{u}=\mathbf{0}} \right) \, \psi_{\beta,\mathbf{p}+\mathbf{k}} \, . \end{aligned} \tag{4.84}$$

Finally, upon rewriting $\psi_{\alpha,\mathbf{p}} = U^{\alpha\ell}_{\mathbf{p}} f_{\ell,\mathbf{p}}$, we identify

$$\widehat{\mathcal{B}}^{a;\ell\ell'}_{\boldsymbol{\eta};\mathbf{p};\mathbf{k}} = (U^\dagger_{\mathbf{p}})^{\ell\alpha} \, (U_{\mathbf{p}+\mathbf{k}})^{\alpha'\ell'} \, \left(e^{i\mathbf{p}\boldsymbol{\eta}} \, \frac{\partial}{\partial \rho^a} K^{\alpha\alpha'}_{\boldsymbol{\rho}} \Big|_{\boldsymbol{\rho}=\boldsymbol{\eta}} + e^{-i\mathbf{k}\boldsymbol{\eta}} \, \frac{\delta}{\delta u^a(\boldsymbol{\eta})} L^{\alpha\alpha'}_{\{\boldsymbol{\eta}'+\boldsymbol{u}(\boldsymbol{\eta}')\}} \Big|_{\boldsymbol{u}=\mathbf{0}} \right), \tag{4.85}$$

as defined in the main text, Eq. (4.30).

4.E.2 Phonon-fermion coupling constants

Considering the particular case Eqs. (4.27), we find

$$\begin{aligned} \widehat{\mathcal{B}}^{a;\ell\ell'}_{\boldsymbol{\eta};\mathbf{p};\mathbf{k}} &:= \left[\textstyle\sum_{b=x,y} \sigma^b_{\alpha\alpha'} \left(e^{i\mathbf{p}\boldsymbol{\eta}} \mathsf{v}^b_{a,\boldsymbol{\eta}} + e^{-i\mathbf{k}\boldsymbol{\eta}} \mathsf{u}^b_{a,\boldsymbol{\eta}} \right) \right. \\ &+ \left. e^{-i\mathbf{k}\boldsymbol{\eta}} \mathsf{u}^z_{a,\boldsymbol{\eta}} \sigma^z_{\alpha\alpha'} + e^{i\mathbf{p}\boldsymbol{\eta}} \mathsf{t}^0_{a,\boldsymbol{\eta}} \delta_{\alpha\alpha'} \right] (U^\dagger_{\mathbf{p}})^{\ell\alpha} (U_{\mathbf{p}+\mathbf{k}})^{\alpha'\ell'}, \end{aligned} \tag{4.86}$$

where

$$\mathsf{t}^0_{a,\boldsymbol{\eta}} = \partial_{\rho^a} \, J^0_{\boldsymbol{\rho}} \big|_{\boldsymbol{\rho}=\boldsymbol{\eta}} \, , \tag{4.87}$$

$$\mathsf{u}^c_{a,\boldsymbol{\eta}} = \frac{\delta}{\delta u^a(\boldsymbol{\eta})} \mathsf{h}^c_{\{\boldsymbol{\eta}'+\boldsymbol{u}(\boldsymbol{\eta}')\}} \big|_{\boldsymbol{u}=\mathbf{0}}, \quad c = x, y, z, \tag{4.88}$$

$$\mathsf{v}^c_{a,\boldsymbol{\eta}} = i\epsilon^{zc\bar{c}} \left(\delta_{a\bar{c}} + \eta_{\bar{c}} \, \partial_{\rho^a}\right) \alpha^{\rm R}_{\boldsymbol{\rho}} \Big|_{\boldsymbol{\rho}=\boldsymbol{\eta}}, \quad c = x, y, \tag{4.89}$$

where $\boldsymbol{\epsilon}$ is the Levi-Civita tensor, $c = x \Leftrightarrow \bar{c} = y$, and $\frac{\delta}{\delta u^a(\boldsymbol{\eta})}$ denotes functional derivation with respect to the ath component of the displacement field at relative position $\boldsymbol{\eta}$.

Hermiticity of H^0_ψ imposes $J^0_{\boldsymbol{\eta}} = (J^0_{-\boldsymbol{\eta}})^*$, $\alpha^{\mathrm{R}}_{\boldsymbol{\eta}} = (\alpha^{\mathrm{R}}_{-\boldsymbol{\eta}})^*$ and $\mathsf{h}^b_{\{\boldsymbol{\eta}\}} \in \mathbb{R}$. We also assume for simplicity that $J^0_{\boldsymbol{\eta}} = J^0_{-\boldsymbol{\eta}}$ and $\alpha^{\mathrm{R}}_{\boldsymbol{\eta}} = \alpha^{\mathrm{R}}_{-\boldsymbol{\eta}}$.

As the gradient of isotropic magnetic exchange, the coefficient $\mathsf{t}^0_{a,\boldsymbol{\eta}}$ is typically the main contribution to spin-lattice coupling, and its role in thermal *longitudinal* conductivity has been considered for a long time in antiferromagnets [Cottam, 1974]. On the other hand, $\mathsf{u}^{x,y,z}_{a,\boldsymbol{\eta}}$ and $\mathsf{v}^{x,y}_{a,\boldsymbol{\eta}}$, which are gradients of the g-tensor and a Rashba exchange, respectively, are typically small but play an important role in the mechanism for phonon *Hall* conductivity which we derive.

4.E.3 Momentum-space rewriting of the unperturbed spinon hamiltonian

We used the convention $\psi_{\mathbf{r},\alpha} = \frac{1}{\sqrt{N_{\mathrm{uc}}}} \sum_{\mathbf{p}} e^{-i\mathbf{p}\mathbf{r}} \psi_{\mathbf{p},\alpha}$. The reciprocal space representation of Eq. (4.26) (in the undistorted lattice) is

$$H^0_\psi = \sum_{\mathbf{p}} \psi^\dagger_{\alpha,\mathbf{p}} \left(\sum_{\boldsymbol{\eta}} e^{i\mathbf{p}\boldsymbol{\eta}} K^{\alpha,\beta}_{\boldsymbol{\eta}} + L^{\alpha,\beta}_{\{\boldsymbol{\eta}\}} \right) \psi_{\beta,\mathbf{p}}. \tag{4.90}$$

With the particular values for $K^{\alpha,\beta}_{\boldsymbol{\eta}}$ and $L^{\alpha,\beta}_{\{\boldsymbol{\eta}\}}$ defined in Eqs. (4.27), this becomes

$$\begin{aligned} H^0_\psi = \sum_{\mathbf{p}} \psi^\dagger_{\alpha,\mathbf{p}} \big(& \sum_{\boldsymbol{\eta}} e^{i\mathbf{p}\boldsymbol{\eta}} J^0_{\boldsymbol{\eta}} \delta_{\alpha\beta} + \sum_a \mathsf{h}^a_{\{\boldsymbol{\eta}\}} \sigma^a_{\alpha\beta} \\ & - i \sum_{\boldsymbol{\eta}} e^{i\mathbf{p}\boldsymbol{\eta}}\, \alpha^{\mathrm{R}}_{\boldsymbol{\eta}} \left(\eta^x \sigma^y_{\alpha\beta} - \eta^y \sigma^x_{\alpha\beta} \right) \big) \psi_{\beta,\mathbf{p}}. \end{aligned} \tag{4.91}$$

We now define

$$w^0_{\mathbf{p}} = \sum_{\boldsymbol{\eta}} e^{i\mathbf{p}\boldsymbol{\eta}} J^0_{\boldsymbol{\eta}}, \tag{4.92}$$

$$\boldsymbol{w}_{\mathbf{p}} = \mathbf{h}_{\{\boldsymbol{\eta}\}} + i \sum_{\boldsymbol{\eta}} e^{i\mathbf{p}\boldsymbol{\eta}}\, \alpha^{\mathrm{R}}_{\boldsymbol{\eta}} (\boldsymbol{\eta} \times \hat{\boldsymbol{z}}), \tag{4.93}$$

such that the spinon hamiltonian in the undistorted lattice reads $H^0_\psi = \sum_{\mathbf{p}} \psi^\dagger_{\mathbf{p}} \cdot (w^0_{\mathbf{p}} \mathbb{1} + \boldsymbol{w}_{\mathbf{p}} \cdot \boldsymbol{\sigma}) \cdot \psi_{\mathbf{p}}$, i.e. more explicitly

$$H^0_\psi = \sum_{\mathbf{p},\alpha\beta} \psi^\dagger_{\mathbf{p},\alpha} \left(\delta_{\alpha\beta} w^0_{\mathbf{p}} + \sum_b w^b_{\mathbf{p}} \sigma^b_{\alpha\beta} \right) \psi_{\mathbf{p},\beta}. \tag{4.94}$$

We note that because of both hermiticity constraints and our simplifying assumptions mentioned above, both $\mathbf{h}$ and $\boldsymbol{w}$ are real vectors, and in addition $\boldsymbol{w}_{\mathbf{p}}(\mathbf{h}) = -\boldsymbol{w}_{-\mathbf{p}}(-\mathbf{h})$. Besides, in the following we consider that the "effective magnetic field" $\mathbf{h}$ is directly proportional to the external magnetic field $\mathbf{h}$ – this is supported by the microscopic derivation in App.4.G. Therefore reversing $\mathbf{h} \to -\mathbf{h}$ is equivalent to reversing $\mathbf{h} \to -\mathbf{h}$. Thus, we rather write $\boldsymbol{w}_{\mathbf{p}}(\mathbf{h}) = -\boldsymbol{w}_{-\mathbf{p}}(-\mathbf{h})$ from now on.

4.E.4 Diagonalization

As a quadratic hamiltonian, H^0_ψ is readily diagonalizable, by a unitary transformation of the spinon operators, $\psi_{\mathbf{p},\alpha} = \sum_\ell U^{\alpha\ell}_{\mathbf{p}} f_{\mathbf{p},\ell}$ such that $H^0_\psi = H^0_f$, as defined in Eq. (4.8). We parametrize the unitary transformation U according to

$$U_{\mathbf{p}}(\mathbf{h}) = \begin{pmatrix} c_{\mathbf{p}}(\mathbf{h}) & -s^*_{\mathbf{p}}(\mathbf{h}) \\ s_{\mathbf{p}}(\mathbf{h}) & c_{\mathbf{p}}(\mathbf{h}) \end{pmatrix}, \tag{4.95}$$

with $c_{\mathbf{p}}(\mathbf{h}) \in \mathbb{R}$ and $c_{\mathbf{p}}(\mathbf{h})^2 + |s_{\mathbf{p}}(\mathbf{h})|^2 = 1$. It is important to note that $c_{\mathbf{p}}$ and $s_{\mathbf{p}}$, and therefore $U^{\alpha\ell}_{\mathbf{p}}$, are not necessarily continuous with respect to $\mathbf{p}$. In fact, infinitely many different wavevector parameterizations can be chosen to diagonalize H^0_ψ. Indeed, an equivalently good choice of diagonalization is $U_{\mathbf{p}} \to U_{\mathbf{p}} \left[\begin{smallmatrix} f_1(\mathbf{p}) & 0 \\ 0 & f_2(\mathbf{p}) \end{smallmatrix}\right] (f_3(\mathbf{p})\mathbb{1} + (1 - f_3(\mathbf{p}))\boldsymbol{\sigma}^x)$ for any $f_{1,2}(\mathbf{p}) \in U(1)$ and $f_3(\mathbf{p}) \in \{0, 1\}$, however singular. Two specific choices will be particularly useful in the following. More precisely, choice I—where the band index coincides with the spin index in all the BZ—is natural in cases where $\mathsf{h}^z \neq 0$, while choice II—where band and spin indices coincide only in half of the BZ—is more natural when $\mathsf{h}^z = 0$. They read as follows:

(i) Choice I: this choice corresponds to a continuous $U^{\alpha\ell}_{\mathbf{p}}$. It reads

$$c^{(\mathrm{I})}_{\mathbf{p}}(\mathbf{h}) = \tfrac{w^z_{\mathbf{p}} + |w_{\mathbf{p}}|}{\sqrt{\underline{w}^2_{\mathbf{p}} + (w^z_{\mathbf{p}} + |\boldsymbol{w}_{\mathbf{p}}|)^2}}; \quad s^{(\mathrm{I})}_{\mathbf{p}}(\mathbf{h}) = \tfrac{w^x_{\mathbf{p}} + i w^y_{\mathbf{p}}}{\sqrt{\underline{w}^2_{\mathbf{p}} + (w^z_{\mathbf{p}} + |\boldsymbol{w}_{\mathbf{p}}|)^2}} \tag{4.96}$$

for all $\mathbf{p}$. The dispersion relation is then

$$\epsilon^{(\mathrm{I})}_{\ell,\mathbf{p}}(\mathbf{h}) = w^0_{\mathbf{p}} + \ell\, |\boldsymbol{w}_{\mathbf{p}}(\mathbf{h})|, \tag{4.97}$$

with $\ell = \pm \equiv \uparrow, \downarrow$. It satisfies $\epsilon^{(\mathrm{I})}_{\ell,\mathbf{p}}(\mathbf{h}) = \epsilon^{(\mathrm{I})}_{\ell,-\mathbf{p}}(-\mathbf{h})$.

(ii) Choice II: this choice corresponds to a $U^{\alpha\ell}_{\mathbf{p}}$ continuous within each of two subsets $\mathsf{D}_\pm$ partitioning the momentum space, but discontinuous at the boundary. More precisely, we divide $\mathbb{R}^3 - \{\mathbf{0}\}$ into two subsets D_+ and $\mathsf{D}_- = \mathbb{R}^3 - \{\mathbf{0}\} - \mathsf{D}_+$ such that $\mathbf{p} \in \mathsf{D}_+ \Leftrightarrow -\mathbf{p} \in \mathsf{D}_-$. For the sake of concreteness, consider $\mathsf{D}_+ = \{p_y > 0\} \cup \{p_y = 0, p_x > 0\} \cup \{\underline{\mathbf{p}} = \mathbf{0}, p_z > 0\}$. Choice II reads

$$\mathbf{p} \in \mathsf{D}_+ : \; c^{(\mathrm{II})}_{\mathbf{p}}(\mathbf{h}) = c^{(\mathrm{I})}_{\mathbf{p}}(\mathbf{h}),\; s^{(\mathrm{II})}_{\mathbf{p}}(\mathbf{h}) = s^{(\mathrm{I})}_{\mathbf{p}}(\mathbf{h}), \tag{4.98}$$

$$\mathbf{p} \in \mathsf{D}_- : \; c^{(\mathrm{II})}_{\mathbf{p}}(\mathbf{h}) = c^{(\mathrm{I})}_{-\mathbf{p}}(-\mathbf{h}),\; s^{(\mathrm{II})}_{\mathbf{p}}(\mathbf{h}) = s^{(\mathrm{I})}_{-\mathbf{p}}(-\mathbf{h}). \tag{4.99}$$

Denoting $\mathsf{s}_{\mathsf{D}}(\mathbf{p}) = \sum_{s=\pm} s \mathbb{1}_{\mathsf{D}_s}(\mathbf{p})$, the dispersion relation then reads

$$\epsilon_{\ell,\mathbf{p}}(\mathbf{h}) = w^0_{\mathbf{p}} + \ell\, \mathsf{s}_{\mathsf{D}}(\mathbf{p})\, |\boldsymbol{w}_{\mathbf{p}}(\mathbf{h})|. \tag{4.100}$$

It satisfies $\epsilon_{\ell,\mathbf{p}}(\mathbf{h}) = \epsilon_{\bar{\ell},-\mathbf{p}}(-\mathbf{h})$, where $\ell = \uparrow \Leftrightarrow \bar{\ell} = \downarrow$.

4.F Symmetries in the specific model

4.F.1 Explicit expansion of $\hat{\mathcal{B}}$

In the microscopic model for phonon-spinon coupling we consider, the auxiliary quantity appearing in the coupling constant, Eq. (4.86) in the previous Appendix and Eq. (4.31) in the main text, reads

$$\begin{aligned}
\widehat{\mathcal{B}}^{a,\ell\ell'}_{\boldsymbol{\eta};\mathbf{p};\mathbf{k}} &= e^{i\mathbf{p}\boldsymbol{\eta}}\mathsf{t}^0_{a,\boldsymbol{\eta}}\begin{pmatrix} c_{\mathbf{p}}c_{\mathbf{p}+\mathbf{k}}+s^*_{\mathbf{p}}s_{\mathbf{p}+\mathbf{k}} & -c_{\mathbf{p}}s^*_{\mathbf{p}+\mathbf{k}}+s^*_{\mathbf{p}}c_{\mathbf{p}+\mathbf{k}} \\ -s_{\mathbf{p}}c_{\mathbf{p}+\mathbf{k}}+c_{\mathbf{p}}s_{\mathbf{p}+\mathbf{k}} & s_{\mathbf{p}}s^*_{\mathbf{p}+\mathbf{k}}+c_{\mathbf{p}}c_{\mathbf{p}+\mathbf{k}}\end{pmatrix}_{\ell,\ell'} \\
&+ e^{-i\mathbf{k}\boldsymbol{\eta}}\mathsf{u}^z_{a,\boldsymbol{\eta}}\begin{pmatrix} c_{\mathbf{p}}c_{\mathbf{p}+\mathbf{k}}-s^*_{\mathbf{p}}s_{\mathbf{p}+\mathbf{k}} & -c_{\mathbf{p}}s^*_{\mathbf{p}+\mathbf{k}}-s^*_{\mathbf{p}}c_{\mathbf{p}+\mathbf{k}} \\ -s_{\mathbf{p}}c_{\mathbf{p}+\mathbf{k}}-c_{\mathbf{p}}s_{\mathbf{p}+\mathbf{k}} & s_{\mathbf{p}}s^*_{\mathbf{p}+\mathbf{k}}-c_{\mathbf{p}}c_{\mathbf{p}+\mathbf{k}}\end{pmatrix}_{\ell,\ell'} \\
&+ Z^{+,a}_{\boldsymbol{\eta};\mathbf{p};\mathbf{k}}\begin{pmatrix} c_{\mathbf{p}}s_{\mathbf{p}+\mathbf{k}} & c_{\mathbf{p}}c_{\mathbf{p}+\mathbf{k}} \\ -s_{\mathbf{p}}s_{\mathbf{p}+\mathbf{k}} & -s_{\mathbf{p}}c_{\mathbf{p}+\mathbf{k}}\end{pmatrix}_{\ell,\ell'} + Z^{-,a}_{\boldsymbol{\eta};\mathbf{p};\mathbf{k}}\begin{pmatrix} s^*_{\mathbf{p}}c_{\mathbf{p}+\mathbf{k}} & -s^*_{\mathbf{p}}s^*_{\mathbf{p}+\mathbf{k}} \\ c_{\mathbf{p}}c_{\mathbf{p}+\mathbf{k}} & -c_{\mathbf{p}}s^*_{\mathbf{p}+\mathbf{k}}\end{pmatrix}_{\ell,\ell'},
\end{aligned} \tag{4.101}$$

where we write $Z^{\pm,a}_{\boldsymbol{\eta};\mathbf{p};\mathbf{k}} = e^{-i\mathbf{k}\boldsymbol{\eta}}(\mathsf{u}^x_{a,\boldsymbol{\eta}} \pm i\mathsf{u}^y_{a,\boldsymbol{\eta}}) + e^{i\mathbf{p}\boldsymbol{\eta}}(\mathsf{v}^x_{a,\boldsymbol{\eta}} \pm i\mathsf{v}^y_{a,\boldsymbol{\eta}})$.

Its behavior in limit cases is explored below. As a consequence of our simplifying assumptions formulated in the main text, all four coefficients $\mathsf{u}^{0,x,y,z}$ hereabove are purely real, while both coefficients $\mathsf{v}^{x,y}$ are purely imaginary.

4.F.2 Detailed symmetry discussion of the microscopic model

In this subsection, we show how the presence of certain symmetries, at the level of the phonon-spinon couplings and the fermions' wavefunctions and dispersions, forbids a phonon Hall conductivity.

Two such particular cases are quite intuitive:

- (i) *Preserved time reversal symmetry:* assume $\mathbf{h} = \mathbf{0}$ and $\mathsf{u}^{x,y,z}_{a,\boldsymbol{\eta}} = 0$. Since $\mathsf{u}^{x,y,z}_{a,\boldsymbol{\eta}} = 0$, the relation Eq.(4.32) with $\xi_{\ell,\ell'} = -(-1)^{\delta_{\ell,\ell'}}$ and $\tilde{\ell} = \overline{\ell}$ holds. Using diagonalization choice II along with $\mathbf{h} = \mathbf{0}$ yields $\epsilon_{\ell,\mathbf{p}} = \epsilon_{\overline{\ell},-\mathbf{p}}$ which concludes.

- (ii) *Absence of spin-orbit coupling:* assume $\alpha^{\mathrm{R}}_{\boldsymbol{\eta}} = 0$, $\mathsf{v}^{x,y}_{a,\boldsymbol{\eta}} = 0$ and $\mathsf{u}^{x,y,z}_{a,\boldsymbol{\eta}} = 0$. Using diagonalization choice I, $U_{\mathbf{p}}$ is independent from $\mathbf{p}$, therefore $\widehat{\mathcal{B}}^{a;\ell\ell'}_{\boldsymbol{\eta};\mathbf{p};\mathbf{k}} = e^{i\mathbf{p}\boldsymbol{\eta}}\mathsf{t}^0_{a,\boldsymbol{\eta}}\delta_{\ell,\ell'}$. Besides, $\epsilon_{\ell,\mathbf{p}} = \epsilon_{\ell,-\mathbf{p}}$. Thus, the relation Eq.(4.32) with $\xi_{\ell,\ell'} = 1$ and $\tilde{\ell} = \ell$ holds.

We also explore two other cases which are less intuitive:

- (iii) *Effectively preserved time reversal symmetry:* assume $\alpha^{\mathrm{R}}_{\boldsymbol{\eta}} = 0$, $\mathsf{v}^{x,y}_{a,\boldsymbol{\eta}} = 0$, $\mathsf{h}^z = 0$ and $\mathsf{u}^z_{a,\boldsymbol{\eta}} = 0$. Using diagonalization choice II, $\epsilon_{\ell,\mathbf{p}} = \epsilon_{\overline{\ell},-\mathbf{p}}$. Besides, $c_{\mathbf{p}} = \frac{1}{\sqrt{2}}$ and $s_{-\mathbf{p}} = -s_{\mathbf{p}}$, so that the relation Eq.(4.32) with $\xi_{\ell,\ell'} = 1$ and $\tilde{\ell} = \overline{\ell}$ holds.

- (iv) *Effective absence of spin-orbit coupling:* assume $\mathsf{h}^{x,y}=0$, $\alpha^{\mathrm{R}}_{\boldsymbol{\eta}}=0$, $\mathsf{v}^{x,y}_{a,\boldsymbol{\eta}}=0$, $\mathsf{u}^{x,y}_{a,\boldsymbol{\eta}}=0$. Then using diagonalization choice I, $U_{\mathbf{p}}=\mathbb{1}_{2\times 2}$ suffices and the relation Eq.(4.32) with $\xi_{\ell,\ell'}=1$ and $\tilde{\ell}=\ell$ holds.

A summary of these four cases is given in Table 4.7.2 in the main text.

In all other physically relevant cases[3], as far as we are aware $\mathfrak{W}^{\ominus,qq'}_{n\mathbf{k},n'\mathbf{k}'}+\mathfrak{W}^{\ominus,qq'}_{n-\mathbf{k},n'-\mathbf{k}'}\neq 0$ for generic $\mathbf{k},\mathbf{k}'$. Therefore $\boldsymbol{\kappa}_{\mathrm{H}}$ does not vanish *a priori*. However, other relations imposed by crystalline symmetries (notably, the mirror symmetries) may still impose a vanishing Hall conductivity. This is still work in progress.

4.F.3 Anti-unitary symmetries

The above particular case (i) highlights the importance of one anti-unitary symmetry $\hat{\mathcal{T}}=\hat{\mathcal{U}}\hat{K}$ defined by $\tilde{\ell}=\bar{\ell},\ \zeta_\ell=(-1)^{\delta_{\ell,\downarrow}}$ (i.e. $\hat{\mathcal{U}}_f=-i\hat{\sigma}^y$). Thus, when $\ell=\uparrow,\downarrow$ identifies with a spin-1/2 index, this $\hat{\mathcal{T}}$ is the traditional time-reversal operator [Wigner, 1959].

The other instance for $\hat{\mathcal{T}}$ identified in (iii) hereabove corresponds to $\tilde{\ell}=\bar{\ell},\ \zeta_\ell=1$ (i.e. $\hat{\mathcal{U}}_f=\hat{\sigma}^x$). Finally, in (ii) and (iv) hereabove, $\hat{\mathcal{T}}$ corresponds to $\tilde{\ell}=\ell,\ \zeta_\ell=1$ (i.e. $\hat{\mathcal{U}}_f=\mathbb{1}$).

It appears that $\tilde{\ell}=\ell,\ \zeta_\ell=(-1)^{\delta_{\ell,\downarrow}}$, i.e.$\hat{\mathcal{U}}_f=\hat{\sigma}^z$, is not represented in the specific cases we have identified.

These results are summarized in Table 4.7.1 in the main text.

4.F.4 Reformulation in the basis of Pauli matrices

Here we identify $\widehat{B}^{\mu}_{a,\boldsymbol{\eta};\mathbf{p};\mathbf{k}}$ for $\mu=0,x,y,z$:

$$\begin{aligned}
\widehat{B}^{0}_{a,\boldsymbol{\eta};\mathbf{p};\mathbf{k}} &= e^{i\mathbf{p}\boldsymbol{\eta}}\mathsf{t}^{0}_{a,\boldsymbol{\eta}}\big(c_{\mathbf{p}}c_{\mathbf{p}+\mathbf{k}}+\mathfrak{Re}[s_{\mathbf{p}}s^*_{\mathbf{p}+\mathbf{k}}]\big)+e^{-i\mathbf{k}\boldsymbol{\eta}}\mathsf{u}^{z}_{a,\boldsymbol{\eta}}\big(i\mathfrak{Im}[s_{\mathbf{p}}s^*_{\mathbf{p}+\mathbf{k}}]\big)\\
&\quad+Z^{+,a}_{\boldsymbol{\eta};\mathbf{p};\mathbf{k}}\tfrac{1}{2}\big(c_{\mathbf{p}}s_{\mathbf{p}+\mathbf{k}}-s_{\mathbf{p}}c_{\mathbf{p}+\mathbf{k}}\big)+Z^{-,a}_{\boldsymbol{\eta};\mathbf{p};\mathbf{k}}\tfrac{1}{2}\big(s^*_{\mathbf{p}}c_{\mathbf{p}+\mathbf{k}}-c_{\mathbf{p}}s^*_{\mathbf{p}+\mathbf{k}}\big) \qquad (4.102)\\
\widehat{B}^{z}_{a,\boldsymbol{\eta};\mathbf{p};\mathbf{k}} &= e^{i\mathbf{p}\boldsymbol{\eta}}\mathsf{t}^{0}_{a,\boldsymbol{\eta}}\big(i\mathfrak{Im}[s^*_{\mathbf{p}}s_{\mathbf{p}+\mathbf{k}}]\big)+e^{-i\mathbf{k}\boldsymbol{\eta}}\mathsf{u}^{z}_{a,\boldsymbol{\eta}}\big(c_{\mathbf{p}}c_{\mathbf{p}+\mathbf{k}}-\mathfrak{Re}[s_{\mathbf{p}}s^*_{\mathbf{p}+\mathbf{k}}]\big)\\
&\quad+Z^{+,a}_{\boldsymbol{\eta};\mathbf{p};\mathbf{k}}\tfrac{1}{2}\big(c_{\mathbf{p}}s_{\mathbf{p}+\mathbf{k}}+s_{\mathbf{p}}c_{\mathbf{p}+\mathbf{k}}\big)+Z^{-,a}_{\boldsymbol{\eta};\mathbf{p};\mathbf{k}}\tfrac{1}{2}\big(s^*_{\mathbf{p}}c_{\mathbf{p}+\mathbf{k}}+c_{\mathbf{p}}s^*_{\mathbf{p}+\mathbf{k}}\big) \qquad (4.103)\\
\widehat{B}^{x}_{a,\boldsymbol{\eta};\mathbf{p};\mathbf{k}} &= e^{i\mathbf{p}\boldsymbol{\eta}}\mathsf{t}^{0}_{a,\boldsymbol{\eta}}\big(c_{\mathbf{p}}i\mathfrak{Im}[s_{\mathbf{p}+\mathbf{k}}]-c_{\mathbf{p}+\mathbf{k}}i\mathfrak{Im}[s_{\mathbf{p}}]\big)\\
&\quad+e^{-i\mathbf{k}\boldsymbol{\eta}}\mathsf{u}^{z}_{a,\boldsymbol{\eta}}\big(-c_{\mathbf{p}}\mathfrak{Re}[s_{\mathbf{p}+\mathbf{k}}]-c_{\mathbf{p}+\mathbf{k}}\mathfrak{Re}[s_{\mathbf{p}}]\big)\\
&\quad+Z^{+,a}_{\boldsymbol{\eta};\mathbf{p};\mathbf{k}}\tfrac{1}{2}\big(c_{\mathbf{p}}c_{\mathbf{p}+\mathbf{k}}-s_{\mathbf{p}}s_{\mathbf{p}+\mathbf{k}}\big)+Z^{-,a}_{\boldsymbol{\eta};\mathbf{p};\mathbf{k}}\tfrac{1}{2}\big(c_{\mathbf{p}}c_{\mathbf{p}+\mathbf{k}}-s^*_{\mathbf{p}}s^*_{\mathbf{p}+\mathbf{k}}\big) \qquad (4.104)\\
\widehat{B}^{y}_{a,\boldsymbol{\eta};\mathbf{p};\mathbf{k}} &= e^{i\mathbf{p}\boldsymbol{\eta}}\mathsf{t}^{0}_{a,\boldsymbol{\eta}}i\big(c_{\mathbf{p}+\mathbf{k}}\mathfrak{Re}[s_{\mathbf{p}}]-c_{\mathbf{p}}\mathfrak{Re}[s_{\mathbf{p}+\mathbf{k}}]\big)\\
&\quad+e^{-i\mathbf{k}\boldsymbol{\eta}}\mathsf{u}^{z}_{a,\boldsymbol{\eta}}\big(-c_{\mathbf{p}+\mathbf{k}}\mathfrak{Im}[s_{\mathbf{p}}]-c_{\mathbf{p}}\mathfrak{Im}[s_{\mathbf{p}+\mathbf{k}}]\big)\\
&\quad+Z^{+,a}_{\boldsymbol{\eta};\mathbf{p};\mathbf{k}}\tfrac{i}{2}\big(s_{\mathbf{p}}s_{\mathbf{p}+\mathbf{k}}+c_{\mathbf{p}}c_{\mathbf{p}+\mathbf{k}}\big)+Z^{-,a}_{\boldsymbol{\eta};\mathbf{p};\mathbf{k}}\tfrac{i}{2}\big(-s^*_{\mathbf{p}}s^*_{\mathbf{p}+\mathbf{k}}-c_{\mathbf{p}}c_{\mathbf{p}+\mathbf{k}}\big) \qquad (4.105)
\end{aligned}$$

[3](in the sense that u^a can only be nonzero if $\mathsf{h}^a\neq 0$ as well, and similarly v^b can only be nonzero if $\alpha^{\mathrm{R}}\neq 0$)

4.G Microscopic derivation of the model

4.G.1 Mean-field derivation of the spinon hamiltonian

Here we show how a quadratic fermion Hamiltonian such as Eq.(4.26) can be obtained from a standard a mean-field treatment of a spin hamiltonian.

We start from the spin hamiltonian

$$H_S^0 = \sum_{\mathbf{r},\mathbf{r}'} J^{ab}_{\mathbf{r},\mathbf{r}'} S^a_{\mathbf{r}} S^b_{\mathbf{r}'} - \sum_{\mathbf{r}} g^{ab}_{\{\mathbf{r}-\mathbf{r}''\}} h^a S^b_{\mathbf{r}}, \tag{4.106}$$

where $a, b = x, y, z$ are the spin directions, $J^{ab}_{\mathbf{r},\mathbf{r}'} = J^{ba}_{\mathbf{r}',\mathbf{r}}$ is a magnetic exchange constant, $\boldsymbol{h}$ is the external magnetic field, and $g^{ab}_{\{\mathbf{r}-\mathbf{r}''\}}$ is the local g-tensor at site $\mathbf{r}$ which in principle depends on the positions $\mathbf{r}''$ of *all* the lattice sites because of crystal fields.

We rewrite the spin operators as $\mathbf{S}_{\mathbf{r}} = \frac{1}{2}\sum_{\alpha\beta} \psi^\dagger_{\mathbf{r}\alpha} \boldsymbol{\sigma}_{\alpha\beta} \psi_{\mathbf{r}\beta}$, where $\psi_{\mathbf{r}\alpha}$ is an Abrikosov fermion at site $\mathbf{r}$ (in the undistorted lattice) and $\alpha = \uparrow, \downarrow$ is the spin-$\frac{1}{2}$ index of the fermion. This provides an exact rewriting of the theory, provided that the constraint $\psi^\dagger_{\mathbf{r}\alpha}\psi_{\mathbf{r}\alpha} = 1 \quad \forall \mathbf{r}$ is enforced exactly at each site. [Baskaran and Anderson, 1988] The latter can be enforced by adding a Lagrange multiplier term $\mathcal{L}_{A^0} = \sum_{\mathbf{r}} A^0_{\mathbf{r}} \left(\psi^\dagger_{\mathbf{r}\alpha}\psi_{\mathbf{r}\alpha} - 1\right)$ to the lagrangian density, where functional integration over $A^0_{\mathbf{r}}(\tau)$ enforces the local constraint. When fluctuations of the scalar field $A^0_{\mathbf{r}}(\tau)$ are neglected, the hereabove constraint is only enforced on average in the ground state, and $A^0_{\mathbf{r}}$ acts only as a local chemical potential for the fermions. Following [Lee and Nagaosa, 1992], we make this approximation in the following.

Expressed in terms of Abrikosov fermions, the spin Hamiltonian Eq.(4.106) reads

$$\begin{aligned} H_S^0 = &\sum_{\mathbf{r},\mathbf{r}'} \frac{1}{4} J^{ab}_{\mathbf{r},\mathbf{r}'} \psi^\dagger_{\mathbf{r}\alpha} \sigma^a_{\alpha\beta} \psi_{\mathbf{r}\beta} \psi^\dagger_{\mathbf{r}'\alpha'} \sigma^b_{\alpha'\beta'} \psi_{\mathbf{r}'\beta'} \\ &- \sum_{\mathbf{r}} g^{ab}_{\{\mathbf{r}-\mathbf{r}''\}} h^a \frac{1}{2} \sum_{\alpha\beta} \psi^\dagger_{\mathbf{r}\alpha} \sigma^b_{\alpha\alpha'} \psi_{\mathbf{r}\alpha'}, \end{aligned} \tag{4.107}$$

i.e. it is a theory of interacting fermions.

We then perform a Hubbard-Stratonovich transform of the four-fermion couplings, in the channel where the expectation values

$$\chi^{\alpha\gamma}_{\mathbf{r},\mathbf{r}'} := \left\langle \psi^\dagger_{\mathbf{r}\alpha} \psi_{\mathbf{r}'\gamma} \right\rangle = (\chi^{\gamma\alpha}_{\mathbf{r}',\mathbf{r}})^* \tag{4.108}$$

can become nonzero, while contractions of the form $\langle \psi^\dagger \psi^\dagger \rangle$ or $\langle \psi \psi \rangle$ remain null. This hypothesis breaks the $SU(2)$ gauge invariance of the initial parton description [Misguich, 2011], but preserves a $U(1)$ gauge symmetry $\psi_{\alpha\mathbf{r}} \to e^{i\theta(\mathbf{r})}\psi_{\alpha\mathbf{r}}$. Note that because of these local gauge transformations, $\chi^{\alpha\gamma}_{\mathbf{r},\mathbf{r}'}$ is only well-defined in a given gauge choice.

The mean-field decoupling, schematically

$$\begin{aligned}&\psi_i^\dagger\psi_j^\dagger\psi_k\psi_l \quad \to \\ &\frac{1}{2}\Big(\left\langle \psi_i^\dagger\psi_k\right\rangle \psi_l\psi_j^\dagger + \psi_i^\dagger\psi_k \left\langle \psi_l\psi_j^\dagger\right\rangle - \left\langle \psi_i^\dagger\psi_k\right\rangle \left\langle \psi_l\psi_j^\dagger\right\rangle \\ &+ \left\langle \psi_i^\dagger\psi_l\right\rangle \psi_j^\dagger\psi_k + \psi_i^\dagger\psi_l \left\langle \psi_j^\dagger\psi_k\right\rangle - \left\langle \psi_i^\dagger\psi_l\right\rangle \left\langle \psi_j^\dagger\psi_k\right\rangle \Big),\end{aligned} \tag{4.109}$$

yields the following rewriting of the spin hamiltonian:

$$\begin{aligned}H_\psi^0 = &-\frac{1}{4}\Big(\chi^{\beta'\beta}_{\mathbf{r}',\mathbf{r}} J^{ab}_{\mathbf{r},\mathbf{r}'}\sigma^a_{\alpha\beta}\sigma^b_{\beta'\alpha'} - \delta_{\mathbf{r},\mathbf{r}'}\chi^{\beta\beta'}_{\mathbf{r}'',\mathbf{r}'} J^{ab}_{\mathbf{r},\mathbf{r}''}\sigma^a_{\alpha\alpha'}\sigma^b_{\beta\beta'}\Big)\psi^\dagger_{\mathbf{r}\alpha}\psi_{\mathbf{r}'\alpha'} \\ &- \sum_{\mathbf{r}} g^{ab}_{\{\mathbf{r}-\mathbf{r}''\}} h^a \frac{1}{2}\sum_{\alpha\beta}\psi^\dagger_{\mathbf{r}\alpha}\sigma^b_{\alpha\alpha'}\psi_{\mathbf{r}\alpha'}.\end{aligned} \tag{4.110}$$

Note that Eq.(4.110) can be understood as an *exact* rewriting of Eq. (4.107) if the Hubbard-Stratonovich field $\chi^{\alpha\gamma}_{\mathbf{r},\mathbf{r}'}$ is treated as an independent bosonic field free to fluctuate. The mean-field approximation we make consists in neglecting amplitude fluctuations, and thus making the ansatz $\chi^{\alpha\gamma}_{\mathbf{r},\mathbf{r}'} = \overline{\chi}^{\alpha\gamma}_{\mathbf{r},\mathbf{r}'} e^{-iA_{\mathbf{r},\mathbf{r}'}}$, where $\overline{\chi}^{\alpha\gamma}_{\mathbf{r},\mathbf{r}'}$ is now a gauge-independent fixed quantity, and the associated $U(1)$ gauge field $A_{\mathbf{r},\mathbf{r}'}$ absorbs the gauge transformations of fermionic fields:

$$\psi_{\alpha\mathbf{r}} \to e^{i\theta(\mathbf{r})}\psi_{\alpha\mathbf{r}} \quad ; \quad A_{\mathbf{r},\mathbf{r}'} \to A_{\mathbf{r},\mathbf{r}'} + \theta(\mathbf{r}) - \theta(\mathbf{r}') \tag{4.111}$$

leaves H_S^0 invariant. Thus Eq.(4.110) is an effective theory for fermions (henceforth called spinons) coupled to a $U(1)$ gauge field. We can identify it as the hamiltonian H_ψ^0 in the main text, Eq.(4.26).

From our mean-field ansatz, the parameters $K^{\alpha\alpha'}_{\mathbf{r}-\mathbf{r}'}$ and $L^{\alpha\alpha'}_{\{\mathbf{r}-\mathbf{r}''\}}$ are given by:

$$K^{\alpha\alpha'}_{\mathbf{r}-\mathbf{r}'} = -(1-\delta_{\mathbf{r},\mathbf{r}'})\frac{1}{4}\chi^{\beta'\beta}_{\mathbf{r}',\mathbf{r}} J^{ab}_{\mathbf{r},\mathbf{r}'}\sigma^a_{\alpha\beta}\sigma^b_{\beta'\alpha'}, \tag{4.112}$$

$$L^{\alpha\alpha'}_{\{\mathbf{r}-\mathbf{r}''\}} = \Big(\frac{1}{4}\sum_{\mathbf{r}''} m^a_{\mathbf{r}''} J^{ab}_{\mathbf{r}'',\mathbf{r}} - \frac{1}{2}h^a g^{ab}_{\{\mathbf{r}-\mathbf{r}''\}}\Big)\sigma^b_{\alpha\alpha'}, \tag{4.113}$$

where we defined the particular quantity

$$m^a_{\mathbf{r}} := \left\langle \psi^\dagger_{\mathbf{r}\alpha}\sigma^a_{\alpha\beta}\psi_{\mathbf{r}\beta}\right\rangle = \sigma^a_{\alpha\beta}\chi^{\alpha\beta}_{\mathbf{r},\mathbf{r}} \tag{4.114}$$

which can become nonzero in presence of an external magnetic field.

4.G.2 Choice of magnetic exchange and mean-field parameters

In this subsection, we show how particular hamiltonian parameters such as those proposed in Eqs.(4.27) can be obtained from Eq.(4.112) for a given choice of magnetic exchange constants $J^{ab}_{\mathbf{r},\mathbf{r}'}$ and of spin liquid ansatz $\chi^{\alpha\gamma}_{\mathbf{r},\mathbf{r}'}$.

We choose the magnetic exchange constants in the form

$$J^{ab}_{\mathbf{r},\mathbf{r}'} = J^{\text{iso}}_{\mathbf{r},\mathbf{r}'}\delta_{ab} + \sum_{\boldsymbol{\eta}} \delta_{\mathbf{r}',\mathbf{r}+\boldsymbol{\eta}}(\hat{z}\times\eta)^c J^D_{|\boldsymbol{\eta}|}\epsilon^{cab}, \tag{4.115}$$

where $J^{\text{iso}}_{\mathbf{r},\mathbf{r}'}$ is the isotropic component (i.e. Heisenberg exchange) and $J^D_{|\boldsymbol{\eta}|}$ is the strength of a Dzyaloshinskii-Moriya interaction with a bond-dependent $\mathbf{D}(\boldsymbol{\eta}) \perp \boldsymbol{\eta}$ vector, where $\boldsymbol{\eta}$ is the bond vector.

We assume that the spin liquid mean-field parameter takes the form

$$\chi^{\beta'\beta}_{\mathbf{r}',\mathbf{r}} = (1-\delta_{\mathbf{r},\mathbf{r}'})\chi^0_{|\mathbf{r}'-\mathbf{r}|}\delta_{\beta\beta'} + \delta_{\mathbf{r},\mathbf{r}'}\chi^{\beta'\beta}_{\mathbf{r},\mathbf{r}}, \tag{4.116}$$

where the $\chi^{\alpha\gamma}_{\mathbf{r},\mathbf{r}}$ ansätze determine the value of $\boldsymbol{m}_{\mathbf{r}}$ the local magnetization. This form, Eq.(4.116), corresponds to the "uniform spin liquid phase" in the terminology of [Ioffe and Larkin, 1989]. Note that if the initial spin model Eq.(4.106) were isotropic (i.e. $J^{ab} = J^{\text{iso}}\delta_{ab}$), this ansatz's isotropy in spin space (i.e. $\delta_{\beta\beta'}$) would signify the absence of spontaneous symmetry breaking. Here, since our initial magnetic model contains anisotropic exchange, it must be understood as a simplifying assumption.

These two assumptions Eqs.(4.115),(4.116) entail

$$\begin{aligned} K^{\alpha\alpha'}_{\mathbf{r}-\mathbf{r}'} = &-\frac{1}{4}J^{\text{iso}}_{\mathbf{r},\mathbf{r}'}\chi^0_{|\mathbf{r}'-\mathbf{r}|}\delta_{\alpha\alpha'} \\ &- \frac{i}{4}\sum_{\boldsymbol{\eta}} \delta_{\mathbf{r}',\mathbf{r}+\boldsymbol{\eta}}\chi^0_{|\boldsymbol{\eta}|}J^D_{|\boldsymbol{\eta}|}(\hat{z}\times\eta)^c\sigma^c_{\alpha\alpha'}, \end{aligned} \tag{4.117}$$

where we used the identities $[\sigma^a,\sigma^b] = i\epsilon^{abc}\sigma^c$ and $\sum_a \sigma^a_{\alpha\beta}\sigma^a_{\alpha'\beta'} = 2\delta_{\alpha\beta'}\delta_{\alpha'\beta} - \delta_{\alpha\beta}\delta_{\alpha'\beta'}$.

We have thus shown that the model for magnetic exchange Eq.(4.115) together with the mean-field ansatz Eq.(4.116) yield a spinon Hamiltonian of the form Eqs.(4.26-4.27), with the parameters

$$J^0_{\mathbf{r}-\mathbf{r}'} = -\frac{1}{4}\chi^0_{|\mathbf{r}-\mathbf{r}'|}J^{\text{iso}}_{\mathbf{r},\mathbf{r}'} \tag{4.118}$$

$$\alpha^{\text{R}}_{\mathbf{r}-\mathbf{r}'} = -\frac{1}{4}\chi^0_{|\mathbf{r}-\mathbf{r}'|}J^D_{|\mathbf{r}-\mathbf{r}'|} \tag{4.119}$$

$$\mathsf{h}^b_{\{\mathbf{r}-\mathbf{r}''\}} = \frac{1}{4}\sum_{\mathbf{r}''} m^a_{\mathbf{r}''}J^{ab}_{\mathbf{r}'',\mathbf{r}} - \frac{1}{2}h^a g^{ab}_{\{\mathbf{r}-\mathbf{r}''\}}. \tag{4.120}$$

Note, in particular, that the inversion-breaking Dzyaloshinskii-Moriya interaction between spins manifests itself as a Rashba interaction between spinons.

4.G.3 Magnetization mean-field Ansatz

It is possible to derive $m^a_{\mathbf{r}}$, or equivalently $\chi_{\mathbf{r},\mathbf{r}}$, as a function of the applied magnetic field and other parameters of the problem. We start from the spin hamiltonian

$$H^0_S = \sum_{\mathbf{r},\mathbf{r}'} J^{ab}_{\mathbf{r},\mathbf{r}'}S^a_{\mathbf{r}}S^b_{\mathbf{r}'} - \sum_{\mathbf{r}} g^{ab}_{\{\mathbf{r}-\mathbf{r}''\}}h^a S^b_{\mathbf{r}}, \tag{4.121}$$

and in a mean-field approximation we replace $S^a_{\mathbf{r}} \to m^a_{\mathbf{r}}$. Further assuming that $\boldsymbol{\chi}_{\mathbf{r},\mathbf{r}} =: \boldsymbol{\chi}$ is uniform, one obtains the following result:

$$m^a_{\mathbf{r}} = \left[\left(\sum_{\mathbf{r}'}\boldsymbol{J}_{\mathbf{r},\mathbf{r}'}\right)^{-1}\right]_{ab} h^c g^{cb}_{\{\mathbf{r}-\mathbf{r}''\}}. \tag{4.122}$$

This is the *classical* value of the magnetization, which we use as a consistent Ansatz parameter.

4.G.4 Further simplification

We start again from Eq.(4.110). Because we know that the mean-field magnetization $\boldsymbol{m}$ satisfies

$$\sum_{\mathbf{r}''} m^a_{\mathbf{r}''} J^{ab}_{\mathbf{r}'',\mathbf{r}} = h^a g^{ab}_{\{\mathbf{r}-\mathbf{r}''\}}, \tag{4.123}$$

we have, in real space and then in reciprocal space,

$$\begin{aligned} H^0_\psi = -\frac{1}{4}\sum_{\mathbf{r},\mathbf{r}'} \psi^\dagger_{\mathbf{r},\alpha} \Big(\chi^0_{|\mathbf{r}-\mathbf{r}'|} \left\{ J^{\text{iso}}_{\mathbf{r},\mathbf{r}'}\delta_{\alpha\alpha'} - iJ^D_{|\mathbf{r}-\mathbf{r}'|}\ \hat{\mathbf{z}}\cdot\left([\mathbf{r}-\mathbf{r}']\times\boldsymbol{\sigma}_{\alpha\alpha'}\right)\right\} \\ +\delta_{\mathbf{r},\mathbf{r}'} h^a g^{ab}_{\{\mathbf{r}-\mathbf{r}''\}}\sigma^b_{\alpha\alpha'}\Big)\,\psi_{\mathbf{r}',\alpha'} \end{aligned} \tag{4.124}$$

$$\begin{aligned} H^0_\psi = -\frac{1}{4}\sum_{\mathbf{p},\mathbf{p}'} \psi^\dagger_{\mathbf{p},\alpha} \Bigg[\frac{1}{N}\sum_{\mathbf{r},\mathbf{r}'} e^{i(\mathbf{p}\mathbf{r}-\mathbf{p}'\mathbf{r}')} \left\{ J^{\text{iso}}_{\mathbf{r},\mathbf{r}'}\delta_{\alpha\alpha'} - iJ^D_{|\mathbf{r}-\mathbf{r}'|}\ \hat{\mathbf{z}}\cdot\left([\mathbf{r}-\mathbf{r}']\times\boldsymbol{\sigma}_{\alpha\alpha'}\right)\right\} \\ +h^a g^{ab}_{\{\boldsymbol{\eta}\}}\sigma^b_{\alpha\alpha'}\delta_{\mathbf{p},\mathbf{p}'}\Bigg]\,\psi_{\mathbf{p}',\alpha'} \end{aligned} \tag{4.125}$$

Now we assume

$$J^{\text{iso}}_{\mathbf{r},\mathbf{r}'} \longrightarrow J_{\text{iso}}\ \mathbb{1}_{\mathbf{r},\mathbf{r}'\ \text{n.n.}}, \tag{4.126}$$

$$J^D_{|\boldsymbol{\eta}|} \longrightarrow J_D\ \mathbb{1}_{\boldsymbol{\eta}\ \text{n.n.}}, \tag{4.127}$$

$$\chi^0_{|\mathbf{r}-\mathbf{r}'|} \longrightarrow \chi_0\ \mathbb{1}_{\mathbf{r},\mathbf{r}'\ \text{n.n.}}. \tag{4.128}$$

Note also that as long as only the hamiltonian in the undistorted lattice, H^0_ψ, is considered, we may just as well consider $g_{\{\mathbf{r}-\mathbf{r}''\}} \to g_0$ as a constant tensor. Indeed the set of vectors $\{\mathbf{r}-\mathbf{r}''\}$ is constant, and simply given by the definition of the undistorted lattice. Consequently,

$$\begin{aligned} H^0_\psi = -\frac{1}{4}\sum_{\mathbf{r}}\sum_{\boldsymbol{\eta}} \psi^\dagger_{\mathbf{r},\alpha}\Big[\delta_{\boldsymbol{\eta}} h^a g^{ab}_0 \sigma^b_{\alpha\beta} \\ +\mathbb{1}_{\boldsymbol{\eta}\ \text{n.n.}}\left\{J_{\text{iso}}\delta_{\alpha\beta} + iJ_D\ \hat{\mathbf{z}}\cdot(\boldsymbol{\eta}\times\boldsymbol{\sigma}_{\alpha\beta})\right\}\chi_0\Big]\psi_{\mathbf{r}+\boldsymbol{\eta},\beta} \end{aligned} \tag{4.129}$$

where $\sum_{\boldsymbol{\eta}}$ spans the entire lattice and $\mathbb{1}_{\boldsymbol{\eta}\ \text{n.n.}}$ is 1 if $\boldsymbol{\eta}$ is a nearest-neighbor vector, 0 otherwise, and

$$\begin{aligned} H^0_\psi = -\frac{1}{4}\sum_{\mathbf{p}} \psi^\dagger_{\mathbf{p},\alpha}\Big[h^a g^{ab}_0 \sigma^b_{\alpha\beta} \\ +\sum_{\boldsymbol{\eta}\ \text{n.n.}} e^{-i\mathbf{p}\boldsymbol{\eta}}\left\{J_{\text{iso}}\delta_{\alpha\beta} + iJ_D\ \hat{\mathbf{z}}\cdot(\boldsymbol{\eta}\times\boldsymbol{\sigma}_{\alpha\beta})\right\}\Big]\psi_{\mathbf{p},\beta} \end{aligned} \tag{4.130}$$

in reciprocal space.

4.H Phonons coupled to an electric field : details

Hereabove, we considered the coupling of phonons to fermions, which can be charged under a certain $U(1)$ gauge field – be it the usual electromagnetism if the fermions are electrons, or an emergent gauge field enforcing some local population constraint. Yet we have not considered the field line (or Aharonov-Bohm phase) accumulated by the fermions as they move. Cases where this can no longer be neglected, and the physics becomes that of charged fermions in an electromagnetic field, are not considered in this paper.

Meanwhile, the gauge field can still couple to the *phonons*, and contribute to the phonon scattering rates. In this section, we compute the latter in the case of the emergent electric field in a spinon Fermi surface spin liquid. We find the diagonal scattering rate Eqs.(4.37).

4.H.1 Definitions

We use the definition of the strain tensor in terms of phonon operators:

$$\begin{aligned}\mathcal{E}^{bc}(\tau,\mathbf{r}) = \frac{i}{2}\sum_{\mathbf{k}n}\sqrt{\frac{\hbar/N_{\rm uc}}{2M\omega_{\mathbf{k}n}}}\left(k^b\varepsilon^c_{n\mathbf{k}}+k^c\varepsilon^b_{n\mathbf{k}}\right)\\ \times\left(a_{\mathbf{k}n}\,e^{-\omega_{n\mathbf{k}}\tau}+a^\dagger_{-\mathbf{k}n}e^{\omega_{n\mathbf{k}}\tau}\right)e^{i\mathbf{k}\cdot\mathbf{r}}.\end{aligned} \tag{4.131}$$

The electric field is

$$\begin{aligned}E_a(\mathbf{r},\tau) = \partial_0 A_a(\mathbf{r},\tau)-\partial_a A_0(\mathbf{r},\tau)\\ =\frac{1}{\sqrt{N_{\rm uc}}}\frac{1}{\beta}\sum_{\mathbf{k}}\sum_{i\omega_p}\left(\omega_p A^a_{\mathbf{k},i\omega_p}-ik_aA^0_{\mathbf{k},i\omega_p}\right)e^{i(\mathbf{k}\mathbf{r}-\omega_p\tau)}\end{aligned} \tag{4.132}$$

4.H.2 Model of interaction

We start with a generic coupling hamiltonian between the electric field and the strain tensor:

$$H_{\mathcal{E}E}=\sum_{\mathbf{r}}\sum_{a,b,c}\lambda_{a;bc}\big[\partial_0A_a(\tau,\mathbf{r})-\partial_aA_0(\tau,\mathbf{r})\big]\mathcal{E}_{bc}(\tau,\mathbf{r})\Big|_{\tau=0} \tag{4.133}$$

where $a,b,c\in\{x,y,z\}$ and $\partial_0=i\partial_\tau$ – we use imaginary time conventions for later convenience. The constant $\lambda_{a;bc}$ is the intensity of the coupling; its first coordinate transforms as a vector, the last two transform as a symmetric tensor.

Note that such a coupling assumes the breaking of inversion, since an electric field is inversion-odd. Meanwhile, we do not consider a coupling involving the emergent *magnetic* field. Indeed the latter, being time-reversal odd, cannot couple directly to the strain tensor but only to the lattice momentum, which is not considered in this paper (recall the discussion in Sec. 4.B.1).

By definition,

$$\boldsymbol{A}(\tau,\mathbf{r})=\frac{1}{\sqrt{N_{\rm uc}}}\sum_{\mathbf{k}}\frac{1}{\beta}\sum_{i\omega_p}e^{-i\omega_p\tau}\boldsymbol{A}_{\mathbf{k},i\omega_p}e^{i\mathbf{k}\mathbf{r}} \tag{4.134}$$

Now, we consider that the space component of the vector potential is in-plane and parameterized by

$$A^a_{\mathbf{k},i\omega_p} = A^{\parallel}_{\mathbf{k},i\omega_p}\frac{k^a}{|\underline{\mathbf{k}}|} + A^{\perp}_{\mathbf{k},i\omega_p}\sum_{b=x,y}\epsilon_{zba}\frac{k^b}{|\underline{\mathbf{k}}|}, \tag{4.135}$$

for $a = x, y$. Fixing the Coulomb gauge, one then has $A^{\parallel}_{\mathbf{k},i\omega_p} = 0$. Thus the phonons are coupled to

$$\begin{aligned} Q^+_{\mathbf{k}n} = &\frac{1}{2\sqrt{N_{\rm uc}}}\sum_{abc}\frac{i\,\lambda_{a;bc}}{\sqrt{2M_{\rm uc}\omega_{n\mathbf{k}}}}\left[(\varepsilon^b_{n\mathbf{k}})^* k_c + (\varepsilon^c_{n\mathbf{k}})^* k_b\right] \\ &\times\Big(\sum_d \epsilon^{azd}\frac{k_d}{|\underline{\mathbf{k}}|}\,\partial_0 A^{\perp}_{\mathbf{k}}(0) - ik_a A^0_{\mathbf{k}}(0)\Big). \end{aligned} \tag{4.136}$$

4.H.3 Dynamics and correlations of the gauge field

4.H.3.1 Definitions

The low-energy theory of the electric field is given in this gauge by $\mathcal{S}_A = \mathcal{S}_{A^\perp} + \mathcal{S}_{A^0}$, with

$$\mathcal{S}_{A^\perp} = \frac{1}{2}\sum_{i\omega_p}\sum_{\mathbf{k}} A^{\perp}_{\mathbf{k},i\omega_p}\left(\gamma\frac{|\omega_p|}{|\underline{\mathbf{k}}|} + \chi\underline{\mathbf{k}}^2\right)A^{\perp}_{-\mathbf{k},-i\omega_p}, \tag{4.137}$$

$$\mathcal{S}_{A^0} = \frac{1}{2}\sum_{i\omega_p}\sum_{\mathbf{k}} A^{0}_{\mathbf{k},i\omega_p}\frac{-m_s}{2\pi}\left(1 - \frac{|\omega_p|}{v_F|\underline{\mathbf{k}}|}\right)A^{0}_{-\mathbf{k},-i\omega_p}, \tag{4.138}$$

where $\gamma = \frac{2\overline{n}}{k_F}$ with $\overline{n}$ the spinon density, $\chi = \frac{1}{24\pi m_s}$ the spinon gas diamagnetic susceptibility and m_s the spinon effective mass. [Ioffe and Larkin, 1989] The action Eqs.(4.137), (4.138) provides an accurate description of the gauge field dynamics in the limit where $\frac{|\omega_p|}{v_F|\mathbf{k}|} \ll 1$. [Kim et al., 1994]

4.H.3.2 Correlations and results for $A^\perp$

From the definition of the euclidean action, Eq. (4.137), the Matsubara Green's function for the transverse $A^\perp$ component is

$$\mathcal{G}_{A^\perp}(\mathbf{k}, i\omega_p) = -\left(\gamma\frac{|\omega_p|}{|\underline{\mathbf{k}}|} + \chi\underline{\mathbf{k}}^2\right)^{-1}. \tag{4.139}$$

From it, we can deduce the retarded and advanced Green's functions, obtained by replacing $i\omega_p \to \omega \pm i0^+$ in $\mathcal{G}_{A^\perp}(\mathbf{k}, i\omega_p)$ written as a function holomorphic in the corresponding complex half-plane:

$$G^{\rm R/A}_{A^\perp}(\mathbf{k}, \omega) = -\left(\mp i\gamma\frac{\omega}{|\underline{\mathbf{k}}|} + \chi\underline{\mathbf{k}}^2\right)^{-1}. \tag{4.140}$$

The combination $i\left(G^{\rm A}_{A^\perp}(\mathbf{k}, \omega_{n\mathbf{k}}) - G^{\rm R}_{A^\perp}(\mathbf{k}, \omega_{n\mathbf{k}})\right)$, explicitly

$$\int {\rm d}t e^{-i\omega_{n\mathbf{k}}t}\langle[A^\perp_{\mathbf{k}}(t), A^\perp_{-\mathbf{k}}(0)]\rangle = \frac{-2\frac{\gamma}{|\underline{\mathbf{k}}|}\omega_{n\mathbf{k}}}{(\chi\underline{\mathbf{k}}^2)^2 + (\frac{\gamma}{|\underline{\mathbf{k}}|})^2\omega^2_{n\mathbf{k}}}, \tag{4.141}$$

is of particular importance, being directly involved in $D^{(1),A^\perp}_{n\mathbf{k}}$ given in the main text.

4.H.3.3 Correlations and results for A^0

From the definition of the euclidean action, Eq. (4.138), the Matsubara Green's function for the A^0 time component is

$$\mathcal{G}_{A^0}(\mathbf{k}, i\omega_p) = \frac{2\pi}{m_s}\left(1 - \frac{|\omega_p|}{v_F|\underline{\mathbf{k}}|}\right)^{-1}. \tag{4.142}$$

From it, we can deduce the retarded and advanced Green's functions,

$$G^{\mathrm{R/A}}_{A^0}(\mathbf{k}, \omega) = \frac{2\pi}{m_s}\left(1 \pm \frac{i\omega}{v_F|\underline{\mathbf{k}}|}\right)^{-1}, \tag{4.143}$$

then follow the same steps as in the previous subsection, leading to $D^{(1),A^0}_{n\mathbf{k}}$ as given in the main text.

4.H.4 Summary of the results

Here, we only compute the contribution to the diagonal scattering rate (i.e. to the longitudinal conductivity) since $H_{\mathcal{E}E}$ does not break time reversal and therefore the corresponding contribution to the Hall conductivity is vanishing.

The result is $D^{(1),A}_{n\mathbf{k}} = D^{(1),A^\perp}_{n\mathbf{k}} + D^{(1),A^0}_{n\mathbf{k}}$ with

$$D^{(1),A^\perp}_{n\mathbf{k}} = \frac{\gamma\omega^2_{n\mathbf{k}} M^{-1}_{\mathrm{uc}}|\underline{\mathbf{k}}|^{-3}}{\chi^2|\underline{\mathbf{k}}|^4 + \gamma^2\frac{\omega^2_{n\mathbf{k}}}{|\underline{\mathbf{k}}|^2}} \left|\sum_{a;b,c} \epsilon^{za\overline{a}} k_a \lambda_{\overline{a};bc}\varepsilon^b_{n\mathbf{k}} k^c\right|^2, \tag{4.144}$$

$$D^{(1),A^0}_{n\mathbf{k}} = \frac{M^{-1}_{\mathrm{uc}}\omega^{-1}_{n\mathbf{k}}\ 2\pi/m_s}{\frac{v_F|\underline{\mathbf{k}}|}{\omega_{n\mathbf{k}}} + \frac{\omega_{n\mathbf{k}}}{v_F|\underline{\mathbf{k}}|}} \left|\sum_{a;b,c} k_a \lambda_{a;bc}\varepsilon^b_{n\mathbf{k}} k^c\right|^2, \tag{4.145}$$

where $a \in \{x, y\}$, $a = x \Leftrightarrow \overline{a} = y$ and $b, c \in \{x, y, z\}$.

In the small momentum limit, $|\underline{\mathbf{k}}| \ll \sqrt{c_{\mathrm{ph}}\gamma/\chi}$, one finds the scaling $D^{(1),A^\perp}_{n\mathbf{k}} \sim k^3$, while in the "less small" momentum limit, $\sqrt{c_{\mathrm{ph}}\gamma/\chi} \ll |\underline{\mathbf{k}}| \ll k_F$, one finds $D^{(1),A^\perp}_{n\mathbf{k}} \sim k^{-1}$. Besides, $D^{(1),A^0}_{n\mathbf{k}} \sim k^3$.

Note that the time component is screened, while the transverse component is Landau-damped; therefore at low momentum these have the same scaling behavior.

4.I Scaling and orders of magnitude

In this section, we summarize the parameter and temperature scalings of the phonons' longitudinal conductivity and thermal resistivity in a spin liquid with a Fermi surface of $d = 2$-dimensional spinons and an emergent electric field. The form of the phonon-fermion couplings is that of App. 4.E. We recall the

momentum scalings of the scattering rates, first derived generally in App. 4.D and then specified in the given model we study in Sec. 4.I.2. We also include the coupling to the emergent electric field, considered in App. 4.H.

The resulting scalings of physical quantities such as κ_L and ϱ_H are summarized in Table 4.9.1 in the main text.

4.I.1 Parameter scalings away from the specific cases

Starting from each of the specific cases identified in Sec. 4.F.2, we turn slightly off zero all the null parameters in the corresponding line of Tab. 4.7.2. By inspection of Eq. (4.101), we extract the leading-order contributions which break the symmetry relation identified in Sec. 4.F.2 for the said specific case.

We find that the effective skew-scattering rate $\mathfrak{W}^{\ominus,\mathrm{eff}}$ features a combination of at least two small parameters among $\mathsf{h}^a, \mathsf{u}^a, \alpha^{\mathrm{R}}$ in the following way:

$$\begin{aligned}&\mathfrak{W}^{\ominus,\mathrm{eff},qq'}_{n\mathbf{k}n'\mathbf{k}'} \propto \mathcal{O}(\mathsf{t}^0)^3 \times \\ &\mathcal{O}\left(\alpha^{\mathrm{R}}\left(\mathsf{u}^z + \mathsf{u}^{x,y} + \mathsf{h}^z\mathsf{t}^0 + \mathsf{h}^{x,y}\mathsf{t}^0\right)\right. \\ &\left. + \mathsf{u}^{x,y}\mathsf{h}^z\mathsf{h}^{x,y} + \mathsf{u}^z(\mathsf{h}^{x,y})^2 + \mathsf{h}^z\mathsf{v}^{x,y} + \mathsf{h}^{x,y}\mathsf{v}^{x,y}\right)\end{aligned} \tag{4.146}$$

Note that all terms in the first $\mathcal{O}(\dots)$ have the same structure: they are all time-reversal-odd (i.e. they contain an odd number of h or u factors), as befits a contribution to the effective skew-scattering rate; they all contain either one t^0 or one u or one v coefficient arising from magnetic exchange spatial derivatives; they all contain at least one off-diagonal (in spin $\sigma =\uparrow,\downarrow$ space) coefficient among $\mathsf{h}^{x,y}, \mathsf{u}^{x,y}, \mathsf{v}^{x,y}, \alpha^{\mathrm{R}}$.

4.I.2 Scaling results from the phonon-fermion coupling

The scalings of the diagonal and skew scattering rates, in the case of a $d = 2$ spinon Fermi surface with quadratic spinons (with effective mass $m_*^{-1} \sim \mathfrak{a}^2 J^0$ and Fermi velocity $v_F \sim \mathfrak{a} J^0$), were derived in Sec. 4.D.2.

4.I.2.1 Diagonal scattering rate

The coupling coefficient $\mathcal{B}^{n,\ell\ell'}_{\mathbf{p};\mathbf{k}}$ appearing in $D_{n\mathbf{k}}$ is dominated by the contribution of t^0, so that $\mathcal{B}(k) \sim k^{1/2}\mathsf{t}^0$. Consequently, following Eq. (4.20), the parameter and momentum scaling of the diagonal scattering rate is $D^{(1),f}_{n\mathbf{k}} \sim k^1\mathcal{O}(\mathsf{t}^0)^2$.

Note that this is different from the variety of scalings obtained in the case of an ordered antiferromagnet (cf Chapter 3). This is because, in an antiferromagnet, the slow variable, namely the staggered magnetization $\boldsymbol{n}$, and its conjugate momentum, the net magnetization $\boldsymbol{m}$, are expanded in terms of canonical bosons as $\boldsymbol{n}_{\mathbf{p}} \sim \Omega_{\mathbf{p}}^{-1/2} b_{\mathbf{p}}{}^{(\dagger)}$ and $\boldsymbol{m}_{\mathbf{p}} \sim \Omega_{\mathbf{p}}^{1/2} b_{\mathbf{p}}{}^{(\dagger)}$; therefore various powers of momentum appeared in mm, mn and nn terms. Meanwhile, in the present case the spins are simply expressed as $\boldsymbol{S} \sim f^\dagger \boldsymbol{\sigma} f$, thus appearing with no extra powers of momentum in their coupling to phonons.

4.I.2.2 Skew-scattering rate

The various contributions to $\mathfrak{W}^{\ominus,\mathrm{eff}}$ (see above, Sec. 4.I.1.) can scale differently with momentum, because of the momentum dependence of $\boldsymbol{h}$ in the presence of a Rashba coupling. The dominant contribution at low temperatures (which has the smallest power of momentum) comes from cases where $\alpha^{\mathrm{R}} = 0$ and $\mathsf{v}^{x,y} = 0$, for which all four coefficients scale like $\mathcal{B}(k) \sim k^{1/2}$. A crossover occurs at momentum $k \approx \mathsf{u}/(\alpha^{\mathrm{R}}\mathsf{t}^0\mathsf{h})$, above which one of the four $\mathcal{B}$ factors scales like $\mathcal{B}(k) \sim k^{3/2}$; we note this $\mathcal{B}(k) \sim k^{\gamma+1/2}$, where $\gamma = 0, 1$ indexes the two behaviors.

Consequently, following Eq. (4.79), the momentum scaling is $\mathfrak{W}^{\ominus,\mathrm{eff},qq'}_{n\mathbf{k}n'\mathbf{k}'} \sim k^{\gamma+1-2\lambda}$. This means for the inverse skew-scattering time

$$\frac{1}{\tau_{\mathrm{skew}}} \sim k^3 \mathfrak{W}^{\ominus,\mathrm{eff},qq'}_{n\mathbf{k}n'\mathbf{k}'} \sim k^{4-2\lambda+\gamma} \tag{4.147}$$

with

$$\begin{cases} \lambda = 0 & \text{for } \Delta\mu \ll (k_B T/v_F)^2/m_* \\ \lambda = 1 & \text{for } \Delta\mu \gg (k_B T/v_F)^2/m_* \\ \gamma = 0 & \text{for } k < \mathsf{u}/(\alpha^{\mathrm{R}}\mathsf{t}^0\mathsf{h}) \\ \gamma = 1 & \text{for } k > \mathsf{u}/(\alpha^{\mathrm{R}}\mathsf{t}^0\mathsf{h}) \end{cases}. \tag{4.148}$$

4.I.3 Scaling of $\kappa_L(T)$

The longitudinal scattering rate appearing in the general formula for κ_L, Eq. (4.2), which identifies with the inverse typical scattering time τ^{-1}, is the sum of different contributions:

$$D_{n\mathbf{k}} = D^{(1),f}_{n\mathbf{k}} + D^{(1),A}_{n\mathbf{k}} + \breve{D}_{n\mathbf{k}}, \tag{4.149}$$

following Matthiessen's rule [Callaway, 1959]. Here $D^{(1),f}_{n\mathbf{k}}$ and $D^{(1),A}_{n\mathbf{k}}$ are the phonon scattering rates due to their coupling to the fermion bilinears and to the electric field, respectively. Their temperature scaling for typical thermal momenta, such that we may replace $\omega_k \sim v_{\mathrm{ph}} k \sim k_B T$, are $D^{(1),f}_{n\mathbf{k}} \sim T^1$ and $D^{(1),A}_{n\mathbf{k}} \sim T^3$. As already mentioned, $\breve{D}_{n\mathbf{k}}$ is an extra contribution due to other scattering processes, which we consider here to scale like a constant, as results from e.g. boundary scattering. We summarize these different scalings with $\tau^{-1} \sim T^\delta$ where $\delta = 0, 1, 3$.

Using these scalings in Eq. (4.2) which has the form $\kappa_L \sim \frac{1}{T^2}\int d^3k \frac{k^2}{D(k)} F(\frac{k}{T})$ for a generic function F, we obtain the scaling for the phonons' longitudinal thermal conductivity in a spinon Fermi surface spin liquid with quadratic dispersion:

$$\frac{\kappa_L}{T} \sim \frac{T^2}{C_{\mathrm{b}} + C_f T + C_A T^3} \tag{4.150}$$

where C_{b}, C_f and C_A are dimensionful parameters corresponding to the scattering of phonons on boundaries, spinon-hole pairs, and electric field excitations, respectively. In terms of scaling law, $\kappa_L \sim T^{3-\delta}$.

4.I.4 Scaling of $\varrho_H(T)$

As we emphasized in Chapter 2, the thermal Hall resistivity ϱ_H is a much better measure of phonon chirality than the thermal Hall conductivity κ_H, in that its temperature scaling coincides with the momentum scaling of the skew-scattering rate $\mathfrak{W}^{\ominus,\text{eff}}$. A consequence of this is that the phonons' coupling to the electric field does not contribute to ϱ_H, while it does contribute to $\kappa_H \propto \mathfrak{W}^{\ominus,\text{eff}}/D^2$ through the diagonal scattering rate D. Therefore, in a spinon Fermi surface spin liquid described by the model hereabove, we expect

$$\varrho_{\text{H}}(T) \sim T^{\gamma+1-2\lambda}, \tag{4.151}$$

due entirely to the phonon-spinons coupling.

Bibliography

[Abragam and Bleaney, 1970] Abragam, A. and Bleaney, B. (1970). *Electron paramagnetic resonance of transition ions*. Clarendon, Oxford.

[Abrikosov et al., 1976] Abrikosov, A., Gorkov, L., and Dzyaloshinski, I. (1976). *Methods of quantum field theory in statistical physics*. Dover Publications Inc.

[Abrikosov, 1965] Abrikosov, A. A. (1965). Electron scattering on magnetic impurities in metals and anomalous resistivity effects. *Physics Physique Fizika*, 2:5–20.

[Akazawa et al., 2020] Akazawa, M., Shimozawa, M., Kittaka, S., Sakakibara, T., Okuma, R., Hiroi, Z., Lee, H.-Y., Kawashima, N., Han, J. H., and Yamashita, M. (2020). Thermal hall effects of spins and phonons in kagome antiferromagnet cd-kapellasite. *Phys. Rev. X*, 10:041059.

[Akkermans and Montambaux, 2007] Akkermans, E. and Montambaux, G. (2007). *Mesoscopic physics of electrons and photons*. Cambridge University Press.

[Ament et al., 2011] Ament, L. J. P., van Veenendaal, M., Devereaux, T. P., Hill, J. P., and van den Brink, J. (2011). Resonant inelastic x-ray scattering studies of elementary excitations. *Rev. Mod. Phys.*, 83:705–767.

[Anderson, 1952] Anderson, P. W. (1952). An approximate quantum theory of the antiferromagnetic ground state. *Physical Review*, 86(5):694.

[Anderson, 1959] Anderson, P. W. (1959). New approach to the theory of superexchange interactions. *Physical Review*, 115(1):2.

[Anderson, 1973] Anderson, P. W. (1973). Resonating valence bonds: A new kind of insulator? *Materials Research Bulletin*, 8(2):153–160.

[Ashcroft and Mermin, 1976] Ashcroft, N. and Mermin, N. (1976). *Solid state physics*. Saunders College Publishing.

[Atkins and de Paula, 2014] Atkins, P. and de Paula, J. (2014). *Atkins' physical chemistry*. Oxford university press.

[Auerbach, 1994] Auerbach, A. (1994). *Interacting electrons and quantum magnetism*. Springer.

[Auerbach and Arovas, 2011] Auerbach, A. and Arovas, D. P. (2011). Schwinger bosons approaches to quantum antiferromagnetism. *Introduction to Frustrated Magnetism*, pages 365–377.

[Balents, 2010] Balents, L. (2010). Spin liquids in frustrated magnets. *Nature*, 464(7286):199–208.

[Bardeen et al., 1957] Bardeen, J., Cooper, L. N., and Schrieffer, J. R. (1957). Theory of superconductivity. *Physical review*, 108(5):1175.

[Barkeshli et al., 2012] Barkeshli, M., Chung, S. B., and Qi, X.-L. (2012). Dissipationless phonon hall viscosity. *Physical Review B*, 85(24):245107.

[Bartsch and Brenig, 2013] Bartsch, C. and Brenig, W. (2013). Thermal drag in spin ladders coupled to phonons. *Phys. Rev. B*, 88:214412.

[Baskaran and Anderson, 1988] Baskaran, G. and Anderson, P. W. (1988). Gauge theory of high-temperature superconductors and strongly correlated fermi systems. *Physical Review B*, 37(1):580.

[Baym, 1969] Baym, G. (1969). *Lectures on quantum mechanics*. Taylor & Francis.

[Baym and Kadanoff, 1961] Baym, G. and Kadanoff, L. P. (1961). Conservation laws and correlation functions. *Phys. Rev.*, 124:287–299.

[Bazhenov et al., 1996] Bazhenov, A., Rezchikov, C., and Smirnova, I. (1996). Lattice dynamics of the La_2CuO_4 cmca orthorhombic phase at $\kappa = 0$. *Physica C: Superconductivity*, 273(1):9–20.

[Benfatto and Silva Neto, 2006] Benfatto, L. and Silva Neto, M. B. (2006). Field dependence of the magnetic spectrum in anisotropic and dzyaloshinskii-moriya antiferromagnets. i. theory. *Phys. Rev. B*, 74:024415.

[Berezinskii, 1971] Berezinskii, V. (1971). Destruction of long-range order in one-dimensional and two-dimensional systems having a continuous symmetry group i. classical systems. *Sov. Phys. JETP*, 32(3):493–500.

[Berezinskii, 1972] Berezinskii, V. (1972). Destruction of long-range order in one-dimensional and two-dimensional systems possessing a continuous symmetry group. ii. quantum systems. *Sov. Phys. JETP*, 34(3):610–616.

[Bethe, 1931] Bethe, H. (1931). Zur theorie der metalle. *Zeitschrift für Physik*, 71(3):205–226.

[Bloch, 1929] Bloch, F. (1929). Über die quantenmechanik der elektronen in kristallgittern. *Zeitschrift für physik*, 52(7):555–600.

[Bloch, 1930] Bloch, F. (1930). Zum elektrischen widerstandsgesetz bei tiefen temperaturen. *Zeitschrift für Physik*, 59(3):208–214.

[Boulanger et al., 2020] Boulanger, M.-E., Grissonnanche, G., Badoux, S., Allaire, A., Lefrançois, É., Legros, A., Gourgout, A., Dion, M., Wang, C., Chen, X., et al. (2020). Thermal hall conductivity in the cuprate mott insulators nd2cuo4 and sr2cuo2cl2. *Nature communications*, 11(1):1–9.

[Boulanger et al., 2022] Boulanger, M.-E., Grissonnanche, G., Lefrançois, É., Gourgout, A., Xu, K.-J., Shen, Z.-X., Greene, R. L., and Taillefer, L. (2022). Thermal hall conductivity of electron-doped cuprates. *Physical Review B*, 105(11):115101.

[Bourgeois-Hope et al., 2019] Bourgeois-Hope, P., Laliberté, F., Lefrançois, E., Grissonnanche, G., de Cotret, S. R., Gordon, R., Kitou, S., Sawa, H., Cui, H., Kato, R., Taillefer, L., and Doiron-Leyraud, N. (2019). Thermal conductivity of the quantum spin liquid candidate etme$_3$Sb[Pd(dmit)$_2$]$_2$: No evidence of mobile gapless excitations. *Phys. Rev. X*, 9:041051.

[Bruin et al., 2022a] Bruin, J., Claus, R., Matsumoto, Y., Kurita, N., Tanaka, H., and Takagi, H. (2022a). Robustness of the thermal hall effect close to half-quantization in α-rucl3. *Nature Physics*, 18(4):401–405.

[Bruin et al., 2022b] Bruin, J. A. N., Claus, R. R., Matsumoto, Y., Nuss, J., Laha, S., Lotsch, B. V., Kurita, N., Tanaka, H., and Takagi, H. (2022b). Origin of oscillatory structures in the magnetothermal conductivity of the putative kitaev magnet α-rucl$_3$.

[Bruus and Flensberg, 2004] Bruus, H. and Flensberg, K. (2004). *Many-Body Quantum Theory in Condensed Matter Physics*. Oxford Graduate Texts.

[Buttiker, 1988] Buttiker, M. (1988). Symmetry of electrical conduction. *IBM Journal of Research and Development*, 32(3):317–334.

[Callaway, 1959] Callaway, J. (1959). Model for lattice thermal conductivity at low temperatures. *Phys. Rev.*, 113:1046–1051.

[Callen, 1985] Callen, H. B. (1985). *Thermodynamics and an introduction to thermostatistics*. Wiley, New York.

[Carruthers, 1961] Carruthers, P. (1961). Theory of thermal conductivity of solids at low temperatures. *Rev. Mod. Phys.*, 33:92–138.

[Casimir, 1938] Casimir, H. (1938). Note on the conduction of heat in crystals. *Physica*, 5(6):495–500.

[Casimir, 1945] Casimir, H. B. G. (1945). On onsager's principle of microscopic reversibility. *Rev. Mod. Phys.*, 17:343–350.

[Chaikin et al., 1995] Chaikin, P. M., Lubensky, T. C., and Witten, T. A. (1995). *Principles of condensed matter physics*, volume 10. Cambridge University Press.

[Chen et al., 2020] Chen, J.-Y., Kivelson, S. A., and Sun, X.-Q. (2020). Enhanced thermal hall effect in nearly ferroelectric insulators. *Phys. Rev. Lett.*, 124:167601.

[Chen et al., 2021] Chen, L., Boulanger, M.-E., Wang, Z.-C., Tafti, F., and Taillefer, L. (2021). Large phonon thermal hall conductivity in a simple antiferromagnetic insulator.

[Chen and Su, 1989] Chen, L.-Y. and Su, Z.-B. (1989). Quantum boltzmann equation and kubo formula for electronic transport in solids. *Physical Review B*, 40(13):9309.

[Chen et al.,] Chen, X., Iaconis, J., Balents, L., and Savary, L. Scaling and methodology for thermal conductivity in quantum magnets. *to appear*.

[Chernyshev and Brenig, 2015] Chernyshev, A. L. and Brenig, W. (2015). Thermal conductivity in large-J two-dimensional antiferromagnets: Role of phonon scattering. *Phys. Rev. B*, 92:054409.

[Chowdhury et al., 2021] Chowdhury, D., Georges, A., Parcollet, O., and Sachdev, S. (2021). Sachdev-ye-kitaev models and beyond: A window into non-fermi liquids. *arXiv preprint arXiv:2109.05037*.

[Christensen et al., 2007] Christensen, N. B., Rønnow, H. M., McMorrow, D. F., Harrison, A., Perring, T. G., Enderle, M., Coldea, R., Regnault, L. P., and Aeppli, G. (2007). Quantum dynamics and entanglement of spins on a square lattice. *Proceedings of the National Academy of Sciences*, 104(39):15264–15269.

[Cohen-Tannoudji et al., 1997] Cohen-Tannoudji, C., Dupont-Roc, J., and Grynberg, G. (1997). *Photons and Atoms-Introduction to Quantum Electrodynamics*. Wiley.

[Coleman, 2015] Coleman, P. (2015). *Introduction to many-body physics*. Cambridge University Press.

[Cottam, 1974] Cottam, M. G. (1974). Spin-phonon interactions in a Heisenberg antiferromagnet. II. The phonon spectrum and spin-lattice relaxation rate. *Journal of Physics C: Solid State Physics*, 7(16):2919–2932.

[Czajka et al., 2022] Czajka, P., Gao, T., Hirschberger, M., Lampen-Kelley, P., Banerjee, A., Quirk, N., Mandrus, D. G., Nagler, S. E., and Ong, N. P. (2022). The planar thermal hall conductivity in the kitaev magnet α-rucl3.

[Czajka et al., 2021] Czajka, P., Gao, T., Hirschberger, M., Lampen-Kelley, P., Banerjee, A., Yan, J., Mandrus, D. G., Nagler, S. E., and Ong, N. (2021). Oscillations of the thermal conductivity in the spin-liquid state of α-rucl3. *Nature Physics*, 17(8):915–919.

[Dalla Piazza et al., 2015] Dalla Piazza, B., Mourigal, M., Christensen, N. B., Nilsen, G., Tregenna-Piggott, P., Perring, T., Enderle, M., McMorrow, D. F., Ivanov, D., and Rønnow, H. M. (2015). Fractional excitations in the square-lattice quantum antiferromagnet. *Nature Physics*, 11(1):62–68.

[De Groot and Mazur, 1984] De Groot, S. R. and Mazur, P. (1984). *Non-equilibrium thermodynamics*. Dover Publications.

[De Haas et al., 1934] De Haas, W., De Boer, J., and Van den Berg, G. (1934). The electrical resistance of gold, copper and lead at low temperatures. *Physica*, 1(7-12):1115–1124.

[Doki et al., 2018] Doki, H., Akazawa, M., Lee, H.-Y., Han, J. H., Sugii, K., Shimozawa, M., Kawashima, N., Oda, M., Yoshida, H., and Yamashita, M. (2018). Spin thermal hall conductivity of a kagome antiferromagnet. *Phys. Rev. Lett.*, 121:097203.

[Drude, 1900] Drude, P. (1900). Zur elektronentheorie der metalle. *Annalen der Physik*, 306(3):566–613.

[Eliashberg, 1962] Eliashberg, G. (1962). Transport equation for a degenerate system of fermi particles. *Sov. Phys. JETP*, 14:886–892.

[Evans and Steer, 1996] Evans, T. and Steer, D. (1996). Wick's theorem at finite temperature. *Nuclear Physics B*, 474(2):481–496.

[Feng et al., 2022] Feng, K., Swarup, S., and Perkins, N. B. (2022). Footprints of kitaev spin liquid in the fano lineshape of raman-active optical phonons. *Phys. Rev. B*, 105:L121108.

[Feng et al., 2021] Feng, K., Ye, M., and Perkins, N. B. (2021). Temperature evolution of the phonon dynamics in the kitaev spin liquid. *Phys. Rev. B*, 103:214416.

[Ferrari et al., 2021] Ferrari, F., Valentí, R., and Becca, F. (2021). Effects of spin-phonon coupling in frustrated heisenberg models. *Phys. Rev. B*, 104:035126.

[Flebus and MacDonald, 2021] Flebus, B. and MacDonald, A. (2021). Charged defects and phonon Hall effects in ionic crystals. *arXiv preprint arXiv:2106.13889*.

[Forster, 1975] Forster, D. (1975). *Hydrodynamic fluctuations, broken symmetry, and correlation functions*. Benjamin Cummings.

[Fourier et al., 1822] Fourier, J. B. J., Darboux, G., et al. (1822). *Théorie analytique de la chaleur*, volume 504. Didot Paris.

[Fradkin, 2013] Fradkin, E. (2013). *Field theories of condensed matter physics*. Cambridge University Press.

[Franz and Wiedemann, 1853] Franz, R. and Wiedemann, G. (1853). Ueber die wärme-leitungsfähigkeit der metalle. *Annalen der Physik*, 165(8):497–531.

[Fröhlich, 1952] Fröhlich, H. (1952). Interaction of electrons with lattice vibrations. *Proceedings of the Royal Society of London. Series A. Mathematical and Physical Sciences*, 215(1122):291–298.

[Gangadharaiah et al., 2010] Gangadharaiah, S., Chernyshev, A. L., and Brenig, W. (2010). Thermal drag revisited: Boltzmann versus Kubo. *Phys. Rev. B*, 82:134421.

[Garrod and Hurley, 1983] Garrod, C. and Hurley, J. (1983). Symmetry relations for the conductivity tensor. *Phys. Rev. A*, 27:1487–1490.

[Georges et al., 1996] Georges, A., Kotliar, G., Krauth, W., and Rozenberg, M. J. (1996). Dynamical mean-field theory of strongly correlated fermion systems and the limit of infinite dimensions. *Reviews of Modern Physics*, 68(1):13.

[Giamarchi, 1991] Giamarchi, T. (1991). Umklapp process and resistivity in one-dimensional fermion systems. *Physical Review B*, 44(7):2905.

[Giuliani and Vignale, 2005] Giuliani, G. and Vignale, G. (2005). *Quantum Theory of the Electron Liquid*. Cambridge University Press.

[Goldstone et al., 1962] Goldstone, J., Salam, A., and Weinberg, S. (1962). Broken symmetries. *Physical Review*, 127(3):965.

[Goodenough, 1955] Goodenough, J. B. (1955). Theory of the role of covalence in the perovskite-type manganites [la, m (ii)] mn o 3. *Physical Review*, 100(2):564.

[Götze and Wölfle, 1972] Götze, W. and Wölfle, P. (1972). Homogeneous dynamical conductivity of simple metals. *Physical Review B*, 6(4):1226.

[Grissonnanche et al., 2019] Grissonnanche, G., Legros, A., Badoux, S., Lefrançois, E., Zatko, V., Lizaire, M., Laliberté, F., Gourgout, A., Zhou, J.-S., Pyon, S., et al. (2019). Giant thermal hall conductivity in the pseudogap phase of cuprate superconductors. *Nature*, 571(7765):376–380.

[Grissonnanche et al., 2020] Grissonnanche, G., Thériault, S., Gourgout, A., Boulanger, M.-E., Lefrançois, E., Ataei, A., Laliberté, F., Dion, M., Zhou, J.-S., Pyon, S., et al. (2020). Chiral phonons in the pseudogap phase of cuprates. *Nature Physics*, 16(11):1108–1111.

[Grüneisen, 1933] Grüneisen, E. (1933). Die abhängigkeit des elektrischen widerstandes reiner metalle von der temperatur. *Annalen der Physik*, 408(5):530–540.

[Guo et al., 2022] Guo, H., Joshi, D. G., and Sachdev, S. (2022). Resonant thermal Hall effect of phonons coupled to dynamical defects. *arXiv preprint arXiv:2201.11681*.

[Guo and Sachdev, 2021] Guo, H. and Sachdev, S. (2021). Extrinsic phonon thermal Hall transport from Hall viscosity. *Physical Review B*, 103(20):205115.

[Hahn, 2005] Hahn, T. (2005). Cuba—a library for multidimensional numerical integration. *Computer Physics Communications*, 168(2):78–95.

[Haldane, 1983a] Haldane, F. D. M. (1983a). Continuum dynamics of the 1-d heisenberg antiferromagnet: Identification with the o (3) nonlinear sigma model. *Physics letters a*, 93(9):464–468.

[Haldane, 1983b] Haldane, F. D. M. (1983b). Nonlinear field theory of large-spin heisenberg antiferromagnets: semiclassically quantized solitons of the one-dimensional easy-axis néel state. *Physical review letters*, 50(15):1153.

[Han and Lee, 2017] Han, J. H. and Lee, H. (2017). Spin chirality and hall-like transport phenomena of spin excitations. *Journal of the Physical Society of Japan*, 86(1):011007.

[Han et al., 2019] Han, J. H., Park, J.-H., and Lee, P. A. (2019). Consideration of thermal hall effect in undoped cuprates. *Physical Review B*, 99(20):205157.

[Han and Klemens, 1993] Han, Y.-J. and Klemens, P. G. (1993). Anharmonic thermal resistivity of dielectric crystals at low temperatures. *Phys. Rev. B*, 48:6033–6042.

[Hänsch and Mahan, 1983] Hänsch, W. and Mahan, G. (1983). Transport equations for many-particle systems. *Physical Review B*, 28(4):1902.

[Hentrich et al., 2019] Hentrich, R., Roslova, M., Isaeva, A., Doert, T., Brenig, W., Büchner, B., and Hess, C. (2019). Large thermal hall effect in $\alpha-rucl_3$: Evidence for heat transport by kitaev-heisenberg paramagnons. *Phys. Rev. B*, 99:085136.

[Hentrich et al., 2018] Hentrich, R., Wolter, A. U. B., Zotos, X., Brenig, W., Nowak, D., Isaeva, A., Doert, T., Banerjee, A., Lampen-Kelley, P., Mandrus, D. G., Nagler, S. E., Sears, J., Kim, Y.-J., Büchner, B., and Hess, C. (2018). Unusual phonon heat transport in $\alpha-rucl_3$: Strong spin-phonon scattering and field-induced spin gap. *Phys. Rev. Lett.*, 120:117204.

[Hermele et al., 2004] Hermele, M., Senthil, T., Fisher, M. P., Lee, P. A., Nagaosa, N., and Wen, X.-G. (2004). Stability of u (1) spin liquids in two dimensions. *Physical Review B*, 70(21):214437.

[Hirokane et al., 2019] Hirokane, Y., Nii, Y., Tomioka, Y., and Onose, Y. (2019). Phononic thermal hall effect in diluted terbium oxides. *Phys. Rev. B*, 99:134419.

[Hirschberger et al., 2015a] Hirschberger, M., Chisnell, R., Lee, Y. S., and Ong, N. P. (2015a). Thermal hall effect of spin excitations in a kagome magnet. *Physical review letters*, 115(10):106603.

[Hirschberger et al., 2015b] Hirschberger, M., Krizan, J. W., Cava, R., and Ong, N. (2015b). Large thermal hall conductivity of neutral spin excitations in a frustrated quantum magnet. *Science*, 348(6230):106–109.

[Holstein, 1959a] Holstein, T. (1959a). Studies of polaron motion: Part i. the molecular-crystal model. *Annals of Physics*, 8(3):325–342.

[Holstein, 1959b] Holstein, T. (1959b). Studies of polaron motion: Part ii. the "small" polaron. *Annals of Physics*, 8(3):343–389.

[Holstein and Primakoff, 1940] Holstein, T. and Primakoff, H. (1940). Field dependence of the intrinsic domain magnetization of a ferromagnet. *Physical Review*, 58(12):1098.

[Hubbard, 1959] Hubbard, J. (1959). Calculation of partition functions. *Physical Review Letters*, 3(2):77.

[Ideue et al., 2017] Ideue, T., Kurumaji, T., Ishiwata, S., and Tokura, Y. (2017). Giant thermal hall effect in multiferroics. *Nature materials*, 16(8):797–802.

[Ideue et al., 2012] Ideue, T., Onose, Y., Katsura, H., Shiomi, Y., Ishiwata, S., Nagaosa, N., and Tokura, Y. (2012). Effect of lattice geometry on magnon hall effect in ferromagnetic insulators. *Phys. Rev. B*, 85:134411.

[Inyushkin and Taldenkov, 2007] Inyushkin, A. V. and Taldenkov, A. (2007). On the phonon hall effect in a paramagnetic dielectric. *Jetp Letters*, 86(6):379–382.

[Ioffe and Regel, 1960] Ioffe, A. and Regel, A. (1960). Non-crystalline, amorphous and liquid electronic semiconductors. *Prog. Semicond*, 4(89):237–291.

[Ioffe and Larkin, 1989] Ioffe, L. B. and Larkin, A. I. (1989). Gapless fermions and gauge fields in dielectrics. *Phys. Rev. B*, 39:8988–8999.

[Ioselevich and Capellmann, 1995] Ioselevich, A. and Capellmann, H. (1995). Strongly correlated spin-phonon systems: A scenario for heavy fermions. *Physical Review B*, 51(17):11446.

[Kadanoff and Baym, 1962] Kadanoff, L. P. and Baym, G. (1962). *Quantum statistical mechanics: Green's function methods in equilibrium and nonequilibrium problems.* Taylor & Francis.

[Kagan and Maksimov, 2008] Kagan, Y. and Maksimov, L. A. (2008). Anomalous hall effect for the phonon heat conductivity in paramagnetic dielectrics. *Phys. Rev. Lett.*, 100:145902.

[Kaib et al., 2021] Kaib, D. A. S., Biswas, S., Riedl, K., Winter, S. M., and Valentí, R. (2021). Magnetoelastic coupling and effects of uniaxial strain in $\alpha - \mathrm{rucl}_3$ from first principles. *Phys. Rev. B*, 103:L140402.

[Kamenev, 2011] Kamenev, A. (2011). *Field theory of non-equilibrium systems.* Cambridge University Press.

[Kameyama et al., 1973] Kameyama, H., Ishibashi, Y., and Yakagi, Y. (1973). Elastic constants in cupric formate tetrahydrate single crystals. *Journal of the Physical Society of Japan*, 35(5):1450–1455.

[Kanamori, 1959] Kanamori, J. (1959). Superexchange interaction and symmetry properties of electron orbitals. *Journal of Physics and Chemistry of Solids*, 10(2-3):87–98.

[Kasahara et al., 2018a] Kasahara, Y., Ohnishi, T., Mizukami, Y., Tanaka, O., Ma, S., Sugii, K., Kurita, N., Tanaka, H., Nasu, J., Motome, Y., Shibauchi, T., and Matsuda, Y. (2018a). Majorana quantization and half-integer thermal quantum Hall effect in a Kitaev spin liquid. *Nature*, 559(7713):227–231.

[Kasahara et al., 2018b] Kasahara, Y., Sugii, K., Ohnishi, T., Shimozawa, M., Yamashita, M., Kurita, N., Tanaka, H., Nasu, J., Motome, Y., Shibauchi, T., and Matsuda, Y. (2018b). Unusual thermal hall effect in a kitaev spin liquid candidate $\alpha-\mathrm{rucl}_3$. *Phys. Rev. Lett.*, 120:217205.

[Katsura et al., 2010] Katsura, H., Nagaosa, N., and Lee, P. A. (2010). Theory of the thermal hall effect in quantum magnets. *Physical review letters*, 104(6):066403.

[Keldysh et al., 1965] Keldysh, L. V. et al. (1965). Diagram technique for nonequilibrium processes. *Sov. Phys. JETP*, 20(4):1018–1026.

[Kim et al., 1994] Kim, Y. B., Furusaki, A., Wen, X.-G., and Lee, P. A. (1994). Gauge-invariant response functions of fermions coupled to a gauge field. *Physical Review B*, 50(24):17917.

[Kittel, 1953] Kittel, C. (1953). *Solid state physics*. John Wiley and Sons.

[Klemens, 1951] Klemens, P. (1951). The thermal conductivity of dielectric solids at low temperatures (theoretical). *Proceedings of the Royal Society of London. Series A. Mathematical and Physical Sciences*, 208(1092):108–133.

[Klemens, 1955] Klemens, P. (1955). The scattering of low-frequency lattice waves by static imperfections. *Proceedings of the Physical Society. Section A*, 68(12):1113.

[Kohn, 1959] Kohn, W. (1959). Theory of bloch electrons in a magnetic field: the effective hamiltonian. *Physical Review*, 115(6):1460.

[Kolland et al., 2012] Kolland, G., Breunig, O., Valldor, M., Hiertz, M., Frielingsdorf, J., and Lorenz, T. (2012). Thermal conductivity and specific heat of the spin-ice compound $\mathrm{dy_2ti_2o_7}$: Experimental evidence for monopole heat transport. *Phys. Rev. B*, 86:060402.

[Kondo, 1964] Kondo, J. (1964). Resistance minimum in dilute magnetic alloys. *Progress of theoretical physics*, 32(1):37–49.

[Koyama and Nasu, 2021] Koyama, S. and Nasu, J. (2021). Field-angle dependence of thermal hall conductivity in a magnetically ordered kitaev-heisenberg system. *Phys. Rev. B*, 104:075121.

[Krumhansl, 1965] Krumhansl, J. A. (1965). Thermal conductivity of insulating crystals in the presence of normal processes. *Proceedings of the Physical Society (1958-1967)*, 85(5):921.

[Kubo, 1952] Kubo, R. (1952). The spin-wave theory of antiferromagnetics. *Physical Review*, 87(4):568.

[Kubo, 1957] Kubo, R. (1957). Statistical-mechanical theory of irreversible processes. i. general theory and simple applications to magnetic and conduction problems. *Journal of the Physical Society of Japan*, 12(6):570–586.

[Kubo et al., 1957] Kubo, R., Yokota, M., and Nakajima, S. (1957). Statistical-mechanical theory of irreversible processes. ii. response to thermal disturbance. *Journal of the Physical Society of Japan*, 12(11):1203–1211.

[Landau, 1957] Landau, L. D. (1957). The theory of a fermi liquid. *Soviet Physics JETP-USSR*, 3(6):920–925.

[Landau and Lifshitz, 1958] Landau, L. D. and Lifshitz, E. M. (1958). *Quantum mechanics: non-relativistic theory*, volume 3. Pergamon Press.

[Laurence and Petitgrand, 1973] Laurence, G. and Petitgrand, D. (1973). Thermal conductivity and magnon-phonon resonant interaction in antiferromagnetic $FeCl_2$. *Phys. Rev. B*, 8:2130–2138.

[Lee and Nagaosa, 1992] Lee, P. A. and Nagaosa, N. (1992). Gauge theory of the normal state of high-tc superconductors. *Physical Review B*, 46(9):5621.

[Lee et al., 2006] Lee, P. A., Nagaosa, N., and Wen, X.-G. (2006). Doping a mott insulator: Physics of high-temperature superconductivity. *Reviews of modern physics*, 78(1):17.

[Lee, 2008] Lee, S.-S. (2008). Stability of the u (1) spin liquid with a spinon fermi surface in 2+ 1 dimensions. *Physical Review B*, 78(8):085129.

[Li et al., 2013] Li, Q. J., Zhao, Z. Y., Fan, C., Zhang, F. B., Zhou, H. D., Zhao, X., and Sun, X. F. (2013). Phonon-glass-like behavior of magnetic origin in single-crystal $tb_2ti_2o_7$. *Phys. Rev. B*, 87:214408.

[Li et al., 2020a] Li, X., Fauqué, B., Zhu, Z., and Behnia, K. (2020a). Phonon thermal hall effect in strontium titanate. *Phys. Rev. Lett.*, 124:105901.

[Li et al., 2020b] Li, Y., Pustogow, A., Bories, M., Puphal, P., Krellner, C., Dressel, M., and Valentí, R. (2020b). Lattice dynamics in the spin-$\frac{1}{2}$ frustrated kagome compound herbertsmithite. *Phys. Rev. B*, 101:161115.

[Lieb et al., 1961] Lieb, E., Schultz, T., and Mattis, D. (1961). Two soluble models of an antiferromagnetic chain. *Annals of Physics*, 16(3):407–466.

[Lifschitz and Pitajewski, 1983] Lifschitz, E. and Pitajewski, L. (1983). Physical kinetics. In *Textbook of theoretical physics. 10*. Pergamon.

[Lifshitz and Pitaevskii, 1980] Lifshitz, E. and Pitaevskii, L. (1980). Statistical physics 2: theory of the condensed state. In *Textbook of theoretical physics. 9*. Pergamon.

[Lin et al., 2017] Lin, X., Rischau, C. W., Buchauer, L., Jaoui, A., Fauqué, B., and Behnia, K. (2017). Metallicity without quasi-particles in room-temperature strontium titanate. *npj Quantum Materials*, 2(1):1–8.

[London, 1937] London, F. (1937). A new conception of supraconductivity. *Nature*, 140(3549):793–796.

[Lovesey, 1972] Lovesey, S. (1972). Theory of the magnon and phonon interaction in FeF2. *Journal of Physics C: Solid State Physics*, 5(19):2769–2784.

[Lucas and Sachdev, 2015] Lucas, A. and Sachdev, S. (2015). Memory matrix theory of magnetotransport in strange metals. *Physical Review B*, 91(19):195122.

[Luttinger, 1951] Luttinger, J. (1951). The effect of a magnetic field on electrons in a periodic potential. *Physical Review*, 84(4):814.

[Luttinger, 1964] Luttinger, J. M. (1964). Theory of thermal transport coefficients. *Phys. Rev.*, 135:A1505–A1514.

[Luttinger and Kohn, 1955] Luttinger, J. M. and Kohn, W. (1955). Motion of electrons and holes in perturbed periodic fields. *Physical Review*, 97(4):869.

[Mahajan et al., 2013] Mahajan, R., Barkeshli, M., and Hartnoll, S. A. (2013). Non-fermi liquids and the wiedemann-franz law. *Phys. Rev. B*, 88:125107.

[Mahan, 1981] Mahan, G. (1981). *Many-particle physics*. Kluwer Academic.

[Mahan, 1987] Mahan, G. D. (1987). Quantum transport equation for electric and magnetic fields. *Physics Reports*, 145(5):251–318.

[Manenkov and Orbach, 1966] Manenkov, A. A. and Orbach, R. (1966). *Spin-lattice relaxation in ionic solids*. Harper & Row.

[Maradudin and Vosko, 1968] Maradudin, A. A. and Vosko, S. H. (1968). Symmetry properties of the normal vibrations of a crystal. *Rev. Mod. Phys.*, 40:1–37.

[Marino, 2017] Marino, E. C. (2017). *Quantum field theory approach to condensed matter physics*. Cambridge University Press.

[Marston and Affleck, 1989] Marston, J. B. and Affleck, I. (1989). Large-n limit of the hubbard-heisenberg model. *Physical Review B*, 39(16):11538.

[Martelli et al., 2018] Martelli, V., Jiménez, J. L., Continentino, M., Baggio-Saitovitch, E., and Behnia, K. (2018). Thermal transport and phonon hydrodynamics in strontium titanate. *Physical review letters*, 120(12):125901.

[Matsubara, 1955] Matsubara, T. (1955). A new approach to quantum-statistical mechanics. *Progress of theoretical physics*, 14(4):351–378.

[Matsumoto and Murakami, 2011] Matsumoto, R. and Murakami, S. (2011). Rotational motion of magnons and the thermal hall effect. *Physical Review B*, 84(18):184406.

[Matthiessen and Vogt, 1864] Matthiessen, A. and Vogt, C. (1864). Iv. on the influence of temperature on the electric conducting-power of alloys. *Philosophical Transactions of the Royal Society of London*, 154(154):167–200.

[Mattis, 1981] Mattis, D. (1981). *The theory of magnetism, I. Statics and dynamics*. Springer.

[Merzbacher, 1961] Merzbacher, E. (1961). *Quantum mechanics*. Jones & Bartlett Publishers.

[Metavitsiadis and Brenig, 2020] Metavitsiadis, A. and Brenig, W. (2020). Phonon renormalization in the kitaev quantum spin liquid. *Phys. Rev. B*, 101:035103.

[Migdal, 1958] Migdal, A. (1958). Interaction between electrons and lattice vibrations in a normal metal. *Sov. Phys. JETP*, 7(6):996–1001.

[Misguich, 2011] Misguich, G. (2011). Quantum spin liquids and fractionalization. In *Introduction to Frustrated Magnetism*, pages 407–435. Springer.

[Mook et al., 2019] Mook, A., Henk, J., and Mertig, I. (2019). Thermal hall effect in noncollinear coplanar insulating antiferromagnets. *Phys. Rev. B*, 99:014427.

[Mori, 1958] Mori, H. (1958). Statistical-mechanical theory of transport in fluids. *Physical Review*, 112(6):1829.

[Mori, 1965] Mori, H. (1965). A continued-fraction representation of the time-correlation functions. *Progress of Theoretical Physics*, 34(3):399–416.

[Mori et al., 2014] Mori, M., Spencer-Smith, A., Sushkov, O. P., and Maekawa, S. (2014). Origin of the phonon Hall effect in rare-earth garnets. *Phys. Rev. Lett.*, 113:265901.

[Mott, 1960] Mott, N. (1960). *Metal-Insulator Transitions*. Taylor & Francis.

[Murakami and Okamoto, 2017] Murakami, S. and Okamoto, A. (2017). Thermal hall effect of magnons. *Journal of the Physical Society of Japan*, 86(1):011010.

[Mühlbauer et al., 2009] Mühlbauer, S., Binz, B., Jonietz, F., Pfleiderer, C., Rosch, A., Neubauer, A., Georgii, R., and Böni, P. (2009). Skyrmion lattice in a chiral magnet. *Science*, 323(5916):915–919.

[Nabarro, 1951] Nabarro, F. R. N. (1951). The interaction of screw dislocations and sound waves. *Proceedings of the Royal Society of London. Series A. Mathematical and Physical Sciences*, 209(1097):278–290.

[Nagaosa, 1999] Nagaosa, N. (1999). *Quantum field theory in strongly correlated electronic systems*. Springer Science & Business Media.

[Nagaosa and Lee, 1990] Nagaosa, N. and Lee, P. A. (1990). Normal-state properties of the uniform resonating-valence-bond state. *Physical review letters*, 64(20):2450.

[Ni et al., 2019] Ni, J. M., Pan, B. L., Song, B. Q., Huang, Y. Y., Zeng, J. Y., Yu, Y. J., Cheng, E. J., Wang, L. S., Dai, D. Z., Kato, R., and Li, S. Y. (2019). Absence of magnetic thermal conductivity in the quantum spin liquid candidate etme$_3$Sb[Pd(dmit)$_2$]$_2$. *Phys. Rev. Lett.*, 123:247204.

[Nozières, 1974] Nozières, P. (1974). A "fermi-liquid" description of the kondo problem at low temperatures. *Journal of low temperature physics*, 17(1):31–42.

[Onnes, 1911] Onnes, H. (1911). Further experiments with liquid helium. c. on the change of electric resistance of pure metals at very low temperature etc. iv. the resistance of pure mercury at helium temperatures. *Communications of the Physical Laboratory of the University of Leiden*, 4(120b):3–5.

[Onose et al., 2010] Onose, Y., Ideue, T., Katsura, H., Shiomi, Y., Nagaosa, N., and Tokura, Y. (2010). Observation of the magnon hall effect. *Science*, 329(5989):297–299.

[Onsager, 1931] Onsager, L. (1931). Reciprocal relations in irreversible processes. i. *Phys. Rev.*, 37:405–426.

[Pauling, 1935] Pauling, L. (1935). The structure and entropy of ice and of other crystals with some randomness of atomic arrangement. *Journal of the American Chemical Society*, 57(12):2680–2684.

[Peierls, 1929] Peierls, R. (1929). Zur kinetischen theorie der wärmeleitung in kristallen. *Annalen der Physik*, 395(8):1055–1101.

[Peierls, 1955] Peierls, R. E. (1955). *Quantum theory of solids*. Oxford University Press.

[Petersen and Hedegård, 2000] Petersen, L. and Hedegård, P. (2000). A simple tight-binding model of spin–orbit splitting of sp-derived surface states. *Surface science*, 459(1-2):49–56.

[Polyakov, 1977] Polyakov, A. M. (1977). Quark confinement and topology of gauge theories. *Nuclear Physics B*, 120(3):429–458.

[Pottier, 2009] Pottier, N. (2009). *Nonequilibrium statistical physics: linear irreversible processes*. Oxford University Press.

[Prange and Kadanoff, 1964] Prange, R. E. and Kadanoff, L. P. (1964). Transport theory for electron-phonon interactions in metals. *Physical Review*, 134(3A):A566.

[Qin et al., 2012] Qin, T., Zhou, J., and Shi, J. (2012). Berry curvature and the phonon Hall effect. *Physical Review B*, 86(10):104305.

[Rammer, 1991] Rammer, J. (1991). Quantum transport theory of electrons in solids: A single-particle approach. *Reviews of Modern Physics*, 63(4):781.

[Rammer and Smith, 1986] Rammer, J. and Smith, H. (1986). Quantum field-theoretical methods in transport theory of metals. *Reviews of modern physics*, 58(2):323.

[Riedl et al., 2019] Riedl, K., Li, Y., Valentí, R., and Winter, S. M. (2019). Ab initio approaches for low-energy spin hamiltonians. *physica status solidi (b)*, 256(9):1800684.

[Rønnow et al., 2001] Rønnow, H. M., McMorrow, D. F., Coldea, R., Harrison, A., Youngson, I. D., Perring, T. G., Aeppli, G., Syljuåsen, O., Lefmann, K., and Rischel, C. (2001). Spin dynamics of the 2d spin $\frac{1}{2}$ quantum antiferromagnet Copper Deuteroformate Tetradeuterate (CFTD). *Phys. Rev. Lett.*, 87:037202.

[Ross et al., 2011] Ross, K. A., Savary, L., Gaulin, B. D., and Balents, L. (2011). Quantum excitations in quantum spin ice. *Physical Review X*, 1(2):021002.

[Sachdev, 2011] Sachdev, S. (2011). *Quantum phase transitions*. Cambridge university press.

[Saito et al., 2019] Saito, T., Misaki, K., Ishizuka, H., and Nagaosa, N. (2019). Berry phase of phonons and thermal Hall effect in nonmagnetic insulators. *Phys. Rev. Lett.*, 123:255901.

[Sakurai, 1994] Sakurai, J. J. (1994). *Modern quantum mechanics; rev. ed.* Addison-Wesley, Reading, MA.

[Samajdar et al., 2019] Samajdar, R., Chatterjee, S., Sachdev, S., and Scheurer, M. S. (2019). Thermal hall effect in square-lattice spin liquids: A schwinger boson mean-field study. *Physical Review B*, 99(16):165126.

[Savary and Balents, 2016] Savary, L. and Balents, L. (2016). Quantum spin liquids: a review. *Reports on Progress in Physics*, 80(1):016502.

[Savary and Senthil, 2015] Savary, L. and Senthil, T. (2015). Probing hidden orders with resonant inelastic x-ray scattering. *arXiv:1506.04752*.

[Schollwöck et al., 2008] Schollwöck, U., Richter, J., Farnell, D. J., and Bishop, R. F. (2008). *Quantum magnetism*, volume 645. Springer.

[Seifert et al., 2022] Seifert, U. F. P., Ye, M., and Balents, L. (2022). Ultrafast optical excitation of magnetic dynamics in van der waals magnets: Coherent magnons and bkt dynamics in $nips_3$. *Phys. Rev. B*, 105:155138.

[Sekine and Nagaosa, 2020] Sekine, A. and Nagaosa, N. (2020). Quantum kinetic theory of thermoelectric and thermal transport in a magnetic field. *Phys. Rev. B*, 101:155204.

[Sheng et al., 2006] Sheng, L., Sheng, D. N., and Ting, C. S. (2006). Theory of the phonon Hall effect in paramagnetic dielectrics. *Phys. Rev. Lett.*, 96:155901.

[Shimshoni et al., 2003] Shimshoni, E., Andrei, N., and Rosch, A. (2003). Thermal conductivity of spin-$\frac{1}{2}$ chains. *Phys. Rev. B*, 68:104401.

[Sommerfeld, 1928] Sommerfeld, A. (1928). Zur elektronentheorie der metalle auf grund der fermischen statistik. *Zeitschrift für Physik*, 47(1):1–32.

[Squires, 2012] Squires, G. L. (2012). *Introduction to the Theory of Thermal Neutron Scattering*. Cambridge University Press, 3 edition.

[Stein et al., 1996] Stein, J., Entin-Wohlman, O., and Aharony, A. (1996). Weak ferromagnetism in the low-temperature tetragonal phase of the cuprates. *Phys. Rev. B*, 53:775–784.

[Stoner, 1938] Stoner, E. C. (1938). Collective electron ferromagnetism. *Proceedings of the Royal Society of London. Series A. Mathematical and Physical Sciences*, 165(922):372–414.

[Stratonovich, 1957] Stratonovich, R. (1957). On a method of calculating quantum distribution functions. In *Soviet Physics Doklady*, volume 2, page 416.

[Strohm et al., 2005] Strohm, C., Rikken, G. L. J. A., and Wyder, P. (2005). Phenomenological evidence for the phonon hall effect. *Phys. Rev. Lett.*, 95:155901.

[Sugii et al., 2017] Sugii, K., Shimozawa, M., Watanabe, D., Suzuki, Y., Halim, M., Kimata, M., Matsumoto, Y., Nakatsuji, S., and Yamashita, M. (2017). Thermal hall effect in a phonon-glass $ba_3cusb_2o_9$. *Phys. Rev. Lett.*, 118:145902.

[Sun et al., 2021] Sun, X.-Q., Chen, J.-Y., and Kivelson, S. A. (2021). Large extrinsic phonon thermal Hall effect from resonant scattering. *arXiv preprint arXiv:2109.12117*.

[Swingle, 2018] Swingle, B. (2018). Unscrambling the physics of out-of-time-order correlators. *Nature Phys*, 14:988–990.

[Teng et al., 2020] Teng, Y., Zhang, Y., Samajdar, R., Scheurer, M. S., and Sachdev, S. (2020). Unquantized thermal hall effect in quantum spin liquids with spinon fermi surfaces. *Phys. Rev. Research*, 2:033283.

[Toews et al., 2013] Toews, W. H., Zhang, S. S., Ross, K. A., Dabkowska, H. A., Gaulin, B. D., and Hill, R. W. (2013). Thermal conductivity of $ho_2ti_2o_7$ along the [111] direction. *Phys. Rev. Lett.*, 110:217209.

[Tritt, 2004] Tritt, T. M. (2004). *Thermal conductivity.* Kluwer Academic Plenum Publishers.

[Wan and Armitage, 2019] Wan, Y. and Armitage, N. P. (2019). Resolving continua of fractional excitations by spinon echo in THz 2D coherent spectroscopy. *Phys. Rev. Lett.*, 122:257401.

[Wannier, 1950] Wannier, G. (1950). Antiferromagnetism. the triangular ising net. *Physical Review*, 79(2):357.

[Wannier, 1962] Wannier, G. H. (1962). Dynamics of band electrons in electric and magnetic fields. *Reviews of Modern Physics*, 34(4):645.

[Watanabe et al., 2016] Watanabe, D., Sugii, K., Shimozawa, M., Suzuki, Y., Yajima, T., Ishikawa, H., Hiroi, Z., Shibauchi, T., Matsuda, Y., and Yamashita, M. (2016). Emergence of nontrivial magnetic excitations in a spin-liquid state of kagomé volborthite. *Proceedings of the National Academy of Sciences*, 113(31):8653–8657.

[Wen, 2004] Wen, X.-G. (2004). *Quantum Field Theory of Many-body Systems: From the Origin of Sound to an Origin of Light and Electrons.* Oxford University Press.

[White et al., 1965] White, R. M., Sparks, M., and Ortenburger, I. (1965). Diagonalization of the antiferromagnetic magnon-phonon interaction. *Phys. Rev.*, 139:A450–A454.

[Wick, 1950] Wick, G. C. (1950). The evaluation of the collision matrix. *Phys. Rev.*, 80:268–272.

[Wigner, 1959] Wigner, E. P. (1959). *Group theory: and its application to the quantum mechanics of atomic spectra.* Academic Press. (translated by Griffin, J. J.).

[Xiao et al., 2010] Xiao, D., Chang, M.-C., and Niu, Q. (2010). Berry phase effects on electronic properties. *Reviews of modern physics*, 82(3):1959.

[Yamashita et al., 2010] Yamashita, M., Nakata, N., Senshu, Y., Nagata, M., Yamamoto, H. M., Kato, R., Shibauchi, T., and Matsuda, Y. (2010). Highly mobile gapless excitations in a two-dimensional candidate quantum spin liquid. *Science*, 328(5983):1246–1248.

[Ye et al., 2020] Ye, M., Fernandes, R. M., and Perkins, N. B. (2020). Phonon dynamics in the kitaev spin liquid. *Phys. Rev. Research*, 2:033180.

[Ye et al., 2018] Ye, M., Halász, G. B., Savary, L., and Balents, L. (2018). Quantization of the thermal Hall conductivity at small Hall angles. *Phys. Rev. Lett.*, 121:147201.

[Ye et al., 2021] Ye, M., Savary, L., and Balents, L. (2021). Phonon Hall viscosity in magnetic insulators. *arXiv:2103.04223*.

[Yosida, 1957] Yosida, K. (1957). Magnetic properties of cu-mn alloys. *Physical Review*, 106(5):893.

[Zhang et al., 2021a] Zhang, H., Xu, C., Carnahan, C., Sretenovic, M., Suri, N., Xiao, D., and Ke, X. (2021a). Anomalous thermal hall effect in an insulating van der waals magnet. *Phys. Rev. Lett.*, 127:247202.

[Zhang et al., 2010] Zhang, L., Ren, J., Wang, J.-S., and Li, B. (2010). Topological nature of the phonon Hall effect. *Physical Review letters*, 105(22):225901.

[Zhang et al., 2019] Zhang, X., Zhang, Y., Okamoto, S., and Xiao, D. (2019). Thermal Hall effect induced by magnon-phonon interactions. *Phys. Rev. Lett.*, 123:167202.

[Zhang et al., 2021b] Zhang, Y., Teng, Y., Samajdar, R., Sachdev, S., and Scheurer, M. S. (2021b). Phonon Hall viscosity from phonon-spinon interactions. *Physical Review B*, 104(3):035103.

[Zhou et al., 2017] Zhou, Y., Kanoda, K., and Ng, T.-K. (2017). Quantum spin liquid states. *Reviews of Modern Physics*, 89(2):025003.

[Ziman, 1956] Ziman, J. M. (1956). Xvii. the effect of free electrons on lattice conduction. *Philosophical Magazine*, 1(2):191–198.

[Ziman, 1960] Ziman, J. M. (1960). *Electrons and Phonons*. Clarendon Press.

Chapter 5

Appendices

5.1 Field-theoretical approach to phonon thermal conductivity

In this appendix, I re-derive our result for the longitudinal thermal conductivity of phonons, using the Keldysh formalism of nonequilibrium field theory.

5.1.1 General steps toward the kinetic equation

Here is a brief summary the general steps of the Keldysh formalism leading to the quantum Boltzmann equation. A few notations and conventios are also defined.

5.1.1.1 The Schwinger-Baym contour and Keldysh rotation

Nonequilibrium field-theoretical techniques, among which the Keldysh foralism, involve time integration along a contour in the complex time plane from $-\infty+i0$ to $+\infty+i0$, then back from $+\infty-i0$ to $-\infty-i0$. This contour is denoted $\mathcal{C}$ in the next few lines. Then for any field Φ,

$$\int_{\mathcal{C}} \mathrm{d}t\Phi(t) = \int_{-\infty}^{+\infty} \mathrm{d}t \left(\Phi(t+i0) - \Phi(t-i0)\right). \tag{5.1}$$

Then one performs the Keldysh rotation:

$$\Phi^{\mathrm{cl/q}}(t) = \frac{1}{\sqrt{2}} \left(\Phi(t+i0) \pm \Phi(t-i0)\right). \tag{5.2}$$

This defines the "quantum" and "classical" fields, in which language the Keldysh theory is expressed.

5.1.1.2 Free bosonic theory

As an introduction to the method, we first consider the free hamiltonian of the phonons, decribed by the free bosonic field $\phi_{\mathbf{k}}$ and its complex conjugate $\overline{\phi}_{\mathbf{k}}$. This hamiltonian reads $H_0 = \sum_{\mathbf{k}} \omega_{\mathbf{k}} \overline{\phi}_{\mathbf{k}} \phi_{\mathbf{k}}$.

The free action for these bosonic fields, expressed in terms of the classical and quantum fields, reads

$$S_0[\phi^{\rm cl},\phi^{\rm q}] = \sum_{\mathbf{k}} \int_{-\infty}^{+\infty} {\rm d}t\ (\overline{\phi}^{\rm cl},\overline{\phi}^{\rm q}) \begin{pmatrix} 0 & [G_0^{-1}]^{\rm A} \\ [G_0^{-1}]^{\rm R} & [G_0^{-1}]^{\rm K} \end{pmatrix} \begin{pmatrix} \phi^{\rm cl} \\ \phi^{\rm q} \end{pmatrix}. \tag{5.3}$$

The quantum-quantum coefficient is always zero by construction, even in the interacting theory; it is an important feature of the Keldysh theory's structure.

One can check that from the free action Eq.(5.3), the free Green's functions ($\alpha,\beta = {\rm cl},{\rm q}$) can be obtained; they are defined as

$$G_0^{\alpha\beta}(\mathbf{k},\mathbf{k}',t,t') = -i \int \mathbf{D}[\phi^{\rm cl},\overline{\phi}^{\rm cl},\phi^{\rm q},\overline{\phi}^{\rm q}]\ \mathbb{T}\ \phi^{\alpha}(\mathbf{k},t)\overline{\phi}^{\beta}(\mathbf{k}',t')\ e^{iS_0[\phi^{\rm cl},\phi^{\rm q}]}, \tag{5.4}$$

where $\mathbb{T}$ stands for time-ordering of the operators. Thus, the advanced and retarded functions are, in the language of classical and quantum variables, $G^{\rm A} = G^{\rm q,cl}$ and $G^{\rm R} = G^{\rm cl,q}$.

It is customary [Kamenev, 2011] to parameterize the Keldysh Green's function $G^{\rm K}$ in terms of the retarded and advanced functions as

$$G^{\rm K} = G^{\rm R} \circ F - F \circ G^{\rm A}, \tag{5.5}$$

where F is an auxiliary function – which we will later interpret in terms of bosoni populations – and $\circ$ denotes space-time convolution, namely

$$(A \circ B)(\mathbf{x},t;\mathbf{x}',t') := \int {\rm d}^d\mathbf{x}''{\rm d}t'' A(\mathbf{x},t;\mathbf{x}'',t'')B(\mathbf{x}'',t'';\mathbf{x}',t'). \tag{5.6}$$

In the case of free bosons, the Green's functions are simply

$$G_0^{\rm R}(\mathbf{k},t) = -i\langle\phi_{\mathbf{k}}^{\rm cl}(t)\overline{\phi}_{\mathbf{k}}^{\rm q}(0)\rangle = -i\theta(t)e^{-i\omega_{\mathbf{k}}t} \overset{\rm FT}{\to} (\epsilon - \omega_{\mathbf{k}} + i0)^{-1} \tag{5.7}$$

$$G_0^{\rm A}(\mathbf{k},t) = -i\langle\phi_{\mathbf{k}}^{\rm q}(t)\overline{\phi}_{\mathbf{k}}^{\rm cl}(0)\rangle = +i\theta(-t)e^{-i\omega_{\mathbf{k}}t} \overset{\rm FT}{\to} (\epsilon - \omega_{\mathbf{k}} - i0)^{-1} \tag{5.8}$$

$$G_0^{\rm K}(\mathbf{k},t) = -i\langle\phi_{\mathbf{k}}^{\rm cl}(t)\overline{\phi}_{\mathbf{k}}^{\rm cl}(0)\rangle = -iF(\omega_{\mathbf{k}})e^{-i\omega_{\mathbf{k}}t} \overset{\rm FT}{\to} -2i\pi F(\epsilon)\delta(\epsilon - \omega_{\mathbf{k}}) \tag{5.9}$$

Thus, $G_0^{\rm R}$ and $G_0^{\rm A}$ coincide with the usual propagators of quantum field theory. [Coleman, 2015] Here, $[G_0^{-1}]^{\rm K} = 2i0F(\omega_{\mathbf{k}})$ is a pure regularization, because we are only considering the free theory. In the case of an interacting theory, the Keldysh Green's function $G^{\rm K}$ contains nontrivial information about the out-of-equilibrium populations – note that at equilibrium, $F = 2n_B + 1$ with n_B the equilibrium bosonic distribution function.

5.1.1.3 Interacting theory

Within the interacting theory, one has to consider the dressed Green's functions

$$G^{\alpha\beta}(\mathbf{k},\mathbf{k}',t,t') = -i \int \mathbf{D}[\phi^{\rm cl},\phi^{\rm q}]\ \phi^{\alpha}(\mathbf{k},t)\overline{\phi}^{\beta}(\mathbf{k}',t')\ e^{iS[\phi^{\rm cl},\phi^{\rm q}]}, \tag{5.10}$$

with $\alpha,\beta = {\rm q},{\rm cl}$.

These satisfy Dyson's equation, which in the Keldysh formalism reads:

$$\begin{pmatrix} 0 & [G_0^{-1}]^{\mathrm{A}} - \Sigma^{\mathrm{A}} \\ [G_0^{-1}]^{\mathrm{R}} - \Sigma^{\mathrm{R}} & -\Sigma^{\mathrm{K}} \end{pmatrix} \circ \begin{pmatrix} G^{\mathrm{K}} & G^{\mathrm{R}} \\ G^{\mathrm{A}} & 0 \end{pmatrix} = \mathbb{1}, \tag{5.11}$$

where $\Sigma^{\mathrm{R}}, \Sigma^{\mathrm{A}}, \Sigma^{\mathrm{K}}$ are the three self-energies of the problem, defined in the usual way. Note that this equation is written in real-space $(\mathbf{x}, t)$, not in reciprocal space as it is customary to define propagators. Note also that now that self-energies can act as regularizators, the infinitesimals $\pm i0$ of the free theory can be omitted, therefore $[G_0^{-1}]^{\mathrm{A}} = [G_0^{-1}]^{\mathrm{R}} =: G_0^{-1}$ and $[G_0^{-1}]^{\mathrm{K}} = 0$ (see above).

In terms of the "population" function F, defined in Eq.(5.5), Dyson's equation can be recast into the following form:

$$[F \overset{\circ}{,} G_0^{-1}] = \Sigma^{\mathrm{K}} - (\Sigma^{\mathrm{R}} \circ F - F \circ \Sigma^{\mathrm{A}}). \tag{5.12}$$

This equation uses again real-space conventions, and can be interpreted as a self-consistent equation with unknown $F(\mathbf{x}, t; \mathbf{x}', t')$, provided the free propagator G_0 is known and the self-energies are determined with some level of approximation.

5.1.1.4 Derivation of the kinetic equation

The hydrodynamics of the phonon's system is expressed in terms of quasiparticles, which are now "dressed" phonons. As usual, the quasiparticle's energy is shifted by the real part of the self-energy, which also redefines the quasiparticle velocity:

$$\omega_{\mathbf{k}} \mapsto \tilde{\omega}_{\mathbf{k}} = \omega_{\mathbf{k}} + \mathrm{Re}\Sigma^{\mathrm{R}} \tag{5.13}$$

$$\boldsymbol{v}_{\mathbf{k}} \mapsto \tilde{\boldsymbol{v}}_{\mathbf{k}} = \nabla_{\mathbf{k}} \tilde{\omega}_{\mathbf{k}} = \boldsymbol{v}_{\mathbf{k}} + \nabla_{\mathbf{k}} \mathrm{Re}\Sigma^{\mathrm{R}}. \tag{5.14}$$

From Dyson's equation, as expressed hereabove in terms of the F function, it is possible to derive Boltzmann's equation. This involves a few approximations, which are explained in [Kamenev, 2011], and which amount to negleting a certain number of quantum corrections, so as to obtain the hydrodynamic limit of the problem.

These are best explained in the framework of the Wigner transform: for a two-point function $F(\mathbf{x}, t; \mathbf{x}', t')$, the latter (along with its inverse) is defined as

$$F[\mathbf{r}, t; \mathbf{k}, \epsilon] = \sum_{\mathbf{r}'} \int \mathrm{d}t' e^{-i\mathbf{k}\mathbf{r}'} e^{-i\epsilon t'} F(\mathbf{r} + \tfrac{\mathbf{r}'}{2}, \mathbf{r} - \tfrac{\mathbf{r}'}{2}, t + \tfrac{t'}{2}, t - \tfrac{t'}{2}), \tag{5.15}$$

$$F(\mathbf{x}_1, t_1; \mathbf{x}_2, t_2) = \frac{1}{N} \sum_{\mathbf{k}} \int \frac{\mathrm{d}\epsilon}{2\pi} e^{i\mathbf{k}(\mathbf{x}_1 - \mathbf{x}_2)} e^{i\epsilon(t_1 - t_2)} F[\tfrac{\mathbf{x}_1 + \mathbf{x}_2}{2}, \tfrac{t_1 + t_2}{2}, \mathbf{k}, \epsilon]. \tag{5.16}$$

The intepretation of this mixed real space and reciprocal space representation is as follows: $(\mathbf{x}, t)$ are slow "center-of-mass" variables, which describe the smooth variations of the function F in space and time; by contrast, $(\mathbf{k}, \epsilon)$ are the Fourier transformed fast variables. Note that the Fourier transform is a particular case of

Wigner transform where all variations are fast, i.e. where there is no dependence upon the slow variables $(\mathbf{x}, t)$.

A hydrodynamic approximation consists of assuming that the time dependence of F is purely in terms of the slow variable t, which amounts to assuming that F is a constant with respect to its variable ϵ, whose value is determined by its evaluation at the quasiparticle's energy $\epsilon = \omega_{\mathbf{k}} + \mathrm{Re}\Sigma^{\mathrm{R}}$. Thus, "ironing out" fast time dependences is equivalent, in the Wigner transform representation, to considering only the quasiparticle peak's contribution to F; this yields a hydrodynamic description of the system in terms of $\tilde{F}(\mathbf{r}, t, \mathbf{k}) := F(\mathbf{r}, t, \mathbf{k}, \tilde{\omega}_{\mathbf{k}})$, where the energy ϵ is no longer a variable since it is solely determined by $\mathbf{k}$ (and $\mathbf{r}, t$ as well if the nonequilibrium self-energies depend thereupon). The same approximation is made in the self-energies.

It is assumed that $\tilde{F}(\mathbf{r}, t, \mathbf{k})$ contains the relevant information about nonequilibrium populations. From Eq.(5.15), the kinetic equation is then obtained:

$$\left[(1 - \partial_\epsilon \mathrm{Re}\Sigma^{\mathrm{R}})\partial_t + \tilde{\mathbf{v}}_{\mathbf{k}} \nabla_{\mathbf{r}} - (\nabla_{\mathbf{r}} \mathrm{Re}\Sigma^{\mathrm{R}}) \nabla_{\mathbf{k}}\right] \tilde{F}(\mathbf{r}, t, \mathbf{k}) = I^{\mathrm{coll}}[\tilde{F}], \tag{5.17}$$

where the collision integral is

$$I^{\mathrm{coll}}[\tilde{F}] = i\Sigma^{\mathrm{K}}(\mathbf{x}, t, \mathbf{k}) + 2F(\mathbf{x}, t, \mathbf{k})\mathrm{Im}[\Sigma^{\mathrm{R}}(\mathbf{x}, t, \mathbf{k})]. \tag{5.18}$$

At this stage it is interesting to note that in the collision integral, $\tilde{F}$ appears multiplied with the imaginary part of a retarded self-energy, which is typically negative. Thus the collision integral has roughly the form $-\tilde{F}/\tau$, with τ a typical scattering time like in the Drude theory. This is consistent with the second law of thermodynamics, which imposes that the longitudinal thermal conductivity be always positive.

One should also note that the identity $\tilde{F}(\mathbf{r}, t, \mathbf{k}) = iG^{\mathrm{K}}(\mathbf{r}, \mathbf{k}, t, t)$ is exactly true in the free theory, but only approximately true in the interacting theory. On the other hand, $iG^{\mathrm{K}}(\mathbf{r}, \mathbf{k}, t, t) = 2n(\omega_{\mathbf{k}}) + 1$ is always exactly true. [Kamenev, 2011] This means that the phonon's population, as captured by $\tilde{F}$, does only coincide with n_B at equilibrium and for a non-interacting system; both the presence of interactions and the absence of a thermal equilibrium entail deviations from the Bose distribution function.

In the following, I consider the particular case of a coupling between phonons and a generic field $Q_{\mathbf{k}}$.

5.1.2 Model and notations

5.1.2.1 Definitions: turning on interactions

The interaction hamiltonian is defined as $H_{\mathrm{int}} = \sum_{q=\pm} \sum_{n\mathbf{k}} \phi^q_{n\mathbf{k}} Q^q_{n\mathbf{k}}$, where $\phi^- := \phi$ and $\phi^+ := \overline{\phi}$ are used as shorthands like in the bulk of this thesis – and similarly for the $Q_{n\mathbf{k}}$ fields.

The interactions' contribution to the action, $S_{\rm int}$, involves the integral over a time contour, which reads

$$\begin{aligned} -\int_{\mathcal{C}} \mathrm{d}t H_{\rm int}(t) &= -\sum_{s=\pm} s \int_{-\infty}^{+\infty} \mathrm{d}t \sum_{q=\pm,n\mathbf{k}} \phi^q_{n\mathbf{k}}(t+is0) Q^q_{n\mathbf{k}}(t+is0) \qquad (5.19) \\ &= -\int_{-\infty}^{+\infty} \mathrm{d}t \sum_{q,n\mathbf{k}} \left[(\phi^{\rm cl}_{n\mathbf{k}})^q(t)(Q^{\rm q}_{n\mathbf{k}})^q(t) + (\phi^{\rm q}_{n\mathbf{k}})^q(t)(Q^{\rm cl}_{n\mathbf{k}})^q(t) \right] \end{aligned}$$

in terms of the "classical" and "quantum" fields.

The full action of the coupled phonon-Q system is then

$$S[\phi^{\rm cl},\phi^{\rm q},Q^{\rm cl},Q^{\rm q}] = S_0[\phi^{\rm cl},\phi^{\rm q}] + S_0[Q^{\rm cl},Q^{\rm q}] - \int_{-\infty}^{+\infty} \mathrm{d}t \sum_{q,n\mathbf{k}} (\phi^q_{n\mathbf{k}})^\alpha \sigma_x^{\alpha\beta} (Q^q_{n\mathbf{k}})^\beta \ (t), \qquad (5.20)$$

where $\alpha = ({\rm cl},{\rm q})$ and $S_0[Q^{\rm cl},Q^{\rm q}]$ is the proper action of the Q field alone, which (in spite of its notation) is not a free action in principle.

5.1.2.2 Diagrammatic expansion

The dressed phonon's Green's function, in the presence of the interaction with the Q fields, is

$$\begin{aligned} &G^{\alpha\beta}_{n,n'}(\mathbf{k},\mathbf{k}',t,t') = \qquad (5.21) \\ &-i\mathbb{T} \int \mathbf{D}[\phi^{\rm cl},\phi^{\rm q}] \ \phi^\alpha_n(\mathbf{k},t)\overline{\phi}^\beta_{n'}(\mathbf{k}',t') \ e^{iS_0[\phi^{\rm cl},\phi^{\rm q}]} \int \mathbf{D}[Q^{\rm cl},Q^{\rm q}] e^{iS_0[Q^{\rm cl},Q^{\rm q}]} e^{iS_{\rm int}[\phi,Q]}, \end{aligned}$$

where the $\overline{\phi},\overline{Q}$ fields in the measure are implicit, and the time ordering $\mathbb{T}$ acts upon both time integrals.

Then, in $\int \mathbf{D}[Q^{\rm cl},Q^{\rm q}] e^{iS_0[Q^{\rm cl},Q^{\rm q}]} e^{iS_{\rm int}[\phi,Q]}$, we expand the $e^{iS_{\rm int}[\phi,Q]}$ factor perturbatively in powers of Q. Note that at zeroth order in this expansion, we recognize the free partition function

$$Z_0 = \int \mathbf{D}[Q^{\rm cl},Q^{\rm q}] e^{iS_0[Q^{\rm cl},Q^{\rm q}]} = 1; \qquad (5.22)$$

the fact that $Z=1$ is always true in the Keldysh formalism, at all orders in the expansion.

Since terms with an odd number of Q operators are zero, one can expand the dressed Green's function in a perturbative series with only terms of even order, namely

$$G^{\alpha\beta}(\mathbf{k},\mathbf{k}',t,t') = G^{\alpha\beta}_0(\mathbf{k},\mathbf{k}',t,t') + G^{\alpha\beta}_2(\mathbf{k},\mathbf{k}',t,t') + G^{\alpha\beta}_4(\mathbf{k},\mathbf{k}',t,t') + \dots . \qquad (5.23)$$

In particular, straightforward expansion of Eq.(5.21) yields at second order

$$\begin{aligned} G^{\alpha\beta}_2(\mathbf{k},\mathbf{k}',t,t') &= \frac{i}{2} \sum_{\gamma,\bar{\delta}={\rm cl,q}} \sum_{qq'\mathbf{k}_1\mathbf{k}_2} \mathbb{T} \int_{-\infty}^{+\infty} \mathrm{d}t_1 \mathrm{d}t_2 \left\langle (Q^q_{\mathbf{k}_1})^{\bar{\gamma}} \ (t_1) (Q^{q'}_{\mathbf{k}_2})^{\bar{\delta}} \ (t_2) \right\rangle \qquad (5.24) \\ &\times \int \mathbf{D}[\phi^{\rm cl},\phi^{\rm q}] \ e^{iS_0[\phi^{\rm cl},\phi^{\rm q}]} \ (\phi^-_{\mathbf{k}})^\alpha(t) (\phi^+_{\mathbf{k}'})^\beta(t') (\phi^q_{\mathbf{k}_1})^\gamma(t_1) (\phi^{q'}_{\mathbf{k}_2})^\delta(t_2), \end{aligned}$$

and at fourth order

$$G_4^{\alpha\beta}(\mathbf{k},\mathbf{k}',t,t') = \frac{-i}{4!}\sum_{\{q_i,\mathbf{k}_i,\lambda_i\}}\mathbb{T}\int_{-\infty}^{+\infty}\mathbf{\Pi}\mathrm{d}t_i\left\langle\prod_{i=1..4}(Q_{\mathbf{k}_i}^{q_i})^{\bar{\lambda_i}}(t_i)\right\rangle \tag{5.25}$$
$$\times\int\mathbf{D}[\phi^{\mathrm{cl}},\phi^{\mathrm{q}}]\;e^{iS_0[\phi^{\mathrm{cl}},\phi^{\mathrm{q}}]}\;\left((\phi_{\mathbf{k}}^-)^\alpha(t)(\phi_{\mathbf{k}'}^+)^\beta(t')\prod_{i=1..4}(\phi_{\mathbf{k}_i}^{q_i})^{\lambda_i}(t_i)\right).$$

The second-order term is explicitly involved in the leading term of the phonons' diagonal scattering rate, involved in the longitudinal thermal conductivity. This is the term which we will evaluate in the following. The fourth-order term is involved in the phonons' off-diagonal scattering rate, involved in the thermal Hall conductivity; although the presence of four Q operators is reminiscent of the results which we obtained in the bulk of this thesis, the precise identification of the correlation functions between the two approaches is still a work in progress. Note that in the above, some n_i indices were omitted to avoid clutter.

5.1.3 The phonons' self-energy

In this subsection, we compute the phonon self-energies, and show how these can be related to correlation functions of the Q operators.

5.1.3.1 Definition of the self-energy

The self-energy is defined implicitly by Dyson's equation, which in real space notations reads

$$G^{\alpha\beta} = G_0^{\alpha\beta} + G_0^{\alpha\gamma}\circ\Sigma^{\gamma\delta}\circ G_0^{\delta\beta} + G_0\Sigma G_0\Sigma G_0 + \ldots, \tag{5.26}$$

where "$+\ldots$" contains each term with $n \geq 3$ insertions of the self-energy with multiplicity 1.

In particular, the lowest-order (i.e. second order in Q) contribution, written in reciprocal space of positions but still in time variables, is

$$G_2^{\alpha\beta}(\mathbf{k},\mathbf{k}',t,t') = \sum_{\gamma,\delta=\mathrm{cl,q}}\int_{-\infty}^{+\infty}\mathrm{d}t_1\mathrm{d}t_2 G_0^{\alpha\delta}(\mathbf{k},t-t_1)\Sigma_2^{\delta\gamma}(\mathbf{k},\mathbf{k}',t_1,t_2)G_0^{\gamma\beta}(\mathbf{k}',t_2-t'), \tag{5.27}$$

since free boson propagators are only function of one momentum and of time differences. In the hereabove equation, we identified Σ_2, which is the lowest- (i.e. second-) order term in the expansion of Σ in powers of Q. Note that contributions from Σ_4 (defined in a similar way) and $(\Sigma_2)^2$ appear simultaneously in G_4.

Computing the phononic self-energies thus amounts to evaluating correlators of an even number of free bosons; so it is possible to apply Wick's theorem, which has a somewhat direct diagrammatic interpretation. At the order which we consider, there are two distinct contributions, which are now evaluated separately.

5.1.3.2 Disconnected diagram

In equilibrium quantum field theory, disconnected diagrams usually do not contribute in average values because they are exactly cancelled by the partition function appearing in the denominator – this is the content of the linked-cluster theorem. Meanwhile, in the Keldysh formalism, the partition function is exactly $Z = 1$ by construction; therefore it is expected (and we will show that it is indeed the case) that the disconnected diagram actually vanishes in this formalism. It reads

$$\begin{aligned} G^{\alpha\beta}_{2,\text{disc.}}(\mathbf{k},\mathbf{k}',t,t') &= \frac{i}{2!}\sum_{\mathbf{p},\mathbf{p}'}\sum_{q,q'=\pm}\int_{-\infty}^{+\infty}\mathrm{d}t_1\mathrm{d}t_2\left\langle \mathbb{T}(Q^q_{\mathbf{p}})^{\bar\gamma}\,(t_1)(Q^{q'}_{\mathbf{p}'})^{\bar\delta}\,(t_2)\right\rangle \\ &\quad\times\left\langle \mathbb{T}(\phi^-_{\mathbf{k}})^{\alpha}(t)(\phi^+_{\mathbf{k}'})^{\beta}(t')\right\rangle\left\langle \mathbb{T}(\phi^q_{\mathbf{p}})^{\gamma}(t_1)(\phi^{q'}_{\mathbf{p}'})^{\delta}(t_2)\right\rangle \end{aligned} \tag{5.28}$$

This involves the product of two Green's functions with "quantum/classical" indices γ, δ and $\overline{\gamma}, \overline{\delta}$ (i.e. their contrary), respectively. If $\gamma = \delta$ then one of these two is a Keldysh Green's function and the other one is exactly zero (see Eq.(5.3)). Otherwise, one of them is a retarded function and the other an advanced function. But these are at the same time points (t_1, t_2) and therefore cannot be both nonzero. Thus $G^{\alpha\beta}_{2,\text{disc.}}(\mathbf{k},\mathbf{k}',t,t') = 0$. Note that this is true regardless of the nature of the Q operators, and arises purely from the stucture of the Keldysh theory – as could be expected from a property closely related to the statement that $Z = 1$.

5.1.3.3 Connected diagram

Contributions to G_2 come solely from the connected diagram, which reads

$$\begin{aligned} G^{\alpha\beta}_{2,\text{ctd.}}(\mathbf{k},\mathbf{k}',t,t') &= \frac{2i}{2!}\sum_{\mathbf{p},\mathbf{p}'}\sum_{q,q'=\pm}\int_{-\infty}^{+\infty}\mathrm{d}t_1\mathrm{d}t_2\left\langle \mathbb{T}\,(Q^q_{\mathbf{p}})^{\bar\gamma}\,(t_1)(Q^{q'}_{\mathbf{p}'})^{\bar\delta}\,(t_2)\right\rangle \\ &\quad\left\langle \mathbb{T}(\phi^-_{\mathbf{k}})^{\alpha}(t)(\phi^{q'}_{\mathbf{p}'})^{\delta}(t_2)\right\rangle\left\langle \mathbb{T}(\phi^q_{\mathbf{p}})^{\gamma}(t_1)(\phi^+_{\mathbf{k}'})^{\beta}(t')\right\rangle \\ &= -i\int\mathrm{d}t_1\mathrm{d}t_2\left\langle \mathbb{T}(Q_{\mathbf{k}'})^{\bar\gamma}(t_2)(Q^\dagger_{\mathbf{k}})^{\bar\delta}(t_1)\right\rangle G_0^{\alpha\delta}(\mathbf{k},t-t_1)G_0^{\gamma\beta}(\mathbf{k}',t_2-t') \end{aligned} \tag{5.29}$$

Thus one can identify the self-energy at this order:

$$\Sigma_2^{\delta\gamma}(\mathbf{k},\mathbf{k}',t_2,t_1) = -i\left\langle \mathbb{T}\,(Q^\dagger_{\mathbf{k}})^{\bar\delta}\,(t_2)(Q_{\mathbf{k}'})^{\bar\gamma}\,(t_1)\right\rangle \tag{5.30}$$

The next step is to perform hydrodynamic approximations so as to obtain the collision integral for the phonons.

5.1.3.4 Wigner transform and hydrodynamic approximations

The Wigner-transformed self-energy is

$$\Sigma_2^{\delta\gamma}[\mathbf{r},t;\mathbf{k},\epsilon] = -i\int\mathrm{d}t' e^{-i\epsilon t'}\sum_{\mathbf{p}} e^{i\mathbf{p}\mathbf{r}}\left\langle \mathbb{T}\,(Q^\dagger_{\mathbf{k}+\mathbf{p}})^{\bar\delta}\,(t+\tfrac{t'}{2})(Q_{\mathbf{k}-\mathbf{p}})^{\bar\gamma}\,(t-\tfrac{t'}{2})\right\rangle \tag{5.31}$$

Because of time-translational invariance of the statistical average, which is defined using the bare action $S_0[Q]$, there is obviously no t-dependence in Σ_2. We now absorb $+\mathrm{Re}\Sigma^{\mathrm{R}}$ into the redefinition of $\omega_{\mathbf{k}}$ (henceforth identified to $\tilde{\omega}_{\mathbf{k}}$), since only the renormalized phonons' energy is the experimentally accessible quantity. Importantly, we perform a hydrodynamical approximation by assuming that Σ_2 is well approximated by its value at the quasiparticle peak, $\epsilon = \omega_{\mathbf{k}}$. Consequently,

$$\tilde{\Sigma}_2^{\delta\gamma}[\mathbf{r}, \mathbf{k}, \omega_{\mathbf{k}}] = -i \int \mathrm{d}t e^{-i\omega_{\mathbf{k}} t} \sum_{\mathbf{p}} e^{i\mathbf{pr}} \left\langle \mathbb{T}\ (Q^\dagger_{\mathbf{k}+\mathbf{p}})^{\bar{\delta}}(t)\ (Q_{\mathbf{k}-\mathbf{p}})^{\bar{\gamma}}(0) \right\rangle \tag{5.32}$$

A last hydrodynamical approximation, which I have already mentioned above in the case of time dependences of the F function, consists of assuming that the self-energy depends solely from fast variables, and that the smooth variations – which contain information beyond the quasiparticle picture – can be neglected. If this approximation is well-founded, then it is legitimate to average over positions $\mathbf{r}$; one thus obtains

$$\widetilde{\Sigma}^{\delta\gamma}(\mathbf{k}, \omega_{\mathbf{k}}) = -i \int \mathrm{d}t e^{-i\omega_{\mathbf{k}} t} \left\langle \mathbb{T}\ (Q^\dagger_{\mathbf{k}})^{\bar{\delta}}(t)\ (Q_{\mathbf{k}})^{\bar{\gamma}}(0) \right\rangle, \tag{5.33}$$

where again δ, γ are q, cl variables.

5.1.4 Quantum Boltzmann equation

5.1.4.1 Self-energies and interpretation

The phonon's retarded self-energy is

$$\widetilde{\Sigma}^{\mathrm{R}}(\mathbf{k}, \omega_{\mathbf{k}}) = \widetilde{\Sigma}^{\mathrm{q,cl}}(\mathbf{k}, \omega_{\mathbf{k}}) = -i \int \mathrm{d}t e^{-i\omega_{\mathbf{k}} t} \left\langle \mathbb{T}\ (Q^\dagger_{\mathbf{k}})^{\mathrm{cl}}\ (t)(Q_{\mathbf{k}})^{\mathrm{q}}\ (0) \right\rangle. \tag{5.34}$$

One shoud notice that the retarded self-energy of the phonons involves a "cl-q" correlation, i.e. an *advanced* Green's function of the Q operators, decoupled from the phonons. In the following we will refer to it as $\widetilde{\Sigma}^{\mathrm{R}}(\mathbf{k}, \omega_{\mathbf{k}}) = G^{\mathrm{A}}_Q(\mathbf{k}, \omega_{\mathbf{k}})$. Therefore the Q bosons should not be interpreted as particles but rather as "holes"; this, of course, is consistent with the fact that for energy to be conserved along a scattering process with interaction $a^\dagger_{n\mathbf{k}} Q^\dagger_{n\mathbf{k}} + \mathrm{h.c.}$, the Q operator should be understood as a bosonic *destruction* operator.

Similarly, the phonons' Keldysh self-energy is

$$i\widetilde{\Sigma}^{\mathrm{K}}(\mathbf{k}, \omega_{\mathbf{k}}) = i\widetilde{\Sigma}^{\mathrm{q,q}}(\mathbf{k}, \omega_{\mathbf{k}}) = \int \mathrm{d}t e^{-i\omega_{\mathbf{k}} t} \left\langle \mathbb{T}\ (Q^\dagger_{\mathbf{k}})^{\mathrm{cl}}(t)\ (Q_{\mathbf{k}})^{\mathrm{cl}}(0) \right\rangle, \tag{5.35}$$

and involves a "cl-cl" correlation, a.k.a Keldysh Green's function, of the Q operators; we write $\widetilde{\Sigma}^{\mathrm{K}}(\mathbf{k}, \omega_{\mathbf{k}}) = G^{\mathrm{K}}_Q(\mathbf{k}, \omega_{\mathbf{k}})$.

Besides, from Eq.(5.12) one can derive the following property:

$$G^{\mathrm{K}}(\mathbf{k}, \omega_{\mathbf{k}}) = F(\omega_{\mathbf{k}}) \left(G^{\mathrm{R}}(\mathbf{k}, \omega_{\mathbf{k}}) - G^{\mathrm{A}}(\mathbf{k}, \omega_{\mathbf{k}}) \right), \tag{5.36}$$

valid for any Green's functions G, be they bare or dressed. We use this in particular in the case of the G_Q functions, since the Q operators decoupled

from the phonons are not necessary free bosons. Thus, using the property that $G^{\mathrm{A}} = \left[G^{\mathrm{R}}\right]^*$, we obtain $i\widetilde{\Sigma}^{\mathrm{K}}(\mathbf{k},\omega_{\mathbf{k}}) = -2F_Q(\omega_{\mathbf{k}})\mathrm{Im}G^{\mathrm{R}}_Q(\mathbf{k},\omega_{\mathbf{k}})$, where F_Q is the F function of the Q excitations, de two variables instead of four – as is also the case in Eq.(5.36).

5.1.4.2 Collision integral

Consequently, and marking explicitly the difference between F_ϕ the phonon "population" function and F_Q that of the Q operators, we obtain

$$\begin{aligned} I^{\mathrm{coll}}[\tilde{F}] &= i\widetilde{\Sigma}^{\mathrm{K}}(n\mathbf{k},\omega_{n\mathbf{k}}) + 2\mathrm{Im}\widetilde{\Sigma}^{\mathrm{R}}(n\mathbf{k},\omega_{n\mathbf{k}})F_\phi(\omega_{n\mathbf{k}}) \\ &= -2\left(F_\phi(\omega_{n\mathbf{k}}) + F_Q(\omega_{n\mathbf{k}})\right)\mathrm{Im}G^{\mathrm{R}}_Q(n\mathbf{k},\omega_{n\mathbf{k}}). \end{aligned} \tag{5.37}$$

(From now on, I specify again the n indices.)

At this stage, both the phonons ϕ and the Q operators could be out-of-equilibrium. Provided that one derived a kinetic equation for F_Q – not necessarily based on the concept of quasiparticles, since the Q field can be more general –, one would have to solve a system of coupled kinetic equations for ϕ and Q simultaneously. This approach is pursued in the "phonon drag" methods.

Here, we will make a similar assumption as in the bulk of this thesis: we assume that the Q fields relax fast to equilibrium, so that the F_Q function is not an unknown but a parameter of the theory. Thus the term proportional to F_Q in the collision integral is a constant, which is absorbed in the definition of thermal equilibrium as the set of parameters, and the definition of thermal equilibrium as the set of variables such the collision integral vanishes (in the permanent regime where $\partial_t = 0$). The phonon's "population" function can be parameterized as $F_\phi = F^{\mathrm{eq}}_\phi + \delta F_\phi$, where F^{eq}_ϕ is the equilibrium function and δF_ϕ the out-of-equilibrium part, which alone is responsible for the net phonon thermal current. The effective collision integral thus reads $I^{\mathrm{coll}}[\tilde{F}] = -2\delta\tilde{F}(\omega_{n\mathbf{k}})\ \mathrm{Im}G^{\mathrm{R}}_Q(n\mathbf{k},\omega_{n\mathbf{k}})$.

Here a physical remark is in order. The imaginary part of a retarded Green's function is usually negative, because of the constraint of causality which puts constraints on the location of the poles. If this were correct, then the collision integral would not entail relaxation to equilibrium, but instability and a divergence of the out-of-equilibrium population $\delta\tilde{F}(\omega_{n\mathbf{k}})$.

However, in the present case, we have already emphasized that the Q (resp. $Q^\dagger$) should rather be thought of like a bosonic creation (resp. destruction) operator; therefore the retarded function of Q has the analytic properties of an usual advanced function. This, of course, is purely a notational issue, which could be easily overcome by exchanging $Q \leftrightarrow Q^\dagger$ when defining the theory, Sec.5.1.2.1.

Finally, recalling the textbook definition of a retarded function,

$$G^{\mathrm{R}}_Q(\mathbf{k},t) \quad = \quad -i\theta(t)\left\langle [Q_{n\mathbf{k}}(t), Q^\dagger_{n\mathbf{k}}(0)]\right\rangle, \tag{5.38}$$

and after some easy algebra, the collision integral can be rewritten as

$$I^{\mathrm{coll}}[\tilde{F}] = \delta\tilde{F}(\omega_{n\mathbf{k}}) \int \mathrm{d}t e^{-i\omega_{n\mathbf{k}}t}\left\langle [Q_{n\mathbf{k}}(t), Q^\dagger_{n\mathbf{k}}(0)]\right\rangle. \tag{5.39}$$

This identifies the longitudinal scattering rate of the phonons $D_{n\mathbf{k}}$, which is exactly that which we obtained in Sec.2 via scattering theory.

5.2 Spin wave expansion from spin-spin interactions

5.2.1 Various representations of the spin operators

To derive the time evolution and correlation function of the spins, in Sec.3 I presented a phenomenological expansion of the spin hamiltonian in terms of two slow fields, $\boldsymbol{m}$ and $\boldsymbol{n}$, whose effective theory was then a nonlinear sigma-model. This semiclassical approach proves very efficient when the low-energy modes are Golstone modes due to a spontaneously broken continuous symmetry of the spin hamiltonian, but fails to capture the upper part of the spin wave dispersion, especially for anisotropic models.

Another semiclassical approach, which sometimes permits a more accurate description of spin models with anisotropies, especially at intermediate energies, consists of rewriting the spin operators in terms of boson creation-annihilation operators directly within the tight-binding spin hamiltonian. [Mattis, 1981] This is the essence of the Holstein-Primakoff procedure for mapping spins onto bosons [Holstein and Primakoff, 1940], by rewriting the spin operators as $S^z_{\mathbf{r}} = S - b^\dagger_{\mathbf{r}} b_{\mathbf{r}}$ and $S^-_{\mathbf{r}} = b^\dagger_{\mathbf{r}} \sqrt{2S - b^\dagger_{\mathbf{r}} b_{\mathbf{r}}} = (S^+_{\mathbf{r}})^\dagger$, where $b^\dagger_{\mathbf{r}}$ creates a boson. From the boson algebra $[b_{\mathbf{r}}, b^\dagger_{\mathbf{r}'}] = \delta_{\mathbf{r},\mathbf{r}'}$, the spin algebra $[S^\alpha, S^\beta] = i\epsilon^{\alpha\beta\gamma} S^\gamma$ is *exactly* enforced. Besides, the square root factor ensures that the boson number cannot exceed $2S+1$, so that the dimensions of the Hilbert spaces also match – or, put more properly: the dimension of that subspace of the Hilbert space accessible by multiple applications of spin operators onto the ground state.

There exist other mappings of spins on bosons which are well-suited to describe ordered phases, like the Dyson-Maleev representation [Schollwöck et al., 2008]: $S^z_{\mathbf{r}} = S - b^\dagger_{\mathbf{r}} b_{\mathbf{r}}$ and $S^+_{\mathbf{r}} = (\sqrt{2S} - b^\dagger_{\mathbf{r}} b_{\mathbf{r}}/\sqrt{2S}) b_{\mathbf{r}} = (S^-_{\mathbf{r}})^\dagger$. This mapping appears to be slightly different from the Holstein-Primakoff one, but they are equivalent in the case of $S = 1/2$ spins.

As an aside, it is also possible to use a representation in terms of Schwinger bosons – which is the analogue to the Abrikosov fermions' construction, with $f_\alpha \to b_\alpha$ and a bosonic algebra instead of a fermionic one. The latter is usually used to describe magnetically disordered phases, although the boson condensation makes it possible to study as well the transition to an ordered phase using this representation. [Auerbach and Arovas, 2011]

5.2.2 Spin wave approximation as a semiclassical limit

In the following I will focus on the Holstein-Primakoff and Dyson-Maleev methods. Because each spin operator contains one-boson, three-boson, five-boson, etc, terms – only one and three bosons in the Dyson-Maleev case –, the tight-binding spin hamiltonian is mapped onto a theory of interacting bosons. The spin-wave approximation consists in keeping only the one-boson term in each

spin operator, so that the spin hamiltonian is approximately described by a theory of *free bosons* – or magnons, or spin wave operators. The dynamics of the system thus becomes that of free particles with a gaussian action. These have the property that their correlation functions are exactly given by the solution to the saddle-point equation, that is to say, by the classical path. Therefore this is known as a classical approximation. [Auerbach, 1994]

From the above formulae, it is clear that this approximation is equivalent to taking the $S \to \infty$ limit in the mapping. One way to understand why this is equivalent to a classical approximation is that, in the path integral formulation of the problem, S appears in front of the integral at the very place where $1/\hbar$ usually sits; the limit $\hbar \to 0$ selects those integrands which minimize the action, i.e. the classical paths. A more handwaving way to understand this is from the spin algebra: in the large-S limit, the rhs of $[S^\alpha, S^\beta] = i\epsilon^{\alpha\beta\gamma}S^\gamma$ is $O(1/S)$ of the lhs, which means that the S^α operators become asymptotically classical (in the sense that they asymptotically commute) when $S \to \infty$.

A practical manifestation of this is that when only the one-boson term in each spin operator is kept, the spin algebra is no longer exactly enforced – however it is recovered in the limit $S \to \infty$.

5.2.3 Equivalence with the nonlinear sigma-model approach

The above mapping of a spin hamiltonian onto a boson hamiltonian does not use the concept of a lagrangean or an action: the bosonic theory is already written in its quantized form, with the bosonic commutation relation $[b, b^\dagger] = 1$ and the bosonic (restricted) space of states defined directly from the mapping. While this might look like a very different approach to that of the nonlinear sigma-model, written as a field theory in terms of a lagrangian with a kinetic term $i\boldsymbol{m}\partial_\tau\boldsymbol{n}$, the two approaches are in fact equivalent.

This can be seen from a description of spins in terms of real bosons, or equivalently in terms of two local real fields u, v. [Ross et al., 2011] These are defined in the local basis $(\mathbf{e}_t, \mathbf{e}_u, \mathbf{e}_v)$ dependent on position $\mathbf{r}$, where $\mathbf{e}_t(\mathbf{r})$ is collinear with the local spin orientation in the ordered state, and $\mathbf{e}_u, \mathbf{e}_v$ are chosen orthogonal to it so as to form an orthonormal basis. The spins can then be parameterized as

$$\mathbf{S}_\mathbf{r} = (-1)^\mathbf{r}\left[S - (u_\mathbf{r}^2 + v_\mathbf{r}^2 - 1)/2\right]\mathbf{e}_t(\mathbf{r}) + \sqrt{S}u_\mathbf{r}\mathbf{e}_u(\mathbf{r}) + (-1)^\mathbf{r}\sqrt{S}v_\mathbf{r}\mathbf{e}_v(\mathbf{r}). \quad (5.40)$$

The real-bosons (a.k.a position-momentum) commutation relation $[u_\mathbf{r}, v_{\mathbf{r}'}] = i\delta_{\mathbf{r},\mathbf{r}'}$ recovers the spin algebra up to $O(1/S)$ corrections. Their kinetic term in the Lagrangian is $u\partial_t v$, as befits a couple of position and momentum operators.

Thus the u, v fields are analogous to the lattice displacement and momentum fields $\boldsymbol{u}, \boldsymbol{p}$ in elasticity theory. In the latter case, quantizing the lattice theory expresses it in terms of phonon operators. [Ashcroft and Mermin, 1976] Similarly, quantizing the magnetic theory expresses it in terms of magnon operators, which appear to be equivalent to the Holstein-Primakoff bosons after the classical approximation. Notice that the number of degrees of freedom between

phonons and magnons is different: there are three phonon polarizations while only one magnon polarization.

So far it appears that the Holstein-Primakoff construction is equivalent to a representation in terms of local real bosons u, v as defined in Eq.(5.40). Now how are these fields u, v related to the nonlinear sigma-model in terms of $\boldsymbol{m}, n$ fields? The difference lies in the fact that the u, v fields are defined in the lattice unit cell, or equivalently in the "large" Brillouin zone defined by the lattice in its paramagnetic phase. By contrast, the $\boldsymbol{m}, \boldsymbol{n}$ fields are defined in the magnetic unit cell, which because of Néel antiferromagnetic order is twice as large as the lattice unit cell – and equivalently they are defined in the "small" Brillouin zone. Therefore the number of modes is in fact the same in the two descriptions: in the nonlinear sigma-model with a Néel order along the $\hat{\boldsymbol{x}}$ axis, there are two slow modes n^y, n^z and two fast modes n^y, n^z, while in the real-boson description there are one slow (say, $u_{\mathbf{k}}$) and one fast (say, $v_{\mathbf{k}}$) modes in the $(0, 0)$ valley, and one slow ($v_{\mathbf{k}+\boldsymbol{\pi}}$) and one fast ($u_{\mathbf{k}+\boldsymbol{\pi}}$) modes in the $\boldsymbol{\pi} = (\pi, \pi)$ valley. Thus the two descriptions are equivalent in the case considered.

Résumé

Dans cette thèse, l'on étudie la diffusion intrinsèque des phonons par un degré de liberté quantique générique, c'est-à-dire un champ Q dont les corrélations, a priori complètement générales, sont restreintes uniquement par l'unitarité et l'invariance par translation. Les taux de diffusion résultant de cette interaction ont des conséquences sur le tenseur de conductivité thermique des phonons ; nous les calculons dans le cadre de la théorie quantique de la diffusion. La dynamique hors d'équilibre des phonons, elle, est étudiée dans le cadre de la théorie cinétique via l'équation de Boltzmann.

À l'ordre le plus bas, le taux de diffusion diagonal, qui détermine la conductivité longitudinale, est contrôlé par les fonctions de corrélation à deux points du champ Q. Les taux de diffusion off-diagonaux, quant à eux, impliquent des fonctions de corrélation à aux moins trois points, voire quatre dans le cas d'interactions à un phonon. Nous avons obtenu des formes générales et explicites pour ces corrélations, qui isolent les contributions spécifiques à la conductivité de Hall. Nous en tirons une discussion générale des conséquences d'une symétrie du système et de l'équilibre thermodynamique local sur le tenseur de conductivité.

Nous calculons ensuite ces fonctions de corrélation à deux et quatre points, et les coefficients de transport thermique qui en résultent, pour une interaction à un phonon et deux opérateurs de création ou d'annihilation bosoniques quelconques. Le couplage, générique, est contraint seulement par l'hermiticité et l'invariance par translation. Afin d'illustrer ce formalisme par l'exemple, nous considérons ensuite le cas particulier d'un matériau antiferromagnétique bidimensionnel, où le champ Q est un opérateur composite de créations-annihilations de magnons, généré par le couplage entre les spins et le réseau. Nous considérons un modèle sigma pour la dynamique de basse énergie des spins, et un couplage des spins au réseau aussi général que possible compte tenu des symétries ; ce modèle permet un calcul analytique des taux de diffusion.

Par une analyse des intégrales impliquées dans l'expression des résultats théoriques, nous extrayons la dépendance en température des conductivités thermiques, en fonction de divers paramètres du modèle. Ces intégrales sont ensuite calculées numériquement. Nous prouvons ainsi explicitement que nos résultats, tout en satisfaisant à toutes les contraintes de symétrie du système, impliquent un effet Hall thermique non nul par diffusion inélastique des phonons par les magnons. En outre, l'effet Hall obtenu est d'amplitude comparable pour des courants thermiques dans le plan de l'ordre magnétique, et perpendiculairement à celui-ci.

Nous calculons ensuite les mêmes fonctions de corrélation à deux et quatre points, et les coefficients de transport thermique qui en résultent, pour une interaction à un phonon et deux opérateurs fermioniques quelconques préservant le nombre total de fermions. Le couplage, générique, est contraint seulement par l'hermiticité et l'invariance par translation. Nous calculons les taux de diffusion diagonaux et off-diagonaux qui en résultent, à la fois pour une dispersion linéaire (et pour tout remplissage) et pour une dispersion quadratique (en présence d'une surface de Fermi) des fermions, où une résolution analytique est possible.

Afin d'élucider le rôle des corrélations dans une phase magnétiquement désordonnée, nous considérons ensuite le cas particulier d'une surface de Fermi de spinons dans un liquide de spin U(1). Après une étude du rôle des symétries dans l'intégrale de collision, nous proposons un modèle d'interaction entre les spins et le réseau, permettant de rendre compte d'un effet Hall thermique par les phonons, que nous avons calculé explicitement. Enfin, le champ électromagnétique émergent associé aux spinons peut lui aussi fluctuer et interagir avec le réseau. Nous proposons donc un couplage phénoménologique entre les phonons et les photons émergents, dont nous déduisons une contribution à la conductivité thermique des phonons.